ISSN 0100-736X (Print)
ISSN 1678-5150 (Online)
Volume 40 Number 12
December 2020

PESQUISA VETERINÁRIA BRASILEIRA

Brazilian Journal of Veterinary Research



Colégio Brasileiro de Patologia Animal

www.pvb.com.br

PESQUISA VETERINÁRIA BRASILEIRA - Brazilian Journal of Veterinary Research (http://www.pvb.com.br/), edited by the scientific association Colégio Brasileiro de Patologia Animal (CBPA) in collaboration with institutions, such as Universidade de Brasília (UnB) and Universidade Federal Rural do Rio de Janeiro (UFRRJ). Pesq. Vet. Bras publishes original papers on animal diseases and related subjects divided by the following areas: **Livestock Diseases (LD), Small Animal Diseases (SA), Wildlife Medicine (WM) and Animal Morphophysiology (MF).**

Pesq. Vet. Bras. is edited from 1981, in continuation to the "Archives of the Institute of Animal Biology" (1959-1961) and the Veterinary Series (1968-1976) of the "Pesquisa Agropecuária Brasileira".

Pesq. Vet. Bras. publishes subjects about natural and experimental diseases. The journal details the diagnostic investigations of natural and emerging diseases of animals; especially herd diseases with occurrence in Brazil. The submission of topics on animal diseases related to public health is encouraged. Pathology in its broad sense is the flagship of the journal, including laboratory diagnostic, epidemiology, clinics and others. Each issue features Original Articles, Reviews or Topics of General Interest; Case Reports are only accepted in the area of Wildlife Medicine (WM). These articles aim a public consisting of veterinary practitioners, pathologists, veterinary diagnostic laboratory staff, toxicologic pathologists, comparative pathologists, medical pathology researchers, environmental scientists, and others involved in veterinary diagnostics and animal research across domestic species and wildlife.

For the preparation of the manuscript, authors must follow the format indicated by the journal, which can be found under "Instructions for Authors," "Submission of articles" in the journal webpage (http://www.pvb.com.br/instructions_to_authors.pdf). Submission of articles outside the presentation standards will be disregarded.

Critical review articles should only be submitted upon invitation by the Chief-Editor and should be supported by original publications of the author on the subject. The editors assume that papers submitted are not being considered for publication in other journals and do not contain material which has already been published. Submitted papers are peer reviewed.

Articles as of January, 2019 will be published in English, including a Portuguese Abstract when Portuguese is the native language of one of the authors.

The journal is indexed and/or abstracted by: SciELO-Scientific Electronic Library Online (www.scielo.br/pvb); ISI/Thomson Reuters, in its products Science Citation Index Expanded and BIOSIS Previews; CABI, in its key-databases CAB Abstracts and Global Health, and in several derived databases, such as: Animal Science Database and VetMedResources (for the internet), Index Veterinarius and Veterinary Science Database (abstract databases), and Veterinary Bulletin (printed), DOAJ-Directory of Open Access Journals (http://www.doaj.org).

Founding General Editor, 1981-2018
Jürgen Döbereiner

Editorial Board

Chief-Editor: David Driemeier (UFGRS), Porto Alegre, RS (davetpat@ufrgs.br).
Managing Editor: Daniel G. Ubiali (UFRRJ), *Seropédica, RJ* (daniel.ubiali@pvb.com.br).
Image-Editor: Asheley H.B. Pereira (UFRRJ), *Seropédica, RJ* (imagens@pvb.com.br).
Publisher: Grillo Tecnologia & Colégio Brasileiro de Patologia Animal (CBPA)

Livestock Diseases

Editor: David Driemeier (UFGRS), Porto Alegre, RS (davetpat@ufrgs.br).
Associate Editors: Ana Lucia Schild (UFPel), *Pelotas, RS* (alschild@terra.com.br); David Driemeier (UFRGS), *Porto Alegre, RS* (davetpat@ufrgs.br); Francisco A. Uzal, (UCDavis), *San Bernardino, CA, USA* (fuzal@cahfs.ucdavis.edu); Franklin Riet-Correa (Instituto Nacional de Investigación Agropecuaria), *La Estanzuela*, *Uruguay* (frcorrea@inia.org.uy); Leticia Trevisan Gressler (IF Farroupilha), Frederico Westphalen, RS (letrevi@gmail.com); Mateus M. Costa (Univasf), *Petrolina, PE* (mmatiuzzi@hotmail.com); Raquel Rech (Texas A&M University), *College Station, TX, USA* (rrech@cvm.tamu.edu); Ricardo A.A. Lemos (UFMS), *Campo Grande, MS* (ricardo.lemos@ufms.br); Roselene Ecco (UFMG), *Belo Horizonte, MG* (eccoro.ufmg@gmail.com).

Small Animal Diseases

Editor: Claudio S.L. Barros (UFMS), *Campo Grande, MS* (cbarros@pvb.com.br).
Associate Editors: Alexandre Mazzanti (UFSM), *Santa Maria, RS* (alexamazza@yahoo.com.br); Corrie Brown (University of Georgia), *Athens, GA, USA* (corbrown@uga.edu); Daniel R. Rissi (Athens Vet. Diagn. Lab.), *Athens, GA, USA* (danielricardorissi@yahoo.com.br); Ingeborg M. Langohr (Louisiana State University), *Baton Rouge, USA* (langohri@dcpah.msu.edu); Leticia Trevisan Gressler (IF Farroupilha), Frederico Westphalen, RS (letrevi@gmail.com); Luciana Sonne (UFRGS), *Porto Alegre, RS* (lusonne@yahoo.com.br); Saulo P. Pavarini (UFRGS), *Porto Alegre, RS* (sauloppvet@yahoo.com.br); Ticiana N. França (UFRRJ), *Seropédica, RJ* (ticianafranca19@gmail.com).

Wildlife Medicine

Editor: Pedro M.O. Pedroso (UnB), *Brasília, DF* (pedrosovet@yahoo.com.br).
Associate Editors: Juliana T.S.A. Macêdo (UnB), *Brasília, DF* (jtsam_targino@yahoo.com.br); Mauro Pereira Soares (UFPel), *Pelotas, RS* (gmpsoares@gmail.com); Ricardo B. Lucena (UFPB), *Areia, PB* (lucena.rb@gmail.com).

Animal Morphophysiology

Editor: Carlos Eduardo Ambrósio (USP), *FZEA-Pirassununga, SP* (ceambrosio@usp.br).
Associate Editors: Antônio C. Assis Neto (USP), *São Paulo, SP* (antonioassis@usp.br); Daniele S. Martins (USP), *FZEA-Pirassununga, SP* (daniele@usp.br); Maria Angélica Miglino (USP), *São Paulo, SP* (miglino@usp.br); Tatiana C. Santos (UEM), *Maringá, PR* (tcsantos@uem.br).

Apoio:

Pesq. Vet. Bras. also has resources from the *Conselho Federal de Medicina Veterinária* (CFMV).

Advisory Board

Adivaldo H. Fonseca (UFRRJ), Seropédica, RJ
Aldo Gava (UDESC), Lages, SC
Alessandra E.S. Lima (UFBA), Salvador, BA
Alexandre Mazzanti (UFSM), Santa Maria, RS
Alexandre S. Borges (Unesp), Botucatu, SP
Aline M. Viott (UFPR), Palotina, PR
Aline R. Hoffmann, Diplomada ACVP (Texas A&M University), College Station, TX, USA
Amauri A. Alfieri (UEL), Londrina, PR
Ana Lucia Schild (UFPel), Pelotas, RS
Angélica T.B. Wouters (UFLA), Lavras, MG
Aníbal G. Armién, Diplomado ACVP (Univeristy of Minnesota), St. Paul, USA
Antônio F.M. Dantas (UFCG), Patos, PB
Axel Colling (CSIRO), Gueelong, Australia
Bruno L. Anjos (Unipampa), Uruguaiana, RS
Carlos L. Massard (UFRRJ), Seropédica, RJ
Caroline A. Pescador (UFMT), Cuiabá, MT
Cláudio E.F. Cruz (UFRGS), Porto Alegre, RS
Claudio S.L. Barros, Membro honorário ACVP (UFMS), Campo Grande, MS
Claudio W. Canal (UFRGS), Porto Alegre, RS
Corrie Brown, Diplomada ACVP (University of Georgia), Athens, GA, USA
Daniel A. Balthazar (UFRRJ), Seropédica, RJ
Daniel C.L. Linhares (Iowa State University), Ames, USA
Daniel G. Ubiali (UFRRJ), Seropédica, RJ
Daniel R. Rissi, Diplomado ACVP (University of Georgia), Athens, GA, USA
Daniela I.B. Pereira (UFPel), Pelotas, RS
Danilo C. Gomes (UFMS), Campo Grande, MS
David Driemeier (UFRGS), Porto Alegre, RS
David E.S.N. Barcellos (UFRGS), Porto Alegre, RS
Djeison L. Raymundo (UFLA), Lavras, MG
Eduardo F. Flores (UFSM), Santa Maria, RS
Edson M. Colodel (UFMT), Cuiabá, MT
Fabiana M. Boabaid (Univ. La Republica), Tacuarembo, Uruguay
Fabiano J.F. Sant'Ana (UnB), Brasília, DF
Fábio S. Mendonça (UFRPE), Recife, PE
Felício G. Júnior (UFCG), Patos, PB
Felipe Pierezan, Diplomado ACVP (UFMG), Belo Horizonte, MG
Félix Gonzáles (UFRGS), Porto Alegre, RS
Fernando H. Furlan (UFMT), Cuiabá, MT
Fernando R. Spilki (Univ. Feevale), Novo Hamburgo, RS
Flademir Wouters (UFLA), Lavras, MG
Francisco A. Uzal, Diplomado ACVP (UCDavis), San Bernardino, CA, USA
Franklin Riet-Correa (Instituto Nacional de Investigación Agropecuaria), La Estanzuela, Uruguay
Glaucia D. Kommers (UFSM), Santa Maria, RS
Glauco J.N. Galiza (UFCG), Patos, PB
Guilherme G. Verocai (Texas A&M University), College Station, TX, USA
Gustavo S. Silva (Iowa State University), Ames, USA
Huarrison A. Santos (UFRRJ), Seropédica, RJ
Ingeborg M. Langohr, Diplomada ACVP (Louisiana State University), Baton Rouge, LA, USA
Iveraldo S. Dutra (Unesp), Araçatuba, SP
Janildo L. Reis Júnior, Diplomado ACVP (UFJF), Juiz de Fora, MG
Jean Carlos R. Silva (UFRPE), Recife, PE
Jeann Leal de Araujo (Texas A&M University), College Station, TX, USA
John Edwards, Diplomado ACVP (Texas A&M University), College Station, TX, USA
José Diomedes Barbosa (UFPA), Castanhal, PA
José Luiz Catão-Diaz (USP), São Paulo, SP
José M.V. Garcia (Univ. La Republica), Montevideo, Uruguay
José R.J. Borges (UnB), Brasília, DF
Josué Díaz-Delgado, Diplomado ACVP (USP), São Paulo, SP
Juliana S. Brum (UFPR), Curitiba, PR
Juliana T.S.A. Macêdo (UnB), Brasília, DF
Luciana Sonne (UFRGS), Porto Alegre, RS
Luciano A. Pimentel (UFRB), Cruz das Almas, BA
Luciano Nakazato (UFMT), Cuiabá, MT
Luciano S. Alonso (UFRRJ), Seropédica, RJ
Luis Fernando Pita Gondim, (UFBA), Salvador, BA
Marcelo B. Labruna (USP), São Paulo, SP
Mauro Pereira Soares (UFPel), Pelotas, RS
Mateus M. Costa (Univasf), Petrolina, PE
Paula R. Giaretta, Diplomada ACVP (Texas A&M University), College Station, TX, USA
Paulo César Maiorka (USP), São Paulo, SP
Paulo M. Roehe (UFRGS), Porto Alegre, RS
Paulo V. Peixoto (UFRRJ), Seropédica, RJ
Pedro M.O. Pedroso (UnB), Brasília, DF
Pedro Malafaia (UFRRJ), Seropédica, RJ
Pedro S. Bezerra Junior (UFPA), Castanhal, PA
Peres R. Badial (Mississipi State University), Starkville, MS, USA
Raquel R. Rech, Diplomada ACVP (Texas A&M University), College Station, TX, USA
Renata A. Casagrande (UDESC), Lages, SC
Ricardo A.A. Lemos (UFMS), Campo Grande, MS
Ricardo B. Lucena (UFPB), Areia, PB
Roberto M.C. Guedes (UFMG), Belo Horizonte, MG
Roselene Ecco (UFMG), Belo Horizonte, MG
Rudi Weiblen (UFMS), Santa Maria, RS
Saulo A. Caldas (UFRRJ), Seropédica, RJ
Saulo P. Pavarini (UFRGS), Porto Alegre, RS
Tatiane T.N. Watanabe, Diplomada ACVP (North Carolina State University), Raleigh, NC, USA
Tessie B. Martins (UFMS), Campo Grande, MS
Tiago C. Peixoto (UFBA), Salvador, BA
Ticiana N. França (UFRRJ), Seropédica, RJ
Valéria Dutra (UFMT), Cuiabá, MT
Welden Panziera (UFRGS), Porto Alegre, RS

Pesquisa Veterinária Brasileira. - - vol.1, n.1 (1981) - . - - Rio de Janeiro: Colégio Brasileiro de Patologia Animal, 1981 -

il.; 28 cm

Mensal.

Resumos em inglês e português.

ISSN 0100-736X (*Print*).

ISSN 1678-5150 (*Online*).

Título traduzido: *Brazilian Journal of Veterinary Research*.

Continuação de: "Arquivos do Instituto de Biologia Animal" (1959-1961) e à Série Veterinária (1968-1976) da "Pesquisa Agropecuária Brasileira".

I. Colégio Brasileiro de Patologia Animal.

Tiragem: 100 exemplares.

ISSN 0100-736X (*Print*)
ISSN 1678-5150 (*Online*)

PESQUISA VETERINÁRIA BRASILEIRA

Brazilian Journal of Veterinary Research

The "Pesquisa Veterinária Brasileira" scientific journal is edited from 1981 in continuation to the "Arquivos do Instituto de Biologia Animal" (1959-1961) and the Veterinary Series (1966-1976) of "Pesquisa Agropecuária Brasileira".

Colégio Brasileiro de Patologia Animal

www.pvb.com.br

Cover illustration: Proliferation of epithelial cells arranged in multiple nests with keratin pearls in a hamster with squamous cell carcinoma (Wentz et al., pag. 1032)

PESQUISA VETERINÁRIA BRASILEIRA
Brazilian Journal of Veterinary Research
ISSN 0100-736X (Print)
ISSN 1678-5150 (Online)

Pesq. Vet. Bras. 40(12):947-954, December 2020
DOI: 10.1590/1678-5150-PVB-6658

Original Article
Livestock Diseases
BY-NC

Gangrenous mastitis in sheep caused by multidrug-resistant *Staphylococcus haemolyticus*[1]

Guilherme S. Moura[2], Rinaldo A. Mota[2], Michele F.S. Marques[2], Atzel C.A. Abad[2], Luciana B.B.C. Costa[3], Fernando N. Souza[4], Valdir M. Almeida[5], Givaldo B. Silva Filho[6], Hisadora A.S.C. Bom[6], Francine Klaumann[6], Francisco A.L. Souza[6] and Fábio S. Mendonça[6]*

ABSTRACT.- Moura G.S., Mota R.A., Marques M.F.S., Abad A.C.A., Costa L.B.B.C., Souza F.N., Almeida V.M., Silva Filho G.B., Bom H.A.S.C., Klaumann F., Souza F.A.L. & Mendonça F.S. 2020. **Gangrenous mastitis in sheep caused by multidrug-resistant *Staphylococcus haemolyticus*.** *Pesquisa Veterinária Brasileira 40(12):947-954.* Laboratório de Diagnóstico Animal, Universidade Federal Rural de Pernambuco, Rua Dom Manoel de Medeiros s/n, Dois Irmãos, Recife, PE 52171-900, Brazil. E-mail: fabio.mendonca@ufrpe.br

Mastitis is a multifactorial disease and considered one of the most critical problems in the dairy industry worldwide. The condition is characterized by reduced milk and several abnormalities in the mammary gland. This study aimed to report an outbreak of gangrenous mastitis caused by multidrug-resistant *Staphylococcus haemolyticus* in a Santa Inês sheep herd. Eighteen sheep were affected, and five of them with severe clinical pictures were examined. The clinical and pathological picture were variable and characterized by apathy, anorexia, emaciation, opaque and brittle hair, apparent and congested episcleral vessels, and hyperthermia. These ewes had enlarged, firm, and painful mammary glands. Macroscopically, these lesions consisted of severe gangrenous mastitis, and microscopically, the primary lesions consisted of necrosis, thrombosis, and fibrosis of the mammary parenchyma. Milk samples from one of the five severely affected ewes were collected and cultured under aerobic or microaerophilic incubation at 37°C for 24 hours on sheep blood agar. The obtained colonies were then submitted to MALDI-TOF for speciation. The colonies were also submitted to an antimicrobial susceptibility test, genotyping of virulence factors and resistance genes were also performed. The isolates showed antimicrobial multiresistance since they were resistant to seven out of 13 tested antibiotics. The isolates were also positive for two staphylococcal enterotoxigenic genes (*sec* and *see*) and fibronectin-binding protein B (*fnbB*).

INDEX TERMS: Gangrene, mastitis, sheep, multidrug-resistant, *Staphylococcus haemolyticus*, non-*aureus* staphylococci, small ruminant, ovine.

[1] Received on July 18, 2020.
Accepted for publication on September 4, 2020.

[2] Departmento de Medicina Veterinária, Universidade Federal Rural de Pernambuco (UFRPE), Rua Dom Manoel s/n, Dois Irmãos, Recife, PE 52171-900, Brazil.

[3] Department of Veterinary Preventive Medicine, College of Veterinary Medicine, Ohio State University, 281 W Lane Ave, Columbus, OH 43210, USA.

[4] Departamento de Ciências Clínicas, Universidade de São Paulo (USP), Rua da Reitoria 374, Cidade Universitária, Butantã, SP 05508-220, Brazil.

[5] Hospital Veterinário, Universidade Federal de Campina Grande (UFCG), Avenida Universitária s/n, Bairro Santa Cecília, Cx. Postal 61, Patos, PB 58708-110, Brazil.

[6] Laboratório de Diagnóstico Animal, Universidade Federal Rural de Pernambuco (UFRPE), Rua Dom Manoel s/n, Dois Irmãos, Recife, PE 52171-900, Brazil. *Corresponding author: fabio.mendonca@ufrpe.br

RESUMO.- [**Mastite gangrenosa em ovinos causada por *Staphylococcus haemolyticus* multirresistente.**] A mastite é uma doença multifatorial e é considerada um dos problemas mais importantes na indústria de laticínios no mundo todo. A condição é caracterizada pela redução de leite e várias anormalidades na glândula mamária. O objetivo deste estudo foi relatar um surto de mastite gangrenosa causada por *Staphylococcus haemolyticus* multirresistente em um rebanho ovino Santa Inês. Dezoito ovelhas foram afetadas e cinco delas com quadro clínico severo foram examinadas. O quadro clínico-patológico era variável quanto a severidade e consistia em apatia, anorexia, magreza, pelos opacos e quebradiços e vasos episclerais aparentes e ingurgitados. As ovelhas apresentavam glândulas aumentadas, firmes e

dolorosas. Macroscopicamente, as principais lesões consistiam em mastite gangrenosa e microscopicamente havia necrose do parênquima glandular, trombose e fibrose. Amostras de leite de uma das cinco ovelhas severamente afetadas foram coletadas e cultivadas sob incubação aeróbica ou microaerofílica a 37°C por 24 horas em ágar sangue de ovelha. As colônias obtidas foram então submetidas ao MALDI-TOF para especiação. Além disso, as colônias foram submetidas a um teste de suscetibilidade antimicrobiana e foi realizada a genotipagem de fatores de virulência e genes de resistência. Os isolados apresentaram multirresistência antimicrobiana por serem resistentes a sete dos 13 antibióticos testados. Os isolados também foram positivos para dois genes enterotoxigênicos estafilocócicos (*sec* e *see*) e proteína B de ligação à fibronectina (*fnbB*).

TERMOS DE INDEXAÇÃO: Mastite, gangrena, ovinos, *Staphylococcus haemolyticus*, multirresistente, estafilococos não-aureus, pequenos ruminantes.

INTRODUCTION

Mastitis is an inflammation of the mammary gland tissue frequently found in ruminants during lactation. In addition to in cattle, mastitis in small ruminants is one of the most critical problems causing significant economic losses in sheep flocks and the dairy industry (Giadinis et al. 2012, Gelasakis et al. 2015). The disease, characterized by reduced milk, pain, anxiety, restlessness, and feeding behavior changes, is developed based on three processes: invasion of an organism, infection, and inflammation (Murphy 1947). Several pathogens have been associated with clinical or subclinical mastitis in ewes (Contreras et al. 2007), in most cases, different bacteria species. For dairy ruminants, *Streptococcus agalactiae* and *Staphylococcus aureus* were considered the primary causes of the disease during previous decades (Ruegg 2017). Currently, pathogens such as *Mannheimia haemolytica* are also included as mastitis causal agents (Omaleki et al. 2010).

In subclinical disease, non-*aureus* staphylococci (NAS) are the most prevalent pathogens found in udders of ewes affected by mastitis (Bergonier et al. 2003, Mørk et al. 2005, Contreras et al. 2007, Gelasakis et al. 2015). Although less pathogenic than *S. aureus*, NAS can also produce persistent subclinical mastitis progressing to clinical disease (Deinhofer & Pernthaner 1995, Contreras et al. 1997, Ariznabarreta et al. 2002). Among NAS, *Staphylococcus epidermidis* is a common species associated with ovine mastitis (Onni et al. 2011), followed by *Staphylococcus chromogenes*, *Staphylococcus simulans*, and *Staphylococcus xylosus*. Other infrequently isolated species, including *Staphylococcus auricularis*, *Staphylococcus capitis*, *Staphylococcus caprae*, *Staphylococcus cohnii*, *Staphylococcus equorum*, *Staphylococcus haemolyticus*, *Staphylococcus hominis*, *Staphylococcus lentus*, *Staphylococcus muscae*, *Staphylococcus saprophyticus*, *Staphylococcus sciuri*, and *Staphylococcus warneri*, were reported in other studies (Fthenakis 1994, Bergonier et al. 2003).

There are no NAS reports causing gangrenous mastitis in sheep to the best of our knowledge. Several studies using molecular tools have suggested that NAS are acquiring virulence factors that might be able to facilitate their transformation into potential clinical mastitis agents (Cunha et al. 2006, Pyörälä & Taponen 2009, Dando et al. 2014). Therefore, this study aimed to report an outbreak of gangrenous mastitis caused by multidrug-resistant *S. haemolyticus* in a sheep flock.

MATERIALS AND METHODS

Sheep farm and animals. This study was performed on a herd of 60 Santa Inês adult sheep located in Limoeiro, Pernambuco, northeastern Brazil (07°52'29" S 35°27'0" W). Epidemiological and clinical data were obtained from the owner and veterinarian during technical visits. A total of eighteen ewes were affected by clinical mastitis at different levels of intensity. Five of them, which were severely affected, were selected and examined in detail according to the clinical condition. Additionally, parameters such as behavior, appetite, mucous membrane color, rectal temperature, heart and respiratory rates, abdominal morphology, reticulum-rumen motility, and the physical appearance of their feces, urine, and skin were also observed. The physical examination identified a disease based on the mammary gland by palpation and visible abnormalities, including the milk's coloration and consistency concerning clinical mastitis.

As the clinical signs evolved, three sheep worsened and died spontaneously, so the owner allowed the necropsy to be performed.

Milk sampling, bacterial speciation and antibiotic resistance patterns. Two milk samples from one ewe were aseptically collected after scrubbing the teat ends with 2% iodine solution. Ten microliters of samples were cultured on 5% sheep blood agar (Oxoid) and incubated for 24 hours at 37°C. We considered an intramammary infection (IMI) to be present if more than 100 colony forming units / mL were detected in the bacteriological culture. Then, colonies were submitted to matrix-assisted laser desorption/ionization - time of flight (MALDI-TOF) for speciation. Bacterial samples were prepared as previously described (Cameron et al. 2017). Measurements were performed on a Microflex LT mass spectrometer (Bruker Daltonics) with a standard pattern-matching algorithm (BioTyper 2.0 Software).

The isolate was submitted to an antimicrobial susceptibility test through a VITEK® automated system using the methodology previously described (Spoor et al. 2013). All the minimum inhibitory concentrations (MIC) were interpreted in accordance with performance standards for antimicrobial disk and dilution susceptibility tests for bacteria isolated from animals of the Clinical and Laboratory Standards Institute (CLSI 2018).

DNA extraction and conventional PCR to detect virulence genes. Sixteen virulence genes (*fnbA, fnbB, clfA, clfB, sea, seb, sec, sed, see, seg, seh, sei, tsst, blaZ, mecA, mecC*) were analyzed (Table 1). Briefly, the DNA was extracted from 300µL of milk using a Wizard® Genomic DNA Purification kit (Promega, Madison/WI) according to the manufacturer's instructions. To detect virulence factor gene fragments in the tested samples, a conventional PCR assay was performed based on the protocol previously described (Mehrotra et al. 2000). All primers (Mehrotra et al. 2000, Sabat et al. 2003) used for amplification are displayed in Table 1. The PCR products were run on a 2% TAE agarose gel stained with Blue Green Loading Dye I (LGC Biotecnologia, São Paulo, Brazil) and photographed under a UV illuminator (L.PIX Molecular Imaging- Loccus biotecnologia, São Paulo, Brazil).

Gross and microscopy lesions. At necropsy, tissue sections from the central nervous system, thorax, abdominal organs and mammary gland were obtained and fixed in 10% buffered formalin. For histopathological observations, sections of the fixed tissues were processed routinely, embedded in paraffin, sectioned (4µm), stained with hematoxylin and eosin (HE) and examined under a light microscope.

RESULTS

Clinical, gross and histopathological findings

Eighteen out of 60 (30%) ewes showed clinical signs characterized by apathy, anorexia, emaciation (Fig.1), opaque and brittle hair, apparent and congested episcleral vessels, and hyperthermia. The owner reported that mammary glands were enlarged and that a purulent discharge was observed when ewes were milked. The ewes were treated for two weeks with oxytetracycline (10mg/kg/12h, IM) and amoxicillin with clavulanic acid (10mg/kg/12h, IM) without an efficient response. Thirteen out of 18 sheep (72.2%) were moderately affected, and five out of 18 sheep (27.8%) were severely affected by the clinical signs described above. Five sheep somewhat affected presented unilateral mastitis, and in these ewes, the uninfected sides were also swollen and tense, with reduced secretion. In general, the affected udders were swollen and tense, hot and firm, and very painful. There was complete stagnation of secretion in severe cases, and only a few milliliters of brown, blood-stained, or purulent secretion was observed when sheep were milked. In these cases, the clinical picture evolved to sternal recumbency, adipsia, cold extremities, mean temperature of 36°C, tachycardia, tachypnea, and comatose state. The signs progressed to spontaneous death in five affected ewes.

Macroscopically, the primary lesions consisted of severe gangrenous mastitis that presented an intense necrohemorrhagic characteristic. In the external examination of three ewes that



Fig.1. Ewe with gangrenous mastitis exhibiting a clinical picture characterized by apathy, prolonged recumbency, anorexia, emaciation and opaque and brittle hair.

Table 1. Target gene, initiator oligonucleotides and size of the amplification product of virulence genes for *Staphylococcus*

Target gene	Name	Oligonucleotide sequence (5´- 3´)	Expected size (bp)	Tm (°C)
fnbA	fnbA_R	ACTTCACCTGTCGCCATTAC	539 bp	61
	fnbA_F	GCAGTACAAGCACCACAAAC		
fnbB	fnbB_F	AGGCGACGGCAAAGATAAA	317 bp	57
	fnbB_R	TAGTAACCTGACCACCACCT		
*clfA**	clfA_F	GATTCTGACCCAGGTTCAGA	945 bp	60
	clfA_R	CTGTATCTGGTAATGGTTCTTT		
*clf**	clfB_F	ATGGTGATTCAGCAGTAAATCC	880 bp	55
	clfB_R	CATTATTTGGTGGTGTAACTCTT		
sea	sea_F	CCGAAGGTTCTGTAGAAGTATG	269 bp	55
	sea_R	GCTTGTATGTATGGTGGTGTA		
seb	seb_F	CCCGTTTCATAAGGCGAGTT	314 bp	55
	seb_R	ACGTAGATGTGTTTGGAGCTAAT		
sec†	sec_F	AGATGAAGTAGTTGATGTGTATGG	451 bp	57
	sec_R	CACACTTTTAGAATCAACCG		
sed	sed_F	GTCACTCCACACGAAGGTAATAA	255 bp	57
	sed_R	GAGACTTTAGACCCATCAGAAGAA		
see†	see_F	GCTGGAGGCACACCAAATA	301 bp	55
	see_R	CATAACTTACCGTGGACCCTTC		
seg	seg_F	GCCAGTGTCTTGCTTTGTAATC	491 bp	57
	seg_R	GAATGCTCAACCCGATCCTAA		
she	seh_F	CACATCATATGCGAAAGCAGAAG	365 bp	56
	seh_R	CCCAAACATTAGCACCAATCAC		
sei	sei_F	AGGCAGTCCATCTCCTGTATAA	568 bp	60
	sei_R	TGCTCAAGGTGATATTGGTGTAG		
tss†	tsst_F	ACCCCTGTTCCCTTATCATC	326 bp	55
	tsst_R	TTTTCAGTATTTGTAACGCC		
blaZ	blaZ_F	AAGAGATTTGCCTATGCTTC	102 bp	55
	blaZ_R	GCTTGACCACTTTTATCAGC		
mecA	mecA1	AAAATCGATGGTAAAGGTTGG	533 bp	52
	mecA2	AGTTCTGCAGTACCGGATTTGC		
mecC	$mec_{ALGA251}$ 1A	CATTAAAATCAGAGCGAGGC	188 bp	59
	$mec_{ALGA251}$ 1B	TGGCTGAACCCATTTTTGAT		

bp = Base pairs, Tm = primer melting temperature; * Primers described by Sabat et al. (2003); † Primers described by Mehrotra et al. (2000).

were severely affected, the udders very firm, enlarged and asymmetric (Fig.2A). The color of the skin was blue, ranging from black. The skin aspect was soft; ulcerations were also observed, and one or both teats were absent due to necrosis (Fig.2B). The affected glandular tissue was swollen and turgid, whereas the lobular parenchyma was necrotic, hemorrhagic, and contained bloody-purulent discharge (Fig.2C). The periductal tissues were white, rigid due to the lack of glandular tissue and fibrosis. The lactiferous sinus and larger ducts had a thickened lining and small rounded polypoid projections into the lumen (Fig.2D). Additionally, reactive supramammary lymph nodes were also observed. Other lesions consisted of congestion of the small intestine's blood vessels; the livers were enlarged, congested, and friable and had rounded edges, with enlarged gallbladders. In the epicardium, areas of petechiae were observed, and both sides of the cranial lobes of the lungs generally had a dark-red coloration with a smooth and shiny surface. Microscopically, the main lesions were characterized by necrosis, thrombosis and fibrosis of the mammary parenchyma (Fig.3A). The periacinar epithelium was vacuolated, necrotic, and large amounts of intralesional bacterial colonies widespread into proteinaceous eosinophilic material were noted. In the necrotic areas, severe inflammatory cell infiltration is composed mainly of degranulated neutrophils, macrophages, epithelioid macrophages, and Langhans giant cells, as well as a small number of lymphocytes and plasma cells (Fig.2C and 3B). Lymphocytes and plasma cells were observed mainly in the interstitium, and sometimes lymphoid follicles were noted, especially around the lactiferous sinus and ducts. Granulation and fibrosis were noted, obliterating many of the acini and lobules, and in these areas, severe thrombosis was remarkable (Fig.3D). The glandular ducts and lactiferous sinus were filled with many neutrophils and necrotic epithelioid macrophages. Other lesions less specific



Fig.2. Gangrenous mastitis in ewes. (**A**) Three ewes showing enlarged and asymmetrical udders. (**B**) Ewe with gangrenous mastitis. The aspect of the skin was friable and ulcerated; the udder was firm and one teat is lacking due to necrosis. (**C**-**D**) The mammary gland had a bloody to purulent content and the affected glandular tissue was swollen and turgid whereas the lobular parenchyma was intensely necrohemorrhagic. The lactiferous sinus is thickened and lining and obstructed by polypoid projections into the lumen.

included mild to moderate infiltration of neutrophils and lymphocytes and plasma cells that were usually seen in the perisinusoidal spaces and among hepatocytes. They were often focally concentrated in sites of mild necrosis at the centrilobular areas. In the lungs, a severe neutrophilic and lymphoplasmacytic inflammatory infiltrate was frequently observed. The alveolar spaces, septa, and bronchioles contained scattered neutrophils, lymphocytes, plasma cells, fibrin, few erythrocytes (hemorrhage), and necrotic cellular debris. Additionally, there was dilated lymphatics and amorphic, homogenous, eosinophilic material (edema) expanding the alveolar lumen.

Bacteriological results

The bacteriological results revealed a pure round, gram-positive, catalase positive and coagulase negative colony in the growth conditions. The obtained isolate was identified by MALDI-TOF as *Staphylococcus haemolyticus*, which showed antimicrobial multiresistance characteristics since resistance was observed in nine out of 15 (60%) tested antibiotics (benzylpenicillin, clindamycin, erythromycin, oxacillin, rifampicin, tetracycline and vancomycin). MIC values and the antimicrobial resistance pattern are shown in Table 2.

Virulence factors

PCR results revealed that the isolate was positive for two staphylococcal enterotoxigenic genes (*sec* and *see*) and fibronectin-binding protein B (*fnbB*). In contrast, the isolate was negative for *fnbB, clfA, clfB, sea, seb, sed, seg, seh, sei, tsst, blaZ, mecA* and *mecC*.

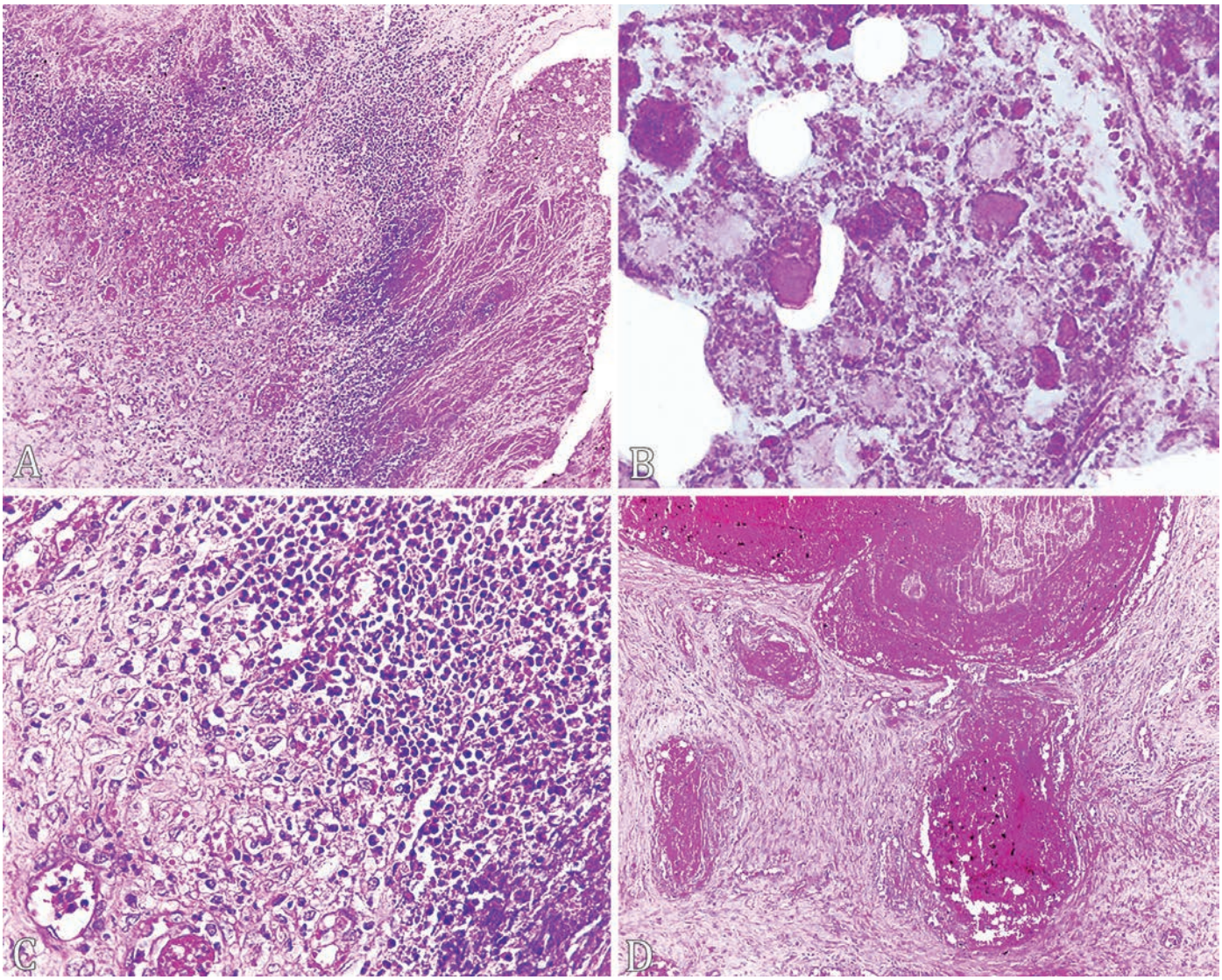


Fig.3. Ewe mammary gland affected by gangrenous mastitis. (**A**) Predominantly, the main lesions were characterized by necrosis, thrombosis and fibrosis of the mammary parenchyma. HE, obj.10x. (**B**) The periacinar epithelium was necrotic and large amounts of intralesional bacterial colonies widespread into proteinaceous eosinophilic material was noted. HE, obj.10x (**C**) Necrotic areas had severe inflammatory cell infiltration composed mainly by degranulated neutrophils, macrophages, lymphocytes and plasma cells. HE, obj.40x. (**D**) Replacement of the glandular parenchyma by fibrous connective tissue and a remarkable thrombosis. HE, obj.10x.

Table 2. Antibiotic resistance pattern of *Staphylococcus haemolyticus* isolated from a mastitis in a sheep

Antibiotics	MIC	Interpretation
Benzylpenicillin	≥0.5	R
Clindamycin	≥8	R
Chloramphenicol	8	S
Enrofloxacin	≤0.5	S
Erythromycin	≥8	R
Gentamicin	≤0.5	S
Kanamycin	≤4	S
Marbofloxacin	≤0.5	S
Oxacillin	≥4	R
Rifampicin	≥32	R
Tetracycline	≥16	R
Trimethoprim/ Sulfamethoxazole	≤10	S
Vancomycin	≥4	R

MIC = minimum inhibitory concentrations, R = resistant, S = sensitive.

DISCUSSION

This study reports a severe and uncommon clinical condition in a flock of meat sheep characterized by gangrenous mastitis and presented systemic clinical signs caused by *Staphylococcus haemolyticus*. The NAS have been isolated in many cases of sheep mastitis (Pyörälä & Taponen 2009). For this reason, the importance of this group of bacteria has been reviewed, and they are presently considered the most important etiologic agents of subclinical mastitis in sheep (Bergonier et al. 2003, Contreras et al. 2007). However, there have been no reports of gangrenous mastitis cases in sheep caused by multidrug-resistant non-*aureus* staphylococci.

In meat production systems, most clinical mastitis cases are associated with *Staphylococcus aureus* or *Mannheimia haemolytica* (Mavrogianni et al. 2007, Arsenault et al. 2008, Kopp 2010, Omaleki et al. 2010, Gelasakis et al. 2015), including gangrenous mastitis (Vautor et al. 2009). The proportion of NAS among bacteria isolated from clinical mastitis cases remains very low in many countries (Pyörälä & Taponen 2009). However, although less pathogenic than *S. aureus* and *M. haemolytica*, NAS can also produce persistent subclinical mastitis, significantly increasing milk somatic cell counts, which could cause clinical mastitis (Deinhofer & Pernthaner 1995, Contreras et al. 1997, Ariznabarreta et al. 2002), as well as producing thermostable enterotoxins (Meyrand et al. 1998, Udo et al. 1999).

Nevertheless, despite the accepted role of these bacteria as major intramammary infection-causing pathogens in small ruminants, the different NAS species' pathogenicity varies widely (Gonzalo et al. 2002, Bergonier et al. 2003). The most commonly isolated NAS species in persistent subclinical intramammary infection in goats and sheep are *Staphylococcus epidermidis*, *Staphylococcus caprae*, *Staphylococcus simulans*, *Staphylococcus chromogenes*, and *Staphylococcus xylosus* (Gonzalo et al. 2002, Bergonier et al. 2003, Contreras et al. 2003). *S. epidermidis* and *S. caprae* are among the most prevalent causal microorganisms in goats, and *S. epidermidis* and *S. simulans* are commonly found in ewes (Contreras et al. 2007).

MALDI-TOF identified the isolate as *S. haemolyticus*. MALDI-TOF was used to determine the *Staphylococcus* isolate at the species level. This approach is vital because this differentiation into species gives us essential information since, in veterinary medicine, we often assume that all NAS form a group with the same characteristics, which is not correct. *S. haemolyticus* is one of the most commonly isolated NAS from bovine mastitis (Hosseinzadeh & Dastmalchi Saei 2014); however, in small ruminants, they are not considered a significant pathogen (Leitner et al. 2009). Gangrene in the mammary gland is the result of marked necrosis caused by β-toxin and often progresses to septicemia. Most *S. haemolyticus* isolates show β-hemolytic activity that leads to an escape of bacteria from the host immune system, permitting the pathogen's survival (Pinheiro et al. 2015). In PCR results, the isolate was negative for the *mec*A and *mec*C genes but positive for the *bla*Z gene. We also detected two staphylococcal enterotoxigenic genes (*sec* and *see*) and fibronectin-binding protein B (*fnbB*).

S. haemolyticus isolates showed antimicrobial multiresistance characteristics, resistant to seven of the 13 antibiotics tested (Table 2). This feature is a result, among other factors, of the relationship between bacterial pathogenicity, host physical resistance, and the resulting selection of interventions such as antimicrobial therapy (Geisinger & Isberg 2017), a condition that hinders response to treatment and, under varying conditions, may become a risk to human health. This multidrug resistance pattern might be the result of selective pressure from the frequent use of antibiotics. These animals received indiscriminate treatment by the farmer. Resistance to benzylpenicillin is common in *S. haemolyticus* (Taponen et al. 2016), and resistance against β-lactams or aminoglycosides is the most common trait observed in *Staphylococcus* spp. Although the isolate was not favorable for the *mec*A and *mec*C genes, it showed phenotypic resistance to oxacillin and vancomycin, a trait that is not common. Multidrug and methicillin-resistant strains are particularly challenging because they narrow therapeutic options, increasing the risk of treatment failure and costs. In this study, genotypic testing for vancomycin resistance was not possible.

Interestingly, compiled data in the molecular analysis showed two staphylococcal enterotoxigenic genes (*sec* and *see*) and fibronectin-binding protein B (*fnbB*). The presence of the sec and see genes correspond to two of the five major types of staphylococcal enterotoxins (*sea, seb, sec, sed*, and *see*) (Johler et al. 2016). Staphylococcal toxins known to be pyrogenic and related to important human diseases, such as food poisoning and septic shock, are commonly associated with *S. aureus*. However, other species have already been shown to be enterotoxigenic (Frey et al. 2013), as in the case reported here. Fibronectin-binding protein B (*fnbB*) belongs to the MSCRAMM (microbial surface components recognizing adhesive matrix molecules) family, adhesins that are well described in *S. aureus* isolates and are known to mediate the adhesion of *Staphylococcus* spp. to fibrinogen, elastin, and fibronectin (Murai et al. 2016), mediating immune evasion mechanisms (Burke et al. 2010), hindering their action. However, the identification of MSCRAMM in non-*aureus* staphylococci (NAS) is poorly described.

Histopathological findings were possible to observe a granulomatous inflammatory process, chronic active in the mammary gland, in addition to areas of necrosis. This is also a characteristic observed in mastitis caused by coagulase-negative *Staphylococcus* in ruminants (Benites et al. 2002).

CONCLUSION

The current study provides evidence of gangrenous mastitis in sheep flocks caused by multidrug-resistant *Staphylococcus haemolyticus*, a non-*aureus* staphylococci. Further studies are needed to clarify the epidemiological, clinical, and histological association of bacterial presence in small ruminants in gangrenous mastitis cases.

Acknowledgments.- In particular, we would like to acknowledge the technical assistants and all farmers who collaborated during the farm work. This work was financially supported by the "Coordenação de Aperfeiçoamento de Pessoal de Nível Superior" (CAPES), process no. 88881.189204/2018-01 and for grant 8887.357759/2019-00. This work was also funded by "Fundação de Amparo à Pesquisa do Estado de São Paulo" (FAPESP), fellowship (process no. 2014/23189-4).

Conflict of interest statement.- The authors declare that the research was conducted in the absence of any commercial or financial relationships that could be construed as a potential conflict of interest.

REFERENCES

Ariznabarreta A., Gonzalo C. & San Primitivo F. 2002. Microbiological quality and somatic 1 cell count of ewe milk with special reference to *staphylococci*. J. Dairy Sci. 85(6):1370-1375. <https://dx.doi.org/10.3168/jds.S0022-0302(02)74203-3> <PMid:12146466>

Arsenault J., Dubreuil P., Higgins R. & Bélanger D. 2008. Risk factors and impacts of clinical and subclinical mastitis in commercial meat-producing sheep flocks in Quebec, Canada. Prev. Vet. Med. 87(3/4):373-393. <https://dx.doi.org/10.1016/j.prevetmed.2008.05.006> <PMid:18656275>

Benites N.R., Guerra J.L., Melville P.A. & Da Costa E.O. 2002. Aetiology and histopathology of bovine mastitis of espontaneous occurrence. J. Vet. Med. Bras. 49(8):366-370. <https://dx.doi.org/10.1046/j.1439-0450.2002.00566.x> <PMid:12449243>

Bergonier D., De Crémoux R., Rupp R., Lagriffoul G. & Berthelot X. 2003. Mastitis of dairy small ruminants. Vet. Res. 34(5):689-716. <https://dx.doi.org/10.1051/vetres:2003030> <PMid:14556701>

Burke F.M., Mccormack N., Rindi S., Speziale P. & Foster T.J. 2010. Fibronectin-binding protein B variation in *Staphylococcus aureus*. BMC Microbiol. 10:160. <https://dx.doi.org/10.1186/1471-2180-10-160> <PMid:20515471>

Cameron M., Barkema H.W., De Buck J., De Vliegher S., Chaffer M., Lewls J. & Keefe G.P. 2017. Identification of bovine-associated coagulase-negative *staphylococci* by matrix-assisted laser desorption/ionization time-of-flight mass spectrometry using a direct transfer protocol. J. Dairy Sci. 100(3):2137-2147. <https://dx.doi.org/10.3168/jds.2016-12020> <PMid:28041734>

CLSI 2018. Performance Standards for Antimicrobial Disk and Dilution Susceptibility Tests for Bacteria Isolated From Animals. 4th ed. CLSI supplement VET08, Clinical and Laboratory Standards Institute, Wayne, PA.

Contreras A., Corrales J.C., Sanchez A. & Sierra D. 1997. Persistence of subclinical intrammary pathogens in goats throughout lactation. J. Dairy Sci. 80(11):2815-2819. <https://dx.doi.org/10.3168/jds.s0022-0302(97)76245-3> <PMid:9406073>

Contreras A., Luengo C., Sánchez A. & Corrales J.C. 2003. The role of intramammary pathogens in dairy goats. Livest. Prod. Sci. 79(2/3):273-283. <https://dx.doi.org/10.1016/S0301-6226(02)00172-0>

Contreras A., Sierra D., Sánchez A., Corrales J.C., Marco J.C., Paape M.J. & Gonzalo C. 2007. Mastitis in small ruminants. Small Ruminant Res. 68(1/2):145-153. <https://dx.doi.org/10.1016/j.smallrumres.2006.09.011>

Cunha M.L.R., Rugolo L.M.S.S. & Lopes C.A.M. 2006. Study of virulence factors in coagulase-negative staphylococci isolated from newborns. Mem. Inst. Oswaldo Cruz 101(6):661-668. <https://dx.doi.org/10.1590/s0074-02762006000600014> <PMid:17072480>

Dando S.J., Mackay-Sim A., Norton R., Currie B.J., St John J.A., Ekberg J.A.K., Batzloff M., Ulett G.C. & Beacham I.R. 2014. Pathogens penetrating the central nervous system: infection pathways and the cellular and molecular mechanisms of invasion. Clin. Microbiol. Rev. 27(4):691-726. <https://dx.doi.org/10.1128/CMR.00118-13> <PMid:25278572>

Deinhofer M. & Pernthaner A. 1995. *Staphylococcus* spp. as mastitis-related pathogens in goat milk. Vet. Microbiol. 43(2/3):161-166. <https://dx.doi.org/10.1016/0378-1135(95)92532-g> <PMid:7740755>

Frey Y., Rodriguez J.P., Thomann A., Schwendener S. & Perreten V. 2013. Genetic characterization of antimicrobial resistance in coagulase-negative staphylococci from bovine mastitis milk. J. Dairy Sci. 96(4):2247-2257. <https://dx.doi.org/10.3168/jds.2012-6091> <PMid:23415536>

Fthenakis G.C., Marples R.R., Richardson J.F. & Jones J.E. 1994. Some properties of coagulase-negative staphylococci isolated from cases of ovine mastitis. Epidemiol. Infect. 112(1):171–176. <https://dx.doi.org/10.1017/s0950268800057538> <PMid:8119356>

Geisinger E. & Isberg R.R. 2017. Interplay between antibiotic resistance and virulence during disease promoted by multidrug-resistant bacteria. J. Infect. Dis. 215(Supl.1):S9-S17. <https://dx.doi.org/10.1093/infdis/jiw402> <PMid:28375515>

Gelasakis A.I., Mavrogianni V.S., Petridis I.G., Vasileiou N.G.C. & Fthenakis G.C. 2015. Mastitis in sheep: the last 10 years and the future of research. Vet. Microbiol. 181(1/2):136-146. <https://dx.doi.org/10.1016/j.vetmic.2015.07.009> <PMid:26216457>

Giadinis N.D., Arsenos G., Tsakos P., Psychas V., Dovas C.I., Papadopoulos E., Karatzias H. & Fthenakis G.C. 2012. "Milk-drop syndrome of ewes": investigation of the causes in dairy sheep in Greece. Small Ruminant Res. 106(1):33-35. <https://dx.doi.org/10.1016/j.smallrumres.2012.04.018>

Gonzalo C., Ariznabarreta A., Carriedo J.A. & San Primitivo F. 2002. Mammary pathogens and their relationship to somatic cell count and milk yield losses in dairy ewes. J. Dairy Sci. 85(6):1460-1467. <https://dx.doi.org/10.3168/jds.S0022-0302(02)74214-8>

Hosseinzadeh S. & Dastmalchi S.H. 2014. Staphylococcal species associated with bovine mastitis in the North West of Iran: emerging of coagulase-negative staphylococci. Int. J. Vet. Sci. Med. 2(1):27-34. <https://dx.doi.org/10.1016/j.ijvsm.2014.02.001>

Johler S., Sihto H.M., Macori G. & Stephan R. 2016. Sequence variability in staphylococcal enterotoxin genes seb, sec, and sed. Toxins, Basel, 8(6):169. <https://dx.doi.org/10.3390/toxins8060169> <PMid:27258311>

Kopp M. 2010. Speciation and the neutral theory of biodiversity. BioEssays 32(7):564-570. <https://dx.doi.org/10.1002/bies.201000023> <PMid:20586053>

Leitner G., Sela S., Hammer-Muntz O., Zivotofsky D., Weisblit L., Chaffer M. & Zamir S. 2009. Outbreak of subclinical mastitis in a flock of dairy goats associated with atypical *Staphylococcus haemolyticus*. J. Dairy Res. 76(1):1-5. <https://dx.doi.org/10.1017/S0022029908003646> <PMid:18922198>

Mavrogianni V.S., Cripps P.J. & Fthenakis G.C. 2007. Bacterial flora and risk of infection of the ovine teat duct and mammary gland throughout lactation. Prevent. Vet. Med. 79(2/4):163-173. <https://dx.doi.org/10.1016/j.prevetmed.2006.11.014> <PMid:17208321>

Mehrotra M., Wang G. & Johnson W.M. 2000. Multiplex PCR for detection of genes for *Staphylococcus aureus* enterotoxins, exfoliative toxins, toxic shock syndrome toxin 1, and methicillin resistance. J. Clin. Microbiol. 38(3):1032-1035. <https://dx.doi.org/10.1128/JCM.38.3.1032-1035.2000> <PMid:10698991>

Meyrand A., Boutrand-Loei S., Ray-Gueniot S., Mazuy C., Gaspard C.E., Jaubert Perrin G., Lapeyre C. & Vernozy-Rozand C. 1998. Growth and enterotoxin production of *Staphylococcus aureus* during the manufacture and ripening of Camembert-type cheeses from raw goats' milk. J. Appl. Microbiol. 85(3):537-544. <https://dx.doi.org/10.1046/j.1365-2672.1998.853531.x> <PMid:9750284>

Mørk T., Tollersrud T., Kvitle B., Jørgensen H.J. & Waage S. 2005. Genetic diversity of *Staphylococcus aureus* isolated from ovine intramammary infections in Norway. Vet. Microbiol. 106(3/4):265-273. <https://dx.doi.org/10.1016/j.vetmic.2004.12.020> <PMid:15778033>

Murai M., Moriyama H., Hata E., Takeuchi F. & Amemura-Maekawa J. 2016. Variation and association of fibronectin-binding protein genes fnbA and fnbB in *Staphylococcus aureus* Japanese isolates. Microbiol Immunol. 60(5):312-325. <https://dx.doi.org/10.1111/1348-0421.12377> <PMid:26990092>

Murphy J.M. 1947. The genesis of bovine udder infection and mastitis; the occurrence of streptococcal infection in a cow population during a seven-year period and its relationship to age. Am. J. Vet. Res. 8(26):29-42. <PMid:20284858>

Omaleki L., Barber S.R., Allen J.L. & Browning G.F. 2010. Mannheimia species associated with ovine mastitis. J. Clin. Microbiol. 48(9):3419-3422. <https://dx.doi.org/10.1128/JCM.01145-10> <PMid:20660220>

Onni T., Sanna G., Larsen J. & Tola S. 2011. Antimicrobial susceptibilities and population structure of *Staphylococcus epidermidis* associated with ovine mastitis. Vet. Microbiol. 148(1):45-50. <https://dx.doi.org/10.1016/j.vetmic.2010.07.024> <PMid:20817422>

Pinheiro L., Brito C.I., De Oliveira A., Martins P.Y., Pereira V.C. & Da Cunha M. 2015. *Staphylococcus epidermidis* and *Staphylococcus haemolyticus*: molecular detection of cytotoxin and enterotoxin genes. Toxins 7(9):3688-3699. <https://dx.doi.org/10.3390/toxins7093688> <PMid:26389954>

Pyörälä S. & Taponen S. 2009. Coagulase-negative staphylococci-emerging mastitis pathogens. Vet. Microbiol. 134(1/2):3-8. <https://dx.doi.org/10.1016/j.vetmic.2008.09.015> <PMid:8848410>

Ruegg P.L. 2017. A 100-year review: mastitis detection, management, and prevention. J. Dairy Sci. 100(12):10381-10397. <https://dx.doi.org/10.3168/jds.2017-13023> <PMid:29153171>

Sabat A., Krzyszton-Russjan J., Strzalka W., Filipek R., Kosowska K., Hryniewicz W., Travis J. & Potempa J. 2003. New method for typing *Staphylococcus aureus* strains: multiple-locus variable number tandem repeat analysis of polymorphism and genetic relationships of clinical isolates. J. Clin. Microbiol. 41(4):1801-1804. <https://dx.doi.org/10.1128/jcm.41.4.1801-1804.2003> <PMid:12682193>

Spoor L.E., Mcadam P.R., Weinert L.A., Rambaut A., Hasman H., Aarestrup F.M., Kearns A.M., Larsen A.R., Skov R.L. & Fitzgerald J.R. 2013. Livestock origin for a human pandemic clone of 5 community- associated methicillin-resistant *Staphylococcus aureus*. MBio 4(4): e00356-13. <https://dx.doi.org/10.1128/mBio.00356-13> <PMid:23943757>

Taponen S., Nykäsenoja S., Pohjanvirta T., Pitkälä A. & Pyörälä S. 2016. Species distribution and in vitro antimicrobial susceptibility of coagulase - negative -staphylococci isolated from bovine mastitic milk. Acta Vet. Scand. 58:12. <https://dx.doi.org/10.1186/s13028-016-0193-8> <PMid:26852389>

Udo E.E., Al-Bustan M.A., Jacob L.E. & Chugh T.D. 1999. Enterotoxin production by coagulase-negative staphylococci in restaurant workers from Kuwait City may be a potential cause of food poisoning. J. Med. Microbiol. 48(9):819-823. <https://dx.doi.org/10.1099/00222615-48-9-819> <PMid:10482292>

Vautor E., Cockfield J., Le Marechal C., Le Loir Y., Chevalier M., Robinson D.A., Thiery R. & Lindsay J. 2009. Difference in virulence between *Staphylococcus aureus* isolates causing gangrenous mastitis versus subclinical mastitis in a dairy sheep flock. Vet. Res. 40(6):56. <https://dx.doi.org/10.1051/vetres/2009039> <PMid:19576164>

PESQUISA VETERINÁRIA BRASILEIRA
Brazilian Journal of Veterinary Research
ISSN 0100-736X (Print)
ISSN 1678-5150 (Online)

Pesq. Vet. Bras. 40(12):955-962, December 2020
DOI: 10.1590/1678-5150-PVB-6675

Original Article
Livestock Diseases
BY-NC

Lesions of the sheep reproductive system found in a slaughterhouse in the state of Bahia, Brazil[1]

Reanne M.M. Silva[2], Juliana T.S.A. Macêdo[3], Maira S.C. Lacerda[3], João Paulo M.V.B. Azevedo[3], Jair A. Ferreira Júnior[3], Robson B. Cerqueira[4] and Pedro Miguel O. Pedroso[2,3]*

ABSTRACT.- Silva R.M.M., Macêdo J.T.S.A., Lacerda M.S.C., Azevedo J.P.M.V.B., Ferreira Júnior J.A., Cerqueira R.B. & Pedroso P.M.O. 2020. **Lesions of the sheep reproductive system found in a slaughterhouse in Bahia state, Brazil**. *Pesquisa Veterinária Brasileira 40(12):955-962*. Laboratório de Patologia Veterinária, Fundação Universidade de Brasília, Campus Universitário Darcy Ribeiro, Via L4 Norte s\n, Brasília, DF, 70910-970, Brazil. E-mail: pedrosovet@yahoo.com.br

The present study aimed to evaluate and diagnose pathologies of the reproductive system of slaughtered sheep in slaughterhouses in the state of Bahia since there are few data on the subject as well as it is important to note the diagnosis of these diseases to apply appropriate control and prophylaxis measures. The research was carried out in slaughterhouses in the state of Bahia according to the "Serviço de Inspeção Federal" and "Serviço de Inspeção Estadual" for sheep slaughter. From July 2018 to February 2019, visits and monitoring of 1,072 slaughtered sheep were carried out. The animals came from 22 municipalities in the state of Bahia, aged from six to 18 months. During slaughter, the sheep reproductive systems were sectioned for evisceration and lesion collection. Additionally, epidemiological surveys related to origin, age, and race were obtained. For bacteriological examination, collections were performed with sterile scalpel slides and swabs in Stuart medium sterile tubes and refrigerated in a thermal box. For histopathological analysis, fragments were fixed in 10% formaldehyde and routinely processed for histology, stained with Hematoxylin and Eosin (HE). A study of the sheep's main pathological changes in slaughterhouses in the state of Bahia was carried out, in which 1.072 genital systems were evaluated, and 211 alterations were identified. The most affected reproductive organs were the ovaries (65.3%), followed by the uterus (29.4%) and uterine tubes (5.3%). In the ovaries, the most frequent lesion was a follicular cyst (34.1%); in the fallopian tubes, the cysts represented 3.3% of the lesions, and in the womb, endometritis was observed in 9% of the animals. Other pathologies identified in the ovaries were: luteinized cyst (2.3%); cystic granulosa cell tumor (0.5%); benign lesion (0.5%); agenesis unilateral (0.5%), in addition to other changes of little clinical significance, such as corpus luteum cysts (11.8%) and paraovarian cysts (15.6%). In the fallopian tubes, hydrosalpinx was observed (1%), as well as adenoma (0.5%), agenesis (0.5%), and cysts (3.3%). Uterine lesions included hydrometra (2.3%); Cystic Endometrial Hyperplasia (CEH), abscess, and pyometra (1.4% each); adenomyosis, womb sera petechiae, and total segmental aplasia (1% each); two pregnant uterus, in early pregnancy, presented pyometra (0.9%), however, no change was observed in the fetuses; and uterine polyp (0.5%). Ectopic pregnancy with fetal maceration (0.5%) was observed; vaginitis occurred in 0.5% of the animals, and endometrial melanosis in 8.5%. The high incidence of follicular cysts and endometritis are characterized as diseases that reduce the reproductive efficiency in herds, causing infertility and economic losses in production.

INDEX TERMS: Sheep, reproductive system, slaughterhouse, Brazil, ovaries, pathology, follicular cysts, endometritis.

[1] Received on July 21, 2020.
Accepted for publication on July 30, 2020.
Part of Doctoral Dissertation of the first author.

[2] Graduate Program in Animal Science in the Tropics, Universidade Federal da Bahia (UFBA), Medicina Veterinária, Av. Adhemar de Barros 500, Ondina, Salvador, BA 40170-110, Brazil.

[3] Laboratório de Patologia Veterinária, Fundação Universidade de Brasília (UnB), Campus Universitário Darcy Ribeiro, Via L4 Norte s\n, Brasília, DF 70910-970, Brazil. *Corresponding author: pedrosovet@yahoo.com.br

[4] Laboratório de Doenças Infecciosas, Hospital Universitário de Medicina Veterinária, Universidade Federal do Recôncavo da Bahia (UFRB), Rua Rui Barbosa 710, Cruz das Almas, BA 44380-000, Brazil.

RESUMO.- [Lesões do sistema reprodutor em ovelhas de abatedouros frigoríficos no estado da Bahia.] O objetivo do presente trabalho foi avaliar e diagnosticar alterações do sistema reprodutor de ovelhas abatidas em abatedouros frigoríficos no estado da Bahia. A pesquisa foi realizada em abatedouros frigoríficos do estado da Bahia com Serviços de Inspeção Federal e Estadual no abate de ovinos. No período de julho de 2018 a fevereiro de 2019 foram realizadas visitas e acompanhamento do abate de 1.072 ovelhas. Os animais eram provenientes de 22 municípios do estado da Bahia, com idade entre 6 a 18 meses. Durante o abate, na evisceração foram seccionados os sistemas reprodutores das ovelhas para avaliação e coleta das lesões. Adicionalmente foram obtidos inquéritos epidemiológicos relacionados à procedência, idade e raça. Para o exame bacteriológico, as coletas foram realizadas com lâminas de bisturi estéreis e *swabs* em tubos estéreis com meio Stuart e refrigeradas em caixa térmica. Para análise histopatológica, os fragmentos foram fixados em formol a 10% e processados de forma rotineira para histologia e corados pela hematoxilina e eosina (HE). Entre 1.072 sistemas genitais avaliados, identificou-se 211 alterações. Os órgãos do sistema reprodutor mais acometidos foram os ovários (65,3%), útero (29,4%) e tubas uterinas (5,3%). Nos ovários, a lesão mais frequente foi o cisto folicular (34,1%); no útero a endometrite (9%) e nas tubas uterinas, os cistos representaram (3,3%). Outras lesões identificadas nos ovários foram: cisto luteinizado (2,3%); tumor de células da granulosa (0,5%); adenoma (0,5%); agenesia unilateral (0,5%), além de outras alterações de pouco significado clínico, como cistos paraovarianos (15,6%) e corpo lúteo cístico (11,8%). Nas tubas uterinas observou-se, além dos cistos tubo-ovarianos (3,3%), hidrossalpinge (1%), adenoma (0,5%) e agenesia (0,5%). As lesões uterinas foram endometrite (9%), hidrometra (2,3%); hiperplasia endometrial cística, abscesso e piometra (1,4% cada); adenomiose, petéquias na serosa do útero e aplasia segmentar (1% cada); dois úteros gravídicos, em início de gestação, apresentaram piometra (0,9%), porém os fetos não apresentaram alterações; e pólipo uterino (0,5%). Observou-se uma gestação ectópica com maceração fetal (0,5%); a vaginite ocorreu em 0,5%, e melanose endometrial em 8,5%. Destaca-se a elevada incidência de cistos foliculares e endometrite que são doenças que reduzem a eficiência reprodutiva dos rebanhos, provocando infertilidade e perdas econômicas na produção.

TERMOS DE INDEXAÇÃO: Sistema reprodutor, ovelhas, abatedouro, frigorífico, Brasil, ovários, patologia, cistos foliculares, endometrite, ovinos.

INTRODUCTION

Brazil has the largest flock of sheep in Latin America, with approximately 18.9 million head, with the Northeast region and the state of Bahia occupying both the 1st place (IBGE 2018). In Brazil, sheep farming is extensive, with low technological investment and reduced zootechnical indicators, formed mainly by mixed or native sheep (Santos 2001, Osório & Rassi 2011). However, the exploration of small ruminants is a growing activity and important for the Northeast region, mainly due to its adaptability to the arid and semi-arid regions of the country, characterized by long periods of drought, high temperatures, and shallow soils that are difficult to drain (Santos 2001, Leite & Simplício 2005, Holanda Júnior & Martins 2007, Monte 2008). It is essential to highlight that some studies have been carried out in slaughter sheep in Brazil to diagnose the main parasitic and infectious lesions, demonstrating that these studies are also important to reduce errors in slaughter condemnations in animals and guarantee the quality of products for consumers (Souza et al. 2011, Higino et al. 2013, Panziera et al. 2018). Reproductive efficiency is one of the most critical factors that promote productivity of sheep farming and economic viability, being essential for developing the herd. However, injuries to the reproductive system have significant limitations, which causes a drop in production (Agrawal 2010, Carvalho Júnior et al. 2010). Thus, diagnosis is necessary to prevent and control the main diseases that affect the sheep reproductive system.

The objective of this study was to evaluate the main changes found in the reproductive system of slaughtered sheep in slaughterhouses in the state of Bahia to identify the main injuries that cause losses in sheep farming and facilitate the development of prevention and control measures.

MATERIALS AND METHODS

The research was carried out in three slaughterhouses for sheep and goats in the state of Bahia according to the "Serviço de Inspeção Federal" and "Serviço de Inspeção Estadual". In the period from July 2018 to February 2019, 1,072 emaciated sheep were slaughtered. During slaughter, the evisceration (removal of internal organs) begins, i.e., the sheep reproductive system was sectioned to evaluate and collect material for anatomopathological and bacteriological examinations. In addition, epidemiological information related to the origin, age, and race of the animals was obtained. The changes were grouped into six categories based on macroscopic and microscopic descriptions: inflammatory, degenerative and proliferative changes, developmental abnormalities, and others.

Reproductive systems with lesions were analyzed macroscopically; then fragments were collected and fixed in 10% buffered formaldehyde, cleaved, processed routinely for histology, and stained with Hematoxylin and Eosin (HE). For the bacteriological examination, collections were performed with sterile scalpel slides and swabs in sterile tubes with Stuart medium and refrigerated in a thermal box. In addition, they were sent to the laboratory for isolation and identification of the etiological agent. The culture media used for primary seeding of uterine secretion were blood agar, chocolate agar, McConkey agar, and Thioglycolate. The biochemical tests used for bacterial identification were Rugai medium, citrate, malonate, urea, lysine, ornithine decarboxylase, Sulfide, Indole, Motility (SIM) medium, catalase, coagulase, Bile Esculin Agar (BEA), Brain Heart Infusion (BHI) Agar, NaCl, and mannitol.

The statistics were based on descriptive analysis as a percentage of the frequency of macroscopic and histopathological changes in the results obtained.

RESULTS

During the studied period, 196 (18.3%) samples of sheep with alterations in the reproductive system were analyzed, with 2.2% of the animals showing concomitant lesions; the total number of injuries corresponded to 19.6% (211/1,072). The animals were consisted of Dorper, Santa Inês, Mestiço, and no defined breeds, aged from six to 18 months and came from 22 municipalities in the state of Bahia, mainly in the North Central region.

The most affected organs of the reproductive system were the ovaries 65.3% (138/211), followed by the uterus 29.4% (62/211) and fallopian tubes 5.3% (11/211). In the ovaries, the most evident lesion was the follicular cyst 34.1% (72/211); in utero, endometritis with 9.0% (19/211) and regarding the uterine tubes, cysts with 3.3% (7/211). The classification and number of the identified injuries are shown in Table 1.

Ovarian changes

In addition to the follicular cyst, the following lesions were diagnosed in the ovaries: paraovarian cysts 15.6% (33/211) and corpus luteum cysts 11.8% (25/211). Findings of little clinical significance were also diagnosed, such as: 2.3% luteinized cyst (5/211); granulosa cell tumor 0.5% (1/211); adenoma 0.5% (1/211) and agenesis 0.5% (1/211).

In the follicular cyst, this cyst consisted of cystic dilatations filled with translucent fluid in the cortical region of ovary and absence of corpus luteum (Fig.1A). It was observed in the microscopic evaluation of follicular cysts a condition of ovaries with the absence of corpus luteum, follicles without visualization of oocytes; and it could also be described fibrosis and vacuolization in the cells of the teak layer or its absence; as well as a layer of cells of the degenerate, flattened, thin granulosa and, some folded cells and cellular debris. Regarding the paraovarian cysts, which were located close to the ovaries (Fig.1B), under the microscopy, they were covered by simple cuboidal epithelium and their wall composed of smooth muscle cells; and corpus luteum cysts, which, when cut, identified a cavity in the center filled with translucent material (Fig.1C). The luteinized cyst, also evaluated, showed areas with an absence of the granular layer, a layer of lutein cells in the cyst wall, with yellowish color.

Regarding proliferative changes, one case of granulosa cell tumor was diagnosed. It did not show macroscopic changes. Microscopically, the neoplastic proliferation of granulosa cells was observed, forming structures similar to follicles. Ovarian adenoma, a benign neoplasm, was characterized by cuboid cells arranged into cords and shaped like arboriform papillae.

Ovarian agenesis, a developmental abnormality characterized by the absence of the right ovary, occurred in a sample analyzed simultaneously with the absence of the right uterine tube.

Table 1. Distribution of 211 lesions in the reproductive system of 1072 sheep in slaughterhouses in the state of Bahia

Alterations	No. of cases	Frequency (%)
	138	65.3
Ovarian changes		
Follicular cyst	72	34.1
Paraovarian cyst	33	15.6
Corpus luteum cyst	25	11.8
Luteinized cyst	5	2.3
Adenoma	1	0.5
Granulosa cell tumor	1	05
Agenesis	1	0.5
Uterine changes	62	29.4
Endometritis	19	9
Melanosis	18	8.5
Hydrometra	5	2.3
Pyometra	5	2.3
Abscess	3	1.4
Cystic Endometrial Hyperplasia (CEH)	3	1.4
Adenomyosis	2	1.0
Petechiae in the serosa	2	1.0
Segmental aplasia	2	1.0
Ectopic pregnancy with fetal maceration	1	0.5
Vaginitis	1	0.5
Polyp	1	0.5
Changes in uterine tubes	11	5.3
Ovarian tube cyst	7	3.3
Hydrosalpinx	2	1.0
Agenesis	1	0.5
Adenoma	1	0.5
TOTAL	211	100

Uterine changes

Uterine inflammatory changes were the most common lesion. In addition, the endometritis was the most observed lesion in the uterus with 9% (19/211). The macroscopic characteristics of endometritis were organ distension, in some cases, from the uterine horns to the cervix, and when cut, with a yellowish-white and paste-like content (Fig.2A). Microscopic evaluation showed a marked inflammatory infiltrate composed of plasmocytes, macrophages, and neutrophils in the submucosa. In one case, in addition to endometritis, dilation and an increase in the number of endometrial glands were observed, which characterizes Cystic Endometrial Hyperplasia (CEH). Pyometra was diagnosed in 2.3% (5/211). Macroscopically, it could be observed an enlarged uterus consisting of yellowish and paste-like content, and of more than 50% purulent exudate.

Among the evaluated cases, two pregnant uteri presented pyometra, where the fetus was located in one of the uterine horns, and the other had content formed by whitish striations. Microscopic analysis showed marked inflammation areas composed of plasma cells, macrophages, and neutrophils in the submucosa. In the bacteriological examination, of the nine samples sent for bacteriological examination, *Escherichia coli* was the most isolated microorganism (6/9), in addition to the following bacteria: *Streptococcus* sp. (1/9) and *Pseudomonas aeruginosa* (1/9). In a sample sent, there was no bacterial growth. The cases of abscesses were located in the uterine wall (Fig.2B) 1.4% (3/211), both presented 1cm in diameter, characterized by purulent or caseous material that varied from yellowish-white or greenish, with odor or odorless, surrounded by a fibrous capsule. Under the microscopy, the abscess was located in the muscular and serous tissue of the uterine wall. A fibrous connective tissue capsule was observed, with moderate inflammatory infiltrate composed of lymphocytes, macrophages, and plasmocytes, and around the area of inflammatory infiltrate necrosis formed by degenerated

macrophages and neutrophils. In the vagina, it could be observed vaginitis in 0.5% (1/211) of the animals. Microscopic evaluation showed moderate mixed inflammatory infiltrate composed of lymphocytes, plasmocytes, and neutrophils located under the Basement Membrane (BM).

In hydrometra 2.3% (5/211) of degenerative lesion and the second major pathology were diagnosed, the uterus was dilated and cut, and it was replete with clear fluid accumulation in the lumen. Microscopy showed dilation of the endometrial glands.

With respect to the CEH (1.4%, 3/211), among the proliferative lesions, there was an intense proliferation of endometrial glands with preservation of the morphological pattern. Adenomyosis in 1% (2/211) was identified in the microscopic analysis by distributing the endometrial glands among the myometrial muscle fibers without macroscopic changes. The uterine polyp (0.5%, 1/211) was diagnosed by a pedunculated formation. Microscopically, it had a digitiform shape with the center filled with fibrous connective tissue.

The developmental abnormality was related to total segmental aplasia in 1% (2/211), absence of the formation of a segment of the uterus, the animals presented only one uterine horn. Melanosis in 8.5% (18/211) was characterized by pigmentation distributed in the endometrium areas (Fig.2C). Microscopy showed the distribution of black pigment in the submucosa and loose connective tissue of the endometrium.

Regarding other changes, ectopic pregnancy with fetal maceration was observed in one case, 0.5% (1/211). A whole normal uterus was found, but it was accompanied and connected to the organ removed from the abdominal cavity, a bag of encapsulated fatty tissue, and in its interior bone structures, a macerated fetus.

Fallopian tubes changes

The pathologies in the uterine tube were as following: tube-ovarian cyst in 3.3% (7/211), hydrosalpinx in 1% (2/211), adenoma in 0.5% (1/211) and agenesis in 0.5% (1/211). Macroscopy of the cysts was located on the external surface of the wall (Fig.3A), close to the insertion of mesosalpinx. The walls were composed of simple cylindrical ciliated epithelium, basement membrane, and smooth muscle on microscopic examination. Hydrosalpinx, an inflammatory disease, was identified by the unilateral dilation of 0.9cm in diameter of the lumen of uterine tube by liquid content (Fig.3B), under microscopy, absence of folds in the mucosa and, due to distension, the cells exhibited a flattened morphology. The developmental abnormality observed in one case was agenesis of the right uterine tube (Fig.3C). A proliferative lesion found in this organ was the adenoma. Microscopically, cuboid cells were observed grouped in cords and formed the shape of arboriform papillae.



Fig.1. Sheep reproductive system. (**A**) Follicular cysts. Cystic dilations filled with translucent fluid in the cortical region of the ovary and absence of corpus luteum. (**B**) Bilateral paraovarian cysts (white arrows). Mesometrial cysts. (**C**) Corpus luteum cysts. Cutting surface, a cavity in the center is identified, filled with translucent material.



Fig.2. Sheep reproductive system. (**A**) Endometritis - an enlarged organ, mainly in the cervix. When cut, it could be observed yellowish-white content. (**B**) Adherence and fibrosis of the uterine horn, fallopian tube, and left ovary. Petechiae are observed distributed from the body of the uterus to the horns, with a prominent protruding abscess on the right bottom of the body of the uterus (white arrow). (**C**) Melanosis. Caruncular pigmentation and edema.



Fig.3. Sheep reproductive system. (**A**) Right ovarian tube cyst (white arrow). (**B**) Distension of the uterine tube (hydrosalpinx) with liquid and translucent content, 0.9cm in diameter (arrow). (**C**) Agenesis of the ovary and right uterine tube.

DISCUSSION

In this study, injuries occurred in 19.5% (211/1,072) of the cases, similar to that observed in other studies of the same nature carried out in the state of Ceará (20.35%) (Santa Rosa et al. 1987), in Iran (25.8%) (Moghaddam & Gooraninejad 2007) and 16.6% (Khodakaram-Tafti & Davari 2013), India (14.98%) (Agrawal 2010) and Himalayas (19.47%) (Sharma et al. 2014).

The ovaries were the most affected organs, with the follicular cyst being the most relevant lesion in this study, presenting results similar to the research by Sharma et al. (2014) as following: 13.56% of lesions in the ovaries was registered (Santa Rosa et al. 1987), in the studies by Moghaddam & Gooraninejad (2007), the highest rates of abnormalities were also in the ovaries consisting of 20.1%, with a predominance of follicular cysts. The etiopathogenesis of follicular cysts may be related to disorders in the Hypothalamic-Pituitary-Gonadal (HPG) axis. If the gonadotropin-releasing hormone (GnRH) is not released from the hypothalamus due to estradiol stimulation, or the anterior pituitary does not release the Luteinizing Hormone (LH), they will cause cyst formation and an increase in progesterone (Silva et al. 2002). The absence of LH receptors in the mature follicle or deficiency of GnRH receptors in the pituitary gland is also related to cyst formation (Santos et al. 2016). Similar results were identified in the ovaries of cows in the microscopic evaluation, such as the absence of oocyte, pellucid zone, and granulosa cells, in addition to internal teak fibrosis and partial luteinization of the cystic wall (Ramos et al. 2010).

The granulosa cell tumor is an ovarian neoplasm of the sexual cords, initially formed by cells similar to the follicle granulosa cells (Santos et al. 2016), and it could be observed in a sheep in this study. Similar data were described in three cows, in which in one case, no macroscopic changes were observed. However, microscopy showed rosette formation in the granulosa cells (Hatipoglu et al. (2002).

The adenoma, a lesion identified in one case in this research, is characterized as an epithelial neoplasia derived from the germinal epithelium, from the Subsurface Epithelial Structures (SES), or the *rete ovarii*. It did not occur in similar studies by other authors (Santa Rosa et al. 1987, Moghaddam & Gooraninejad 2007, Agrawal 2010, Khodakaram-Tafti & Davari 2013, Sharma et al. 2014). Under the microscopic examination, they tend to have cuboid cells grouped into cords, with a pycnotic nucleus, a sparse cytoplasm grouped in the shape of arboriform papillae (Akihara et al. 2007).

Among the findings with little clinical significance, the paraovarian cyst represented 15.6% and the corpus luteum cysts 11.8%. In a study conducted by Khodakaram-Tafti & Davari (2013), it could be found 0.9% paraovarian cysts in sheep, and in a research performed with cows, this cyst was identified in eight cases (Hatipoglu et al. 2002). The corpus luteum cyst is characterized by the formation of a cystic cavity in the center of the lutein tissue, present in 25% of the corpus luteum (Santos et al. 2016). In studies with cows, 0.74% (Ramos et al. (2010) and 2.51% (Hatipoglu et al. 2002) of corpus luteum cysts were identified.

Endometritis was the most identified uterine pathology in the present study, comprising 9% of changes in the uterus characterized by yellowish-white mucus. In other studies carried out with sheep, endometritis was predominant in 2.93% (Khodakaram-Tafti & Davari 2013) and 0.34% of cases (Agrawal 2010). In the macroscopic evaluation, the presence of mucus, which can vary from serous to purulent and also from varying degrees of purulent striations (Schlafer & Miller 2007), hyperemia and endometrial edema (Santos et al. 2016). Microscopically, an inflammatory infiltrate formed by lymphocytes, histiocytes, and neutrophils in periglandular and perivascular regions could be identified, and it was possible to verify fibrosis in these areas as well (Bonnett et al. 1993, Bondurant 1999). It is a frequent alteration in the uterus of several domestic females that reduces reproductive efficiency of herds, increases the occurrence of estrous repetition and birth interval, and causes a drop in milk production (Nascimento & Santos 2011).

Pyometra, acute or chronic infection of the uterus, with deposition of purulent material and persistence of a corpus luteum, can occur due to endometritis or metritis (Dow 1960, Sheldon et al. 2008, Schlafer & Foster 2015). When it forms purulent exudate, infection is usually caused by *Staphylococcus* sp. and *Streptococcus* sp. (Johnson 2006, Foster 2013, Schlafer & Foster 2015). In this work, the bacteria *Escherichia coli* and *Streptococcus* sp could be detected.

Hydrometra was the second pathology diagnosed in this research with 2.3%. It is described as the accumulation of clear and aseptic fluid in the lumen of the uterus (Nascimento & Santos 2011, Foster 2013), which may be concomitant to the development of endometrial hyperplasia (Santos et al. 2016), as well as being characterized as widespread pathology in

goats and also diagnosed in sheep (Bretzlaff 1993, Wittek et al. 1997). If the hydrometra or mucometra are chronic, they cause atrophy of the endometrium, contributing to subfertility or infertility (Smith 1980, Schlafer & Miller 2007, Foster 2013, Schlafer & Foster 2015). Other work performed could register 0.3% (Moghaddam & Gooraninejad 2007), 0.15% (Khodakaram-Tafti & Davari 2013) and 2.99% of this pathology (Agrawal 2010).

In this study, the CEH was observed in 1.4% of the diseases. According to Santa Rosa et al. (1987), in a study carried out with sheep in the state of Ceará, this disease was identified in 0.85% of the animals; in another survey in Iran, it was identified in 0.15% (Khodakaram-Tafti & Davari 2013); and in a study performed with cattle, eight cows showed CEH (Hatipoglu et al. 2002). CEH is caused by hyperestrogenism in ruminants, usually due to the ingestion of phytoestrogenic plants in sheep and goats, and also owing to follicular cysts or granulosa cell tumors in cows, which can promote mucometra, hydrometra, or pyometra (Santos et al. 2016). Macroscopically, a slight, irregular, or diffuse thickening of the endometrium is observed (Foster 2013). It is usually associated with ovarian neoplasms (Maclachilan 1987, Cardilli et al. 2007). Microscopic findings are characterized by the proliferation of endometrial glands, which can preserve their morphological pattern or be dilated, cystic, and covered by a cuboidal epithelium (Pereira et al. 2015).

The accumulation of melanin in the uterine caruncles and caruncular pigmentation is a finding with little clinical significance that mainly affects black-skinned sheep, with a greater tendency in animals with pigmentation on the face. This heterotopic pigmentation occurs due to the accumulation of melanin in a not pigmented organ, such as the lung, but can occur in other organs. This pathology is developed owing to the irregular migration of melanocytes from the neural groove but does not interfere with the function of the organs (Santos et al. 2016). In the present study, 18 cases of melanosis were diagnosed, corresponding to 8.5% of uterine lesions. Other studies have also recorded this finding, where hyperpigmentation has been reported due to deposition of melanin in the uterine caruncles and the intercaruncular endometrium (Smith et al. 1999, Khodakaram-Tafti & Davari 2013).

In this study, 3.3% of cysts located in the fallopian tube were diagnosed. According to Santos et al. (2016), it is located on the external surface of the wall and, in most cases, adjacent to the insertion of the mesosalpinx, which can cause stenosis of the lumen by compression. When located in the fimbriated region of the infundibulum, they cause infertility by impairing the oocyte uptake.

Hydrosalpinx represented 1% of pathologies. The oviduct inflammatory process may cause this degenerative alteration, characterized by the distension of the lumen of uterine tubes by the accumulation of transudate (Santos et al. 2016). It can also occur due to adhesions of the uterine tube to nearby organs (Grunert et al. 2005). In other studies, this lesion was observed with a variation in the incidence of 1.69%, where the cases of hydrosalpinx were bilateral and affected the middle portion of the fallopian tubes (Santa Rosa et al. 1987); it could be observed in 1.1% (Moghaddam & Gooraninejad 2007) and 0.35% in cows located in the right uterine tube (Lenzi 2017); and 0.36% (Hatipoglu et al. 2002).

A case of adenoma was also diagnosed in the fallopian tube. Epithelial and mesenchymal neoplasms of this organ are rare in domestic animals. There are reports of benign epithelial neoplasms in dogs (Pierezan et al. 2016, Gelberg & McEntee 1986, Marino et al. 2007). The principal differential diagnosis of adenoma is related to the adenocarcinoma, and implantation in other organs and peritoneal cavities should be considered (Gelberg & McEntee 1986, Pierezan et al. 2016).

CONCLUSION

Infertility and reduction in reproductive efficiency of sheep can be caused mainly by follicular cysts, endometritis, and cysts in the uterine tubes. These important pathologies interfere in the productivity of sheep farming. Early diagnosis of these changes prevents probable losses in production.

Acknowledgments.- To the "Serviço de Inspeção Federal" (SIF) and "Serviço de Inspeção Estadual" (SIE), and also to the slaughterhouse professionals, the "Coordenação de Aperfeiçoamento de Pessoal de Nível Superior" (CAPES) for granting the first author's scholarship, and the "Universidade Federal da Bahia" (UFBA).

Conflict of interest statement.- The authors have no competing interests.

REFERENCES

Agrawal J.K. 2010. Genital status and reproductive disorders in small ruminants-an abattoir investigation. Doctoral Dissertation, Chaudhary Sarwan Kumar Himachal Pradesh Krishi Vishvavidyalaya Palampur, India, 80p.

Akihara Y., Shimoyama Y., Kawasako K., Komine M., Hirayama K., Kagawa Y., Omachi T., Matsuda K., Okamoto M., Kadosawa T. & Taniyama H. 2007. Inmunohistochemical evaluation of canine ovarian tumors. J. Vet. Med. Sci. 69(7):703-708. <https://dx.doi.org/10.1292/jvms.69.703> <PMid:17675800>

Bondurant R.H. 1999. Inflammation in the bovine female reproductive tract. J. Animal Sci. 77(supl.2):101-110. <https://dx.doi.org/10.2527/1999.77suppl_2101x> <PMid:15526785>

Bonnett B.N., Martins S.W. & Meek A.H. 1993. Associations of clinical findings, bacteriological and histological results of endometrial biopsy with reproductive performance of postpartum dairy cows. Prev. Vet. Med. 15(2/3):205-220. <https://dx.doi.org/10.1016/0167-5877(93)90114-9>

Bretzlaff K.N. 1993. Development of hydrometra in a ewe flock after ultrasonography for determination of pregnancy. J. Am. Vet. Med. Assoc. 203(1):122-125. <PMid:8407445>

Cardilli D.J., Toniollo G.H., Mostachio G.Q., Motheo T.F., Lima I.G. & Vicente W.R. 2007. Disgerminoma ovariano em cadela: relato de caso. Clín. Vet. 66:64-66.

Carvalho Júnior C.A., Xavier M.N., Costa L.F. Silveira S.S., Sant'Anna F.M., Borges A.M., Gouveia A.M.G. & Santos R.L. 2010. Agentes infecciosos que podem promover infertilidade em machos da espécie ovina. Rev. Bras. Reprod. Anim. 34(3):160-167.

Dow C. 1960. The cystic hyperplasia-pyometra complex in the bitch. Doctoral Dissertation, University of Glasgow, United Kingdom. 72p.

Foster R.A. 2013. Sistema Reprodutivo da Fêmea, p.1088-1099. In: McGavin M.D. & Zachary J. F. Bases da Patologia Veterinária. 5. ed. Elsevier, Rio de Janeiro.

Gelberg H.B. & Mcentee K. 1986. Pathology of the canine and feline uterine tube. Vet. Pathol. 23(6):770-775. <https://dx.doi.org/10.1177/030098588602300617> <PMid:3811142>

Grunert E., Birgel E.H., Vale W.G. & Birgel Junior E.H. 2005. Patologia e Clínica da Reprodução dos Animais Domésticos: Ginecologia. São Paulo: Varela. 551p.

Hatipoglu F., Kiran M.M., Ortatatli M., Erer H. & Çiftçi M.K. 2002. An abattoir study of genital pathology in cows: I. Ovary and oviduct. Rev. Méd. Vet., 153(1):29-33.

Higino S.S.S., Pinheiro S.R., Rocha V.C.M., Souza G.O., Portela R.A., Alves C.J., Vasconcellos S.A., Dib C.C., Rosário T.R., Melville P.A. & Azevedo S.S. 2013. Tuberculose em caprinos e ovinos abatidos no semiárido da Paraíba, Brasil. Arqs. Inst. Biológico. 80(3):281-287. <https://dx.doi.org/10.1590/S1808-16572013000300004>

Holanda Júnior E.V. & Martins E.C. 2007. Análise da produção e do mercado de produtos caprinos e ovinos: o caso do território do sertão do Pajeú em Pernambuco. Anais VII Congresso Brasileiro de sistemas de produção, Fortaleza, CE, p.5-6. (Resumo)

IBGE. Instituto Brasileiro de Geografia e Estatística. 2018. Pecuária: Efetivos / Rebanhos. Available at <www.sidra.ibge.gov.br> Accessed on Aug. 25, 2019.

Johnson C.A. 2006. Distúrbios do sistema reprodutivo, p.811-912. In: Nelson R.W. & Couto C.G. Medicina Interna de Pequenos Animais. 3ª ed. Elsevier, Rio de Janeiro.

Khodakaram-Tafti A. & Davari A. 2013. Congenital and acquired abnormalities of reproductive tract of non-pregnant ewes slaughtered in Fars province, Iran. Iran. J. Vet. Res. 14(2):140-144. <https://dx.doi.org/10.22099/IJVR.2013.1588>

Leite E.R. & Simplício A.A. 2005. Sistema de produção de caprinos e ovinos de corte para o Nordeste brasileiro: Importância econômica. [S.I.]: Embrapa. Disponível em <http://www.cnpc.embrapa.br/importancia.htm>. Acesso em: 01 dez. 2018.

Lenzi G.P. 2017. Caracterização macroscópica, microscópicas e ultrassonográfica de patologias do trato reprodutivo de fêmeas bovinas provenientes de abatedouro. Dissertação de Mestrado, Universidade Federal de Minas Gerais, Belo Horizonte. 30p.

Maclachilan N.J. 1987. Ovarian disorders in domestic animals. Environ. Health Perspec. 73:27-33. <https://dx.doi.org/10.1289/ehp.877327> <PMid:3665869>

Marino G., Quartuccio M., Cristarella S., Nicòtina P.A. & Zanghì A. 2007. Adenoma of the uterine tube in the bitch: two case reports. Vet. Res. Commu. 31(supl.1):173-175. <https://dx.doi.org/10.1007/s11259-007-0025-4> <PMid:17682868>

Moghaddam A. & Gooraninejad S. 2007. Abattoir survey of gross abnormalities of the ovine genital tracts in Iran. Small Rum. Res. 73(1/3):259-261. <https://dx.doi.org/10.1016/j.smallrumres.2006.10.022>

Monte H.L.B.D. 2008. Gestão técnico-econômica da produção de leite de cabra nos cariris paraibanos. Tese de doutorado, Universidade Federal da Paraíba, Areia, 211p.

Nascimento E.F. & Santos L.S. 2011. Patologia da Reprodução dos Animais Domésticos. 3ªed. Guanabra Koogan, Belo Horizonte, p.174.

Osório A. & Rassi L. 2011. A carne ovina e o abate clandestino: quais são as causas da informalidade? Disponível em: <http://www.farmpoint.com.br/cadeia-produtiva/espaco-aberto/a-carne-ovina-e-o abate-clandestino-quais-sao-as-causas-da-informalidade-70459n.aspx> Acesso em: 10 fev. 2019.

Panziera W., Vielmo A., De Lorenzo C., Heck L.C., Pavarini S.P., Sonne L., Soares J.F. & Driemeier D. 2018. Caracterização das lesões parasitárias de ovinos observadas na linha de abate. Pesq. Vet. Bras. 38(8):1491-1504. <https://dx.doi.org/10.1590/1678-5150-pvb-5549>

Pereira J.V.T.N., Pinho R.O., Meneses R.M., Mendes V.R.A., Pereira E.C.M. & Guimarães J.D. 2015. Hiperplasia endometrial cística e hidrossalpinge associada à cisto folicular em bovinos. Rev. Bras. Med. Vet. 37(1):1-6.

Pierezan F., Trost M.E. & Barros C.S.L. 2016. Uterine tube adenoma in a bitch. Brazilian J. Vet. Pathol., 9(1):27-30.

Ramos E.M., Oliveira C.M., Silva S.M.M.S., Silva L.S., Maruo V.M., Minharro S. & Cavalcante T.V. 2010. Alterações ovarianas em vacas zebuínas criadas na Amazônia Oriental. Rev. Cient. Eletr. Med. Vet. 8(15):1-18.

Santa Rosa J., Santos L.F.L. & Simplício A.A. 1987. Alterações anátomo-histopatológicas no sistema reprodutivo de ovelhas adultas, não prenhes, no município de Sobral, Ceará. Rev. Bras. Reprod. Anim. 11(14):179-186.

Santos R.L. 2001. Diagnóstico da cadeia produtiva da caprinocultura de corte no estado da Bahia. 2001. Monografia de Especialização em Administração em Agribusiness, Faculdade São Francisco de Barreiras, Barreiras. 40p.

Santos R.L., Nascimento E.F. & Edwards J.F. 2016. Sistema Reprodutivo Feminino, p.1206. In: Santos R.L. & Alessi A.C. Patologia Veterinária. 2ª ed. Roca, Rio de Janeiro.

Schlafer D.H. & Foster R.A. 2015. Female genital system, p.358-464. In: Maxie M.G., Jubb K.V.F., Kennedy P.C. & Palmer's N.C. Pathology of Domestic Animals. Vol.3. 6ª ed. Elsevier, St. Louis.

Schlafer D.H. & Miller R.B. 2007. Female genital system, p.424-564. In: Jubb K.V.F., Kennedy P.C. & Palmer's N.C. Pathology of Domestic Animals. Vol. 3. 5ed. Elsevier Saunders, Philadelphia.

Sharma A., Kumar P., Singh M. & Vasishta M.K. 2014. Reproductive health status of north western Himalayan Gaddi sheep: An abattoir study. Open Vet. J. 4(2):103-106. <PMid:26623348>

Sheldon I.M., Willians E.J., Miller A.N.A., Nash D.M. & Herath S. 2008. Uterine diseases in cattle after parturition. Vet. J. 176(3):115-121. <https://dx.doi.org/10.1016/j.tvjl.2007.12.031> <PMid:18329302>

Silva J.R.V., Ferreira M.A.L., Costa S.H.F., Santos R.R., Carvalho F.C.A., Rodrigues A.P.R., Lucci C.M., Báo S.N. & Figueiredo J.R. 2002. Degeneration rate of preantral follicles in the ovaries of goats. Small Ruminant Res. 43(3):203-209. <https://dx.doi.org/10.1016/S0921-4488(02)00017-2>

Smith K.C., Parkinson T.J. & Long S.E. 1999. Abattoir survey of acquired reproductive abnormalities in ewes. Vet. Rec. 144(18):491-496. <https://dx.doi.org/10.1136/vr.144.18.491> <PMid:10358887>

Smith M.C. 1980. Caprine production, p.969-1004. In: Morrow D.A. Current Therapy in Theriogenology: Diagnosis, Treatment and Prevention of Reproductive Diseases in Animals. WB Saunders, Philadelphia.

Souza M.F., Carvalho A.Q., Garino Jr F. & Riet-Correa F. 2011. Linfadenite caseosa em ovinos deslanados abatidos em um frigorífico da Paraíba. Pesq. Vet. Bras. 31(3):224-230. <https://dx.doi.org/10.1590/S0100-736X2011000300007>

Wittek T., Richter A., Erices J. & Elze K. 1997. Incidence, diagnosis, therapy and subsequent fertility in goats with hydrometra. Tierarztl. Prax. Ausg. G. Grosstiere/Nutztiere. 25(6):576-582. <PMid:9451762>

PESQUISA VETERINÁRIA BRASILEIRA
Brazilian Journal of Veterinary Research
ISSN 0100-736X (Print)
ISSN 1678-5150 (Online)

Pesq. Vet. Bras. 40(12):963-969, December 2020
DOI: 10.1590/1678-5150-PVB-6674

Original Article
Livestock Diseases
BY-NC

Testicular and seminal evaluation of goats fed hay *Cenostigma pyramidale*[1]

Maria V.B. Santos[2], Ana K.S. Cavalcante[4], Juliana T.S.A. Macêdo[3], Marilúcia C. Santos[2], Laiara F. Rocha[5], Alessandro L. Machado[5] and Pedro M.O. Pedroso[2,3]*

ABSTRACT.- Santos M.V.B., Cavalcante A.K.S., Macêdo J.T.S.A., Santos M.C., Rocha L.F., Machado A.L. & Pedroso P.M.O. 2020. **Testicular and seminal evaluation of goats fed hay *Cenostigma pyramidale*.** *Pesquisa Veterinária Brasileira 40(12):963-969.* Laboratório de Patologia Veterinária, Universidade de Brasília, Campus Universitário Darcy Ribeiro, Via L4, Norte s/n, Brasília, DF 70910-970, Brazil. E-mail: pedrosovet@yahoo.com.br

This study aimed to assess the possible occurrence of reproductive changes in male goats associated with ingestion of *Cenostigma pyramidale* hay. Sixteen animals divided into two experimental groups, G1 and G2 (control group) were used. Animals in G1 received 2% of forage, based on live weight (LW), composed of 100% of *C. pyramidale*, and animals in G2 received 2% of *Panicum maximum* "Massai' grass hay, based on LW. Both groups received 1% of concentrated feed supplementation based on LW, along with mineralized salt and water *ad libitum*. The goats were subjected to weighing, testicular biometry, and semen and blood collection every 30 days. After 120 days, the animals were castrated and their testes were collected. Testicular measurements were performed and fragments were collected for histological processing to determine the gonadosomatic index (GSI), diameter of the seminiferous tubules, height of the germinal epithelium (HGE), volumetric proportion and volume of the testicular parenchyma components, total length of the seminiferous tubules, length of the seminiferous tubules per gram of testis, and leydigosomatic and tubulosomatic indexes. The data were evaluated for normality using the Student's *t*-test. Data with normal distribution were assessed using analysis of variance (ANOVA) and the non-parametric data were evaluated using the Kruskal-Wallis test, both at 5% probability. Statistically significant differences ($p<0.05$) were observed for GSI (G1=0.48 ±0.08 and G2=0.34 ±0.09) and HGE (G1=52.95 ±2.99 and G2=.47.63 ±2.67) between treatments. Consumption of *C. pyramidale* hay increased LW and, consequently, testicular weight, contributing to high GSI. In conclusion, ingestion of *C. pyramidale* has no toxic effect on the testicular, seminal and histological parameters of goat testis. Due to its nutritional characteristics, consumption of this plant improves animal body development. Because *C. pyramidale* is adapted to semi-arid regions, it can be an alternative source of feed for goats during periods of shortage.

INDEX TERMS: Goats, hay, *Cenostigma pyramidale*, toxic plant, animal reproduction, male, testicle.

RESUMO.- [**Avaliação testicular e seminal de caprinos alimentados com feno de *Cenostigma pyramidale*.**] Para avaliar a possível ocorrência de alterações reprodutivas em caprinos machos associado ao consumo de *Cenostigma pyramidale*, foram utilizados 16 animais divididos em dois grupos experimentais, G1 e G2 (grupo controle). Animais

[1] Received on June 22, 2020.
Accepted for publication on July 4, 2020.

[2] Graduate Program in Animal Sciences in the Tropics (PPGCAT), Faculdade de Medicina Veterinária e Zootecnia, Universidade Federal da Bahia (UFBA), Av. Adhemar de Barros 500, Ondina, Salvador, BA 40170-110, Brazil.

[3] Laboratório de Patologia Veterinária, Universidade de Brasília (UnB), Campus Universitário Darcy Ribeiro, Via L4 Norte s/n, Brasília, DF 70910-970, Brasil. *Corresponding author: pedrosovet@yahoo.com.br

[4] Laboratório de Estudos em Morfofunção Animal, Prédio Elismar V. Adorno (Biologia), Centro de Ciências Agrárias, Ambientais e Biológicas, Universidade Federal do Recôncavo da Bahia (UFRB), Rua Rui Barbosa 710, Campus Universitário, Cruz das Almas, BA 44380-000, Brazil.

[5] Hospital Universitário de Medina Veterinária, Centro de Ciências Agrárias, Ambientais e Biológicas, Universidade Federal do Recôncavo da Bahia (UFRB), Rua Rui Barbosa 710, Campus Universitário, Cruz das Almas, BA 44380-000, Brazil.

pertencentes ao G1 receberam 2% de volumoso, com base no peso vivo (PV), constituído de 100% de *C. pyramidale* e o G2 receberam 2%, com base no PV, de feno de *Panicum maximum* 'Massai'. Todos os grupos receberam 1%, com base no PV, de suplementação concentrada, além de sal mineralizado e água *ad libitum.* A cada 30 dias os animais eram submetidos à pesagem, biometria testicular e coletas de sêmen. O sêmen foi avaliado quanto ao volume, turbilhonamento, vigor, motilidade, concentração espermática, defeitos maiores, menores e totais. Após 120 dias os animais foram castrados e os testículos coletados. Foram realizadas as mensurações testiculares e coletados fragmentos para o processamento histológico, para determinação do índice gonadossomático, diâmetro dos túbulos seminíferos, altura do epitélio germinativo, proporção volumétrica e volume dos componentes do parênquima testicular, comprimento total dos túbulos seminíferos, comprimento de túbulo seminífero por grama de testículo, índices leydigossomático e tubulossomático. Os dados foram avaliados quanto à normalidade pelo teste t de Student, os dados com distribuição normal foram analisados por análise de variância com 5% de probabilidade e os não paramétricos, pelo teste de Kruskal-Wallis, a 5% de probabilidade. Houve diferenças significativas (p<0,05) para índice gonadossomático (G1=0,48±0,08 e G2=0,34±0,09) e altura do epitélio germinativo (G1=52,95±2,99 e G2=47,63±2,67) entre os tratamentos. O feno de catingueira promoveu aumento no peso corporal e consequentemente maior peso testicular, o que contribui para elevação do IGS. Concluiu-se que o consumo da *C. pyramidale* não possui efeito tóxico sobre os parâmetros testiculares, seminais e histológicos do testículo dos caprinos e que a planta, por suas características nutricionais promoveu melhora no desenvolvimento corporal dos animais e por ser uma planta adaptada ao clima do semiárido, se constitui uma fonte alternativa de alimentação para esta categoria animal, durante períodos de escassez de alimento.

TERMOS DE INDEXAÇÃO: Caprinos, feno, *Cenostigma pyramidale*, planta tóxica, reprodução animal, caprino, testículo.

INTRODUCTION

Cenostigma pyramidale species, originally cataloged as *Caesalpinia pyramidalis* (Tul.) or *Poincianella pyramidalis* (Tul.) L.P. Queiroz (Flora do Brasil 2020), is popularly called "catingueira", "catinga-de-porco" or "pau-de-rato". These names are due to the unpleasant odor of their green leaves. It is a xerophilous, arboreal, medium-sized Fabaceae (Matias et al. 2017). *C. pyramidale* presents wide distribution in the Brazilian northeastern semi-arid region and is considered endemic in the Caatinga biome (Silva et al. 2009, Maia 2012). It is among the forage species most used by animals in the Caatinga (Araujo et al. 2010). Its hay has good nutritional value, presenting high protein concentrations (10.82%) even in long periods of drought (Mendonça Jr. et al. 2008), which makes this species an important feed source for animals during the critical periods of forage scarcity in the dry season (Vieira et al. 2005).

In the Northeast region of Brazil, consumption of *C. pyramidale* is related to the occurrence of reproductive changes in female sheep and goats (Reis et al. 2016, Lopes et al. 2017). This plant is associated with one of the leading causes of abortion, embryonic mortality, and malformation in goats and sheep in the northeastern semi-arid region, being necessary to keep it out of the reach of females during pregnancy (Marcelino et al. 2017, Souza et al. 2018). Reproduction experiments conducted with goats (Reis et al. 2016) and sheep (Lopes et al. 2017) have proved that this plant causes congenital malformations, embryonic losses, and abortion and that the malformations observed in the animals studied were similar to those described by producers of the semi-arid region of the state of Bahia in cases of natural poisoning.

In the semi-arid region, where cases of natural poisoning have occurred (Marcelino et al. 2017), in addition to the toxic effects on females, many small ruminant producers reported that *C. pyramidale* also causes reproductive problems in male sheep and goats (Souza et al. 2018). Until then, reproductive changes due to consumption of *C. pyramidale* had only been proven in pregnant goats and sheep (Reis et al. 2016, Lopes et al. 2017), but toxic effects on the reproductive parameters in males had been observed.

This study aimed to carry out an experiment on pubescent male goats to determine whether *C. pyramidale* has a toxic effect on the reproductive system of male goats.

MATERIALS AND METHODS

The experiment was carried out in the premises of the "Setor de Caprinocultura" of the "Centro de Ciências Agrárias, Ambientais e Biológicas" of the "Universidade Federal do Recôncavo da Bahia" (CCAAB-UFRB) located in the municipality of Cruz das Almas, state of Bahia, Brazil. The project was approved by the Ethics Committee on the Use of Animals (CEUA) of UFRB under protocol no. 23007.000119352019-60.

Cenostigma pyramidale leaves were previously harvested manually from November to February 2019 in the Tupiaçú district (12°33'07.8" S; 39°17'35.1" W), municipality of Cabaceiras do Paraguaçu, Recôncavo da Bahia. After drying in the shade for 6 h for three days, the leaves were crushed, weighed, and stored in plastic bags for daily supply to the animals.

A total of 16 male, crossbred goats with mean age >1 year and initial average live weight (LW) of 33 kg were used in the study. Initially, the animals were dewormed, vaccinated, and submitted to physical examination with measurement of heart and respiratory rates, ruminal movements and temperature, verification of mucous membranes and integrity of the common integument, palpation of lymph nodes to prove health, and andrological examination. All examinations were performed following the recommendations of the "Colégio Brasileiro de Reprodução Animal" (CBRA) and the animals underwent an adaptation period of 15 days. The goats were randomly assigned to two groups of eight animals each (G1 and G2). G1 was fed 1% concentrated supplementation (CS) based on LW and 2% roughage based exclusively on *C. pyramidale* hay. In G2, the feed consisted of 1% CS based on LW and 2% roughage based on *Panicum maximum* 'Massai' hay. Both groups received CS prepared with corn and soy bran enriched with vitamins and minerals, in addition to mineralized salt and water *ad libitum*. The hay was homogenized with the CS and ingested spontaneously.

Samples of *C. pyramidale* and Massai grass hay were sent for bromatological analysis at the "Laboratório de Nutrição Animal" of UFRB. The bromatological composition of the diets was prepared according to the Association of Official Analytical Chemists (AOAC, 1992) to determine the levels of dry matter (DM), mineral matter (MM), and crude protein (CP). Determination of neutral detergent

fiber (NDF) and acid-detergent fiber (ADF) was carried out according to Van Soest et al. (1991).

Every 30 days, the animals were weighed individually and testicular biometry (TB) was performed, always by the same operator. The scrotal perimeter (SP) was measured using a measuring tape. The length, width, and thickness of the right and left testes were measured using a caliper. Testicular consistency was assessed through qualitative analysis by palpation and was classified as fibro-elastic (normal), firm, or flaccid (abnormal). The animals were submitted to semen collection every 30 days since the beginning of plant supply using the artificial vagina method and a female in estrus as a mannequin. After obtaining the ejaculate, the following seminal characteristics were evaluated: volume of the ejaculate, seminal color and aspect, and semen swirl, vigor, motility and concentration, as well as semen morphology including major and minor defects.

After 120 days of supplying the diets to each group, the animals were submitted to bilateral surgical orchiectomy. After removal, the testes were weighed, measured, and dissected. Tissue fragments were collected and fixed in 10% buffered formaldehyde. Subsequently, testicular fragments were processed routinely by histological techniques, stained with hematoxylin-eosin (HE), and analyzed by optical microscopy.

The following testicular morphometric parameters were analyzed: right and left testicular weight, gonadosomatic index (GSI), diameter of seminiferous tubules, height of the germinal epithelium (HGE), volumetric proportion of the components of the testicular parenchyma, total length of seminiferous tubules, length of seminiferous tubule per gram of testis, and leydigosomatic and tubulosomatic indexes.

The tubular diameter and height of the epithelium were measured using a 10x micrometric eyepiece and a 10x objective under an optical microscope. Twenty cross-sections chosen at random through horizontal scanning - the ones with the most circular contour - were measured and had their mean determined for each animal.

Height of the epithelium was obtained in the same tubules used to measure the diameter, considering the epithelial thickness from the basal membrane to the luminal border. Two measurements from each cross-section were obtained, referring to the two contralateral points. The mean between the two measurements was considered a representative measure.

The volumetric proportion data of the testicular parenchyma components were obtained using a graticule with 408 intersections considered as points, with 400x magnification. Ten random fields were evaluated and, for each animal, evaluation of the coincident points was performed on the different constituent elements of the testicular parenchyma. Approximately 2,040 points were counted per animal. The following testicular parenchyma components were recorded: seminiferous tubule (tunica propria, seminiferous epithelium, and tubular lumen), Leydig interstitial cells, blood vessels, and connective tissue.

The total length of seminiferous tubules was obtained using the formula (França et al. 2000):

$$LST = \frac{vst}{\pi r^2}$$

where, LST = total length of seminiferous tubules, VST = total volume of seminiferous tubules, previously calculated by the volumetric proportion of seminiferous tubules in the testicular volume, and r^2 = base area corresponding to the cross-section area of the seminiferous tubule, considering the radius (r) as half the average diameter.

The final result referring to the total tubule length was expressed in meters for each animal. The GSI, which represents the percentage of body mass allocated in the testis, was calculated from the average weight of the two tests divided by the live weight. The leydigosomatic and tubulosomatic indexes represent the percentage of body mass allocated in the Leydig cells and seminiferous tubules. The percentage of testicular parenchyma of the Leydig cells and seminiferous tubules was calculated using the GSI.

All parameters were initially tested for normality using the Student's *t*-test. THe parameters with normal distribution were assessed using analysis of variance (ANOVA) and the non-parametric data were evaluated by the Kruskal-Wallis test, both at 5% probability.

RESULTS

A sample of Massai grass hay supplied to the animals showed percentages of CP, NDF, and ADF of 3.02, 84.12 and 47.24, respectively, whereas a sample of *Cenostigma pyramidale* hay showed percentages of CP, NDF, and ADF of 10.82, 63.2, and 28.09%, respectively (Table 1).

Regarding the testicular biometric parameters and LW of goats in the evaluated periods, no differences were found between the groups ($p>0.05$), and it was observed that the averages were close in all parameters studied, except for live weight, which presented variation between the periods. In both groups, SP varied with LW and increased as a result of it. In G1, in 60 days, the mean SP was 20.1 cm with 26.6 kg LW, and in 120 days, the mean SP was 22.6 cm with 36.2 kg LW. In G2, the mean SP values were 21.3 cm over 60 days with 28.5 kg LW and 33.9 cm over 120 days with a 35.5 kg LW (Table 2).

Testicular consistency was the same in both experimental groups ($p>0.05$). In all periods evaluated, the testicles were tenso-elastic, which indicates normal testicular constitution.

As for the seminal aspect characteristic, in all evaluations, color was uniform with predominance of yellow ivory, and the consistency varied between creamy and milky.

When considering the semen characteristics in the evaluated periods, it was observed that G1 and G2 were similar, and that there was no difference ($p>0.05$) in all the variables analyzed, presenting parameters adequate for the goat species. However, in the first semen collection both in G1 and G2, minor defects corresponded to 23.21 and 21.85% and total defects accounted for 29.28 and 27.85%, respectively (Table 3).

Table 4 shows that there was statistically significant difference between the groups for the characteristics of the gonadosomatic index (GSI) and HGE ($p<0.05$), in which G1 showed higher values than G2. For GSI, G1 showed 0.48%, while G2 presented 0.34%, and for HGE, the values were 52.95 and 47.63 μm for G1 and G2, respectively. No effect of the

Table 1. Chemical composition of the diets supplied to the animals

Parameters	*Cenostigma pyramidale*	*Panicum maximum*
Dry matter (%)	91.06	91.07
Mineral matter (%)	2.70	7.3
Crude protein (%)	10.82	3.02
Neutral detergent fiber (%)	63.62	84.12
Acid-detergent fiber (%)	28.09	47.24

diets provided was found for the other parameters ($p>0.05$). However, testicular weight was greater in G1 compared with G2, with mean values of 87 and 63 g, respectively.

When considering the volumetric proportions of the testicular parenchyma components, no treatment was effective on the constituents of the seminiferous tubules or the intertubular tissue ($p>0.05$). However, higher proportions of seminiferous tubules compared with intertubular tissue were observed in both experimental groups (Table 5).

In the histological study, no changes were observed after ingestion of *C. pyramidale* by goats for 120 days in both groups.

DISCUSSION

Cenostigma pyramidale has been proved to be toxic for goats and sheep, with effects observed in the organogenesis phase (Reis et al. 2016, Souza et al. 2018). However, results of this study demonstrated that its consumption for 120 days by pubescent male goats did not result in toxicity to the reproductive system, not causing changes in the gametes. Because this plant presents good nutritional value with adequate protein concentrations, it constituted an excellent feed source for the animals.

Testicular measurements are considered as parameters in the evaluation of goat semen production. The scrotal perimeter (SP) is an excellent parameter to evaluate the size of the testes and the semen production capacity of goats, thus serving as a way to select a breeder for the herd. This variable does not dependent on breed or climate, but it has a close relationship with age and LW (Almeida et al. 2010). In the present study, the increase in LW positively influenced the SP indexes, and these were presented according to age and LW for both experimental groups. A similar finding was described by Souza et al. (2011) when studying Anglo-Nubian goats aged from 20-44 weeks, who observed average SP values of 21.1 and 25.5 cm, and LW values of 25.75 and 43.6 kg, respectively, and by Rodrigues (2010) in Alpine goats at 12 months of age, with a LW of 27 kg and SP of 22 cm.

The ejaculate volume of goats varies from 0.1 to 1.5 mL according to the CBRA (2013). For this variable, the means of experimental groups ranged from 0.4 to 0.7 mL and 0.2 to 0.9 mL in G1 and G2, respectively. This range indicates good functioning of the accessory sexual glands, associated with androgen production and libido of the animal, reflecting in seminal volume increase.

Greater development of the testes was observed in both experimental groups overtime. Growth of the testicular parenchyma and the consequent expansion of the diameter of the seminiferous tubules, as a result of proliferation of the germ cells and differentiation of the Sertoli cells, provided an increase in semen concentration. According to Aguiar et al. (2006), semen concentration gradually increases with advancing age, since it is directly related to development of the seminiferous tubules, as semen remain inactive until puberty when they start to divide and proliferate.

Increase in the percentages of minor and total defects at baseline occurred as a result of the high frequency of bent tail

Table 2. Testicular biometrics and body weight of goats in the different periods of supply of *Cenostigma pyramidale*

Group	Period (days)	SP (cm)	Length LT (cm)	Length RT (cm)	Width LT (cm)	Width RT (cm)	Thickness LT (cm)	Thickness RT (cm)	BW (kg)
G1	0	21.9±1.9	6.7±0.8	6.8±0.9	3.8±0.4	3.8±0.4	4.3±0.5	4.3±0.4	34.1±6.6
	30	21.1±2.1	6.4±0.9	6.6±0.9	3.9±0.5	3.8±0.3	4.3±0.7	4.3±0.6	34.3±9.5
	60	20.1±2.9	6.2±0.9	6.3±0.8	3.5±0.6	3.6±0.5	4.3±0.6	4.2±0.6	26.6±6.5
	90	22.1±2.1	6.5±0.6	6.6±0.6	4.0±0.4	4.0±0.4	4.1±0.7	4.2±0.8	28.0±6.6
	120	22.6±2.1	6.7±0.9	6.8±0.8	4.3±0.38	4.3±0.3	4.2±0.6	4.2±0.7	36.2±7.3
G2	0	21.8±2.5	6.0±0.8	6.2±0.8	3.8±0.4	3.7±0.3	4.1±0.6	4.0±0.6	33.6±8.1
	30	21.3±2.6	6.2±0.8	6.2±0.8	3.7±0.5	3.7±0.6	4.0±0.7	4.0±0.7	34.8±7.0
	60	21.3±3.2	6.2±1.0	6.3±1.0	3.9±0.6	3.9±0.7	4.3±0.6	4.2±0.7	28.5±8.2
	90	21.6±3.7	6.2±0.9	6.2±1.0	3.9±0.6	3.8±0.6	4.3±1.1	4.3±1.2	27.8±8.9
	120	23.9±3.6	6.2±1.0	6.1±1.0	4.4±0.6	4.5±0.6	4.2±0.7	4.2±0.8	35.5±7.1

G1 = goats fed *C. pyramidale* hay, G2 = control group, SP = scrotal perimeter, BW = body weight, RT = right testis, LT = left testis.

Table 3. Seminal physical and morphological parameters of goats in the different periods of supply of *Cenostigma pyramidale*

Group	Period	Volume (mL)	Swirl (0-5)	Vigor (0-5)	Motility (%)	Conc. (x109/ mL)	DMaj (%)	DMin (%)	DTot (%)
G1	0	0.7±0.3	3.6±0.4	3.4±0.4	81.4±6.9	3.6±1.2	6.1±3.1	23.2±8.1	29.3±7.4
	30	0.5±0.3	2.9±1.4	3.3±1.6	73.0±29.9	4.7±1.4	2.2±1.6	15.7±5.7	17.9±6.0
	60	0.7±0.6	3.3±1.2	4.2±0.8	85.0±15.2	4.7±1.8	2.9±2.4	12.3±3.5	15.2±5.3
	90	0.4±0.3	3.7±0.8	3.5±0.6	82.0±4.5	4.2±1.6	1.6±0.8	11.6±3.8	13.3±3.3
	120	0.7±0.3	3.0±1.6	3.8±1.2	78.3±17.2	4.4±1.4	3.3±0.5	8.5±3.0	11.0±2.9
G2	0	0.8±0.4	3.3±1.0	3.0±0.8	74.3±12.7	3.2±0.8	6.0±1.9	21.9±9.8	27.9±9.3
	30	0.4±0.3	3.0±1.4	3.2±1.3	71.4±16.5	4.0±1.4	2.4±3.2	9.3±4.4	11.6±5.8
	60	0.8±0.6	3.0±1.3	3.3±1.4	75.7±19.0	4.2±2.5	2.6±1.5	12.0±4.9	14.6±5.7
	90	0.2±0.1	4.0±0.6	3.9±0.4	77.9±8.1	4.9±0.9	1.4±1.2	8.9±4.1	10.3±5.1
	120	0.9±0.5	4.1±0.7	4.9±0.4	92.9±7.6	5.0±0.9	3.9±1.2	8.2±2.3	12.1±2.7

G1 = goats fed *C. pyramidale* hay, G2 = control group, Conc. = concentration, DMaj = major defects, DMin = minor defects, DTot = total defects.

and distal cytoplasmic gout pathologies in both experimental groups. These defects were considered less important. These values stabilized after 30 days.

Semen defects with a bent or coiled tail can be caused by failures in thermoregulation, testicular degeneration, hypoosmotic conditions, failures in epididymal transit, or thermal shock, especially when using cold formaldehyde to fix semen (Souza et al. 2011). Distal cytoplasmic gout and tail pathologies are associated with immaturity or reproductive rest (Arruda et al. 2015). Thus, these data corroborate the percentage of pathologies found in the present study, justifying that they were possibly caused by sexual rest and heat stress.

A relationship between testicular and live weight was observed in both groups. The animals in G1 presented higher means than those in G2. In domestic animals, testicular weight varies between species. It is determined by several factors, such as establishment of semen activity, increase in the population of germ cells, and number of Sertoli cells, directly affecting semen production. According to Rodrigues (2010), there is a fast growth of testicular weight between four and six months of age due to the accelerated growth of the tubular diameter and length and, consequently, of the volume of the seminiferous tubules in the testicular parenchyma. After this period, testicular growth stabilizes. Variations in testicular weight of goats at other ages are attributed to genetic characteristics and environmental, feeding and handling conditions.

The GSI corresponds to the somatic investment in gonadal mass, being a parameter that represents semen production from the high correlation between semen volume and testicular weight. The animals in G1 showed a higher percentage of LW allocated in the testes. This variable has a high correlation with live and testicular weights, and these averages were higher in G1 than in G2, which influenced the GSI found. Van Soest (1994) recommend at least 6-8% CP for rumen microbial fermentation efficiency, which may explain the higher LW verified G1 compared with G2. *Cenostigma pyramidale* hay exhibited a percentage of 10.82% of CP, higher than the recommended to meet the demand for nutrients, providing balance in feed use by ruminal microorganisms compared with Massai grass hay, with a CP percentage of 3.02%. According to Urbano et al. (2015), reducing CP consumption negatively influences weight gain and carcass quality. Also, higher percentages of NDF were observed in Massai grass hay compared with *C. pyramidale* hay. According to Ribeiro et al. (2020), increased NDF levels harms feeding efficiency and reduces weight gain. Therefore, ingestion of *C. pyramidale* hay promoted an increase in LW and, consequently, greater testicular weight, which contributed to increasing the GSI.

Table 4. Testicular weight and testicular morphometric parameters of goats fed *Cenostigma pyramidale* hay

Parameters	G1	G2
Testicular weight (g)	87.00±20.40	63.00±26.67
GSI (%)	0.48±0.08*	0.34±0.09
DST (μm)	226.61±7.96	225.25±5.96
LD (μm)	107.86±11.38	118.75±15.89
HGE (μm)	52.95±2.99*	47.63±2.67
LSI (%)	0.0009±0.0005	0.0007±0.0003
TSI (%)	0.2755±0.0481	0.2836±0.0634
LST (m)	2.407.34±144.81	2.442.32±139.52
LGT (m/g)	14.52±3.56	22.24±8.76

* Statistical difference (p>0.05); G1 = goats fed *C. pyramidale* hay, G2 = control group, GSI = gonadosomatic index, DST = diameter of seminiferous tubules, LD = lumen diameter, HGE = height of the germinal epithelium, LSI = leydigosomatic index, TSI = tubulosomatic index, LST = total length of seminiferous tubules, LGT = total length of seminiferous tubules per gram of testis.

Table 5. Volumetric proportion of the components of the testicular parenchyma of goats fed *Cenostigma pyramidale* hay

Parameters (%)	G1	G2
Lumen	21.55±4.28	19.87±3.23
Germinal epithelium	73.89±3.28	75.65±3.11
Basement membrane	1.37±0.40	1.58±0.53
Connective tissue	2.62±1.78	2.38±1.00
Leydig cells	0.44±0.23	0.42±0.23
Blood vessel	0.14±0.5	0.10±0.3

G1 = goats fed *C. pyramidale* hay, G2 = control group.

Diameter measurements of the seminiferous tubules indicate spermatogenic activity, testicular function, and development of the germinal epithelium. There are significant variations in these dimensions among the different domestic species (França & Godinho 2003). In this study, this measure was similar to that observed by Rodrigues (2010) for Alpine goats at one year of age, who found an average of 228 μm. A higher value was reported by Mohammed et al. (2011) in goats at two years of age, who reported an average of 258 μm. According to Morais et al. (2012), variation in the tubular diameter of mammals can be observed between different breeds, strains, and mating systems, remaining relatively constant in non-seasonal and sexually mature animals. According to Avelar et al. (2010), the diameter of the seminiferous tubules depends on the tubular lumen size and on the total number of cells per cross-section of the seminiferous tubule. Various factors collaborate in the tubular diameter, such as the number of layers of germ cells and the efficiency and secretion of fluids by the Sertoli cells, which influence the tubular lumen size.

The morphometric study of the testes showed that the animals fed *C. pyramidale* hay presented higher means for the height of the seminiferous epithelium. According to Hoshino et al. (2002) this variable is higher in adult animals. This finding occurs because of the greater stimulus of mitosis and greater spermatogenesis, generating an extensive epithelium resulting from the larger number of cells.

Studies conducted with *C. pyramidale* extract revealed its cytotoxic effect through the Allium cepa test, which showed higher mitotic indices as a consequence of increased cell division and proliferation (Queiroz et al. 2018). Therefore, the height of seminiferous epithelium in G1 was possibly stimulated by ingestion of the plant, which acted on the germ cells, increasing cell division. However, it is not possible to conclude that the components of *C. pyramidale* were cytotoxic, which requires more detailed studies.

Mean proportional values referring to the testicular parenchyma components revealed similarity to the seminiferous tubules and intertubular tissue between the experimental groups, demonstrating that consumption of *C. pyramidale* did not alter the composition of the testicular parenchyma. Concerning the seminiferous tubules, the animals in this

study showed proportional values slightly above the average of most species, which vary between 60 and 90% (Russell et al. 1993). This fact is directly associated with the volumetric proportion occupied by the testis intertubular tissue, for which the animals in this study showed greater investment in seminiferous tubules compared with their intertubular space.

The tubulosomatic index is associated with volume of the seminiferous tubules in the testis and with animal LW. This parameter proposes quantifying the percentage of body investment in seminiferous tubules, allowing intra- and inter-specific comparison between animals of different body sizes (Leite et al. 2006). A higher percentage than that observed in both experimental groups was described by Rodrigues (2010) in Alpine goats at 12 months of age with an average LW of 27 kg, where tubulosomatic index was 0.36%. This difference can be explained by the higher LW of the animals of the present study.

Variations in diameter and volume of the seminiferous tubules in the testicular parenchyma are reflected in the LST value variation. Thus, the larger the diameter of the seminiferous tubules, the smaller the LST value. The goats in G1 and G2 showed values higher than those of the crossbred goats studied by Lents et al. (2018), which presented LST of 1,769.48 m and LGT of 13.06 m/g. This difference occurred because of the greater tubular diameter and volume values used to obtain these results.

CONCLUSION

Ingestion of *Cenostigma pyramidale* has no toxic effect on the testicular, seminal and histological parameters of goat testis. Due to its nutritional characteristics, consumption of this plant improves animal body development. Because *C. pyramidale* is adapted to semi-arid regions, it can be an alternative source of feed for goats during periods of shortage.

Acknowledgments.- The first author would like to thank the "Fundação de Amparo à Pesquisa do Estado da Bahia" (FAPESB) for the grant of the master's scholarship. This study was supported by "Instituto Nacional de Ciência e Tecnologia", "Conselho Nacional de Desenvolvimento Científico e Tecnológico" (INCT-CNPq) for the Control of Poisoning by Plants (Proc. No. 573534/2008-0).

Conflict of interest statement.- The authors declare having no competing interests.

REFERENCES

Aguiar G.V., Araújo A.A. & Moura A.A.A. 2006. Desenvolvimento testicular, espermatogênese e concentrações hormonais em touros Angus. Revta Bras. Zootec. 35(4supl.):1629-1638. <https://dx.doi.org/10.1590/S1516-35982006000600008>

Almeida M.M., Machado Jr A.A.N., Ambrósio C.E., Menezes C.E., Righi D.A., Nascimento I.M.R. & Carvalho M.A.M. 2010. Influência do grau de bipartição escrotal sobre parâmetros reprodutivos de caprinos. Pesq. Vet. Bras. 30(4):345-350. <https://dx.doi.org/10.1590/S0100-736X2010000400011>

AOAC 1992. Official Methods of Analysis. 12nd ed. Association of Official Analytical Chemists, Washington. 1094p.

Araujo K.D., Dantas R.T., Andrade A.P., Parente H.N. & Silva E.E. 2010. Uso de espécies da caatinga na alimentação de rebanhos no município de São João do Cariri-PB. RA'E GA 20:157-171.

Arruda R.P., Celeghini E.C.C., Garcia A.R., Santos G.C., Leite T.G., Oliveira L.Z., Lançoni R. & Rodrigues M.P. 2015. Morfologia espermática de touros: interpretação e impacto na fertilidade. Revta Bras. Reprod. Anim. 39(1):47-60.

Avelar G.F., Oliveira C.F.A., Soares J.M., Silva I.J., Dobrinski I., Hess R.A. & França L.R. 2010. Postnatal somatic cell proliferation and seminiferous tubule maturation in pigs: a non-random event. Theriogenology 74(1):11-23. <https://dx.doi.org/10.1016/j.theriogenology.2009.12.014> <PMid:20189235>

CBRA 2013. Manual para Exame Andrológico e Avaliação de Sêmen Animal. 3ª ed. Colégio Brasileiro de Reprodução Animal, Belo Horizonte. 87p.

Flora do Brasil 2020. Jardim Botânico do Rio de Janeiro. Available at <http://floradobrasil.jbrj.gov.br> Accessed on Jun., 2019. (in Construction)

França L.R. & Godinho C.L. 2003. Testis morphometry, seminiferous epithelium cycle length, and daily sperm production in domestic cats (*Felis catus*). Biol. Reprod. 68(5):1554-1561. <https://dx.doi.org/10.1095/biolreprod.102.010652> <PMid:12606460>

França L.R., Silva Jr V.A., Chiarinigarcia H., Garcia S.K. & Debeljuk L. 2000. Cell proliferation and hormonal changes during postnatal development of the testis in the pig. Biol. Reprod. 63(6):1629-1636. <https://dx.doi.org/10.1095/biolreprod63.6.1629> <PMid:11090429>

Hoshino P., Nakaghi L.S.O., Pacheco M.R., Lui J.F. & Malheiros E.B. 2002. Morfometria dos túbulos seminíferos e ductos epididimários de cães e gatos provenientes de cirurgia de castração. Revta Biotemas 15(1):97-110. <https://dx.doi.org/10.5007/%25x>

Leite F.L.G., Paula T.A.R., Matta S.L.P., Fonseca C.C., Neves M.T.D. & Barros J.B.G. 2006. Cycle and duration of the seminiferous epithelium in puma (*Puma concolor*). Anim. Reprod. Sci. 91(3/4):307-316. <https://dx.doi.org/10.1016/j.anireprosci.2005.04.003>

Lents M.P., Barbosa L.P., Santana A.L.A., Pinheiro E.E.G., Mugabe L.C., Biscarde C.E.A. & Souza R.S. 2018. Immunocastration of goats using anti gonadotrophin releasing hormone vaccine. Theriogenology 114:7-13. <https://dx.doi.org/10.1016/j.theriogenology.2018.03.013> <PMid:29574307>

Lopes J.R.G., Santos J.R.S., Medeiros M.A., Campos E.M., Medeiros R.M.T. & Riet-Correa F. 2017. Reproductive losses caused by the ingestion of *Poincianella pyramidalis* in sheep. Toxicon 138:98-101. <https://dx.doi.org/10.1016/j.toxicon.2017.08.020> <PMid:28843661>

Maia G.N. 2012. Caatinga: árvores e arbustos e suas utilidades. 2ª ed. Printcolor, Fortaleza, p.159-169.

Marcelino S.A.C., Macêdo J.T.S.A., Reis S.D.S., Lacerda M.S.C., Silva A.R.S., Riet-Correa F., Pimentel L.A. & Pedroso P.M.O. 2017. Malformações em pequenos ruminantes no semiárido da Bahia: aspectos epidemiológicos, clínico-patológicos e radiológicos. Pesq. Vet. Bras. 37(12):1437-1442. <https://dx.doi.org/10.1590/s0100-736x2017001200013>

Matias J.R., Silva F.F.S. & Dantas B.F. 2017. Catingueira-verdadeira *Poincianella pyramidalis* [Tul.] L.P. Queiroz. Nota Técnica nº 6, ABRATES, Londrina. Available at <http://www.alice.cnptia.embrapa.br> Accessed on Jun., 2019.

Mendonça Jr A.F., Braga A.P. & Galvão R.J.D. 2008. Composição bromatológica, consumo e digestibilidade in vivo de dietas com diferentes níveis de feno de catingueira (*Caesalpinea pyramidalis* Tul.), fornecidas para ovinos SRD. Revta Biol. Ciênc. Terra 8(1):135-142.

Mohammed A.H.S., Kadium D.A.H & Ebed A.K. 2011. Some morphometric and histological description of the seminiferous, striaghted and rete testis tubules in the testis of indogenous male goats (two years old). J. Vet. Med. Sci. 2(1):19-29.

Morais D.B., Barbosa L.P., Melo B.E.S., Matta S.L.P., Neves M.M., Balarini M.K. & Rodrigues M.V. 2012. Microscopy and morphometry of tubular components of rabbit testis supplemented with royal jelly. Arq. Bras. Med. Vet. Zootec. 64(4):810-816. <https://dx.doi.org/10.1590/S0102-09352012000400004>

Queiroz A.C.P, Sousa M.S.A.S & Sousa M.A.N. 2018. Atividade genotóxica de *Cenostigma pyramidale* (Tul.) Gagnon & G.P. Lewis (Fabaceae) sob *Allium cepa* (Amaryllidaceae). III Congresso Nacional de Pesquisa e Ensino em Ciências, Campina Grande, PB. 12p.

Reis S.D.S., Oliveira R.S., Marcelino S.A., Macêdo J.T.S., Riet-Correa F., Pimentel L.A. & Pedroso P.M.O. 2016. Congenital malformations and other reproductive losses in goats due to poisoning by *Poincianella pyramidalis* (Tul.) L.P. Queiroz (=*Caesalpinia pyramidalis* Tul.). Toxicon 118:91-94. <https://dx.doi.org/10.1016/j.toxicon.2016.04.043> <PMid:27125469>

Ribeiro P.H.C., Lima V., Urbano S.A., Menezes M.S., Tavares Neta M.D.L., Costa M.G., Aguiar E.M. & Inácio J.G. 2020. Consumo e desempenho de cordeiros confinados alimentados com diferentes níveis de fibra em detergente neutro. Braz. J. Develop. 6(4):16964-16975. <https://dx.doi.org/10.34117/bjdv6n4-023>

Rodrigues M.H. 2010. Análise morfométrica e funcional do desenvolvimento testicular de caprinos da raça alpina criados em condições semi-intensivas. Doctoral Dissertation, Universidade Estadual do Norte Fluminense Darcy Ribeiro, Goytacazes, Rio de Janeiro. 159p.

Russell L.D., Ettlin R.A., Sinha Hikim A.P. & Clegg E.D. 1993. Histological and histopathological evaluation of the testis. Int. J. Androl. 16(1):83-84. <https://dx.doi.org/10.1111/j.1365-2605.1993.tb01156.x>

Silva L.B., Santos F.A.R., Gasson P. & Cutler D. 2009. Anatomia e densidade básica da madeira de *Caesalpinia pyramidalis* Tul. (Fabaceae), espécie endêmica da caatinga do Nordeste do Brasil. Acta Bot. Bras. 23(2):436-445. <https://dx.doi.org/10.1590/S0102-33062009000200015>

Souza L.E.B., Cruz J.F., Teixeira Neto M.R., Ferraz R.C.N. & Cruz M.H.C.C. 2011. Puberty and sexual maturity in Anglo-Nubian male goats raised in semi-intensive system. Revta Bras. Zootec. 40(7):1533-1539. <https://dx.doi.org/10.1590/S1516-35982011000700019>

Souza M.F., Bezerra I.T.F., Barbosa F.M.S., Rocha V.C., Sousa M.S., Oliveira Neto T.S., Lacerda-Lucena P.B. & Lucena R.B. 2018. Abortos, malformações congênitas e falhas reprodutivas espontâneas em caprinos causados na intoxicação pelas folhas da catingueira, *Poincianella pyramidalis* (sin. *Caesalpinia pyramidalis*). Pesq. Vet. Bras. 38(6):1051-1057. <https://dx.doi.org/10.1590/1678-5150-pvb-5243>

Urbano S.A., Ferreira M.A., Véras R.M.L., Azevedo P.S., Santos Filho H.B., Vasconcelos G.A. & Oliveira J.P.F. 2015. Características de carcaça e composição tecidual de ovinos Santa Inês alimentados com manipueira. Revta Bras. Ciênc. Agrár. 10(3):466-472. <https://dx.doi.org/10.5039/agraria.v10i3a4812>

Van Soest P.J. 1994. Nutritional Ecology of the Ruminant. 2nd ed. Cornell University Press, Ithaca, p.290-311.

Van Soest P.J., Robertson J.B. & Lewis B.A. 1991. Methods for dietary fiber, neutral detergent fiber, and nonstarch polyssacharides in relation to animal nutrition. J. Dairy Sci. 74(10):3583-3597. <https://dx.doi.org/10.3168/jds.S0022-0302(91)78551-2> <PMid:1660498>

Vieira E.L, Carvalho F.F.R., Batista A.M.V., Ferreira R.L.C., Santos M.V.F., Lira M.A., Silva M.J. & Silva E.M.B. 2005. Composição química de forrageiras e seletividade de bovinos em bosque de Sabiá (*Mimosa caesalpiniifolia* Benth.) nos períodos chuvoso e seco. Revta Bras. Zootec. 34(5):1505-1511. <https://dx.doi.org/10.1590/S1516-35982005000500010>

PESQUISA VETERINÁRIA BRASILEIRA
Brazilian Journal of Veterinary Research
ISSN 0100-736X (Print)
ISSN 1678-5150 (Online)

Pesq. Vet. Bras. 40(12):970-976, December 2020
DOI: 10.1590/1678-5150-PVB-6679

Original Article
Livestock Diseases
BY-NC

Use of oral fluids to detect anti *Lawsonia intracellularis* antibodies in experimentally infected pigs[1]

Michelle P. Gabardo[2], José Paulo H. Sato[2], Talita P. Resende[2], Luisa V.A. Otoni[2], Lucas A. Rezende[2], Amanda G.S. Daniel[2], Carlos E.R. Pereira[2] and Roberto M.C. Guedes[2]*

ABSTRACT.- Gabardo M.P., Sato J.P.H., Resende T.P., Otoni L.V.A., Rezende L.A., Daniel A.G.S, Pereira C.E.R. & Guedes R.M.C. 2021. **Use of oral fluids to detect anti-*Lawsonia intracellularis* antibodies in experimentally infected pigs.** *Pesquisa Veterinária Brasileira 40(12):970-976*. Departamento de Clínica e Cirurgia, Escola de Medicina Veterinária, Universidade Federal de Minas Gerais, Av. Antônio Carlos 6627, Belo Horizonte, MG 31270-901, Brazil. E-mail: guedesufmg@gmail.com

Several pathogens and antibodies derived from serum or produced in tissues associated with the oral cavity are present in the oral fluid (OF). Considering the applicability of this alternative sample, recent studies in veterinary medicine have tested OF as a replacement for serum in diagnostic assays. The aim of this study was to standardize the immunoperoxidase monolayer assay (IPMA) to detect anti-*Lawsonia intracellularis* immunoglobulin A (IgA) and immunoglobulin G (IgG) in OF samples from experimentally infected pigs. Sixty-two pigs were divided into two groups: control (T1, n=30) and inoculated with *L. intracellularis* (T2, n=32). Blood, OF and fecal samples were collected at 0, 7, 14, 21, 28 and 42 days post-inoculation (dpi). Some adaptations of the standard technique for serum were made to IPMA for the detection of IgA and IgG in OF. The IPMA showed high specificity and sensitivity for serum samples and high specificity and moderate sensitivity for the detection of IgA and IgG in OF. There was high agreement between the results of serum IgG and OF IgA and IgG. Based on our results, oral fluid samples may be used for the evaluation and determination of anti-*L. intracellularis* antibodies in pigs, but not for individual diagnosis of swine proliferative enteropathy.

INDEX TERMS: Oral fluid, *Lawsonia intracellularis*, antibody, pigs, diagnostic, enteric disease, porcine proliferative enteropathy, serology, swine.

RESUMO.- [Utilização de fluidos orais para detecção de anticorpos anti *Lawsonia intracellularis* em suínos experimentalmente infectados.] Vários patógenos e anticorpos derivados do soro ou produzidos em tecidos associados a cavidade oral estão presentes no fluido oral (FO). Considerando a aplicabilidade dessa amostra alternativa, estudos recentes em medicina veterinária têm testado o FO como substituto do soro para testes diagnósticos. O objetivo desse estudo foi padronizar a imunoperoxidase em monocamada de célula (IPMC) para a detecção de imunoglobulina A e imunoglobulina G anti-*Lawsonia intracellularis* em amostras de FO de suínos experimentalmente infectados. Um total de 62 suínos foram divididos em dois grupos: controle (T1, n=30) e inoculados com *L. intracellularis* (T2, n=32). Sangue, FO e amostras de fezes foram coletados aos 0, 7,14, 21, 28 e 42 dias após a inoculação (dpi). Algumas adaptações da técnica foram realizadas na técnica padrão da IPMC para a detecção de IgA e IgG. A IPMC demostrou alta especificidade e sensibilidade para amostras de soro e alta especificidade de moderada sensibilidade para a detecção de IgA e IgG em FO. Houve alta concordância entre resultados de detecção de IgG em soro com a IgA e IgG em amostras de FO. Baseado em nossos resultados, amostras de fluido oral podem ser usadas em avaliações e detecção de anticorpos anti-*L. intracellularis* em suínos, porém não de forma individual.

TERMOS DE INDEXAÇÃO: Fluido oral, anticorpo, *Lawsonia intracellularis*, suínos, diagnóstico, doenças entéricas, enteropatia proliferativa, sorologia.

[1] Received on July 11, 2020.
Accepted for publication on September 4, 2020.
[2] Departamento de Clínica e Cirurgia, Escola de Medicina Veterinária, Universidade Federal de Minas Gerais (UFMG), Av. Antônio Carlos 6627, Belo Horizonte, MG 31270-901, Brazil. E-mails: michelle.gabardo@ifmg.edu.br, jose.sato@agroceres.com, talitaresendevet@gmail.com, luisavianna.vet@gmail.com, rezendeavelino65@gmail.com, amandavet2007-1@hotmail.com, carlos.pereira@ufv.br
*Corresponding author: guedesufmg@gmail.com

INTRODUCTION

Lawsonia intracellularis is an obligate intracellular bacterium that causes porcine proliferative enteropathy (PPE) (McOrist et al. 1995). PPE is an intestinal infectious disease of grow-finishing pigs. PPE has three manifestations: acute, characterized by bloody diarrhea and death of the pigs at slaughter age; chronic, characterized by a performance decrease and transitory diarrhea in pigs from 6 to 20 weeks of age; and subclinical, characterized mainly by decreased production performance (Guedes 2007).

Among *ante mortem* diagnostic tests, PCR is highly specific; however, there are inhibitory factors that interfere with sensitivity in fecal samples. Additionally, the results are influenced by the course of the disease and variations in fecal shedding (Vannucci et al. 2012). Serological tests, such as ELISA, indirect immunofluorescence and the immunoperoxidase monolayer assay (IPMA), are also used (Kroll et al. 2005). Seroconversion occurs approximately 14 days after exposure to the agent and lasts for a long period; serology can be used to evaluate the kinetics of infection in the herd and to establish disease control strategies (Walter et al. 2004).

Traditionally, serum is used in diagnostic tests, but there are an increasing number of studies in veterinary medicine that used oral fluid (OF) to detect viruses, bacteria and specific antibodies against these agents (Prickett et al. 2008). OF samples may provide practical and economic advantages, including easier collection and reduced stress (Prickett & Zimmerman 2010).

Additionally, several studies have shown a high correlation between the detection of infectious agents and antibodies from serum and OF (Kittawornrat et al. 2013, Panyasing et al. 2014, 2013). Tests based on OF have demonstrated good sensitivity, specificity and reproducibility (Kittawornrat et al. 2013, Ouyang et al. 2013). To date, there have been no reports of the use of OF to detect anti-*L. intracellularis* antibodies in experimentally infected pigs. This study aimed to detected immunoglobulin A (IgA) and immunoglobulin G (IgG) anti-*L. intracellularis* antibodies in OF and to verify the persistence of the detection of these isotypes in OF in experimentally infected pigs. [e]

MATERIALS AND METHODS

Animals and experimental design. The experiment was approved by the Animal Experimentation Ethics Committee of the "Universidade Federal de Minas Gerais" (#77/2011 - June 8, 2011). Sixty-two 5-week-old pigs (10.0±0.64kg/b.w.) from a commercial swine herd free of clinical signs of PPE and other enteric diseases were used. All pigs were weighed, ear-tagged and randomly divided into the control (T1) and infected (T2) groups (30 and 32 pigs each, respectively). Each group was housed in separated rooms with four suspended pens with plastic floors, meshed-wired separations, deposit feeders and nipple drinkers. Four pigs were grouped per pen; however, there were only three pigs in two pens of the T1.

Management of temperature, and feeding were the same for all pens. All daily management activities were initially performed in control rooms, changing boots and overalls between the control room and infected challenge pigs. No parenteral or feed antimicrobial agents were used throughout the experimental period.

At 42 days post inoculation (dpi), all pigs were individually weighed. Pigs in poor clinical condition were euthanased and necropsied. The remaining pigs were euthanased and postmortem evaluated at 49 dpi. At necropsy, gross lesions were evaluated and ileum and cecum samples were collected to histopathologic and immunohistochemistry (IHC) to confirm *Lawsonia intracellularis* infection (Guedes et al. 2002a). For the IHC the labeled streptavidin[3] method with polyclonal antibodies specific for *L. intracellularis* was used (Guedes & Gebhart 2003a).

Preparation of inoculum and inoculation. The inoculum was prepared from porcine intestines affected by PPE, according to a previously described model (Guedes et al. 2002c). On day 0, pigs in T2 received 1 dose of 60mL of the inoculum via stomach tube. The total dose was approximately 8.8×10^{10} *L. intracellularis*/pig. Pigs in T1 received a sham inoculum. Bacteriologic testing of the inoculum did not detect any other confounding enteropathogenic organisms, such as *Salmonella* sp., *Brachsypira* spp. or enteropathogenic *Escherichia coli*.

Clinical evaluation and sample collection. Clinical observations of diarrhea were made by the same person twice a week. The scoring was based on Guedes et al. (2002d). The OF, blood and fecal samples were collected individually 0, 7, 14, 21, 28, 35 and 42 dpi. The pen OF sample was collected 0, 4, 14, 21, 28, 35 and 42 dpi. To collect OF, 15cm long cotton ropes were individually provided for pig. To prevent other pigs in the pen to have access to the rope of a given individual, the cotton ropes were marked and provided directly into the mouth of the animal. To collect pen samples, rope bundles were tied to the side of each pen for a time period sufficient to acquire an average of 10mL of OF per pen or until the pigs lost interest in the rope, in general for 30min. OF were extracted by twisting the damp part in plastic bags, then transferring to 50mL conical tubes, centrifuged at 1000x g for 10min, aliquoted and stored at -20˚C until tested. Blood samples were collected at the same days, processed and serum stored at -20˚C until tested.

Individual fecal samples from all pigs were collected at the same days and stored at -20°C for PCR testing. DNA of fecal was extracted from fecal samples using a commercial kit[4] according to the manufacturer's protocol, and subsequently tested by PCR (Jones et al. 1993).

Serum and oral fluid analysis. Serum samples were tested by IPMA for anti-*L. intracellularis* IgG (Guedes et al. 2002b, 2002c). For the verification of titers, positive serum samples at the 1:30 cut-off point were serially diluted to 1:120, 1:480 and 1:1920.

The IPMA used for detection of *L. intracellularis*-specific IgA and IgG in OF was a modified version of the IPMA used for serum described by Guedes et al. (2002b). The standardization of the IPMA for both isotypes in OF was initially performed on samples from a farm with PPE cases and pigs with high serum antibody titers. To for standardization, briefly, 96-well plates containing acetone fixed monolayer of McCoy cells highly infected with *L. intracellularis* were rehydrated with distilled water or PBS Tween 0.05% (PBS with 0.05% Tween 20, pH 7.2) for 10 and 45 minutes at 37°C. OF and secondary antibody (anti-pig IgA[5] and IgG[6] -peroxidase conjugate) were diluted in phosphate-buffered saline (PBS; pH 7.2), or 0.25% skimmed milk 1x PBS solution or PBS Tween 0.05%. Secondary antibodies were also diluted in IPMA buffer (PBS with 2.5% serum

[3] K675 Dako, Corporation, CarpintariaI. CA 93013 USA.
[4] PSP Stool DNA Spin Kit, Molecular STRATEC Campus Berlin-Buch, Germany.
[5] Bethyl Laboratories, Montgomery, Texas, USA.
[6] Sigma-Aldrich, St. Louis, MO.

fetal bovine, 1% rabbit serum, and 0.08% Tween 80) (Guedes et al. 2002b). OF were tested undiluted and diluted 1:2 and 1:3, and the secondary antibodies were tested using 1:45, 1:50, 1:100 and 1:200 dilutions. OF samples were gradually thawed in the refrigerator at 4°C for 12 hours to avoid interference of temperature on the integrity of the antibodies (Prickett et al. 2010, Decorte et al. 2013, Jones & Muehlhauser 2014) and to sediment gross material.

Statistical analysis. Comparisons of serum anti-*L. intracellularis* IgG, and OF anti- *L. intracellularis* IgA and IgG between the groups were performed by the Kaplan-Meier test in the statistical program STATA. The level of significance was 5% ($P<0.05$). The sensitivity and specificity of IPMA were calculated in Microsoft Excel using the control and infected groups, at 28 dpi, for the determination of negative and positive samples, respectively. The Spearman correlation test was used to evaluate the correlation between the detection of serum IgG and IgA and IgG in OF. The Kappa method was used to verify agreement between the tests and the agreement between the detection of specific IgA and IgG in individual and collective samples. The program used was BioEstata 5.0. The pens were considered positive if at least one animal tested positive for the studied immunoglobulin isotype in the individual collection.

RESULTS

Animals and inoculation

All pigs were seronegative and PCR negative for *Lawsonia intracellularis* in fecal samples on day 0.

In the third week post-inoculation an animal in T2 had bloody diarrhea from 19 to 23 dpi, and watery diarrhea until 34 dpi, when it was euthanased due to its poor clinical condition and persistent diarrhea. At necropsy, there were typical PPE lesions confirmed by IHC. *L. intracellularis* fecal shedding was first detected in T2 pigs 7 dpi and peaked at 14 dpi. Pigs in the T1 remained negative up to 28 dpi (Fig.1). At the end of the experiment, macroscopic lesions were more frequent, extensive and severe, as well as IHC scores were more intense in the T1 group.

Four pigs from each group died or were euthanized in the first and second week of the study due to conditions not related to the challenge.

IPMA in serum and oral fluid

The main modifications of IPMA for OF were the hydration of the plates with PBS Tween 0.05%, no dilution of the samples, and the time of incubation of OF sample was extended to 45 min, as described by Barrera-Zarate (2019). All tested concentrations of anti-pig IgA and anti-pig IgG secondary antibodies were adequate, but the 1:100 dilution in PBS 0.05% Tween had less background; thus, specific immunostaining was easier to visualize.

One animal in T2 seroconverted 14 dpi, and 100% of the pigs were seropositive at 42 dpi. T1 pigs seroconverted at 35 dpi, and an increasing number of seropositive pigs were detected at 42 dpi, but the proportion of seropositive pigs was significantly lower ($P<0.05$) than T2 from 14-42 dpi (Fig.1).

The first detection of specific *L. intracellularis* IgA and IgG, respectively, in OF occurred at 14 dpi and 21 dpi in T2,

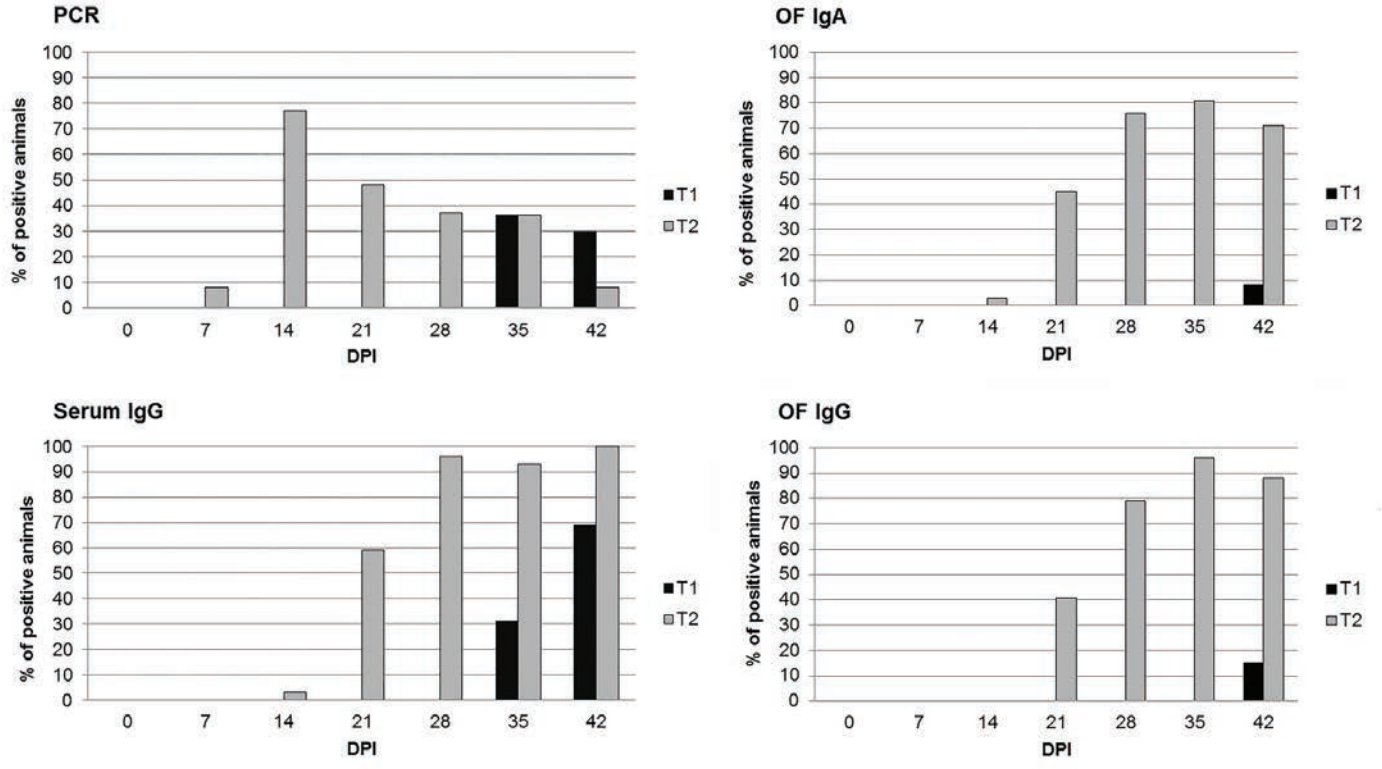


Fig.1. Percentage of positive pigs by PCR for *Lawsonia intracellularis* in fecal samples, percentage of positive pigs using immunoperoxidase monolayer assay (IPMA) to detect IgG in serum samples and Percentage of positive pigs using IPMA to detect IgA and IgG in oral fluids (OF) samples. All pigs used in the experiment were considered in these analyses. There was a difference ($P<0.05$) in positive animals for *L. intracellularis* between groups on 7 to 28 dpi. There was a difference ($P<0.05$) in the detection of serum IgG between the groups on 21 to 42 dpi.

with higher percentages of positive pigs at 35 dpi for both isotypes. In T1, both isotypes were detected in OF at 42 dpi. The detection of both isotypes in this group remained different from T2 from 14 and 21 dpi until 42 dpi (P<0.05) for IgA and IgG (Fig.2), respectively. Figure 2 shows the curve of serum IgG titers and the percentage of IgA and IgG positive pigs in OF.

The IPMA sensitivity and specificity for the detection of serum IgG and OF IgA and IgG were determined using 52 samples (26 pigs from each group) at 28 dpi. The IPMA sensitivity for detecting IgG in serum was 100% and 84.62% and 88.46% for OF IgA and IgG, respectively. The specificity was 100% for both serum and OF.

There was an increase in the number of IgA- and IgG-positive pigs based on the OF analysis concomitant with the increase in IgG serum titers. There was a high correlation between the detection of serum IgG and the detection of IgA and IgG in the OF (rs = 0.82 and rs = 0.89, respectively).

There was high agreement between the IPMA results for specific *L. intracellularis* IgG in serum and OF IgA and IgG at 28 dpi in individual samples (Table 1). In the OF pen samples, the IPMA detected one positive pig housed together with three negative animals (Table 2 and 3), and there was high agreement between the pen samples IPMA results and the individual animal samples.

DISCUSSION

The naive condition of the pigs used in this study was confirmed by serology and PCR of samples collected on the day of inoculation. The success of the challenge was confirmed by the high number of pigs that shed *Lawsonia intracellularis* in their feces, the seroconversion rate and the detections of lesions at the end of the experiment. Although the T1 was housed in separate room with strict management, due to the long period of the experiment, there was indirect contamination confirmed by *L. intracellularis* fecal shedding and seroconversion at 35 dpi. This period of T1 contaminations was confirmed with detection of more evident macroscopic lesions and immunolabelling compared to T2. The period between the inoculation of T2 pigs and euthanasia (49 dpi) justify the regression of gross lesions by the end of the trial, as previous demonstrated by Guedes & Gebhart (2004).

Both clinical manifestations and the detection of *L. intracellularis* in feces of T2 were consistent with other experimental challenge studies using mucosal homogenate as the inoculum (Guedes et al. 2002b, 2002d). Fecal and serum samples from pigs of both groups were negative by PCR and serology during the first two weeks and remained PCR negative until 35 dpi in T1.

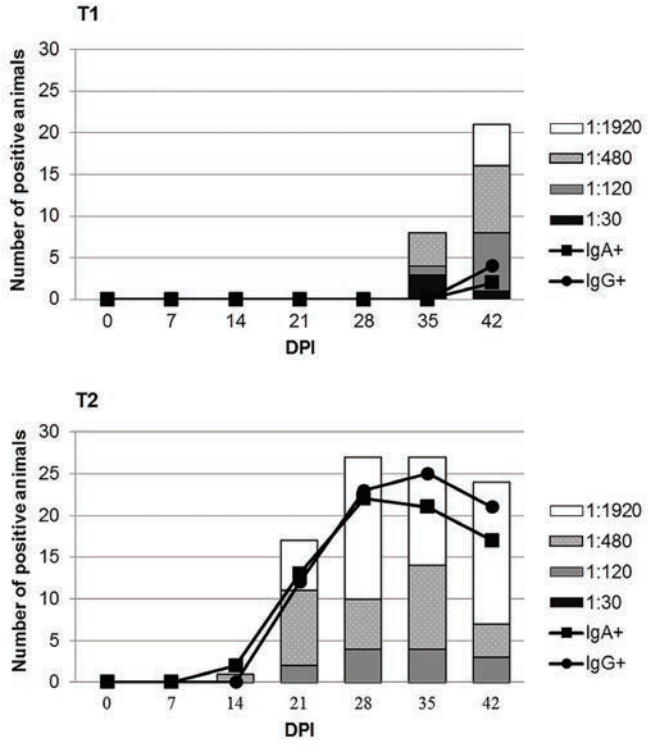


Fig.2. Positivity of pigs detected in serum and oral fluids (OF). Numbers and titers of *Lawsonia intracellularis* IgG seropositive pigs (bars) and numbers of positive pigs and specific *L. intracellularis* IgA and IgG titers (lines) in OF samples. T1 = control group and T2 = inoculated group.

Table 1. Percentage of agreement between immunoperoxidase monolayer assay (IPMA) results for specific *Lawsonia intracellularis* IgG in serum and IgA and IgG in oral fluid (OF) at 21 and 28 dpi

	21 dpi	28 dpi
Serum IgG/IgA OF	79.00[a] (0.46)[b]	90.38 (0.81)
Serum IgG/IgG OF	80.77 (0.50)	94.23 (0.88)
IgA OF/IgG OF	86.54 (0.58)	92.31 (0.84)
Individual pig IgA/pen IgA	93.75 (0.86)	100.00
Individual pig IgG /pen IgG	100.00	100.00

Twenty-six animals were used in each group; [a] percentage of agreement, [b] Kappa-index.

Table 2. Number of positive animals per pen and pan positive for IgA in individual and collective samples, respectively, of pig oral fluid on different days post-inoculation with *Lawsonia intracellularis*

	Pen	0 dpi	7 dpi	14 dpi	21 dpi	28 dpi	35 dpi	42 dpi
Control pen	1A	0/4	0/4	0/4	0/4	0/4	1/4	2/4
	1B	0/4	0/4	0/4	0/4	0/4	2/4	3/4[a]
	1C	0/4	0/4	0/4	0/4	0/4	1/4	0/4
	1D	0/4	0/4	0/4	0/4	0/4	1/4	1/4
	2A	0/3	0/2	0/2	0/2	0/2	1/2	0/2
	2B	0/3	0/2	0/2	0/2	0/2	2/2	1/2[a]
	2C	0/4	0/4	0/4	0/4	0/4	1/4	0/4[a]
	2D	0/4	0/2	0/2	0/2	0/2	0/2	1/2[a]
Inoculated pen	3A	0/4	0/4	1/3	3/3[a]	2/3[a]	2/2[a]	2/3[a]
	3B	0/4	0/4	1/4	2/4[a]	3/4[a]	4/4[a]	4/4[a]
	3C	0/4	0/4	0/4	1/4[a]	2/4[a]	1/4[a]	1/4[a]
	3D	0/4	0/4	0/4	0/4	4/4[a]	4/4[a]	2/4[a]
	4A	0/4	0/3	0/3	0/3	1/3[a]	0/2[a]	0/2[a]
	4B	0/4	0/4	0/4	3/3[a]	3/3[a]	3/3[a]	3/3[a]
	4C	0/4	0/4	0/4	3/4[a]	4/4[a]	3/3[a]	3/3[a]
	4D	0/4	0/4	0/4	1/4	3/4[a]	3/4[a]	2/4a

[a] Positive pens in collective oral fluid, [b] cells surround indicates pens with negative pens in collective samples, but positive results in individual samples; * Positive in collective sample, but negative in individual samples.

OF contains pathogens and antibodies derived from serum or produced in tissues associated with the oral cavity. A number of studies in animals have demonstrated the usefulness of OF compared to serum (Pacheco et al. 2010, Pricket et al. 2011, Giménez-Lirola et al. 2013, Vosloo et al. 2015). These studies used ELISA for the detection of serum and OF antibodies. IPMA was chosen in the present study because this methodology was already established in our laboratory and had demonstrated high sensitivity and specificity in previous studies (Guedes et al. 2002b, 2002c).

Similar to serum samples, the present study also demonstrated high specificity of IPMA in OF, as no false positive animal was detected (at 21 and 28 dpi). Despite the low concentrations of antibodies detectable in OF (Escribano et al. 2012), the IPMA showed moderate sensitivity for detecting IgA (84.62%) and IgG (88.46%) in OF. Kittawornrat et al. (2012) also obtained good sensitivity and specificity for the detection of anti-PRRSV IgG in field samples after standardization of ELISA in OF. Control pigs showed positive OF after indirect infection, demonstrated by positive PCR and increase of seropositive pigs. This result demonstrated that even naturally infected pigs have detectable antibodies specific for *L. intracellularis* in the OF. Although not planned, this result demonstrated that this type of sample might also be applicable in field conditions.

Due to IgA antibodies representing mucosal immunity, we expected the detection of IgA prior to IgG, however, as observed that there was no time difference in the detection of both, only two pigs were positive one week before IgG detection in T2. In T2, the percentage of IgG detection in OF was higher than IgA from 21 to 42 dpi. This difference may be explained by the influence of the rope material used (cotton). In two studies using synthetic (i.e., polyamide) and natural fiber (i.e., cotton) rope material, higher detection of IgA was observed using the synthetic materials. However, there was no difference between the materials for the detection of IgG (Olsen et al. 2013, Decorte et al. 2014). Another explanation is that sick pigs have higher concentrations of total immunoglobulin in their OF compared to healthy pigs; this is especially true for IgG, which significantly increases among immunoglobulins (Escribano et al. 2012) and remains useful for a longer time in standard concentrations for the diagnosis in both experimental and field samples (Kittawornrat et al. 2012, 2014). Therefore, it can be inferred that the use of cotton rope for the detection IgG anti-*L. intracellularis* in OF may be used for the monitoring the disease.

The first detection and the peak of antibodies occurred at the same time in the OF and serum in T2 group. Our findings support those Nogueira et al. (2013), who demonstrated that the peak of detection for serum and mucosal IgG against *L. intracellularis* were correlated. A similar correlation between serum and OF IgG was observed in other studies (Prickett et al. 2011, Kittawornrat et al. 2013, Mur et al. 2013). In general, the kinetics of antibodies response in the OF is dependent on the kinetics of antibodies in the serum and mucosa (Prickett & Zimmerman 2010). In the present study, there was a significant correlation between the serum IgG and the two isotypes in the OF. The percentage of agreement between the IPMA results in serum and OF was high at 28 dpi, with 90% for IgA and 94% for IgG. In agreement with our result, Kittawornrat et al. (2013) observed a high correlation between serum and OF and high agreement of positive results using ELISA to detect anti-PRRSV-specific antibodies.

In the present study, the majority of the pigs with IgG titers lower than <1:480 in serum were negative for IgA and IgG in the OF. Similar results were observed in the study of Mur et al. (2013) for African swine fever. The low initial antibody serum titers in control pigs could be explained by the low number of pigs with positive OF one week after IgG seroconversion

Table 3. Number of positive animals per pen and pan positive for IgG in individual and collective samples, respectively, of pig oral fluid on different days post-inoculation with *Lawsonia intracellularis*

	Pen	0 dpi	7 dpi	14 dpi	21 dpi	28 dpi	35 dpi	42 dpi
Control pen	1A	0/4	0/4	0/4	0/4	0/4	0/4	1/4[b]
	1B	0/4	0/4	0/4	0/4	0/4	0/4	1/4[b]
	1C	0/4	0/4	0/4	0/4	0/4	0/4	0/4
	1D	0/4	0/4	0/4	0/4	0/4	0/4	0/4
	2A	0/4	0/3	0/3	0/3	0/3	0/3	0/3
	2B	0/3	0/2	0/2	0/2	0/2	0/2	0/2
	2C	0/4	0/4	0/4	0/4	0/4	0/4	1/4[a]
	2D	0/2	0/2	0/2	0/2	0/2	0/2	1/2[a]
Inoculated pen	3A	0/4	0/4	0/3	2/3[a]	2/2[a]	2/2[a]	2/2[a]
	3B	0/4	0/4	0/4	1/4[a]	2/3[a]	4/4[a]	4/4[b]
	3C	0/4	0/4	0/4	1/4[a]	4/4[a]	4/4[a]	3/4[a]
	3D	0/4	0/4	0/4	0/4	4/4[a]	4/4[a]	2/2[a]
	4A	0/4	0/3	0/3	3/3[a]	1/3[a]	1/2[a]	2/2[a]
	4B	0/4	0/4	0/4	3/3[a]	3/3[a]	3/3[a]	3/3[a]
	4C	0/4	0/4	0/4	1/4[a]	4/4[a]	3/3[a]	3/3[a]
	4D	0/4	0/4	0/4	0/4	2/4[a]	4/4[a]	3/4[a]

[a] Gray marking indicates the positive pens in collective oral fluid, [b] cells surround indicates pens with negative results in collective samples, but positive results in individual samples.

Table 4. Number of PCR positive animals per pen in individual fecal collect and qPCR positive pen in collective oral fluids (OF) on different days post-inoculation with *Lawsonia intracellularis*

	Pen	14 dpi	21 dpi	28 dpi	35 dpi	42 dpi
Control pen	1A	0/4[a]	0/4[a]	0/4[a]	1/4[a]	2/4[a]
	1B	0/4[a]	0/4[a]	0/4[a]	2/4[a]	3/4[a]
	1C	0/4[a]	0/4[a]	0/4[a]	1/4[a]	0/4*
	1D	0/4[a]	0/4[a]	0/4[a]	1/4[a]	1/4[a]
	2A	0/2[a]	0/2[a]	0/2[a]	1/2[a]	0/2*
	2B	0/2[a]	0/2[a]	0/2[a]	2/2[a]	1/2[a]
	2C	0/4[a]	0/4[a]	0/4[a]	1/4[a]	0/4*
	2D	0/2[a]	0/2[a]	0/2[a]	0/2[b]	0/2*
Inoculated pen	3A	2/3[a]	1/3[a]	0/3[a]	2/3[a]	0/3
	3B	2/4[a]	2/4[a]	2/4[a]	2/4[a]	0/4[a]
	3C	4/4[a]	1/4[a]	1/4[a]	1/4[a]	0/4[a]
	3D	4/4[a]	2/4[a]	1/4[a]	2/4[b]	0/4[a]
	4A	2/3[a]	1/3[a]	1/3[a]	0/2[a]	0/2[a]
	4B	3/4[a]	2/3[a]	1/3[a]	1/3[a]	1/3[b]
	4C	3/4[a]	3/4[a]	3/4[a]	1/4[a]	0/3*
	4D	1/4[a]	2/4[a]	1/4[a]	1/4[a]	0/4*

[a] Gray marking indicates the positive pens in collective oral fluid, [b] cells surround indicates pens with negative pens in collective samples, but positive results in individual samples; * Positive in collective sample, but negative in individual samples.

compared to the inoculated pigs. The difference in the infective initial dose of *L. intracellularis* (which was presumably lower in the control group due to natural exposure) could explain the difference in the initial immune response of the control pigs, as humoral and mucosal responses are dose dependent (Nogueira et al. 2013).

The application of OF-based testing facilitates the monitoring, surveillance and detection of diseases in animal populations. The samples can be collected from various pigs in pens at the same time, thereby facilitating collection and increasing the sample size (Prickett & Zimmerman 2010). In a study of the detection of anti-PRRSV-specific antibodies in OF collected in pens, it was observed that IgM, IgG and IgA were readily detected in populations in which the infection was controlled by experimental challenge. However, this was not observed in field samples (Kittawornrat et al. 2012). Natural exposure in the T1 group may have resulted in pigs at different stages of the humoral response. Thus, in the present study, we compared individuals with pen OF to verify whether collective samples could be representative of the group. The results demonstrated high agreement between individual OF and pen OF samples, and IPMA could detect one positive housed together with three negative pigs (Table 2-4).

Similar results were found by Barrera-Zarate et al. (2019) that detected IgG positive oral fluid collected in the pen that not all pigs tested were positive in serum samples. However, just the correlation of positivity of FO and serum was possible in farms with clinical signs, in the growth and finishing pigs.

CONCLUSIONS

The immunoperoxidase monolayer assay (IPMA) technique has demonstrated moderate sensitivity and high specificity for the detection of anti-*Lawsonia intracellularis* IgA and IgG in oral fluids (OF) in experimentally inoculated pigs and has the ability to detect positive pigs in OF pen samples.

The simultaneous detection of antibodies in both serum and OF samples and the high agreement between the IPMA in serum and OF demonstrate that OF may be used for serologic profile analysis, but not for individual diagnosis of EPS.

In addiction, IgG antibodies remain in the oral fluid for a minimum of three weeks.

Acknowledgements.- The authors thank "Pró de Reitoria de Pesquisa" of the "Universidade Federal de Minas Gerais" (PRPq-UFMG), "Conselho Nacional de Desenvolvimento Científico e Tecnológico" (CNPq), "Coordenação de Aperfeiçoamento de Pessoal de Nível Superior" (CAPES) and "Fundação de Amparo à Pesquisa do Estado de Minas Gerais" (Fapemig) for their financial support. R.M.C.G. is a recipient of a fellowship from CNPq. Rafaela Andrade collaborated with processed samples. João Paulo Haddad collaborated with data analysis.

Conflict of interest statement.- The authors declare that there is no conflict of interest.

REFERENCES

Barrera-Zarate J.A., Andrade M.R., Pereira C.E.R., Vasconcelos A., Wagatsuma M.M., Sato J.P.H., Daniel A.G.S., Rezende L.A., Otoni L.A.V., Laub R.P., Macedo N.R., Costa C.M., Haddad J.P.A. & Guedes R.M.C. 2019. Oral fluid for detection of exposure to *Lawsonia intracellularis* in naturally infected pigs. Vet. J. 244:34-36. <https://dx.doi.org/10.1016/j.tvjl.2018.12.003> <PMid:30825892>

Decorte I., Breedam W.V., Stede Y.V., Nauwync H.J., Regge N.D. & Cay A.B. 2014 Detection of total and PRRSV-specific antibodies in oral fluids collected with different rope types from PRRSV-vaccinated and experimentally infected pigs. BMC Vet. Res. 10:134. <https://dx.doi.org/10.1186/1746-6148-10-134> <PMid:24938323>

Decorte I., Van der Stede Y., Nauwynck H., De Regge N. & Cay A.B. 2013. Effect of saliva stabilisers on detection of porcine reproductive and respiratory syndrome virus in oral fluid by quantitative reverse transcriptase real-time PCR. Vet. J. 197(2):224-228. <https://dx.doi.org/10.1016/j.tvjl.2013.02.001> <PMid:23489844>

Escribano D., Gutiérrez A.M., Martínez Subiela S., Tecles F. & Cerón J.J. 2012. Validation of three commercially available immunoassays for quantification of IgA, IgG, and IgM in porcine saliva samples. Res. Vet. Sci. 93(2):682-687. <https://dx.doi.org/10.1016/j.rvsc.2011.09.018> <PMid:22019471>

Giménez-Lirola L.G., Xiao C.T., Zavala M., Halbur P.G. & Opriessnig T. 2013. Improving ante mortem diagnosis of *Erysipelothrix rhusiopathiae* infection by use of oral fluids for bacterial, nucleic acid, and antibody detection. J. Microbiol. Methods 92(2):113-121. <https://dx.doi.org/10.1016/j.mimet.2012.11.014> <PMid:23201482>

Guedes R.M.C. & Gebhart C.J. 2003a. Preparation and characterization of polyclonal and monoclonal antibodies against *Lawsonia intracellularis*. J. Vet. Diagn. Invest. 15(5):438-446. <https://dx.doi.org/10.1177/104063870301500506> <PMid:14535543>

Guedes R.M.C. & Gebhart C.J. 2004. Progression of *L. intracellularis* infection and mucosal immune response in pigs. Proceedings of the International Pig Veterinary Society, 18th International Pig Veterinary Society, Congress Hamburg, Germany, p.250.

Guedes R.M.C. 2007. Diarreias e enterites em leitões de recria e terminação. Suinocultura, Proceedings of the AveSui Regiões, VII Seminário de Aves e Suínos, Belo Horizonte, MG, p.39-43.

Guedes R.M.C., Gebhart C.J., Armbruster G.A. & Roggow B.D. 2002d. Serologic follow-up of a repopulated swine herd after an outbreak of proliferative hemorrhagic enteropathy. Can. J. Vet. Res. 66(4):258-263. <PMid:12418781>

Guedes R.M.C., Gebhart C.J., Deen J. & Winkelman N.L. 2002b. Validation of an immunoperoxidase monolayer assay as a serologic test for porcine proliferative enteropathy. J. Vet. Diagn. Invest. 14(6):528-530. <https://dx.doi.org/10.1177/104063870201400618> <PMid:12423042>

Guedes R.M.C., Gebhart C.J., Winkelman N.L. & Mackie-Nuss R.A. 2002c. A comparative study of an indirect fluorescent antibody test and an immunoperoxidase monolayer assay for the diagnosis of porcine proliferative enteropathy. J. Vet. Diagn. Invest. 14(5):420-423. <https://dx.doi.org/10.1177/104063870201400512> <PMid:12296397>

Guedes R.M.C., Gebhart C.J., Winkelman N.L., Mackie-Nuss R.A.C., Marsteller T.A. & Deen J. 2002a. Comparison of different methods for diagnosis of Porcine Proliferative Enteropathy. Can. J. Vet. Res. 66(2):99-107. <PMid:11989741>

Jones G.F., Ward G.E., Murtaugh M.P., Lin G. & Gebhart C.J. 1993. Enhanced detection of intracellular organism of swine proliferative enteritis, Ileal symbiont intracellularis, in faeces by polymerase chain reaction. J. Clin. Microbiol. 31(10):2611-2615. <https://dx.doi.org/10.1128/JCM.31.10.2611-2615.1993> <PMid:8253956>

Jones T.H. & Muehlhauser V. 2014. Effect of handling and storage conditions and stabilizing agent on the recovery of viral RNA from oral fluid of pigs. J. Virol. Methods 198:26-31. <https://dx.doi.org/10.1016/j.jviromet.2013.12.011> <PMid:24384096>

Kittawornrat A., Engle M., Panyasing Y., Olsen C., Schwartz K., Rice, A., Lizano S., Wang C. & Zimmerman J. 2013. Kinetics of the porcine reproductive and respiratory syndrome virus (PRRSV) humoral immune response in swine serum and oral fluids collected from individual boars. BMC Vet. Res. 9:61. <https://dx.doi.org/10.1186/1746-6148-9-61> <PMid:23537175>

Kittawornrat A., Panyasing Y., Goodell C., Wang C., Gauger P., Harmon K., Rauh R., Desfresne L., Levis I. & Zimmerman J. 2014. Porcine reproductive and respiratory syndrome virus (PRRSV) surveillance using pre-weaning

oral fluid samples detects circulation of wild-type PRRSV. Vet. Microbiol. 168(2/4):331-339. <https://dx.doi.org/10.1016/j.vetmic.2013.11.035> <PMid:24393634>

Kittawornrat A., Prickett J., Wang C., Olsen C., Irwin C., Panyasing Y., Ballagi A., Rice A., Main R., Johnson J., Rademacher C., Hoogland M., Rowland R. & Zimmerman J. 2012. Detection of porcine reproductive and respiratory syndrome virus (PRRSV) antibodies in oral fluid specimens using a commercial PRRSV serum antibody enzyme-linked immunosorbent assay. J. Vet. Diagn. Invest. 24(2):262-269. <https://dx.doi.org/10.1177/1040638711435679> <PMid:22379043>

Kroll J.J., Roof M.B., Hoffman L.J., Dickson J.S. & Harris D.L. 2005 Proliferative enteropathy: a global enteric disease of pigs caused by *Lawsonia intracellularis*. Anim. Health Res. Rev. 6(2):173-197. <https://dx.doi.org/10.1079/ahr2005109> <PMid:16583781>

McOrist S., Gebhart C.J., Boid R. & Barns S.M. 1995. Characterization of *Lawsonia intracellularis* gen. nov., sp. nov., the obligately intracellular bacterium of porcine proliferative enteropathy. Int. J. Syst. Bacteriol. 45(4):820-825. <https://dx.doi.org/10.1099/00207713-45-4-820> <PMid:7547305>

Mur L., Gallardo C., Soler A., Zimmermman J., Pelayo V., Nieto R., Sánchez-Vizcaíno J.M. & Arias M. 2013 Potential use of oral fluid samples for serological diagnosis of African swine fever. Vet. Microbiol. 165(1/2):135-139. <https://dx.doi.org/10.1016/j.vetmic.2012.12.034> <PMid:23374655>

Nogueira M.G., Collins A.M., Donahoo M. & Emery D. 2013. Immunological responses to vaccination following experimental *Lawsonia intracellularis* virulent challenge in pigs. Vet. Microbiol. 164(1/2):131-138. <https://dx.doi.org/10.1016/j.vetmic.2013.02.004> <PMid:23478250>

Olsen C., Karriker L., Wang C., Binjawadagi B., Renukaradhya G., Kittawornrat A., Lizano S., Coetzee J., Main R., Meiszberg A., Panyasing Y. & Zimmerman J. 2013. Effect of collection material and sample processing on pig oral fluid testing results. Vet. J. 198(1):158-163. <https://dx.doi.org/10.1016/j.tvjl.2013.06.014> <PMid:24011474>

Ouyang K., Binjawadagi B., Kittawornrat A., Olsen C., Hiremath J., Elkalifa N., Schleappi R., Wu J., Zimmerman J.J. & Renukaradhya G. 2013 Development and validation of assay to detect porcine reproductive and respiratory syndrome virus-specific neutralizing antibody titers in pig oral fluid samples. Clin. Vaccine Immunol. 20(8):1305-1313. <https://dx.doi.org/10.1128/CVI.00276-13> <PMid:23784856>

Pacheco J.M., Butler J.E., Jew J., Ferman G.S., Zhu J. & Golde W.T. 2010. Iga antibody response of swine to Foot-and-Mouth Disease virus infection and vaccination. Clin. Vaccine Immunol. 17(4):550-558. <https://dx.doi.org/10.1128/CVI.00429-09> <PMid:20107003>

Panyasing Y., Goodell C.K., Giménez-Lirola L., Kittawornrat A., Wang C., Schwartz K.J. & Zimmerman J.J. 2013. Kinetics of influenza A virus nucleoprotein antibody IgM, IgA, and IgG in serum and oral fluid specimens from pigs infected under experimental conditions. Vaccine 31(52):6210-6215. <https://dx.doi.org/10.1016/j.vaccine.2013.10.040> <PMid:24200976>

Panyasing Y., Goodell C.K., Wang C., Kittawornrat A., Prickett J.R., Schwartz K.J., Ballagi A., Lizano S. & Zimmerman J.J. 2014. Detection of influenza A virus nucleoprotein antibodies in oral fluid specimens from pigs infected under experimental conditions using a blocking ELISA. Transbound. Emerg. Dis. 61(2):177-184. <https://dx.doi.org/10.1111/tbed.12019> <PMid:23046061>

Prickett J., Simer R., Christopher-Hennings J., Yoon K.J., Evans R.B. & Zimmerman J.J. 2008. Detection of Porcine reproductive and respiratory syndrome virus infection in porcine oral fluid samples: a longitudinal study under experimental conditions. J. Vet. Diagn. Invest. 20(2):156-163. <https://dx.doi.org/10.1177/104063870802000203> <PMid:18319427>

Prickett J.R. & Zimmerman J.J. 2010. The development of oral fluid-based diagnostics and applications in veterinary medicine. Anim. Health Res. Rev. 11(2):207-216. <https://dx.doi.org/10.1017/S1466252310000010> <PMid:20202287>

Prickett J.R., Cutler S., Kinyon J.M., Naberhaus N., Stensland W.R., Yoon K.-J. & Zimmerman J.J. 2010. Stability of porcine reproductive and respiratory syndrome virus and antibody in swine oral fluid. J. Swine Health Prod. 18(4):187-195.

Prickett J.R., Johnson J., Murtaugh M.P., Puvanendiran S., Wang C., Zimmerman J.J. & Opriessnig T. 2011. Prolonged detection of PCV2 and anti-PCV2 antibody in oral fluids following experimental inoculation. Transbound. Emerg. Dis. 58(2):121-127. <https://dx.doi.org/10.1111/j.1865-1682.2010.01189.x> <PMid:21223532>

Vannucci F.A., Pusterla N., Mapes S.M. & Gebhart C. 2012. Evidence of host adaptation in *Lawsonia intracellularis* infections. Vet. Res. 43(1):53. <https://dx.doi.org/10.1186/1297-9716-43-53> <PMid:22715937>

Vosloo W., Morris J., Davis A., Giles M., Wang J., Nguyen H.T., Kim P.V., Quach N.V., Le P.T., Nguyen P.H., Dang H., Tran H.X., Vu P.P., Hung V.V., Le Q.T., Tran T.M., Mai T.M., Le Q.T. & Singanallur N.B. 2015. Collection of oral fluids using cotton ropes as a sampling method to detect Foot-and-Mouth Disease virus infection in pigs. Transbound. Emerg. Dis. 62(5):e71-75. <https://dx.doi.org/10.1111/tbed.12196> <PMid:24325543>

Walter D., Gebhart C., Kroll J., Holck J.T. & Chittick W. 2004. Serologic profiling and vaccination timing for *Lawsonia intracellularis*. J. Swine Health Prod. 12(6):310-313.

PESQUISA VETERINÁRIA BRASILEIRA
Brazilian Journal of Veterinary Research
ISSN 0100-736X (Print)
ISSN 1678-5150 (Online)

Pesq. Vet. Bras. 40(12):977-984, December 2020
DOI: 10.1590/1678-5150-PVB-6731

Original Article
Livestock Diseases
BY-NC

Indirect ELISA (iELISA) standardization for the diagnosis of bovine enzootic leukosis[1]

Cláudia F. Resende[2], Grazielle C. F. Galinari[2], Raphael M. Victor[3], Telissa C. Kassar[2], Thiago L.M. Arcebispo[4], Emília Delarmelina[2], Romulo C. Leite[2] and Jenner K.P. Reis[2]*

ABSTRACT.- Resende C.F., Galinari G.C.F., Victor R.M., Kassar T.C., Arcebispo T.L.M., Delarmelina E., Leite R.C. & Reis J.K.P. 2020. **Indirect ELISA (iELISA) standardization for the diagnosis of bovine enzootic leucosis**. *Pesquisa Veterinária Brasileira 40(12):977-984*. Laboratório de Retroviroses, Departamento de Medicina Veterinária Preventiva, Escola de Veterinária, Universidade Federal Minas Gerais, Campus Pampulha, Av. Antonio Carlos 6627, Belo Horizonte, MG 31270-901, Brazil. E-mail: jenner@ufmg.br

Enzootic bovine leukosis (EBL) is an infectious disease caused by bovine leukemia virus (BLV) that affects cattle worldwide. Agar gel immunodiffusion (AGID) was the reference test for EBL diagnosis for many years, but enzyme-linked immunosorbent assay (ELISA) showed higher sensitivity, was faster to perform, and resulted in an objective reading. However, the importation of ELISA kits is lengthy and expensive, and currently, no AGID kits are available in Brazil. The aim of this work was to standardize an indirect ELISA (iELISA) for EBL diagnosis using BLV antigens produced in *Tadarida brasiliensis* lung (Tb1Lu) cells, which are Bovine viral diarrhea virus (BVDV) free, unlike fetal lamb kidney (FLK) cells, currently used for this purpose. Following standardization, iELISA results were compared with those obtained by AGID and the commercial Chekit Leucose-Serum ELISA. Compared to AGID, iELISA had 94,44% sensitivity, 75.68% specificity, 79.10% positive predictive value (PPV) and 93.30% negative predictive value (NPV), with 84% concordance and a Kappa index of 0.699. Compared to the Chekit Leucose-Serum ELISA, iELISA showed 92.60% sensitivity, 87.09% specificity, 90.27% PPV and 90,00% NPV, with 90.27% concordance and a Kappa index of 0.801. Taking into account the high agreement with the traditional tests and the absence of non-specific reactions with BVDV, the developed assay could be used as diagnostic method to control EBL in Brazil.

INDEX TERMS: iELISA, bovine, enzyme-linked immunosorbent assay, Enzootic bovine leukosis, diagnosis, control, cattle.

RESUMO.- [**Padronização de um ELISA indireto (iELISA) para diagnóstico da leucose enzoótica bovina.**] A leucose enzoótica bovina (LEB) é uma doença infecciosa natural dos bovinos com distribuição mundial causada pelo "bovine leukemia virus" (BLV). A imunodifusão em gel de ágar (IDGA) foi considerada por muitos anos o teste de eleição, porém ensaios imunoenzimáticos (ELISA) apresentam sensibilidade mais elevada e leitura mais rápida e objetiva. No entanto, a importação de *kits* de ELISA é um processo dispendioso e demorado, e atualmente não há kits de IDGA comercialmente disponíveis no Brasil. Desta forma, o objetivo deste trabalho foi padronizar um ELISA indireto (iELISA) para diagnóstico da LEB utilizando antígenos produzidos a partir do cultivo do BLV em linhagem celular *Tadarida brasiliensis "*lung" (Tb1Lu) livre de "bovine viral diarrhea virus" (BVDV), diferentemente do que acontece com as linhagens "fetal lamb kidney" (FLK) atualmente utilizadas na produção desses antígenos para uso em ensaios sorológicos. Após a padronização do iELISA, os resultados foram comparados com aqueles obtidos por IDGA e pelo ELISA comercial "Chekit Leucose-Serum". Comparado ao IDGA, o iELISA apresentou 94,44% de sensibilidade, 75,68% de especificidade, valor preditivo positivo (VPP)

[1] Received on September 11, 2020.
Accepted for publication on September 28, 2020.
[2] Graduate Program in Animal Science, Laboratório de Retroviroses, Departamento de Medicina Veterinária Preventiva, Escola de Veterinária, Universidade Federal Minas Gerais (UFMG), Campus Pampulha, Av. Antônio Carlos 6627, Belo Horizonte, MG 31270-901, Brazil. *Corresponding author: jenner@ufmg.br
[3] Ministério da Agricultura Pecuária e Abastecimento (MAPA), Manaus, AM, Brazil.
[4] Ministério da Agricultura Pecuária e Abastecimento (MAPA), Brasília, DF, Brazil.

de 79,1% e valor preditivo negativo (VPN) de 93,3%, com concordância entre os testes de 84% e o índice Kappa 0,699. Quando comparado ao ELISA "Chekit Leucose-Serum", o iELISA apresentou sensibilidade de 92,6%, especificidade de 87,09%, VPP de 90,27% e VPN de 90%, com concordância de 90,27% e o índice Kappa 0,801. Portanto, devido à alta concordância com os testes tradicionais e ausência da ocorrência de reações inespecíficas com BVDV, o ensaio desenvolvido pode ser utilizado como ferramenta diagnóstica para o controle da LEB no Brasil.

TERMOS DE INDEXAÇÃO: iELISA, bovinos, ensaio de imunoadsorção enzimática, leucose enzoótica bovina, diagnóstico, controle.

INTRODUCTION

Enzootic bovine leukosis (EBL) is an infectious and contagious disease of cattle caused by bovine leukemia virus (BLV), a B-cell lymphotropic virus of the genus *Deltaretrovirus*, family Retroviridae. The disease is characterized by a long incubation period, with 1-5% of infected animals developing lymphosarcoma, an often-fatal clinical form of the disease, while approximately 30% develop persistent lymphocytosis. However, the inapparent form is the most frequent, with the asymptomatic animal being an important source of BLV transmission (Camargos et al. 2004, De Oliveira et al. 2016).

The disease is debilitating in animals that develop lymphosarcoma, leading to death within weeks or months after the onset of clinical manifestations. BLV infection compromises the immune response of the host, predisposing the host to secondary infections, leading to earlier animal disposal and increasing costs of production due to carcass condemnation, veterinary services, medication and treatment of sick animals (Trainin & Brenner 2005, OIE 2012, Leite et al. 2013). The dairy industry is directly affected, both by the lower survival of EBL positive cows and by decreases in milk production, especially among animals with persistent lymphocytosis (Nekouei et al. 2016). Rajão et al. (2014) estimates that in Brazil, BLV infection results in losses higher than 100 dollars per cow per lactation, which represents a significant economic loss, especially for small producers. There is also economic loss related to restrictions in exportation. Some countries, especially those in the European Union, have a ban on BLV-infected animals and biological products of animal origin, such as semen and embryos (Larsen et al. 2013). In addition to its economic relevance, in recent years BLV has been studied in relation to human health. There is some evidence that suggest BLV infection in women that is likely associated with the development of breast cancer (Buehring et al. 2014, 2017, Khalilian et al. 2019).

The prevalence of BLV infection in dairy herds may reach 60-90% in many countries. Serological surveys revealed that EBL is endemic, with high prevalence rates in North America, South America, Africa, Asia and Australia. In Brazil, it has been detected in several states, with serological prevalence varying from 8.9% to 53.2% (Romero & Rowe 1981, Molnár et al. 1999, Camargos et al. 2002, 2004, Carneiro et al. 2003, Megid et al. 2003, Poletto et al. 2004). Identification and isolation of seropositive animals is necessary to control virus dissemination, and serological tests should be performed periodically for this purpose. The gp51 glycoprotein of the viral envelope is highly immunogenic and therefore widely used in serological diagnostic tests. The protein p24 is also used since it is the main viral capsid protein and induces a strong immune response (Troiano et al. 2013, De Oliveira et al. 2016).

For many years the agar gel immunodiffusion (AGID) test, used for individual serum or plasma samples, was the test of choice for the diagnosis of EBL, especially for its practicality and low cost. However, despite its easy applicability, it failed to detect low titers of antibodies, especially in recent infections or in animals with a reduced antibody response, which implied the occurrence of false-negative results. In recent years, enzyme-linked immunosorbent assay (ELISA) tests have been developed for pooled use or in individual serum and milk samples. When compared to the AGID, these tests have higher sensitivity and an objective reading, allowing the testing of a large number of samples simultaneously, with results in a few hours (OIE 2012, Troiano et al. 2013, Bai et al. 2019).

The AGID is still the most used test for the diagnosis of EBL in Brazil, but there is no national commercial test available and international tests use antigen produced in fetal lamb kidney (FLK) cells persistently infected with BLV. However, it is known that this cell line is susceptible to Bovine viral diarrhea virus (BVDV) contamination, which may negatively influence the specificity of the test due to potential non-specific reactions (Camargos et al. 2007). In 1995, BLV-free bovine herds were vaccinated against BVDV and subsequently an increasing number of positive results for this disease were detected by ELISA, but analyzes of these reactions by other serological tests and PCR provided negative results for EBL. Thus, false positive results have been associated with cross-reactivity against anti-BVDV antibodies induced by vaccination (Beier & Conraths 1996 apud Beier et al. 2004).

A BVDV-free and BLV-permissive cell line would be an alternative for antigen production for diagnostic use, as it eliminates the likely occurrence of non-specific reactions. Previous studies have shown that *Tadarida brasiliensis* lung (TB1Lu) bat cells are highly permissive to BLV, with a progressively increased production of viral particles, reaching high levels of replication after a short culture period, (Graves & Ferrer 1976, Patrascu 1988, Suzuki et al. 2018). In addition, these cells are also resistant to BVDV infection according to the American Type Culture Collection manual (ATCC® CCL-88™), presenting a suitable source for the research and production of virus-related antigens. Thus, the aim of the present study was to develop an indirect ELISA that used antigen produced in a Tb1Lu cell line infected with a Brazilian BLV isolate to be used as a diagnostic tool, in addition to AGID, for the control of EBL.

MATERIALS AND METHODS

Bovine serum. Seventy-three serum samples of same-farmed calves, kindly provided by Professor Elias Jorge Facury Filho from the "Universidade Federal de Minas Gerais" (UFMG), were collected before (n=32) and after (n=41) colostrum suckling. Considering the high prevalence of EBL in Brazilian cattle and the difficulty of obtaining samples from a BLV-free herd, we adopted the strategy of obtaining serum from non-colostrum-fed (NCF) calves to be used as a negative control. All procedures for handling and collecting animal samples were approved by the Ethics Committee on the Use of Animals of the UFMG under protocol number 151/2015.

AGID. Serum samples were tested using the AGID test, as a reference for this standardization, and for comparison purposes. A commercial AGID kit for enzootic bovine leucosis diagnosis (TECPAR, Brazil) was used for anti-gp51 antibody detection, using

crude antigen produced in a FLK cell line persistently infected with bovine leukemia virus (BLV), following the manufacturer's recommendations. The reading was performed after 72 hours of incubation at 25°C (room temperature-RT).

Chekit Leucose-Serum ELISA (IDEXX Laboratories, USA). All samples were tested using the commercial ELISA (Chekit Leucose-Serum), an indirect ELISA using microplates coated with inactivated BLV crude antigen. Tests were performed following the manufacturer's recommendations.

Virus. The Tb1Lu cell line (ATCC® CCL-88™ - American Type Culture Collection, USA), pre-infected with a Brazilian BLV field isolate (GenBank accession number: KU255419) was used. To guarantee the absence of BVDV, the cells, fetal bovine serum (FBS), trypsin and Minimum Essential Medium Eagle (MEM) (Sigma, USA) were previously tested by polymerase chain reaction (PCR) at the "Laboratório Federal de Defesa Agropecuária" (LFDA), and were all negative for this virus. Cultivation was carried out in MEM containing 1% penicillin/streptomycin, 0.5% fungizon, and 25mM HEPES, supplemented with 5% FBS. The cells were incubated in a 5% CO_2 atmosphere at 37°C until reaching approximately 80% confluence, when the cells were subcultured. At the time of each passage, the medium supernatant was collected and stored at -20°C for virus purification.

BLV antigen (BLV-Ag) production. Supernatants and monolayers of the cell cultures were subjected to three cycles of freezing and thawing for cell disruption and release of viral particles and proteins. The cell suspension was centrifuged at 925 × *g* for 30 min at 4°C, the supernatant was collected and 0.318g of ammonium sulfate was added to each 1mL of supernatant, which was stirred for 1 hour at 4°C. Then, centrifugation was performed again at 4000 × *g* for 30 min at 4°C. The precipitate was dissolved in a small volume of phosphate buffered saline (PBS) and transferred to a dialysis membrane. The antigen preparation was dialyzed against 1× PBS, at a volume of 100× the membrane-contained volume, at 4°C, stirring. The first dialysis lasted for 12 to 14 hours and the second dialysis, for approximately four hours. After this procedure, the dialysis membrane was covered with polyethylene glycol (PEG 6000) at 4°C to concentrate the antigen. The concentrated antigen solution was then transferred to a microtube and 10% Triton X-100 and 1% protease inhibitor (Sigma, USA) was added. The total protein concentration of the final antigen preparation was estimated using the Total Protein Monoreagent Kit (Bioclin, Brazil), following the manufacturer's recommendations. The final antigenic product was stored at -20°C until use.

Polyacrylamide gel electrophoresis. For disaggregation and analysis of protein content, the antigen produced was subjected to polyacrylamide gel electrophoresis using a 10% Amersham™ ECL™ Gel (GE Healtcare Life Sciences, USA), according to the manufacturer's recommendations. After electrophoresis, the Amersham™ ECL™ Gel was stained with Coomassie Blue Brilliant R-350.

Indirect ELISA (iELISA) standardization. Polystyrene 96-well plates (Maxsorb, Nunc, Hampton, NH, USA) were coated with 0.5ng or 1.0ng per well BLV-Ag produced in Tb1Lu cells, diluted in 0.05M carbonate buffer pH 9.6 (containing 0.015M sodium carbonate and 0.035M sodium bicarbonate); 100µL diluted BLV-Ag was added per well and incubated overnight at 4°C. The next day, the plate was washed twice with 200µL per well 1× PBS with 0.05% Tween 20 (PBST), followed by incubation for 1 hour at RT with 100µL PBST containing 5% skim milk to block non-specific binding sites, and three washes with 200µL PBST. Then, 100µL serum samples, two-fold serially diluted in PBST with 1% skim milk, were added in duplicate wells and the plate was kept at RT for 1 hour, followed by three washes with PBST. Two positive controls (a pool of positive samples and one colostrum-fed calf serum) and two negative controls (BFS and one NCF calf serum) were added to each plate. After the washes, 100µL anti-bovine IgG peroxidase conjugated (Sigma), tested at dilutions of 1:5000 and 1:7500, in PBST with 1% skim milk, was added per well and the plate was incubated at RT for 1 hour. Three further washes with 200µL PBST were performed, followed by incubation with 100µL per well 0.5mg/mL o-phenylenediamine (OPD) substrate, diluted in acid buffer pH 5.0 (citric acid 0.1M, sodium phosphate 0.2M and 0.003% of 30 volumes hydrogen peroxide) at RT for 20 min, in the dark. The reaction was stopped with 40µL of 1M sulfuric acid in each well. Plates were read in an ELISA reader (Thermo Plate TP-Reader) at an absorbance of 492nm. The cut-off point was calculated using the MedCalc program, version 13.0.0.0 (MedCalc Software, Mariakerke, Belgium) based on the receiver operating characteristic (ROC) curve analyses.

Statistical analysis. A contingency table (2×2) was used to compare tests. The positive predictive value (PPV), negative predictive value (NPV), sensitivity, and specificity values for AGID and the Chekit Leucose-serum ELISA, the concordance between tests and the Kappa index were evaluated.

RESULTS

Antigen production (BLV-Ag)

The BLV-Ag produced in this study had a total protein concentration estimated at 6.19µg/µL. To verify the presence of viral proteins, BLV-Ag was separated by sodium dodecyl sulfate-polyacrylamide gel electrophoresis (SDS-PAGE). A unique band corresponding to 51kDa was detected in the gel, indicating the presence of the viral envelope glycoprotein gp51 (Fig.1).

iELISA and comparative analysis with commercial tests

The standardized iELISA was performed under the following conditions: 1.0µg BLV-Ag per well, a serum dilution of 1:25 and conjugate dilution of 1:5000. Under these conditions, a higher discrimination between positive and negative sera was obtained, based on the AGID results, used as reference test. Figure 2 shows the relationship between the optical density (OD), frequency, and the distribution of 36 (49.31%) positive and 37 (50.69%) negative sera in AGID. Twenty-seven negative sera by AGID and two positive sera had an OD lower than 0.100; when the OD values were between 0.100 and 0.150, the number of positives in AGID increased to 12, while the amount of negatives dropped to six; readings above 0.200 were all positive.

The ROC curve analysis using the field samples indicated a cutoff point of an OD equal to 0.104 (Fig.3A). Thus, the field samples were considered positive when they presented an OD above 0.104. The diagnostic capacity of the test was measured by assessing its sensitivity and specificity for AGID, which were 94.44% and 75.68%, respectively, with a 95% confidence level. The PPV was 79.1% and the NPV was 93.3%. The agreement between tests was 84% and the Fleiss' Kappa index was 0.699, classified as substantial (0.61-0.80) (Lage et al. 2016) (Table 1).

Of the 73 serum samples tested, 43 (58.9%) were positive in the iELISA, of which, nine (12.32%) were negative by AGID. Thirty samples (41.09%) were considered negative by iELISA, two of which (2.73%) were positive by AGID (Fig.3B).

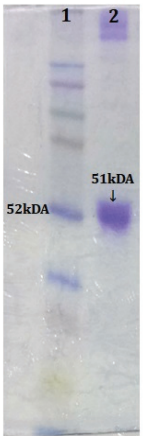
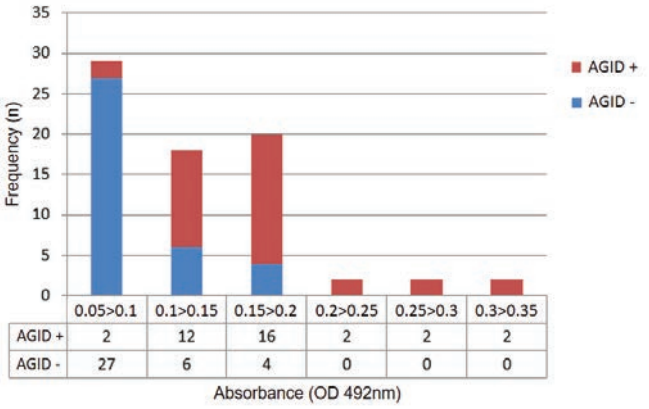


Fig.1. Sodium dodecyl sulfate-polyacrylamide gel electrophoresis of the bovine leukemia virus antigen (BLV-Ag) stained using Coomassie Blue Brilliant R350 *Tadarida brasiliensis* lung (Tb1Lu) cells. Molecular weight marker (column 1), BLV-Ag preparation (column 2).



	0.05>0.1	0.1>0.15	0.15>0.2	0.2>0.25	0.25>0.3	0.3>0.35
AGID +	2	12	16	2	2	2
AGID -	27	6	4	0	0	0

Fig.2. Sera distribution by optical density (OD) in the indirect enzyme-linked immunosorbent assay (iELISA) compared to agar gel immunodiffusion (AGID).

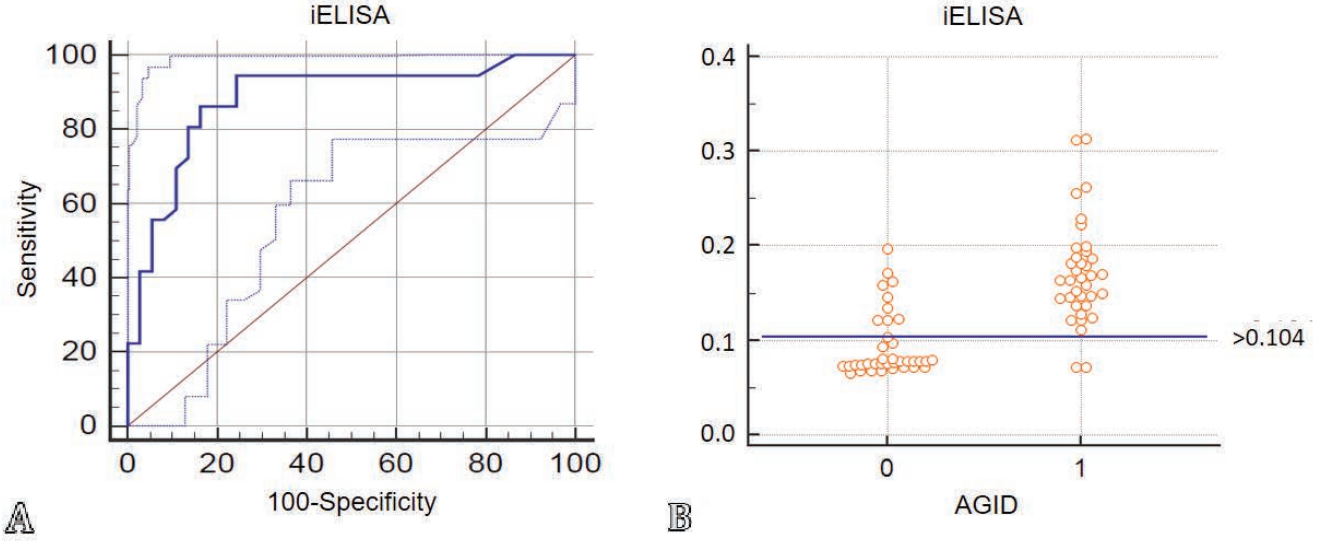


Fig.3. Determination of the cut-off point of the indirect enzyme-linked immunosorbent assay (iELISA) with reference to agar gel immunodiffusion (AGID). (**A**) Receiver operating characteristic (ROC) curve analysis based on results obtained from tested field samples. The area under the curve is calculated as 0.883, with a 95% confidence interval. (**B**) Comparison of results from the sera of 73 calves tested by iELISA and AGID. Negative samples by AGID (0), positive samples by AGID (1).

Figure 4 shows the comparison of the results of the 72 samples tested by iELISA and the Chekit ELISA. For analysis of the sensitivity, specificity, concordance and kappa values, the sample with an undetermined result by the Chekit ELISA was excluded. Thus, iELISA showed a sensitivity of 92.6% and a specificity of 87.09% compared to the Chekit ELISA, with a PPV of 90.27%, and a NPV of 90%. The concordance between the tests was 90.27% and the Kappa value was 0.801 (Table 2).

Overall analysis of the results

As expected, most colostrum-fed (CF) calf serum samples were positive and the NCF calves were negative in all three assays. However, a small number of CF calves were diagnosed as negative and NCF calves as positive (Table 3). There was a disagreement between 11 (15.06%) serum samples; one sample positive by iELISA had a negative result by AGID and was undetermined using the Chekit ELISA. Five samples, two of non-colostrum fed animals, were positive by iELISA and negative in the other two tests. Unexpectedly, one NCF serum was positive by AGID and negative by ELISA.

DISCUSSION

Currently AGID is the only test used for EBL diagnosis in Brazil and in many other countries. Although there is no national kit available, this technique continues to be the most practical and economical, and it has been adopted by most governments as the official test used in importation processes. However, due to the high prevalence of bovine leukemia virus (BLV) in Brazilian herds, it is not feasible to use it in epidemiological studies and control programs, since a large number of samples have to be tested (Camargos et al. 2007, Troiano et al. 2013). For many years, only one manufacturer produced the AGID

kit for EBL testing in Brazil, even though it was produced in an insufficient amount to supply the full demand for tests in the country, since the antigen used was dependent on viral cultures in cell lines, a time consuming and complex production process when performed at a large scale, as required for the AGID. Aditionally the production of this kit has been discontinued. According to our estimate for the AGID test, 25µL of pure antigen is required for three samples each, while in the iELISA, the same amount of antigen was sufficient for 96 samples simultaneously. There are no national commercial ELISA kits available in Brazil and the importation of these kits is an expensive and often time-consuming process, making it an unfeasible method to be used at a large scale. Furthermore, many of these assays utilize antigen preparations from cultures of persistently BLV-infected FLK cells, which are susceptible to BVDV contamination. In studies by Oliveira et al. (2013), 88 samples belonging to 32 cell cultures of different species, obtained from eight laboratories, were tested for different contaminants. Of the 88 samples, 21 (23.9%) were positive for BVDV by PCR, including three FLK samples from the three different batches analyzed. To minimize nonspecific reactions and to increase the specificity of the test, a BVDV-free Tb1Lu cell line was infected with BLV and was used to produce antigen for the standardization of the iELISA, which proved to be an efficient alternative for this purpose.

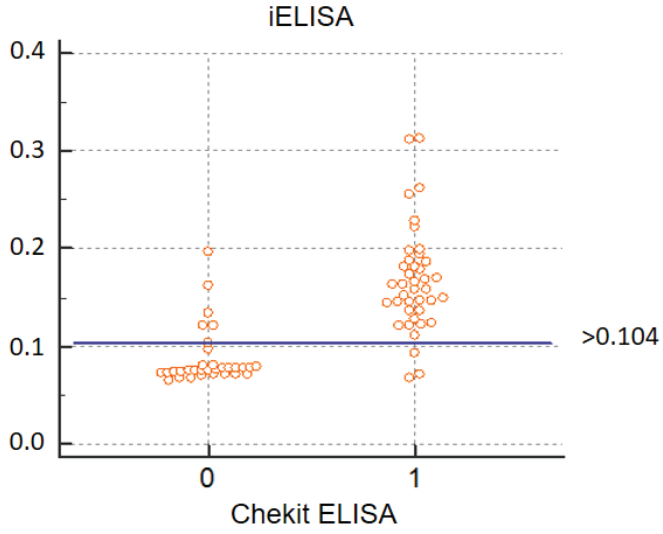


Fig.4. Comparison of the results of 72 samples tested by indirect enzyme-linked immunosorbent assay (iELISA) and the Chekit ELISA. Negative samples by Chekit ELISA (0), positive samples by Chekit ELISA (1).

Viral protein gp51 is the main partially-purified protein in the antigen preparation used in this work, as determined by SDS-PAGE (Fig.1). BLV-infected animals develop a humoral response characterized by the production of high titers of antibodies, especially against the p24 and gp51 proteins. This justifies the widespread use of these antigens in serological diagnostic tests, mainly gp51, considering that antibodies against it reach higher titers and are detected earlier than those produced against p24 (Gutiérrez et al, 2009).

BLV appears to exhibit less genetic variability when compared to other retroviruses; however, phylogenetic studies of the *env* gene of strains isolated from several countries have

Table 1. Comparative analysis between the iELISA and AGID tests on 73 bovine samples

AGID	iELISA		
	Positive	Negative	Total
Positive	34	2	36
Negative	9	28	37
Total	43	30	73
Sens.%		94.44	
Spec.%		75.68	
PPV%		79.1	
NPV%		93.3	
Agree.%		84	
Kappa		0.699	

iELISA = indirect enzyme-linked immunosorbent assay, Sens. = sensitivity, Spe. = specificity, PPV = positive predictive value, NPV = negative predictive value, Agree. = agreement, Kappa = Fleiss' Kappa index, AGID = agar gel immunodiffusion.

Table 2. Comparative analysis between the iELISA and Chekit ELISA tests on 72 bovine samples

Chekit ELISA	iELISA		
	Positive	Negative	Total
Positive	38	3	41
Negative	4	27	31
Total	42	30	72
Sens.%		92.6	
Spec.%		87.09	
PPV%		90.47	
NPV%		90.0	
Agree.%		90.27	
Kappa		0.801	

iELISA = indirect enzyme-linked immunosorbent assay, Sens. = sensitivity, Spec. = specificity, PPV = positive predictive value, NPV = negative predictive value, Agree. = agreement, Kappa = Fleiss' Kappa index.

Table 3. Relation of the results obtained in the AGID, iELISA and commercial Chekit ELISA tests of serum samples from CF and NCF calves

Sera	AGID		iELISA		ELISA Chekit	
	Positive	Negative	Positive	Negative	Positive	Negative
CF	34 (46.6%)	7 (9.6%)	40 (54.8%)	1 (1.4%)	37 (51.4%)	3 (4.2%)
NCF	2 (2.7%)	30 (41.1%)	3 (4.1%)	29 (39.7%)	3 (4.2%)	29 (40.2%)
Total	73		73		72	

AGID = agar gel immunodiffusion, iELISA = indirect enzyme-linked immunosorbent assay, CF = colostrum-fed, NCF = non-colostrum-fed.

shown that this virus is classified into, at least, ten distinct genotypes according to variations in gp51. These variations are preferentially located in the conformational epitopes F, G and H of the gp51 protein (Camargos et al. 2004, Gautam et al. 2018). These epitopes induced the production of neutralizing antibodies and it was speculated that they may influence the antigenic characteristics of the virus and reduce the sensitivity of the diagnostic methods, especially serological methods. The use of antigen from a BLV Brazilian isolate for indirect ELISA may be an advantage, as the variability among strains is associated with different geographic regions. In addition, glycosylation sites, important for cell recognition processes, such as virus binding to cell receptors and cell-cell fusion, are highly conserved among the different BLV strains, maintaining the essential functions of the protein (Camargos et al. 2004, Polat et al. 2016). However, to better assess this interference, it would be necessary to test a larger number of samples from different geographic origins.

The iELISA developed in this study had high sensitivity (94.44%) and considerable specificity (75.68%), identifying nine positive results more than AGID. This could be explained by the increased sensitivity related to the use of a BLV Brazilian strain or by a low titer of antibodies in the serum of these animals that was undetectable by the AGID. Additionally, it could have even been a reading error, as the reading of these test results are subjective and susceptible to misinterpretation, which may compromise the diagnostic accuracy and consequently, impair the efficiency of control programs. Furthermore, four (5.47%) samples with a weak positive result in AGID showed a high OD reading in the iELISA, and thus were classified as positive. The ability of our iELISA to detect positive animals is one of the main advantages of the test and is in agreement with other ELISAs previously described in the literature (Troiano et al. 2013, Larsen et al. 2017). Weak reactions to AGID that are positive in the iELISA are an important intrinsic feature of the test, since this type of reaction is more difficult to detect and can easily go unnoticed due to reader errors in the AGID.

Unexpectedly, two samples collected from NCF animals were positive by AGID and negative in the iELISA. These results were considered as false positives in AGID. It was also hypothesized that these calves were born from infected cows and BLV was transmitted during pregnancy or childbirth. Animals fed colostrum and negative by AGID, were positive in at least one of the ELISAs, which likely indicated a false negative result of the AGID test in these cases.

Compared to the Chekit Leucose Serum ELISA, the iELISA showed a higher sensitivity and classified one sample as positive that was undetermined by the commercial test. This demonstrated that the developed assay had a similar performance to the commercial assay and could be used as an alternative to the Chekit Leucose-Serum ELISA, with the advantage of being more economically feasible and accessible to producers and laboratories.

EBL control is difficult due to its wide distribution, slow evolution, and the presence of a large number of asymptomatic animals that go unnoticed by breeders. In addition, the lack of knowledge among producers and technicians on the real importance of the disease as a source of damage contributes to the spread of the virus. In the United States, where the low risk of tumor development is not seen as a reason to control the spread of the virus, there are no efforts to do appropriate controls; thus, the annual economic loss associated with this infection is estimated at 500 million dollars (Ott et al. 2003, Rajão et al. 2014). The identification of positive animals is necessary to control virus propagation; in this perspective, the developed iELISA allows a better understanding of the true serological status of the herds in Brazil and studies of the impact of the disease on productivity, contributing to a better control of EBL.

Another important issue regarding BLV infection and its widespread distribution is its zoonotic potential as a causative agent of breast cancer in humans. Buehring et al. (2003) identified for the first time the presence of antibodies against the viral capsid protein p24 in human serum samples. After this finding, several studies have shown the presence of proviral DNA in the blood (Buehring et al. 2019) and breast tissue of women diagnosed with cancer in the USA, Australia, Iran and Brazil (Buehring et al. 2014, 2017, Khalilian et al. 2019, Schwingel et al. 2019). How virus transmission occurs remains unclear, but it is speculated that it is by ingestion of bovine products, such as milk and meat infected with BLV (Buehring et al. 2015, Cuesta et al. 2018). The genome of BLV has been detected in unpasteurized milk and raw meat, supporting this hypothesis (Olaya-Galán et al. 2017). Considering this information and the high prevalence of BLV in herds, especially dairy cattle, the use of an efficient diagnostic test to detect positive animals is fundamental, not only because of the economic importance of the disease, but also because it represents a possible problem of food safety and public health.

CONCLUSION

The indirect ELISA standardized using gp51 antigen produced in *Tadarida brasiliensis* lung (Tb1Lu) cells infected with a bovine leukemia virus Brazilian isolate presented high sensitivity for the diagnosis of enzootic bovine leukosis (EBL) and could be used as a screening test in serological surveys. To increase the accuracy of EBL diagnosis, we suggest that the iELISA should be used as a screening test, and positive cases should be confirmed in a complementary test, such as AGID, based on its high specificity.

Acknowledgements.- This work was supported by the "Conselho Nacional de Desenvolvimento Científico e Tecnológico" (CNPq, grant no. 481772.2013-8), "Coordenação de Aperfeiçoamento de Pessoal de Nível Superior" (CAPES), "Fundação de Amparo à Pesquisa de Minas Gerais" (FAPEMIG) and "Instituto Nacional de Ciência e Tecnologia" (INCT - Pecuária).

Conflict of interest statement.- The authors declare that they have no competing interests.

REFERENCES

Bai L., Yokoyama K., Watanuki S., Ishizaki H., Takeshima S.N. & Aida Y. 2019. Development of a new recombinant p24 ELISA system for diagnosis of bovine leukemia virus in serum and milk. Arch Virol. 164(1):201-211. <https://dx.doi.org/10.1007/s00705-018-4058-5> <PMid:30311076>

Beier D. & Conraths F.J. 1996. Abkl¨arung fraglicher und falsch-positiver Ergebnisse in einem Testbesteck zum Nachweis von Antik¨orpern gegen das bovine Leukosevirus (BLV) und m¨ogliche Zusammenh¨ange zu BVD/MD-Impfungen. Mitteilungsblatt zur Tierseuchensituation der Bundesrepublik Deutschland, BFAV, I. Halbjahr. (apud Beier D., Riebe R., Blankenstein P., Starick E., Bondzio A. & Marquadt O. 2004. Establishment of a new bovine leukosis virus producing cell line. J. Virol. Methods 121(2):239-246. <https://dx.doi.org/10.1016/j.jviromet.2004.06.017> <PMid:15381362>)

Buehring G.C., DeLaney A., Shen H., Chu D.L., Razavian N., Schwartz D.A., Demkovich Z.R. & Bates M.N. 2019. Bovine leukemia virus discovered in human blood. BMC Infect Dis. 19(1):297. <https://dx.doi.org/10.1186/s12879-019-3891-9> <PMid:30940091>

Buehring G.C., Philpott S.M. & Choi K.Y. 2003. Humans have antibodies reactive with bovine leukemia virus. AIDS Res. Hum. Retroviruses 19(12):1105-1113. <https://dx.doi.org/10.1089/088922203771881202> <PMid:14709247>

Buehring G.C., Shen H., Schwartz D.A. & Lawson J.S. 2017. Bovine leukemia virus linked to breast cancer in Australian women and identified before breast cancer development. Plos One 12(6)e0179367. <https://dx.doi.org/10.1371/journal.pone.0179367> <PMid:28640828>

Buehring G.C., Shen H.M., Jensen H.M., Choi K.Y., Sun D. & Nuovo G. 2014. Bovine leukemia virus DNA in human breast tissue. Emerg. Infect. Dis. 20(5):772-782. <https://dx.doi.org/10.3201/eid2005.131298> <PMid:24750974>

Buehring G.C., Shen H.M., Jensen H.M., Jin D.L., Hudes M. & Block G. 2015. Exposure to bovine leukemia virus is associated with breast cancer: a case-control study. PLoS One 10(9)e0134304. <https://dx.doi.org/10.1371/journal.pone.0134304> <PMid:26332838>

Camargos M.F., Feliziani F., De Giuseppe A. & Lessa L.M. 2007. Evaluation of diagnostic tests to bovine leukemia vírus. Revta Port. Ciênc. Vet. 102(561-562):169-173.

Camargos M.F., Melo C.B., Leite R.C. & Stancek D. 2002. Frequência de soropositividade para a leucose enzoótica bovina em rebanhos de Minas Gerais. Ciênc. Vet. Trop. 5:20-26.

Camargos M.F., Reis J.K.P. & Leite R.C. 2004. Bovine leukemia virus. Virus Rev. Res. 9(1):44-59.

Carneiro P.A.M., Araujo W.P., Birgel E.H. & Souza K.W. 2003. Prevalência da infecção pelo Vírus da Leucose dos Bovinos em rebanhos leiteiros criados no estado do Amazonas, Brasil. Acta Amaz. 33(1):111-125. <https://dx.doi.org/10.1590/1809-4392200331125>

Cuesta L.M., Lendez P.A., Farias M.V.N., Dolcini G.L. & Ceriani M.C. 2018. Can bovine leukemia virus be related to human breast cancer? A review of the evidence. J. Mammary Gland Biol. Neoplasia 23(3):101-107. <https://dx.doi.org/10.1007/s10911-018-9397-z> <PMid:29777406>

De Oliveira C.H.S., Resende C.F., Oliveira C.M., Barbosa J.D., Fonseca Junior A.A., Leite R.C. & Reis J.K.P. 2016. Absence of bovine leukemia virus (BLV) infection in buffaloes from Amazon and southeast region in Brazil. Prev. Vet. Med. 129:9-12. <https://dx.doi.org/10.1016/j.prevetmed.2016.05.002> <PMid:27317318>

Gautam S., Mishra N., Kalaiyarasu S., Jhade S.K. & Sood R. 2018. Molecular characterization of Bovine leukaemia virus (BLV) strains reveals existence of genotype 6 in cattle in India with evidence of a new subgenotype. Transbound. Emerg. Dis. 65(6):1968-1978. <https://dx.doi.org/10.1111/tbed.12979> <PMid:30044055>

Graves D.C. & Ferrer J.F. 1976. In vitro transmission and propagation of the bovine leukemia virus in monolayer cell cultures. Cancer Res. 36(11 Pt):4152-4159. <PMid:61801>

Gutiérrez G., Alvarez I., Fondevila N., Politzki R., Lomónaco M., Rodríguez S., Dus Santos M.J. & Trono K. 2009. Detection of Bovine leukemia virus specific antibodies using recombinant p24-ELISA. Vet. Microbiol. 137(3/4):224-234. <https://dx.doi.org/10.1016/j.vetmic.2009.01.022> <PMid:19201553>

Khalilian M., Hosseini S.M. & Madadgar O. 2019. Bovine leukemia virus detected in the breast tissue and blood of Iranian women. Microb. Pathog. 135:103566. <https://dx.doi.org/10.1016/j.micpath.2019.103566> <PMid:31252065>

Lage D.P., Martins V.T., Duarte M.C., Costa L.E., Garde E., Dimer L.M., Kursancew A.C.S., Chávez-Fumagalli M.A., Magalhães-Soares D.F., Menezes-Souza D., Roatt B.M., Machado-de-Ávila R.A., Soto M., Tavares C.A.P. & Coelho E.A.F. 2016. A new Leishmania-specific hypothetical protein and its non-described specific B cell conformational epitope applied in the serodiagnosis of canine visceral leishmaniasis. Parasitol. Res. 115(4):1649-1658. <10.1007/s00436-016-4904-x> <PMid:26782811>

Larsen A., Corva S., Panei J., Geisler C. & Mortola E. 2017. Enzyme-linked immunosorbent assays using the recombinant gp51 and p24 of Bovine leukemia virus for immunodetection of the disease. OJAS 7(3):241-253. <https://dx.doi.org/10.4236/ojas.2017.73019>

Larsen A., Gonzalez E.T., Serena M.S., Echeverría M.G. & Mortola E. 2013. Expression of p24 gag protein of Bovine leukemia virus in insect cells and its use in immunodetection of the disease. Mol. Biotechnol. 54(2):475-483. <https://dx.doi.org/10.1007/s12033-012-9587-7> <PMid:22829115>

Leite R.C., Reis J.K.P., Oliveira A.P., Nascimento P.M.P., Oliveira F.G., Naves J.H.F.F., Rodrigues A.P.S., Gasparini M.S., Alves F., De Oliveira C.H.S., Rajão D.S. & Galinari G.C.F. 2013. Retroviroses dos animais domésticos. Vet. Zootec. 20:73-92.

Megid J., Nozaki C.N., Kuroda R.B.S., Cruz T.F. & Lima K.C. 2003. Ocorrência de leucose enzoótica bovina na microrregião da Serra de Botucatu. Arq. Bras. Med. Vet. Zootec. 55(5):645-646. <https://dx.doi.org/10.1590/S0102-09352003000500021>

Molnár É., Molnár L., Dias H.T., Silva A.O.A. & Vale W.G. 1999. Ocorrência da leucose enzoótica dos bovinos no estado do Pará, Brasil. Pesq. Vet. Bras. 19(1):7-11. <https://dx.doi.org/10.1590/S0100-736X1999000100002>

Nekouei O., VanLeeuwen J., Stryhn H., Kelton D. & Keefe G. 2016. Lifetime effects of infection with Bovine leukemia virus on longevity and milk production of dairy cows. Prev. Vet. Med. 133:1-9. <https://dx.doi.org/10.1016/j.prevetmed.2016.09.011> <PMid:27720022>

OIE 2012. Enzootic bovine leucosis, p.721-731. In: Ibid. (Eds), Manual of Diagnostic Tests and Vaccines for Terrestrial Animals (mammals, birds and bees). Vol.1. 7th ed. World Organisation for Animal Health, Paris.

Olaya-Galán N.N., Corredor-Figueroa A.P., Guzmán-Garzón T.C., Ríos-Hernandez K.S., Salas-Cárdenas S.P., Patarroyo M.A. & Gutierrez M.F. 2017. Bovine leukaemia virus DNA in fresh milk and raw beef for human consumption. Epidemiol. Infect. 145(15):3125-3130. <https://dx.doi.org/10.1017/S0950268817002229> <PMid:28956522>

Oliveira T. F.P., Fonseca Junior A.A., Camargos M.F., de Oliveira A.M., Cottorello A.C.P., Ados R.S., Almeida I.G. & Heinemann M.B. 2013. Detection of contaminants in cell culture, sera and trypsin. Biologicals 41(6):407-414. <https://dx.doi.org/10.1016/j.biologicals.2013.08.005> <PMid:24071554>

Ott S.L., Johnson R. & Wells S.J. 2003. Association between bovine leukosis soroprevalence and herd level productivity on US dairy farms. Prev. Vet. Med. 61(4):249-262. <https://dx.doi.org/10.1016/j.prevetmed.2003.08.003> <PMid:14623410>

Patrascu I.V. 1988. Bovine leukemia virus. VII. In vitro replication of virus in bat lung cell culture NBL BLV 2. Virologie 39(3):199-205. <PMid:2848358>

Polat M., Takeshima S.N., Hosomichi K., Kim J., Miyasaka T., Yamada K., Arainga M., Murakami T., Matsumoto Y., de la Barra Diaz V., Panei C.J., González E.T., Kanemaki M., Onuma M., Giovambattista G. & Aida Y. 2016. A new genotype of bovine leukemia virus in South America identified by NGS-based whole genome sequencing and molecular evolutionary genetic analysis. Retrovirology 13:4. <https://dx.doi.org/10.1186/s12977-016-0239-z> <PMid:26754835>

Poletto R., Kreutz L.C., Gonzales J.C. & Barcellos L.J.G. 2004. Prevalência de tuberculose, brucelose e infecções víricas em bovinos leiteiros do município de Passo Fundo, RS. Ciênc. Rural 34(2):595-598. <https://dx.doi.org/10.1590/S0103-84782004000200043>

Rajão D.S., Heinemann M.B., Reis J.K.P., Braz G.F., Haddad J.P.A., Ribeiro A.C.C.L. & Leite R.C. 2014. Effects of bovine leukemia virus infection on crossbred and purebred dairy cattle productive performance in Brazil. Semina, Ciênc. Agrárias 35(2):891-900. <https://dx.doi.org/10.5433/1679-0359.2014v35n2p891>

Romero C.H. & Rowe C.A. 1981. Enzootic bovine leukosis virus in Brazil. Trop. Anim. Health Prod. 13(2):107-111. <https://dx.doi.org/10.1007/BF02237902> <PMid:6262958>

Schwingel D., Andreolla A.P., Erpen L.M.S., Frandoloso R. & Kreutz L.C. 2019. Bovine leukemia virus DNA associated with breast cancer in women from South Brazil. Nature 9:2949. <https://dx.doi.org/10.1038/s41598-019-39834-7>

Suzuki T., Ikeda H. & Mase M. 2018. Restricted viral cDNA synthesis in cell lines that fail to support productive infection by bovine leukemia virus. Arch Virol. 163(9):2415-2422. <https://dx.doi.org/10.1007/s00705-018-3887-6> <PMid:29796925>

Trainin Z & Brenner J. 2005. The direct and indirect economics impacts of bovine leukemia virus infection on dairy cattle. Israel J. Vet. Med. 60:94-105.

Troiano L.D.C., Thomaz-Soccol V., Agottani J.V.B., Brodzinski J., Penha T.R. & Ozaki S.C. 2013. Production, characterization, and use of monoclonal antibodies against gp51 protein to diagnose bovine leukemia virus infection. Biores Open Access 2(1):55-60. <https://dx.doi.org/10.1089/biores.2012.0295> <PMid:23515423>

PESQUISA VETERINÁRIA BRASILEIRA
Brazilian Journal of Veterinary Research
ISSN 0100-736X (Print)
ISSN 1678-5150 (Online)

Pesq. Vet. Bras. 40(12):985-991, December 2020
DOI: 10.1590/1678-5150-PVB-5998

Original Article
Livestock Diseases
BY-NC

Welfare during pre-slaughter handling and carcass lesions of beef cattle submitted to different loading densities[1]

Käthery Brennecke[2]*, Cynthia P. Zeferino[2], Vando Edésio Soares[2], Cássia M.B. Orlandi[2], Liandra M.A. Bertipaglia[2], Sarah Sgavioli[2], Paulo H.M. Dian[2] and Weberson D.C. Amâncio[2]

ABSTRACT.- Brennecke K., Zeferino C.P., Soares V.E., Orlandi C.M.B., Bertipaglia L.M.A., Sgavioli S., Dian P.H.M. & Amâncio W.D.C. 2020. **Welfare during pre-slaughter handling and carcass lesions of beef cattle submitted to different loading densities**. *Pesquisa Veterinária Brasileira 40(12):985-991.* Departamento de Produção Animal, Universidade Brasil, Avenida Hilário da Silva Passos 950, Parque Universitário, Descalvado, SP 13690-000, Brazil. E-mail: kathery.brennecke@universidadebrasil.edu.br

Inadequate pre-slaughter handling conditions can compromise animal welfare and productivity. This study aimed to evaluate the animal welfare (AW) indexes during pre-slaughter handling and quantify the carcass lesions of beef cattle submitted to different loading densities. A total of 270 Nellore cattle, at 30 months of age, from three farms were used in the study. Each farm presented a different loading density: higher density (500kg/m^2), intermediate density (450kg/m^2), and lower density (420kg/m^2). Three shipments of cattle from each farm with 30 animals each were used in the AW analysis. Ten animals from each shipment were considered for quantification of carcass bruises. The AW indexes were classified according to the five-freedom criterion (physiological, environmental, sanitary, behavioral, and psychological). After slaughter, the carcasses were inspected in the routine line and evaluated for the presence of lesions. Statistically significant differences (p<0.001) were found for all variables studied as a function of AW and bruises. The best AW index and the lowest mean weight of lesions were found at the loading density of 450kg/m^2. The highest carcass weight was observed at the loading density of 500kg/m^2. Lesions were found in 100% of the animals at the loading densities of 500 and 420kg/m^2. In conclusion, the best AW indexes and the smallest occurrence of bruises were verified at the loading density of 450kg/m^2. This study confirmed the importance of adequate pre-slaughter handling to ensure cattle welfare and, consequently, greater profitability for producers and slaughterhouses.

INDEX TERMS: Welfare, pre-slaughter, carcass, lesions, beef cattle, loading density, animal behavior, transport.

RESUMO.- [**Bem-estar durante o manejo pré abate e lesões em carcaça de bovinos submetidos às diferentes densidades de carregamento.**] Condições de manejo pré-abate inadequadas podem comprometer o bem-estar e a produtividade animal. O objetivo deste estudo foi avaliar os índices de bem-estar animal (BEA) durante o manejo pré-abate e quantificar as lesões em carcaça de bovinos submetidos às diferentes densidades de carregamento. Para isto, foram utilizados 270 bovinos Nelore, aos 30 meses de idade, provenientes de três fazendas. Cada fazenda apresentou diferente densidade de carregamento: maior densidade (500kg/m^2), densidade intermediária (450kg/m^2) e menor densidade (420kg/m^2). Foram realizados três carregamentos de cada fazenda, compostos por 30 animais cada. Para análise do BEA e quantificação de lesões nas carcaças bovinas foram considerados 10 animais de cada carregamento. Os índices de BEA foram classificados segundo o critério das cinco liberdades (fisiológica, ambiental, sanitária, comportamental e psicológica). Após o abate, as carcaças foram inspecionadas na linha de rotina e avaliadas quanto à presença de lesões. Foram encontradas diferenças significativas (P<0,001) para todas as variáveis estudadas em função do BEA e das lesões. O melhor índice de bem-estar e o menor peso médio de lesão foi encontrado na densidade de carregamento de

[1] Received on June 15, 2020.
Accepted for publication on September 4, 2020.
[2] Stricto sensu Professional Master's Program in Animal Production, Departamento de Produção Animal, Universidade Brasil, Avenida Hilário da Silva Passos 950, Parque Universitário, Descalvado, SP 13690-000, Brazil. *Corresponding author: kathery.brennecke@universidadebrasil.edu.br

450kg/m^2. O maior peso da carcaça foi encontrado na densidade de carregamento de 500kg/m^2. Em 100% dos animais nas densidades de carregamento de 500 e 420kg/m^2 foram encontradas lesões. Pode-se concluir que a densidade de carregamento de bovino de 450kg/m^2 obteve os melhores índices de bem-estar e menor ocorrência de lesões. Este estudo confirma a importância do manejo pré-abate adequado na garantia do bem-estar aos bovinos e, consequentemente, na maior rentabilidade ao produtor e ao frigorífico.

TERMOS DE INDEXAÇÃO: Bem-estar animal, pré abate, lesões, carcaça de bovinos, densidade de carregamento, comportamento animal, bovinos de corte, transporte.

INTRODUCTION

In 2017, Brazil led the world production of beef, with a commercial herd of 221.8 million head of cattle. Of the total meat produced, 20% was exported and 80% supplied the domestic market, guaranteeing a consumption of approximately 37.5 kg of beef per inhabitant (USDA 2018). Currently, the agricultural sector is undergoing a modernization process related to productive aspects and pre-slaughter logistics aiming to improve animal living conditions and quality of the final product (Mendonça et al. 2016).

Animal welfare (AW) is of paramount importance for ensuring good quality of the meat produced and, therefore, high economic return for producers and slaughterhouses. AW should be considered from the beginning of pre-slaughter handling, which starts on the farm with the separation and fasting of the animals and extends throughout the *ante mortem* period (Souza 2005).

Practices such as the use of stingers or electric shocks force animals to drive and enter the transport truck during the loading and unloading stage. This type of handling results in large carcass losses resulting from bruises, being more harmful than the distance traveled (Rebagliati et al. 2008). In contrast, when the basic principles of AW are followed - these steps are carried out by professionals who respect animal rights - higher carcass yield and better quality of the final product are obtained (Andrade et al. 2004).

The transport of cattle from the farm to the slaughterhouse is an important pre-slaughter handling step that involves many factors: type of vehicle, loading density, distance and time traveled, road conditions, driver's driving behavior, and temperature. Association between two or more of these factors is determining and can stress the animals and cause bruises on their carcasses (Mendonça et al. 2016). According to Strappini et al. (2009), transport conditions (vehicle design, loading density, climatic conditions, transport time and distance, handlers' training, road conditions, and animal behavior, sex, and breed) can interfere with the level of cattle welfare.

The importance of properly carrying out the transport arises from losses on the quality of the meat produced (Schwartzkopf-Genswein et al. 2012), as it represents the second largest cause of bruises in bovine carcasses, with an index of 33.08%, second only to pre-slaughter handling and vaccination lesions (Moro et al. 2001).

Problems with loading density are commonly cited, but there are few studies on the subject. The Farm Animal Welfare Council establishes a formula for calculating the minimum area occupied by an animal, recommending an average of 360kg/m^2 (Knowles 1999). However, from an economic point of view, high animal density transport is expected. In Brazil, the loading density used ranges from 390 to 410kg/m^2 (Roça 2002); a loading density >550kg/m^2 is considered inadequate (Tarrant et al. 1988).

The quantification and classification of bruises present in the carcasses of slaughtered animals is an important indicator of inadequate handling - a fact that can occur at any stage of the process: loading on the farm, transport, unloading at the slaughterhouse, and slaughter (Polizel Neto et al. 2015). However, Braggion & Silva (2004) consider that lesions in carcasses during transport occur as a result of association of high loading density with greater stress reaction, bruises, large number of falls and other causes such as horns, kicking, and trampling, which are usually linked to handling problems. Bruises are characterized by traumatic lesions caused by vessel bleeding with consequent accumulation of blood and serum in the tissues (Nanni Costa et al. 2006).

Carcass bruises are a way to assess cattle handling and, therefore, are indicative of AW problems. Suppression of the immune system and physiological changes in animals are consequences of stress and may indicate a pre-pathological state (Moberg 1985). Measurements of behavior and physiological evidence are of great value, as they provide data on animal feelings. However, there is not sufficient information in the scientific literature aimed at improving animal welfare. Therefore, developing methods to analyze AW, with emphasis on behavioral characteristics, becomes a great challenge.

Although the stressful effects of pre-slaughter practices on cattle have been widely studied in some regions of the world, the topic still receives limited attention in Latin America (Romero et al. 2013). Thus, little updated information is available in the literature about the impact of transport and pre-slaughter conditions on AW and carcass quality in Brazil. Despite the existence of risk analysis protocols associated with cattle welfare during transport (Marahrens et al. 2011), further studies are needed to identify the harmful effects of these steps on AW and carcass quality. In this way, it is possible to recommend appropriate changes in handling routines that can minimize the biological cost to animals during the pre-slaughter process and improve the product quality (Romero et al. 2013).

In this context, the present study aimed to evaluate the AW indexes during pre-slaughter handling and quantify the carcass lesions of beef cattle subjected to different loading densities.

MATERIALS AND METHODS

Animals and experimental conditions. The study was conducted in a slaughterhouse located in the interior of the state of São Paulo, Brazil, accredited and supervised by the "Serviço de Inspeção de São Paulo" (SISP). All legal slaughtering recommendations were followed. The procedures involving the animals were approved by the Ethics Committee on the Use of Animals (CEUA) of the "Universidade Brasil", Descalvado campus, state of São Paulo, Brazil, under protocol no. 004/6 - 2016.

A total of 270 castrated male and female, not dehorned, pure and crossbred Nellore cattle at approximately 30 months of age were used in the study. These animals came from three farms (A, B, and C) where they were reared on pasture. Three shipments of cattle from each farm with 30 animals each (total 90 animals per

farm) were used. However, for the experiment's composition and analysis, only 10 cattle per shipment were taken at random, totaling 30 animals per farm.

The average distance traveled to the slaughterhouse was about 55 km on paved roads. The transport was carried out in the morning's early hours (between 4:30 and 5:30 a.m.) during the winter. According to the Köppen classification, climate in the study region is Cwb (humid subtropical) characterized by dry winters and mild summers, with an average temperature <22 °C during the hottest months (Setzer 1966).

Low-capacity, two-axle, livestock, crate trucks were used to transport the cattle. According to Tarrant et al. (1988), the three farms showed an average loading density. However, due to the difference in individual weight between the animals (400 to 500 kg, on average), farm A had the highest density (500.1 ±14.5 kg/m^2), farm B presented intermediate density (450.8 ±26.5 kg/m^2), and farm C showed the lowest loading density (419.9 ±10.9 kg/m^2). Approximate values of 500, 450, and 420 kg/m^2 were adopted for farms A, B, and C loading densities, respectively.

According to the procedures required by the current legislation, pre-slaughter and slaughter handling procedures were carried out with rest and a water diet, and were the same for all farms. The cattle were stunned following the requirements of humane slaughter using penetrating captive dart pistols and subsequently hoisted to proceed with the bleeding process and slaughter flow to reduce the economic losses in the carcasses.

The experiment followed a completely randomized design, with three loading densities and ten repetitions per loading, for the characteristics of AW and bruises in bovine carcasses.

Assessment of welfare indexes. The AW indices were evaluated according to the five-freedom criterion (physiological, environmental, health, behavioral, and psychological) proposed by the World Society for the Protection of Animals (WSPA 2009). For each freedom, the farm's condition characteristics, the truck (depending on the transport), and the slaughterhouse were evaluated (Table 1).

Each assessment was carried out by a single strategically positioned evaluator. The evaluator was able to visualize the animals secretly and without interfering with the handlers' activities. For the characteristics analyzed in each location (farm, truck, and slaughterhouse), assessment was carried out following the Welfare Quality® (WSPA 2009) recommendations, with adaptations. Thus, scores from 1 to 5 were generated and averages were obtained.

Evaluation of carcass bruises. The cattle were submitted to a 10-h fast and then transported to the slaughterhouse. The animals belonging to each shipment were allocated and separated from each other and from the rest of the slaughter line to prevent possible occurrence of other types of lesions that could compromise the objectives of this study.

After slaughter, the entire carcass was sawn lengthwise. Each half carcass was weighed and inspected according to Decree no. 9013 of March 29, 2017 (Brasil 2017) and to the Regulation of Industrial and Sanitary Inspection of Products of Animal Origin (Brasil 1997).

Assessment of carcass bruises was performed in the slaughter inspection routine line and followed the criterion described by Aus-Meat Limited (2001). Purple or blue-red bruises were considered aslesions that occurred within less than 24 hours (Andrade et al. 2008). The lesions were quantified and grouped according to carcass location in forequarter, ribs, and hindquarter, observing the medial and lateral faces of the cranial and caudal parts. Vaccination lesions were also quantified. After counting, the lesions were removed using curved knives, stored in plastic bags with a previously determined weight, and weighed on a digital scale with accuracy of 0.0005 kg.

Statistical analysis. The AW indices and the quantification of bovine carcass bruises were evaluated according to the three different loading densities. The data were processed using the Statistica 12 (StatSoft Power Solutions, Inc., 2014). The model included both the fixed loading density and the random bovine effects. The data were evaluated for normality and homogeneity of variance by residual analysis. For the nonparametric data, comparison of the means was performed by the Kruskal-Wallis test. A significance level of 5% (p<0.05) was adopted for all statistical analyses.

RESULTS AND DISCUSSION

Proper handling during the pre-loading and unloading stages and ideal transport conditions are essential in the productive chain of cattle destined for slaughter. However, these stages are still one of Brazil's main cattle handling problems (Brunel et al. 2018). Although there are limitations to assessing AW, indicators in slaughterhouses have the potential to reduce chronic painful conditions to the animals caused by poor handling or damage due to inadequate housing conditions (Grandin 2017).

Table 1. Conditions evaluated for the animal welfare (AW) index in the pre-slaughter handling of beef cattle from three loading densities

Location	Features*
Farm	Handling - handlers' technique
	Handling - loading time
	Installation - condition of the cattle chute and syringe
	Installation - boarding ramp conditions
	Installation - corral floor conditions
	Installation - lairage conditions prior to loading
	Installation - farm corral floor
Truck (during transport)	Handling - driving technique
	Handling - truck crate cleaning
	Installation - truck crate floor conditions
	Installation - crate conditions
	Installation - hatch conditions
	Installation - partition conditions
Slaughterhouse	Handling - handlers' technique in unloading
	Handling - unloading time
	Handling - technique in guiding the animal to the corral
	Installation - access ramp
	Installation - slaughterhouse corral floor
	Installation - shading
	Installation - water availability
	Installation - sprinkler operation
	Installation - gate conditions and lot divisions
	Installation - corral space
	Handling - handler's technique in conducting slaughter
	Installation - animal access to the slaughter ramp
	Handling - stunning technique
	Installation - stunning box conditions

* Evaluation according to the 5-freedom criterion WELFARE QUALITY® (adapted from WSPA 2009).

Currently, there is no universally accepted protocol for assessing AW. Those available in the scientific literature describe a variety of methods and measures used in slaughter assessment. Although each of them has strengths and weaknesses, it is necessary to consider each slaughter plant's particularities, as the layout of the facilities can lead to difficulties in visual observation and physical measurement of parameters based on welfare. Commercial pressures and the need for speed during the processing step can also prevent these parameters from being measured (Wigham et al. 2018).

In the present study, the highest mean AW index was found at the loading density of 450kg/m^2, as shown in Table 2. This result stems from the higher AW rates of the farm, truck, and slaughterhouse at this density.

The scientific literature shows that the most critical, stressful, and bruising stage for the animal is the transport and the association of factors intrinsic to it (Moro et al. 2001, Dalla Costa et al. 2007, Mendonça et al. 2016). Findings of present experiment show that AW at the slaughterhouse obtained the lowest index compared with those on the farm and truck.

Paranhos da Costa (2002) carried out ethological observations of the procedures involved in transporting cattle to the slaughterhouse (from handling on the farm to slaughter), described the handling and facilities conditions, the behavior of the animals, and the frequency, and concluded that detailed studies are needed to detect critical points and establish a cattle handling quality of service program. The way to achieve the necessary cultural change to improve AW, handler safety, and the sector's profitability is through training and knowledge transfer (Huertas et al. 2018).

The lowest AW index on the truck was found at the loading density of 500kg/m^2 (Table 2). According to Tarrant et al. (1988), high animal loading densities are associated with a greater stress reaction, risk of injury, and number of falls compared with low or moderate loading densities. Their study corroborates the values found in the present study, in which a statistically significant difference was observed between the loading density (p<0.0001) and the worst AW rates on the truck at the densities of 500 and 420kg/m^2 (Table 2).

Transport to the slaughterhouse compromises the welfare of beef cattle. A tool to measure the AW level is observation of carcass bruises. The frequency of these bruises reflects the transport conditions and, consequently, the animals' welfare, which can be observed to avoid economic losses (Huertas et al. 2018). In this study, the lowest weight of lesions was found at the loading density of 450kg/m^2 (p<0.0001; Table 2).

Huertas et al. (2018) evaluated the unloading conditions associated with the average number of carcass bruises in cattle and found no significant correlation results. Andrade et al. (2008) found lesions in cattle subjected to different transport types as a function of time. They verified a higher proportion of lesions in lots subjected to road transport for more than an hour and distances greater than 70 km, most of them on unpaved roads, but observed a lower proportion of lesions in animals belonging to the lot transported on paved roads over distances up to 50 km. This result was not related to space provided to the animals - the loading density to which the cattle were subject during the transport on crate trucks.

Results of this study also show that the largest number of lesions was found at both high- and low-densities, which corresponded to 100% of the animals evaluated (Table 3). In addition, the average values of tissue removal were 0.81 and 0.80kg/bovine for the loading densities of 500 and 420kg/m^2. Values of 24.30 and 23.40kg of removed tissue were obtained for the loading densities considered high and low, respectively, whereas a tissue removal value of 11.18 kg was verified at the loading density of 450kg/m^2.

Andrade et al. (2008), when studying cattle carcass bruises caused by transport in the Pantanal region, without considering loading density, observed 82 and 45% of lesions in batches of cattle transported over distances of 50km.

Tarrant et al. (1988), Warriss (1990), and Gonzalez et al. (2012) have reported that inappropriate loading densities (either high or low) increase the frequency of falls, lesions, bruises, and mortality, as well as hormonal concentrations due to stress, with consequent reduced meat quality. Tarrant et al. (1988) classify the loading densities of as 600, 400, and 200kg/m^2 as high, average, and low, respectively. Tarrant & Grandin (1993) qualify the availability of 1.11m^2 as a high loading density for 500 kg of body weight, and explain that cattle fall as a result of reduced mobility under these conditions, preventing them from taking their preferred guidance.

According to Mendonça et al. (2016), long vehicles present a more significant centrifugal displacement effect, caused by the vehicle's traction distance - in this case, the front - causing

Table 2. Minimum mean square error (MMSE) of AW indexes in pre-slaughter handling and lesion weight of beef cattle from three loading densities

Parameters	Loading density (kg/m^2)			Probability (P)[E]
	500	450	420	
AW farm[A]	3.40±0.10^c	3.70±0.00^a	3.60±0.03^b	<0.0001
AW truck[B]	2.60±0.10^c	3.10±0.40^a	2.80±0.00^b	<0.0001
AW slaughterhouse[C]	2.10±0.00^b	2.30±0.20^a	2.10±0.00^b	<0.0001
AW mean[D]	2.70±0.10^b	3.00±0.20^a	2.80±0.10^a	<0.0001
Average carcass weight (kg)	290.30±18.60^a	236.50±37.10^b	236.60±34.40^b	<0.0001
Mean weight of lesions (kg)	0.80±0.60^a	0.30±0.40^b	0.80±1.30^{ab}	<0.0001

[A AW] farm = animal welfare on the farm, during pre-slaughter handling, according to the five-freedom criterion, [B] AW truck = animal welfare in the truck (transport stage), during pre-slaughter handling, according to the five-freedom criterion, [C] AW slaughterhouse = animal welfare in the slaughterhouse, during pre-slaughter handling, according to the five-freedom criterion, [D] AW mean = average animal welfare during pre-slaughter handling according to the five-freedom criterion. For AW evaluation and average weight of carcass and lesions, 10 cattle from each shipment were used; [E] Probability (P) = probability of type I error; [a,b,c] means followed by the same letter on the line do not differ by the Kruskal Wallis test at 5% probability; average carcass weight = total carcass weight (kg) after removal of lesions; mean weight of lesions = specific lesion quantity (kg).

greater vibration to the animals, and, as a consequence, greater possibility of bruises or lesions.

Regardless of the loading density, there was predominance of bruises in the forequarter, with a total of 89 lesions (55%), compared with the hindquarter, with a total of 72 lesions (45%). In the forequarter, the ribs showed 31 lesions, which represented 35% of the forequarter's total lesions (Table 3). Huertas et al. (2018), when classifying the prevalence lesion location in the carcass, reported results opposite to those of the present study, with the highest prevalence in the thigh and hip region (29.3%), followed by the forequarter (22.4%), hindquarter (17.3%), flank (14.1%), rump (10.1%), and loin (6.8%).

Regarding the total weight of the lesions in different locations in the bovine carcasses, there was no effect of the loading density to the hindquarter (P=0.2041), ribs (P=0.4989), and vaccine site (p=0.3535). However, for the forequarter, there was a statistically significant difference (p=0.0006) with greater and smaller lesion weight at the loading densities of 500 and 450kg/m^2 (0.9±0.3 *vs*. 0.4±0.5kg, per animal), respectively (Table 4).

Andrade et al. (2008), when working with the stunning of cattle slaughtered in the Pantanal region and checking the occurrence of bruises, found a larger number of lesions in the caudal hindquarter and in the hindquarter of the right half-carcasses. However, Ghezzi et al. (2008) reported that the scapula and hindquarters are risk factors for lesions during transport.

Tarrant et al. (1988) observed that the animal's stress level increased according to its location at the rear of the truck crate. The stocking density influenced orientation on the truck. Those authors also observed that loss of balance of the animals was associated with specific driving events, especially braking and cornering. Small losses of balance were recorded at all stocking densities, but large losses of balance, including falling animals, were associated with high loading density.

Andrade et al. (2004) observed that 60.40% of the bruises in half carcasses in less than 24 h suggest that these lesions had occurred during transport or at the slaughterhouse. This observation corroborates the findings of the present study, since a high rate of lesions was obtained, and the lowest AW rates were verified at the slaughterhouse and on the truck.

Animal bruises have a multifactorial origin. However, there is a consensus in the scientific literature that bruises acquired during the pre-slaughter period occur mainly during the loading, transport, and unloading stages (Dalla Costa et al. 2007), as well as through physical contact, trampling, falls,

Table 3. Number and total weight of lesions in bovine carcasses from three loading densities

Parameters	Loading density (kg/m^2)[A]		
	500	450	420
Total number of lesions	64	44	53
Number of carcasses with lesion	30	26	30
Number of carcasses without lesion	00	04	00
Number of carcasses with more than one lesion	27	14	17
Number of lesions in the forequarter	35	26	28
Number of lesions in the ribs (forequarter)	10	12	09
Number of lesions in the hindquarter	29	18	25
Percentage of carcasses with lesion[B] (%)	100	87	100
Average weight of tissue removed/bovine (kg)	0.81	0.43	0.80

[A] Loading densities refer to the average weight of cattle, from each farm, depending on the truck crate area. For the parameters of lesions in bovine carcasses, 10 animals from each shipment were used. [B] The percentage of carcasses with lesion was obtained by the ratio of number of carcasses evaluated to number of carcasses with lesions. Average weight of tissue removed/bovine = Weight of lesion + weight of bruised tissue.

Table 4. Total weight of lesions (kg) in bovine carcasses from three loading densities

Variable	Loading density[A] (kg/m^2)	Weight (kg)	95% CI	p-value[B]
Lesion in the forequarter	500	0.9 ±0.3^a	0.8-1.0	0.0006
	450	0.4 ±0.5^b	0.2-0.6	
	420	0.6 ±0.5^{ab}	0.4-0.8	
Lesion in the hindquarter	500	0.8 ±0.4^a	0.7-1.0	0.2041
	450	0.8 ±0.4^a	0.6-0.9	
	420	0.9 ±0.3^a	0.8-1.0	
Lesion in the ribs	500	0.4 ±0.5^a	0.2-0.5	0.4989
	450	0.2 ±0.4^a	0.1-0.4	
	420	0.3 ±0.4^a	0.1-0.4	
Vaccination lesion	500	0.0 ±0.0^a	0.0-0.0	0.3535
	450	0.0 ±0.1^a	0.0-0.1	
	420	0.0 ±0.0^a	0.0-0.0	

[A] Load densities based on the average weight of the cattle, from each farm, depending on the truck crate area, [B] P-value = type I error probability; ^{a,b} means followed by the same letter in the column do not differ by the Kruskal Wallis test at 5% probability.

and possible confrontations (Nanni Costa et al. 1999, Grandin 2001). In other words, handling failures and, mainly, the animals' reaction in response to the handlers' aggressiveness result in a greater occurrence of carcass lesions. Care should be taken mainly at the time of separation, as it constitutes a naturally stressful stage. It is necessary to handle the animals according to the welfare requirements so that new routine and balanced normal activities can be reestablished (Paranhos da Costa 2002). Finally, minimizing the stressful effects on cattle to ensure AW and reduce carcass losses is a significant challenge.

CONCLUSIONS

The best animal welfare indexes and the lowest occurrence of bruises were verified for the cattle loading density of 450kg/m^2.

The average weight and number of lesions in all treatments confirm the importance of adequate pre-slaughter handling to guarantee cattle welfare, good quality of the meat produced, and higher profitability for producers and slaughterhouses.

The need to adopt professional training programs, supervision and improvement of cattle handling conditions is reinforced.

Conflict of interest statement.- The authors declare having no competing interests.

REFERENCES

Andrade E.N., Filho Ojeda O., Silva B.S. & Silva R.A.M.S. 2004. Influência do transporte fluvial em carcaças de bovinos no Pantanal. Corumbá, Embrapa Pantanal, 3p. (Comunicado Técnico, 43).

Andrade E.N., Roça R.O., Silva R.A.M.S., Gonçalves H.C. & Pinheiro R.S.B. 2008. Prevalência de lesões em carcaças de bovinos de corte abatidos no Pantanal Sul Mato-Grossense transportados por vias fluviais. Ciênc. Tecnol. Aliment. 28(4): 822-829. <https://dx.doi.org/10.1590/S0101-20612008000400010>

Aus-Meat Limited. 2001. Beef & veal language. South Brisbane, 4p.

Braggion M. & Silva R.A.M.S. 2004. Quantificação de lesões em carcaças de bovinos abatidos em frigoríficos no Pantanal Sul-Mato-Grossense. Corumbá, Embrapa Pantanal, p.1-4. (Comunicado Técnico, 45)

Brasil. 1997. Ministério da Agricultura e do Abastecimento. Secretaria de Defesa Agropecuária – DAS. Departamento de Inspeção de Produtos de Origem Animal – DIPOA. DNT– Divisão de Normas Técnicas. Regulamento da Inspeção Industrial e Sanitária de Produtos de Origem Animal. Brasília, DF. 241p.

Brasil. 2017. Decreto 9013 de 29 de março de 2017. Regulamenta a Lei nº 1.283, de 18 de dezembro de 1950, e a Lei nº 7.889, de 23 de novembro de 1989, que dispõe sobre a inspeção industrial e sanitária de produtos de origem animal. Disponível em <http://www.planalto.gov.br/ccivil_03/_ato2015-2018/2017/decreto/D9013.htm> Acesso em 15 jun. 2020.

Brunel H.S.S., Dallago B.S.L., Almeida A.M.B., Assis A.Z., Calzada R.J.B., Alvarenga A.B.B., Menezes A.M., Barbosa J.P., Lopes P.R., González F.H.D., McManus C., Broom D. & Bern F.E.M. 2018. Hemato-biochemical profile of meat cattle submitted to different types of pre-loading handling and transport times. International Journal of Veterinary Science and Medicine. 6:90-96. <https://dx.doi.org/10.1016/j.ijvsm.2018.04.002>

Dalla Costa O.A., Faucitano L., Coldebella A., Ludke J.V., Peloso J.V., Dalla Roza D. & Paranhos da Costa M.J.R. 2007. Effects of the season of the year, truck type and location on truck on skin bruises and meat quality in pigs. Livest. Sci. 107(1):29-36. <https://dx.doi.org/10.1016/j.livsci.2006.08.015>

Ghezzi M.D., Acerbi R., Ballerio M., Rebagliati J.E., Diaz M.D., Bergonzelli P., Civit D., Rodríguez E.M., Passucci J.A., Cepeda R., Sañudo M.E., Copello M., Scorzielo J., Caló M., Camussi E., Bertoli J. & Aba M.A. 2008. Evaluacion de las practicas relacionadas com el transporte terrestre de hacienda que causan perjuicios econômicos en la cadena de ganados y carnes. *Sítio Arg Prod Anim*, 5: 01-29.

Gonzalez L.A., Schamartzkopf-Genswein K.S., Bryan M., Silasi R. & Brown F. 2012. Factors affecting body weight loss during commercial long haul transport of cattle in North America. J. Anim. Sci. 90(10):3630-3639. <https://dx.doi.org/10.2527/jas.2011-4786> <PMid:22665642>

Grandin T. 2001. Perspectives on transportations issues: the importance of having physically fit cattle and pigs. J. Anim. Sci. 79(E. Suppl.):E201-E207. <https://dx.doi.org/10.2527/jas2001.79E-SupplE201x>

Grandin T. 2017. On-farm conditions that compromise animal welfare that can be monitored at the slaughter plant. Meat Sci. 132:52-58. <https://dx.doi.org/10.1016/j.meatsci.2017.05.004>

Huertas S.M., Kempener R.E.A.M. & van Eerdenburg F.J.C.M. 2018. Relationship between methods of loading and unloading, carcass bruising, and animal welfare in the transportation of extensively reared beef cattle. Animals, 8(7):119. <https://dx.doi.org/10.3390/ani8070119> <PMid:30018193>

Knowles T.G. 1999. A review of the road transport of cattle. Veterinary Record, London, 144(8):197-201. <https://dx.doi.org/10.1136/vr.144.8.197> <PMid:10097341>

Marahrens M., Kleinschmidt N., Di Nardo A., Velarde A., Fuentes C., Truar A., Otero J.L., Di Fede E. & Dalla Villa P. 2011. Risk assessment in animal welfare – especially referring to animal transport. Preventive Veterinary Medicine, 102(2):157-163. <https://dx.doi.org/10.1016/j.prevetmed.2011.04.010> <PMid:21601298>

Mendonça F.S., Vaz R.Z., Costa O.A.D., Gonçalves G.V.B. & Moreira S.M. 2016. Fatores que afetam o bem-estar de bovinos durante o período pré-abate. Arch. Zootec. 65(250):279-287. <https://dx.doi.org/10.21071/az.v65i250.500>

Moberg G.P. 1985. Biological response to stress: key to assessment of animal well-being?, p.27-49. In: Moberg, G.P. Animal Stress. Bethesda: American Physiological Society.

Moro E., Junqueira J.O.B. & Umehara O. 2001. Levantamento da incidência de reações vacinais e/ou medicamentosas em carcaças de bovinos na desossa em frigoríficos no Brasil. *A Hora Veterinária* 21(123):1-5.

Nanni Costa L., Fiego D.P., Dall'Olio S., Davoli R. & Russo V. 1999. Influence of loading method and stocking density during transport on meat and dry-cured ham quality in pigs with different halothane genotypes. Meat Sci. 51(4):391-399. <https://dx.doi.org/10.1016/S0309-1740(98)00160-0>

Nanni Costa L., Lo Fiego D.P., Tassone F. & Russo V. 2006. The relationship between carcass bruising in bulls and behaviour observed during pre-slaughter phases. Vet. Res. Commun. 30(1):379-381. <https://dx.doi.org/10.1007/s11259-006-0086-9>

Paranhos da Costa M.J.R. 2002. Ambiência e qualidade de carne. Anais do 5º Congresso das Raças Zebuínas-ABCZ, Uberaba, MG, p.170-174.

Polizel Neto A., Zanco N., Lolatto D.C.J., Moreira P.S.A. & Dromboski T. 2015. Perdas econômicas ocasionadas por lesões em carcaças de bovinos abatidos em matadouro-frigorífico do norte de Mato Grosso. Pesq. Vet. Bras. 35(4):324-328. <https://dx.doi.org/10.1590/S0100-736X2015000400002>

Rebagliati J.E., Ballerio M., Acerbi R., Diaz M., Alvarez M.M., Bigatti F., Cruz J.A., Scitelli L., Ergonzelli P., Gonzalez C., Civit D. & Ghezzi M.D. 2008. Evaluación de las prácticas ganaderas en bovinos que causan perjuicios económicos en plantas frigoríficas de la República Argentina (2005). REDVET - Revista Electrónica Veterinária 9(10B):1-40.

Roça R.O. 2002. Abate humanitário de bovinos. In: I Conferência virtual global sobre produção orgânica de bovinos de corte. Embrapa Pantanal, Corumba-MS. Brazil.

Romero M.H., Uribe-Velásquez L.F., Sánchez J.A. & Miranda-de la Lama G.C. 2013. Risk factors influencing bruising and high muscle pH in Colombian

cattle carcasses due to transport and pre-slaughter operations. Meat Sci. 95(2):256-263. <https://dx.doi.org/10.1016/j.meatsci.2013.05.014> <PMid:23747620>

Schwartzkopf-Genswein K.S., Faucitano L., Dadgar S., Shand P., González L.A. & Crowe T.G. 2012. Road transport of cattle, swine and poultry in North America and its impact on animal welfare, carcass and meat quality: a review. Meat Sci, 92(3):227-243. <https://dx.doi.org/10.1016/j.meatsci.2012.04.010> <PMid:22608833>

Setzer J. 1966. Atlas Climático e Ecológico do Estado de São Paulo. Comissão Interestadual da Bacia Paraná-Uruguai, 61p.

Souza P. 2005. Exigências atuais de bem-estar animal e a sua relação com a qualidade da carne. Embrapa Suínos e Aves. Disponível em <https://www.agencia.cnptia.embrapa.br/Repositorio/exigencias_atuais_de_bem_estar_animal_e_sua_relacao_com_qualidade_da_carne_000fz75urw702wx5ok0cpoo6agbfbiwd.pdf> Acesso em 15 jun. 2020.

StatSoft Power Solutions, Inc. (2014). STATISTICA (data analysis software system), version 12. Disponível em:<http://www.statsoft.com> Acesso em 15 jun. 2020.

Strappini A.C., Metz J.H.M., Gallo C.B. & Kemp B. 2009. Origin and assessment of bruises in cattle at slaughter. Animal, 3(5):728-736. <https://dx.doi.org/10.1017/S1751731109004091> <PMid:22444452>

Tarrant P.V. & Grandin T. 1993. Cattle transport. In: Grandin, T. Livestock Handling and Transport. 1. ed. Cabi International. Wallingford. UK. pp. 109-126

Tarrant P.V., Kenny F.J. & Harrington D. 1988. The effect of stocking density during 4-hour transport to slaughter on behaviour, blood constituents and carcass bruising in Friesian steers. Meat Sci. 24(3):209-222. <https://dx.doi.org/10.1016/0309-1740(88)90079-4> <PMid:22055952>

USDA. United States Department of Agriculture. 2018. Foreign Agricultural Service. Livestock and Poultry: World Markets and Trade. Available at <https://apps.fas.usda.gov/psdonline/app/index.html#/app/downloads> Accessed on Jun. 15, 2020.

Warriss P.D. 1990. The handling of cattle pre-slaughter and its effects on carcass meat quality. Applied Animal Behaviour Science, Amsterdan, 28, (1/2):171-186. <https://dx.doi.org/10.1016/0168-1591(90)90052-F>

Wigham E.E., Butterworth A., Wotton S. 2018. Assessing cattle welfare at slaughter – Why is it important and what challenges are faced? Meat Sci. 145:171-177. <https://dx.doi.org/10.1016/j.meatsci.2018.06.010> <PMid:29982070>

WSPA Brasil. 2009. World Society for the Protection of Animals. Programa Nacional de Abate Humanitário (Steps): Melhorando o Bem-Estar Animal no Abate. Rio de Janeiro, 2009. 1 CD-ROM, p.33.

PESQUISA VETERINÁRIA BRASILEIRA
Brazilian Journal of Veterinary Research
ISSN 0100-736X (Print)
ISSN 1678-5150 (Online)

Pesq. Vet. Bras. 40(12):992-1001, December 2020
DOI: 10.1590/1678-5150-PVB-6710

Original Article
Livestock Diseases
BY-NC

Physiological and biochemical responses and hydration status in equines after two barrel racing courses[1]

Cláudio L.N. Gomes[2]*, Andressa M. Alves[3], José D. Ribeiro Filho[4], Felipe J. Moraes Júnior[2], Raimundo A. Barreto Júnior[5],Rodrigo S. Fucuta[6], Bruna M. Ribeiro[7] and Leandro M. Miranda[8]

ABSTRACT.- Gomes C.L.N., Alves A.M., Ribeiro Filho J.D., Moraes Júnior F.J., Barreto Júnior R.A., Fucuta R.S., Ribeiro B.M. & Miranda L.M. 2020. **Physiological and biochemical responses and hydration status in equines after two barrel racing courses**. *Pesquisa Veterinária Brasileira 40(12):992-1001*. Departamento de Clínicas Veterinárias, Universidade Estadual do Maranhão, Cidade Universitária Paulo VI, Bairro Tirirical, São Luis, MA 65055-970, Brazil. E-mail: claudioninagomes@uol.com.br

Studies on biochemical constituents and hydration of horses in training or competitions are essential for the knowledge of their adaptive physiological and metabolic responses to the type of exercise inherent to the sport. The present research evaluated the effects of exercise on hydric status and physiologic and biochemical profiles in Quarter Horses during a barrel race training session. The design consisted of three evaluation times (T): at rest, before the start of physical activity (T0); immediately after a 10-minute warm-up trot and then running the barrel race courses twice with a 10-minute interval (T1); and after one hour's rest after the second course (T2). The parameters analyzed were: heart rate (HR), respiratory rate (RR), body temperature (BT) and mucose color; the capillary refill time (CRT), packed cell volume (PCV), total plasma proteins (TPP), serum creatinine (CRE) and blood urea nitrogen (BUN) were evaluated and used to infer water status; plasma osmolarity (Osm) was measured; the electrolytes sodium (Na), potassium (K), chloride (Cl), total calcium (tCa), total magnesium (tMg) and phosphorus (P), plasma glucose (Glu) and lactate (Lac) and the muscle enzymes creattine kinase (CK) and aspartate aminotransferase (AST) completed the evaluated parameters. The data for the variables studied were submitted to ANOVA and the Tukey test at 5% probability. After exercise (in T1), HR, RR, BT, PCV, TPP, Glu, Lac, Cre increased (P<0.05), there was also increase in phosphorus and decrease in K (P<0.05), but there was no hypophosphatemia and hipokalemia, respectively. After rest (in T2), only glucose returned to baseline levels (T0) and, with lower mean values, HR, RR, BT, PCV, K and Lac did not return to baseline levels (T0), while P decreased (P<0.05). Osm, BUN, Na, Cl, tCa, tMg, CK and AST did not change between times (P>0.05). It was concluded that the maximum intensity exercise performed on two barrel race courses caused mild hemoconcentration, did not changed plasma osmolality or concentrations of important electrolytes and muscle enzymes of horses, but caused hyperlactatemia without the plasma lactate concentrations being fully recomposed after resting.

INDEX TERMS: Physiology, biochemistry, equines, barrel race, exercise.

[1] Received on September 13, 2020.
Accepted for publication on October 1, 2020.

[2] Departamento de Clínicas Veterinárias, Universidade Estadual do Maranhão (UEMA), Cidade Universitária Paulo VI, Bairro Tirirical, São Luís, MA 65055-970, Brazil. E-mail: fmoraesjr@hotmail.com; *Corresponding author: claudioninagomes@uol.com.br

[3] Master Program in Animal Science, Centro de Ciências Agrárias, Universidade Estadual do Maranhão (UEMA), Cidade Universitária Paulo VI, Bairro Tirirical, São Luís, MA 65055-970, Brazil. E-mail: andressamalves@outlook.com

[4] Departamento de Medicina Veterinária, Universidade Federal de Viçosa (UFV), Avenida PH Rolfs s/n, Campus Universitário, Viçosa, MG 36571-000, Brazil. E-mail: dantas@ufv.br

[5] Departamento de Medicina Veterinária, Universidade Federal Rural do Semi-Árido (UFERSA), Av. Francisco Mota, 572, bairro Costa e Silva, Mossoró, RN 59625-900, Brazil. E-mail: barreto@ufersa.edu.br

[6] Veterinarian. São Luís, MA, Brazil. E-mail: fucuta_2@hotmail.com

[7] Curso de Medicina Veterinária, Centro Universitário do Sul de Minas (UNIS), Varginha, Minas Gerais, Brazil. bruna.ribeiro.vet@gmail.com

[8] Laboratório de Patologia Clínica, Universidade Estadual do Maranhão (UEMA), Cidade Universitária Paulo VI, Bairro Tirirical, São Luís, MA 65055-970, Brazil. E-mail: macedo.mir@gmail.com

RESUMO.- [**Respostas fisiológicas e bioquímicas e status de hidratação em equinos após dois percursos de três tambores**]. O perfil bioquímico e o status de hidratação de equinos em treinamentos ou competições fornecem dados importantes das suas respostas fisiológicas e metabólicas em relação ao tipo específico de exercício em uma modalidade esportiva. No presente estudo, o status hídrico e o perfil fisiológico-bioquímico de equinos foram avaliados durante treinamento de três tambores, em três tempos (T): em repouso, antes do início da atividade física (T0); imediatamente após 10 minutos de aquecimento ao trote seguido de duas corridas na pista de tambor, intervaladas em 10 minutos (T1); e após uma hora de descanso do segundo percurso (T2). Os parâmetros avaliados foram: frequência cardíaca (FC), frequência respiratória (FR), temperatura corporal (BT) e cor da mucosa; o tempo de enchimento capilar (TEC), volume globular ou hematócrito (VG), proteínas plasmáticas totais (TPP), creatinina sérica (Cre) e a ureia (Ure) foram avaliados e utilizados para inferir o estado hídrico dos animais; a osmolaridade plasmática (Osm) também foi mensurada; as concentrações dos eletrólitos sódio (Na), potássio (K), cloreto (Cl), cálcio total (tCa), magnésio total (tMg) e fósforo (P), e das enzimas musculares foram mensurados no soro, e as de glicose (Gli) e lactato (Lac) no plasma. Os dados das variáveis estudadas foram submetidos à ANOVA e ao teste de Tukey a 5% de probabilidade. Após o exercício (T1), a FC, FR, TC, VG, TPP, Gli, Lac, Cre aumentaram. O P também aumentou (P<0,05), mas não alcançou nível de hiperfosfatemia, e o K diminuiu (P<0,05), mas não ao nível de hipocalemia. Embora com médias menores, a FC, FR, TC, VG, K e o Lac não retornaram aos níveis basais (T0) após o repouso (T2), apenas a Gli, enquanto o fósforo diminuiu (P<0,05). A Osm, ureia, Na, Cl, tCa, tMg, CK e AST não variaram entre os tempos (P>0,05). Concluiu-se que, o exercício de intensidade máxima realizado em dois percursos de três tambores causou leve hemoconcentração, não alterou a osmolaridade plasmática nem importantes concentrações de eletrólitos e de enzimas musculares dos equinos, porém, causou hiperlactatemia, sem completa recomposição da concentração do lactato após uma hora de descanso.

TERMOS DE INDEXAÇÃO: Fisiologia, bioquímica, equinos, corrida de tambor, exercício.

INTRODUCTION

The type, intensity, and duration of exercise in equestrian modalities cause transitory physiological and metabolic changes in horses. Knowing these changes, it is possible to understand the responses of horses to the type of exercise and to monitor their adaptations to training (Padilha et al. 2017, Hunka et al. 2018). For this, in addition to a careful physiological examination, biochemical responses obtained in laboratory tests are essential in assessing the physical conditioning of a racing horse (Gomes et al. 2020).

During exercise, the water in the horse's body commonly varies due to the large amount of heat generated in the muscle that causes dehydration. In addition to water loss, there is loss of electrolytes such as sodium, potassium, chloride, calcium, and magnesium in the sweat. This hydroelectrolytic alteration alters plasma osmolarity, as it depends on the osmotic strength of the components present in the plasma that include, glucose, proteins, blood urea nitrogen and creatinine, in addition to the electrolytes (Lacerda-Neto et al. 2003).

High intensity exercise in short duration requires rapid energy production and consumption to support muscle work. In this metabolic process, the body intensifies anaerobic mechanisms, particularly anaerobic glycolysis, where lactic acid is generated and can increase rapidly in horses (Barbosa et al. 2016). Lactic acid is broken down into hydrogen and lactate ions, so the lactate concentrations in these tissues can infer about the levels of lactic acid in them, thus lactate has been used to indicate the capacity physical and adaptation of horses to the exercises imposed on them (Rodrigues et al. 2016, Binda et al. 2016, Gomes et al. 2019).

The Quarter Horse equine breed is classic in barrel racing competitions, in which the exercise is high intensity and of short duration, with predominance of anaerobic metabolism. The Quarter Horse breed they are present in approximately 45% of muscle fibers IIx (Snow & Valberg 1994), what justifies it as the preferred breed for this activity. Fast-twitch muscle fibers (type IIx) have a significant capacity to store glycogen, thriving mainly in anaerobic glycolysis. These fibers are essential in performing intense and "explosive" exercises over short distances. The energy of anaerobic glycolysis starts seconds after the beginning of the exercise, however, the moles of ATP generated by glucose are low in anaerobic glycolysis when compared to aerobic glycolysis, and the accumulation of lactic acid and rapid depletion of glycogen muscle, resulting from anaerobic glycolysis, would generate early muscle fatigue (Vermeulen et al. 2017).

On the other hand, based on studies carried out on human muscle fibers, Westerblad (2016) pointed out results contesting acidosis as a factor underlying the impairment of muscle contraction in fatigued muscles, and that there is no obvious causal relationship between acidosis and reduced production of fatigue strength, therefore, acidosis would not be a significant cause of skeletal muscle fatigue. The involvement of acidosis in skeletal muscle fatigue would occur in combination with other changes induced by fatigue or indirectly. For example, extensive production of lactic acid would cause a reduction in the amount of ATP acquired from glycogen stored in muscle fiber, which would limit performance during exercises in which glycogen depletion is a key factor. Post-exercise measurements of lactate and muscle enzymes in the blood of equine athletes have been commonly used in assessing the effectiveness of training and in the diagnosis of muscle injuries as result of exercise (Janicki et. 2012).

In Brazil, the barrel racing events have official circuits endorsed by the "Associação Brasileira de Criadores de Cavalos Quarto de Milha" (ABQM) and is quite widespread in different regions of the country. only a few studies have shown physiological and laboratory results of horses in this modality (Capelleto et al. 2009, Barbosa et al. 2016, Rodrigues et al. 2016, Souza et al. 2018, Binda et al. 2016, Gomes et al. 2019, 2020), Therefore, it is important and necessary to obtain results that express the organic responses of these animals under specific climatic conditions, so that a more scientific basis can be applied in the preparation of these animals during training.

Based on this reality, the present research studied laboratory parameters of Quarter Horse in barrel race training (three barrel) in the northeast of Brazil where the modality

is a highlight among equestrian sports. The evaluation of animals in barrel racing training will be useful to inform about the physiological and biochemical profiles of horses and, in particular, their hydration status after two courses, and whether resting for one hour is sufficient to recompose the possible homeostatic changes caused by exercise.

MATERIALS AND METHODS

The research was carried out at the "Haras Quatro Irmãos", located in the municipality of Raposa, Latitude -6.51667, Longitude -44.1833 6°31'0" South, state of Maranhão, Brazil.

The horses´ daily diet consisted of bulk: Tifton 85 hay (2% of the bodyweight of the horse), divided in two supplies a day at 9 a.m. and 5 p.m.; and concentrate (Equimax Premium - IRCA Nutrição Animal, associated to Equimax Balance - IRCA Nutrição Animal), with 135g/Kg crude protein and 3.970Kcal Kg^{-1}) digestible energy, supplied at 4.0kg/day: 1.5kg at 6 a.m.; 1.0kg at 11 a.m.; 1.5kg at 3 p.m.; 60g daily of mineral salt (Ircafós Equos 72 ADE - IRCA Nutrição Animal) associated with the concentrate, supplied to the animals in the morning and water *ad libitum*.

Ten Quarter Horses were used in the research, all raised in the same stud farm where the study was carried out. Horses were housed individually in 4.5 X 5.0 meters (m) masonry stalls, with floors covered by sawdust, a feeder, and automatic water cooler. The animals had participated in the last race in January 2016 and remained in training the following month, five days a week. The study was conducted in March 2016.

The equines were assessed (five animals/day, on two consecutive mornings): seven males and three females, five to eight years old (mean age 7.1), 360-492kg body weight (mean weight = 419.60), healthy and adapted to barrel racing tests. Temperature and relative humidity (T/RH) at the beginning and at the end of the training were, respectively: 27°C/67% and 30°C/66% (day 1); 25°C/68% and 30°C/67% (day 2).

The clinical assessments and venous blood samples collect were performed at the times (T): at rest, before the start of physical activity (T0); immediately after (at most three minutes) the horses complete two three-drum racing courses, with an interval of 10 minutes between the courses in which the animals were led at a pace in a shaded and covered area. Before the first course, the horses performed a 10-minute warm-up.; and after one hour's rest, held by the halter and kept in a shaded place (T2).

The track for the barril race was prepared in a similar way to that used in competition of this modality: on soft terrain, three barrels were positioned to form a triangle. Barrels 1 and 2 formed the base of the triangle and were 27.5m equidistant. Barrel 3, positioned as the top of the triangle, was 32.0m away from each of the other barrels. The start-finish line was marked parallel to an imaginary line between barrels 1 and 2, at 18.30m from these, in the opposite direction to the top of the triangle. On each course, the horse and rider sets bypassed the first barrel in a 360° turn from left to right, then the second and third barrels also in a 360° turn, but from right to left, and then headed for the finish line. In each course the horse-rider sets rounded the first drum in a 360° turn from left to right, then the second and third turns also at 360°, but from right to left, and headed for the finish line. They then immediately proceeded to a covered sandy area next to the course to evaluate the animals and collect the samples.

Clinical parameters such as heart rate (HR), respiratory rate (RR), body temperature (BT), mucous color, capillary refill time, absence of pain and inappetence, and laboratory tests such as packed cell volume (PCV) or hematocrit, glycemia and proteinemia were evaluated. These parameters were normal in all ten animals. Heart rate and respiratory rate were evaluated by auscultation using a stethoscope (Accumed Rappaport Premium Stethoscope) for one minute immediately after completing the second course, and the rectal temperature for three minutes.

Blood samples were collected, after antisepsis, by puncturing the jugular vein, placed in a flask containing sodium fluoride to obtain plasma (vacuum siliconized flask - 4.0ml - sodium fluoride - Vacuette), and in siliconized flasks without anticoagulant to obtain serum (vacuum siliconized flask - 4.0ml without anticoagulant - Vacuette).

The serum and plasma aliquots were kept frozen at -20°C until the time of the laboratory analyses, at the Laboratory of Clinical Analyses at the Federal University of Viçosa, State of Minas Gerais, Brazil. The following were measured in the serum: concentrations ([ ]) of the sodium ions (Na^+) and potassium ions (K^+) by flame photometry (B462 Flame Photometer Micronal, São Paulo, Brazil); concentrations of serum chloride (Cl^-), total calcium (tCa), total magnesium (tMg), blood urea nitrogen (BUN), creatinine (Cre), phosphorus (P), and aspartate aminotransferase (AST). Concentration of plasma glucose (GLU) and total proteins (TPP) were measured by multi-biochemical analyzer (HumanStar 300), and plasma osmolarity (Osm) was determined using freezing-point depression (Advanced Micro-Osmometer Model 3320 - Advanced Instruments Inc., Norwood/MA, USA).

Plasma lactate, serum creatine kinase (CK) and were measured in a semi-automatic biochemical analyzer model BIO-200 (Bioplus Products for Laboratories Ltda) at the "Laboratório de Patologia Clínica", "Universidade Estadual do Maranhão" (UEMA), Maranhão, Brazil.

In the statistical analysis, a completely randomized block design was used with three treatments (T0, T1 and T2) in 10 replications (number of animals). The data for the variables studied were submitted to the normality test. The normality test for variables that were not normal (glucose, CK and AST) was the Shapiro-Wilk test. Glucose and AST mathematically transformed by LOG on base 10 (LOG10) and CK by 1/CK (inverse). The normal data and the data normalized were submitted to ANOVA and the Tukey test at 5% probability. The analyses were made using the statistical analysis software program 9.4/2015 (Statistical Analysis System Institute - SAS Institute, SAS/STAT, USA).

RESULTS AND DISCUSSION

All values obtained in the pre-exercise or baseline (T0) time for the studied parameters were within normal limits, demonstrating that the animals presented normality (Table 1-4).

The heart rate (HR), respiratory rate (RR) and body temperature (BT) increased ($P<0.05$) after exercise (T1). Although they decreased after 1 hour's rest (T2), theses parameters were still higher than at the baseline time (T0) (Table 1). CRT did not change in the animals between times ($P>0.05$), although the means at T2 and T3 were greater than in T1 (Table 1).

Increase in the HR, RR and BT in the present study was similar to results found by Allaam et al. (2014) when evaluating Thoroughbred Horses after exercises at the same times established in the present study. These parameters also increased in Quarter Horses immediately after a barrel racing session, and after 30 and 120 minutes (min) recovery from exercise (Binda et al. 2016). These increases can be justified by because the increase in HR in the horse during exercise

occurs due to the increase in metabolic rates, as responses to adrenaline and glycolysis (Allaam et al. 2014), but also, to increased strength of cardiac contraction to maintain an adequate blood flow for perfusion and tissue oxygenation. Increase in RR is a response conditioned by the increase in pulmonary ventilation, the accumulation of metabolism products, decreased blood pH and increase in body temperature due exercise (Janicki et. 2012). The increase in body temperature is a fact commonly observed in horses after exercise. It is an expected answer, because horses have a high metabolic capacity and small surface area for heat dissipation. When exercising, approximately 20% of the metabolism in the horse's muscle cells is used for work and 80% becomes heat, increasing the body's internal heating (Wallsten et al. 2012).

The PCV increased (P<0.05) after exercise (T1) (Table 2). Capelleto et al. (2009) also found an increase in PCV in Quarter Horses after a three-barrel test, with slightly higher mean values than those obtained in the present study. Although slightly recomposed in T2, it was still increased in relation to the baseline time. The increase in PCV after exercise in the horses studied can be justified based on the following: when at rest, the horses maintain a splenic reserve of erythrocytes that, depending on the exercise, can be sent to the circulating blood by the response of the spleen to stimuli that alter sympathetic activity or as responses to plasma adrenaline concentrations. Thus, splenic erythrocytes are added to circulating ones, thus increasing the PCV in the blood and, effectively, the oxygen storage and transport capacity in erythrocyte hemoglobins. Concomitantly, blood viscosity increases. PCV also increases due to the change of fluids from the plasma to the tissues, and the increase in blood pressure and osmolarity in the muscles (Wickler & Anderson 2000, Böning et al. 2012).

The TPP increased at T2 (P<0.05) in relation to the other times (Table 2). PCV and TPP are used to diagnose dehydration in horses. Their values can characterize the hemoconcentration caused by water losses in sweat during exercise. So, it is possible that the increase in PPT in horses may have been generated by the greater loss of water in sweat and breathing that reduced the plasma volume. On the other hand, A slight increase in this marker (TPP) can be caused by a reduction in plasma volume and not by real dehydration, which can be caused by sweating (Zobba et al. 2011). Therefore, hemoconcentration can be explained by changes in intercompartmental fluid rather than a loss of corporeal fluid (McKeever et al. 1993). Demirtas (2018) considered that displacement of intercompartmental fluids may have been the reason for an increase in TPP concentrations in Arabian horses after exercises. Therefore, the increase in PCV and TPP in T1 was probably a result of water loss and, or displacement in the body, and the reductions that subsequently occurred after resting (T2), due to the return of fluids to the extracellular space that diluted the concentrations of solutes in the plasma.

Although PCV and PPT increased, signaling the presence of dehydration, this was not reflected by CRT. The CRT is also a useful parameter to infer dehydration in horses, and its increase has been seen in horses after exercise in different equestrian modalities (Wallsten et al. 2012, Binda et al. 2016, Demirtas 2018). The PCV, PPT and CRT values, analyzed together, characterized only the presence of mild dehydration in the horses (Table 1), so that the water status

Table 1. Mean values and standard deviations of heart rate, respiratory rate, rectal temperature, capillary refill time and mucous color in horses after two barrel racing courses

Parameter	Reference ranges	Evaluation time (T)		
		T0	T1	T2
Heart rate	30 - 40bpm	37.60±3.37^{C}	106.40±12.54^{A}	50.00±8.89^{B}
Respiratory rate	18 - 20 rpm	19.20±2.53^{C}	65.40±9.43^{A}	36.40±8.93^{B}
Rectal temperature	37.0 - 38.5ºC	37.21±0.39^{B}	39.49±0.71^{A}	38.86±0.80^{A}
Capillary refill time	< 2 seconds	1.20±0.42^{A}	1.60±0.52^{A}	1.60±0.70^{A}
Mucous color	Rose (normal)	Rose (normal)	Rose (normal)	Rose (normal)

T0 = time before training starts, T1 = immediately after training, T2 = one hour rest after T1; ^{A,B,C} Mean values on the same line followed by different uppercase letters differ between times (P<0.05) by the Tuckey test.

Table 2. Mean values and standard deviations of packed cel volume (PCV), total plasma proteins (TPP), creatinine, blood ureic nitrogen (BUN) and osmolality (Osm) in horses after two barrel racing courses

Parameter	Reference ranges	Evaluation time (T)		
		T0	T1	T2
PCV	32 - 50 %	33.60±2.88^{B}	48.70±5.50^{A}	41.60±4.79A^{B}
TPP	5.2 - 7.9 g dL^{-1}	7.55±0.31^{AB}	8.85±0.40^{A}	7.04±0.64^{B}
Creatinine	1.1 - 1.9 mg dL^{-1}	1.41±0.17^{B}	1.66±0.02^{A}	1.58±0.25^{AB}
BUN	22 - 48 mg dL^{-1}	34.70±7.45^{A}	36.90±6.57^{A}	36.30±6.78^{A}
Osm	270 - 310 mMol L^{-1}	298.60±16.87^{A}	312.50±19.54^{A}	299.20±21.47^{A}

T0 = time before training starts, T1 = immediately after training, T2 = one hour rest after T1; ^{A,B,AB} Mean values on the same line followed by tdifferent uppercase letters differ between times (P<0.05) by the Tuckey test.

may not have reached a degree of hypovolemia to the point of compromising the tissue perfusion of the animals, and therefore did not alter the CRT significantly.

There was an increase (P<0.05) in creatinine concentration after exercise (Table 2), corroborating results found in horses under exercise in the studies by Allann et al. (2014) and Monteiro et al. (2018). According to Toribio (2008), exercise can induce a slight increase in Cre concentrations, which is a creatine metabolism-derived product synthesized mainly in the kidneys, liver, and pancreas. In muscle, Cre is a non-enzymatic by-product derived from phosphocreatine (CPi) and its concentration is related to muscle mass and renal function. Large horses or those with large muscle mass, such as Quarter Horses, tend to have higher concentrations of creatinine. In the horse, Cre secretion and reabsorption are minimal. Therefore, increased Cre metabolism during intense physical exercise (Table 2), and the concomitant decrease in renal glomerular filtration (RGF) may have influenced its increase in T1.

Blood Urea Nitrogen (BUN) did not vary (P>0.05) between the times (Table 2), corroborating with Gomes et al. (2019) who also did not detect variations in the BUN in Quarter Horses during three-barrel training, although, McGowan & Hodgson (2014) reported that the BUN can exceed the normal limits in high or low exercise intensity, due to reduced renal blood flow or fluid loss. However, this did not occur in the present study.

There was no change in plasma osmolarity (Table 2). Osmolarity did not change between the times (P>0.05) because concentrations of important osmotically active substances in the extracellular space such as sodium, BUN and glucose did not exceed normal physiological limits. A similar fact was observed by Gomes et al. (2019) in Quarter Horses after a barrel race, in which plasma osmolarity remained at normal limits and the sodium, potassium, glucose and urea values remained at normal physiological limits. The maintenance of osmolarity in exercised horses can be explained based on physiological mechanisms. Increased osmolarity and reduced blood volume are, respectively, conditions for increased secretion and release of ADH into the circulation, which stimulates was reabsorption in the kidneys, partially helping to conserve fluid in the body. Therefore, the renal adjustment of water and salt excretion corrects the plasma volume and adjustment of the plasma osmolarity (Feher 2017).

The change in blood volume as hyper or hypovolemia induces a hormonal contraction, involving renin, aldosterone, vasopressin, and natriuretic peptide, among others. However, the effects of exercise may differ with respect to sprint (short) vs endurance (long duration). Therefore, a distinct change in osmolarity does not occur in all cases. For example, in prolonged exercises, the plasma volume decreases, generating hemoconcentration, while the plasma osmolarity remains practically unchanged (Coenen 2005). This may justify the fact that dehydration occurred in the horses in the post-exercise period, without significant changes in plasma osmolarity.

There was no change in serum sodium concentrations (P>0.05) between the studied times (Table 3). The results found for sodium corroborated those of Prado et al. (2019) who also did not find significant alterations in sodium in English Thoroughbred horses under intense effort. Gomes et al. (2019) also found no change in sodium concentrations in horses after a barrel race training session. Considering that the horses were already well conditioned for barrel racing, little loss of sweat sodium and renal resorption of the sodium supported the stability of this electrolyte in the test performed.

Another justification for the non-variation in sodium in exercised horses is based on systemic and renal hormonal processes. The hypothalamic-pituitary-adrenal axis (HPAA) is influential in renal sodium homeostasis, by increasing the synthesis of mineralocorticoid and by acting on the mineralocorticoid and glucocorticoid receptors in the kidneys. In this process, cortisol plays an imperative role, as it stimulates renal transport processes attributed to the renin-angiotensin-aldosterone system (RAAS), and its high concentration during exercise helps to maintain the stability of sodium in the blood (Prado et al. 2019). These results suggest that there is an important mechanism for maintaining osmolarity in horses during exercise, especially in relation to sodium, the most abundant component in the extracellular space.

The potassium concentration decreased (P<0.05) at the post-exercise (T1) and post-rest (T2) times (Table 3) but it remained within normal reference limits, not characterizing hypokalemia. As for potassium, the reduction of this electrolyte in horse serum was also verified by Di Filippo et al. (2009), after resistance competition, and by Linhares et al. (2017), in Mangalarga Machador horses, after completing a cavalcade, which are long duration equestrian events. These researchers raised the possibility that the decrease in potassium may also

Table 3. Mean values and standard deviations of sodium, potassium, chloride, total calcium and total magnesium in horses after two barrel racing courses

Parameter	Reference ranges	Evaluation time (T)		
		T0	T1	T2
Sodium	132 - 145 mMol L^{-1}	136.40±2.86^{A}	137.30±3.06^{A}	135.80±2.49^{A}
Potassium	2.4 - 4.7 mMol L^{-1}	3.78±0.21^{A}	3.52±0.21^{B}	3.45±0.26^{B}
Chloride	99 - 109 mMol L^{-1}	98.90±3.75^{A}	97.40±3.24^{A}	95.20±3.08^{A}
Total calcium	2.8 - 3.4 mMol L^{-1}	2.97±0.26^{A}	3.02±3.24^{A}	3.02±0.29^{A}
Total magnesium	0.9 - 1.5 mg dL^{-1}	0.90±0.08^{A}	0.95±0.15^{A}	0.86±0.14^{A}

T0 = time before training starts, T1 = immediately after training, T2 = one hour rest after T1; ^{A,B} Mean values on the same line followed by different uppercase letters differ between times (P<0.05) by the Tuckey test.

come from metabolic control in the kidneys, in which there is renal excretion of the potassium cation (K^+) and hydrogen proton (H^+), and reabsorption of the sodium cation (Na^+).

On the other hand, a decrease in post-exercise serum potassium was also observed in horses by Lacerda-Neto et al. (2003), after the animals performed low intensity exercise. Barbosa et al. (2016) also found a decrease in this electrolyte in horses, after a barrel race, but the concentration remained within normal concentrations for the species, similar to the results found in the present study. Another reason to justify this fact was presented by Muriel (2007) who stated that decrease in potassium can occur due to its rapid entry into the muscle cell after the interruption of exercise, by the action of the Na^+-K^+ pump that reduces its concentration in the blood.

In the present study, there was no change in chloride concentrations between the times (P>0.05) (Table 3). Chloride is the most concentrated electrolyte in the horse's sweat. More intense exercises cause greater chloride losses in sweating, which can reduce its serum concentration (Lacerda-Neto et al. 2003). A reduction in serum chloride was also observed in horses submitted to polo (Monteiro et al. 2018). However, Walker & Collins (2017) also did not observe changes in chloride in horses immediately following 20 minutes trotting, and immediately following a 2 min race. In the present study, the intensity of the exercise during two courses may not have caused significant chloride losses in the animals' sweat, preserving its normal blood concentrations. On the other hand, there are organic mechanisms that favor the cation-anion balance in the body, since [Cl^-] tends to be regulated secondarily to [Na^+] (Muriel 2007), which may also have influenced the results found, since sodium also did not vary during the three evaluation times adopted in this research.

The total calcium concentrations assessed in the horses also did not vary between times (P>0.05) (Table 3). Brazilian sport horses adapted and trained in a tropical climate, when submitted to training that consisted of flatwork exercises, aerobic conditioning and jumping over track and nature obstacles, also showed no serum calcium variations (Padilha et al. 2017). On the other hand, Crocomo et al. (2009) verified increased calcium in the blood of PSI horses after high intensity and long duration exercise. According to Coenen (2005), the influence of exercise on requirements for calcium is low, because it is possible that, due to the action of parathormone, the mobilization of calcium from the tissue to the blood is maintained, preserving its concentrations. So, it is also possible that [Ca] did not vary in the animals because the effort was not long, causing little perspiration and little loss of calcium in the sweat.

The total magnesium concentrations also did not vary significantly in the present study (P>0.05) (Table 3). Likewise, in a polo game, Monteiro et al. (2018) found no variation in serum magnesium in horses. On the other hand, Crocomo et al. (2009) found increased values of serum magnesium in PSI horses submitted to a 2000 meters gallop. In high-intensity exercise, the magnesium concentration increases because adenosines mono and diphosphate have much less affinity for magnesium than for ATP ions (Demirtas et al. 2015). The evaluation of magnesium in the blood of horses during physical activities is of great importance, because during muscle activity its concentration increases in the sarcoplasm, which reduces the flow of calcium through the sarcoplasmic reticulum membrane, generating muscle fatigue (Demirtas et al. 2015). However, as there are few studies on serum magnesium in horses and the results obtained are still mixed, further studies are needed to understand the effects of physical effort on magnesium concentrations in horses.

The phosphorus concentration was increased at T1 (P<0.05) (Table 4). Similar results were obtained in horses after intense exercise by Piccione et al. (2007) in PSI. Results without phosphorus variation after intense and maximum exercise in PSI horses were reported by Crocomo et al. (2009). This increase may be subsequent to ATP dephosphorylation to provide high energy phosphate for muscle contraction, due to the greater loss of vascular compartment fluid in proportion to phosphorus (Rose et al. 1993) or by adrenergic stimulation during intense physical exercise inducing parathyroid hormone (PTH), with subsequent increase in circulation phosphorus (Piccione et al. 2007, Crocomo et al. 2009). Moreira et al. (2015) found an increase in phosphorus in military horses after urban patrolling carried out both in the morning and afternoon, and considered that the increase may have occurred due to the reduction in the glomerular filtration rate (GFR) of this ion as a result of the exercise, because, during exercise, renal blood flow is reduced to supplement an increase in cardiac output and, subsequently, peripheral blood flow, especially in the muscles. They also pointed out that, as GFT decreases, there is approximately 85% phosphorus reabsorption in the contoured proximal tubules. All the justifications of the

Table 4. Mean values and standard deviations of phosphorum, glucose, lactate, creatine kinase (CK) and aspartate aminotransferase (AST) in horses after two barrel racing courses

Parameter	Reference ranges	Evaluation time (T)		
		T0	T1	T2
Phosphorum	2.5 - 5.6 mg dL^{-1}	2.89±0.39^B	3.38±0.46^A	2.16±0.37^C
Glucose	75 - 115 mg dL^{-1}	78.80±6.71^B	99.30±22.10^A	82.90±17.53^{AB}
Lactate	0.5 - 1.5 mMol L^{-1}	0.43 ± 0.09^C	20.71±4.99^A	6.24±1.98^B
CK	90 - 307 UI L^{-1}	177±49.38^A	185.20±26.77^A	160.00±27.77^A
AST	226 - 366 UI L^{-1}	250.40±34.88^A	282.20±46.30^A	254.60±21.56^A

T0 = time before training starts, T1 = immediately after training, T2 = one hour rest after T1; ^{A,B,C,AB} Mean values on the same line followed by different uppercase letters differ between times (P<0.05) by the Tuckey test.

respective authors mentioned in the paragraph also serve to support the increase in post-exercise phosphorus in the animals of the present study.

Phosphorus decreased at T2 in relation to T0 and T1 (P<0.05) (Table 3). Considering that phosphorum is extremely important for the formation of the ATP used as a source of energy in body aerobic metabolismo (Rose et al. 1993, Piccione et al. 2007), it is possible that this electrolyte was returned to the intracellular medium, thereby decreasing the serum concentrations previously increased by T1. Therefore, a physiological variation.

The glucose concentration increased in T1 (P<0.05), differing from T0 and T2 (Table 4) but it remained within normal reference limits, not characterizing hyperglicemia. Despite the significant variation in glucose, its mean values remained within the normal limits of reference at the three evaluation times, corroborating with Rodrigues et al. (2016) who also did not obtain an increase in the plasma glucose of Quarter Horses after a simulated barrel race exercise. On the other hand, the average values of the present study are still lower than those reported by McGowan & Hodgson (2014), of concentrations of 180 to 206mg dL^{-1} in horses that performed high intensity short duration exercises. Barbosa et al. (2016) also found an increase in blood glucose in horses immediately after a barrel race exercise, as also Souza et al. (2018), in Quarter Horses, immediately after the second three-barrel course.

Some studies have reported that the increase in blood glucose after exercise may be due to hepatic glycogenolysis and gluconeogenesis, in response to the energetic need to maintain muscle activity (Allaam et al. 2014), and because of the increase in blood cortisol and catecholamines, with concomitant reduction insulin, causing an increase in blood glucose (Barbosa et al. 2016). However, the lactate is the main non-glycidic substrate for glucose synthesis (gluconeogenesis) during high intensity exercises. In high intensity and short duration exercise - such as the barrel race - the excess of pyruvic acid produced is biotransformed into lactate. In red blood cells as well as the exercising muscle tissue that favors anaerobic metabolism, glucose is converted to pyruvate and subsequently to lactate. Lactate is secreted into plasma and picked up by the liver for conversion into glucose in Cori cycle via a redox reaction catalyzed by lactate dehydrogenase (Draoui & Feron 2011).

Plasma lactate concentration increased at T1 (P<0.05) (Table 4), reaching limits of hyperlactatemia: >5mMol L^{-1} (Goméz e Mizok. 2017). Comparing lactate increases after exercise in the horses studied, similar results were seen in Quarter Horses during barrel race (Rodrigues et al. 2016, Souza et al. 2018) and "vaquejada" (Binda et al. 2016). This increase occurred because anaerobic glycolysis is a rapid ATP production pathway caused by the partial break down of glucose. In this process, lactic acid is fractioned into hydrogen and lactate as the product of this glycolytic metabolismo (Barbosa et al. 2016) and both increase in the blood.

It is of great importance to highlight that the increase in blood lactate concentration is called hyperlactatemia, which may or may not be associated with acidemia (pH<7.35). Lactic acidosis is a situation where lactate production exceeds clearance and acidemia and hyperlactatemia occur simultaneously. Although used as a marker of anaerobic metabolism and tissue hypoxia, lactate is not a "malignant" molecule and not only a residual product of anaerobiosis, but a fundamental participant in metabolism and energy homeostasis, being produced from pyruvate reduction by the action of the enzyme lactate dehydrogenase (LDH) in different cells in the body, mainly in skeletal muscle, skin, brain and red blood cells (Goméz e Mizok 2017).

A slight recomposition of lactate concentration was observed after resting. But, although decreased in T2 compared to T1 (P<0.05), it remained higher than at T0 (P<0.05), and at levels of discrete hyperlactatemia (Table 4). Similarly, Gomes et al. (2019, 2020) also did not find recovery of the plasma lactate concentration in Quarter Horses after resting for 40 min at the end of a course, and after resting for 60 min at the end of two three-drum courses, respectively. However, Allaam et al. (2014) obtained a significant increase in lactate in Throroughbred Horses, five minutes after exercise, which returned to baseline levels after one hour of rest. Lactate recomposition after rest is attributed to gluconeogenesis that metabolizes lactate to glucose. As for the consumption of lactate circulating in the body, its uptake and daily release occur mainly in the liver and kidneys, which use it as a substrate for the regeneration of glucose through the process of gluconeogenesis. But, during resting conditions, it is also partially metabolized by oxidation in many organs such as the heart, brain, and skeletal muscle, through the Krebs cycle, to generate adenosine triphosphate (ATP) (Goméz and Mizok 2017).

Plasma lactate concentrations depend on your turnover (lactate synthesis minus its uptake in tissues). At the end of the exercise, it is lower than that produced during the exercise due to the uptake of lactate by the tissues, including neoglycogenesis (Benetti et al. 2000). Based on this, an athlete under frequent training could have a greater capacity for neoglycogenesis than an untrained one. So, this can be useful for Veterinarians and trainers in conditioning sports horses during training and equestrian events, not with the sole concern that horses show less post-exercise lactate production, but the ability to consume and recompose concentrations of lactate after the end of the exercise. This can be accomplished by comparing the neoglycogenic activity of the equine athlete to the type of exercise, verifying whether after an exercise under a specific intensity and duration, plasma lactate concentrations in trained horses are lower in relation to those of untrained, suggesting an increase in neoglycogenic activity.

CK and AST are proteins released after the increased permeability of sarcolemma in the musculoskeletal cell, due to physical effort, which, when intense, can generate acute muscle damage (Padilha et al. 2017). Binda et al. (2016), also did not find variation in the enzymes CK and AST in horses after barrel race exercise in tropical conditions, and neither did Hunka et al. (2018) in puller or vaquejada helper horses, and attributed this to the fact that the animals were in good physical condition for this purpose. Likewise, the horses in the present study were also adapted and in continuous barrel racing activity, with good adaptation and good muscle conditioning.

The values of CK and AST did not differ between the evaluated times (P>0.05) and were within normal limits (Table 4). Rodrigues et al. (2016) found a higher mean serum CK concentration in horses in a simulated barrel race, after a four-hour rest at the end of the exercise, even greater than that

obtained immediately after the exercise. These researchers also found no significant variations for [AST]. Assessing serum amyloid A (SAA) protein, CK and AST in ten horses that had jumped over a meter high obstacles, Carvalho Filho et al. (2019), found no significant difference in the biomarkers SAA and AST between the pre-exercise moments, and 30 min, 60 min and 24h post-exercise, the CK increased after 30 min from the end of the exercise, but was already stabilized in 24h.

According to Barrelet & Ricketts (2002), repetitive and adequate exercises induce the physiological adaptation of horses to stress exercise, reducing extracellular changes harmful to muscle cells. So, as [CK] and [AST] are related to exercise type and intensity, it is possible that, by the end of two barrel races, the intensity did not reach a degree of effort beyond the physical conditioning that the animals were already adapted to perform and there was no influence on the values of these enzymes. However, it is important to consider that the maximum CK peak occurs between 6 and 12 hours after muscle injury, and AST, between 24 and 36 hours, and since measurements were taken inf this study only until one hour after exercise, it is possible that their enzyme levels would have not yet reached higher concentrations in animals.

Although CK and AST have been commonly used as skeletal muscle (SKM) injury biomarkers, the certainty of the occurrence of muscle injuries based on these enzymes has been reassessed. Second Chanoit et al. (2001), the plasma CK value, which is a standard clinical marker, may be interpreted differently depending on the physical performance of the subject, and peak plasma CK activity does not provide a realistic assessment of the amount of damaged muscle, and, thus, it is a relatively crude indicator of muscle damage.

Gondin et al. (2013) analyzed the acute phase response (APR) in fifteen clinically healthy "high-goal" polo ponies of a Brazilian elite polo team by quantifying the physiological variables of venous blood and acute phase proteins (APP) 5 minutes, 6 and 12 hours after a pole training, which is of high intensity for all positions of the game in which horses are used. The researchers found that changes in muscle membrane permeability occurred in all horses, based on that of CK without correlation with APR, and a significant increase in total serum proteins, albumin, ceroplasmin, haptoglobin, alpha-1 antitrypsin, and 23-kDa proteins during the physical effort of the match, demonstrating that high intensity exercise at the equestrian pole causes an acute phase response of relatively short duration and non-inflammatory, and that the change in APR was just a variation related to physiological stress as a function of exercise.

Skeletal troponin I (sTnI), myosin light chain 3 (Myl3), and creatine kinase muscle isoform (CKm) proteins have been shown recently to be biomarkers more sensitive and specific for monitoring drug-induced SKM injury in rat toxicology studies (Vlasakova et al. 2017). Quantitative measurement of sTnI, Myl3, CKm and lipid transport protein fatty acid binding protein 3 (FABP3) were studied by Burch et al. (2015) in human serum with important muscular dystrophies and compared with the plasma CK concentration, aiming to verify if these proteins would better reflect the patients' disease state than the CK activity. The authors concluded that the different profiles of these proteins in the three muscular dystrophies suggested different mechanisms that regulate their release in the circulation. The potentially increased specificity for skeletal muscle injury and the correlation with clinical outcomes in the patients studied suggested that these biomarkers could be a valuable non-invasive tool for monitoring the progression of muscle disease. Vlasakova et al. (2017), obtained findings that supported the conclusion that sTnI, Myl3, and CKm are sensitive early tissue leakage biomarkers for monitoring SKM injury and effects of exercise in dog. Future research may elucidate the value of these proteins in monitoring horses with the possibility of musculoskeletal injuries, guiding the directions of clinical biochemistry regarding the use of biomarkers in equine physiology.

CONCLUSION

The maximum intensity exercise performed in two drum runs did not alter the plasma osmolality, the electrolyte and muscle enzyme concentrations of the horses, and caused only a mild hemoconcentration that was already recomposed after resting for an hour. However, it caused hyperlactatemia without the plasma lactate concentrations being fully recomposed after resting.

Acknowledgements.- The authors thank the "Fundação de Amparo à Pesquisa e ao Desenvolvimento Científico e Tecnológico do Maranhão" (FAPEMA), Maranhão, Brazil, for funding research grants for Alves A.M. (FAPEMA-BIC 02415/15) and Fucuta R.S, (FAPEMA-BIC 04190/16); "Coordenação de Aperfeiçoamento de Pessoal de Nível Superior" (CAPES), Brazil, for partial financing/Finance code 001; "Haras Quatro Irmãos", Maranhão, Brazil, for granting the location and the horses for the animal experiment; "Laboratório de Patologia Clínica" (LPC), of the "Universidade Estadual do Maranhão" (UEMA), Maranhão, Brazil; and "Laboratório de Pesquisa em Patologia Clínica Veterinária" (LPPCV) of the "Universidade Federal de Viçosa" (UFV), Minas Gerais, Brazil, for carrying out the laboratory analyzes.

Bioethics and biossecurity committee approval.- The research was approved by the Ethics Commission on Animal Experimentation (CEEA) of the Veterinary Medicine Course at the "Universidade Estadual do Maranhão" (UEMA), Maranhão state, Brazil, protocol number 10/2016.

Conflict of interest statement.- The authors declare there are no conflicts of interest. The founding sponsors had no role in the design of the study, in the collection, analysis, or data interpretation, in the writing of the manuscript, and in the decision to publish the results.

REFERENCES

Allaam M., Elseady Y., Nayel M., Elsify A., Salama A., Hassan H., Hassan M. & Kamar A. 2014. Physiological and hemato-chemical evaluation of thoroughbred race horse after exercise. IJAVMS 8(3):81-93.

Barbosa J.P.B., Denadai D.S., Gerardi B., Pereira M.A., Chaves A.A., Gomide L.M.W., Peiró J.R. & Mendes L.C.N. 2016. Endoscopic airway, blood gas, electrolytes, and acid-base in equine submitted to three-barrel training. Arq. Bras. Med. Vet. Zootec. 68(5):1152-1158. <https://dx.doi.org/10.1590/1678-4162-8739>

Barrelet A. & Ricketts S. 2002. Haemnatology and blood biochemnistry in the horse: a guide to interpretation. In Practice 24(6):318-327. <https://dx.doi.org/10.1136/inpract.24.6.318>

Benetti M., Santos R.T. & Carvalho T. 2000. Cinética de lactato em diferentes intensidades de exercícios e concentrações de oxigênio. Revta Bras. Med. Esporte 6(2):50-56. <https://dx.doi.org/10.1590/S1517-86922000000200004>

Binda M.B., Teixeir F.A., Carvalho R.S., Macedo L.P., Conti L.M.C., Manso Filho H.C. & Coelho C.S. 2016. Effects of 3-Barrel racing exercise on electrocardiographic

and on blood parameters of Quarter Horses. J. Equine Vet. Sci. 47:71-76. <http://dx.doi.org/10.1016/j.jevs.2016.08.001>

Böning D., Maassen N. & Pries A.R. 2012. The optimal hematocrit increases during exercise. J. Appl. Physiol. 113(7):1168. <http://dx.doi.org/10.1152/japplphysiol.00957.2012>

Burch P.M., Pogoryelovac O., Goldsteina R., Bennettb D., Guglieric M., Straubc V., Bushbyc K., Lochmuller H. & Morrisb C. 2015. Muscle-derived proteins as serum biomarkers for monitoring disease progression in three forms of muscular dystrophy. J. Neuromuscul. Dis. 2(3):241-255. <https://dx.doi.org/10.3233/JND-140066> <PMid:26870665>

Capelleto E.C., Angeli A.L. & Graff H. 2009. Physiological answers in quarter horses after barrel racing. Revta Acad. Ciênc. Agrár. Ambient. 7(3):299-304.

Carvalho Filho W.P., Fonseca L.A., Girardi F.M., Bento L.D., Souto P.C. & Orozco A.M.O. 2019. Serum amyloid A and muscle activity biomarkers in horses submitted to equestrian show jumping. Pesq. Vet. Bras. 39(8):668-671. <https://dx.doi.org/10.1590/1678-5150-PVB-6218>

Chanoit G.P., Lefebvre, H.P., Orcel K., Laroute V., Toutain P.L. & Braun J. 2001. Use of plasma creatine kinase pharmacokinetics to estimate the amount of exercise-induced muscle damage in Beagles. Am. J. Vet. Res. 62(9):1375-1380. <http://dx.doi.org/10.2460/ajvr.2001.62.1375> <PMid:11560263>

Coenen M. 2005. Exercise and stress: impact on adaptive processes involning water and electrolytes. Livest. Prod. Sci. 92(2):131-135. <https://dx.doi.org/10.1016/j.livprodsci.2004.11.018>

Crocomo L.F., Balarin M.R.S., Takahira R.K. & Lopes R.S. 2009. Serum macro minerals in adults thoroughbred horses, before and after the high intensity exercise. Revta Bras. Sáude Prod. Anim. 10(4):11-16.

Demirtas B. 2018. Physical, haematological and biochemical responses of arabian horses to jereed (Javelin Swarm) competition. Kafkas Univ. Vet. Fak. Derg. 24(2):219-226. <http://dx.doi.org/10.9775/kvfd.2017.18674>

Demirtas B., Yaramis C.P. & Atmaca M. 2015. Exercise-induced physiological fatigue in horses: review. Turkiye Klinikleri J. Vet. Sci. 6(2):60-66. <http://dx.doi.org/10.5336/vetsci.2016-51263>

Di Filippo P.A., Gomide L.M.W., Orozco C.A.G., Silva M.A.G., Martins C.B., Lacerda Neto J.C. & Santana Á.E. 2009. Changes in electrolytes and blood gases in arabian horses during 60 km endurance race. Ciênc. Anim. Bras. 10(3):840-846. <http://dx.doi.org/10.5216/cab.v10i3.1535>

Draoui N. & Feron O. 2011. Lactate shuttles at a glance: from physiologigal paradigms to anti-cancer treatments. Dis. Model Mech. 4(6):727-732. <https://dx.doi.org/101242/dmm.007724> <PMid:22065843>

Feher J. 2017. Hypothalamus and pituitary gland, p.870-882. In: Ferrer J. (Ed.), Quantitative Human Physiology: an introdution. 2nd ed. Academic Press, U.S.A.

Gomes C.L.N., Ribeiro Filho R.F., Silva L.P., Aranha R.M.C., Moraes Júnior F.J., Cardoso J.K.M. & Monteiro L.C. 2019. Physiological and biochaemical parameters of horses in three-barrel training: post-warm-up, post-exercise and post-rest. Arq. Bras. Med. Vet. Zootec. 71(2):631-639. <https://dx.doi.org/10.1590/1678-4162-10270>

Gomes C.L.N.G., Alves A.M., Ribeiro Filho J.D., Moraes Junior F.J., Chaves R.M., Aranha R.M.C., Fucuta R.S. & Ribeiro B.M. 2020. Exercise training session-induced metabolic acidosis in barrel racing horses Acidose metabólica induzida por sessão de treinamento em equinos de tambor. Ciênc. Rural 50(5):e20180887 <http://dx.doi.org/10.1590/0103-8478cr20180887>

Goméz H. & Mizok B.A. 2017. Hyperlactatemia and lactic acidosis, p.394-404. In: Ronco C., Bellomo R., Kellum J.A. & Ricci Z. (Eds,), Critical Care Nephrology. 3rd ed. Elsevier, Philadelphia.

Gondin M.R., Foz N.S.B., Pereira M.C., Flagliari J.J., Orozco C.A.G., D'Angelis F.H.F., Queiroz-Neto A. & Ferraz G.C. 2013. Acute Phase responses of different positions of high-goal (elite) polo ponies. J. Equine Vet. Sci. 33(11):956-961. <https://dx.doi.org/10.1016/j.jevs.2013.02.005>

Hunka M.M., Souza L.A., Almeida T.H.S., Nery P.C.R., Manso H.E.C.C.C. & Manso Filho H.C. 2018. Metabolic and physiological changes during and after vaquejada exercise in horses. Med. Vet., Recife, 12(4):254-262. <https://dx.doi.org/10.26605/medvet-v12n4-2454>

Janicki B., Kochowicz A., Cigan-Szczezielniak D. & Krumrych W. 2012. Fundamental of exercise physiology in horse. Med. Weter. 68(6):326-327.

Lacerda-Neto J.C., Sampaio R.C.L., Ferraz G.C., Teixeira-Neto A.R., Pereira D.M., Titto E.A.L., Carvalho M.B. & Queiroz-Neto A. 2003. Effects of intermittent water cooling and electrolyte supplements on serum osmolality and electolytes of horses during low-intensity exercise. Revta Port. Ciênc. Vet. 98(548):189-195.

Linhares J.M., Di Filippo P.A., Bogossian P.M., Guerra R.V.B.A., Bustamante S.R.B., Carvalho C.B. & Ferreira F.S. 2017. Physical exercise on serum electrolytes and acid base balance in mangalarga marchador horses submitted to cavalcade of 4, 8 and 20km. Ciênc. Rural 47(5):1-6. <https://dx.doi.org/10.1590/0103-8478cr20160277>

McGowan C.M. & Hogdson D.R. 2014. Haematology and biochemistry, p.56-68. In: Hodgson D.R., McKeever K.H. & McGowan C.M. (Eds), The Athletic Horse. 2nd ed. Elsevier Saunders, China.

McKeever K.H., Hinchcliff K.W., Reed S.M. & Robertson J.T. 1993. Role of decreased plasma volume in hematocrit alterations during incremental treadmill exercise in horses. Am. J. Physiol. 265(2 Pt 2):404-408. <https://dx.doi.org/10.1152/ajpregu.1993.265.2.R404> <PMid:8368395>

Monteiro L.C., Ribeiro Filho J.D., Dantas W.M.F., Ribeiro B.M., Silva M.O, Costa C.M., Ermita P.A.N., Silva G.M.M. & Campos C.H.C. 2018. Effect of ad libitum intake of an electrolyte repository in horses that underwent a polo game. Semina, Ciênc. Agrárias 39(1):187-198. <https://dx.doi.org/10.5433/1679-0359.2018v39n1p187>

Moreira D.O., Leme F.O.P., Marques M.M., Leão N.F., Viana W.S., Faleiros R.F. & Alves G.E.S. 2015. Concentrações de proteínas totais, glicose, cálcio, fósforo, lactato, ureia e creatinina em equinos de cavalaria militar antes e após trabalho de patrulhamento urbano. Ciênc. Anim. Bras. 16(1):73-80. <https://dx.doi.org/10.1590/1089-6891v16i115233>

Muriel M.G. 2007. Equilíbrio hidroeletrolítico, p.87-101. In: Boffi F.M. (Ed.), Fisiolgia del Ejercicio en Equinos. Inter-Médica, Buenos Aires.

Padilha F.G.F., Dimache L.A.G., Almeida F.Q. & Ferreira A.M.R. 2017. Blood biochemical parameters of Brazilian sport horses under training in tropical climate. Revta Bras. Zootec. 46(8):678-682. <https://dx.doi.org/10.1590/s1806-92902017000800008>

Piccione G., Giannetto C., Costa A., Fazio F. & Caola G. 2007. Effects of high intensity exercise on serum electrolytes and protein in thoroughbred horses. Magy Allatorvosok Lapja 129(4):208-213.

Prado R.O.F., Morales B.J.E., García M.L., Molina-Ochoa J., Valpuesta S.G., Hernández R.J.A. & García C.A.C. 2019. Effects of exercise on cations/anions in blood serum of English Thoroughbred horses. Arq. Bras. Med. Vet. Zootec. 71(3):909-916. <https://dx.doi.org/10.1590/1678-4162-10830>

Rodrigues I.M.S.M.M., Spindola B.F. & Botteon P.T.L. 2016. Biochemical and oxidative profile of horses used in simulated three-barrel test. Revta Bras. Med. Vet. 38(supl.2):93-100.

Rose R.J., Allen J.R., Hodgson D.R. & Stewart J.H. 1983. Responses to sumaximal treadmill exercise in the horses: changes in haematology, arterial blood gas and acid base measurements, plasma biochemical values and heart rate. Vet. Rec. 113(26/27):612-618. <PMid:6665971>

Snow D. & Valberg S. 1994. Muscle anatomy, physiology and adaptations to exercise and training, p.145-179. In: Hodgson D.R. & Rose R.J. (Eds), The Atletic Horse: principles and practice of equine sports medicine. W.B. Saunders, Philadelphia.

Souza L.A., Hunka M.M., Nery P.C.R., Coelho C.S., Manso H.E.C.C.C. & Manso Filho H.C. 2018. The effect of repeated barrel racing on blood biomarkers and physiological parameters in Quarter Horses. Comp. Exerc. Physiol. 14(1):47-54. <https://dx.doi.org/10.3920/CEP170019>

Toribio R. 2008. Essentials of equine renal and urinary tract physiology. Vet. Clin. N. Am., Equine Pract. 23(3):533-561. <https://dx.doi.org/10.1016/j.cveq.2007.09.006> <PMid:8061849>

Vermeulen R., Meeûs C., Plancke L., Boshuizen B., Bruijn M. & Delesalle C. 2017. Effects of training on equine muscle physiology and muscle adaptations in response to different training approaches. Vlaams Diergen. Tijds. 86:224-230. <https://dx.doi.org/10.21825/vdt.v86i4.16183>

Vlasakova K., Lane P., Michna L., Muniappa N., Sistare F.D. & Glaab W.E. 2017. Response of novel skeletal muscle biomarkers in dogs to drug-induced skeletal muscle injury or sustained endurance exercise. Toxicol. Sci. 156(2):422-427. <https://dx.doi.org/10.1093/toxsci/kfw262>

Walker E.J. & Collins S.A. 2017. The effect of exercise intensity and use of an electrolyte supplement on plasma electrolyte concentrations in the standardbred horse. Can. J. Anim. Sci. 97(4):668-672. <https://dx.doi.org/10.1139/CJAS-2016-0189>

Wallsten H., Olsson K. & Dahlborn K. 2012. Temperature regulation in horses during exercise and recovery in a cool environment. Acta Vet. Scand. 54(1):42. <https://dx.doi.org/10.1186/1751-0147-54-42> <PMid:22805591>

Westerblad H. 2016. Acidosis is not a significant cause of skeletal muscle fatigue. Med. Sci. Sports Exerc. 48(11):2339-2342. <https://dx.doi.org/10.1249/MSS.0000000000001044> <PMid:27755383>

Wickler S.J. & Anderson T.P. 2000. Hematological changes and athletic performance in horses in response to high altitude (3.800 m). Am. J. Physiol. Regul. Integr. Comp. Physiol. 279(4):R1176-R1181. <https://dx.doi.org/10.1152/ajpregu.2000.279.4.R1176> <PMid:11003981>

Zobba R., Ardu M., Niccolini S., Cubeddu F., Dimauro C., Bonelli P., Dedola C., Stefano V, & Parpaglia M.L.P. 2011. Physical, hematological, and biochemical responsesto acute intense exercise in polo horses. J. Equine Vet. Sci. 31(9):542-548. <https://dx.doi.org/10.1016/j.jevs.2011.03.010>

PESQUISA VETERINÁRIA BRASILEIRA
Brazilian Journal of Veterinary Research
ISSN 0100-736X (Print)
ISSN 1678-5150 (Online)

Pesq. Vet. Bras. 40(12):1002-1009, December 2020
DOI: 10.1590/1678-5150-PVB-6739

Original Article
Small Animal Diseases
BY-NC

Clinical-pathological and immunohistochemical evaluations of cardiac lesions in cats with chronic kidney disease[1]

Gabriela C. Cid[2]*, Mariana P.B. Jardim[3], Amanda C. Jesus[3], Samay Z.R. Costa[4], Ilka N. Gonçalves[5], Tiago C. Peixoto[6], Heloisa J.M. Souza[7] and Vivian A. Nogueira[8]

ABSTRACT.- Cid G.C., Jardim M.P.B., Jesus A.C., Costa S.Z.R., Gonçalves I.N., Peixoto T.C., Souza H.J.M. & Nogueira V.A. 2020. **Clinical-pathological and immunohistochemical evaluations of cardiac lesions in cats with chronic renal disease.** *Pesquisa Veterinária Brasileira 40(12):1002-1009.* Universidade Federal Rural do Rio de Janeiro, Rodovia BR-465 Km 7, Zona Rural, Seropédica, RJ 23890-000, Brazil. E-mail: gabrieladecarvalhocid@gmail.com

Chronic kidney disease (CKD) is characterized by irreversible morphostructural lesions that can progressively evolve to chronic renal insufficiency and kidney failure. It is known that the heart and kidneys are closely related, and that communication between these organs occurs through a variety of pathways; subtle physiological changes in one of them are compensated by the other. Histopathological cardiac evaluation through routine staining presents a limitation to identify specific or discreet lesions in the cardiomyocytes. This study aimed to evaluate serum troponin levels in cats with CKD, associated with clinical and pathological findings, as well as to correlate the morphostructural cardiac lesions to determine their distribution through macroscopic and histological assessments and anti-cardiac troponin C (cTnC) immunohistochemistry (IHC). To this end, 20 cats (18 diagnosed with CKD and two controls) were selected. Anti-human cTnC IHC was conducted after necropsy and separation in eight regions of each collected heart. Heart fragments from two cats without CKD were used as controls. The anti-human cTnC antibody is useful in detecting cardiac lesions and has shown decreased expression in cardiomyocytes of cats with CKD. Serum troponin was above the reference values in 11/18 (61.11%) animals and decreased expression for the cTnC antibody was observed in individual cardiomyocytes in 9/18 (50%) animals. It was verified that the number of regions with decreased expression for the cTnC antibody in cardiomyocytes is significantly correlated with serum troponin. The anti-human cTnC antibody has been found effective in detecting cardiac lesions and has shown decreased expression in the cardiomyocytes of cats with CKD. Correlation was observed between increased serum cTnI and loss of immunoreactivity at anti-cTnC antibody IHC in cats with CKD, which proves damage to cardiomyocytes secondary to kidney disease.

INDEX TERMS: Clinics, pathology, immunohistochemistry, cardiac lesions, cats, renal disease, troponin, biomarker, cardiology, nephrology.

[1] Received on July 30, 2020.
Accepted for publication on August 10, 2020.

[2] Graduate Program in Veterinary Medicine, Departamento de Epidemiologia e Saúde Pública (DESP), Universidade Federal Rural do Rio de Janeiro (UFRRJ), Rodovia BR-465 Km 7, Zona Rural, Seropédica, RJ 23890-000, Brazil. *Corresponding author: gabrieladecarvalhocid@gmail.com

[3] Graduate Program in Veterinary Medicine, Departamento de Medicina e Cirurgia Veterinária (DMCV), Universidade Federal Rural do Rio de Janeiro (UFRRJ), Rodovia BR-465 Km 7, Zona Rural, Seropédica, RJ 23890-000, Brazil. E-mails: jardim.marii@gmail.com, amanda.ufpr@yahoo.com.br

[4] Laboratório de Ensino Pesquisa Extensão e Produção (LEPEP), Patologia Veterinária do Instituto Federal Farroupilha, Campus Frederico Westphalen, Rodovia BR-386 Km 40, Frederico Westphalen, RS 98400-000, Brazil. E-mail: samayzillmann@gmail.com

[5] Veterinarian, Salvador, BA, Brazil. E-mail: ilkavet@gmail.com

[6] Departamento de Anatomia, Patologia e Clínicas Veterinárias, Escola de Medicina Veterinária e Zootecnia, Universidade Federal da Bahia (UFBA), Av. Adhemar de Barros s/n, Bairro Ondina, Salvador, BA 40170-110, Brazil. E-mail: tcpeixoto@ufba.br

[7] Departamento de Medicina e Cirurgia Veterinária (DMCV), Universidade Federal Rural do Rio de Janeiro (UFRRJ), Rodovia BR-465 Km 7, Zona Rural, Seropédica, RJ 23890-000, Brazil. E-mail: heloisajusten@yahoo.com.br

[8] Departamento de Epidemiologia e Saúde Pública (DESP), Universidade Federal Rural do Rio de Janeiro (UFRRJ), Rodovia BR-465 Km 7, Zona Rural, Seropédica, RJ 23890-000, Brazil. E-mail: vivianmedvet@yahoo.com.br

RESUMO.- [**Avaliações clínico-patológica e imuno-histoquímica de lesões cardíacas em gatos com doença renal crônica.**] A doença renal crônica (DRC) é caracterizada por lesões morfoestruturais irreversíveis, que podem evoluir progressivamente para insuficiência renal crônica e falência renal. Sabe-se que o coração e os rins mantêm estreita relação e a comunicação entre esses órgãos ocorre por uma variedade de vias; alterações fisiológicas sutis em um desses órgãos são compensadas pelo outro. A avaliação histopatológica cardíaca mediante a colorações rotineiras são limitadas para identificar lesões específicas ou discretas em cardiomiócitos. O presente trabalho teve como objetivos avaliar os níveis séricos de troponina em gatos com DRC, associados aos achados clínico-patológicos, bem como correlacionar as lesões cardíacas morfoestruturais, a fim de determinar a distribuição destas, por meio da avaliação macroscópica, histológica e imuno-histoquímica com anti-cTnC. Neste estudo foram selecionados 20 gatos (18 diagnosticados com DRC e 2 animais controle). Para a aplicação da técnica de imuno-histoquímica anti-troponina C humana, necropsias foram realizadas e cada coração coletado separadamente em 8 regiões. Fragmentos do coração de 2 gatos sem lesão cardíaca foram utilizados como controle. O anticorpo anti-TnC humano é útil na detecção de lesões cardíacas e apresentou expressão diminuída em cardiomiócitos de gatos com DRC. Em 11/18 animais (61,11%) a troponina sérica encontrava-se acima dos valores de referência e foram observadas diminuição da expressão para anticorpo-cTnC em cardiomiócitos individuais em 9/18 (50%). Notou-se que o número de regiões com diminuição da expressão para anticorpo-cTnC em cardiomiócitos está significativamente correlacionado com a troponina sérica. O anticorpo anti-TnC humano se mostrou eficaz para detectar lesões cardíacas e demonstrou diminuição da expressão nos cardiomiócitos de gatos com DRC. Houve correlação entre o aumento da CTnI sérica e perda da imunorretividade na avaliação imuno-histoquímica com anticorpo anti-TnC em gatos com DRC o que comprova danos em cardiomiócitos secundários a doença renal.

TERMOS DE INDEXAÇÃO: Clínica, patologia, imuno-histoquímica, lesões cardíacas, gatos, doença renal, troponina, biomarcador, cardiologia, nefrologia, felinos.

INTRODUCTION

Chronic kidney disease (CKD) is characterized by irreversible morphostructural lesions that can progressively evolve to chronic renal insufficiency and kidney failure. Kidney failure leads to disruption of metabolic and endocrine functions, hydroelectrolytic and acid-base disorders (Ribeiro et al. 2008), and changes in cardiac function (Martin & Franco 2005). CKD occurs with high frequency in pets, with a prevalence of 30-40% in feline species (Polzin et al. 2005). Consequently, there is a decrease in the ability of this organ to concentrate and eliminate certain toxic substances that, under normal conditions, are eliminated from the body by renal excretion (Polzin et al. 2005).

It is known that the heart and kidneys are closely related, and that communication between these organs occurs through a variety of pathways; subtle physiological changes in one of them are not always compensated by the other (Viswanathan & Gilbert 2011). Cardiac alterations in humans with chronic renal insufficiency were first described in 1947. Macroscopically, there was marked ventricular hypertrophy and fibrosis, and intense interstitial edema was observed on histological examination of the myocardium. That study suggested that the cause of death had been uremia, given that routine clinical dialysis was not available at the time (Langendorf & Pirani 1947). Heart diseases, when associated with nephropathies, can develop more quickly and are difficult to control. CKD can cause anemia, uncontrolled cholesterol and triglycerides levels, and hinders the control of arterial blood pressure. In humans, it accelerates the process of atherosclerosis, with subsequent mineralization and formation of atheromatous plaques in the cerebral and coronary arteries, which can cause myocardial infarction (Ronco et al. 2008).

Routine staining is limited to showing specific or discrete lesions in the cardiomyocytes (Stigger et al. 2001, Carmo et al. 2011). Several immunohistochemical techniques with high specificity and sensitivity have been developed aiming to detect damage to the cardiomyocytes. Among these, cardiac troponin has shown promising results in cattle (Ortmann et al. 2000, Pavarini et al. 2012, Bandinelli et al. 2014, Santos et al. 2016), sheep (Costa et al. 2016), and dogs (D'avila et al. 2016). Necrotic cardiomyocytes, detectable or not by routine optical microscopy exams, show negative immunostaining, while those unaffected are positive for troponin (Jenkins et al. 2010, Bandinelli et al. 2014, Santos et al. 2016 Costa et al. 2016, D'avila et al. 2016).

To date, there have been no studies evaluating immunohistochemistry (IHC) with anti-cTnC to detect cardiac lesions in domestic cats. Thus, the present study aimed to evaluate the serum levels of troponin I in cats with CKD, associated with clinical and pathological findings, as well as to correlate the morphostructural cardiac lesions to determine their distribution through macroscopic and histological assessments and anti-cardiac troponin C (cTnC) IHC.

MATERIALS AND METHODS

This study was approved by the Ethics Committee on Animal Use (EAUC) of "Universidade Federal Rural do Rio de Janeiro" (UFRRJ) under the process no. 7430260817, and was carried out at the Histopathology and Immunohistochemistry Laboratories of the "Setor de Patologia Animal" (PAS), located in Annex I of the "Instituto de Veterinária" of UFRRJ. Laboratory tests (blood count, biochemistry, and troponin I) were performed in a private clinical pathology laboratory.

The study sample was composed of 20 cats (*Felis catus*) - 12 females and eight males: 18 diagnosed with CKD and 2 controls, regardless of breed, sex, and age. After necropsy, fragments from all organs were macroscopically evaluated, collected, and processed for histopathology.

The following inclusion criteria were adopted: cats with biochemical profile of azotemia, at stage II or higher of the International Renal Interest Society (IRIS), with serum creatinine concentrations >1.6mg/dL (IRIS 2019), and record of clinical signs and complementary exams consistent with the diagnosis of CKD. Animals with primary heart disease or other conditions that could elevate serum troponin levels, such as hypertrophic cardiomyopathy, hyperthyroidism, primary or metastatic cardiac neoplasia, were excluded from the study. This exclusion was based on a thorough clinical evaluation with the aid of imaging and laboratory tests to diagnose CKD. Histological analysis of the thyroid gland was performed in the 20 animals, and usual morphology was observed, without hyperplasia or any other changes. Arterial blood pressure was measured on 12 of the 18 cats with CKD.

Laboratory tests including biochemistry, blood count, and serum troponin were performed in all cats in this study. Blood samples were collected from each cat to perform blood count and biochemistry tests in all consultations within the sample collection period in this study until death. Collection for serum troponin measurement was performed in animals at CKD stages II, III, or IV.

During this study, 18 cats with CKD and two control animals were necropsied. On macroscopic examination, several organs were evaluated in detail, and the data were recorded in forms prepared for this research. At necropsy, the hearts were collected whole for gross evaluation according to the technique described by Bandinelli et al. (2014). Then they were cross-sectioned in a total of four complete sections equidistant from each other. Eight fragments from different regions of each heart were collected separately and placed in previously identified flasks containing 10% buffered formalin solution. Fragments were collected from the apex, interventricular septum, left and right ventricles, left and right papillary muscles, and left and right atria. Heart fragments from two cats without renal and cardiac injuries were used as control. For histopathological examination, each sample was fixed and routinely processed for histology, the sections were stained with hematoxylin and eosin (HE), and the slides were examined under an optical microscope.

Anti-human troponin C IHC was performed on serial slides obtained from sections of the eight heart regions. The histological sections were dewaxed in two xylene baths (20 min each), hydrated in four alcohol baths (5 min each), and incubated for 15 min in 3% hydrogen peroxide diluted on the spot. They remained for another 15 min in the same solution and were then diluted to block endogenous peroxidases. After washing the slides with distilled water, they were kept in a water bath with citrate buffer (pH 6.0) at approximately 98 °C for 15 min for antigen recovery. Blocking of nonspecific reactions was performed using 5% skimmed milk (Molico® - Brazilian industry) for 30 min. The sections were incubated overnight with anti-human troponin C antibody (Novocastra® clone 1A2) in a 1:100 dilution (1µl antibody to 100µl PBS or ADS-125 antibody diluent). The REVEAL biotin-free polymer-HRP detection system (Spring) was used with diaminobenzidine (DAB) as chromogen. All sections were stained with Harris' hematoxylin and evaluated under an optical microscope.

The Spearman's correlation coefficients were calculated to measure the relationship between the laboratory variables and the number of heart regions with decreased expression for cTnC antibody in individual cardiomyocytes. The Fisher's exact test was applied to assess whether plasma troponin was independent of the IRIS stages. The data were processed using the *R* 3.6.12 software. A significance level of 5% ($p<0.05$) was adopted for all statistical analyses.

RESULTS

A total of 18 cats diagnosed with CKD and 2 control animals were assessed between March 2016 and November 2018. Of these 18 cats, 11 (61.15%) were female and 7 (38.9%) male, with ages varying from 4 to 23 years (mean of 10.5 years). Eleven (11, 61.1%) cats were weighed using the body score with a scale ranging from 1 to 5 (1 = cachectic, 2 = underweight, 3 = ideal, 4 = overweight, and 5 = obese). With regard to breed, varied patterns were observed: most cats were crossbred (14, 77.8%), two were Persian (11.1%), one was Birman (5.55%), and one Siamese (5.55%).

In the analysis of creatinine and urea, parameters above the reference values were found in the 18 animals with CKD. In the serum troponin test, data above the reference values were found in 10/18 (55.6%) animals. The highest values for creatinine and urea, as well as for serum troponin, the classification of animals according to IRIS, the presence or absence of cardiac injury at HE, and the loss of cardiac troponin at IHC are described in Table 1.

Clinically, 14/18 (77.7%) animals presented reduced appetite, 16/18 (88.8%) showed weight loss, and 6/18

Table 1. Classification of IRIS and laboratory tests

Cat	IRIS stage	Creatinine 0.51.6mg/dL (reference)	Urea 42.854.2mg/dL (reference)	Troponin serum 0.030.16ng/L (reference)	Cardiac lesion (HE)	Areas with troponin loss (IHC)
1	II	2.0	53.0	0.03	No	No
2	III	2.91	72.7	0.09	Yes	(+)
3	IV	13.0	130.0	0.673	No	No
4	IV	6.81	308.2	39,497	Yes	+++
5	IV	6.6	152	0.11	No	No
6	IV	11.3	430.6	0.120	No	No
7	II	2.2	188.5	1,558	Yes	(+)
8	IV	6.33	206.1	0.448	Yes	(+)
9	IV	6.8	226	0.990	Yes	(+)
10	IV	8.8	241	0.085	No	No
11	IV	8.2	325	0.023	No	No
12	IV	17.0	276.0	0.166	No	No
13	II	2.8	-	9,332	Yes	(+)
14	IV	8.40	226	1,237	Yes	(+)
15	IV	9.4	276	51,019	Yes	+++
16	IV	8.0	200.0	0.046	No	No
17	IV	10.9	309	0.206	Yes	(+)
18	II	2.8	47	0.131	No	No
19*	-	-	-	-	No	No
20*	-	1.6	-	0.11	No	No

* Control animals; (+) Discrete, + mild, ++ moderate, +++ marked.

(33.33%) had vomiting episodes. All cats that had arterial blood pressure measured (12/18) showed values within normality (120-140 mmHg).

In the macroscopic analysis of the cats, the main findings were pale mucous membrane (8/18, 44.44%), kidneys reduced in size (13/18, 72.2%) and with irregular capsular surface (15/18, 83.3%). The main histological lesions in the kidneys included predominantly diffuse interstitial lymphoplasmacytic infiltrate in the corticomedullary region (18/18, 100%), Bowman's capsule thickening (15/18, 83.3%), atrophy and glomerular sclerosis (16/18, 88.8%), mineralization (9/18, 50%), vacuolar degeneration of contorted tubular epithelial cells (6/18, 33.3%), and interstitial fibrosis (5/18, 27.7%).

Histopathological analysis of the heart revealed hypereosinophilic cardiomyocytes in 9/18 (50%) cats, presented singly in seven (38.8%) (Fig.1A) and in large areas in two (11.11%) (Fig.2A) animals; foci of fibrosis in 3/18 (16.6%) felines; mineralization of myocytes and tunica intima of heart vessels also in 3/18 (16.6%) animals; deposition of amorphous eosinophilic substance with reduction of the vascular lumen, characterizing arteriosclerosis, in 1/18 (5.5%) cat. Control animals did not show any important changes (Fig.3A,B).

Decreased expression for cTnC antibody was observed in cardiomyocytes (affected areas) in 9/18 cats (50%), singly in seven (38.8%) (Fig.1B) and in extensive areas in two (11.11%) cats (Fig.2B). Of these 18 animals, 11 showed increased serum troponin I levels: six (66.7%) with only one affected region and three (33.3%) with two affected regions. Of the eight heart areas observed, the most frequently affected region was the apex (27.8%), followed by the left ventricle (16.7%), right papillary muscle (11.1%), left papillary muscle (5.6 %), and right ventricle (5.6%).

It was observed that the number of regions with decreased expression for cTnC antibody in cardiomyocytes is strongly and significantly correlated only with serum troponin I. There were no significant correlations with the other variables of the laboratory tests (Table 2).

Of the 18 cats analyzed, five (27.77%) were in stage II, one (5.55%) in stage III, and 13 (72.2%) in stage IV of the IRIS. A *p*-value of 0.6998 was obtained in the Fisher's exact test, suggesting independence between IRIS stage and the number

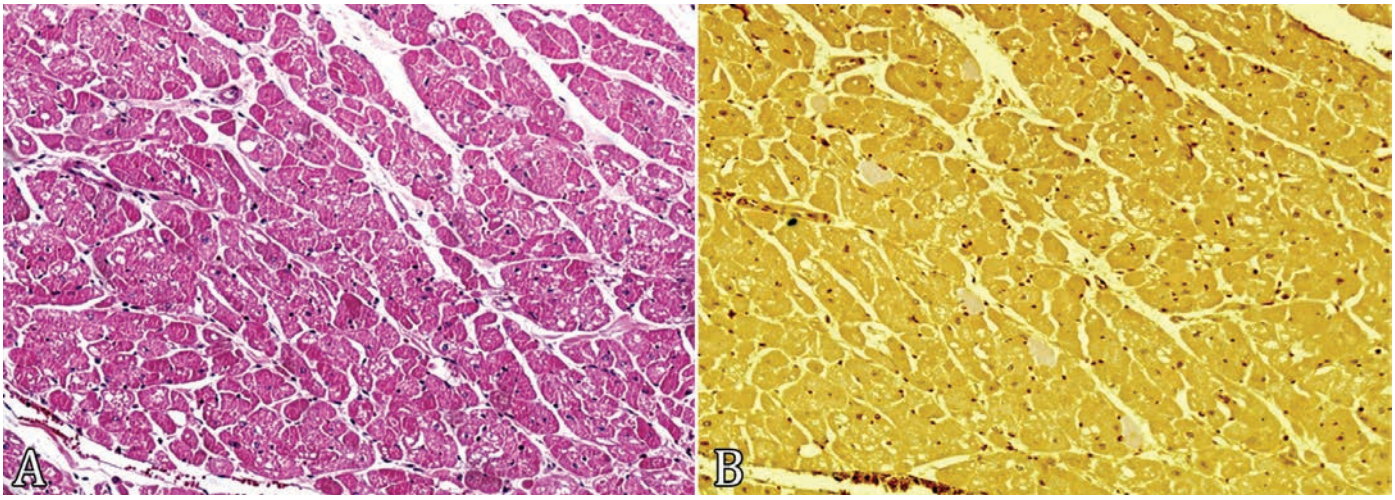


Fig.1. (**A**) Few individual hypereosinophilic cardiomyocytes. Cat 2. HE, obj.20x. (**B**) Decrease in expression for anti-human cTnC antibody corresponding to the area with hypereosinophilic cardiomyocytes. Cat 2. IHC, obj.20x.

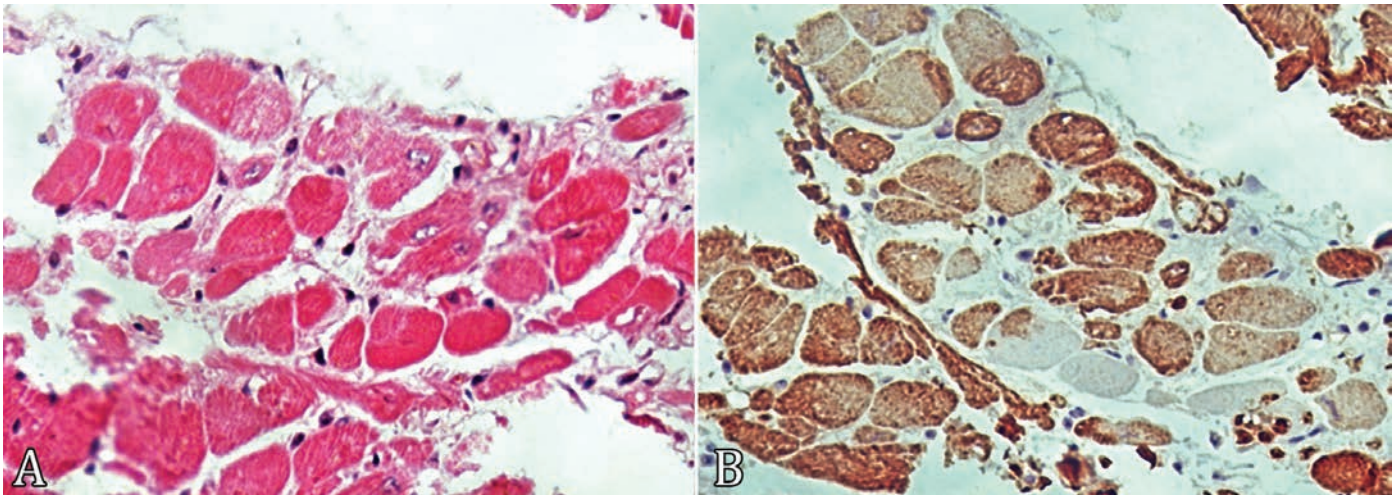


Fig.2. (**A**) Area delimited with individual hypereosinophilic cardiomyocytes . Cat 2. HE, obj.40x. (**B**) Moderate decrease in expression for anti-human cTnC antibody corresponding to the area with hypereosinophilic cardiomyocytes. Cat 2. IHC, obj.40x.

of regions with decreased expression for cTnC antibody in cardiomyocytes, that is, the number of affected regions was not associated with the IRIS stage.

DISCUSSION

Cardiorenal syndrome (CRS) is widely studied in medicine (Martin & Franco 2005). In veterinary medicine, CRS has gained notoriety because of its high prevalence and wide variety among dogs and cats (Pouchelon et al. 2015). According to the classification by Pouchelon et al. (2015), animals developed cardiovascular disease/dysfunction secondary to primary CKD and concomitant with impairment of both systems. Kidney-mediated systemic hypertension can result in increased afterload, left ventricular hypertrophy, worsening of mitral or aortic insufficiency, arrhythmia, vasculopathy, or retinopathy. In addition, volume overload generates systemic arterial hypertension, hypokalemia, or hyperkalemia and, consequently, cardiac arrhythmia (Pouchelon et al. 2015). In this study, the animals showed signs, clinical exams, laboratory findings, and images compatible with CKD. However, they did not present impairment of the cardiovascular system, which confirms the classification as primary kidney disease.

The use of serum cTnI as a biomarker of cardiac injury in this study assisted with identifying cardiomyocyte injury in the feline species. Langhorn et al. (2019) observed an increase in serum cTnI concentration in cats with compromised renal function without evidence of structural cardiac injury, which confirms its possible prognostic indicator in cats with CKD. These data corroborate the findings of the present study, since cats with CKD showed a significant increase in serum cTnI. The results reported by Langhorn et al. (2019) reinforce the hypothesis that increased impairment of renal function reflects myocardial injury or, at least partially, damage to the myocytes induced by a non-cardiac disease. This damage is correlated with codependency of the cardiorenal system, where its interaction involves shared mechanisms (Ronco et al. 2014, Keller et al. 2016), as well as with the causes of cardiac remodeling by CKD that would include activation of the renin-angiotensin-aldosterone system (RAAS) of the sympathetic nervous system (SNS) after a decline in glomerular filtration rate (GFR), which induce heart disease and fibrosis, in addition to uremic toxins, hyperphosphatemia, and non-anemia. Regenerative hypotheses have been recently raised (Langhorn et al. 2019).

In the animals of this study, only one serum cTnI measurement was performed because of the high costs of the exam and the lack of availability of the owners to collect the material. However, according to the literature, increased serum cTnI concentration occurs 4-6 h after an injury or acute necrosis of the human myocardium (Nelson & Thompson 2006, Jenkins et al. 2010), and can remain elevated for an average of 7-10 days after an acute episode (Sleeper et al. 2001), which demonstrates that its prolonged release time allows confirmation of the diagnosis up to three weeks (Godoy et al. 1998). A retrospective study conducted by Porciello et al. (2008) showed that dogs and cats with acute or chronic renal failure generally have high levels of cTnI, with an average of 72% of

Table 2. Spearman's correlation coefficient between the number of regions with decreased expression for cTnC antibody in cardiomyocytes of cats with chronic kidney disease (CKD) and laboratory test variables

Laboratory tests	Spearman's correlation	*p*-value	N
Maximum creatinine	-0.1203	0.6345	18
Maximum urea	0.2015	0.4381	17
Hematocrit	0.1797	0.4900	17
Leukogram	0.1966	0.4656	16
Troponin	0.7754	0.0002	18
Creatinine 1	0.1101	0.6636	18
Creatinine 2	-0.2848	0.3457	13
Creatinine 3	-0.2062	0.6242	8
Creatinine 4	-0.2236	0.7177	5
Creatinine 5	-1,0000	1,0000	2
Urea 1	0.3243	0.2041	17
Urea 2	-0.1927	0.5938	10
Urea 3	-0.4743	0.4195	5
Urea 4	0	1,0000	3
Urea 5	*	*	1

N = Number of cats subjected to the examination; * It was not possible to calculate because there was only one observation.

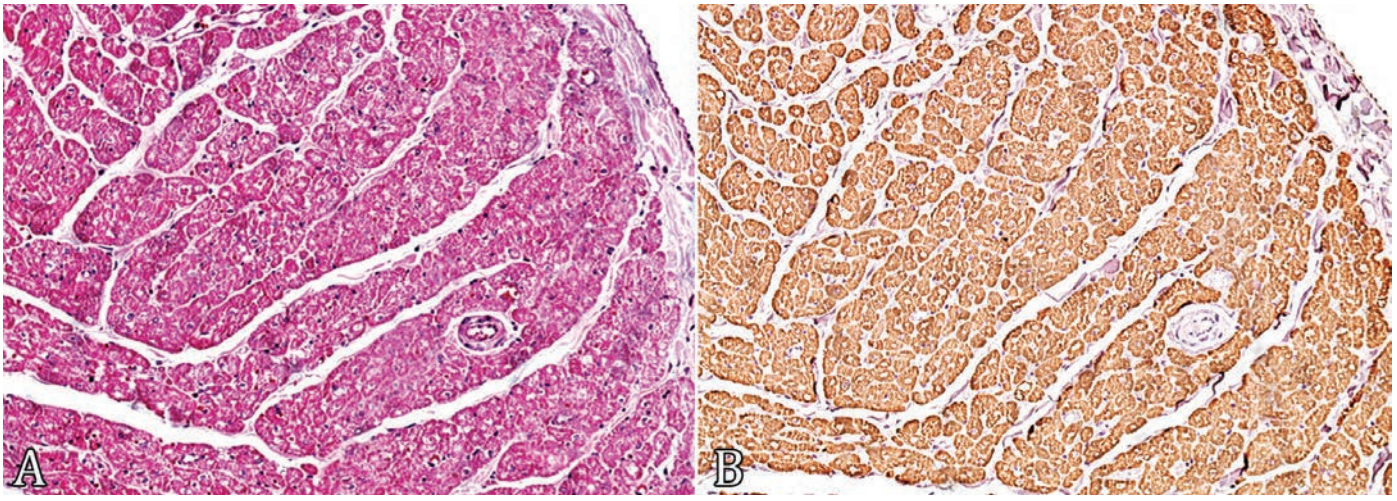


Fig.3. (**A**) Histological section of the heart. Control animal. HE, obj.20x. (**B**) Histological section of the heart with expression for the anti-human cTnC antibody. Control area. IHC, obj.20x .

cats with renal failure without a clear primary heart disease clinical condition. As in the present study, both previously mentioned studies justified the viability and application of serum cTnI in cats diagnosed with primary CKD for possible assistance and verification of early secondary cardiac injuries.

The primary histological lesions found in the hearts of the cats diagnosed with CKD included cardiomyocyte necrosis, foci of fibrosis, and mineralization both of myocytes and of the tunica intima of heart vessels, with both alterations observed in 3/18 animals, in addition to arteriosclerosis, found in only 1/18 cat. Although these were random findings, interstitial and/or perivascular fibrosis was observed secondarily in animals with renal dysfunction. This imbalance can be explained by homeostasis (Bagshaw et al. 2013), where volume overload contributes to increased preload and cardiac output changes. Increased afterload, such as activation of the SNS and RAAS, which lead to the development of systemic arterial hypertension (Bagshaw et al. 2013), and angiotensin II can induce cardiac fibrosis (Kawano et al. 2000).

In this study, both animals that presented foci of interstitial and/or perivascular fibrosis were in stage IV of the IRIS, with classic signs of uremia of advanced CKD. These findings in cats (Langendorf & Pirani 1947) contrast with those reported by D'avila et al. (2016), who found that most dogs with CKD presented interstitial and/or perivascular fibrosis at different IRIS stages of the disease.

The mineralization observed in both myocytes and tunica intima of the vessels, in 3/18 animals can be correlated to the deposition of minerals in tissues submitted to previous necrosis injury, that is, to dystrophic mineralization (Alfrey 2004, Cardoso et al. 2019). D'avila et al. (2016) verified that 100% of dogs evaluated showed endothelial lesions of different intensities, which was observed in only 1/18 of the cats in this study; however, it corroborates the study by Dantas & Kommers (1997), who reported that only 18% of the dogs had extrarenal uremic lesions such as vascular alteration associated with myocardial necrosis and mineralization. Coagulation necrosis and cardiac dystrophic mineralization were also observed in 43.7 and 25% of dogs with CKD, respectively, in the study conducted by Cardoso et al. (2019). Lesions of this nature were attributed to cardiac vessel changes in cats with uremia and/or metabolic and hemodynamic changes caused by CRS, since it reinforces the hypothesis that a dystrophic lesion precedes mineralization in cases of degenerative, inflammatory, or necrotic lesions in uremic dogs.

In 9/18 cats with CKD, there was a reduction in the levels and even total loss of cTnC expression in the sarcoplasm of groups of isolated cardiomyocytes or myocytes. At histopathological examination, cardiomyocytes presented a significant decrease in immunoreactivity, which, in histopathology, showed an increase in cytoplasmic eosinophilia, associated with nuclear pyknosis/karyorrhexis. Marked immunoreactivity was observed in the remaining and intact myocytes of both animals with CKD and those used as negative controls. Few studies have reported the use of IHC with anti-troponin antibody to detect cardiac lesions in veterinary medicine. Recently, through IHC for the human cTnC antibody, degenerative-necrotic lesions have been observed in the heart of cattle poisoned by *Amorimia exotropica* (Pavarini et al. 2012, Bandinelli et al. 2014) and of sheep poisoned by *Amaranthus spinosus* (Costa et al. 2016). Foci of hypereosinophilic cardiomyocytes with coagulation necrosis, neutrophilic inflammation, and subtle to mild variation in the staining pattern of some fibers with part of them showing a total loss of troponin I were found in the myocardium of dogs infected with *Dirofilaria immitis* (Carretón et al. 2012). D'avila et al. (2016) performed IHC on the heart fragments of 22 dogs with a previous diagnosis of CKD and found, in the heart of 16 animals, groups of hypereosinophilic cardiomyocytes with homogeneous cytoplasm and, in some cases, loss of striation and pyknosis, and IHC also revealed, in all dogs, several groups of myocytes with significant or absence of immunoreactivity for the cTnC antibody.

This study demonstrates a relationship between increased serum cTnI, increased cytoplasmic cardiomyocyte eosinophilia, and confirmed incipient cardiac injury due to loss of immunoreactivity to cTnC in the sarcoplasm and cardiomyocytes of cats diagnosed with CKD. There was an increase in eosinophilic cardiomyocytes confirmed by the loss of troponin from cardiac myocytes through IHC using human cTnC antibody. These findings corroborate those observed in dogs with CKD and heartworm disease (Carretón et al. 2012, D'avila et al. 2016), sheep with acute and subacute nephrotoxic injury (Costa et al. 2016), and cattle (Pavarini et al. 2012, Bandinelli et al. 2014) with cardiac injuries, which confirm the viability of this technique for these species. Regarding the extent of cardiac injury in cats, small foci of isolated necrosis or individual cardiomyocytes were observed, demonstrating that, even in advanced stages of CKD, cardiac lesions manifest differently in this species, which can be explained by the different pathophysiology and consequent clinical-pathological behavior of the feline species (Bagshaw et al. 2013). There is little evidence of this in the literature, both in dogs and cats (Sampedrano et al. 2006). In humans (Ronco et al. 2008), pathophysiology, especially concerning CKD, is a primary disease. Among the hypotheses addressed, systemic hypertension secondary to kidney disease is one of the leading causes of cardiac injuries. It can affect the heart of cats through injuries adaptive to the increased pressure of the heart load that, in some cases, promotes myocyte ischemia and consequent necrosis (Carr & Egner 2009).

In this study, each heart region was assessed separately to map the main affected areas, and 9/18 animals (50%) presented specific areas with incipient necrosis of cardiomyocytes in routine staining, confirmed by IHC, with the loss of staining for the human cTnC antibody. Among the observations, the apex (41.7%) was the main affected area, followed by left ventricle (25%), right papillary muscle (16.7%), left papillary muscle (8.3%), and right ventricle (8.3%), which indicates a greater predisposition of the species to damage in these regions of the heart. In the study conducted by Bandinelli et al. (2014) when mapping the hearts of cattle poisoned by *Amorimia exotropica*, the most affected area, the left papillary muscle, was found to be predisposed to this disease. In previous studies using of the cTnC antibody in the myocardial fragments of dogs (D'avila et al. 2016) and sheep (Costa et al. 2016), no mapping of the heart areas was performed.

In the present work, the animals were classified into the different IRIS stages by establishing the history, anamnesis, and clinical signs compatible with CKD over more than three months of evolution, as well as laboratory tests and serum measurements of creatinine and urea performed at different times throughout the clinical evolution of each cat. Creatinine

was used as the primary marker for IRIS classification since it is the most used substance for biochemical assessment of glomerular filtration (Junior & Williams 2010). There were 4/18 animals (2.25%) in stage II, 1/18 (5.6%) in stage III, and the vast majority, 13/18 (72.2%), were in stage IV. Clinical signs and laboratory findings for each animal confirm the standards stipulated by IRIS for each category. The predominance CKD stage IV is characterized by the presence of intense azotemia (serum creatinine >5.0 mg/dL), with significant loss of renal function and several systemic manifestations of uremia. However, no correlation was observed between the stages of IRIS and increased serum cTnI and loss of immunoreactivity at IHC by statistical analysis (*p*-value of 0.5252 by the Fisher's exact test), which suggests independence between IRIS staging and the number of regions with decreased expression for cTnC antibody in cardiomyocytes, that is, the number of affected regions is not associated with IRIS staging. In addition to the different pathophysiology of each species for CKD and CRS, Porciello et al. (2008) suggest that this response is individual, which justifies the independence and response to disease and the consequent data for the cardiovascular system for each animal.

CONCLUSIONS

Increased serum cTnI levels occur in cats with compromised renal function regardless of the IRIS stages, and this increase is correlated with the extent of cardiac injury observed at IHC.

The anti-human cTnC antibody demonstrated considerable viability for use in the feline species and IHC proved to be an effective tool to assist with detection and extension of cardiac injury in cats diagnosed with chronic kidney disease (CKD).

Acknowledgments.- This study was finaced in part by the "Coordenação de Aperfeiçoamento de Pessoal de Nível Superior" (CAPES), Brazil, Finance Code 001. The authors are also grateful to "Fundação de Amparo à Pesquisa do Estado do Rio de Janeiro" (FAPERJ).

Conflict of interest statement. The authors declare having no conflicts of interest.

REFERENCES

Alfrey A.C. 2004. The role of abnormal phosphorus metabolism in the progression of chronic kidney disease and metastatic calcification. Kidney Intern. 66(Supl.90):S13-S17. <https://dx.doi.org/10.1111/j.1523-1755.2004.09003.x> <PMid:15296502>

Bagshaw S.M., Hoste E.A., Braam B. Briguori C., Kellum J.A. & McCullough P.A. 2013. Cardiorenal Syndrome Type 3: pathophysiologic and epidemiologic considerations. ADQI Consensus on AKI Biomarkers and Cardiorenal Syndromes 182, Karger Publishers, p.137-157.

Bandinelli M.B, Bassuino D.M, Fredo G., Mari C., Driemeier D., Sonne L. & Pavarini S.P. 2014. Identificação e distribuição de lesões cardíacas em bovinos intoxicados por *Amorimia exotropica*. Pesq. Vet. Bras. 34(9):837-844. <https://dx.doi.org/10.1590/S0100-736X2014000900006>

Cardoso P.G., Pinto M.P., Moroz L.R., Fontes T.N., Santos R.S., Freitas J.L. Nogueira V.A., & Peixoto T.C. 2019. Dystrophic mineralization in uremic dogs: an update. Pesq. Vet. Bras. 39(11):889-899. <https://dx.doi.org/10.1590/1678-5150-pvb-6250>

Carmo P.M.S., Irigoyen L.F., Lucena R.B., Fighera R.A., Kommers G.D. & Barros C.S.L. 2011. Spontaneous coffee senna poisoning in cattle: report on 16 outbreaks. Pesq. Vet. Bras. 31(2):139-146. <https://dx.doi.org/10.1590/S0100-736X2011000200008>

Carr A.P & Egener B. 2009. Blood Pressure in Small Animals, Part 2: Hypertension-target organ damage, heart and kidney. European J. Companion Anim. Pract. 19(1):13-17.

Carretón E., Grandi G., Morchón R., Simón F., Passeri B., Cantoni A.M. & Montoya-Alonso J.A. 2012. Myocardial damage in dogs affected by heartworm disease (*Dirofilaria immitis*): immunohistochemical study of cardiac myoglobin and troponin I in naturally infected dogs. Vet. Parasitol. 189(2/4):390-393. <https://dx.doi.org/10.1016/j.vetpar.2012.04.013> <PMid:22571834>

Costa S.Z., Peixoto P.V., Brust L.A.C., D'avila M.S., Santos A.M., Driemeier D., Nogueira V.A. & França T.N. 2016. Troponina C na detecção imuno-histoquímica de alterações regressivas precoces no miocárdio de ovinos naturalmente intoxicados por *Amaranthus spinosus* (Amaranthaceae). Pesq. Vet. Bras. 36(2):83-89. <https://dx.doi.org/10.1590/S0100-736X2016000200004>

D'avila M.S., Franca T.N., Peixoto P.F.V., Peixoto T.C., Santos A.M., Costa S.Z.R., Santos R.S., Gonçalves T. & Nogueira V.A. 2016. Avaliações morfológica e imuno-histoquímica (Troponina C) de lesões cardíacas em cães com doença renal crônica. Revta Bras. Med. Vet. 38(Supl.2):128-138.

Dantas A.F.M & Kommers G.D. 1997. Lesões extra-renais de uremia em 72 cães. Ciênc. Rural 27(2):301-306. <https://dx.doi.org/10.1590/S0103-84781997000200022>

Godoy M.F., Braile D.M., Neto J.P. & Purini Neto J. 1998. A troponina como marcador de injúria celular miocárdica. Arq. Bras. Cardiol. 71(4):629-633. <https://dx.doi.org/10.1590/S0066-782X1998001000013>

IRIS 2019. Staging of CKD. International Renal Interest Society, United Kingdom. 5p. Available at <http://www.iris-kidney.com/>

Jenkins C.P., Cardona D.M., Bowers J.N., Oliai B.R., Allan R.W. & Normann S.J. 2010. The utility of C4d, C9, and troponin T immunohistochemistry in acute myocardial infarction. Arch. Pathol. Lab. Med. 134(2):256-263. <https://dx.doi.org/10.1043/1543-2165-134.2.256> <PMid:20121615>

Junior K.J.K. & Williams R.D. 2010. Exames laboratoriais em urologia, p.46-57. In: Tanagho E.A. & Mcaninch J.W. (Eds), Urologia Geral Smith. 17ª ed., AMGH, Rio Grande do Sul.

Kawano H., Do Y.S., Kawano Y., Starnes V., Barr M., Law R.E., & Hsueh W.A. 2000. Angiotensin II has multiple profibrotic effects in human cardiac fibroblasts. Circulation 101(10):1130-1137. <https://dx.doi.org/10.1161/01.cir.101.10.1130> <PMid:10715259>

Keller S.P., Kovacevic A. & Howard J. 2016. Evidence of cardiac injury and arrhythmias in dogs with acute kidney injury. J. Small Anim. Pract. 57(8):402-408. <https://dx.doi.org/10.1111/jsap.12495> <PMid:27357259>

Langendorf R. & Pirani C.L. 1947. The heart in uremia - an electrocardiographic and pathologic study. Am. Heart J. 33(3):282-307. <https://dx.doi.org/10.1016/0002-8703(47)90657-1> <PMid:20286348>

Langhorn R., Jessen L.R., Kloster A.S., Jensen A.P., & Koch J. 2019. Cardiac troponin I in cats with compromised renal function. J. Feline Med. Surg. 21(10):985-991. <https://dx.doi.org/10.1177/1098612X18813427> <PMid:31551016>

Martin L.C & Franco R.J. 2005. A doença renal como fator de risco cardiovascular. Arq. Bras. Cardiol. 85(6):432-436. <https://dx.doi.org/10.1590/S0066-782X2005001900011>

Nelson O.L. & Thompson P.A. 2006. Cardiovascular dysfunction in dogs associated with critical illnesses. J. Am. Anim. Hosp. Assoc. 42(5):344-349. <https://dx.doi.org/10.5326/0420344> <PMid:6960037>

Ortmann C., Pfeiffer H. & Brinkmann B. A. 2000. Comparative study on the immunohistochemical detection of early myocardial damage. Int. J. Legal Med.113(4):215-220. <https://dx.doi.org/10.1007/s004149900094> <PMid:10929237>

Pavarini S.P., Bandinelli M.B., Juffo G.D., Souza S.O.D., Driemeier D. & Cruz C.E.F.D. 2012. Decreased expression of cardiac troponin C is associated with cardiac lesions in *Amorimia exotropica* poisoned cattle. Pesq. Vet. Bras. 32(10):1005-1008. <https://dx.doi.org/10.1590/S0100-736X2012001000010>

Polzin D.J., Osborne C.A. & Ross S. 2005. Chronic kidney disease, p.1756-1785. In: Ettinger S.J. & Feldman E.C. (Eds), Textbook of Veterinary Internal Medicine. Vol. 2. 6th ed. St. Louis, Elsevier Saunders.

Porciello F., Rishniw M., Herndon W.E., Birettoni F., Antognoni M.T. & Simpson K.W. 2008. Cardiac troponin I is elevated in dogs and cats with azotaemia renal failure and in dogs with non-cardiac systemic disease. Australian Vet. J. 86(10):390-394. <https://dx.doi.org/10.1111/j.1751-0813.2008.00345.x> <PMid:18826510>

Pouchelon J.L., Atkins C.E., Bussadori C., Oyama M.A., Vaden S.L., Bonagura J.D. & Grauer G.F. 2015. Cardiovascular–renal axis disorders in the domestic dog and cat: a veterinary consensus statement. J. Small Anim. Pract. 56(9):537-552. <https://dx.doi.org/10.1111/jsap.12387> <PMid:26331869>

Ribeiro R.C.H.M., Oliveira G.A.S.A., Ribeiro D.F., Bertolin D.C. Cesarino C.B., Lima L.C.E.Q. & Oliveira S.M. 2008. Caracterização e etiologia da insuficiência renal crônica em unidade de nefrologia do interior do Estado de São Paulo. Acta Paul. Enferm. 21(Número Especial):207-211 <https://dx.doi.org/10.1590/S0103-21002008000500013>

Ronco C. & Di lullo L. Cardiorenal syndrome. 2014. Heart Failure Clin. 10(2):251-280. <https://dx.doi.org/10.1016/j.hfc.2013.12.003> <PMid:24656104>

Ronco C., Haapio M., House A.A., Anavekar N. & Bellomo R. 2008. Cardiorenal syndrome. J. Am. Coll. Cardiol. 52(19):1527-1539. <https://dx.doi.org/10.1016/j.jacc.2008.07.051> <PMid:19007588>

Sampedrano C.C., Chetboul V., Gouni V., Nicolle A.P., Pouchelon J-.L., & Tissier R. 2006. Systolic and diastolic myocardial dysfunction in cats with hypertrophic cardiomyopathy or systemic hypertension. J. Vet. Intern. 20(5):1106-1115. <https://dx.doi.org/10.1892/0891-6640(2006)20[1106:sadmdi]2.0.co;2> <PMid:17063702>

Santos A.M., Peixoto P.V., D'Ávila M.S., Peixoto T.C., França T.N., Costa S.Z., Cid G.C. & Nogueira V.A. 2016. Troponin C in immunohistochemical detection of early regressive myocardial lesions in cattle and sheep poisoned with sodium monofluoroacetate. Pesq. Vet. Bras. 36(2):67-72. <https://dx.doi.org/10.1590/S0100-736X2016000200001>

Sleeper M.M., Clifford C.A. & Laster L.L. 2001. Cardiac troponin I in the normal dog and cat. J. Vet. Intern. Med. 15(5):501-503. <https://dx.doi.org/10.1892/0891-6640(2001)015<0501:ctiitn>2.3.co;2> <PMid:11596740>

Stigger A.L., Barros C.S.L., Langohr I.M. & Barros S.S. 2001. Intoxicação experimental por *Ateleia glazioviana* (Leg. Papilionoideae) em ovinos. Pesq. Vet. Bras. 21(3):98-108. <https://dx.doi.org/10.1590/S0100-736X2001000300002>

Viswanathan G. & Gilbert S. 2011. The Cardiorenal syndrome: making the connection. Int. J. Nephrol. 2011:1-10. <https://dx.doi.org/10.4061/2011/283137> <PMid:21151533>

PESQUISA VETERINÁRIA BRASILEIRA
Brazilian Journal of Veterinary Research
ISSN 0100-736X (Print)
ISSN 1678-5150 (Online)

Pesq. Vet. Bras. 40(12):1010-1017, December 2020
DOI: 10.1590/1678-5150-PVB-6377

Original Article
Small Animal Diseases
BY-NC

Evaluation of galectins 1 and 3 expression in canine melanoma[1]

Jéssica S. Garcia[2]*, Nicolle G.T.Q. Hazarbassanov[2], Júlia C. Nakamura[3], Victor Nowosh[3], Bruno Cogliati[4], Lilian Rose Marques de Sá[4] and Cristina O. Massoco[4]

ABSTRACT.- Garcia J.S., Hazarbassanov N.G.T.Q., Nakamura J.C., Nowosh V., Cogliati B., Marques de Sá L.R. & Massoco C.O. 2020. **Evaluation of galectins 1 and 3 expression in canine melanoma**. *Pesquisa Veterinária Brasileira 40(12):1010-1017*. Departamento de Patologia, Faculdade de Medicina Veterinária e Zootecnia, Universidade de São Paulo, Avenida Prof. Dr. Orlando Marques de Paiva 87, Cidade Universitária, São Paulo, SP 05508-270, Brazil. E-mail: jessica.sg@hotmail.com

Canine melanoma is a frequently-occuring neoplasm in dogs and presents as malignant and highly metastatic in this context, studies that contribute to the understanding of the tumor microenvironment in melanoma include the role of galectins. Galectins are proteins of the family of animal lectins that display carbohydrate recognition domains. Galectin-1 and galectin-3 are associated with neoplastic transformation, neoplastic cell survival, angiogenesis, immune system evasion, and metastasis. The goal of this study was to establish a correlation between expression patterns of galectin-1 and galectin-3 and the different degrees of aggressiveness of canine melanoma, as well as to determine serum concentration of galectin-3 in dogs with melanoma. Galectin-1 and galectin-3 expression was analyzed by immunohistochemistry in 30 canine melanomas, six melanocytomas and nine metastatic lymph nodes from patients whose primary tumors were also processed and analyzed. Serum samples from 30 dogs were collected and galectin-3 concentration was determined by ELISA and compared to the samples of 10 healthy dogs. Canine melanoma samples expressed galectin-1 in the cytoplasm and presented a variable pattern of galectin-3 staining depending on melanoma aggressiveness. We observed a decrease in the percentage of cells with cytoplasmic galectin-3 immunolabeling simultaneous to the increased nuclear staining intensity, while there was also a decrease in the percent frequency of nuclear galectin-3 immunolabeled cells according to progression of melanoma, comparing the least to the most aggressive cases. Dogs with melanoma had increased serum levels of galectin-3 when compared to healthy animals, suggesting its potential biomarker of patients with melanoma.

INDEX TERMS: Galectin-1, galectin-3, canine, melanoma, lectins, neoplasms, immunohistochemistry, tumor microenvironment, dogs.

[1] Received on October 29, 2019.
Accepted for publication on August 28, 2020.
Master's research of the first author with support from CAPES and FAPESP.

[2] Departamento de Patologia, Faculdade de Medicina Veterinária e Zootecnia (FMVZ), Universidade de São Paulo (USP), Avenida Prof. Dr. Orlando Marques de Paiva 87, Cidade Universitária, São Paulo, SP 05508-270, Brazil. *Corresponding author: jessica.sg@hotmail.com

[3] Graduate Program, Departamento de Patologia, Faculdade de Medicina Veterinária e Zootecnia (FMVZ), Universidade de São Paulo (USP), Avenida Prof. Dr. Orlando Marques de Paiva 87, Cidade Universitária, São Paulo, SP 05508-270, Brazil.

[4] Professor, Departamento de Patologia, Faculdade de Medicina Veterinária e Zootecnia (FMVZ), Universidade de São Paulo (USP), Avenida Prof. Dr. Orlando Marques de Paiva 87, Cidade Universitária, São Paulo, SP 05508-270, Brazil.

RESUMO.- [**Avaliação da expressão das galectinas 1 e 3 no melanoma canino.**] O melanoma canino é uma neoplasia frequente em cães que apresenta um potencial maligno e metastático. Neste contexto, investigar o microambiente tumoral é fundamental para compreender os mecanismos intercelulares e intracelulares envolvidos no desenvolvimento e progressão da doença. Neste estudo, destacamos as galectinas, proteínas da família das lectinas animais que exibem domínios de reconhecimento à carboidratos; a galectina-1 e a galectina-3 estão associadas a transformação neoplásica, sobrevivência de células neoplásicas, angiogênese, evasão do sistema immune e desenvolvimento de metástases. O objetivo deste estudo foi

determinar os padrões de expressão de galectina-1 e galectina-3 em diferentes graus de agressividade do melanoma canino, bem como dosar a concentração sérica de galectina-3 em cães com melanoma e comparar com cães saudáveis. A expressão de galectina-1 e galectina-3 foi analisada em 30 melanomas caninos, seis melanocitomas e nove linfonodos metastáticos. A galectina-3 sérica foi mensurada em 30 cães com melanoma e comparada a 10 cães saudáveis. No melanoma canino a expressão de galectina-1 foi citoplasmática e a expressão de galectina-3 foi variável de acordo com o grau de agressividade. Notou-se uma redução na porcentagem de células com imunomarcação de galectina-3 citoplasmática e um aumento simultâneo da intensidade de imunomarcação nuclear, enquanto houve também uma diminuição na frequência percentual de células com imunomarcação nuclear de acordo com a progressão do melanoma comparando-se os casos menos com os mais agressivos. Cães com melanoma apresentaram níveis séricos aumentados de galectina-3 quando comparados a animais saudáveis, mostrando seu uso potencial como biomarcador em pacientes com melanoma.

TERMOS DE INDEXAÇÃO: Galectinas 1, galectina 3, melanoma, caninos, lectinas, neoplasia, imunoistoquímica, microambiente tumoral.

INTRODUCTION

Galectin plays a key role in tumor microenvironment, contributing to neoplastic transformation, neoplastic cell survival, angiogenesis and metastasis development (Liu & Rabinovich 2005). Galectins are carbohydrate-binding proteins of the lectin family that are present in the nucleus, cytoplasm, cell surface and secreted by cells in several tissues. Galectin-1 (gal-1) and galectin-3 (gal-3) are strongly related to neoplastic progression and metastasis development (Barondes et al. 1994, Van den Brûle et al. 2002, Liu & Rabinovich 2005).

Expression of gal-1 and gal-3 has been studied in different types of human tumors, such as breast cancer (Khaldoyanidi et al. 2003, Moreno et al. 2013, Simone et al. 2014), prostate carcinomas (Wang et al. 2009, Knapp et al. 2013, Compagno et al., 2014), glioma (BINH et al. 2013, Verschuere et al. 2014) and melanoma (Prieto et al. 2006, Mourad-Zeidan 2008, Lefranc et al. 2011, Mathieu et al. 2012, Brown et al. 2012, Borges et al. 2013), but there are few studies about galectin expression in different types of canine tumors (Woo et al. 2001, Johnson et al. 2007, Oliveira et al. 2014, Ribeiro et al. 2016, Vargas et al. 2018). These studies evaluated the expression of galectin-3 by the immunohistochemistry technique in gastric carcinoma, hemangiosarcoma, various canine tumors and mammary carcinomas respectively, showing the expression according to the different cell types present in these tumors and the difference between cell compartments.

Some studies have pointed out the use of galectins as biomarkers of tumor progression and as a prognostic factor in humans with cutaneous melanoma and hepatocellular carcinoma (Vereecken et al. 2005, Matsuda et al. 2008) and dogs with mammary carcinoma (Ribeiro et al. 2016). Serum gal-3 was measured prior to surgery and then one month and three months after tumor resection in dogs with mammary carcinoma (Ribeiro et al. 2016). The highest concentrations of gal-3 were detected one month after surgery in all patients and, in subsequent examination, only animals with metastasis had persistently increased levels of serum gal-3 (Ribeiro et al. 2016). Also, in canine mammary carcinomas, an increase in gal-3 expression by immunohistochemistry has been detected in intravascular neoplastic cells and metastatic cells in lymph nodes, suggesting that increased expression of gal-3 contributes to metastasis development (Oliveira et al. 2014). Even though progress has been made regarding mammary carcinomas, there is little information about galectin expression patterns in canine melanoma, which is just as aggressive, highly metastatic and difficult to treat.

Comprehensive studies about galectin expression patterns in canine melanoma have not been published, so the present study verified the expression patterns of galectin-1 and galectin-3 on melanoma samples and assessed serum concentration of galectin-3 in canine patients with naturally-occurring melanoma.

MATERIALS AND METHODS

Case selection and samples. All animals were included in the study after owner's consent. The study was approved by the Ethics Committee on Animal Use (CEUA/FMVZ-USP) under protocol 4360110815. Tumor samples were collected prospectively from 54 canine patients with melanomas from several teaching veterinary hospitals and private clinics and six samples of canine melanocytoma obtained retrospectively from the Veterinary Pathology Service at the "Universidade de São Paulo" (USP). Of the melanoma patients, 24 animals were removed from the study due to the presence of other diseases, and 30 animals met the inclusion criteria. These animals had no other disease that could interfere with the study. Animals were staged at the pre-surgery with physical examination, complete blood count, complete serum biochemistry, triple thoracic radiographs views, abdominal ultrasound examination and echocardiogram. Tumor samples were fixed in 10% formaldehyde for 48 hours and later included in paraffin blocks.

To analyze and compare gal-3 expression among samples, 4 groups were formed according to the degree of aggressiveness: melanocytoma (M, n=6), non-metastatic melanoma (NM, n=9), metastatic melanoma (MM, n=21). The metastatic lymph nodes (LN) were harvested from 9 of the patients from the MM group. The degree of aggressiveness was defined according to the progression of melanocytomas to melanomas and metastatic tissues and the groups represent different stages of disease evolution. Melanocytomas were considered the least aggressive tumors due to their benign behavior. Melanomas from non-metastatic patients (group NM) were considered less aggressive than melanomas from metastatic patients (group MM). LN groups of metastatic lymph nodes from patients in group MM were considered the most aggressive because they are metastatic tissues. Table 1 shows the epidemiological information regarding breed, age, sex, site of melanoma, pigmentation and aggressiveness.

Serum dosage of gal-3. Serum samples were collected from the same 30 melanoma-bearing dogs prior to excision of the neoplasia and kept under refrigeration at 2 to 8°C for 24 hours after collection. Serum samples were also collected from 10 animals considered clinically healthy after clinical examination, blood cell count and biochemical analyses (control group). All samples were stored at -70°C until quantification of gal-3. Serum concentrations of gal-3 were determined using a commercial kit according to manufacturer's instructions (R&D Systems-Quantikine® ELISA, Minneapolis/MN, USA).

Immunohistochemistry (IHC) for gal-1 and gal-3. Histological sections of tumor tissues (5µm width) were placed over silanized slides, then tissue melanin removal was performed as described (Silva et al. 2011). Slides were incubated for 12 to 24 hours at room

temperature in TrisHCL buffer (pH 7.4, 0.2M) with 10% hydrogen peroxide. Following dewaxing, antigen retrieval was carried out in a pascal pan (S2800, Dako Cytomation-Carpinteria, CA) for 19 minutes at 125°C temperature with citrate buffer (pH 6.0, 10mM) and blocking endogenous peroxidase was achieved with 6% hydrogen peroxide for 30 minutes at room temperature. Anti-gal-1 antibody (Galectin-1/LGALS1-D608T- Cell Signaling) was incubated for 1 hour at 37°C at 1:3000 dilution in PBS with 3% BSA, and anti-gal-3 antibody (Galectin-3/LGALS3-D4I2R- Cell Signaling) was incubated overnight refrigerated in the 1:600 dilution in PBS with 1% BSA. The detection system used was SuperPicture™ (Thermo Fisher Scientific, Waltham/MA, USA). Diaminobenzidine was used as chromogen and the sections were counterstained with Harris hematoxylin, mounted and assessed in an optical microscope.

Immunohistochemical analysis was performed by two evaluators on a Nikon microscope (model 80i) in 400x high power throughout the tumor. For gal-3, four scores were assigned according to the frequency of labeled cells: score 1 = 0-5% cells, score 2 = 6-25% cells, score 3 = 26-75%, and score 4 = >75% cells. Regarding the intensity of labeled cells, a scale from 1 to 3 was established: 1 = weakly stained, 2 = moderately stained, and 3 = heavily stained. These parameters were analyzed separately for both nuclear labeling and cytoplasmic labeling and compared among the four groups formed. Since all samples were very homogeneous for gal-1 staining no score was assigned.

Western blot for gal-3. The validation of the human antibody used for canine galectin-3 was performed by using the western blot technique on five canine melanoma samples and two cell lines MeLn and CF41 (canine melanoma and one of canine mammary carcinoma, respectively).

Tumor samples were transported from the veterinary hospitals to our laboratory in refrigerated RPMI-1640 cell culture medium (Gibco, Thermo Fisher Scientific, Waltham/MA, USA). The tumors were fragmented and incubated with 1mg/mL collagenase II (Gibco, Thermo Fisher Scientific, Waltham/MA, USA) in RPMI for 90 minutes in water bath at 37°C under constant magnetic stirring. Then, the solution was filtered using a nylon filter (70µm - Cell Strainer, BD Biosciences). Cells were stored in cryoprotectant solution (fetal bovine serum, Sigma-Aldrich) with 10% dimethyl sulfoxide (Sigma-Aldrich) and placed in liquid nitrogen. The next step was protein extraction from canine melanoma cells and two other cell lines used as controls: CF41.Mg (canine breast carcinoma - ATCC) and MeLn (melanoma cell line derived from a metastatic lymph node which was established in our laboratory and tested positive for MelanA

Table 1. Characterization of dogs with melanoma according to breed, age, sex, site of melanoma, degree of pigmentation, aggressiveness and site of metastasis

Animal	Breed	Age (years)	Gender	Site of tumor	Pigmentation	Aggressiveness	Site of metastasis
1	English Bulldog	8	Male	Digit	Melanic	MM	Lymph node
2	Cocker Spaniel	14	Female	Oral	Melanic	NM	-
3	Schnauzer	12	Female	Digit	Melanic	NM	-
4	Poodle	8	Male	Skin	Melanic	MM	Lymph node
5	Mixed breed	10	Male	Oral	Melanic	MM	Lymph node
6	Chow	8	Male	Oral	Melanic	MM	Lymph node
7	Golden Retriever	9	Male	Oral	Melanic	MM	Lymph node
8	Mixed breed	13	Male	Oral	Melanic	NM	-
9	Poodle	10	Male	Oral	Melanic	MM	Lymph node
10	Labrador Retriever	11	Female	Oral	Melanic	MM	Lymph node, lung
11	Yorkshire Terrier	12	Female	Oral	Amelanic	NM	-
12	Dachshund	12	Female	Oral	Melanic	MM	Lymph node
13	Cocker Spaniel	12	Female	Digit	Melanic	MM	Lymph node
14	German Sheperd	10	Male	Oral	Melanic	MM	Lymph node
15	Mixed breed	15	Female	Oral	Melanic	MM	Lymph node
16	Yorkshire Terrier	12	Female	Oral	Melanic	NM	-
17	Mixed breed	13	Male	Oral	Melanic	MM	Lymph node
18	Poodle	15	Male	Oral	Melanic	MM	Lymph node
19	Mixed breed	13	Male	Oral	Melanic	NM	-
20	Mixed breed	13	Male	Oral	Amelanic	MM	Lymph node
21	Golden Retriever	1	Female	Oral	Amelanic	NM	-
22	Schnauzer	11	Female	Oral	Melanic	NM	-
23	Dachshund	14	Female	Oral	Melanic	MM	Lymph node
24	Mixed breed	15	Male	Oral	Melanic	NM	-
25	Akita	13	Male	Oral	Melanic	MM	Lung
26	Pug	11	Female	Oral	Amelanic	MM	Lymph node
27	Poodle	13	Male	Oral	Melanic	MM	Lymph node
28	Mixed breed	12	Male	Oral	Amelanic	MM	Lung
29	Mixed breed	17	Male	Skin	Melanic	MM	Lymph node, lung
30	Golden Retriever	11	Female	Oral	Amelanic	MM	Lymph node

NM = non-metastatic melanoma, MM = metastatic melanoma.

and PNL2 (Giudice et al. 2010). Proteins were extracted using RIPA buffer (Sigma-Aldrich) with 1x protease and phosphatase inhibitors (Halt™ single-use cocktail, EDTA-free, 100x, Thermo Fisher Scientific, Waltham/MA, USA). Protein quantification was performed by Quick Start™ Bradford Protein Assay (Bio-Rad).

Thirty micrograms total protein were resolved in 12% SDS-PAGE gels and run in standard PAGE running buffer for 90 minutes at 90V. Proteins were transferred to PDVF membranes in a Transblot Turbo™ (Bio-Rad), standard 30-minute protocol, and the membranes were blocked with 5% bovine serum albumin fraction V (BSA, ICN Biomedicals) in Tris-buffered saline-Tween 20 (TBS-T) at room temperature for 1 hour. Gal-3 was detected using a human anti-gal-3 antibody (Galectin-3/LGALS3-D4I2R- Cell Signaling) 1:1000. Secondary anti-rabbit IgG antibody conjugated to HRP was then added at 1:50000 dilution (Bio-Rad). β-actin was used as loading control (monoclonal anti-mouse β-actin antibody (Sigma-Aldrich) 1:50000 dilution and anti-mouse IgG HRP 1:50000 dilution (Bio-Rad). Membranes were visualized using ECL substrate (Clarity™, Bio-Rad) in the Bio-Rad ChemiDoc®, and band intensity was quantified using Scion software.

Statistical analysis. Serum levels of gal-3 were compared between healthy and melanoma-bearing dogs using Student's t-test. Normality was assessed using the Shapiro-Wilk test. The Fisher's exact test was used in this study to identify differences in gal-3 immunohistochemistry staining scores between groups. The significance level was set at $p<0.05$) and statistical analysis was performed using GraphPad Prism version 6 (San Diego/CA, USA).

RESULTS

Epidemiological information

In this study, the median age was 12 years (minimum value 1 and maximum value 17) and there was no gender prevalence (17 males and 13 female dogs). The number of animals and their proportion in relation to the racial definition, melanic and amelanotic form, anatomical location and staging are illustrated in Table 1. The control group for the serum dosage of gal-3 was formed by 10 dogs, 50% male and 50% female. The median age was 9 years (minimum value 7 and maximum value 13). The patients had a predominance of melanotic (80%) followed by 20% amelanotic tumors and the oral mucosa was the most common location for melanoma (83%) followed by digit (10%) and skin (7%).

Expression of gal-1

The pattern of gal-1 expression in the tumor samples was predominantly cytoplasmic. Frequency of labeled cells was predominantly greater than 75% (Fig.1).

Expression of gal-3

All tumor samples expressed immunoreactivity for gal-3 and their expression pattern was analyzed according to the scores assigned for cytoplasmic and nuclear immunolabeling intensity and according to the frequency of immunolabeled cells. This expression was compared among study groups: melanocytoma (M, n=6) (Fig.2A), non-metastatic melanoma (NM, n=9) (Fig.2B), metastatic melanoma (MM, n=21) (Fig.2C) and metastatic lymph nodes (LN, n=9) (Fig.2D). Fisher's exact test was used to compare intensity of both cytoplasmic and nuclear immunolabeling (Table 2 and 3) and frequency of positive cells for both cytoplasmic and nuclear immunolabeling (Table 4 and 5).

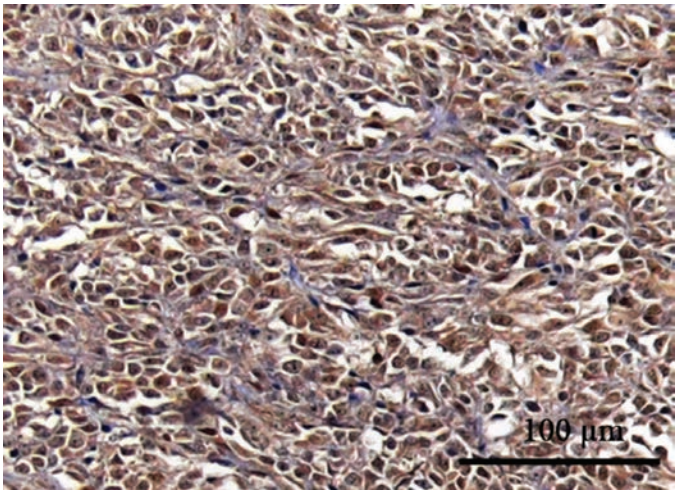


Fig.1. Canine melanoma immunolabelled for galectin-1. Positive staining in brown and counter-staining in Harris haematoxylin, obj.20x.

Serum gal-3

Gal-3 serum levels of melanoma-bearing dogs (mean = 14.55 ± 3.48ng/mL) were compared with healthy animals (mean = 10.76 ± 2.23ng/mL) by parametric Student's t-test and there was a statistically significant difference (p-value=0.0027) (Fig.3).

Western Blot for gal-3

Validation of human antibody to gal-3 was performed using western blot. The blot shows that human anti-gal-3 antibody was able to detect gal-3 in protein samples from five canine tumors used in this study, as well as in canine tumor cell lines described. Additionally, gal-3 expression was variable among cell lines and tumor samples within the same aggressiveness degree (Fig.4).

DISCUSSION

This is the first prospective study that evaluated expression patterns of gal-1 and gal-3 in canine melanomas of different degrees of aggressiveness and compared serum levels of gal-3 in melanoma-bearing dogs with healthy dogs. It has been increasingly recognized that galectins play an important role in modulating tumor cell proliferation and evolution by their interaction with the proteins encoded by the Ras oncogene that control cell proliferation, differentiation and survival (Paz et al. 2001).

In this study, the expression of gal-1 in tumor samples was predominantly cytoplasmic, since we observed more than 75% of immunolabeled cells in the majority of samples. The decision to not perform a semi-quantitative analysis on gal-1 expression was determined because tumor samples showed a very homogeneous expression pattern in frequency and a small variation in stain intensity. In human medicine, cytoplasmic expression of gal-1 can contribute to the transformation of tumor cells by interaction with proteins encoded by the Ras oncogene (Paz et al. 2001). Gal-1 can also be associated with angiogenesis, metastasis development by mechanisms of cell adhesion,

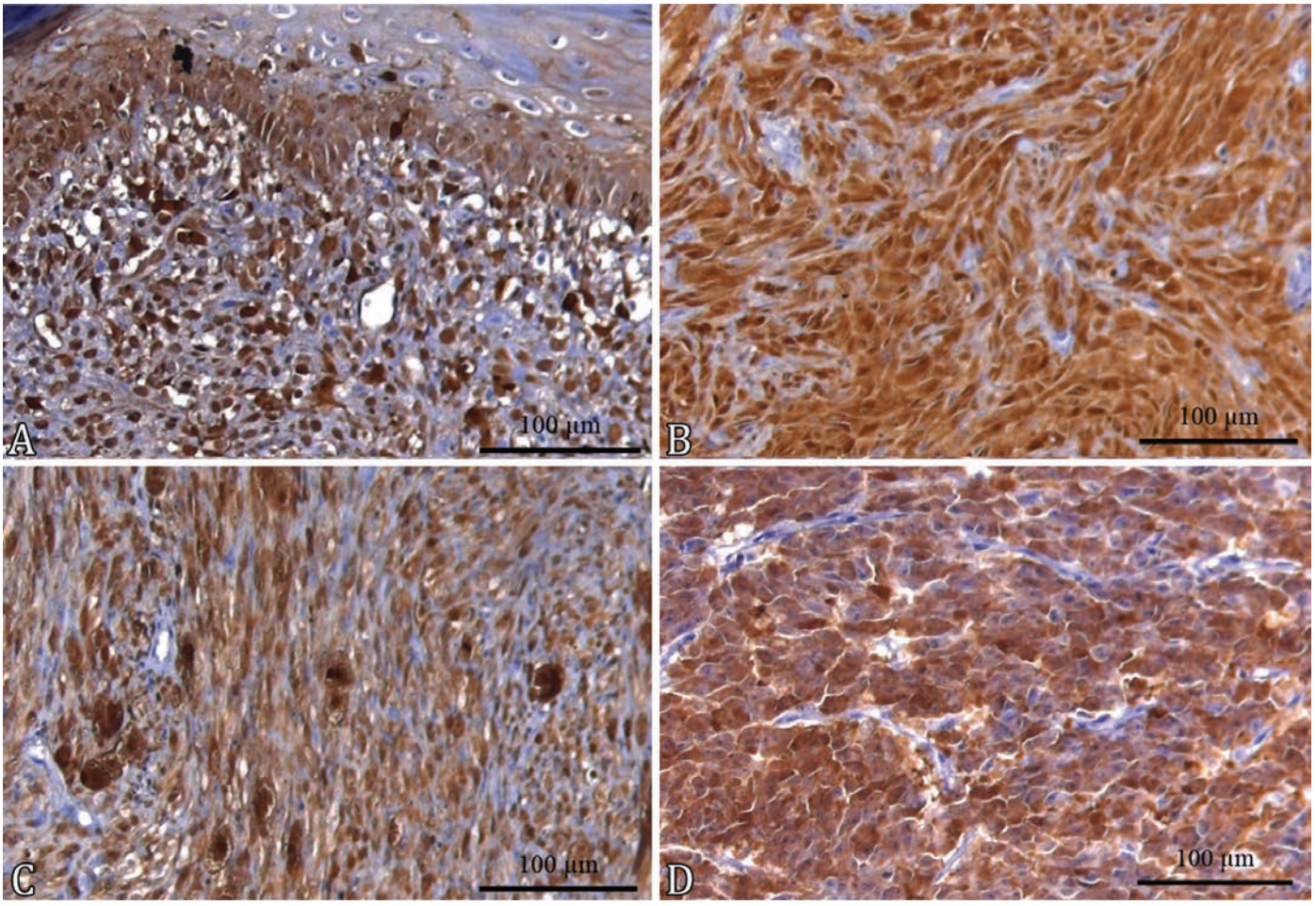


Fig.2. Canine melanoma according degree of aggressiveness immulabelled for galectin-3 (gal-3). (**A**) Canine melanocytoma immunolabelled for gal-3, cytoplasmic immunolabeling intensity score 3, cytoplasmic immunolabeling frequency score 3, nuclear immunolabeling intensity score 3 and nuclear immunolabeling frequency score 3. (**B**) Canine non-metastatic melanoma immunolabelled for gal-3, cytoplasmic immunolabeling intensity score 2, cytoplasmic immunolabeling frequency score 4, nuclear immunolabeling intensity score 2 and nuclear immunolabeling frequency score 3. (**C**) Canine metastatic melanoma immunolabelled for gal-3, cytoplasmic immunolabeling intensity score 2, cytoplasmic immunolabeling frequency score 4, nuclear immunolabeling intensity score 3 and nuclear immunolabeling frequency score 3. (**D**) Canine metastatic melanoma lymph nodes immunolabelled for gal-3, cytoplasmic immunolabeling intensity score 2, cytoplasmic immunolabeling frequency score 4, nuclear immunolabeling intensity score 2 and nuclear immunolabeling frequency score 3. Positive staining in brown and counter-staining in Harris haematoxylin, obj.20x.

Table 2. Contingency table with number of animals (n) and frequency of distribution in percentage for the different cytoplasmic immunolabeling intensity scores of gal-3 in relation to M, NM, MM and LN comparison groups

Cytoplasmic intensity	M (n) %	NM (n) %	MM (n) %	LN (n) %	Total	*P*-value
1	(2) 33	(1) 11	(5) 24	(1) 11	9	*P*<0.0001
2	(3) 50	(7) 78	(14) 67	(8) 89	32	
3	(1) 17	(1) 11	(2) 10	(0) 0	4	

M = melanocytoma, NM = non-metastatic melanoma, MM = metastatic melanoma, LN = metastatic lymph nodes.

Table3. Contingency table with number of animals (n) and frequency of distribution in percentage for the different gal-3 nuclear immunolabeling intensity scores compared to M, NM, MM and LN comparison groups

Nuclear intensity	M (n) %	NM (n) %	MM (n) %	LN (n) %	Total	*P*-value
1	(0) 0	(0) 0	(0) 0	(0) 0	0	*P*<0.0001
2	(5) 83	(4) 44	(10) 48	(4) 44	23	
3	(1) 17	(5) 56	(11) 52	(5) 56	22	

M = melanocytoma, NM = non-metastatic melanoma, MM = metastatic melanoma, LN = metastatic lymph nodes.

Table 4. Contingency table with number of animals (n) and frequency of distribution in percentage for the different cytoplasmic immunolabeling frequency scores of gal-3 compared to M, NM, MM and LN comparison groups

Frequency of labeled cytoplasmic	M (n) %	NM (n) %	MM (n) %	LN (n) %	Total	*P*-value
1	(0) 0	(0) 0	(0) 0	(0) 0	0	*P*<0.0001
2	(0) 0	(3) 33	(2) 10	(3) 33	8	
3	(5) 83	(2) 22	(14) 67	(5) 56	26	
4	17	(4) 44	(5) 24	(1) 11	11	

M = melanocytoma, NM = non-metastatic melanoma, MM = metastatic melanoma, LN = metastatic lymph nodes.

Table 5. Contingency table with number of animals (n) and frequency of distribution in percentage for the different gal-3 nuclear immunolabelling frequency scores compared to M, NM, MM and LN comparison groups

Frequency of labeled nuclear	M (n) %	NM (n) %	MM (n) %	LN (n) %	Total	*P*-value
1	(0) 0	(0) 0	(0) 0	(0) 0	0	*P*<0.0001
2	(0) 0	(4) 44	(5) 24	(5) 56	14	
3	(6) 100	(5) 56	(16) 76	(4) 44	31	
4	0	0	0	0	0	

M = melanocytoma, NM = non-metastatic melanoma, MM = metastatic melanoma, LN = metastatic lymph nodes.

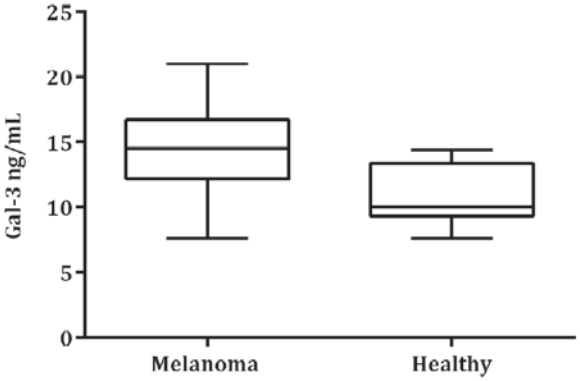


Fig.3. Mean serum concentrations of galectin-3 from melanoma-bearing dogs and healthy dogs. Box plots $p<0.05$.

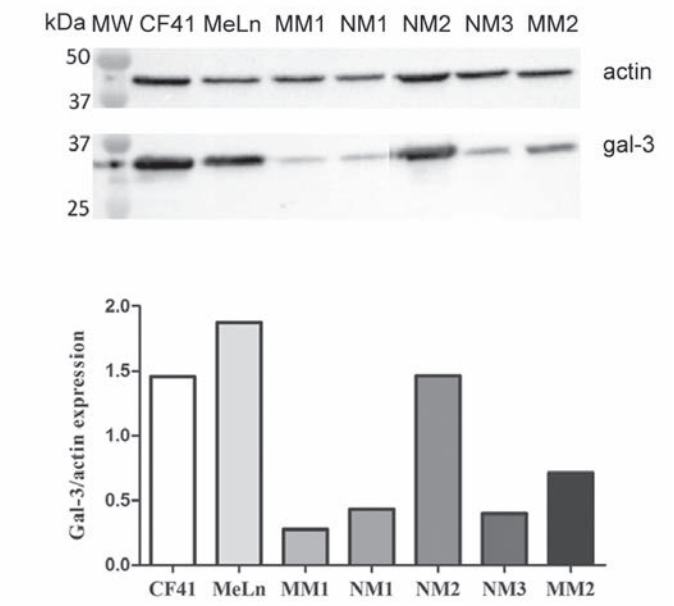


Fig.4. Western blot analysis of galectin-3 (gal-3) expression in canine primary melanomas. Blots were exposed to anti-gal-3 and anti-actin antibodies. For each sample, gal-3 protein bands density was quantified and relativized to their respective beta-actin loading control. Canine mammary gland carcinoma cell line (CF41), canine lymph node metastatic melanoma cell line (MeLn), non-metastatic melanoma (NM), metastatic melanoma (MM).

regulating immune evasion mechanisms, and immune system evasion that occurs due to T lymphocyte turnout (Rabinovich 2005, Camby et al. 2006). In addition, gal-1 expression in human melanomas has been correlated with increased tumor resistance to radiotherapy and chemotherapy treatments, due to modulation of angiogenesis and immunosuppressive cells infiltrating the tumor microenvironment (Brown et al. 2012, Borges et al. 2013). Gal-1 expression was also reported in canine mammary tumors, in which an increased staining in tumor and stromal cells (Oliveira et al. 2014) was observed. Even though gal-1 may play a significant role in tumor regulation and might be a novel therapeutic target for canine melanoma, further studies are necessary to elucidate the underlying mechanisms involved in tumor development.

In contrast to gal-1, expression of gal-3 was observed in a heterogeneous cellular location among groups, suggesting a shift in its pattern during melanoma progression, since our immunohistochemistry slides were analyzed according to the degree of aggressiveness and not by clinical stage (Owen 1980).

Surprisingly, no sample of the LN group fell under the heavily stained category, suggesting that cytoplasmic intensity of gal-3 expression significantly decreases throughout progression of melanoma and metastasis formation. Regarding the frequency of cytoplasmic immunolabeling, a decrease of labeled cells in the MM and LN groups was observed when compared to the NM and M groups, showing that there is a negative correlation between cytoplasmic staining of gal-3 and melanoma progression. According to Brown et al. (2012), high expression of gal-3 in early primary melanomas may contribute to resistance to apoptosis of these cells and metalloproteinases that are released by these cells during melanoma progression use gal-3 as a substrate, causing depletion of intracellular stocks (Brown et al. 2012). Our findings corroborate the hypothesis of Brown et al. (2012), where the depletion of intracellular gal-3 stores in melanoma progression was associated with an unfavorable prognosis and increased risk of developing metastasis (Brown et al. 2012).

Regarding nuclear immunolabeling intensity, a higher expression of gal-3 was observed in more aggressive tumors in NM, MM, LN groups when compared to benign tumors in group M. These findings corroborate those of Mourad-Zeidan (2008), who showed that metastatic lesions in human melanoma patients display high nuclear expression of gal-3 (Mourad-Zeidan 2008). Concomitant to this increase in nuclear immunolabeling intensity, a reduction in frequency of nuclear immunolabeled cells was observed in samples of the most aggressive tumors of NM, MM, LN groups when compared to benign tumors of group M. Brown et al. (2012) showed that human patients with melanoma presented worse prognosis when nuclear gal-3 expression was less frequent (Brown et al. 2012). Prieto et al. (2006) found opposing results when comparing benign neoplasms with cutaneous melanomas in different stages of evolution in human patients since he suggested that, as melanoma progresses, there is an increase in gal-3 expression (Prieto et al. 2006). This disagreement of results can be explained by the difference between the methodologies, especially in relation to the antibody used, since gal-3 can be cleaved by extracellular matrix metalloproteinases.

The present study suggests that gal-3 expression in canine melanomas is similar to gal-3 expression in human cutaneous melanomas as noted by previous studies, in which, during melanoma progression, there was a decrease in expression of gal-3 when comparing benign melanocytic lesions with melanomas at degrees of aggressiveness.

Serum gal-3 has been proposed as a prognostic biomarker in humans with skin melanoma (Vereecken et al. 2005). In our study, dogs with melanoma had a higher serum concentration of gal-3 when compared to healthy dogs. This data is in accordance with Vereecken et al. (2005), which found increased serum gal-3 concentrations in human patients with skin melanoma, suggesting that neoplastic cells are responsible for releasing gal-3 in the blood (Vereecken et al. 2005). Serum concentration of gal-3 could also be used to predict the presence of metastasis in dogs, since Ribeiro et al. (2016) showed that only mammary carcinoma patients that developed metastasis continued to have elevated serum gal-3 concentrations (Ribeiro et al. 2016) after mastectomy. In the present study, it was impossible to evaluate the potential of serum concentration of gal-3 as a prognostic factor and predictor of metastasis, because blood samples were collected at only one time point (before tumor removal).

We demonstrated that human anti-gal-3 antibody used in immunohistochemistry assays was detected in western blots and the protein possesses the expected molecular weight. This analysis was performed only in a few samples to confirm the specificity of antibody, so it was not possible to perform an extensive comparison between samples.

In human medicine, gal-3 inhibitors are being studied. These molecules are modified citrus pectin which can compete with glycans and block gal-3, mediating cell survival (Glinsky & Raz 2009, Demotte et al. 2014). Therefore, further studies are needed to better understand the contribution of these molecules to the development of canine melanoma and to investigate galectins as potential therapeutic targets.

CONCLUSIONS

Expression pattern of gal-1 in canine melanoma was predominantly cytoplasmic regardless of the degree of aggressiveness.

Our findings suggest that during canine melanoma progression, there was a decrease in expression of gal-3 when comparing benign melanocytic lesions with melanomas at degrees of agressiveness.

Dogs with spontaneous melanoma had increased serum levels of gal-3 before the excision of the neoplasia when compared to the clinically healthy animals, indicating a potential use as a monitoring and prognostic tool in patients with melanoma.

Acknowledgements.- This work is based on a Master thesis supported by "Coordenação de Aperfeiçoamento de Pessoal de Nível Superior" (CAPES) and "Fundação de Apoio à Pesquisa do Estado de São Paulo" (FAPESP, grant no. 2015/14758-8). Special thanks to clinical veterinarians who provided samples for this work.

Conflict of interest statement.- There are no conflicts of interest.

REFERENCES

Barondes S.H., Cooper D.N.W., Gitts M.A. & Lefflerm H. 1994. Galectins: structure and function of a large family of animal lectins. J. Biol. Chem. 269(33):20807-20810. <PMid:8063692>

Binh N.H., Satoh K., Kobayashi K., Takamatsu M., Hatano Y., Hirata A., Tomita H., Kuno T. & Hara A. 2013. Galectin-3 in preneoplastic lesions of glioma. J. Neurooncol. 111(2):123-132. <https://dx.doi.org/10.1007/s11060-012-1005-2> <PMid:23179497>

Borges B.E.,Teixeira V.R., Appel M.H., Steclan C.A., Rigo F., Filipak Neto F., Da Costa Ferreira A.M., Chammas R., Zanata S.M. & Nakao L.S. 2013. De novo galectin-3 expression influences the response of melanoma cells to isatin-Schiff base copper (II) complex-induced oxidative stimulus. Chem. Biol. Interact. 206(1):37-46. <https://dx.doi.org/10.1016/j.cbi.2013.08.005> <PMid:23994248>

Brown E.R., Doig T., Anderson N., Brenn T., Doherty V., Xu Y., Bartlett J.M., Smyth J.F. & Melton D.W. 2012. Association of galectin-3 expression with melanoma progression and prognosis. Eur. J. Cancer 48(6):865-874. <https://dx.doi.org/10.1016/j.ejca.2011.09.003> <PMid:22071132>

Camby I., Le Mercier M., Lefranc F. & Kiss R. 2006. Galectin-1: a small protein with major functions. Glycobiology 16(11):137R-157R. <https://dx.doi.org/10.1093/glycob/cwl025> <PMid:16840800>

Compagno D., Gentilini L.D., Jaworski F.M., Pérez I.G., Contrufo G. & Laderach D.J. 2014. Glycans and galectins in prostate cancer biology, angiogenesis and metastasis. Glycobiology 24(10):899-906. <https://dx.doi.org/10.1093/glycob/cwu055> <PMid:24939371>

Demotte N., Bigirimana R., Wieërs G., Stroobant V., Squifflet J.L., Carrasco J., Thielemans K., Baurain J.F., Van der Smissen P., Courtoy P.J. & van der Bruggen P. 2014. A short treatment with galactomannan GM-CT-01 corretcs the functions of freshly isolated human tumor-infiltrating lymphocytes. Clin. Cancer Res. 20(7):1823-1833. <https://dx.doi.org/10.1158/1078-0432.CCR-13-2459> <PMid:24526733>

Giudice C., Ceciliani F., Rondena M., Stefanello D. & Grieco V. 2010. Immunohistochemical investigation of PNL2 reactivity of canine melanocytic neoplasms and comparison with Melan A. J. Vet. Diagn. Invest. 22(3):389-394. <https://dx.doi.org/10.1177/104063871002200307> <PMid:20453212>

Glinsky V.V. & Raz A. 2009. Modified citrus pectin anti-metastatic properties: one bullet, multiple targets. Carbohydr. Res. 344(14):1788-1791. <https://dx.doi.org/10.1016/j.carres.2008.08.038> <PMid:19061992>

Johnson K.D., Glinskii O.V., Mossineb V.V., Turk J.R., Mawhinneyb T.P., Anthony D.C., Henry C.J., Huxleyz V.H., Glinsky G.V., Pienta K.J., Razbb A. & Glinsky V.V. 2007. Galectin-3 as a potential therapeutic target in tumors arising from malignant endothelia. Neoplasia 9(8):662-670. <https://dx.doi.org/10.1593/neo.07433> <PMid:17786185>

Khaldoyanidi S.K., Glinsky V.V., Sikora L., Glinskii A.B., Mossine V.V., Quinn T.P., Glinsky G.V. & Sriramarao P. 2003. MDA-MB-435 Human breast carcinoma cell homo- and heterotypic adhesion under flow conditions is mediated in part by *Thomsen-Friedenreich* antigen-galectin-3 interactions. J. Biol. Chem. 278(6):4127-4134. <https://dx.doi.org/10.1074/jbc.M209590200> <PMid:12438311>

Knapp J.S., Lokeshwar S.D., Vogel U., Hennenlotter J., Schwentner C., Kramer M.W., Stenzl A. & Merseburger A.S. 2013. Galectin-3 expression in prostate cancer and benign prostate tissues: correlation with biochemical recurrence. World J. Urol. 31(2):351-358. <https://dx.doi.org/10.1007/s00345-012-0925-y> <PMid:22892876>

Lefranc F., Mathieu V. & Kiss R. 2011. Galectin-1-mediated biochemical controls of melanoma and glioma aggressive behavior. World J. Biol. Chem. 2(9):193-201. <https://dx.doi.org/10.4331/wjbc.v2.i9.193> <PMid:21949569>

Liu F.T. & Rabinovich G.A. 2005. Galectins as modulators of tumor progression. Nat. Rev. Cancer 5(1):29-41. <https://dx.doi.org/10.1038/nrc1527> <PMid:15630413>

Mathieu V., De Lassalle E.M., Toelen J., Mohr T., Bellahcène A., Van Goietsenoven G., Verschuere T., Bouzin C., Debyser Z., De Vleeschouwer S., Van Gool S., Poirier F., Castronovo V., Kiss R. & Feron O. 2012. Galectin-1 in melanoma biology and related neo-angiogenesis processes. J. Invest. Dermatol. 132(9):2245-2254. <https://dx.doi.org/10.1038/jid.2012.142> <PMid:22622427>

Matsuda Y., Yamagiwa Y., Fukushima K., Ueno Y. & Shimosegawa T. 2008. Expression of galectin-3 involved in prognosis of patients with hepatocellular carcinoma. Hepatol. Res. 38(11):1098-1111. <https://dx.doi.org/10.1111/j.1872-034X.2008.00387.x> <PMid:18684128>

Moreno T.D., Croci D.O., Cerliani J.P., Martinez-Allo V.C., Dergan-Dylon S., Méndez-Huergo S.P., Stupirski J. C., Mazal D., Osinaga E., Toscano M.A., Sundblad V., Rabinovich G.A. & Salatino M. 2013. Targeting galectin-1 overcomes breast cancer-associated immunosuppression and prevents metastatic disease. Cancer Res. 73(3):1107-1117. <https://dx.doi.org/10.1158/0008-5472.CAN-12-2418> <PMid:23204230>

Mourad-Zeidan A.A. 2008. Role of galectin-3 in melanoma progression. Doctoral Dissertation, Faculty of Medicine, Ludwig-Maximilians-University, Munich. 164p.

Oliveira J.T., De Matos A.J., Barros R., Ribeiro C., Chen A., Hespanhol V., Rutteman G.R. & Gärtner F. 2014. Differential expression of galectin-1 and galectin-3 in canine non-malignant and malignant mammary tissues and in progression to metastasis in mammary tumors. Anticancer Res. 34(5):2211-2222. <PMid:24778023>

Owen L.N. 1980. TNM classification of tumours in domestic animals. Veterinary Public Health Unit, WHO Collaborating Center for Comparative Oncology, World Health Organization, Genebra.

Paz A., Haklai R., Elad-Sfadi G., Ballan E. & Kloog Y. 2001. Galectin-1 binds oncogenic H-Ras to mediate Ras membrane anchorage and cell transformation. Oncogene 20(51):7486-7493. <https://dx.doi.org/10.1038/sj.onc.1204950> <PMid:11709720>

Prieto V.G., Mourad-Zeidan A.A., Melnikova V., Johnson M.M., Lopez A., Diwan AH., Lazar A.J., Shen S.S., Zhang P.S., Reed J.A., Gershenwald J.E., Raz A. & Bar-Eli M. 2006. Galectin-3 expression is associated with tumor progression and pattern of sun exposure in melanoma. Clin. Cancer Res. 12(22):6709-6715. <https://dx.doi.org/10.1158/1078-0432.CCR-06-0758> <PMid:17121890>

Rabinovich G.A. 2005. Galectin-1 as a potencial cancer target. Brit. J. Cancer 92(7):1188-1192. <https://dx.doi.org/10.1038/sj.bjc.6602493> <PMid:15785741>

Ribeiro C., Santos M.S., De Matos A.J., Barros R., Gärtner F., Rutteman G.R. & De Oliveira J.T. 2016. Serum galectin-3 levels in dogs with metastatic and non-metastatic mammary tumors. In Vivo 30(1):13-16. <PMid:26709123>

Silva A.P., Silva R.G., Cogliati B., Dias A.S.M., Le Bas A.E. & Hernandez-Blazquez F.J. 2011. Bleaching of melanin in the epidermis of South American fur seal and its application on enzyme immunohistochemistry. Pesq. Vet. Bras. 31(3):267-270. <https://dx.doi.org/10.1590/S0100-736X2011000300014>

Simone G., Malara N., Trunzo V., Renne M., Perozziello G., Di Fabrizio E. & Manz A. 2014. Galectin-3 coats the membrane of breast cells and makes a signature of tumours. Mol. Biosyst. 10(2):258-265. <https://dx.doi.org/10.1039/c3mb70359b> <PMid:24281352>

Van Den Brûle F., Califice S. & Castronovo V. 2002. Expression of galectins in cancer: a critical review. Glicoconj. J. 19(7/9):537-542. <https://dx.doi.org/10.1023/B:GLYC.0000014083.48508.6a> <PMid:14758077>

Vargas T.H.M., Pulz L.H. & Strefezzi R.F. 2018. Immunohistochemical expression of Galectin-3 in canine tumors. Braz. J. Vet. Pathol. 11(1):1-6. <https://dx.doi.org/10.24070/bjvp.1983-0246.v11i1p1-6>

Vereecken P., Zouaoui Boudjeltia K., Debray C., Awada A., Legssyer I., Sales F., Petein M., Vanhaeverbeek M., Ghanem G. & Heenem M. 2005. High serum galectin-3 in advanced melanoma: preliminary results. Clin. Exp. Dermatol. 31(1):105-109. <https://dx.doi.org/10.1111/j.1365-2230.2005.01992.x> <PMid:16309497>

Verschuere T., Toelen J., Maes W., Poirier F., Boon L., Tousseyn T., Mathivet T., Gerhardt H., Mathieu V., Kiss R., Lefranc F., Van Gool S.W. & De Vleeschouwer S. 2014. Glioma-derived galectin-1 regulates innate and adaptive antitumor immunity. Int. J. Cancer. 134(4):873-884. <https://dx.doi.org/10.1002/ijc.28426> <PMid:23929302>

Wang Y., Nangia-Makker P., Tait L., Balan V., Hogan V., Pienta K.J. & Raz A. 2009. Regulation of prostate cancer progression by galectin-3. Am. J. Pathol. 174(4):1515-1523. <https://dx.doi.org/10.2353/ajpath.2009.080816> <PMid:19286570>

Woo H.J., Joo H.G., Song S.W., Sohn Y.S. & Chae C. 2001.Immunohistochemical detection of galectin-3 in canine gastric carcinomas. J. Comp. Pathol.124(2/3):216-218. <https://dx.doi.org/10.1053/jcpa.2000.0442> <PMid:11222020>

PESQUISA VETERINÁRIA BRASILEIRA
Brazilian Journal of Veterinary Research
ISSN 0100-736X (Print)
ISSN 1678-5150 (Online)

Pesq. Vet. Bras. 40(12):1018-1028, December 2020
DOI: 10.1590/1678-5150-PVB-6543

Original Article
Small Animal Diseases
BY-NC

Effects of canine adipose-derived mesenchymal stem cells on the epithelialization of rabbits' skin autograft (*Oryctolagus cuniculus*)[1]

Jorge L. Alvarez Gómez[2]*, Josiane M. Pazzini[2], Michele A. Barros[3], Bruna P. Morais[3], Bruna Firmo[2], Andresa Matsui[3], Roberto Ampuero[2] and Andrigo B. De Nardi[2]

ABSTRACT.- Alvarez Gómez J.L., Pazzini J.M., Barros M.A., Morais B.P., Firmo B., Matsui A., Ampuero R. & De Nardi A.B. 2020. **Effects of canine adipose-derived mesenchymal stem cells on the epithelialization of rabbits' skin autograft (*Oryctolagus cuniculus*)**. *Pesquisa Veterinária Brasileira 40(12):1018-1028*. Departamento de Clínica e Cirurgia Veterinária, Faculdade de Ciências Agrárias e Veterinárias, Universidade Estadual Paulista "Júlio de Mesquita Filho", Via de Acesso Prof. Paulo Donatto Castellane s/n, Jaboticabal, SP 14884-9900, Brazil. E-mail: jorgeluisalgo@gmail.com

The present study aimed to evaluate the effects of mesenchymal stem cells derived from canine adipose tissue in the healing process of full-thickness mesh skin grafts in rabbits. The stem cells were collected from young dogs; and, after characterization, remained in cryopreservation, in independent doses containing 2 x 10^6 cells. The mesh distal limb graft technique was performed in 60 rabbits, divided into three groups, CG (Control Group), GT1 (Intralesional Stem Cell Treated Group), and GT2 (Intravenous Stem Cell Treated Group), containing 20 animals each. After grafting, each group was randomly divided into four subgroups according to euthanasia time 3, 7, 14, and 30 days, containing five animals in each group. Animals of GT1_14, GT1_30, and GT2_14, GT2_30 subgroups received a second dose of xenogeneic cells on the seventh day. Meanwhile, animals from GT1_30 and GT2_30 received the third dose of xenogeneic cells on day 14. The groups treated with xenogeneic stem cells positively affected type III collagen re-epithelialization and deposition, and possibly GT1 had a controlled inflammatory response. However, no effect on angiogenesis. Thus, it was possible to demonstrate tolerance and therapeutic action of mesenchymal stem cells from canine adipose tissue in skin grafts in rabbits.

INDEX TERMS: Canine, stem cells, epithelialization, rabbits, skin autograft, *Oryctolagus cuniculus* xenogens, mesh grafts, healing, revascularization, angiogenesis, rabbits.

RESUMO.- [**Efeitos das células-tronco mesenquimais derivadas do tecido adiposo de cães na epitelização de autoenxertos de pele em coelhos (*Oryctolagus cuniculus*).**] O presente estudo teve como principal objetivo avaliar os efeitos das células-tronco mesenquimais derivadas do tecido adiposo de cães no processo de cicatrização de autoenxertos de pele de espessura total em malha em coelhos. As células-tronco foram coletadas de cães jovens, após a caracterização estas permaneceram em criopreservação, em doses individuais contendo 2 x 10^6 células. A técnica de enxerto em malha na região distal do membro foi realizada em 60 coelhos, divididos em três grupos, GC (Grupo Controle), GT1 (Grupo tratado com células-tronco intralesional) e GT2 (Grupo tratado com células-tronco via endovenosa), contendo 20 animais cada. Imediatamente após a enxertia, cada grupo foi dividido aleatoriamente em quatro subgrupos, de acordo com o tempo de eutanásia 3, 7, 14 e 30 dias contendo cinco animais cada. Animais dos subgrupos GT1_14, GT1_30 e GT2_14, GT2_30 receberam uma segunda dose de células xenógenas no sétimo dia. Ademais, animais do GT1_30 e do

[1] Received on June 21, 2020.
Accepted for publication on September 10, 2020.
Master's Research with support from CAPES.

[2] Departamento de Clínica e Cirurgia Veterinária, Faculdade de Ciências Agrárias e Veterinárias, Universidade Estadual Paulista "Júlio de Mesquita Filho" (Unesp), Via de Acesso Prof. Paulo Donato Castellane s/n, Jaboticabal, SP 14884-9900, Brazil. *Corresponding author: jorgeluisalgo@gmail.com

[3] Regenera Stem Cells, Rua Baguaçu 26, Ed. Business Center II, Sala 101, Alphaville Empresarial, Campinas, SP 13098-327, Brazil. E-mails: michele@regeneravet.com.br, bruna@regeneravet.com.br

GT2_30 receberam a terceira dose de células xenógenas no dia 14. Os grupos tratados com células-tronco xenógenas tiveram um efeito positivo na reepitelização e deposição de colágeno tipo III, e possivelmente, o GT1 teve uma resposta inflamatória controlada, entretanto o efeito na angiogênese não foi observado. Dessa forma, foi possível demonstrar que houve tolerância e ação terapêutica das células-tronco mesenquimais derivadas do tecido adiposo de cães em enxertos de pele em coelhos.

TERMOS DE INDEXAÇÃO: Células-tronco, cães, autoenxertos, pele, coelhos, *Oryctolagus cuniculus*, xenógenas, enxertos em malha, cicatrização, revascularização, angiogênese, coelhos.

INTRODUCTION

Full-meshed skin autografts are a cutaneous segment that includes the epidermis and the entire dermis. This grafting technique is commonly used to cover large defects after excision of neoplasms, trauma, or burns, mainly when the wounds are located in the limbs' distal region or on flexor surfaces (Bohling & Swaim 2012, MacPhail 2013). Traditionally, a recipient site with granulation tissue is recommended for the technique's success; however, this recommendation does not seem to influence graft survival (Tong & Simpson 2012, Riggs et al. 2015). Severe inflammation, the presence of clots, or the formation of seroma between the graft and recipient site site during the first week of grafting interfere negatively in phases of adherence, inosculation, and revascularization, causing delay of the regenerative process, failure of technique, and death of the graft (Andreassi et al. 2005, Bohling & Swaim 2012, MacPhail 2013). To improve the fixation and adherence of skin graft in the recipient site, and consequently to stimulate epithelialization and angiogenesis, some studies have evaluated negative vacuum pressure therapy (Nolff & Meyer-Lindenberg 2015, Or et al. 2017), platelet-rich plasma sponge (Pazzini et al. 2018) and laser therapy (Reis Filho et al. 2017), showing promising results.

In the field of regenerative medicine, it has been shown that mesenchymal adipose-derived stem cell (ADSCs) accelerates the stages of the skin wound healing process (Kim et al. 2007), including ischemic wounds caused by diabetes (Kim et al. 2011) and wounds caused by burns (Franck et al. 2019), with increased collagen secretion and deposition (Kim et al. 2007, Franck et al. 2019). Autologous ADSCs have also been shown to improve skin autografts' survival in diabetic rats (Zografou et al. 2013). Studies on ischemia and reperfusion models of axial skin flaps have reported a favorable effect of ADSCs, decreasing necrosis and associated complications (Suartz et al. 2014, Pu et al. 2017).

These facts corroborate that autogenous or allogeneic mesenchymal stem cells have a reparative effect, either by direct transdifferentiation compatible with the cells of the injured tissue or, indirectly by a paracrine effect (Rehman et al. 2004) by several growth factors with antifibrotic or anti-apoptotic action (Rehman et al. 2004), angiogenic action (Kim et al. 2011, Hamada et al. 2019, Franck et al. 2019), anti-inflammatory and immunomodulatory action (Pu et al. 2017, Oliveira et al. 2018, Pinto-Filho et al. 2018). Concerning xenogenous mesenchymal stem cells, experimental studies reported that transplantation of pig adipose-derived stem cells (ADSCs) into joints of dogs with osteoarthritis was favorable in controlling the disease (Tsai et al. 2014). Human ADSCs were also effective in healing skin wounds in rabbits (Rodriguez et al. 2015, Kim et al. 2017) and mice (Kim et al. 2011), without showing clinical signs of intolerance to xenogen transplantation. According to Li et al. (2012), only six (6.4%) of 88 published experiments showed failure in stem cells' function, constituting a possible therapeutic alternative with potential clinical use. In this sense, the present study aimed to evaluate the effects of mesenchymal stem cells derived from dogs' adipose tissue in the healing process of full-thickness skin autografts in rabbits.

MATERIALS AND METHODS

The experiment was approved by the Ethics Committee on the Use of Animals (ECUA/FCAV), protocol number 173466/15, of "Faculdade de Ciências Agrárias e Veterinárias", "Universidade Estadual Paulista "Júlio de Mesquita Filho" (Unesp), Campus of Jaboticabal/SP, Brazil.

Animals. Sixty New Zealand White female rabbits (*Oryctolagus cuniculus*), fourteen weeks of age and average weight of 3.0kg (standard deviation 0.14), clinically healthy and without physical changes. The animals were divided into three groups, CG (Control Group), GT1 (Group treated with adipose-derived stem cells (ADSCs), intralesional), and GT2 (Group treated with ADSCs, intravenously), containing 20 animals each. Immediately after grafting, each group was randomly divided into four subgroups, according to the time of euthanasia: 3, 7, 14, and 30 days (GC_3, GC_7, GC_14, GC_30; GT1_3, GT1_7, GT1_14, GT1_30 and GT2_3, GT2_7, GT2_14, GT2_30) with five animals each. Before the experimental procedure, all rabbits were kept in individual cages for an adaptation period of four weeks, in a controlled environment to reduce the stress response, receiving water ad libitum and 100 grams per day of commercial feed for fattening (Agromix Animal Nutrition, Jaboticabal/SP, Brazil) and 100 grams of hay every 48 hours. The rabbits were handed at the same hours and by the same staff.

Xenogenous stem cells. The mesenchymal stem cells derived from dogs' adipose tissue were obtained from the stem cell bank of the company Regenera Stem Cells® (Campinas/SP, Brazil), cryopreserved in individual flasks containing doses of 2×10^6 cells, ready for use. According to company information, the origin of the adipose tissue is periovarian (10-15g) collected during the castration of young donors (≤2 years) and healthy (negative for distemper, parvovirus, and leishmania). The collected adipose tissue was washed, fragmented, and incubated for one hour in a saline solution buffered with Dulbecco's phosphate (DPBS) with a 0.1% type I Collagenase, and centrifuged. Subsequently, the cell precipitate was resuspended in culture (modified Eagle medium with high glucose concentration (LGC Biotechnology, São Paulo, Brazil), 15% fetal bovine serum (Hyclone Inc., Logan/UT, USA), 1% penicillin/streptomycin, 1% of non-essential amino acids and 1% L-glutamine (LGC Biotechnology) and incubated at 37°C and 5% CO_2. When it reached approximately 70% confluence, the cells were trypsinized and expanded. Part of the material was separated for characterization, where the potential for differentiation of mesenchymal stem cells (MSC) was assessed through its ability to differentiate into three different cell lines (osteogenic, adipogenic, and chondrogenic) under specific culture conditions. The immunophenotypic profile of MSCs was evaluated through flow cytometry by expression of CD44, CD73, CD90, CD105, and the absence of CD34 and CD45.

Anesthetic procedure. Rabbits were pre-anesthetized with 0.07mg/kg of acepromazine (Acepran®Vetnil, São Paulo, Brazil) and 0.5mg/kg of morphine (Dimorf®, Cristália, São Paulo, Brazil)

intramuscularly. After 15 minutes, the animals were oxygenated for one minute using a face mask attached to a semi-open system connected to the anesthesia machine. Afterward, isofluorane (Isoflorine®, Cristália, São Paulo, Brazil) was supplied 5V% until the animal allowed to instill oral spray Lidocaine (Xylestesin®, Cristália, São Paulo, Brazil). In lateral decubitus and with the head extended, the orotracheal intubation with a Magil probe number 3.0 was performed. Subsequently, the concentration of isofluorane was then adjusted to maintain an adequate anesthetic plan. The atrial artery was catheterized (22G BD Insyte catheter, Minas Gerais, Brazil) to monitor blood pressure throughout the procedure.

Surgical procedure. With the animal in an adequate anesthetic plane, trichotomy of the right lateral wall of the chest (local donor) and the distal region of the right radio (recipient site) was performed, followed by antisepsis and asepsis. A 2cm x 2cm square wound was created in the recipient site, leaving the tendons of the radial carpal extensor muscle, common digital extensor, and lateral digital extensor exposed. Then, at the donor site, a 2cm x 2cm incision was made to obtain the skin fragment and transform it into a full-thickness mesh graft. Subsequently, the graft edges were fixed with 4-0 nylon suture in a particular simple suture pattern. The donor site wound was also closed with 4-0 nylon thread, in a simple interrupted suture pattern, in a centripetal way. Finally, to compress the graft to the recipient site, non-adherent compressive bandages were performed, the first contact layer consisting of a non-sterile adherent gauze moistened with lubricating gel (K-Y® Johnson & Johnson, Brazil), the second layer of sterile dry gauze, and cotton bandage, and the third layer of protection with waterproof adhesive. All animals received a prophylactic dose of 5mg/kg of enrofloxacin (injectable Chemitril 2.5%, Chemitec, Brazil) subcutaneously, 20 minutes before the start of surgery.

Analgesia with tramadol hydrochloride (Tramal® ampoule 50mg/ml), dosage of 3mg/kg/subcutaneously, every 8 hours for three days postoperatively. The evaluation of acute pain was performed based on changes in behavior and facial expression in rabbits recommended by Leach et al. (2009) and Keating et al. (2012). No anti-inflammatory drugs were injected. The bandage swap was repeated every 72 hours, followed by the macroscopic assessment of the grafts recommended by Reis Filho et al. (2017) by a single evaluator blindly.

Xenogenous stem cell transplantation. In all GT1 animals, the first dose of 2 x 10^6 adipose-derived stem cell (ADSC) cells was intralesional before positioning the graft at the recipient site. Immediately after thawing the ADSC and later dilution of 2 x 10^6 ADSCs in 0.5 mL of lactated ringer's solution, 0.1 ml was injected in five different locations (confluent lateral edges of the wound and in the middle of the lesion) using a 21 G needle. GT1_14 animals received the second dose on the seventh postoperative day. The GT1_30 animals received the second and third doses on the seventh and fourteenth postoperative day, respectively, through the grafts' lateral slits. All GT2 animals received the first dose of 2 x 10^6 ADSC cells, diluted in 1.0mL of lactated ringer's solution, slowly through the ear's marginal vein using a 22 G catheter and a 21G needle, immediately after graft fixation at the recipient site. GT2_14 animals received the second dose on the seventh postoperative day. GT2_30 animals received the second and third doses on the seventh and fourteenth postoperative day, respectively. However, in the CG animals, only skin autograft was performed. The thawing and washing of the ADSCs were performed using the same company's defrosting kit that guarantees the viability of ADSC above 70%; for this reason, after thawing the ADSC, a viability test was not performed at the time of intralesional transplantation or intravenous infusion.

Histopathological evaluation. After euthanasia on the previous days, the grafts were excised with an extra 0.5cm lateral margin of intact skin and a deep facial plane. The samples were immersed for 36 hours in buffered formaldehyde 10%. After this period, they were transferred to a 70% alcohol solution (70% ethyl alcohol) until the moment of paraffin inclusion processing. The 4µm cross-sections were stained with hematoxylin and eosin (HE). The evaluation of inflammation, vascularization, and fibroblasts was the quantitative method of counting mononuclear and polymorphonuclear cells, blood vessels, and fibroblasts both in the superficial and deep dermis, selecting five histological fields at 40x magnification, and was expressed as the average number of vessels per sample. The evaluation of re-epithelialization and necrosis was performed as recommended by Reis Filho et al. (2017). For the evaluation of collagen, picrosirius was used (Easy Path - Picrosirius Red Staining). The sections were analyzed under an optical microscope under polarized light (Olympus BX-53®, Japan). From each slide, 5 histological fields were selected and photomicrographed at a 20x magnification. The images were analyzed with the *software* Image J®, with the plug-in Threshold Colour. The observation of type I collagen fibers (yellow-orange to orange and red birefringence) and type III collagen (green or yellow-birefringence) was identified as recommended by Bedoya et al. (2016).

Immunohistochemistry. The cuts were extended on glass sheets previously cleaned and degreased, prepared with an organosilane-based adhesive (3-aminopropyltriethoxysilane, Sigma Chemical, C.O., USA). Monoclonal antibody CD31 evaluated Immunomarking of vascular endothelium for angiogenesis (Abcam), 1:50 dilution, antigenic recovery with porcine gastric mucous pepsin (Sigma life the science-United Kingdom) 37°C greenhouse, incubation 120 min, a detection system for polymer kit method (Novolinktm Polymer Detection Systems, Leica Biosystems New Castle Ltda-United Kingdom). The immunomarking evaluation of the vascular endothelium (angiogenesis) was performed by the quantitative method of microvascular counting, according to Pazzini et al. (2017), analyzing the areas with the largest number of vessels in the superficial and deep dermis, selecting five fields for analysis in the 40x magnification and was expressed as the average number of vessels in each sample.

Macroscopic evaluation and statistical analysis. The eight continuous variables (macrophages, neutrophils, monocytes, fibroblasts, vascularization, type I collagen, type III collagen, CD31) were categorized into three levels considering the position of the values of each variable: lowest (0<25% first quartile), medium (>25-75% second quartile) and highest (>75% third quartile). This division was performed for each group (GC, GT1, GT2). For categorical variables such as necrosis, re-epithelialization, secretion, and crust, they were cataloged in four classes: absent, discreet, moderate, and accentuated. The graft color variable was classified as usual pink-red, blue, and ischemic. Burt's tables were created, and multivariate multiple correspondence analysis (MCA) for times 3, 7, 14, to determine the association and total variation between the categorical variables and 30 for GC, GT1, and GT2 (general correspondence). After the general correspondence analysis, the variables were grouped into three classes: inflammatory cells (macrophages, neutrophils, monocytes), proliferation (fibroblasts, vascularization, type III collagen, type I collagen, CD31), and external appearance (graft color, secretion, crust, necrosis, re-epithelialization) performing a new ACM analysis for each class by groups including the four times in the same analysis. The Statistical program (STATSOFT, Version 7) was used with a significance level of 0.05.

RESULTS

During the experiments, the animals of GT1 and GT2 did not show local or systemic clinical signs suggestive of rejection or hypersensitivity after transplantation of xenogenic stem cells. On the third day of the macroscopic evaluation, serosanguinolent secretion was moderate in all groups but gradually decreased over the first week of evaluation (Fig.1). However, the animals of GT1_14 continued to present a discreet serous secretion, possibly because they received the second dose of intralesional stem cells on the seventh postoperative day. In most cases, the re-epithelialization of the graft slits was prominent after the seventh day (Fig.1). The grafts' color was similar between all groups; however, grafts in GT2 had a better macroscopic appearance (no crusts) after the second week of evaluation (Fig.1).

Through multiple correspondence analysis (MCA) of the variables grouped in the external appearance class, it was possible to identify a significant correspondence ($p<0.05$) of the re-epithelialization with GT1_3, GT1_30, and GT2_3 (Fig.2)

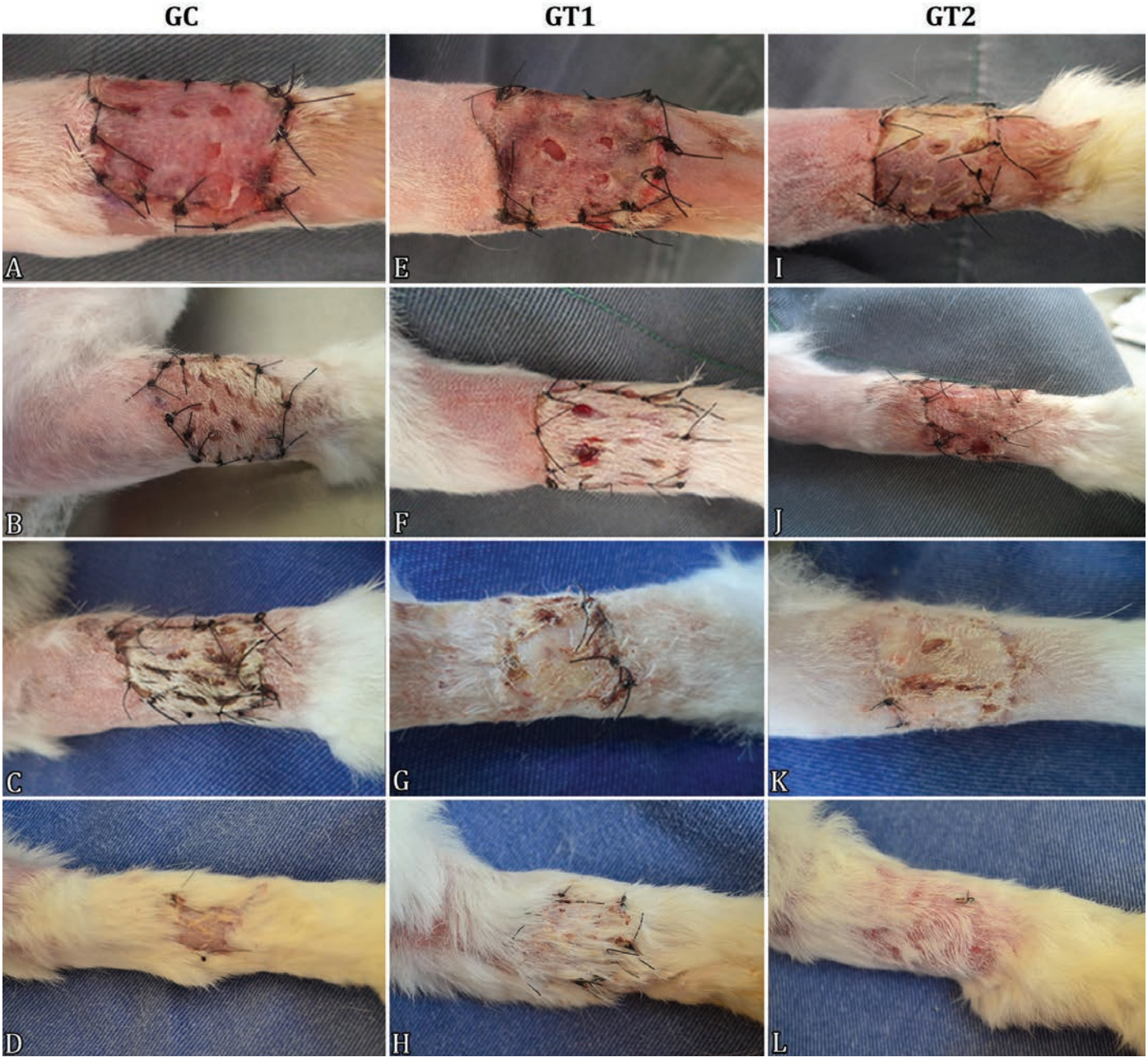


Fig.1. Macroscopic evaluation and clinical evolution of mesh skin grafts in the distal region of the right thoracic limb in rabbits (*Oryctolagus cuniculus*). The presence of secretion through the open slits and the reddish-pink color mixed with the blue or ischemic color was notorious on the third day of evaluation (**A**) GC_3, (**E**) GT1_3, (**I**) GT2_3. On the seventh day, the secretion decreased, and the cracks started to heal (**B**) GC_7, (**F**) GT1_7, (**J**) GT2_7. On the fourteenth day, the grafts' color was similar to normal tissue, with the presence of crusts and healing of the slits in the grafts. (**C**) GC_14, (**G**) GT1_14, (**K**) GT2_14. In general, on the 30th, there was hair growth, showing the treated groups better appearance (**H**) GT1_30, (**L**) GT2_30 than the control group (**D**) GC_30.

and re-epithelialization with GT1_7 and GT2_7 (p<0.10). Although there are other correspondences described in table 1, they were not significant. Regarding the infiltration of inflammatory cells, formed by neutrophils, macrophages, and monocytes, were present in most samples of GC, GT1, and GT2. The cellular infiltrate in the superficial and deep dermis was more evident in samples from the seventh day, gradually decreasing until the 30th. There were some inflammatory foci in the superficial dermis. Through the MCA of the variable inflammatory cells, summarized in table 1, a significant correspondence (p<0.05) of macrophages and GT1_3 and GT1_14 was observed (Fig.3). Other significant associations between the variable high neutrophils with high monocytes and low neutrophils with low monocytes were observed in GT2_7 and GT1_14, respectively. Regarding the control group, there were no significant matches.

During the microscopic evaluation of the samples on the third day, it was possible to observe incomplete epithelialization, predominant in the not re-epithelialized area, especially in grafts from the control group. (Fig.4). The integration of the graft at the recipient site was evident after the seventh day. Necrosis was similar between CG, GT1, and GT2, being on the third day multifocal in most samples and with discrete signs on the seventh day. In all groups. Fibroblast proliferation was marked on the seventh and moderate on the fourteenth day of evaluation. Samples from animals treated with xenogenous adipose-derived stem cells (ADSCs) had a more significant presence of keratinocytes proliferating on day 14. Evaluation of vascularization/angiogenesis by the quantitative counting method microvascular in HE stained samples (Fig.4) and immunostaining with CD31 antibody, respectively, were similar.

Regarding collagen fibers, after histochemical evaluation with picrosirius (Fig.5), it was observed that type III collagen

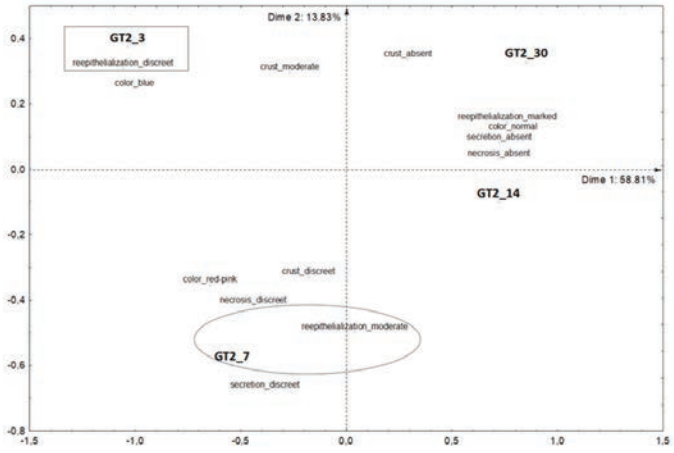


Fig.2. Multiple correspondence analysis of the variables grouped in the external appearance class (graft color, secretion, crust, necrosis, re-epithelialization) for treatment group 2 (GT2), including the four times in the same analysis. There was a significant correspondence (p<0.05) of the variables within the rectangle. However, the variables within the circle were significant for p<0.10.

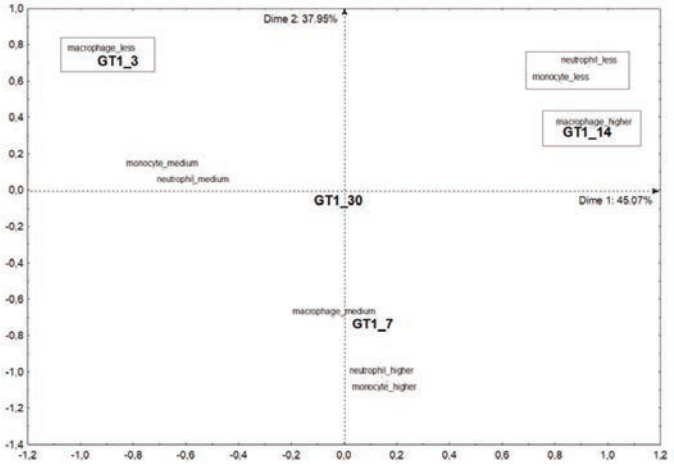


Fig.3. Analysis of multiple correspondences of the variables grouped in the class inflammatory cells (macrophages, neutrophils, monocytes) for treatment group 1 (GT1), including the four times in the same analysis. There was a significant correspondence (p<0.05) of the variables within the rectangle. Although there were other correspondences, they were not significant.

Table 1. Summary of the multiple correspondence analysis of variables grouped into three classes: inflammatory cells, proliferation and external appearance

Grouped variables	Group	Evaluation day			
		3	7	14	30
Macro/Neutral/Mono	GC	L/L/L	H/H/H	M/-/M	M/M/-
	GT1	L/M/M	M/H/H	H/L/L	M/M/-
	GT2	L/M/L	H/H/H	M/L/M	M/-/-
Fibro/Vasc/COL-I/COL-III/CD31	GC	L/L/-/-/L	H/H/-/M/M	M/M/-/-/H	-/-/L/H/-
	GT1	M/-/-/L/-	-/M/H/-/H	L/L/-/-/-	H/H/L/H/-
	GT2	L/L/-/-/-	M/M/-/H/-	H/H/-/-/L	M/M/-/H/-
Necros/reepitel/color/secretion/crust	GC	mo/-/-/mo/-	-/-/r/d/d	-/mo/-/-/mo	-/ch/n/a/a
	GT1	-/d/is/-/-	d/mo/r/-/-	-/-/-/d/mo	a/ch/n/a/a
	GT2	-/d/bl/-/-	d/mo/r/d/d	a/ch/n/a/a	a/ch/n/a/a

Macro = macrophages, Neutral = neutrophils, Mono = monocytes, Fibro = fibroblasts, Vasc = vascularization, COL I = collagen type I, COL-III = collagen type III, CD31 = angiogenesis, L = low, M = medium, H = high, a = absent, d = discrete, mo = moderate, ch = checked, n = normal, r = red-rose, bl = blue, is = ischemic.

fibers predominated at all times of assessment and in all groups. However, edema in the deep dermis was frequently observed in GT1_7 and GT1_14, dissociating the collagen fibers. In this same group, there were also hemorrhage foci on the third, seventh, and fourteenth day of the microscopic evaluation (Fig.4).

Through the multiple correspondence analysis (MCA) of the proliferation variables (fibroblasts, vascularization, collagen type III, collagen type I, CD31), several matches were found (Table1). However, a significant correspondence ($p<0.05$) of the vascularization was observed in the control group (GC_7, GC_14); in the group treated with intralesional stem cells (GT1_30) and, in the group treated with stem cells intravenously (GT2_3, GT2_14) (Fig.6). There was also a significant correspondence of type III collagen in GT1_3, GT1_30, and GT2_30. On the other hand, fibroblast proliferation was significant only in GT2_3 (Fig.6).

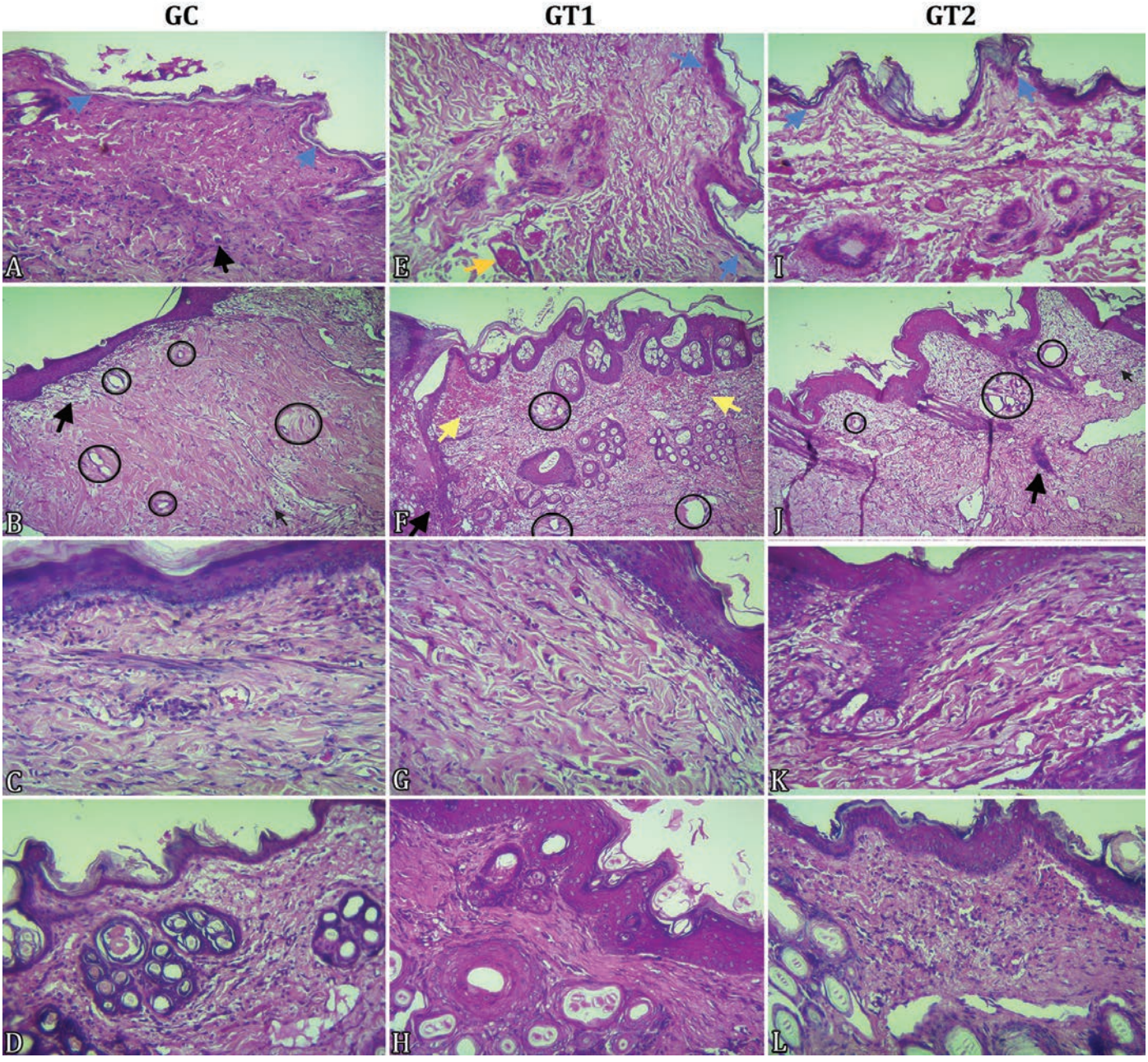


Fig.4. Microscopic evaluation of full-thickness mesh skin grafts in rabbits (*Oryctolagus cuniculus*). On the third day, the formation of discontinuous and thin epithelium is observed - epidermis (blue arrow), hemorrhage foci (yellow arrow) and slight presence of inflammatory cells (black arrow) (**A**) GC_3, (**E**) GT1_3, (**I**) GT2_3. On the seventh day, there was a predominance of the re-epithelialized area, neoangiogenesis (black circle), mild hemorrhage (yellow arrow) (**B**) GC_7, (**F**) GT1_7, (**J**) GT2_7. On the fourteenth day, the re-epithelialization was complete on the connective tissue (**C**) GC_14, (**G**) GT1_14, (**K**) GT2_14. On day 30, a complete formed epithelium is observed, showing follicles developed in the treated groups (**H**) GT1_30, (**L**) GT2_30 than in the control group (**D**) GC_30. (**B**, **F**, **J**) HE, obj.10x. (**A**, **C**, **D**, **E**, **G**, **H**, **I**, **K**, **L**) HE, obj.20x.

DISCUSSION

According to Andreassi et al. (2005) and Liptak (2012), fibrin, leukocytes, and fibroblasts play essential roles in the adherence and plasma imbibition of grafting. However, the adherence phase can be compromised by excess fluids in the recipient site (Yucel et al. 2016) or by the presence of xenogenic biological material (Reis Filho et al. 2017), interfering with graft adhesion to the recipient site, causing chronic inflammation, purulent secretion, ischemic necrosis and consequent failure of graft integration and healing (Bohling & Swaim 2012, MacPhail 2013, Reis Filho et al. 2017). However, grafts treated with intralesional xenogenous stem cells did not demonstrate these harmful clinical signs despite delayed serous secretion in GT1 (GT1_14), similar to another study (Rodriguez et al. 2015). Edema, dissociation of collagen fibers, and foci of hemorrhage in GT1 samples possibly occurred due to the dilution volume (Yucel et al. 2016). Due to repeated local trauma after intralesional injection (in the second and third doses) with a 21G gauge needle, both the dilution volume and repeated injections did not hinder the success of the mesh grafts. Recently, a study demonstrated that a local injection of 200μL of 0.9% saline solution in full-thickness grafts in

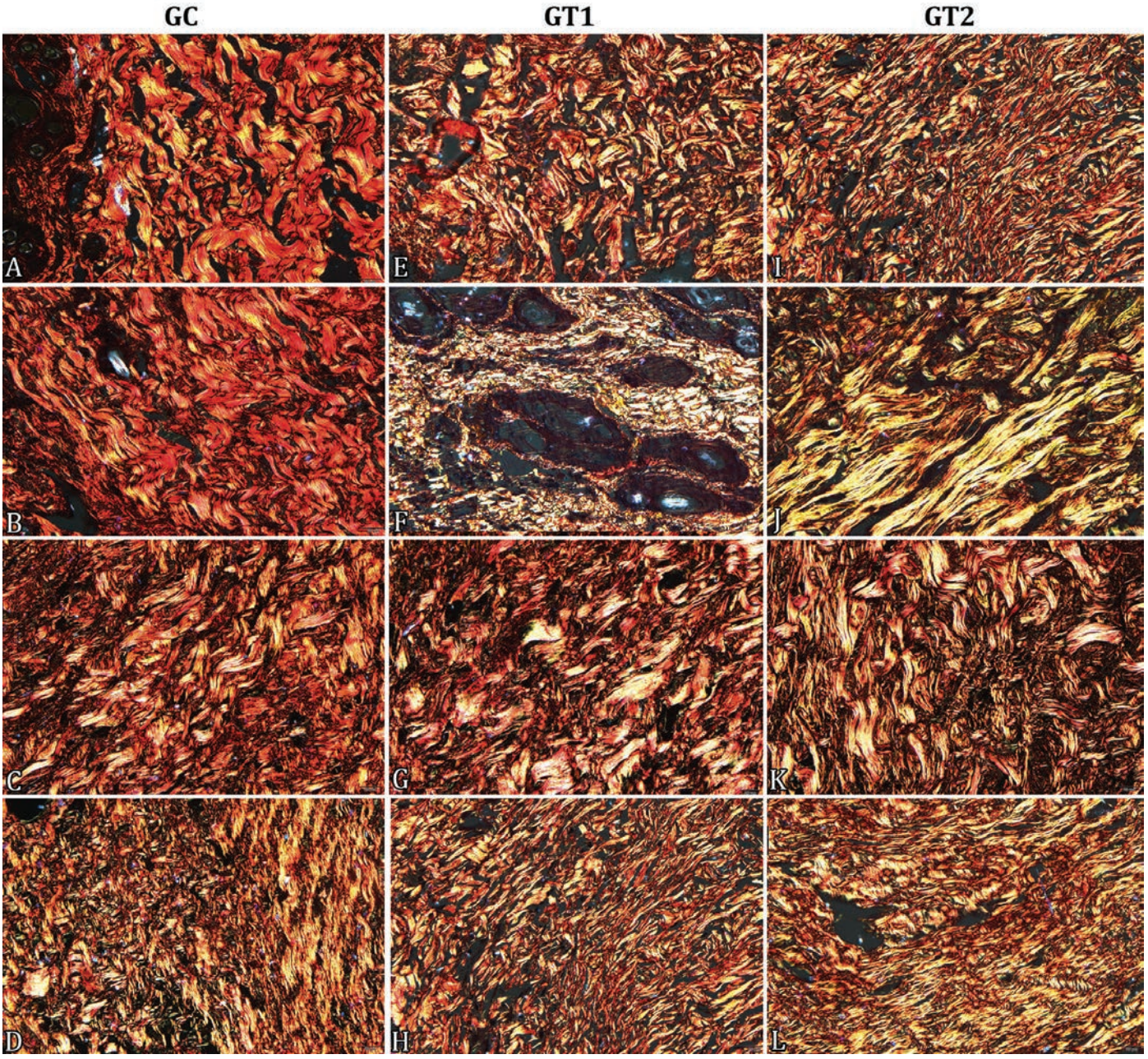


Fig.5. Photomicrography under polarized light of the evaluation of collagen fibers, analysis with Image J® software with the Threshold Color plug-in. The organization of collagen fibers in the central region of the skin graft in rabbits (*Oryctolagus cuniculus*) is shown in samples from the third day (**A**) GC_3, (**E**) GT1_3, (**I**) GT2_3, from the seventh day (**B**) GC_7, (**F**) GT1_7, (**J**) GT2_7, on the fourteenth (**C**) GC_14, (**G**) GT1_14, (**K**) GT2_14 and the 30th, (**D**) GC_30, (**H**) GT1_30, (**L**) GT2_30. Picrosirius staining, obj.20x.

rats caused a more significant inflammatory reaction than a negative control group (without injection) (Vidor et al. 2018).

Nevertheless, when allogeneic adipose-derived stem cells (ADSCs) were transplanted simultaneously, this inflammatory process was attenuated at the graft site (Vidor et al. 2018). This fact explains why the GT1 grafts managed to overlap the inflammatory process caused by the intralesional injection. Possibly there was an interaction between the inflammatory cells and the transplanted stem cells, activating a paracrine mechanism with pro-inflammatory and anti-inflammatory cytokines (Kim et al. 2013, Vidor et al. 2018), creating a favorable transition from the inflammatory to the proliferative phase (Kim et al. 2013). Regarding the presence of polymorphonuclear cells at the lesion site, Oliveira et al. (2018) report that mesenchymal stem cells promote chemotaxis of polymorphonuclear cells to the injury site, but for Ma et al. (2014) and Zachar et al. (2016), the actions of mesenchymal stem cells seem to vary according to the inflammatory process and between animal species.

Studies have established that macrophages play a central role in the different phases of physiological wound repair (Zhang et al. 2010, Heo et al. 2011). Depending on the phenotype, macrophages are classified as activated M1 or pro-inflammatory macrophages and, in alternative activated macrophages M2 or anti-inflammatory with regenerative functions that promote tissue homeostasis (Das et al. 2015, Krzyszczyk et al. 2018). Mesenchymal stem cells exert their modulating effect on M1 phenotype macrophages' polarization for the M2 phenotype (Blázquez et al. 2016). A study carried out in rats demonstrated that the macrophages phenotype M2 with the macrophages phenotype M1 were statistically significant on the second day of grafting, with low levels of pro-inflammatory cytokines IL-1β, and FNT-α and high levels of IL-10, thus regulating the local inflammation of cutaneous autografts treated with adipose-derived stem cells (ADSCs) (Wang et al. 2016). Other studies suggest that mesenchymal stem cells can induce monocyte (M0) polarization to acquire phenotype macrophage characteristics M2 (Zhang et al. 2010, Heo et al. 2011), or in the absence of IL-6, mesenchymal stem cells can induce M0 polarization for the phenotype M1 (Wang et al. 2016).

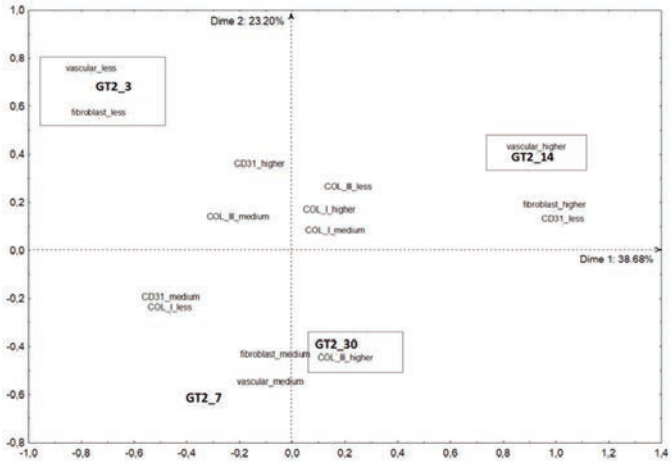


Fig.6. Multiple correspondence analysis of the grouped proliferation variables (fibroblasts, vascularization, type III collagen, type I collagen, CD31) for treatment group 2 (GT2) including the four times in the same analysis. There was a significant correspondence (p<0.05) of the variables within the rectangle.

According to MacPhail (2013), blood flow is reestablished from the recipient site to the skin graft during the inoculation phase, 24 hours after grafting. While revascularization occurs in the next 48 or 72 hours, the dark coloration of the graft's fades, and a reddish-pink tonality appears (Bohling & Swaim 2012), like the macroscopic appearance observed in grafts of the three groups. It is known that some cytokines, particularly vascular endothelial growth factor (VEGF), stimulates vascular proliferation on the fifth or seventh day of grafting (Bohling & Swaim 2012, MacPhail 2013). This fact was corroborated in the control group, where angiogenesis was significant in GC_7 and GC_14. However, it was also significant in GT2_3 and GT2_14, and GT1_30, similar to another xenogen study in rabbits (Kim et al. 2017). However, other studies on skin autografts in rats have reported that intralesional transplantation of autogenous adipose-derived stem cells (ADSCs) have a local paracrine effect on VEGF, stimulating angiogenesis and anti-apoptotic action on the seventh day of grafting (Zografou et al. 2013), thus reducing ischemic necrosis on the fourteenth postoperative day (Wang et al. 2016, Vidor et al. 2018). Regarding the method of assessing vascular proliferation, according to Pazzini et al. (2017), the CD31 antibody did not have an advantage over the H&E method.

The effect of xenogenic mesenchymal stem cells on cutaneous autografts of GT1 and GT2 was similar both in microscopic re-epithelialization (GT1_3, GT1_7, GT2_3, GT2_7) and in collagen deposition type III (GT1_30 and GT2_30), in agreement with another xenogenous study in skin wounds that showed an acceleration of healing after the seventh day of treatment (Rodriguez et al. 2015). This result demonstrated that autologous adipose-derived stem cells (ADSCs) stimulated collagen deposition in skin grafts through the expression of the VEGF factor or by the transforming growth factor β3 (TGF-β3), which also stimulates epithelialization (Zografou et al. 2013, Wang et al. 2016) possibly through a paracrine effect (Kim et al. 2007, Pelizzo et al. 2015). The TGF-β3 expression is also associated with smaller scars and better collagen organization (Hamada et al. 2019). Furthermore, ADSCs seem to significantly influence the tensile strength of wounds after the second week of treatment (Stoff et al. 2009). Usually, during the wound healing and remodeling process, type III collagen gradually decreases as type I collagen increases (Bohling & Swaim 2012, MacPhail 2013). However, in GT1 and GT2, collagen type III predominated in all periods of evaluation. For Franck et al. (2019), the persistent increase in type III collagen in skin wounds treated with ADSCs possibly happens because ADSCs interrupt the regulation of growth factors. Together with a more significant number of type III collagen molecules, this interruption generates extracellular matrix formation and early reduction of scars.

In principle, most of the xenogen type experimental studies were with bone marrow-derived mesenchymal stem cells (BMSC) in models of autoimmune diseases or ischemia and reperfusion (Li et al. 2012). According to Lin et al. (2012), since liposculpture is performed more frequently, more xenotransplantation studies with human adipose-derived stem cells (ADSCs) have been carried out with different animal species with no evidence of inflammation or rejection.

Niemeyer et al. (2008) proved in mice that the subcutaneous injection of undifferentiated human ADSCS and human BMSCs survived for eight weeks; however, when human ADSCS and human BMSC had osteogenic differentiation, they survived only four weeks in a xenogenous environment. Stoff et al. (2009) reported that on the third day and seventh day after intradermal injection of 1.5 x10^6 human mesenchymal stem cells (hMSCs), they observed a diffuse dispersion pattern of hMSCs in the immediate area to the wound; on day 14, they found hMSCs at the dermo-epidermal interface and 21 days after the injection the cells persisted, but to a lesser extent in the dermis and underlying fascia in skin wounds in rabbits.

According to Li et al. (2012), determining the ideal number of xenogenic mesenchymal stem cells required to guarantee the effectiveness of the treatment is complicated due to the many variations between the origin of the mesenchymal stem cells, doses, routes of administration, recipient species, and objectives of experimental models (Lin et al. 2012). Thus, the idea of using three applications of xenogenic mesenchymal stem cells came from the hypothesis that a dose increase, that is, the presence of more cells in the site after the initial stimulus, could increase and/or accelerate the response obtained. Moreover, two analyses were performed between the first and second doses (3 and 7 days). We can assess whether after the second application (analysis with 14 days) there was an increase or improvement in the response compared to the analysis of 3 and 7 days. The same principle was used for the third dose. However, the results observed in this healing model of cutaneous autografts in acute wounds demonstrated few full advantages between the evaluation periods after the second and third injection of xenogenous stem cells, when compared with other studies that administered a single intralesional dose of autogenous stem cells (Zografou et al. 2013, Wang et al. 2016) or allogenous (Vidor et al. 2018). Recently, a study carried out in mice with skin wounds compared three administration methods (intravenous, intramuscular, and topical) containing 1 x 10^6 allogeneic adipose-derived stem cells (ADSCs). On the first day of the evaluation, no differences were found between the three treated groups and the control group without ADSCs. However, on the third day (intravenous and topical group) and fourth day (intramuscular group), they observed that the healing process was significantly accelerated until the seventh day when compared with the control group (Kim et al. 2019). Only one bone regeneration model in rabbits has carried out a comparative and proven study that the transplantation of autologous mesenchymal stem cells (rabbits) shows better results compared with the xenogenous transplant (human). However, the xenogenous transplant was superior to the control group (Niemeyer et al. 2010), justifying its application.

The literature shows that mesenchymal stem cells are non-immunogenic, able to protect themselves from the immune system without the risk of rejection after extrinsic transplantation because they present low expression of the class I histocompatibility complex (MHC I) and, absence of molecules of the class II histocompatibility complex (MHC II) (Li et al. 2012, Kim et al. 2013, Ma et al. 2014). In general, mesenchymal stem cells (MSC) use several molecular mechanisms to suppress innate immune cells, intelligently orchestrate this entire immune system. This action by MSC is possible, as they secrete several soluble factors such as IL-4, IL-6, IL-1, TGF-β, HGF, IDO, and PGE2 (Spaggiari et al. 2009, Spaggiari & Moretta 2013), the latter being the primary central mediator of the immunomodulatory response on other cells of the immune system (Lee et al. 2016). Dendritic cells (DC) unite the innate and adaptive immune systems, as they function both as producers of cytokines and potent antigen presenters (Spaggiari & Moretta 2013). DCS absorb the antigen and, during maturation and activation, increase the expression of co-stimulatory molecules (CD40, CD80, CD83, and CD86), migrate to secondary lymphoid organs, and present the antigen to T cells (Spaggiari & Moretta 2013). During T cells' initiation, the DCs also produces a mixture of cytokines that affect the T cells' evaluating function. MSCs affect most of these processes: they inhibit endocytosis by the DCs, increase the regulation of major histocompatibility complex (MHC), CD40, CD80, CD83, and CD86 during differentiation, and prevent the further expression of CD40, CD83, and CD86 during maturation. MSCs also interfere with CD's ability to produce IL-12 and activate allogeneic T cells (Nauta et al. 2006, Spaggiari et al. 2009). Also, MSCs block the generation of dermal CD from precursors of CD14 + CD1a derived from CD34 and those derived from immature monocytes (Nauta et al. 2006).

Mesenchymal stem cells (MSCs) also antagonize the macrophage M1 phenotype expression and reduce the expression of CD86 and MHCII of these cells, thus decreasing their stimulatory power (Maggini et al. 2010). MSCs also antagonize the macrophage M1 phenotype expression and reduce the expression of CD86 and MHCII of these cells, thus decreasing their stimulatory power (Di Nicola et al. 2002, Zappia et al. 2005). This inhibition is also independent of the major histocompatibility complex (MHC) since autologous and allogeneic mesenchymal stem cells (MSC) have this same anti-proliferative effect. This T cell suppression mechanism occurs because MSC regulates the synthesis of inducible nitric oxide (iNOS), which produces nitrous oxide (Ren et al. 2008). Another important event is that MSC modulate the production of cytokines released by T cells through the production of immunomodulatory molecules, such as hepatocyte growth factor (HGF), TGF-B, and PGE2 (Di Nicola et al. 2002), being able to suppress IFNy production from TH1 cells, they promote IL-4 secretion from TH2 cells and increase the proportion of Treg (Aggarwal & Pitenger 2005). These MSC actions are well observed in responses to autoimmune diseases where pathology control only occurs when there is severe immunosuppression and immunomodulation (Ben-Ami et al. 2011).

Among the present study's limitations, we have not marked the adipose-derived stem cells (ADSCs) of dogs to track their migration and exact location in the wound and skin graft in rabbits treated by the intravenous intralesional route. Besides, to corroborate, the effects of stem cells on macrophages have not been evaluated for specific markers or evaluation of interleukins involved in the process of acute inflammation and other growth factors using flow cytometry.

CONCLUSIONS

The study demonstrates no rejection even across species, suggesting that xenogenous transplantation is safe after intralesional or intravenous injection of mesenchymal stem cells derived from adipose tissue in dogs in rabbits.

Regarding therapeutic efficacy, treatment with xenogeneic stem cells did not influence fibroblasts' angiogenesis and

proliferation compared to the control group. There was possibly a favorable effect on re-epithelialization in the first week and deposition of type III collagen, both in the group treated by the intravenous route and the group treated by the intralesional route. Further studies are necessary to assess xenogenous adipose-derived stem cells (ADSCs) immunomodulatory, anti-inflammatory, and angiogenic actions in grafting.

Acknowledgements.- To the "Coordenação de Aperfeiçoamento de Pessoal de Nível Superior" (CAPES), for granting the financial support to Jorge Luis Alvarez Gómez, to carry out activities in Brazil and to the "Faculdade de Ciências Agrárias e Veterinárias", Unesp, Campus de Jaboticabal, for the structure and laboratory support.

Conflict of interest statement.- The authors declare no conflict of interest.

REFERENCES

Aggarwal S. & Pittenger M.F. 2005. Human mesenchymal stem cells modulate allogeneic immune cell responses. Blood. 105(4):1815-1822. <https://dx.doi.org/10.1182/blood-2004-04-1559> <PMid:15494428>

Andreassi A., Bilenchi R., Biagioli M. & D'Aniello C. 2005. Classification and pathophysiology of skin grafts. Clin Dermatol. 23(4):332-337. <https://dx.doi.org/10.1016/j.clindermatol.2004.07.024> <PMid:16023927>

Bedoya S.A.O., Conceição L.G., Viloria M.I.V., Loures F.H., Valente F.L., Amorim R.L. & Silva F.F. 2016. Caracterização de colágenos tipo I e III no estroma do carcinoma de células escamosas cutâneo em cães. Arq. Bras. Med. Vet. Zootec. 68(1):147-154. <https://dx.doi.org/10.1590/1678-4162-8484>

Ben-Ami E., Berrih-Aknin S. & Miller A. 2011. Mesenchymal stem cells as an immunomodulatory therapeutic strategy for autoimmune diseases. Autoimmunity Rev. 10(7):410-415. <https://dx.doi.org/10.1016/j.autrev.2011.01.005> <PMid:21256250>

Blázquez R., Sánchez-Margallo F.M., Álvarez V., Usón A. & Casado J.C. 2016. Surgical meshes coated with mesenchymal stem cells provide an anti-inflammatory environment by a M2 macrophage polarization. Acta Biomater. 31:221-230. <http://dx.doi.org/10.1016/j.actbio.2015.11.057> <PMid:26654766>

Bohling M.W. & Swaim S.F. 2012. Skin Grafts, p.1271-1290. In: Tobias K. & Johnston S. (Eds.), Veterinary Surgery Small Animal. Vol.2. 1ª ed. St. Louis.

Das A., Sinha M., Datta S., Abas M., Chaffee S., Sen C.K. & Roy S. 2015. Monocyte and macrophage plasticity in tissue repair and regeneration. Am. J. Pathol. 185(10):2596-2606. <https://dx.doi.org/10.1016/j.ajpath.2015.06.001> <PMid 26118749>

Di Nicola M., Carlo-Stella C., Magni M., Milanesi M., Longoni P.D., Matteucci P., Grisanti S. & Gianni A.M. 2002. Human bone marrow stromal cells suppress T-lymphocyte proliferation induced by cellular or nonspecific mitogenic stimuli. Blood. 99(10):3838-3843. <https://dx.doi.org/10.1182/blood.v99.10.3838> <PMid:11986244>

Franck C.L., Senegaglia A.C., Leite L.M.B., de Moura S.A.B., Francisco N.F. & Ribas Filho J.M. 2019. Influence of adipose tissue-derived stem cells on the burn wound healing process. Stem Cells Int. 2019(3):1-10. <https://dx.doi.org/10.1155/2019/2340725> <PMid:30886634>

Hamada T., Matsubara H., Yoshida Y., Ugaji S., Nomura I. & Tsuchiya H. 2019. Autologous adipose-derived stem cell transplantation enhances healing of wound with exposed bone in a rat model. PLoS One 14(5):e0214106. <https://dx.doi.org/10.1371/journal.pone.0214106> <PMid:31083652>

Heo S.C., Jeon E.S., Lee I.H., Kim H.S., Kim M.B. & Kim J.H. 2011.Tumor necrosis factor–α-activated human adipose tissue-derived mesenchymal stem cells accelerate cutaneous wound healing through paracrine mechanisms. J. Invest Dermatol. 131(7):1559-1567. <https://dx.doi.org/10.1038/jid.2011.64> <PMid:21451545>

Keating S.C., Thomas A.A., Flecknell P.A. & Leach M.C. 2012. Evaluation of EMLA cream for preventing pain during tattooing of rabbits: changes in physiological, behavioural and facial expression responses. PLoS One. 7(9):e44437. <https://dx.doi.org/10.1371/journal.pone.0044437> <PMid:22970216>

Kim C.M., Oh J.H., Jeon Y.R., Kang E.H. & Lew D.H. 2017. Effects of human adipose-derived stem cells on the survival of rabbit ear composite grafts. Arch Plast. Surg. 44(5):370-377. <https://dx.doi.org/10.5999/aps.2017.44.5.370> <PMid:28946717>

Kim E.K., Li G., Lee T.J. & Hong J.P. 2011. The effect of human adipose-derived stem cells on the healing of ischemic wound in a diabetic nude mouse model. Plast. Reconstr. Surg. 128(2):387-394. <https://dx.doi.org/10.1097/PRS.0b013e31821e6de2> <PMid:21788830>

Kim H., Hyun M.R. & Kim S.W. 2019. The effect of adipose-derived stem cells on wound healing: comparison of methods of application. Stem Cells Int. 2019(4):1-8. <https://dx.doi.org/10.1155/2019/2745640>

Kim J.M., Lee J.H., Lyoo Y.S., Jung D.I. & Park H.M. 2013. The effects of topical mesenchymal stem cell transplantation in canine experimental cutaneous wounds. Vet. Dermatol. 24(2):242-253. <https://dx.doi.org/10.1111/vde.12011> <PMid:23432413>

Kim W.S., Park B.S., Sung J.H., Yang J.M., Park S.B., Kwak S.J. & Park J.S. 2007. Wound healing effect of adipose-derived stem cells: a critical role of secretory factors on human dermal fibroblasts. J. Dermatol. Sci. 48(1):15-24. <https://dx.doi.org/10.1016/j.jdermsci.2007.05.018> <PMid:17643966>

Krzyszczyk P., Schloss R., Palmer A. & Berthiaume F. 2018. The role of macrophages in acute and chronic wound healing and interventions to promote pro-wound healing phenotypes. Front Physiol. 9:419. <https://dx.doi.org/10.3389/fphys.2018.00419> <PMid:29765329>

Leach M.C., Allweiler S., Richardson C., Roughan J.V., Narbe R. & Flecknell P.A. 2009. Behavioural effects of ovariohysterectomy and oral administration of meloxicam in laboratory housed rabbits. Res. Vet. Sci. 87(2):336-347. <https://dx.doi.org/10.1016/j.rvsc.2009.02.001> <PMid:19393122>

Lee B.C., Kim H.S., Shin T.H., Kang I., Lee J.Y., Kim J.J., Kang H.K., Seo Y., Lee S., Yu K.R., Choi S.W. & Kang K.S. 2016. PGE2 maintains self-renewal of human adult stem cell via EP2-mediated autócrino signaling and its production is regulated by cell-to-cell contact. Sci. Rep. 6:26298. <https://dx.doi.org/10.1038/srep26298> <PMid:27230257>

Li J., Ezzelarab M.B. & Cooper D.K. 2012. Do mesenchymal stem cells function across barriers? Relevance for xenotransplantation. Xenotransplantation. 19(5):273-285. <https://dx.doi.org/10.1111/xen.12000> <PMid:22978461>

Lin C.S., Lin G. & Lue T.F. 2012. Allogeneic and xenogeneic transplantation of adipose-derived stem cells in immunocompetent recipients without immunosuppressants. Stem Cells Dev. 21(15):2770-2778. <https://dx.doi.org/10.1089/scd.2012.0176> <PMid:22621212>

Liptak J. M. 2012. Immediate skin grafting following tumour excision. J. Small Anim. Pract. 53(9):493-494. <https://dx.doi.org/10.1111/j.1748-5827.2012.01274.x> <PMid:22943213>

Ma S., Xie N., Li W., Yuan B., Shi Y. & Wang Y. 2014. Imunobiology of mesenchymal stem cell. Cell Death Differ. 21(2):216-225. <https://dx.doi.org/10.1038/cdd.2013.158> <PMid:24185619>

MacPhail C.M. 2013. Surgery of tegumentary system, p.222-272. In: Fossum T.W. (Ed.), Small Animal Surgery. 4ª ed. St. Louis.

Maggini J., Mirkin G., Bognanni I., Holmberg J., Piazzón I.M., Nepomnaschy I., Costa H., Cañones C., Raiden S., Vermeulen M. & Geffner J.R. 2010. Mause bone marrow-derived mesenchymal stromal cells turn activated macrophages into a regulatory-like profile. PLoS One. 5(2):e9252. <https://dx.doi.org/10.1371/journal.pone.0009252> <PMid:20169081>

Nauta A.J., Kruisselbrink A.B., Lurvink E., Willemze R. & Fibbe W.E. 2006. Mesenchymal stem cells inhibit generation and function of both CD34+-derived and monocyte-derived dendritic cells. J Immunol. 177(4):2080-2087. <https://dx.doi.org/10.4049/jimmunol.177.4.2080> <PMid:16887966>

Niemeyer P., Szalay K., Luginbühl R., Südkamp N.P. & Kasten P. 2010. Transplantation of human mesenchymal stem cells in a non-autogenous setting for bone regeneration in a rabbit critical-size defect model. Acta Biomater. 6(3):900-908. <https://dx.doi.org/10.1016/j.actbio.2009.09.007> <PMid:19766744>

Niemeyer P., Vohrer J., Schmal H., Kasten P., Fellenberg J., Suedkamp N.P. & Mehlhom A.T. 2008. Survival of human mesenchymal stromal cells from bone marrow and adipose tissue after xenogenic transplantation in immunocompetent mice. Cytotherapy. 10(8):784-795. <https://dx.doi.org/10.1080/14653240802419302> <PMid:18951271>

Nolff M.C. & Meyer-Lindenberg A. 2015. Negative pressure wound therapy augmented full-thickness free skin grafting in the cat: aoutcome in 10 grafts transferred to six cats. J. Feline Med. Surg. 17(12):1041-1048. <https://dx.doi.org/10.1177/1098612X15569893> <PMid:25656341>

Oliveira A.P.L., Rangel J.P.P., Raposo V., Pianca N.G., Cruz E.P., Neto E.P., Fiorio W.A.B. & Monteiro B.S. 2018. Allogenic mesenchymal stem cell intravenous infusion in reparation of mild intestinal ischemia/reperfusion injury in New Zeland rabbits. Pesq. Vet. Bras. 38(4):710-721. <http://dx.doi.org/10.1590/1678-5150-pvb-5061>

Or M., Van Goethem B., Kitshoff A., Koenraadt A., Schwarzkopf I., Bosmans T. & De Rooster H. 2017. Negative pressure wound therapy using polyvinyl alcohol foam to bolster full-thickness mesh skin grafts in dogs. Vet. Surgery. 46(3):389-395. <https://dx.doi.org/10.1111/vsu.12613> <PMid:28151546>

Pazzini J.M., Serafim E.L., Gärtner F., Amorim I., Faria F., Rêma A., Moraes P.C. & De Nardi A.B. 2017. Histochemical and immunohistochemical evaluation of angiogenesis in rabbits (*Oryctolagus cuniculus*) submitted to skin grafts associated with platelet-rich plasma. Pesq. Vet. Bras. 37(12):1519-1525. <https://dx.doi.org/10.1590/s0100-736x2017001200026>

Pazzini J.M., Serafim E.L., Uscategui R.R.A., Almeida V.T., Oliva C.A.C., Gärtner F., Amorim I., Faria F., Rêma A., Reis Filho N.P., Ferreira M.G.P.A., Silva A.C., Huppes R.R., Moraes P.C., Oliveira J.A. & De Nardi A.B. 2018. Surgical sponge associated with platelets rich plasma in skin mesh grafts and layer in rabbits (Oryctolagus cuniculus). Arq. Bras. Med. Vet. Zootec. 70(5):1339-1348. <https://dx.doi.org/10.1590/1678-4162-9560>

Pelizzo G., Avanzini M.A., Icaro Cornaglia A., Osti M., Romano P., Avolio L., Maccario R., Dominici M., De Silvestri A., Andreatta E., Costanzo F., Mantelli M., Ingo D., Piccinno S. & Calcaterra V. 2015. Mesenchymal stromal cells for cutaneous wound healing in a rabbit model: pre-clinical study applicable in the pediatric surgical setting. J. Transl. Med. 13:219. <https://dx.doi.org/10.1186/s12967-015-0580-3> <PMid:26152232>

Pinto-Filho S.T.L., Dalmolin F., Pillat M.M., Graça D.L., Borges L., Rosa M.P., Danesi C.C., Maciel R.M., Veiga M.LM., Dullius A.I.S. & Pippi N.L. 2018. Analise macroscópica e histopatológica do alotransplante parcial de vesícula urinária com células-tronco mesenquimais alogênicas derivadas do tecido adiposo em coelhos. Arq. Bras. Med. Vet. Zootec. 70(6):1845-1854. <https://dx.doi.org/10.1590/1678-4162-9952>

Pu C.M., Liu C.W., Liang C.J., Yen Y.H., Chen S.H., Jiang-Shieh C.L., Chen Y.C. & Chen Y.L. 2017. Adipose-derived stem cells protect skin flaps against ischemia/reperfusion injury via IL-6 expression. J. Invest. Dermatol. 137(6):1353-1362. <https://dx.doi.org/10.1016/j.jid.2016.12.030> <PMid:28163069>

Rehman J., Traktuev D., Li J., Merfled-Clauss S., Temm-Grove C.J., Bovenkerk J.E., Pell C.L., Johnstone B.H., Considine R.V. & March K.L. 2004. Secretion of angiogenic and antiapoptotic factors by human adipose stromal cells. Circulation. 109(10):1292-1298. <https://dx.doi.org/10.1161/01.CIR.0000121425.42966.F1> <PMid:14993122>

Reis Filho N., Ferreira M., Pascoli A., Viéra R., Pazzini J.M., Oliveira R., Salardani I., Silva P., Rosseto L., Albernaz S., Vasconcelos R.O., Ferraudo A., Moraes P.C. & Nardi A. 2017. Epitelização de enxertos cutâneos em feridas recentes de coelhos tratados com membrana amniótica canina e/ou laserterapia. Arq. Bras. Med. Vet. Zootec. 69(3):603-612. <https://dx.doi.org/10.1590/1678-4162-9337>

Ren G., Zhang L., Zhao X., Xu G., Zhang Y., Roberts A.I., Zhao R.C. & Shi Y. 2008. Mesenchymal stem cell-mediated immunosupreesion occurs via concerted action of chemokines and nitric oxide. Cell Stem Cell. 2(2):141-150. <https://dx.doi.org/10.1016/j.stem.2007.11.014> <PMid:18371435>

Riggs J., Jennings J.L., Friend E.J., Halfacree Z., Nelissen P., Holmes M.A. & Demetriou J.L. 2015. Outcome of full-thickness skin grafts used to close skin defects involving the distal aspects of the limbs in cats and dogs: 52 cases (2005-2012). J. Am. Vet. Med. Assoc. 247(9):1042-1047. <https://dx.doi.org/10.2460/javma.247.9.1042> <PMid:26480014>

Rodriguez J., Boucher F., Lequeux C., Josset-Lamaugarny A., Rouyer O., Ardisson O., Rutschi H, Sigaudo-Roussel D., Damour O. & Mojallal A. 2015. Intradermal injection of human adipose-derived stem cells accelerates skin wound healing in nude mice. Stem Cell Res. Ther. 6:241. <https://dx.doi.org/10.1186/s13287-015-0238-3> <PMid:26645735>

Spaggiari G.M. & Moretta L. 2013. Interactions between mesenchymal stem cells and dendritic cells. Adv. Biochem. Eng. Biotechnol. 130:199-208. <https://dx.doi.org/10.1007/10_2012_154>

Spaggiari G.M., Abdelrazik H., Becchetti F. & Moretta L. 2009. MSCs inhibit monocyte-derived DC maturation and function by selectively interfering with the generation of immature DCs: central role of MSC-derived prostaglandin E2. Blood. 113(26):6576-6583. <https://dx.doi.org/10.1182/blood-2009-02-203943> <PMid:19398717>

Stoff A., Rivera A.A., Sanjib B.N., More S.T., Moore S.T., Numnum M.T., Espinosa de los Monteros A., Richter D.F., Siegal G.P., Chow I.T., Feldman D., Vasconez I.O. & Curiel D.T. 2009. Promotion of incisional wound repair by human mesenchymal stem cell transplantation. J. Compilation. 18(4):362-369. <https://dx.doi.org/10.1111/j.1600-0625.2008.00792.x> <PMid:18803656>

Suartz C.V., Gaiba S., Ftança J.P., Aloise A.C. & Ferreira L.M. 2014. Adipose-derived stem cells (ADSCs) in the viability of random skin flap in rats. Acta Cir. Bras. 29 (upl.2):6-9. <https://dx.doi.org/10.1590/S0102-86502014001700001>

Tong T. & Simpson D.J. 2012. Free skin grafts for immediate wound coverage following tumor resection from the canine distal limb. J. Small Anim. Pract. 53(9):520-525. <https://dx.doi.org/10.1111/j.1748-5827.2012.01250.x> <PMid:22788796>

Tsai S.Y., Huang Y.C., Chueh L.L., Yeh L.S. & Lin C.S. 2014. Intra-articular transplantation of porcine adipose-derived stem cells for the treatment of canine osteoarthriitis: a pilot study. World J. Transplant. 4(3):196-205. <https://dx.doi.org/10.5500/wjt.v4.i3.196> <PMid:25346893>

Vidor S.B., Terraciano P.B., Valente F.S., Rolim V.M., Kuhl C.P., Ayres L.S., Garcez T.N.A., Lemos N.E., Kipper C.E., Pizzato S.B., Driemeier D., Cirne-Lima E.O. & Contesini E.A. 2018. Adipose-derived stem cells improve full-thickness skin grafts in a rat model. Res. Vet. Sci. 118:336-344. <https://dx.doi.org/10.1016/j.rvsc.2018.03.014> <PMid:29621642>

Wang J., Hao H., Huang H., Chen D., Han Y. & Han W. 2016. The effect of adipose-derived stem cells on full-thickness skin grafts. Biomed. Res. Int. 2016:1464725. <https://dx.doi.org/10.1155/2016/1464725> <PMid:27413735>

Yucel E., Alagoz M.S., Eren G.G., Yasar E.K., Izmiril H.H., Duruksu G., Isgoren S., Muezzinoglu B. & Karaoz E. 2016. Use of adipose-derived mesenchymal stem cells to increase viability of composite grafts. J. Craniofacial. Surg. 27(5):1354-1360. <https://dx.doi.org/10.1097/SCS.0000000000002707> <PMid:27258717>

Zachar L., Bačenková D. & Rosocha J. 2016. Activation, homing, and role of the mesenchymal stem cells in the inflammatory environment. J. Inflamm. Res. 15(9):231-240. <https://dx.doi.org/10.2147/JIR.S121994> <PMid:28008279>

Zappia E., Cassazza S., Pedemonte E., Benvenuto F., Bonanni I., Gerdoni E., Giunti D., Ceravolo A., Cazzanti F., Franssoni F., Mancardi G. & Uccelli A. 2005. Mesenchymal stem cells ameliorate experimental autoimmune encephalomyelitis inducing T-cell anergy. Blood. 106(5):1755-1761. <https://dx.doi.org/10.1182/blood-2005-04-1496> <PMid:15905186>

Zhang Q.Z., Su W.R., Shi S.H., Wilder-Smith P., Xiang A.P., Wong A., Nguyen A.L., Know C.W. & Le A.D. 2010. Human gingiva derived mesenchymal stem cells elicit polarization of M2 macrophages and enhance cutaneous wound healing. Stem Cells 28(10):1856-1868. <https://dx.doi.org/10.1002/stem.503> <PMid:20734355>

Zografou A., Papadopoulos O., Tsigris C., Kavantzas N., Michalopoulos E., Chatzistamatiou T., Papassavas A., Stavropoulou-Gioka C., Dontas I. & Perrea D. 2013. Autologous transplantation of adipose-derived stem cells enhances skin graft survival and wound healing in diabetic rats. Ann. Plast. Surg. 71(2):225-232. <https://dx.doi.org/10.1097/SAP.0b013e31826af01a> <PMid:23636118>

PESQUISA VETERINÁRIA BRASILEIRA
Brazilian Journal of Veterinary Research
ISSN 0100-736X (Print)
ISSN 1678-5150 (Online)

Pesq. Vet. Bras. 40(12):1029-1038, December 2020
DOI: 10.1590/1678-5150-PVB-6727

Original Article
Small Animal Diseases
BY-NC

Neoplasms in domestic hamsters in Southern Brazil: epidemiological and pathological aspects of 40 cases[1]

Maria F. Wentz[2], Matheus V. Bianchi[2], Lauren S. Mello[2], Camila Á. Pietzsch[2], Marcelo M. Alievi[3], David Driemeier[2], Luciana Sonne[2] and Saulo P. Pavarini[2]*

ABSTRACT.- Wentz M.F., Bianchi M.V., Mello L.S., Pietzsch C.A., Alievi M.M., Driemeier D., Sonne L. & Pavarini S.P. 2020. **Neoplasms in domestic hamsters in Southern Brazil: epidemiological and pathological aspects of 40 cases**. *Pesquisa Veterinária Brasileira 40(12):1029-1038*. Setor de Patologia Veterinária, Faculdade de Veterinária, Universidade Federal do Rio Grande do Sul, Av. Bento Gonçalves 9090, Porto Alegre, RS 91540-000, Brazil. E-mail: saulo.pavarini@ufrgs.br

Although neoplasms are commonly reported in domestic hamsters, retrospective studies approaching spontaneous tumors with data regarding epidemiological findings are scarce. The present study aimed to describe the epidemiological and pathological findings of 40 cases of tumors in domestic hamsters diagnosed in a veterinary pathology laboratory in Southern Brazil from 2002 to 2019. Chinese hamster (*Cricetulus griseus*) was the most commonly affected species (16/40), followed by Djungarian hamster (*Phodopus sungorus,* 11/40) and Syrian hamster (*Mesocricetus auratus,* 4/40). Among the cases, 57.5% were females (23/40), while 42.5% were males (17/40). The affected hamsters' median age was of 14-months old, with an age range of 8- to 36-months old. Twenty-four cases were assessed as anatomopathological samples (biopsies), while 16 were composed of carcasses submitted to postmortem examination, and, therefore, the neoplasm was related to the cause of death. The integumentary system was frequently affected (60%, 24/40), followed by the female reproductive tract (22.5%, 9/40), hematopoietic system (10%, 4/40), digestive tract (5%, 2/40), and endocrine system (2.5%, 1/40). The most frequent neoplasm was squamous cell carcinoma (35%, 14/40), mostly on the lip/nasal region (50%, 7/14). Other tumors included fibrosarcoma (10%, 4/40), lymphoma (10%, 4/40), mammary cystadenoma (10%, 4/40), apocrine sweat gland adenoma (7.5%, 3/40), hemangiosarcoma (5%, 2/40), leiomyosarcoma (5%, 2/40), and granulosa ovarian cell tumor (5%, 2/40). The five remaining cases occurred individually and were composed of hepatoid gland adenoma, solid thyroid carcinoma, cutaneous melanoma, ovarian teratoma, and cutaneous trichoblastoma. Neoplasms were identified as an important cause of death and major reason to perform biopsy in domestic hamsters in Southern Brazil.

INDEX TERMS: Neoplasms, domestic hamsters, Brazil, epidemiology, pathology, spontaneous tumors, oncopathology, rodents, squamous cell carcinoma, lymphoma, fibrosarcoma.

RESUMO.- [**Neoplasias em hamsters domésticos no Sul do Brasil: aspectos epidemiológicos e patológicos de 40 casos.**] Embora neoplasmas em hamsters domésticos sejam comumente relatados, estudos retrospectivos abordando neoplasias espontâneas e os dados epidemiológicos associados são escassos. O presente estudo teve o objetivo de descrever os principais achados epidemiológicos e patológicos de 40 casos de tumores em hamsters domésticos diagnosticados em um laboratório de patologia veterinária do Sul do Brasil de 2002 a 2019. A principal espécie acometida foi o hamster chinês (*Cricetulus griseus*, 16/40), seguido por hamster anão russo siberiano (*Phodopus sungorus*, 11/40) e hamster sírio (*Mesocricetus auratus*, 4/40). As fêmeas corresponderam a 57,5% dos casos (23/40), enquanto os machos representaram 42,5% (17/40). Foram afetados roedores com uma faixa etária de 8 a 36 meses de idade, e uma mediana de 14 meses. Do total de casos, 24 foram exames anatomopatológicos

[1] Received on June 9, 2020.
Accepted for publication on August 14, 2020.
[2] Setor de Patologia Veterinária, Faculdade de Veterinária, Universidade Federal do Rio Grande do Sul (UFRGS), Av. Bento Gonçalves 9090, Agronomia, Porto Alegre, RS 91540-000, Brazil.
[3] Núcleo de Conservação e Reabilitação de Animais Silvestres (PRESERVAS), Faculdade de Veterinária, Universidade Federal do Rio Grande do Sul (UFRGS), Av. Bento Gonçalves 9090, Agronomia, Porto Alegre, RS 91540-000, Brazil.
*Corresponding author: saulo.pavarini@ufrgs.br

(biopsias) e 16 casos foram examinados através de necropsia e, portanto, relacionados com a causa da morte dos animais. O sistema tegumentar foi o mais frequentemente acometido (60%; 24/40), seguido pelo trato reprodutivo (22,5%; 9/40), sistema hematopoietico (10%; 4/40), trato digestório (5%; 2/40) e sistema endócrino (2,5%; 1/40). A neoplasia mais frequentemente diagnosticada foi o carcinoma de células escamosas (35%; 14/40), localizado principalmente em região labionasal (50%; 7/14). Outros tumores incluíram fibrossarcoma (10%; 4/40), linfoma (10%; 4/40), adenoma cístico de glândula mamária (10%; 4/40), adenoma de glândula sudorípara (7,5%; 3/40), hemangiossarcoma (5%; 2/40), leiomiossarcoma (5%; 2/40) e tumor de células da granulosa (5%; 2/40). Os outros cinco casos remanescentes ocorreram individualmente e eram compostos por adenoma de glândula hepatoide, carcinoma sólido de tireoide, melanoma cutâneo, teratoma ovariano e tricoblastoma cutâneo. Neoplasmas foram identificados como importantes causas de morte ou razões para realização de biopsia em hamsters domésticos no Sul do Brasil.

TERMOS DE INDEXAÇÃO: Neoplasias, hamsters domésticos, Brasil, epidemiologia, patologia, tumores espontâneos, oncopatologia, roedores, carcinoma de células escamosas, linfoma, fibrossarcoma.

INTRODUCTION

Hamsters were initially employed as laboratory animals, with significant importance in a medical investigation (Bampi et al. 2014) owing to a supposed low spontaneous tumor incidence and high susceptibility to administered carcinogens (Homburger 1983, Greenacre 2004). However, it became prevalent in the last few decades as a companion or pet animal (Kamino et al. 2001, Kondo et al. 2008). Consequently, veterinary care, such as surgical procedures, has become standard on these rodent patients, as pet owners have increased their demand for quality services (Capello 2011). Among the main species of domestic hamsters worldwide, the Syrian (golden) hamster (*Mesocricetus auratus*) is the most popular (Lennox & Bauck 2012), followed by dwarf hamsters, such as the Djungarian or Russian dwarf hamster (*Phodopus sungorus*) (Jelinek et al. 2013), and the Campbell's Russian dwarf hamster (*Phodopus campbelli*) (Kondo et al. 2008). Moreover, in Brazil, it seems that the Chinese hamster (*Cricetulus griseus*) has become popular in recent years (Conrado et al. 2013, Conceição et al. 2018).

Among the diseases that occur in hamsters, confusing data has been published regarding neoplastic conditions, with studies that report low frequencies of 3.7% (Van Hoosier & Trentin 1979) to highest levels up to 50% in hamsters older than 2-years old (Greenacre 2004). The knowledge regarding its occurrence is mainly related to comprehensive studies aimed at human comparative carcinogenic models (Van Hoosier & Trentin 1979, De Oliveira et al. 2009, Bampi et al. 2014). Other studies have presented these conditions in hamsters as case reports (Santos et al. 2002, Kondo et al. 2006, 2007, 2011, Ghaffari et al. 2009, Martorell et al. 2010, Golbar et al. 2011, Rainwater et al. 2011, Conrado et al. 2013, Jelinek et al. 2013, Johnson et al. 2014, Conceição et al. 2018), disease outbreaks (Coggin et al. 1983), or as retrospective case series in laboratory hamsters (Homburger 1983, Kamino et al. 2001, McInnes et al. 2013), but few have included case series of spontaneous neoplasms in companion animals (Harvey et al. 1992, Kondo et al. 2008). This diagnostic approach is helpful to clinical veterinarians and pathologists in order to obtain a rapid, practical, and precise diagnosis. Therefore, this study aimed to identify and characterize the main epidemiological, gross, and microscopic features of 40 spontaneous neoplasms diagnosed in domestic hamsters through anatomopathological or necropsy exams in Southern Brazil.

MATERIALS AND METHODS

A retrospective study of the anatomopathological and necropsy database in domestic hamsters was conducted to search for records of neoplastic conditions diagnosed from January 2002 to January 2019 at the "Setor de Patologia Veterinária". The materials submitted to the laboratory [fragments of organs in 10% formalin (excisional or incisional biopsies) or refrigerated carcasses] were originated from the "Núcleo de Conservação e Reabilitação de Animais Silvestres" (PRESERVAS) or private veterinary clinics in the metropolitan area of Porto Alegre, Rio Grande do Sul state. Information surrounding the species affected, sex, age, system affected, and anatomical location of the lesion(s) was retrieved from the anatomopathological or necropsy reports and the clinical medical files when available.

After case selection, gross features were evaluated through photographs and previous descriptions present in the reports. Also, paraffin-embedded tissues from these cases were retrieved, cut at 3μm, stained by hematoxylin and eosin (HE), and assessed under light microscopy. These slides were reevaluated, and histological lesions were reclassified. The cases were grouped into nine categories based on the morphological diagnosis: squamous cell carcinoma, lymphoma, fibrosarcoma, mammary cystic adenoma, sweat gland adenoma, hemangiosarcoma, leiomyosarcoma, ovarian granulosa cell tumor, and other neoplasms.

RESULTS

A total of 40 hamsters was diagnosed with a neoplastic condition at the analyzed period. Of these, 24 were assessed as anatomopathological samples (biopsies), while 16 were composed of carcasses submitted to postmortem examination, wherein the neoplasm was regularly identified as the cause of death.

Females accounted for 57.5% of the cases (23/40), while males compiled 42.5% of the total (17/40). Age was provided in 92.5% of cases (37/40), with an age range of 8- to 36-months old and a median age of 14-months old. The species affected were informed in 77.5% of the cases (31/40), of which 16 were Chinese hamsters (*C. griseus,* 51.6%), 11 were Djungarian hamsters (*P. sungorus,* 35.5%), and four were Syrian hamsters (*M. auratus,* 12.9%).

The integumentary system was most frequently affected, accounting for a total of 24 cases (60%), followed by the female reproductive tract (9 cases; 22.5%; ovary, uterus, or mammary glands), hematopoietic system (4 cases, 10%), digestive tract (2 cases, 5%), and endocrine system (1 case, 2.5%).

The absolute frequency and anatomical location according to each neoplastic morphological diagnosis are presented in Table 1. The age, sex, and species affected were also grouped according to each neoplastic morphological diagnosis and are presented accordingly to the absolute frequency of diagnosis in Table 2.

Table 1. Frequency and anatomical location of neoplasms diagnosed in 40 domestic hamsters in Southern Brazil

Neoplasm	N	Frequency	Anatomical location
Squamous cell carcinoma	14	35%	Lip-nasal region: 7/14 (50%) Ear: 3/14 (21.4%) Cheek pouch: 2/14 (14.3%) Skin (submandibular): 1/14 (7.1%) Skin[1]: 1/14 (7.1%)
Lymphoma	4	10%	Multicentric: 3/4 (75%) Lymph node: 1/4 (25%)
Fibrosarcoma	4	10%	Skin (limb): 2/4 (50%) Skin (mammary gland): 1/4 (25%) Skin[1]: 1/4 (25%)
Mammary cystadenoma	4	10%	Mammary gland
Apocrine sweat gland adenoma	3	7.5%	Skin (prepuce): 1/3 (33.3%) Skin (limb): 1/3 (33.3%) Skin (axillary region): 1/3 (33.3%)
Hemangiosarcoma	2	5%	Skin (abdomen): 1/2 (50%) Skin[1]: 1/2 (50%)
Leiomyosarcoma	2	5%	Uterus
Ovarian granulosa cell tumor	2	5%	Ovary
Hepatoid gland adenoma	1	2.5%	Prepuce
Thyroid solid carcinoma	1	2.5%	Thyroid
Cutaneous melanoma	1	2.5%	Skin[1]
Ovarian teratoma	1	2.5%	Ovary
Cutaneous trichoblastoma	1	2.5%	Skin (limb)

N = number of cases; [1] specific anatomical location was not informed.

Table 2. Median age, age range, sex, and species of 40 domestic hamsters according to each neoplasm in Southern Brazil

Neoplasm	N	Median age	Age range	Sex (M:F)	Species affected			
					CH	DH	SH	NA
Squamous cell carcinoma	14	12 m	8 m - 24 m	7:7	7	7	-	-
Lymphoma	4	19.5 m	10 m - 29 m	2:2	2	-	1	1
Fibrosarcoma	4	21 m	12 m - 24 m	1:3	1	1	-	2
Mammary cystadenoma	4	12 m	9 m - 14 m	0:4	2	1	1	1
Apocrine sweat gland adenoma	3	10 m	9 m - 36 m	3:0	-	2	-	1
Hemangiosarcoma	2	20 m	16 m - 24 m	1:1	1	-	-	1
Leiomyosarcoma	2	21 m	18 m - 24 m	0:2	-	-	1	1
Ovarian granulosa cell tumor	2	36 m	36 m - 36 m	0:2	-	-	-	2
Hepatoid gland adenoma	1	24 m	24 m	1:0	1	-	-	-
Thyroid solid carcinoma	1	14 m	14 m	1:0	-	-	1	-
Cutaneous melanoma	1	NA	NA	0:1	-	-	-	1
Ovarian teratoma	1	12 m	12 m	0:1	1	-	-	-
Cutaneous trichoblastoma	1	24 m	24 m	1:0	1	-	-	-

N = number of cases, M = male, F = female, CH = Chinese hamster, DH = Djungarian hamster, SH = Syrian hamster, NA = not available, m = months old.

Squamous cell carcinoma

Squamous cell carcinoma (SCC) was the most common neoplasm identified in this study, accounting for 35% of the cases (14/40), of which six originated from biopsies and eight from necropsies. Of these, five hamsters died promptly after or during surgical resection of the mass. The lip/nasal region was most commonly affected, accounting for 50% of the cases (7/14), of which four had a similar gross pattern with the tumor involving the upper lip and extending into the nasal cavity. These were associated with nasal, maxillary, or mandibular deformations (facial swelling), as invasion and obliteration of the surrounding bones and nasal cavity were frequent, in addition to skin ulceration (Fig.1A-C). The ear was affected in three cases, followed by the cheek (buccal) pouch in two hamsters. Microscopically, masses were composed of neoplastic proliferation of epithelial cells forming fingerlike projections towards the superficial/deep dermis, in addition to multiple nests of neoplastic cells occasionally containing concentrically laminated keratin (keratin pearls). Moreover, a variable degree of the desmoplastic reaction was observed (mild to marked) (Fig.1D).

Lymphoma

Most cases (3/4) were represented by multicentric lymphomas, which were concomitantly identified as the cause of death, while the remaining consisted of a lymph node sample assessed through biopsy. The main organs affected included the lymph nodes (4/4), liver (2/4), spleen (2/4),

kidneys (1/4), small intestine (1/4), mediastinum (1/4), and skin (1/4) (Fig.2A-C). At the necropsy, there were multiple, variable-sized, whitish, soft nodules or masses that on the cut surface were smooth and bright intermixed with red areas. These nodules involved and frequently replaced most of the nodal parenchyma, similarly to other organs affected (spleen, kidneys, and small intestine). Hepatic lymphoma was characterized by focal nodular whitish areas within the parenchyma. Mediastinum or thymic lymphoma was characterized by an extensive whitish mass, which occupied the cranial portion of the thoracic cavity (cranial mediastinum) and displaced/compressed the lungs (atelectasis) in a Chinese hamster. Cutaneous involvement occurred as an extensive alopecic area, interspersed with multiple crateriform nodular lesions at the dorsal thoracic region, cervical region, and head in a Chinese hamster. Microscopically, all the masses were composed by a diffuse neoplastic proliferation of large round cells (larger than two erythrocytes) arranged in mantles. The cells had well-defined cytoplasm, round non-cleaved nuclei, and inconspicuous to single visible nucleoli. A mean mitotic count higher than four mitotic figures per high power field (400x) was noted. Frequently, tingible body macrophages were observed intermingled with the neoplastic lymphocytes, consistent with the 'starry sky' microscopical pattern (Fig.2D). The neoplasms were classified in all cases as high grade diffuse large cell lymphomas.

Fibrosarcoma

Fibrosarcoma was mostly diagnosed through samples assessed as biopsies (3/4), while in one case, it was detected

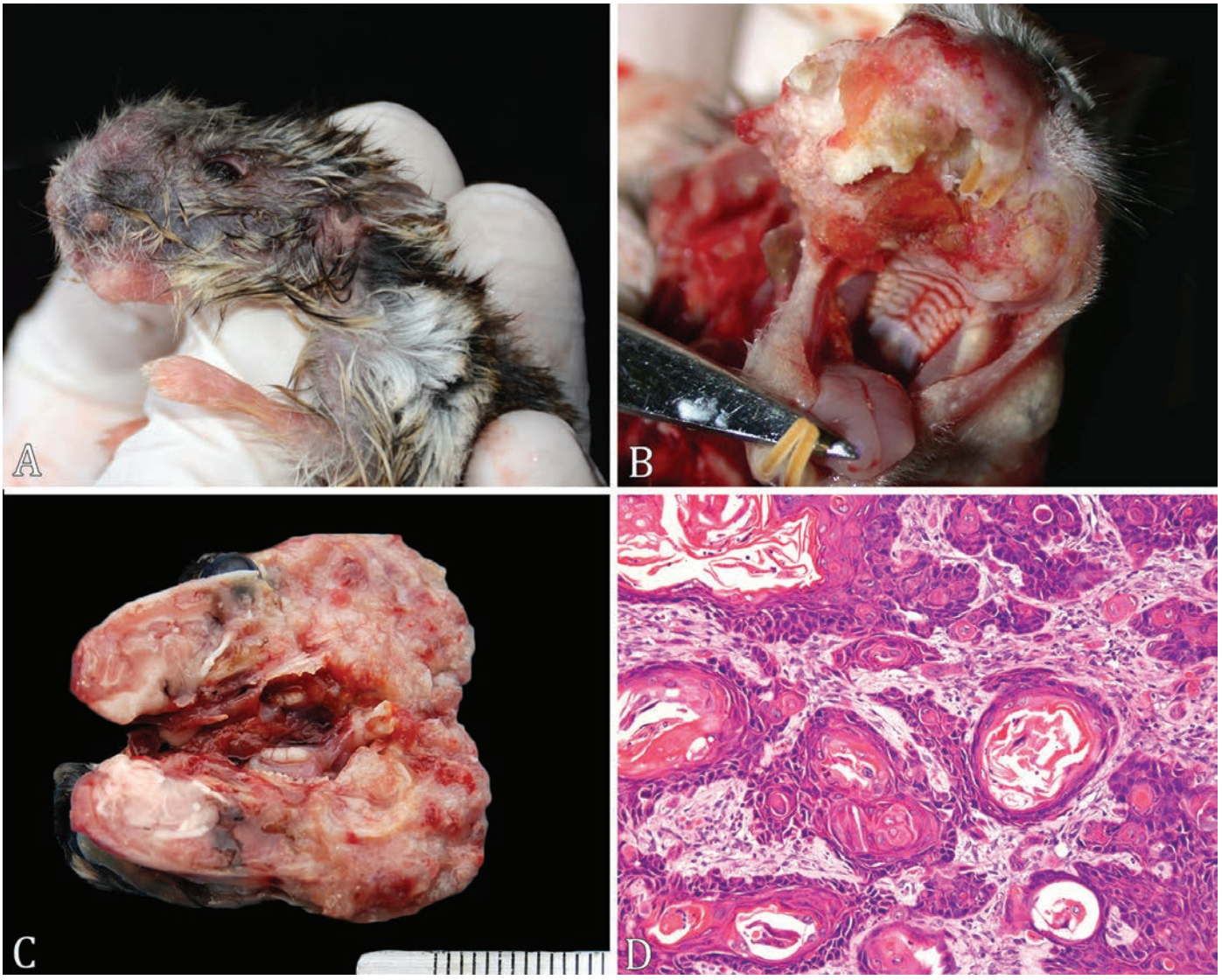


Fig.1. Gross and microscopic findings of squamous cell carcinoma in hamsters in Southern Brazil. (**A**) Djungarian hamster (*Phodopus sungorus*). Facial deformation induced by an increase in volume (mass) at the lip/nasal region. (**B**) Chinese hamster (*Cricetulus griseus*). Whitish mass at the upper lip, which extends into the oral and nasal cavities. (**C**) This mass's cut surface reveals that it completely obliterates the nasal cavity, it is predominantly white, intermixed with red areas, and extends into replacing most of the hard palate. (**D**) Histologically, there is a neoplastic proliferation of epithelial cells arranged in multiple nests with keratin pearls forming at the center. HE, obj.20×.



Fig.2. Gross and microscopic findings of lymphoma in hamsters in Southern Brazil. (**A**) Chinese hamster (*Cricetulus griseus*). The mesenteric lymph node is enlarged and effaced by a predominantly reddish mass intermixed by pinpoint white areas. Besides, the liver presents a focal nodular, white area. (**B**) Chinese hamster (*C. griseus*). A whitish mass occupies the cranial mediastinum at the thoracic cavity, causing pulmonary atelectasis. (**C**) Chinese hamster (*C. griseus*). The dorsum's extensive alopecic area is intermixed with multiple crateriform nodular lesions at the dorsal thoracic region, cervical region, and head. (**D**) Histologically, there is a neoplastic proliferation of large lymphocytes arranged in mantles. Multiple tingible body macrophages are observed intermingled with the neoplastic lymphocytes, giving the lesion a 'starry sky' microscopical pattern. HE, obj.20×.

through necropsy. In all cases, the samples consisted of cutaneous masses, characterized by single, demarcated, and firm to hard nodules, with focal areas of superficial ulceration. Microscopically, the nodules were composed of neoplastic proliferation of spindle cells arranged in bundles in multiple directions. These cells had broad eosinophilic and poorly demarcated cytoplasm, oval nuclei, and evident nucleoli, often multiple per cell. Extensive focal areas of epidermal ulceration associated with neutrophilic infiltrate were frequently noted as well (Fig.3A).

Mammary cystadenoma

Mammary neoplasms were composed solely by benign tumors assessed through biopsy samples, of which mammary cystic adenoma was identified in all cases (4/4). Relatively young females were affected, with a median age of 12-months old. Microscopically, all cases presented multifocal to coalescing areas of adenomatous hyperplasia intermixed with the benign proliferation of epithelial cells, which were frequently arranged in multiple variable size cystic structures (Fig.3B).

Apocrine sweat gland adenoma

Apocrine sweat gland adenoma was diagnosed in three cases, which were assessed through biopsy of skin samples. Grossly, these lesions presented as single and soft nodules that on the cut surface exuded a translucid fluid through cavitations. Histologically, there was a proliferation of columnar epithelial cells arranged in well-differentiated tubular structures,

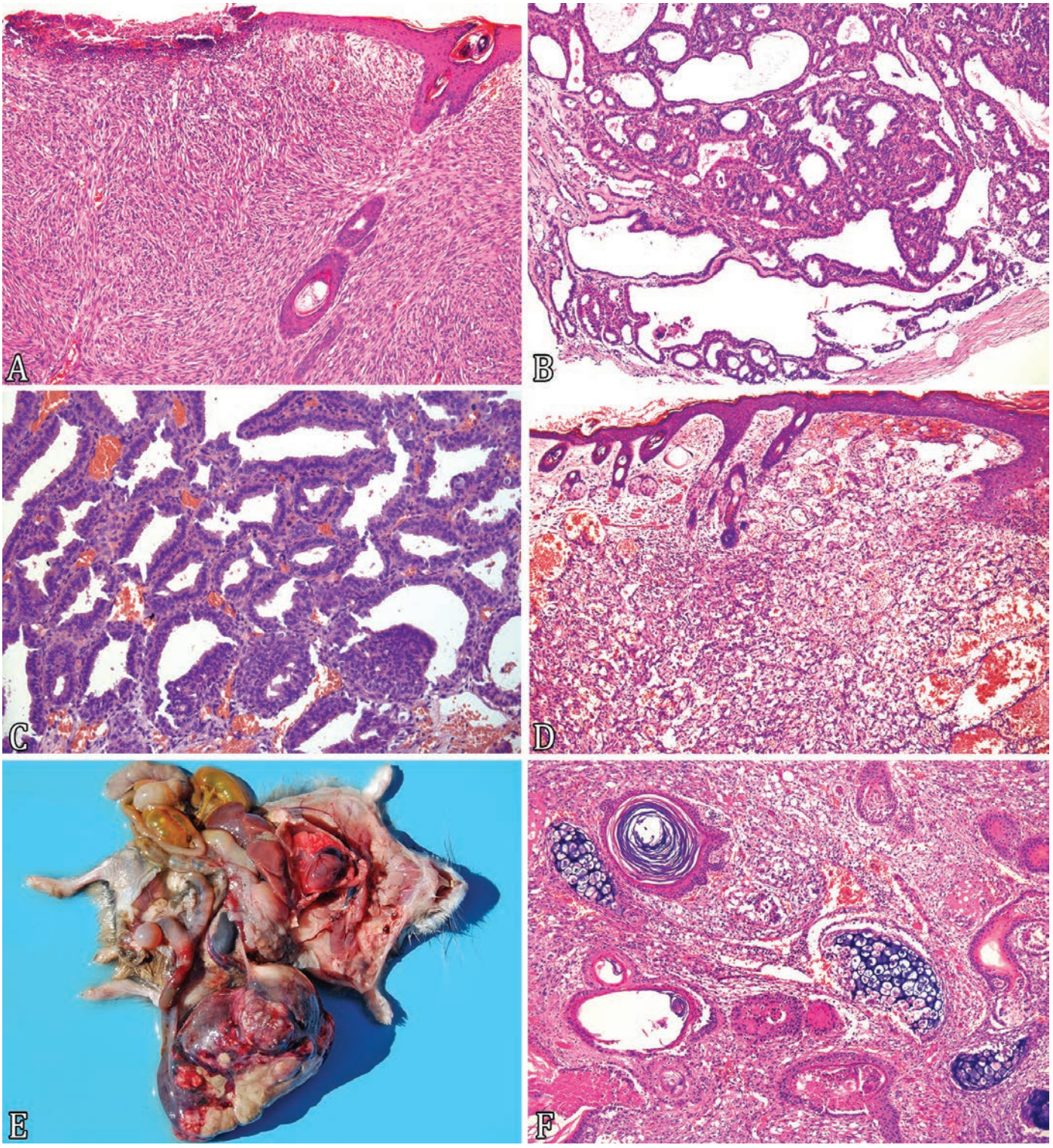


Fig.3. Gross and microscopic findings of other neoplasms diagnosed in hamsters in Southern Brazil. (**A**) Cutaneous fibrosarcoma. The malignant neoplastic proliferation of spindle cells is arranged in bundles in multiple directions at the superficial and deep dermis. A focally extensive area of ulceration at the epidermis is also observed. HE, obj.10×. (**B**) Mammary cystadenoma. The benign neoplastic proliferation of epithelial cells is arranged in multiple cystic areas. HE, obj.10×. (**C**) Sweat gland adenoma. The benign neoplastic proliferation of columnar epithelial cells has abundant granular cytoplasm and is arranged in acinar structures. HE, obj.20×. (**D**) Cutaneous hemangiosarcoma. The neoplastic proliferation of spindle cells at the superficial and deep dermis is arranged in multiple primitive vascular structures filled by erythrocytes. HE, obj.10×. (**E-F**) Ovarian teratoma. Chinese hamster (*Cricetulus griseus*). (**E**) The left ovary is effaced by a whitish-reddish mass, which occupies almost the entire abdominal cavity. (**F**) Microscopically, there is a neoplastic proliferation of cells with multiple germinative origins. The neoplasm forms multifocal random areas of stratified epithelium containing keratin at the center, cartilaginous tissue, muscle fibers, and adipose tissue intermixed with multifocal areas of necrosis. HE, obj.20×.

which contained small amounts of basophilic material within the lumen. Moreover, the cells had an abundant granular cytoplasm, and occasionally apical blebs (characteristic of apocrine glands) were observed (Fig.3C).

Hemangiosarcoma

Hemangiosarcoma was diagnosed through samples assessed as biopsies in two cases, which affected only the skin and were grossly characterized by non-limited red nodular structures. On the cut surface, these exhibited multiple cystic red areas that microscopically consisted of a proliferation of mesenchymal spindle cells arranged in primitive vascular structures filled by variable amounts of erythrocytes. Also, there were extensive areas of epidermal ulceration associated with hemorrhage (Fig.3D).

Leiomyosarcoma

Leiomyosarcoma was diagnosed in two samples of uterus (biopsies) obtained through hysterectomy in older females (median age of 21-months old). Histologically, these were characterized by a highly cellular neoplastic proliferation of spindle cells arranged in bundles in multiple directions, with moderate amounts of eosinophilic and poorly limited cytoplasm, and moderate pleomorphism.

Ovarian granulosa cell tumor

Ovarian granulosa cell tumor was diagnosed in two cases assessed as biopsies of the ovaries of two older females (median age of 36-months old). Microscopically, there was proliferation of cells arranged radially, which were lined and surrounded by moderate amounts of fibrous stroma, forming follicle-like structures.

Other neoplasms

Other neoplasms were identified individually, accounting for 2.5% (1/40) of the total of cases each: hepatoid gland adenoma, solid thyroid carcinoma, cutaneous melanoma, ovarian teratoma, and cutaneous trichoblastoma. Among these, ovarian teratoma was associated with the death of a 12-months old female Chinese hamster, while the other cases were diagnosed through biopsy. The ovarian teratoma featured an oval white mass occupying almost the entire abdominal cavity at the necropsy, measuring 5 × 3 × 3cm. This mass originated from the left ovary and displaced/compressed most of the abdominal cavity organs (Fig.3E). On the cut surface, it was predominantly soft, intermixed with firm to hard areas. Microscopically, the neoplasm was composed of cells of distinct germinative lines: epithelial, mesenchymal, and neuronal. The neoplastic cells formed multifocal random areas of stratified epithelium containing keratin, cartilaginous tissue, mineralized bone tissue, dentigerous tissue, muscle fibers, adipose tissue, glandular epithelium, and nervous tissue, which were intermixed with multifocal areas of necrosis (Fig.3F).

DISCUSSION

The diagnosis of neoplastic lesions in 40 hamsters in the present investigation was mainly based on the samples' gross and microscopic features, which were obtained either through anatomopathological or necropsy examination. Some factors, such as age range and sex predisposal, have been previously analyzed compared to the frequency and type of neoplasm detected, but there are still some controversies in the literature, as neoplasms tend to occur mostly in older hamsters, with an incidence of 70% reported in animals older than 2 years (Van Hoosier & Trentin 1979). Considering that hamsters may have a life span of 18- to 36-months old (Kamino et al. 2001, Kondo et al. 2008, Lennox & Bauck 2012), the hamsters of the present study were relatively younger with a median age of 14-months old, differing from a previous study wherein 19.8-months old was the median age of domestic hamsters affected by neoplasms. Male hamsters have been previously considered more prone to neoplasm development (Kamino et al. 2001, Kondo et al. 2008). However, another study conducted on Syrian control hamsters found a higher incidence of tumors in females (McInnes et al. 2013), similar to the current investigation. Previous studies focusing on spontaneous neoplasms have described these conditions mostly in Djungarian and Syrian hamsters (Kamino et al. 2001, Kondo et al. 2008, McInnes et al. 2013). In the present work, however, most of the neoplasms were detected in Chinese hamsters, possibly associated with the increasing popularity of the species as pet hamsters in Brazil (Conrado et al. 2013, Conceição et al. 2018).

Among the neoplasms detected, most of them (60%) involved the integumentary system, as observed previously in an investigation of spontaneous neoplasms in domestic Djungarian hamsters (Kondo et al. 2008). Similarly, a clinical retrospective study focused on hamsters' dermatological diseases observed that nodule formation (abscesses and neoplasms) was typical (White et al. 2019). It is believed that domestic hamsters are more affected by integumentary tumors when compared to laboratory specimens, wherein neoplasms tend to affect multiple organs (Kamino et al. 2001). In the present investigation, a higher level of cutaneous tumors may be related to the fact that SCC was frequently detected, accounting for 35% of the neoplasms. This differed from a previous study in which the primarily identified neoplasm was papilloma (Kondo et al. 2008), which was not detected in the present work, while SCC accounted for 8% of the cases in that study (Kondo et al. 2008). Nonetheless, other investigations conducted on Syrian laboratory hamsters reported a higher prevalence of spontaneous adrenal neoplasms (Kamino et al. 2001, McInnes et al. 2013). However, no adrenal gland neoplasm was identified in the current work, which could be related to the small number of Syrian hamsters in the analyzed population.

Squamous cell carcinoma (SCC) is relatively common in Syrian hamsters submitted as experimental models in research in order to evaluate chemical carcinogens effects at the buccal pouch, such as dimethylbenzanthracene (DMBA) or carbamide peroxide (De Oliveira et al. 2009, Bampi et al. 2014). The buccal pouch is the primary location for chemical carcinogenesis studies in hamsters because of the low cost and easy anatomical access, which can be readily everted for gross evaluation (Mognetti et al. 2006). Nonetheless, the spontaneous occurrence of the condition is poorly described, with most of the reports focused on the cheek pouch (Martorell et al. 2005, Ghaffari et al. 2009, Capello 2011), while the involvement of lips, gingiva, mandible, and maxilla, as detected in the current investigation, is relatively uncommon (Conceição et al. 2018). The hamsters affected in the present work had an age range of 8- to 24-months old, with a median age of

12-months old, which are data quite similar to those previously reported in other studies (Ghaffari et al. 2009, Conceição et al. 2018). Djungarian, Chinese, and Syrian hamsters appear to be equally susceptible to SCC development (Martorell et al. 2005, Ghaffari et al. 2009, Conceição et al. 2018). Although the current study did not detect any SCC in Syrian hamsters, this is possibly related to the small number of rodents from this species analyzed in the current work.

Squamous cell carcinoma (SCC) development in other domestic species is often related to ultraviolet light chronic exposure, lack of skin pigment, and scarcity or absence of hair at the sites affected (Goldschmidt & Goldschmidt 2017). Although hamsters are nocturnal rodents usually maintained in environments where sunlight exposure is minimal (Martorell et al. 2010), these factors were most likely associated with SCC occurrence in the present investigation, as non-pigmented regions and areas less covered by hairs were mostly affected, such as lips, nasal region, and ears. The oral region has also been identified as a common location for SCC development in adult African pigmy hedgehogs (*Atelerix albiventris*) (Aguila et al. 2019) and the second most common in the oral cavity of dogs, while in cats, it mainly involves the facial and nasal regions (Goldschmidt & Goldschmidt 2017). In the lips, the condition usually begins as erythematous, squamous, and, often, ulcerative lesions that progress to highly infiltrative masses, which are rarely able to metastasize (Gardner 1996). Similarly, no metastases were detected in the hamsters of the present study at the regional lymph nodes. It is presumed that death was mostly related to the neoplasm's infiltrative behavior, which was able to cause facial deformities and dysphagia, similarly to that described in Chinese and Syrian hamsters in other studies (Ghaffari et al. 2009, Conceição et al. 2018). This pathogenesis is similar to that reported in African pigmy hedgehogs affected by oral SCC, in which masses diagnosed as SCC caused facial deformation, dysphagia, and infiltration of the nasal cavity induced characteristic clinical signs (Aguila et al. 2019). Considering that many pet rodents are experts in hiding signs of illness and those pet hamsters are less likely to be presented for veterinary treatment with spontaneous tumors than other small rodents, the diagnosis of unusual diseases is often reduced or retarded (Greenacre 2004, Ghaffari et al. 2009, Rainwater et al. 2011). Additionally, pursue diagnostic investigations in hamsters is often constrained by economic reasons, as owners are inclined not to spend money on a small rodent with a short life span (White et al. 2019), and, therefore, these animals usually do not undergo full gross and histopathologic examinations (Rainwater et al. 2011). Thus, the current study highlights the importance of SCC early diagnosis because out of eight hamsters submitted to necropsy; five died promptly after or during surgical resection of the mass.

Lymphoma was the second most common neoplasm in this investigation, and, similarly, the occurrence of the condition has been extensively reported in hamsters, (Van Hoosier & Trentin 1979, Coggin et al. 1983, Harvey et al. 1992, De Alencar et al. 2012). In another study conducted with laboratory hamsters, lymphoma prevalence reached 8% (Kamino et al. 2001), which is quite similar to the frequency observed in this study (10%). Lymphoma involvement in the species is usually referred as multicentric, because multiple organs may be affected simultaneously. Peripheral and visceral lymph nodes are the primary sites affected (Santos et al. 2002), as in the current work. Nonetheless, the small intestine and liver are also commonly involved (Santos et al. 2002, Coggin et al. 1983), as observed. The liver was affected in two cases and the small intestine in one case. Other organs inflicted may include the spleen, kidneys (Santos et al. 2002), and mediastinum (thymus) (Coggin et al. 1983), which were also affected in this study. Grossly, lymphoma usually presents as soft, round, yellow-white masses, often with central necrosis, involving the lymph nodes, liver, and kidneys (Coggin et al. 1983), as observed in this investigation. On the other hand, spleen and hepatic involvement are characterized by diffuse enlargement (splenomegaly) and whitish foci within the parenchyma (Coggin et al. 1983), similar to the present work.

Histologically, lymphomas may be classified into multiple histological and phenotypical patterns, being large cell lymphoma the most common pattern in Syrian hamsters (Santos et al. 2002). Accordingly, the cases of the present work were classified as high grade diffuse large cell lymphomas. Additionally, lymphomas in hamsters generally contain conspicuous amounts of karyorrhectic debris and tingible bodies within histiocytic cells, which indicates a "starry sky" morphologic appearance (Coggin et al. 1983) similarly to the cases in the current investigation. Multicentric lymphoma may be induced by hamster polyomavirus (HaPV), a Papovaviridae virus, in young Chinese and Syrian hamsters during outbreaks of HaPV (Coggin et al. 1983, Simmons et al. 2001). In the present study, we could not assert if HaPV was involved in the cases detected, as all samples were already paraffin-embedded and, thus, molecular detection was not performed. Nevertheless, considering that lymphoma affected hamsters with a median age of 19-months old in this study, a viral etiology is less likely for these cases because HaPV infection is related to lymphoma in young hamsters (5-weeks old). In contrast, older animals usually develop immune resistance to lymphoma development (Coggin et al. 1983). Additionally, lymphoma induced by HaPV infection mostly occurs in research colonies (Hocker et al. 2017), but rarely in pet hamsters (Simmons et al. 2001).

Fibrosarcomas often have an infiltrative and recurrent behavior, but metastases are rare in domestic animals (Hendrick 2017), similarly to the present study wherein single nodules restricted to the skin were observed. These lesions involved mainly the limbs and ventrum (mammary gland), which are referred as the most common locations for fibroma or fibrosarcoma development in hamsters (Kondo et al. 2011, Hocker et al. 2017). Differential diagnosis of fibrosarcoma in hamsters should include atypical fibroma/fibrosarcoma, a neoplasm derived from ganglion cell-like (GL) cells characterized by large amounts of GL cells, which are similar to histiocytes or neurons and intermixed with collagen fibers (Baba et al. 2003). Considering that GL cell levels in the dermis and subcutaneous tissue is dependent on circulating androgen levels, most atypical fibromas are detected in sexually mature male hamsters older than 7-months (Hocker et al. 2017), while most of the cases of the present work occurred in females. Additionally, the cases herein were differentiated through the neoplastic cells' histological features, as these were predominantly spindle. At the same time, atypical fibromas/fibrosarcomas present polygonal to angular to spindle-shaped and medium-large neoplastic cells, as well as large amounts of collagen fibers (Kondo et al. 2011). Moreover, extraskeletal osteosarcoma should

also be considered a differential in these cases, as previously reported in a one-year old Chinese hamster (Conrado et al. 2013) and this was obtained by the absence of osteoid within the neoplasms diagnosed.

When mammary tumors are examined, only benign neoplasms corresponding to mammary cystadenomas were identified. Similarly, in rats, mammary tumors are mostly composed of benign mammary fibroadenomas, which rarely metastasizes, and, thus, surgical treatments are related to good prognosis (Capello 2011), as in the present study wherein all samples were obtained through biopsies and were not related to death in the affected hamsters. Mammary tumors are widely reported in hamsters, with adenoma and adenocarcinoma identified as the most frequent (Kondo et al. 2009). A genetic predisposal was suggested in Djungarian hamsters (Jelinek et al. 2013). Despite the report of other studies of the occurrence of mammary tumors solely in Djungarian hamsters (Kamino et al. 2001, Kondo et al. 2009, Jelinek et al. 2013), this study identified the neoplasm in Syrian and Chinese hamsters as well. Besides, a previous study identified that mammary adenomas accounted for 12% of the neoplasms in domestic hamsters (Kamino et al. 2001), which is similar to the present study's frequency (10%). Moreover, young hamsters with a median age of 12-months old were mostly affected in the present investigation, similarly to previous studies (Kamino et al. 2001, Yoshimura et al. 2015).

The reproductive system was the second most commonly affected in this study, after skin neoplasms. These systems are the most commonly involved in surgical procedures in both female and male rodent patients. Ovariohysterectomy may be recommended in females to prevent reproductive disease, such as mammary tumors, or as a therapeutic measure in debilitated animals (Capello 2011). In the present work, reproductive tumors were represented mostly by mammary neoplasms, followed by uterine and ovarian neoplasms, such as leiomyosarcoma, ovarian granulosa cell tumor, and teratoma. Although uterine tumors are widely described in laboratory animals and leiomyomas are regarded as the most common uterine neoplasms in hamsters (Kamino et al. 2001), two uterine cases of leiomyosarcoma were diagnosed in the present study. Differential diagnosis should rely on tumoral pleomorphism and mitotic index (Kondo et al. 2007), as performed in the current investigation. Other differentials include uterine adenocarcinomas (Kamino et al. 2001) and collision tumors with mixed granular cell tumor and uterine adenocarcinoma (Golbar et al. 2011), which was obtained through the microscopical features of the neoplasm. Uterine tumors are common in aged hamsters (Kamino et al. 2001, Golbar et al. 2011), similar to the present study, wherein the animals had a median age of 21-months old.

A considerable high incidence of ovarian granulosa cell tumor was previously detected in approximately 25-month old female laboratory hamsters (McInnes et al. 2013), similarly to the present study in which the two females affected by this neoplasm were 36-months old. Moreover, we report a novel case of ovarian teratoma in a Chinese hamster, and, although it has not been previously detected as a spontaneous neoplasm in domestic hamsters (Kondo et al. 2008), it may be induced in male Syrian hamsters through intratesticular inoculation of zinc chloride (Guthrie & Guthrie 1974). Ovarian teratomas are rare neoplasms in domestic animals and are originated from pluripotent germ cells of the ovaries or testicles, being mostly described in dogs and horses. These cells may differentiate into multiple tissues, such as bone, cartilage, teeth, or skin and its adnexa (Agnewl & Maclahlan 2017), as observed in the present case. Most teratomas are benign tumors, but some tissue components may have malignant features (Agnewl & Maclahlan 2017). In the present study, however, no malignant feature of metastasis was identified.

CONCLUSIONS

Neoplasms are important causes of death or a major reason to perform biopsy in domestic hamsters in Southern Brazil. The hamsters affected in this study had a median age of 14-months old, and females were slightly more affected than males.

Cutaneous neoplasms were most commonly identified, and Squamous cell carcinoma (SCC) was the most frequent tumor, wherein the lip/nasal region was mostly affected. Other identified neoplasms included lymphoma, fibrosarcoma, and mammary cystadenoma, in addition to less common neoplasms, such as uterine leiomyosarcoma, ovarian granulosa cell tumor, and ovarian teratoma.

Acknowledgements.- We thank the "Conselho Nacional de Desenvolvimento Científico e Tecnológico (CNPq)" and the "Coordenação de Aperfeiçoamento de Pessoal de Nível Superior (CAPES)" for supporting this study.

Animal welfare/ethical statement.- We authors of the article entitled "Neoplasms in domestic hamsters in Southern Brazil: epidemiological and pathological aspects of 40 cases" declared, for all due purposes, the project that gave rise to the present data of the same has not been submitted for evaluation of the Ethics Committee of the "Universidade Federal do Rio Grande do Sul" (UFRGS), but we are aware of the content of the Brazilian resolutions of the "Conselho Nacional de Controle de Experimentação Animal (CONCEA)" <http://www.mct.gov.br/index.php/content/view/310553.html> if it involves animals. Thus, the authors assume full responsibility for the presented data and are available for possible questions, should they be required by the competent authorities.

Conflict of interest statement.- The authors have no competing interests.

REFERENCES

Agnewl D.W. & Maclahlan N.J. 2017. Tumors of the genital systems, p.689-722. In: Meuten D.J. (Ed.), Tumors in Domestic Animals. 5th ed. John Wiley and Sons, Ames.

Aguila G.D., Torres C.G., Carvallo F.R., Gonzalez C.M. & Cifuentes F.F. 2019. Oral masses in African pygmy hedgehogs. J. Vet. Diagn. Invest. 31(6):864-867. <https://dx.doi.org/10.1177/1040638719878870> <PMid:31585523>

Baba Y., Takahashi K. & Nakamura S. 2003. Androgen-dependent atypical fibromas spontaneously arising in the skin of Djungarian hamsters (*Phodopus sungorus*). Comp. Med. 53(5):527-531. <PMid:14655996>

Bampi V.F., Vilela W.F., Gonçalves R.V., Rheingantz M.G.T., Minello L.F., Da Silva J.L.B & De Oliveira L.B.O. 2014. The promoting effect of carbamide peroxide teeth bleaching gel in a preclinical model of head and neck cancer in hamster buccal pouch. Clin. Exp. Otorhinolaryngol. 7(3):210-215. <https://dx.doi.org/10.3342/ceo.2014.7.3.210> <PMid:25177438>

Capello V. 2011. Common surgical procedures in pet rodents. J. Exot. Pet. Med. 20(4):294-307. <https://dx.doi.org/10.1053/j.jepm.2011.07.002>

Coggin J.H. Jr., Bellomy B.B., Thomas K.V. & Pollock W.J. 1983. B-cell and T-cell lymphomas and other associated diseases induced by an infectious

DNA viroid-like agent in hamsters (*Mesocricetus auratus*). Am. J. Pathol. 110(3):254-266. <PMid:6600884>

Conceição A.M., Andrade R.L.F.S., Sarmento C.A.P., Souza K.S. & Fioretto E.T. 2018. Squamous cell carcinoma in Chinese hamsters (*Cricetulus griseus*). Acta Sci. Vet. 46(supl.1):267.

Conrado F.O., Bruno S.F. & De Alencar N.X. 2013. What is your diagnosis? Scapular mass in a Chinese hamster. Vet. Clin. Pathol. 42(4):533-534. <https://dx.doi.org/10.1111/vcp.12083> <PMid:24117501>

De Alencar N.X., Bruno S.F., Campos S.D.E., De Queiroz G.B., De Souza A.M. & Macieira D.B. 2012. Lymphoma on Chinese hamster (*Cricetulus griseus*) - two case reports. Braz. J. Vet. Med. 34(2):141-145.

De Oliveira L.B., Bampi V.F., Gomes C.F & De Souza M.A. 2009. Angioarchitecture of squamous cell carcinoma from hamster buccal pouch: a scanning electron microscopy study. Scanning 31(5):188-194. <https://dx.doi.org/10.1002/sca.20161> <PMid:20039331>

Gardner D.G. 1996. Spontaneous squamous cell carcinomas of the oral region in domestic animals: a review and consideration of their relevance to human research. Oral Dis. 2(2):148-154. <https://dx.doi.org/10.1111/j.1601-0825.1996.tb00216.x> <PMid:8957928>

Ghaffari S., Moayer F. & Dezfoulian O. 2009. Spontaneous differentiated squamous cell carcinoma of cheek pouch in a Syrian hamster. Iran. J. Vet. Res. 10(1):84-86.

Golbar H.M., Izawa T., Kuwamura M., Okamura K., Fujita D., Tagami Y., Sasai H. & Yamate J. 2011. A collision tumor consisting of granular cell tumor and adenocarcinoma in the uterus of an aged djungarian hamster. J. Toxicol. Pathol. 24(4):233-237. <https://dx.doi.org/10.1293/tox.24.233> <PMid:22319236>

Goldschmidt M.H. & Goldschmidt K.H. 2017. Epithelial and melanocytic tumors of the skin, p.88-141. In: Meuten D.J. (Ed.), Tumors in Domestic Animals. 5th ed. John Wiley and Sons, Ames.

Greenacre C.B. 2004. Spontaneous tumors of small mammals. Vet. Clin. N. Am., Exot. Anim. Pract. 7(3):627-651. <https://dx.doi.org/10.1016/j.cvex.2004.04.009> <PMid:15296867>

Guthrie J. & Guthrie O.A. 1974. Embryonal carcinomas in Syrian hamsters after intratesticular inoculation of zinc chloride during seasonal testicular growth. Cancer Res. 34(10):2612-2614. <PMid:4413223>

Harvey R.G., Whitbread T.J., Ferrer L. & Cooper J.E. 1992. Epidermotropic cutaneous T-cell Lymphoma (mycosis fungoides) in Syrian Hamsters (*Mesocricetus auratus*). A report of six cases and the demonstration of T-cell specificity. Vet. Dermatol. 3(1):13-19. <https://dx.doi.org/10.1111/j.1365-3164.1992.tb00138.x>

Hendrick M.J. 2017. Mesenchymal tumors of the skin and soft tissues, p.142-175. In: Meuten D.J. (Ed.), Tumors in Domestic Animals. 5th ed. John Wiley and Sons, Ames.

Hocker S.E., Eshar D. & Wouda R.M. 2017. Rodent oncology: diseases, diagnostics, and therapeutics. Vet. Clin. N. Am., Exot. Anim. Pract. 20(1):111-134. <https://dx.doi.org/10.1016/j.cvex.2016.07.006> <PMid:27890286>

Homburger F. 1983. Background data on tumor incidence in control animals (Syrian hamsters). Prog. Expo. Tumor Res. 26:259-265. <https://dx.doi.org/10.1159/000407264> <PMid:6844644>

Jelinek F., Felsberg J. & Mestan M. 2013. Familial incidence of mammary gland tumours in the Djungarian hamster (*Phodopus sungaros*): a case report. Vet. Med. Czech. 58(8):442-448. <https://dx.doi.org/10.17221/6985-VETMED>

Johnson J.G. III., Blair R., Brandão J., Tully T.N.Jr. & Gaunt S.D. 2014. Atypical fibrosarcoma in the skin of a Roborovski hamster (*Phodopus roborovskii*). Vet. Clin. Pathol. 43(2):281-284. <https://dx.doi.org/10.1111/vcp.12146> <PMid:24829077>

Kamino K., Tillmann T. & Mohr U. 2001 Spectrum and age-related incidence of spontaneous tumours in a colony of Han:AURA hamsters. Exp. Toxicol. Pathol. 52(6):539-544. <https://dx.doi.org/10.1016/S0940-2993(01)80012-9> <PMid:11256756>

Kondo H., Kimoto H., Shibuya H., Shirai W., Matsuo K. & Sato T. 2007. Spontaneous uterine leiomyosarcoma in a golden hamster (*Mesocricetus auratus*). J. Vet. Med. A, Physiol. Pathol. Clin. Med. 54(1):27-29. <https://dx.doi.org/10.1111/j.1439-0442.2007.00912.x> <PMid:17359451>

Kondo H., Onuma M., Shibuya H. & Sato T. 2008. Spontaneous tumors in domestic hamsters. Vet. Pathol. 45(5):674-680. <https://dx.doi.org/10.1354/vp.45-5-674> <PMid:18725472>

Kondo H., Onuma M., Shibuya H. & Sato T. 2009. Morphological and immunohistochemical studies of spontaneous mammary tumors in Siberian hamsters (*Phodopus sungorus*). J. Comp. Pathol. 140(2/3):127-131. <https://dx.doi.org/10.1016/j.jcpa.2008.09.012> <PMid:19110261>

Kondo H., Onuma M., Shibuya H., Sato T. & Abbott J.R. 2011. Atypical fibrosarcomas derived from cutaneous ganglion cell-like cells in 2 domestic Djungarian hamsters (*Phodopus sungorus*). J. Am. Assoc. Lab. Anim. Sci. 50(4):523-525. <PMid:21838983>

Kondo H., Takada M., Shibuya H., Shirai W., Matsuo K. & Sato T. 2006. Cutaneous plasmacytoma in three golden hamsters (*Mesocricetus auratus*). J. Vet. Med. A, Physiol. Pathol. Clin. Med. 53(2):74-76. <https://dx.doi.org/10.1111/j.1439-0442.2006.00796.x> <PMid:16466459>

Lennox A.M. & Bauck L. 2012. Basic anatomy, physiology, husbandry, and clinical techniques, p.339-354. In: Quesenberry K.E. & Carpenter J.W. (Eds), Ferrets, Rabbits, and Rodents: clinical medicine and surgery. 3rd ed. Elsevier Saunders, St. Louis.

Martorell J., Fondevila D. & Ramis A. 2005. Spontaneous squamous cell carcinoma of the cheek pouch in two dwarf hamsters (*Phodopus sungorus*). Vet. Rec. 156(20):650-651. <https://dx.doi.org/10.1136/vr.156.20.650> <PMid:15894733>

Martorell J., Martínez A. & Soto S. 2010. Complete ablation of vertical auditive conduct and ear pinna in a Dwarf hamster (*Phodopus sungorus*) with an aural spontaneous squamous cell carcinoma. J. Exot. Pet Med. 19(1):96-100. <https://dx.doi.org/10.1053/j.jepm.2009.06.015>

McInnes E.F., Ernst H. & Germann P.G. 2013. Spontaneous neoplastic lesions in control Syrian hamsters in 6-, 12-, and 24-month short-term and carcinogenicity studies. Toxicol. Pathol. 41(1):86-97. <https://dx.doi.org/10.1177/0192623312448938> <PMid:22707381>

Mognetti B., Di Carlo F. & Berta G.N. 2006. Animal models in oral cancer research. Oral Oncol. 42(5):448-460. <https://dx.doi.org/10.1016/j.oraloncology.2005.07.014> <PMid:16266822>

Rainwater K.A.E., Hawkins M.G., Crabs T. & Malka S. 2011. An anaplastic sarcoma of probable salivary origin in a Teddy-bear hamster (*Mesocricetus auratus*). J. Exot. Pet Med. 20(2):144-150. <https://dx.doi.org/10.1053/j.jepm.2011.02.010>

Santos V.M., Lima M.A., Marquez D.S., Cabrine-Santos M., Lages-Silva E., Matheus J.M., Oliveira-Junior J.V. & Ramírez L.E. 2002. Spontaneous B-cell lymphoma in hamster. Medicina, Ribeirão Preto, 35:179-183.

Simmons J.H., Riley L.K., Franklin C.L. & Besch-Williford C.L. 2001. Hamster Polyomavirus infection in a pet Syrian hamster (*Mesocricetus auratus*). Vet. Pathol. 38(4):441-446. <https://dx.doi.org/10.1354/vp.38-4-441> <PMid:11467479>

Van Hoosier G.L.Jr. & Trentin J.J. 1979. Naturally occurring tumors of the Syrian hamster. Prog. Exp. Tumor Res. 23:1-12. <https://dx.doi.org/10.1159/000401419> <PMid:392586>

White S.D., Bourdeau P.J., Brément T., Bruet V., Gimenez-Acosta C., Guzman D.S.M., Paul-Murphy J. & Hawkins M.G. 2019. Companion hamsters with cutaneous lesions; a retrospective study of 102 cases at two university veterinary teaching hospitals (1985-2018). Vet. Dermatol. 30(3):243-e74. <https://dx.doi.org/10.1111/vde.12730>

Yoshimura H., Kimura-Tsukada N., Ono Y., Michishita M., Ohkusu-Tsukada K., Matsuda Y., Ishiwata T. & Takahashi K. 2015. Characterization of spontaneous mammary tumors in domestic Djungarian hamsters (*Phodopus sungorus*). Vet. Pathol. 52(6):1227-1234. <https://dx.doi.org/10.1177/0300985815583097> <PMid:25967136>

PESQUISA VETERINÁRIA BRASILEIRA
Brazilian Journal of Veterinary Research
ISSN 0100-736X (Print)
ISSN 1678-5150 (Online)

Pesq. Vet. Bras. 40(12):1039-1047, December 2020
DOI: 10.1590/1678-5150-PVB-6544

Original Article
Animal Morphophysiology
BY-NC

Assessment of fetal lung maturity using analysis of amniotic fluid from ewes that gave birth prematurely and at term[1]

Natália Cristina de Souza[2]*, Fernanda Bovino[3], Larissa Gabriella Avilla[4], Maurício Deschk[5], Jefferson F. Alcindo[6], Maria Fernanda C.B. Fink[7], Luiz Cláudio N. Mendes[8] and Francisco Leydson F. Feitosa[8]

Abstract.- Souza N.C., Bovino F., Avilla L.G., Deschk M., Alcindo J.F., Fink M.F.C.B., Mendes L.C.N. & Feitosa F.L.F. 2020. **Assessment of fetal lung maturity using analysis of amniotic fluid from ewes that gave birth prematurely and at term.** *Pesquisa Veterinária Brasileira 40(12):1039-1047*. Departamento de Clínica, Cirurgia e Reprodução Animal, Faculdade de Medicina Veterinária de Araçatuba, Universidade Estadual Paulista, Rua Clóvis Pestana 793, Cx. Postal 533, Jardim Dona Amélia, Araçatuba, SP 16050-680, Brazil. E-mail: souzanataliancs@gmail.com

The aim of this study was to evaluate the lung maturity of premature and full-term lambs by analyzing amniotic fluid using the following methods: Clements test, Nile blue cytology test, hematoxylin-Shorr stain, lamellar body count, and radiographic tests. The use of these methods is intended to identify high-risk newborns and provide immediate clinical intervention after birth. Altogether, 56 animals (24 ewes and 32 lambs) were included in the study and divided into 3 groups. Group I consisted of 8 ewes that were at approximately 145 days of gestation; this group delivered 10 lambs naturally. Group II consisted of 8 ewes that were at 138 days' gestation; this group delivered 11 lambs by cesarean section. Group III consisted of 8 ewes at 138 days' gestation; this group was administered intramuscular dexamethasone (16mg/animal) 36 hours prior to a cesarean section. Group III delivered11 lambs. Cytological tests were performed using a microscope with a maximum magnification of 1000x, while the Clements test was visually observed by one of the researchers. Amnioticfluid lamellar body counts were measured using transmission electron microscopy. Among the staining methods, hematoxylin-Shorr was reliable, and Group III had a greater number of orangeophilic cells when compared to Group II, probably due to corticoid administration. The Clements test showed pulmonary maturity in approximately 20% of Group I lambs and Group II showed 9.1% of bubbles; however, Group III had the highest pulmonary maturity percentage (36.4%). The lamellar bodies were measured, and all groups had sizes between 0.019 and 0.590μm. Radiographic evaluation revealed that the majority of lambs presented some level of pulmonary radiodensity, indicating an acinar pattern at birth. These results are in line with the expectations of each group. We found that the normal group showed greater pulmonary maturity, whereas Group II presented pulmonary immaturity, which is expected because this group comprised lambs born prematurely and Group III showed pulmonary

[1] Received on August 17, 2020.
Accepted for publication on September 10, 2020.

[2] Graduate Program in Animal Science, Departamento de Clínica, Cirurgia e Reprodução Animal, Faculdade de Medicina Veterinária, Universidade Estadual Paulista "Júlio de Mesquita Filho" (Unesp), Campus Araçatuba, Rua Clóvis Pestana 793, Jardim Dona Amélia, Araçatuba, SP 16050-680, Brazil. *Corresponding author: souzanataliancs@gmail.com

[3] Professor, Faculdade de Ciências Agrárias Andradina (FCAA), Fundação Educacional de Andradina (FEA), Rua Amazonas 571, Stella Maris, Andradina, SP 16901-160SP, Brazil.

[4] Professor, Universidade Federal de Mato Grosso do Sul (UFMS), Cidade Universitária, Av. Costa e Silva s/n, Pioneiros, Campo Grande, MS 79070-900, Brazil.

[5] Veterinarian, Universidade Federal de Juiz de Fora (UFJF), Campus Universitário, Rua José Lourenço Kelmer s/n, São Pedro, Juiz de Fora, MG 36036-900, Brazil.

[6] Professor, Universidade Federal de Juíz de Fora (UFJF), Campus Universitário, Rua José Lourenço Kelmer s/n, São Pedro, Juiz de Fora, MG 36036-900, Brazil.

[7] Graduation in Veterinary Medicine, Faculdade de Medicina Veterinária, Universidade Estadual Paulista "Júlio de Mesquita Filho" (Unesp), Campus Araçatuba, Rua Clóvis Pestana 793, Jardim Dona Amélia, Araçatuba, SP 16050-680, Brazil.

[8] Professor, Departamento Clínica, Cirurgia e Reprodução Animal, Faculdade de Medicina Veterinária, Universidade Estadual Paulista "Júlio de Mesquita Filho" (Unesp), Campus Araçatuba, Rua Clóvis Pestana 793, Jardim Dona Amélia, Araçatuba, SP 16050-680, Brazil.

maturity almost comparable to the normal delivery group (Group I). This is due to the fact that although these animals are premature, the use of dexamethasone helped in pulmonary maturation. Therefore, these pulmonary maturity tests are considered effective when more than one technique is used and can be used routinely in the care of a pregnant ewe in labor, where a simple collection of amniotic fluid can predict a high-risk pregnancy and alert the veterinarian if the newborn needs intensive supportive treatment.

INDEX TERMS: Fetus, lung, amniotic fluid, ewes, sheep, lung fetal maturity, lamb survival, ovine.

RESUMO.- [Avaliação da maturidade pulmonar fetal utilizando a análise de líquido amniótico de ovelhas que deram à luz prematuramente e a termo.] O objetivo deste estudo foi avaliar a maturidade pulmonar de cordeiros prematuros e a termo por meio da análise do líquido amniótico utilizando os seguintes métodos: teste de Clements, teste de citologia do azul do Nilo, coloração de hematoxilina-Shorr, contagem de corpos lamelares e testes radiográficos. Um desses métodos tem por objetivo identificar recém-nascidos de alto risco e fornecer intervenção clínica imediata após o nascimento. Ao todo, 56 animais (24 ovelhas e 32 cordeiros) foram incluídos no estudo e divididos em 3 grupos. O grupo I foi composto por 8 ovelhas com aproximadamente 145 dias de gestação; este grupo deu à luz 10 cordeiros naturalmente. O Grupo II foi composto por 8 ovelhas com 138 dias de gestação; este grupo deu à luz 11 cordeiros por cesariana. Grupo III consistiu de 8 ovelhas com 138 dias de gestação; este grupo recebeu dexametasona intramuscular (16 mg / animal) 36 horas antes de uma cesariana. O Grupo III entregou 11 cordeiros. Os testes citológicos foram realizados em microscópio com aumento máximo de 1000x, enquanto o teste de Clements foi observado visualmente por um dos pesquisadores. A contagem de corpos lamelares de líquido amniótico foi medida usando microscopia eletrônica de transmissão. Dentre os métodos de coloração, o hematoxilina-Shorr foi confiável, sendo que o Grupo III apresentou maior número de células orangeofílicas quando comparado ao grupo II, provavelmente devido à administração de corticóide. O teste de Clements mostrou maturidade pulmonar em aproximadamente 20% dos cordeiros do Grupo I e o Grupo II apresentou 9,1% de bolhas; entretanto, o Grupo III apresentou o maior percentual de maturidade pulmonar (36,4%). Os corpos lamelares foram medidos e todos os grupos apresentaram tamanhos entre 0,019 e 0,590μm. A avaliação radiográfica revelou que a maioria dos cordeiros apresentava algum grau de radiodensidade pulmonar, indicando padrão acinar ao nascimento. Esses resultados estão alinhados com as expectativas de cada grupo. Verificamos que o grupo normal apresentou maior maturidade pulmonar, enquanto o Grupo II apresentou imaturidade pulmonar, o que é esperado por se tratar de cordeiros nascidos prematuramente e o Grupo III apresentou maturidade pulmonar quase comparável ao grupo de parto normal (Grupo I). Isso se deve ao fato de que, embora esses animais sejam prematuros, o uso da dexametasona auxiliou na maturação pulmonar. Portanto, esses testes de maturidade pulmonar são considerados eficazes quando mais de uma técnica são utilizadas e podem ser usadas rotineiramente no cuidado de uma ovelha gestante em trabalho de parto, onde uma simples coleta de líquido amniótico pode prever uma gravidez de alto risco e alertar o veterinário se o recém-nascido precisa de tratamento de suporte intensivo.

TERMOS DE INDEXAÇÃO: Pulmão, feto, líquido amniótico, ovelhas, maturidade pulmonar fetal, sobrevivência de cordeiros.

INTRODUCTION

Neonatology in farm animals is an area with little advancement. In human pediatrics, due to advances in technology and the adequate supportive treatment of premature newborns, the likelihood of survival for these high-risk patients is easily achieved; premature babies under 28 weeks can survive (Patel 2016, Cheong et al. 2018).

The reverse occurs in veterinary medicine; whereas the gestation period in sheep varies between 145 to 148 days (Jainudeen & Hafez 2004) and this period can be modified by maternal, fetal and environmental factors. In other words, lambs born just 7 days before the expected date of delivery are at great risk of dying, even before the first 24 hours of life. Therefore, according the some studies, lambs born with an average of 138 days can be considered premature (Radostits et al. 2007, Avila et al. 2014, Bovino 2015, Feitosa et al. 2017, Miura et al. 2019).

In premature human neonates, one of the primary assessments is lung function, since this function is essential for the survival of the newborn and lung development problems can cause complications, such as respiratory distress syndrome (RDS) among others (Ghartey et al. 2012, Harrison & Goldenberg 2016, Patel 2016).

Based on these data, we must have the same concerns with animal species, and lung function must be assessed since prematurity can lead to impaired lung capacity in premature lambs. One of the important assessments that can be applied right after lamb birth is the Apgar score modified by Born (1981). It is a method that assesses the animals' vitality level through some parameters at birth (Rodrigues et al. 2007, Avila et al. 2014).

In human medicine, the evaluation of amniotic fluid is important in determining the fetal condition. A variety of biochemical, cytological, immunological and biophysical tests can be performed using amniotic fluid to assess pulmonary, renal, and epidermal maturation (Kjeldsberg & Knight 1998, Miron 2012). However, some of these methods have disadvantages such as delay in results, requiring specialized training and are considered expensive (Dubin 1998).

As an alternative in human medicine, the Clements test, lamellar body counts, and Nile blue cytology are fast, cheap, and routine methods that can determine whether the fetus is premature. The Clements test is a qualitative method used to determine the presence of pulmonary surfactant contained in the amniotic fluid (Clements et al.1972, Crockett 1988).

Lamellar bodies store surfactant, which is then released into the alveolar space by fetal breathing movements (Dubin 1998, Jörger et al. 2017). As for the cytological method of Nile blue, the amniotic fluid is rich in epithelial cells originating from the skin and other fetal constituents. The classification of these cells can indicate immaturity or maturity of the fetal epidermis (Rosborg 1970, Morrison 1974, Souza et al. 2000).

Due to the advantages of these methods, there are some studies described in animal species that assessed fetal lung maturity through the analysis of amniotic fluid, including the physical and biochemical analysis of amniotic fluid in sheep (Souza et al. 2000); the use of cytological typification of amniotic fluid at the time of calving (Moya 2005); the analysis of amniotic fluid in neonate horses including the use of lamellar body counts to assess fetal lung maturity (Castagnetti et al. 2007); the evaluation of the efficiency of the Clements test, of the Nile blue cytology and Shorr and lamellar bodies count in the amniotic fluid of goats born by eutocic and premature births (Feitosa et al. 2020).

Since gestational complications such as prematurity are associated with higher mortality rates, directly affecting the productivity of a herd, the use of rapid and routine methods to support these newborns is extremely important, since neglect in treatment of a newborn can cause several economic losses to the producer.

The aim of this study was to assess the degree of vitality, as well as the pulmonary maturity of premature and full-term lambs through the analysis of amniotic fluid, using the Clements test, lamellar body count, and Nile blue cytology, allowing better identification of high-risk newborn lambs and providing immediate clinical intervention after birth.

MATERIALS AND METHODS

Experimental group. A total of 56 animals (24 multiparous ewes and 32 lambs) from a Suffolk crossbreed flock in Araçatuba, São Paulo State, were included in the study. The ewes were divided into 3 experimental groups. Group I consisted of 8 ewes at approximately 145 days gestation. This group produced 10 lambs born naturally. Group II consisted of 8 ewes at 138 days gestation. This group delivered 11 lambs by caesarean section. Group III consisted of 8 ewes at 138 days gestation which were administered intramuscular dexamethasone (16 mg/animal) 36 hours prior to caesarean section. Group III had 11 lambs.

The ewes were left to graze on pasture with corn based silage and other supplements provided to ensure a balanced diet. Prior to their expected due date and/or scheduled cesarean section, the ewes were transferred to a stall in order to enable observations. Group I ewes were monitored 24 hours a day so that adequate support could be given in case of lambing.

To assist animal management on this study and to ensure lambing happened in a condensed time frame, a protocol for the fertilization of the ewes was developed. Estrus was synchronized using vaginal sponges impregnated with progesterone, followed by an intramuscular administration of 0.4mL of prostaglandin (PGF2α) on day 0 (D0). This procedure was followed by an intramuscular administration of 500IU of equine chorionic gonadotropin (eCG) and 0.4mL of prostaglandin on the day 7 (D7). A misture of ink and oil was placed on the breast region of the breeding ram. So when the male covered the female, it was possible to see a paint stain on the rear of the sheep, a different color was used every 15 days, in order to differentiate the females who returned to heat. This type of marking allowed us to facilitate the observation of the females that were covered and from the day of covering it was possible to estimate individual fertilizations dates, and later the pregnancies confirmed using an ultrasound (DP Vet 2200, Mindray) scan 45 to 60 days post fertilization.

For the cesarean sections conducted, the anesthetic procedure used included a proximal paravertebral block, which consisted of 5mL of lidocaine hydrochloride (2% Xylestesin®, Cristália) administered in each dorsal and ventral nerve roots of T13, L1, and L2 combined with epidural administration (L6-S1) of morphine sulfate (Dimorf®, Cristália) at a dose of 0.1mg/kg diluted in 5mL of saline. In cases where the paravertebral anesthesia was not considered effective, lidocaine hydrochloride was used directly at the incision site. After the removal of the fetus, the ewes were sedated using midazolam maleate (Dormonid®, Roche) at a dose of 0.2mg/kg. The caesarean sections were conducted by an incision on the ewes left flank, while they were placed in right lateral decumbency, as described (Tibary & Van Metre 2004).

Amniotic fluid (sample collection). In ewes that delivered naturally (Group I), AF was collected after the expulsion of the amniotic sac. If the amniotic sac remained intact, this was done by puncturing the sac using an 18G hypodermic needle attached to a 20-mL syringe. If the amniotic sac had ruptured, AF was obtained by placing a "Falcon" tube next to the vulva while the ewe was having contractions. After samples had been taken, the AF samples were kept refrigerated in Styrofoam containers with ice packs. They were then subsequently frozen at -18°C. For Groups II and III, the ewes uterus was first exteriorized in order to establish the best place for uterine incision. This avoided excessive bleeding and contamination of AF with blood from the cesarean section. Once the placenta could be observed, the amniotic sac was gently ruptured, and an 18G hypodermic needle coupled to a 20-mL syringe was used to harvest the largest amount of amniotic fluid possible. All the AF samples collected from the 3 groups were evaluated using the same tests, the Clements' test, lamellar body count, and 0.1% Nile blue and hematoxylin-Shorr staining.

Lamb vitality. To evaluate the vitality of the lambs, the Apgar score modified by Born (1981) was used. This included the following items scored from 0 to 2: a) response to cold water on the head (0 = absent, 1 = decreased, 2 = spontaneous and active movements); b) palpebral and interdigital reflex (0 = absent; 1 = weak reaction, one reflex present; 2 = immediate reaction, both reflexes present); c) Respiratory activity (0 = imperceptible, 1 = slow and irregular, 2 = regular and rhythmic); d) mucous membrane color (0 = white or blue, 1 = blue-tinged, 2 = pink-red). The scores were then interpreted using a grading system. A score between 7 and 8 represented good vitality, 4 to 6 was considered moderate vitality, and 0 to 3 was considered low vitality (depressed). Apgar evaluation has been widely used as a routine method in newborn lambs and goats (Feitosa et al. 2020, Avila et al. 2014). Lambs belonging to Groups II and III were closely monitored and bottle-fed (50ml) where possible with colostrum harvested from their mothers. Later, the lambs were put in individual stalls ($9m^2$) with their mothers and observed to see whether they would be accepted by their mother. None of the premature lambs were rejected by their mother. Care was taken to ensure that the temperature and ventilation was at a level to prevent hypothermia and hypoxia of the neonates. Temperature was controlled using an incubator and ventilation was controlled using an Ambu bag.

Mortality rates. The mortality rate of newboen lambs was expressed as a percentage in this study, some lambs that died were submitted to necropsy to diagnose the possible cause of the death.

Pulmonary radiography evaluation. The pulmonary radiographic examination was performed at lambs birth (M0), at 24 (M24) and 48 hours of life (M48), using a fixed X-ray device, placing the animals in the lateral decubitus position side.

Clements's test. Clements' test was performed using the guidelines set out previously (Clements et al. 1972). Five different dilutions of AF in 14 × 100mm glass tubes, that had been chemically

cleaned with ether, were distributed differing amounts of AF, saline (0.9% = S), and ethanol (95% = E). Tube 1 consisted of 1mL of AF and 1mL of E; Tube 2 consisted of 0.75mL of AF, 0.25mL of S, and 1mL of E; Tube 3 consisted of 0.5mL of AF, 0.5mL of S, and 1mL of E; Tube 4 consisted of 0.25mL of AF, 0.75mL of S, and 1mL of E; and tube 5 consisted of 0.2mL of AF, 0.8mL of S, and 1mL of E. All the tubes were closed using a clean rubber stopper, vigorously shaken for 15 seconds, and then placed in an upright rack. After 15 minutes, if there was an intact ring of bubbles at the air/liquid interface, this was considered to be a positive result. For this test, outcomes were divided into two categories: (1) negative or "immature": non-persistent bubbles in the first tube and persistent in the first and second tubes but not in the third and (2) positive or "mature": stable foam in the first 3 tubes.

Lamellar body count. The LB count was performed using platelet channel hematology analyzers, utilizing 0.5mL of AF per sample. The equipment was calibrated using the parameters for platelet count in sheep, which is 25 to 35 fentiliters. The samples were filtered, placed in tubes measuring 12 × 75mm, and the supernatant tested using an automated Coulter STKS® platelet channel. They were assessed by size and volume distribution, and compared to a standard logarithmic curve -carrier flow technology (Fakhoury et al. 1994, Carrillo et al. 1997, Lewis et al. 1999).

Nile blue staining. For the Nile blue staining, approximately 50µl of AF was placed on a microscope slide, on which 50µl of a 0.1% Nile blue sulfate solution was added. The solutions were mixed together and mounted underneath a coverslip in order to facilitate visualization. The cells derived from AF were observed under a light microscope (at a magnification of 400 to 1,000 X). The cells were classified as either cyanophilic (blue cells) which indicates immature fetal cells or orangeophilic (orange cells), which indicates fetal cell maturity (Brosens & Gordon 1966).

Hematoxylin-Shorr staining. For the hematoxylin-Shorr staining samples that contained mucus were placed in a centrifuge at 3,000 rpm for 3 minutes in order to avoid cell lysis. Following this the sample went through a cytospin. Mucus-free samples were directly placed in a cytocentrifuge (REVAM®) at 1000 rpm for 6 minutes. Sample staining was performed according to the recommendations published in previous studies. The cells too were classified as either cyanophilic (blue cells) which indicates immature fetal cells or orangeophilic (orange cells), which indicates fetal cell maturity (Luna 1968,).

Statistical analysis. Data were analyzed for variance using the SAS PROC MIXED (Statistical Analysis System) and covariance structure as defined by Akaike's information criterion. Means were compared multiple times using LSMEANS (Least Squares Means), which was adjusted to Tukey's test. The values of variables (tables with medians) were analyzed using Kruskal-Wallis test. This was done in order to progressively compare the groups. The Friedman test was used to compare times in each group. This was followed by Dunn's multiple comparisons test. The values of each of the variables, the color of the mucous membrane and the results of the Clements' test were analyzed using Fisher's exact test. The significance level was set at 5%.

All procedures such as the administration of anesthetic and conducting a cesarean section were carried out by the same people. Similarly, rating and analyses, whether radiological, laboratory-based, or clinical, were always carried out by the same people on the team.

Research ethics commission. This study was conducted with the approval of the Ethics Committee on Animal Use of the "Faculdade de Medicina Veterinária", Unesp, City of Araçatuba, São Paulo, Brazil (protocol FOA-00121-2013).

RESULTS

Apgar score

In our study, the lambs belonging to Group I, showed statistical difference (p<0.05) in the moments immediately after birth (T0) and 15 minutes after birth (T15), showing greater vitality, reaching the highest Apgar score (score 8) when compared to Group II and III. However, it is possible to visualize in Groups II and III, although there are no significant differences, the Group III showed better vitality at birth (T0) than Group II (3±2.38 and 5±1.5, respectively), and after 15 minutes after birth (T15) the values were equal (Table 1).

Mortality rates

None of the lambs born at term (Group I) died. Although the groups did not differ statistically, in prematurely born lambs, the mortality rate, as expected, was high. This was especially the case for lambs delivered by ewes that did not receive dexamethasone 36 hours before the cesarean section was performed (Group II). In this group, 4 (4/11 = 36%) newborns died within 15 minutes of birth and two more died between 15 minutes and 12 hours after birth. Of the premature lambs born from ewes that received a 16-mg dose of dexamethasone (Group III), a total of 3 animals died (3/11 = 27%), two of them within 15 minutes (T15) and the third within one hour (T60). The dead lambs were submitted to a necropsy examination and hydrostatic docimasia of Galen was performed to prove that lung failure had occurred in animals that died in the first 15 minutes after birth. Necroscopic findings for the lambs that died up until 12 hours after birth were congestion and diffuse edema in both lungs and liver.

Table 1. Evaluation of the Apgar score modified by Born (1981) at birth (T0), and at 15 and 60 minutes after birth, with scores from 0 to 3 (low vitality), 4 to 6 (moderate vitality) and 7 to 8 (good vitality) in lambs born naturally (Group I), premature and caesarean section (Group II), premature and cesarean section + dexamethasone (Group III)

Timepoints	Apgar								
	Group I			Group II			Group III		
	n	Md	Min-Max	n	Md	Min-Max	n	Md	Min-Max
T0	10	8[a]	6 - 8	11	3[b]	0 - 7	11	5[b]	2 - 7
T15	10	8[a]	6 - 8	7	6[b]	1 - 7	10	5[b]	1 - 8
T60	10	7	6 - 8	5	6	6 - 8	8	6	5 - 8

n = Number, Md = median, Min-Max = minimum-maximum; [a,b] Medians followed by different letters in the same row denote statistical difference by the Dunn test (p<0.05).

Pulmonary radiography evaluation

On radiographic evaluations of Group I lambs immediately following birth (M0), most lambs showed increased pulmonary radiodensity along with an alveolar pattern in their diaphragmatic lobes (Fig.1A). Some lambs, however, showed no breathing pattern changes.

For 7 of the lambs in Group II, there was a homogeneous increase in pulmonary radiodensity, which obscured the view of the cardiac silhouette. This is consistent with pleural effusion, which is associated with difficulty in viewing the diaphragmatic dome. A general increase in pulmonary radiodensity with alveolar pattern and the presence of air bronchograms in diaphragmatic lobes was observed in lambs. In these cases, the cardiac silhouette and diaphragmatic domes could be partially seen due to the intense alveolar pattern (Fig.1B). Such results have also been reported in humans, where radiographic findings show that the surfactant deficiency in RDS causes a generalized acinar collapse; thus, decreased lung expansion as well as thinning of the pulmonary vessels and air bronchograms are observed (Agrons et al. 2005).

Three lambs born by cesarean section, whose mothers received dexamethasone 36 hours prior (Group III), showed a slight increase in radiodensity with an alveolar pattern in the diaphragmatic and accessory lobes, with blurring of the caudal vena cava observed. Eight lambs displayed homogeneous radiodensity in their thoracic cavity, which obscured the cardiac silhouette and diaphragmatic domes from view. This suggested the occurrence of atelectasis in these lambs (Fig.1C).

Clements' test

Although it was expected that AF of ewes belonging to Group I would show the greatest bubble stability as they were born at term (Table 2), there were no statistical differences between groups (p<0.05). Bubbles were observed up to the third tube for one ewe from Group II (Fig.2A,B). The AF obtained from 4 ewes in Group III showed a higher percentage of lung maturity (36.4% out of a total of 11 animals) also contained bubbles.

Lamellar body count

Using transmisssion electron microscopy (TEM), we observed that females in Groups II and III had a greater absence of lamellar bodies in the amniotic fluid when compared to full-term sheep (Fig.3). We found that the sheep lamellar bodies belonging to Group III showed variation in the measurements, with the smallest measurement being 0.019 to the largest of 0.590μm, while the size of the lamellar bodies of Groups I and



Fig.1. (**A**) Radiograph showing respiratory pattern of lambs born in a normal birth (Group I). Increased pulmonary radiopacity of the alveolar pattern located in diaphragmatic lobes at 24 hours after birth (M24). (**B**) Toracic radiograph of cesarean section lambs (Group II) at 24 hours(M24) after birth, denotes a general increase in pulmonary radiodensity with alveolar pattern and the presence of air bronchograms in diaphragmatic lobes was observed in lambs. In these cases, the cardiac silhouette and diaphragmatic domes could be partially seen due to the intense alveolar pattern. (**C**) Toracic radiograph of lambs born by cesarean section + dexamethasone (Group III) in 24 hours (M24) after birth, the lambs displayed homogeneous radiodensity in their thoracic cavity, which obscured the cardiac silhouette and diaphragmatic domes from view. This suggested the occurrence of atelectasis in these lambs.

Table 2. Number (n) and percentage (%) of the Clements' test in amniotic fluid of ewes belonging to Groups I, II and III. Results are classified as positives (presence of bubbles), indicative of fetal lung maturity, or negative (absence of bubbles), indicating fetal lung immaturity

Tube	Clements' test	Group I		Group II		Group III		P[a]
		n	%	n	%	n	%	
1st	Positive	2	20.0	1	9.1	4	36.4	0.3313
	Negative	8	80.0	10	90.9	7	63.6	
2nd	Positive	-	-	1	9.1	2	18.2	0.7560
	Negative	10	100.0	10	90.9	9	81.8	
3rd	Positive	-	-	1	9.1	-	-	1.0000
	Negative	10	100.0	10	90.9	11	100.0	
4th	Negative	10	100.0	11	100.0	11	100.0	-
5th	Negative	10	100.0	11	100.0	11	100.0	-

[a] Fisher's exact test.

II remained within the values found in Group III. This explains why counting LB in commercial hematological counters is difficult, as sheep LB are much smaller than platelets. As the exact counting of lamellar bodies was not possible, lamellar bodies were measured to clarify their size and the comparison between groups was observacional.

Nile blue staining

In cytological analysis using Nile blue staining, we found that Group I showed no significant difference in the observation of blue and orange-stained cells compared with Group II. We did, however, observe a statistically significant difference between Groups I and III ($p<0.05$). In the majority of amniotic fluids studied (Table 3), there were more blue-stained cells compared to orange-stained cells. Groups I, II, and III had medians of 96.1%, 90.5%, and 87% respectively.

Hematoxylin-Shorr

In contrast to the results obtained using the Nile blue test, in which a high number of blue cells were observed, the hematoxylin-Shorr method showed a higher number of orange-stained cells (Table 3). The number of these orange-stained cells, which is indicative of fetal maturity was lower in Groups II (Fig.4B) and III (cesarean + dexamethasone) (Fig.4C), as compared to the samples obtained from ewes that delivered naturally (Fig.4A). Table 3 shows a significant difference ($p<0.05$) between Group I when compared to Group III. The Groups I, II and III had medians of 79.0%, 60.0% e 54.4% of orange cells indicative of fetal maturity, respectively.

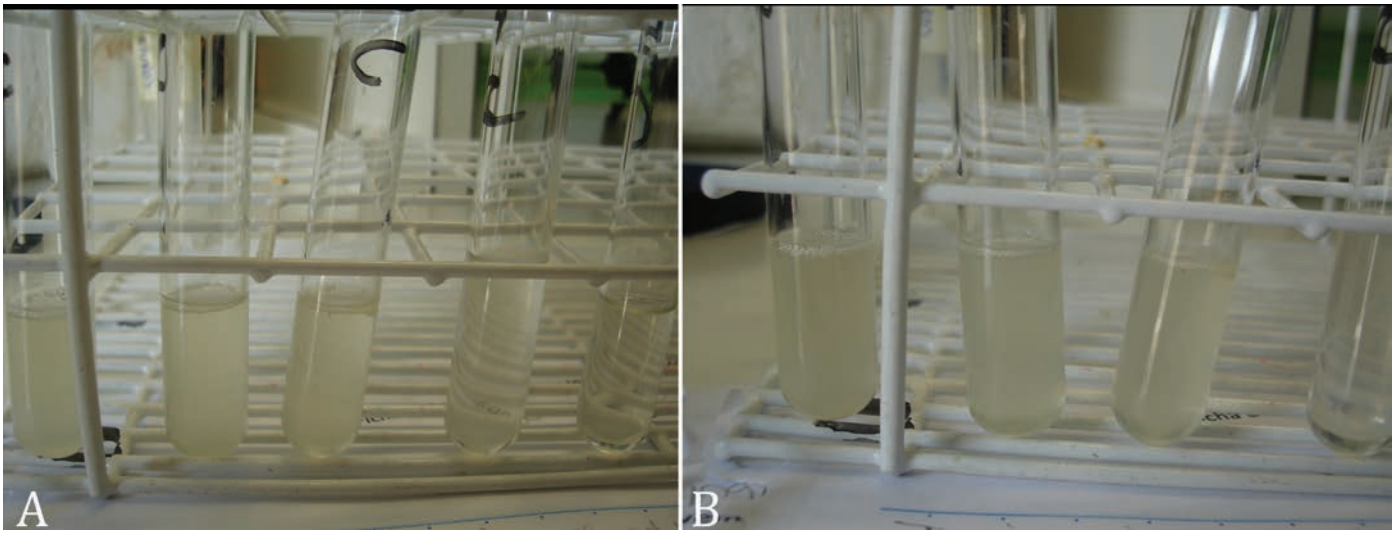


Fig.2. (**A**) Presence of bubbles observed up to the third tube for one ewe from Group II (Caesarian section). (**B**) Maturity pulmonary fetal. If there was an intact ring of bubbles at the air/liquid interface, this was considered to be a positive result; were divided into two categories: (1) negative or "immature": non-persistent bubbles in the first tube and persistent in the first and second tubes but not in the third and (2) positive or "mature": stable foam in the first 3 tubes.

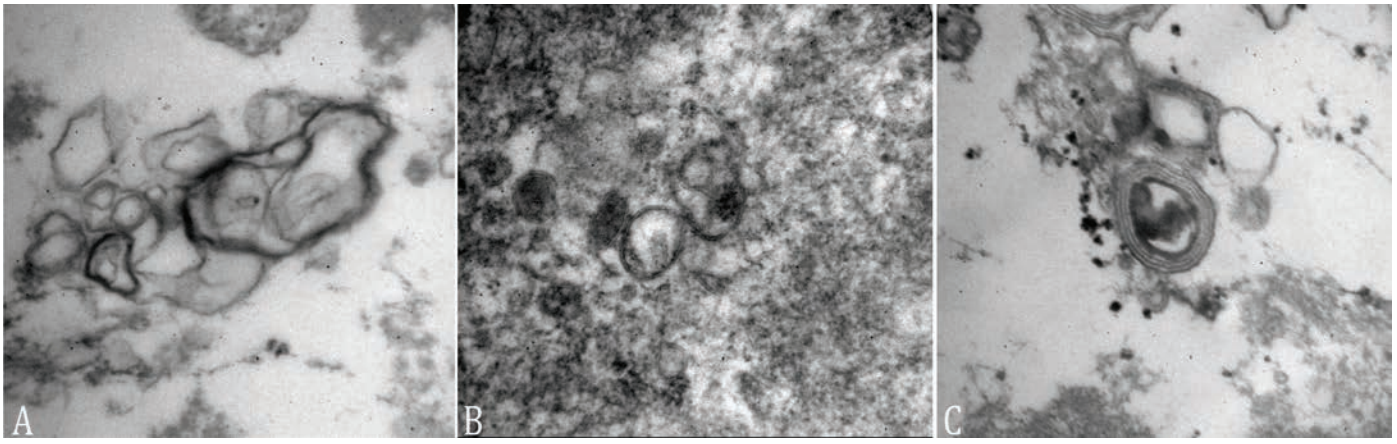


Fig.3. (**A**) Presence of lamellar bodies in amniotic fluid from sheep belonging to Group I (born naturally), in an increase of 75.000x, note that these structures are more open (unrolled), according to Steibel (2008), these structures that store surfactant unwind to take the form of tubular myelin, whose function is to reduce the surface tension of the pulmonary alveoli. (**B**) Presence of lamellar bodies in the amniotic fluid of sheep belonging to Group II (Caesarean section), in an increase of 120.000x, observe the lamellar bodies in a small amount, still coiled, showing their concentric blades. (**C**) Lamellar body belonging to Group III (cesarean section + dexamethasone), in an increase of 50.000x, showing its concentric blades, represented by a thin layer of reduced diameters, accompanied by a center in its structure.'

Table 3. Median (Md), minimum and maximum percentages of blue and orange stained cells present in the amniotic fluid of ewes from Group I (born naturally), Group II (caesarean) and Group III (caesarean + dexamethasone), using Nile blue (0.1%) and hematoxylin-Shorr

Variable	Category	Group I			Group II			Group III		
		n	Md	Min - Max	n	Md	Min - Max	n	Md	Min - Max
Nile blue staining	Blue	10	96.1 ^{A}	84.0 - 98.0	11	90.5 ^{AB}	73.0 - 96.3	11	87.0 ^{B}	80.8 - 96.9
	Orange	10	4.0 ^{A}	2.0 - 16.0	11	9.5 ^{AB}	3.7 - 27.0	11	13.0 ^{B}	3.1 - 19.3
Hematoxilin-Shorr	Blue	10	21.0^{A}	8.0 - 42.7	11	40.0 ^{AB}	19.8 - 66,7	11	45.6 ^{B}	32.0 - 64.9
	Orange	10	79.0^{A}	57.3 - 92.0	11	60.0 ^{AB}	33.3 - 80.2	11	54.4 ^{B}	35.1 - 68.0

n = Number, Md = median, Min-Max = minimum-maximum; ^{A,B,AB} Medians followed by different letters in the same row denote statistical difference by the Dunn test (p<0.05).

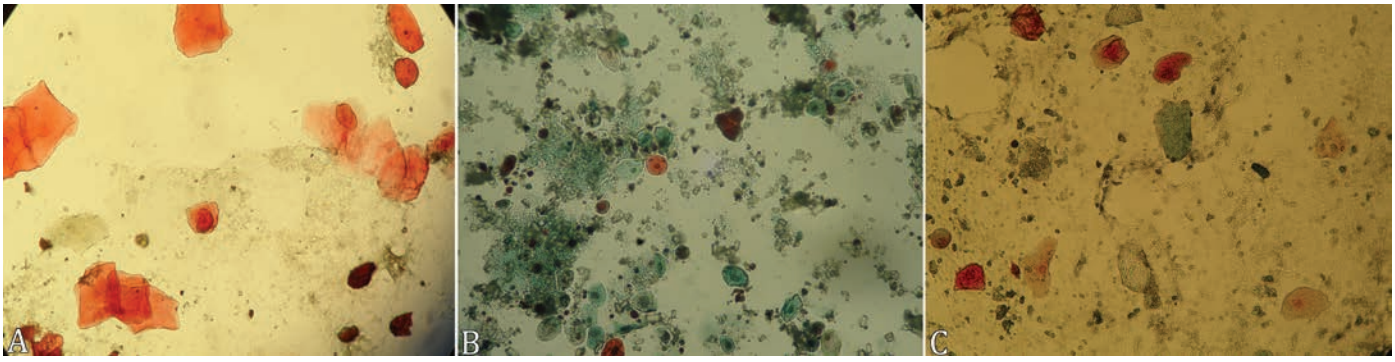


Fig.4. (**A**) Blade belonging to Group I (born naturally), showing reater presence of orangeophilic cells. In this figure the highest incidence is anucleated superficial cells. Hematoxylin-Shorr, obj.40x. (**B**) Blade belonging to Group II (Caesarean section), showing a greater amount of cyanophilic cells (blue /green) than orangeophilic cells. Hematoxylin-Shorr, obj.40x.(**C**) Blade belong to Group III (cesarean section + dexamethasone), showing the presence of orangeophilic as well as cyanophilic cells , indicating that the application of dexamethasone caused greater fetal maturity when compared to Group II that did not receive dexamethasone. Hematoxylin-Shorr, obj.40x.

DISCUSSION

The normal gestation period among sheep varies both between breeds and individual sheep. Breeds that mature early or are prolific tend to have shorter gestation periods when compared to the slower maturing wool breeds of sheep. The average length of gestation is 150 days, with a standard variation of 13 days between individuals. In this study, lambs were considered premature when born by cesarean section at 138 days gestation (Edmondson et al. 2012).

Adequate Apgar scores in the immediate neonatal period (Table 1) vary among domestic species (Carrillo et al. 1997). About the results of Adequate Apgar scores in the immediate neonatal period, While the median score of Group III lambs was not significantly higher than that in Group II, there was a slight increase in the Apgar score of Group I at birth (T0). Presumably, this was due to the administration of dexamethasone in these ewes 36 hours prior to the caesarean section being conducted. In a study on canine neonates, a positive correlation between Apgar scores and the formation of septa and subsaccules in the lungs was found. This clinical improvement may be due to more efficient gas exchange from structural changes in the lung parenchyma due to administration of antenatal glucocorticoids (Regazzi 2011).

Regarding the mortality rate, despite not differing statistically, the percentage of deaths was higher in animals born in Group II than in Group III, assuming that lambs born in both groups were premature (born at 138 days). It is believed that greater survival in Group III probably occurred due to the administration of dexamethasone in the sheep 36 hours before farrowing. It is known that the administration of corticosteroids has positive effects on fetal lung maturation, decreasing the risk of premature births, respiratory distress syndrome (RDS), and other gestational changes (Areia et al. 2018).

Avila et al. (2014) showed that the administration of glucocorticoids, such as dexamethasone, efficiently decreased the mortality rate in premature lambs born at 138 days of life, as it improved the clinical condition and survival of these lambs.

Radiography is a cheap and effective method for visualizing lung changes. It is a complementary examination that helps in the diagnosis of the patient.

The ultrasound of the lung, although it is a relatively new technique, imaging diagnosis using ultrasound of the lung is valuable in predicting newborn respiratory prognosis. Research conducted on humans provides evidence that the analyses of lung ultrasound images can help predict neonatal respiratory morbidity (Bonet-Carne et al. 2015).

The Clements' test showed if a test result is positive, the fetal lung is considered mature (Crockett 1988); however, Clements' test has a high rate of false negative results. Therefore, it is recommended that negative Clements' test results should be reviewed with caution and, where possible, other methods of assessing fetal lung maturity, such as cytological evaluation by hematoxylin-Shorr staining, should be used to confirm the parameters of neonatal viability. A previous study conducted reported that all AF samples obtained from ewes showed little reaction to the Clements' test and were, therefore, considered negative (Souza et al. 2000). This demonstrates the lack of accuracy of this technique when it is applied to ewes and/or there is an absence of surfactant at the corresponding gestational stages in sheep.

In humans, the size of the LB (0.2-2μm) is compatible with the size of a platelet (1-3μm). Therefore, blood counters commonly used to perform complete blood counts can quantify LB. The number corresponding to the platelet count is considered the total quantity of LB. However, due to several unsatisfactory attempts to undertake LB counts using standard hematological counters as well as the lack of studies in this area regarding sheep, we also used transmission electron microscopy (TEM) to evaluate LB in AF. Lamellar bodies can be easily detected in AF through using electron microscopy (Fig.3). Several studies have shown that LB increases over the course of pregnancy and its presence in AF correlates well with other indicators of fetal lung maturity (Lee et al. 1996, DeRoche et al 2002, Castagnetti et al. 2007, Jörger et al. 2017).

Using the Nile blue technique, the cells from amniotic fluid were classified as cyanophilic cells (blue cells) with characteristics of fetal immaturity, as well as the presence of orange cells (orange-colored cells) where their presence is an indicative of fetal maturity. In this study it was observed a larger amount of cyanophilic cells (blue) when compared to orangeophilic cells (orange), with medians of 96.1% in Group I, 90,5% in Group II and 87 % (Group III). Such, these results could be explained by the fact that animals from Groups II and III born by performing elective surgeries at 138 days of age, which would indicate a larger off cells indicative of fetal immaturity. However, when the normal delivery group (Group I) was similar results of those of premature animals, with few orange cells and many blue cells. Therefore, we conclude that in this method most cells stained blue, making this technique unsatisfactory in sheep species. So it was proposed in this research the cytology of Hematoxylin- Shorr described by Moya (2005), for evaluation and comparison results obtained between both techniques. We can see that in Groups II and III, while orangeophilic cells decreased when compared to Group I, cyanophilic cells increased in these two groups, since cyanophilic cells are indicative of fetal immaturity, that is, it becomes the expected result, since these lambs were born premature in Groups II and III. Based on our findings, we believe that cytological study of AF by hematoxylin-Shorr staining should be done for assessing fetal maturity as it is comparatively low-cost, reliable, and easy to perform.

CONCLUSIONS

The assessment of pulmonary and fetal maturity is important in veterinary neonatology so as to predict when a high-risk patient will give birth as well as to enable faster administration of therapy to newborns requiring treatment, helping to increase their survival rates.

Clements' test is inconsistent and unreliable when negative results are obtained, although it is reliable when positive results are obtained and can be used as a strong indicator of lung maturation in newborns. The use of transmission electron microscopy reveals that lamellar bodies in amniotic fluid of sheep ranged from 0.019 to 0.590μm. Therefore, platelet channel of hematology analyzers is not an accurate method to obtain results regarding the amount of LB in sheep. Nile blue staining (0.1%) is not satisfactory in this species for predicting fetal maturity. However, hematoxylin-Shorr staining is effective and can accurately predict the degree of maturity of fetal lambs, especially when it is applied together with other assessment techniques used for evaluating fetal and lung maturity. Radiographic findings play an important role in assessing pulmonary maturity and physiologic condition of premature lambs.

Acknowledgments.- The authors would like to thank the staff of the Department of Electron Microscopy, "Faculdade de Ciências Agrárias e Veterinárias", Unesp, Jaboticabal/SP, the "Departamento de Biologia Celular e Molecular e Bioagentes Patogênicos" (Biocel), "Faculdade de Medicina", USP, RibeirãoPreto/SP, and the "Fundação de Amparo à Pesquisa do Estado de São Paulo" (FAPESP) for granting a master's scholarship (2011/14933-3) and financial support (2011/20219-1).

Declaration of conflict of interest.- The authors declare no conflicts of interest.

REFERENCES

Agrons G.A, Courtney S.E., Stocker T. & Markowitz I. 2005. Lung disease in premature neonates: radiologic-pathologic correlation 1. Radiographics 25(4):1047-1073. <https://dx.doi.org/10.1148/rg.254055019>

Areia A.L., Almeida M.F., Braga A.J.C., Pereira N.B., Macedo C.V. & Nogueira-Silva C. 2018. Corticoterapia para maturação pulmonar fetal. Acta Obst. Ginecol. Port. 12(4):311-313.

Avila G.L., Bovino F., Camargo D.G., Souza N.C., Santos G.G.F., Deschk M., Mendes L.C.N. & Feitosa F.L.F. 2014. Aplicação materna de glicocorticóide nos parâmetros vitais de cordeiros nascidos a termo e prematuros. Ciência Rural 44(6):1106-1112. <https://dx.doi.org/10.1590/S0103-84782014000600025>

Bonet-Carne E., Palacio M., Cobo T., Perez-Moreno A., Lopez M., Piraquive J.P., Ramirez J.C., Botet F., Marques F. & Gratacos E. 2015. Quantitative ultrasound texture analysis of fetal lungs to predict neonatal respiratory morbidity. Ultrasound Obstet. Gynecol. 45(4):427-433. <https://dx.doi.org/10.1002/uog.13441> <PMid:24919442>

Born E. 1981. Untersuchungen über den einfluss der schnittentbindung auf die vitalität neugeborener kälber. Doctoral Dissertation, Tierärztliche Hochschule, Hannover. 47p.

Bovino F. 2015. Abordagem clínica de cordeiros prematuros: avaliação de protocolos terapêuticos emergenciais para estimulação da atividade respiratória. Doctoral Dissertation, Faculdade de Medicina Veterinária de Araçatuba, Universidade Estadual Paulista. 93p.

Brosens I. & Gordon H. 1966. The estimation of maturity by cytological examination of the liquor amnii. J. Obstet. Gynecol. 73(1):88-90. <https://dx.doi.org/10.1111/j.1471-0528.1966.tb05124.x> <PMid:4159951>

Carrillo J.B., García E.A., Lozano C.G., Galache P.V., Lozano de la J.G. & González H.L. 1997. Cuantificación de cuerpos lamelares en líquido amniótico: método de valoración de madurez pulmonar fetal. Ginecol. Obstet. Mex. 65:202-206.

Castagnetti C., Mariella J., Serrazanetti G.P., Grandis A., Merlo B., Fabbri M. & Mari G. 2007. Evaluation of lung maturity by amniotic fluid analysis in equine neonate. Theriogenology 67(9):1455-1462. <https://dx.doi.org/10.1016/j.theriogenology.2007.02.013> <PMid:17448529>

Cheong J.L.Y., Lee K.J., Boland R.A., Spittle A., Opie G.F., Burnett A.C., Hickey L.M., Roberts G., Anderson P.J. & Doyle L.W. 2018. Changes in long-term prognosis with increasing postnatal survival and the occurrence of postnatal morbidities in extremely preterm infants offered intensive care: a prospective observational study. Lancet Child Adolesc. Health 2(12):872-879. <https://dx.doi.org/10.1016/s2352-4642(18)30287-6>

Clements J.A., Platzker A.C.G., Tierney D.F., Hobel C.J., Creasy R.K., Margolis A.J., Thibeault D.W., Tooley W.H. & Willian O.H. 1972. Assessment of the risk of respiratory-distress syndrome by a rapid test for surfactant in amniotic fluid. N. Engl. J. Med. 286(20):1077-1082. <https://dx.doi.org/10.1056/NEJM197205182862004> <PMid:5067186>

Crockett H.H. 1988. A comparison of laboratory tests for assessing fetal maturity. Master's Thesis, University of Utah, Salt Lake City, UT.

DeRoche M.E., Ingardia C.J., Guerette P.J., Wu A.H., LaSala C.A. & Mandavilli S.R. 2002. The use of lamellar body counts to predict fetal lung maturity in pregnancies complicated by diabetes mellitus. Am. J. Obstet. Gynecol. 187(4):908-912. <https://dx.doi.org/10.1067/mob.2002.127122> <PMid:12388975>

Dubin S.B. 1998. Assessment of fetal lung maturity: practice parameter. Am. J. Clin. Pathol. 110(6):723-732. <https://dx.doi.org/10.1093/ajcp/110.6.723> <PMid:9844584>

Edmondson M.A., Roberts J.F., Baird A.N., Bychawski S. & Pugh D.G. 2012. Theriogenology of sheep and goats. Sheep Goat Med. 150-230. <https://dx.doi.org/10.1016/b978-1-4377-2353-10008-3>

Fakhoury G., Daikoku N.H., Benser J. & Dubin N.H. 1994. Lamellar body concentrations and the prediction of fetal pulmonary maturity. Am. J. Obstet. Gynecol. 170(1):72-76. <https://dx.doi.org/10.1016/S0002-9378(13)70282-5>

Feitosa F.L.F., Ávila L.G., Bovino F., Santos G.G.F., Mendes L.C.N., Peiró J.R. & Perri S.H.V. 2017. Efeitos da corticoterapia maternal nos valores hemogasométricos de cordeiros nascidos a termo e prematuros. Pesq. Vet. Bras. 37(5):521-525. <https://dx.doi.org/10.1590/s0100-736x2017000500016>

Feitosa F.L.F., Braga G.I., Mendes L.C.N., Alcindo J.F., Souza N.C., Bovino F., Trein T.A., Trevizan J.T. & Baptista R.S. 2020. Avaliação da maturidade pulmonar de cabritos nascidos a termo e prematuros. Arq. Bras. Med. Vet. Zootec. 72(4):1313-1320. <https://dx.doi.org/10.1590/1678-4162-11522>

Ghartey K., Coletta J., Lizarraga L., Murphy E., Ananth C.V. & Bannerman C.G. 2012. Neonatal respiratory morbidity in the early term delivery. Am. J. Obstet. Gynecol. 207(4):292.e1-292.e4. <https://dx.doi.org/10.1016/j.ajog.2012.07.022> <PMid:22902075>

Harrison S.M. & Goldenberg R.L. 2016. Global burden of prematurity. Seminars Fetal Neonatal Med. 21(2):74-79. <https://dx.doi.org/10.1016/j.siny.2015.12.007> <PMid:26740166>

Jainudeen M.R. & Hafez E.S.E. 2004. Gestação, fisiologia pré-natal e parto, p.141-155. In: Hafez B. & Hafez E.S.E. (Eds), Reprodução Animal. 7ª ed. Manole, Barueri.

Jörger A., Acevedo C., Busley D., Ganter M., Schmiedl A. & Ziehank E.H. 2017. Stereological and biophysical characteristics of the ovine surfactant system and its changes caused by ovine pulmonary adenocarcinoma. Res. Vet. Sci. 114:332-340. <https://dx.doi.org/10.1016/j.rvsc.2017.06.008> <PMid:28651195>

Kjeldsberg C. & Knight J. 1998. Body fluids: laboratory examination of amniotic, cerebrospinal, serous and synovial fluids. 3rd ed. American Society of Clinical Pathologists, Chicago.

Lee I.S., Cho Y.K., Kim A., Min W.K., Kim K.S. & Mok J.E. 1996. Lamellar body count in amniotic fluid as a rapid screening test for fetal lung maturity. J Perinatol. 16(Pt 1):176-180. <PMid:8817425>

Lewis P.S., Lauria M.R., Dzieczkowski J., Utter G.O. & Dombrowski M.P. 1999. Amniotic fluid lamellar body count: Cost-effective screening for fetal lung maturity. Obstet. Gynecol. 93(3):387-391. <https://dx.doi.org/10.1016/s0029-7844(98)00416-5> <PMid:10074985>

Luna L.G. 1968. Manual of histologic staining methods of the Armed Forces Institute of Pathology. 3rd ed. McGraw-Hill Book Company, New York. 258p.

Miron P.M. 2012. Preparation, culture and analysis of amniotic fluid samples. Curr. Protocols Humans Genet. 74(1):e62. <https://dx.doi.org/10.1002/0471142905.hg0804s74> <PMid:22786614>

Miura H., Yamazaki T., Kikichi M. & Sakaguchi M. 2019. Plasma steroid hormone concentrations and their relationships in Suffolk ewes during gestation and parturition. Anim. Sci. J. 90(11):1426-1431. <https://dx.doi.org/10.1111/asj.13286> <PMid:31486265>

Morrison J.C. 1974. Nile blue staining of cells in amniotic fluid for fetal maturity. Part I: a reppraisal. Obstet. Gynecol. 44(3):355-361. <PMid:4137082>

Moya C.F. 2005. Tipificação citológica do líquido amniótico de bezerros oriundos de produção In Vitro, transferência de embrião e inseminação artificial no momento do parto. Master's Thesis, Faculdade de Medicina Veterinária e Zootecnia, Universidade Estadual Paulista, Botucatu, SP. 64p.

Patel R.M. 2016. Short-and-long-term outcomes for extremely preterm infants. Am. J. Perinatol. 33(3):318-328. <https://dx.doi.org/10.1055/s-0035-1571202> <PMid:26799967>

Radostits O.M., Gay C.C., Hinchcliff K.W. & Constable P.D. 2007. Veterinary Medicine: a textbook of the diseases of cattle, horses, sheep, pigs and goats. 10th ed. Elsevier Saunders, Philadelphia. 2156p.

Regazzi F.M. 2011. Modificações pulmonares morfométricas e funcionais de neonatos da espécie canina em resposta à corticoterapia pré-natal. Master's Thesis, Faculdade de Medicina Veterinária e Zootecnia, Universidade Estadual Paulista, Botucatu, SP. 106p.

Rodrigues J.A., Veiga G.A.L., Silva L.C., Lúcio C.F. & Vannuchi C.I. 2007. Avaliação por escore apgar, temperatura e hemogasometria arterial em neonatos da espécie ovina. Annals of Congresso Brasileiro de Reprodução Animal, Curitiba, p.23.

Rosborg J. 1970. Estimation of fetal maturity by amniotic fluid cytology. Acta Obstet. Gynecol. Scand. 49(3):285-287. <https://dx.doi.org/10.3109/00016347009157252> <PMid:4103880>

Souza C., Prestes N.C. & Lopes R.S. 2000. Determinação da maturidade fetal através da análise de parâmetros físicos e bioquímicos do fluido amniótico de ovinos (*Ovis aries*), colhidos em abatedouro. Annals of XXVII Congresso Brasileiro de Medicina Veterinária. Águas de Lindoia, SP, p.29a.

Tibary A. & Van Metre D. 2004. Surgery of the sheep and goat reproductive system and urinary tract, p.527-547. In: Fubini S.L. & Ducharme N.G (Eds), Farm Animal Surgery. W.B. Saunders, St. Louis.

PESQUISA VETERINÁRIA BRASILEIRA
Brazilian Journal of Veterinary Research
ISSN 0100-736X (Print)
ISSN 1678-5150 (Online)

Pesq. Vet. Bras. 40(12):1048-1053, December 2020
DOI: 10.1590/1678-5150-PVB-6716

Original Article
Animal Morphophysiology
BY-NC

Influence of seasonality on the physiological and seminal parameters of buffaloes in the western region of Pará[1]

Sâmia R.S. Castro[2]*, Leticia S. Rebelo[3], Onildo S. Fernandes Junior[3], Alessandra S. Belo-Reis[4], Kedson A.L. Neves[2], Welligton C. Silva[5], Adriana C. Morini[2] and William G. Vale[2]

ABSTRACT.- Castro S.R.S., Rebelo L.S., Fernandes Junior O.S., Belo-Reis A.S., Neves K.A.L., Silva W.C. & Vale W.G. 2020. **Influence of seasonality on the physiological and seminal parameters of buffaloes in the western region of Pará.** *Pesquisa Veterinária Brasileira 40(12):1048-1053.* Departamento de Medicina Veterinária, Universidade da Amazônia, Rua Rosa Vermelha 335, Aeroporto Velho, Santarém, PA 68010-200, Brazil. E-mail: samiarubielle@hotmail.com

Awareness of the physiological changes that occur when animals are subjected to climatic changes that are considered stressful is essential to maintain animal welfare and to be able to exploit their reproductive potential efficiently and rationally. The present study was carried out to evaluate climatic variables' influence on physiological parameters, and Murrah buffalo ejaculates reared in a humid tropical climate in the Amazon. The immediate analyzes pertinent to the physical and morphological characteristics of the ejaculates were carried out and corresponded in the rainy season (RS) volume of 3.4±2.0mL; the mass activity of 4.4±0.5; motility of 80.4±5.6%; vigor of 4.4±0.4; concentration of 657,300±237,865.1 x 106sptz/mL; major defects of 9.0±2.6%; minor defects of 11.2±3.9%; total defects 20.2±5.3% and sperm plasma membrane integrity (SPMI) 84.8±5.6%, whereas in the non-rainy season (nRS), the results were 4.0±2.1mL; the mass activity of 3.0±1.0; motility of 56.2±13.4%; vigor of 3.0±1.0; concentration of 586,000±291,925.9 x 106sptz/mL; major defects of 20.8±9.9%; minor defects of 27.5±6.3%; total defects 48.3±9.3% and SPMI of 57.9±12.4%. Furthermore, a statistical difference (P<0.05) was observed for the parameters mass activity, motility, vigor, major defects, minor defects, total defects, and sperm plasma membrane integrity between both periods. The data on heart frequency, superficial temperature (head, back, groin, and scrotal pouch) showed a statistical difference between both periods (P<0.05). To conclude is necessary specific management in the non-rainy season that thermal stress is not a determining factor in reducing the reproductive quality of buffaloes; it is necessary to use means to improve animal welfare; one alternative is to use baths regularly for these animals or provide constant access to areas of rivers or lakes, as well as shading, preventing the buffaloes from being directly exposed to the unfavorable thermal environment.

INDEX TERMS: Seasonality, physiology, semen, buffaloes, Pará, Amazon, *Bubalus bubalis*, environment, reproductive parameters.

[1] Received on August 15, 2020.
Accepted for publication on September 10, 2020.

[2] Laboratório de Biotecnologia Animal, Universidade Federal do Oeste do Pará (UFOPA), Rua Vera Paz s/n, Tapajós, Bairro Salé, Santarém, PA 68040-255. Brazil. *Corresponding author: samiarubielle@hotmail.com

[3] Centro Acadêmico de Medicina Veterinária, Universidade da Amazônia (UNAMA), Rua Rosa Vermelha 335, Aeroporto Velho, Santarém, PA 68010-200, Brazil. E-mail: leticiarebelo@hotmail.com, jr.asd@hotmail.com

[4] Professor, Curso de Medicina Veterinária, Universidade da Amazônia (UNAMA), Rua Rosa Vermelha 335, Aeroporto Velho, Santarém, PA 68010-200, Brazil. E-mail: alessandra.belo.reis@gmail.com

[5] Master's student in Animal Health and Production, Universidade Federal Rural da Amazônia (UFRA), Av. Presidente Tancredo Neves 2501, Terra Firme, Belém, PA 66077-830, Brazil. E-mail: welligton.medvet@gmail.com

RESUMO.- [**Influência da sazonalidade nos parâmetros fisiológicos e seminais de búfalos da região oeste do Pará.**] O conhecimento das alterações fisiológicas que ocorrem quando os animais são submetidos a alterações climatológicas consideradas estressantes é fundamental para manter o bem-estar animal, e poder explorar o seu potencial reprodutivo de forma eficiente e racional. O presente estudo foi realizado com o objetivo de avaliar a influência de variáveis climáticas sobre parâmetros fisiológicos e de ejaculados de búfalos, da raça Murrah, criados em clima tropical úmido da Amazônia. As análises imediatas pertinentes às características físicas e morfológicas dos ejaculados

foram realizadas e corresponderam no período chuvoso (PCh) o volume de 3,4±2,0mL, turbilhonamento de 4,4±0,5; motilidade de 80,4±5,6%; vigor de 4,4±0,4; concentração de 657.300±237.865,1 x 10^6sptz/mL; defeitos maiores de 9,0±2,6%; defeitos menores de 11,2±3,9%; defeitos totais de 20,2±5,3% e integridade da membrana plasmática (IMP) de 84,8±5,6%, enquanto que no período não chuvoso (PnCh), os resultados foram de 4,0±2,1mL; turbilhonamento de 3,0±1,0; motilidade de 56,2±13,4%; vigor de 3,0±1,0; concentração de 586.000±291.925,9 x 10^6sptz/mL; defeitos maiores de 20,8±9,9%; defeitos menores de 27,5±6,3%; defeitos totais de 48,3±9,3% e IMP de 57,9±12,4%. Observou-se diferença estatística (P<0,05) para os parâmetros movimento de massa, motilidade, vigor, defeitos maiores, defeitos menores, defeitos totais e integridade da membrana plasmática entre os dois períodos. Dados de frequência cardíaca, temperatura superficial (cabeça, dorso, virilha e bolsa escrotal) diferiram estatisticamente entre os períodos (P<0,05). Conclui-se que se faz necessário usar de um manejo específico no período não chuvoso para que o estresse térmico não seja um fator determinante na redução da qualidade reprodutiva dos búfalos, para isto se faz necessário utilizar de meios para melhorar o bem-estar animal, sendo uma das alternativas fazer uso de banhos regularmente para estes animais, ou disponibilizar acesso constante destes a áreas de rios ou lagos, assim como sombreamentos, evitando que os búfalos fiquem expostos diretamente ao ambiente térmico desfavorável.

TERMOS DE INDEXAÇÃO: Sazonalidade, fisiologia, sêmen, búfalos, Pará Amazônia, *Bubalus bubalis*, meio-ambiente, parâmetros reprodutivos.

INTRODUCTION

In Brazil, four breeds of buffalo are recognized: Carabao, Jafarabadi, Mediterranean, and Murrah. According to data from the Ministério da Agricultura (2011), the buffalo herd in Brazil is estimated at around 1.17 million head, with the northern region having the highest concentration with 720 thousand heads, with 39% of the national herd found in the state of Pará, followed by the northeast and southeast regions, with 135 and 104 thousand heads, respectively (Vilela 2013).

Despite being considered rustic animals and easy to adapt to, compared to cattle, buffaloes are more sensitive to direct solar radiation and environments with high temperatures due to their specific morphological characteristics. Among them, such as the high concentration of melanin in the skin and hair that provides low reflectivity, which helps to have a high absorption of heat when exposed directly under the sun, low quantity and efficiency of sweat glands that hinders heat loss through sweating; low hair density and the epidermis layer of thick skin, which reduces heat loss through conduction and irradiation (Joshi et al. 1968, Garcia 2006, Ablas et al. 2007, Barbosa et al. 2007).

In regions of tropics and subtropics, where the climate is hot and humid, buffalo are adapted to live, and this is due to their semi-aquatic nature in which it seeks to keep the body submerged in water to reduce the effect of heat. This occurs mainly when the temperature and humidity index reaches the value of 85 temperature and humidity index (THI), which is common in tropical regions, and when the discomfort of buffaloes is most significant (Ablas et al. 2007). Although the West of Pará has a tropical climate, said to be adaptable by buffaloes, the temperatures reached are higher than the acceptable temperatures. In these regions, the high environmental temperatures are constant (Garcia 2013).

The knowledge of the physiological changes that occur when animals are subjected to climatic changes considered stressful is essential to maintain animal welfare and to be able to exploit their reproductive potential efficiently and rationally. Thus, handling is a determining factor for these animals to reproduce. In addition to the use of biotechnologies, they need an environment closer to their natural environment, with the presence of shading and water, so that their physiological changes resulting from thermal stress do not become determining factors for a decrease in their reproductive quality (Vale 2002, Almeida et al. 2015, Castro et al. 2017).

The buffaloes have gained prominence in meat and milk; with that, the search for biotechnology techniques, such as artificial insemination (AI) and cryopreservation, has become as crucial for buffaloes as they are for cattle. Along with cryopreservation techniques, there was a concern to certify that the semen used in this process was of quality. Furthermore, only morphological aspects of the semen were taken into account, forgetting to analyze the possible influences that external factors such as time and time of harvest that could influence the reproductive performance of these animals (Sally et al. 2015).

Based on this information, this study's objective was to analyze the physiological, behavioral, and seminal changes of buffaloes in the rainy and non-rainy periods in the municipality of Santarém, Pará state, Amazônia.

MATERIALS AND METHODS

All analyses followed the Ethics Committee on the Use of Animals at the "Universidade Federal do Oeste do Pará", filed under number No. 03003-2017. For the present study's execution, seminal processing and laboratory analyses were carried out at the Animal Biotechnology Laboratory of the "Universidade Federal do Oeste do Pará", Santarém, Pará, Amazonia, Brazil and located at 2°25'39.1" S 54°41'48.6" W and altitude of 15 meters. The local climate is of the Af type, characterized by being a rainy tropical climate, being classified as Am3 according to the Köppen system (Köppen & Geiger 1928). Annual rainfall ranges from 2,000 to 2,500mm, with total rainfall below 60mm during the month with less rain. The maximum air temperature ranges from 30.5 to 32.0°C, and the minimum varies between 21.0 and 22.5°C (Köppen & Geiger 1928). The rainy period is from March to June and not rainy from July to November in the study region. In Pará, Vale (1988) observed that the difference in light is small throughout the year. The buffalo behaves as continuous polystyrene; that is, the behavior of seasonal reproductive activity is less pronounced.

As semen donors, five buffalo bulls were selected from a batch of 12, pre-evaluated by andrological examination (the criterion used was concerning the sperm quality presented). The donors were between 2 and 4 years old and had an average weight of 709.5±35.5kg. They were kept in a semi-confinement regime, with access to the Canarana forage (*Echinochloa polystachia*), corn, soy and sorghum ration, water and mineral salt ad libitum, and stalls with natural shade for resting. Before this study, the animals were dewormed and vaccinated.

Semen was obtained routinely from all bulls using the artificial vagina harvesting method. According to Sansone et al. (2000), Vale (2011), buffaloes can be considered easily adaptable animals and be able to collect semen using this method. Ten semen collections

were performed per animal each period, thus totaling 50 samples for the rainy period and 50 for the non-rainy period. A minimum period of two days of rest was maintained for each new harvest of the animal. Immediately after collection, the ejaculate was evaluated by an experienced operator for appearance (milky), color (white, yellowish-white, white-brown), volume (mL, graduated collection tube), sperm motility, mass movement or whirlwind, vigor, following the norms established by the CBRA (2013). The concentration was assessed through the Neubauer chamber with a 1: 200 dilution in formalin saline as described by Vale (2011), sperm morphology by wet drop technique with phase-contrast microscopy evaluation, the integrity of the sperm plasma membrane was assessed by the hyposmotic test (HOST), as Rasul et al. (2000) and Barros et al. (2007).

In animals, physiological parameters such as heart rate (HR), respiratory rate (RR), rectal temperature (RT), superficial temperature (ST - subdivided into areas of the head, back, groin and testicles) were measured. For HR measurements (bpm), a stethoscope was used; the respiratory rate was determined by observing the chest-abdominal area and counting the breathing movements for one minute (mpm); to determine the rectal temperature (°C), a digital thermometer was used, and the body surface temperature (°C) was measured with an infrared digital thermometer with a laser sight (-50°C to 380°C, Benetech®, model: GM300) in the head, back (hip), groin and testicles.

A mini weather station (WS-GP1 Weather Station, AT Delta-Devices Ltda®) was installed at the experiment site to measure room temperature (°C), percentage of relative humidity (%), rainfall (mm), solar radiation (w/m2), and wind speed (m.s-1). The mini station was located near the bays. Due to the different average maximum levels of ambient temperature, rain, and humidity, this study, according to the literature, divided the year into two seasons, according to the harvests carried out: rainy season (RS), from March to June; and non-rainy season (nRS), from August to November.

Meteorological data were evaluated using the general linear model (GLM). In contrast, semen data was examined using the repeated measurement instruction of the MIXED procedure (Proc MIXED) from the Statistical Analysis Systems software (SAS Institute Inc., Cary/NC, USA). The model included the fixed effects of the bull's age, ejaculate (harvest week), season, average maximum temperature, humidity, and the interaction between them. The sperm morphology and plasma membrane integrity data of the ejaculates were transformed into a square root before analysis. Pearson's correlation coefficients were used to analyze the association between semen parameters and age, season, and meteorological data. The generalized estimation equation (GEE) test was used to determine the differences between the individual semen quality variables (categorical). The differences were considered statistically significant at $P<0.05$. The Shapiro-Wilk normality test was applied to test whether the variables under study assumed normal distribution or not, and the data not being standard, the Kruskal-Wallis.

RESULTS

Meteorological data obtained on environmental conditions in different seasons such as temperature, relative humidity, precipitation, and solar radiation ($P<0.05$) were different when comparing the rainy season (RS) and non-rainy season (nRS), while wind speed did not show a significant difference ($P>0.05$) between periods (Table 1). The average physical and morphological characteristics of all buffalo ejaculates described by rainy and non-rainy periods are contained in Table 2.

The immediate analyzes pertinent to the physical and morphological characteristics of the ejaculates were carried out and the volume of 3.4±2.0mL corresponded to the RS, swirling (mass movement) of 4.4±0.5; motility of 80.4±5.6%; a vigor of 4.4±0.4; concentration of 657,300±237,865.1 x 106sptz/mL; major defects 9.0±2.6%; defects smaller than 11.2±3.9%; total defects of 20.2±5.3% and plasma membrane integrity (PMI) of 84.8±5.6%, whereas in nRS, the results were 4.0±2.1mL; a mass movement of 3.0±1.0; motility of 56.2±13.4%; a vigor

Table 1. Variables found in the different seasons based on data obtained by the Meteorological Station WS-GP1 (AT Delta-DevicesLtda, Cambridge, UK) in Santarém, Pará, from March to November 2016 (mean±SD)

Season	Temperature (°C)	Relative humidity (%)	Rainfall (mm)	Solar radiation (W/m^2)	Wind speed (m.s-1)
Rainy season*	28.1±1.8[a]	89.4±10.2[a]	2,418±309[a]	232.7±301.3[a]	1.6±0.7[a]
Non-rainy season**	29.4±1.9[b]	79.0±10.6[b]	381±95[b]	260.6±314.0[b]	2.0±1.0[a]

* Rainy season = March to June, ** non-rainy season = August to November 2016; [a,b] Means with different superscript letters within a column were significantly different between seasons ($P<0.05$).

Table 2. Average physical and morphological characteristics of buffalo ejaculates, in the rainy and non-rainy seasons (n=100), Santarém, Pará, 2016

Seminal parameters	Rainy season*	Non-rainy season**
Volume (ml)	3.4±2.0[a]	4.0±2.1[a]
Whirlwind (0-5)	4.4±0.5[a]	3.0±1.0[b]
Motility (%)	80.4±5.6[a]	56.2±13.4[b]
Vigor(0-5)	4.4±0.4[a]	3.0±1.0[b]
Concentration (x10^6sptz/mL)	657,300±237,865.1[a]	586,000±291,925.9[a]
Major defects (%)	9.0±2.6[a]	20.8±9.9[b]
Minor defects (%)	11.2±3.9[a]	27.5±6.3[b]
Total defects (%)	20.2±5.3[a]	48.3±9.3[b]
Plasma membrane integrity (%)	84.8±5.6[a]	57.9±12.4[b]

* Rainy season = March-June, ** non-rainy season = August to November; [a,b] Different lowercase letters on the same line indicate a significant difference between periods ($P<0.05$).

of 3.0±1.0; concentration of 586,000±291,925.9 x 106sptz/mL; defects greater than 20.8±9.9%; defects smaller than 27.5±6.3%; total defects of 48.3±9.3% and PMI of 57.9±12.4%. There was a statistical difference (P<0.05) for the parameters mass movement, motility, vigor, major defects, minor defects, total defects, and integrity of the plasma membrane between the two periods.

Data on heart rate, surface temperature (head, back, groin, and scrotum) differed statistically between periods (P<0.05). However, the RR and RT referring data did not differ between periods (P>0.05). The HR data showed a statistical difference when comparing the periods, with the highest values observed in the rainy season (54±10.9bpm). While the head region (STH) (36.2±2.4), groin (GST) (34.6±2.2), scrotum (STS) (32.3±2.0), and back region (STB) (35.1±2.1) also showed significant differences (P<0.05), however, the highest values were found in the non-rainy season (Table 3).

DISCUSSION

According to Köppen (Afi) classification, the best air conditions in the region with the hot and humid climate surpass the recommended for creating buffaloes throughout the year, demonstrating that buffaloes can experience thermal discomfort.

In the present study, we can corroborate this research because the animals presented thermal discomfort in the described region, represented by the buffalo's physiological and reproductive changes. We are still considering that the ideal climatic conditions for the growth and reproduction of buffalo are air temperature between 13 and 18ºC, associated with average relative humidity between 55 and 65%, medium heat stroke, and wind speed between 5 and 8km/h (Marai & Haeeb 2010, Garcia 2013). These ideal climatic conditions described were not observed and recorded in the region.

Buffaloes were kept in the same management conditions during the two study periods (rainy and non-rainy), offering the same amount of food (concentrated and voluminous), mineral salt, bathing twice a day, constant shading water supply *ad libitum*. Even maintaining the routine, there were changes in these animals' physiological parameters; the surface temperatures (head, back, groin, and scrotum) were increased during the non-rainy period. The rise in surface temperature may have been an attempt to thermoregulation through cutaneous evaporation of heat conducted from the central core of the body to peripheral vascularization (Almeida et al. 2015). According to Garcia (2013), in bioclimatological terms, an animal can have an elevated body temperature when it absorbs an excessive amount of heat from the medium when its capacity to dissipate body heat is reduced, the association of both factors is established. Regardless of the cause, this temperature rise's consequences are manifested in a cascade of events to try to adjust the animal organism to the imposed challenge.

The increase in the ambient temperature and other physiological variables can alter the vagal tone, intensifying the cardio accelerator and vasoconstrictor centers' activity, thus increasing the HR (Souza et al. 2007). According to Guyton & Hall (2002), this effect presumably results because the excessive heat increases the cell membrane's ionic permeability, resulting in accelerating the self-excitation process, unlike what happened in the experiment, in which the heart rate decreased during the non-rainy period. The increase in heart rate was not associated with an increase in the ambient temperature, which occurred in the non-rainy period; this can be explained by the animals'-controlled thermoregulation mechanism and the handling used, which did not cause thermal discomfort.

The increase in rectal temperature indicates that heat release mechanisms have become insufficient to maintain homeothermy (Matos 2008). In the experiment's case, there were no changes in the rectal temperature or the respiratory rate, which, according to Silva et al. (2011), is the first thermal discomfort indicator. It was deduced that it was due to the handling of the animals subjected to shading installs. They managed to control their thermoregulation only with skin evaporation maintaining thermal balance.

In males, thermal stress translates into reduced seminal quality and lower viability of sperm (Sansone et al. 2000, Vale et al. 2007, Bhakat et al. 2015). Thermal stress can lead to interruptions in reproductive processes through two general mechanisms (Castro et al. 2017); the first is the failure of the homeokinetic mechanisms present in the animal organism, capable of regulating body temperature that can compromise reproductive function. This can cause loss of libido and spermatogenesis disturbances in males (Jöchle & Lamond 1980, Henry et al. 2017, Vale 2007). Because the animal starts to spend its energy maintaining its thermoregulation point due to thermal discomfort, it ends up eating little, impairing the absorption of necessary nutrients essential for the functioning of reproductive hormones. Per second, we have the failure of homeokinetic systems to regulate reproduction, increasing body temperature around its regulated set point, which can compromise cells' function and the consequent reproduction processes. In the present study, we can observe the negative influence of thermal stress on reproductive parameters, as there was a significant difference between rainy and non-rainy periods.

In Brazil, buffaloes reared in the south-central regions tend to show reproductive seasonality (Jacomini 1989). Those reared in the north of the country show continuous polystyrene activity, reproducing throughout the year if they are well-nourished and well managed (Vale 1988). In the hot

Table 3. Average physiological parameters, before the buffalo semen collections, in the rainy and non-rainy seasons (n=100) in Santarém, Pará, 2016

Season	HR (bpm)	RR (mpm)	RT (°C)	STH (°C)	STB (°C)	GST (°C)	STS (°C)
Rainy season	54 ± 10.9[a]	22 ±6.8[a]	38.3 ± 0.8[a]	33.3 ± 2.5[a]	33.6 ± 2.1[a]	32.3 ± 2.2[a]	30.3 ± 2.0[a]
Non-rainy season	48 ± 11.8[b]	23 ± 6.7[a]	38.2 ± 0.8[a]	36.2 ± 2.4[b]	35.1 ± 2.1[b]	34.6 ± 2.2[b]	32.3 ± 2.0[b]

* Rainy season = March to June, ** non-rainy season = August to November; HR = heart rate, RR = respiratory rate, RT = rectal temperature, STH = surface temperature of the head, STB = surface temperature of the back, GST = groin surface temperature, STS = superficial temperature of the scrotum; [a,b] Means with different superscript letters within a column were significantly different between seasons (P<0.005).

and humid tropical region of the Amazon, the best time to obtain semen would be between January and June, as reported by Vale (1994). Therefore, this study aimed to identify the effects of the humid tropical climate on physiological and reproductive aspects of buffalo ejaculates that could alter these aspects between the two climatic periods existing in the Lower Amazon mesoregion (rainy and non-rainy). Relevance studies have demonstrated a significant difference in other regions, as described by Mohan & Sahni (1990), Galli et al. (1993), Sansone et al. (2000).

They claim that in temperate regions of the world, it appears that the semen is of better-quality during winter and spring than in summer and autumn, that is, in milder temperatures, giving more thermal comfort to the animal.

Thus, as reported by Di Francesco (2010), who found a significant number of normal sperm in the spring (69.6%) and also findings by Ferrer et al. (2010), who reported a lower number of normal sperm in summer (66.2%), the experiment had a significant difference between rainy and non-rainy periods.

Sperm volume data did not show significant differences, agreeing with the studies of some authors in swamp buffalo (Koonjaenak et al. 2007) and river buffalo (Heuer et al. 1987, Bahga & Khokar 1991, Khan et al. 1997, Tiwari et al. 2011, Bhakat et al. 2015).

The study carried out by Andrade (2016) showed a significant difference during the year since the data diverge with results obtained by him, which concluded he did not hear significant changes throughout the year, and this may be due to work was carried out in a humid subtropical climate. Like Mayahi et al. (2014), Bhakat et al. (2015) found differences in motility between the winter and summer periods. The present study found differences between the rainy period 80.4 ± 5.6% and the non-rainy period 56.2±13.4%.

Thus, the studies carried out in different regions, the effect of periods considered unfavorable, and the non-rainy period negatively influence the sperm quality of the animals, which makes us think about the importance of including special handling so that buffalo can be appropriately used throughout the year.

CONCLUSIONS

The buffalo reproductive parameters, such as whirling, motility, vigor, significant defects, minor defects, total defects, and plasma membrane integrity, proved to be better in the rainy than non-rainy, overcoming delays between periods.

The physiological parameters that were influenced by the non-rainy period, in comparison to the rainy season, were heart rate and surface temperature, head, back, groin, and scrotum (P<0.05).

Specific management in the non-rainy period is necessary so that the thermal stress is not a determining factor in reducing the reproductive quality of the buffaloes.

Necessary means to improve the animal welfare are important such as regular baths, or provide access to areas of rivers or lakes and shading, preventing buffaloes exposure to the unfavorable thermal environment.

Conflict of interest statement.- The authors declare that there are no conflicts of interest.

REFERENCES

Ablas D.S., Titto E.A.L., Pereira A.M.F., Titto C.G. & Leme T.M.C. 2007. Comportamento de bubalinos a pasto frente a disponibilidade de sombra e água para imersão. Ciênc. Anim. Bras. 8(2):167-175. <https://dx.doi.org/10.5216/cab.v8i2.1339>

Almeida J.C.F., Silva G.P. & Silva J.A.R. 2015. Influência climática nos mecanismos fisiológicos e comportamentais de bubalinos na região amazônica. 42º Congresso Brasileiro de Medicina Veterinária, 1º Congresso Sul-Brasileiro da Anclivepa, Curitiba, PR, p.726-730.

Andrade G.O. 2016. Avaliação da sazonalidade nas características sexuais de touros bubalinos (*Bubalus bubalis*) criados em clima subtropical úmido (19º latitude sul). Master's Thesis, Universidade Federal de Minas Gerais, Escola de Veterinária, Belo Horizonte. 68p.

Bahga C.S. & khokar B.S. 1991. Effect of different seasons on concentration of plasma luteinizing hormone and seminal quality vis-à-vis freezability of buffalo bulls (*Bubalus bubalis*). Int. J. Biometeorol. 35(4):222-224. <https://dx.doi.org/10.1007/bf01047289> <PMid:1778653>

Barbosa O.R., Zeoula L.M., Sirena R.M., Oliveira R.A., Berticelli T. & Ornellas S.A. 2007. Comparação nas respostas termoregulatórias de búfalos e bovinos em confinamento. 1. Temperatura da superfície do corpo e taxa de sudação. Anais 44º Sociedade Brasileira de Zootecnia/Pastagens, Unesp, Jaboticabal, SP. (CD-ROM)

Barros P.M.H., Nichi M., Cortada C.N.M., Carvalho N.A.T., Baruselli P.S., Barnabe R.C. & Barnabe V.H. 2007. Semen evaluation of Murrah buffalo bulls using sperm functional tests. Ital. J. Anim. Sci. 6(Supl.2):772-774. <https://dx.doi.org/10.4081/ijas.2007.s2.772>

Bhakat M., Mohanty T.K., Gupta A.K., Prasad S., Chakravarty A.K. & Khan H.M. 2015. Effect of season on semen quality parameters in Murrah buffalo bulls. Buffalo Bull. 34(1):100-112.

Castro S.R.S., Morini A.C., Silva A.S.L., Neves K.A.L., Minervino A.H.H., Meneses A.A.M. & Vale W.G. 2017. Influence of seasonality on buffalo semen. Anim. Vet. Sci. 5(3):45-51. <https://dx.doi.org/10.11648/j.avs.20170503.12>

CBRA 2013. Manual para Exame Andrológico e Avaliação de Sêmen Animal. 3ª ed. Colégio Brasileiro Reprodução Animal, Belo Horizonte. 104p.

Di Francesco S. 2010. Effect of season on reproductive performances in buffalo species (*Bubalus bubalis).* Doctoral Dissertation in Production and Health of Food of Animal Origin, Universita' Degli Studi di Napoli Federico II, Napoli. 165p.

Ferrer A., Montes I. & Alcalá Y. 2010. Influencia de la época del año en las características del semen fresco del búfalo de agua. Cien. Tecnol. Ganadera 4(1):53-58.

Galli A., Bornaghi V., Balduzzi D., Buttazzoni L. & Aleandri R. 1993. Sexual behaviour and semen quality relating to italian buffalo. Anais Proceedings 3rd World Buffalo Congress, Varna, Bulgaria, p.562-570.

Garcia A.R. 2006. Influência de fatores ambientais sobre as características reprodutivas de búfalos do rio (*Bubalus bubalis*). Revta Ciênc. Agrárias 45(supl.):1-13.

Garcia. A.R. 2013. Conforto térmico na reprodução de bubalinos criados em condições tropicais. Revta Bras. Reprod. Anim. 37(2):121-130.

Guyton A. & Hall J.E. 2002. Tratado de Fisiologia Médica. Guanabara Koogan, Rio de Janeiro. 1014p.

Henry M., Brito M.F., Neves B.P., Auler P.A., Almeida J., Andrade G.O., Becerra V.B. & Bergmann L. 2017. Peculiarities of the buffalo species for andrological evaluation - results of four years of study and weekly semen collection schedule. Anim. Reprod. 14(supl.1):1225-1223. <https://dx.doi.org/10.21451/1984-3143-AR0005>

Heuer C., Tahir M.N. & Amjad H. 1987. Effect of season on fertility of frozen buffalo semen. Anim. Reprod. Sci. 13(1):15-21. <https://dx.doi.org/10.1016/0378-4320(87)90115-1>

Jacomini J.O. 1989. Aspectos do ciclo estral e do comportamento sexual de búfalos (*Bubalus bubalis*, var. *bubalis*). Master's Thesis in Veterinary

Medicine, Escola de Veterinária, Universidade Federal de Minas Gerais, Belo Horizonte. 80p.

Jöchle W. & Lamond D.R. 1980. Control of Reproductive Functions in Domestic Animals. Martinus Nijhoff. 248p.

Joshi B.C., McDowell R.E. & Sadhu D.P. 1968. Body surface evaporation rates at low and high temperatures in Murrah buffalo. J. Dairy. Sci. 51(10):1689-1692. <https://dx.doi.org/10.3168/jds.S0022-0302(68)87253-4> <PMid:5693163>

Khan M.S., Bajwa M.A. & Tahir M. 1997. Effect of diet and season on semen characteristics in Nili-Ravi buffalo bulls. Buffalo Bull. 16(3):60-63.

Koonjaenak S., Chanatinart V., Aiumlamai S., Pinyopumimintr T. & Rodriguez-Martinez H. 2007. Seasonal variation in semen quality of swamp buffalo bulls (*Bubalus bubalis*) in Thailand. Asian. J. Androl. 9(1):92-101. <https://dx.doi.org/10.1111/j.1745-7262.2007.00230.x> <PMid:17187160>

Köppen W. & Geiger R. 1928. Klimate der Erde. Verlag Justus Perthes, Gotha. (Wall-Map 150cmx200cm)

Marai I.F.M. & Haeeb A.A.M. 2010. Buffalo's biological functions as affected by heat stress. Rev. Livest. Sci. 127(2/3):89-109. <https://dx.doi.org/10.1016/j.livsci.2009.08.001>

Matos L.B. 2008. Conforto térmico e eficiência da inseminação artificial em tempo fixo em búfalas leiteiras mantidas em sistemas silvipastoris na Amazônia Oriental. Master's Thesis in Animal Science, Universidade Federal do Pará. Belém. 81p.

Mayahi S., Mamouei M., Tabatabaei S. & Mirzadeh K. 2014. Reproductive characteristics and thyroidal function in relation with season in Khuzestan buffalo (*Bubalus bubalis*) bulls. Vet. Res. Forum 5(3):201–205.

Ministério da Agricultura 2011. Dados de rebanho bovinos e bubalinos do Brasil. Avaiable at <http://www.agricultura.gov.br/arq_editor/file/Dados%20de%20rebanho%20bovino%20e%20bubalino%20do%20Brasil_2011.pdf> Accessed on Feb. 3, 2017.

Mohan G. & Sahni K.L. 1990. Efficiency of semen production in buffalo bulls, p.14-16. In: Acharya R.M., Lokeshwar R.R. & Kumar S. (Eds), Recent Advances in Buffalo Research. Vol.3.

Rasul Z., Anzar M., Jalali S. & Ahmad N. 2000. Effect of buffering systems on post-thaw motion characteristics, plasma membrane integrity, and acrosome morphology of buffalo spermatozoa. Anim. Reprod. Sci. 59(1/2):31-41. <https://dx.doi.org/10.1016/s0378-4320(00)00070-1> <PMid:10804274>

Sally S.A., Aida I.M., Amany A.T. & Mohamed M.AB.D.E. 2015. Effect of seasonal variations on semen quality and fertility of Egyptian water buffalo (*Bubalus Bubalis*) Bulls. Res. J. Pharm. Biol. Chem. Sci. 6(6):1059-1069.

Sansone G., Nastri M.J.F. & Fabbrocini A. 2000. Storage of buffalo (*Bubalus bubalis*) semen. Anim. Reprod. Sci. 62(1/3):55-76. <https://dx.doi.org/10.1016/s0378-4320(00)00154-8> <PMid:10924820>

Silva J.A.R., Araújo A.A., Lourenço Junior J.B., Santos N.F.A., Garcia A.R. & Nahúm B.S. 2011. Conforto térmico de búfalas em sistema silvipastoril na Amazônia Oriental. Pesq. Agropec. Bras. 46(10):1364-1371. <https://dx.doi.org/10.1590/S0100-204X2011001000033>

Souza B.B., Silva R.M.N., Marinho M.L., Silva G.A., Silva E.M.N. & Souza A.P. 2007. Physiological parameters and heat tolerance index of sindi breed bovine in the semi-arid of Paraiba. Ciênc. Agrotec. 31(3):883-888. <https://dx.doi.org/10.1590/S1413-70542007000300040>

Tiwari R., Mishra G.K., Shukla M.K., Singh R.B., Saxena S.K. & Siddiqui M.U. 2011. Seasonal variations in semen production of Murrah buffalo bulls. Indian J. Anim. Reprod. 32(2):5-7.

Vale W.G. 1988. Fisiologia da reprodução na búfala, p.1-28. In: Vale W.G. (Ed.), Bubalinos: fisiologia e patologia da reprodução. Fundação Cargill, Campinas.

Vale W.G. 1994. Collection, processing and deep freezing of buffalo semen. Buffalo J. (supl.2):65-81.

Vale W.G. 2002. Reproductive management of buffalo male aimming semen production for artificial insemination. Proceedings 1st Buffalo Symposium of Americas, Belém, PA, p156-171.

Vale W.G. 2007. Effects of environment on buffalo reproduction. Ital. J. Anim. Sci. 6(2):130-142. <https://dx.doi.org/10.4081/ijas.2007.s2.130>

Vale W.G. 2011. Avances biotecnológicos em reproducción de búfalos. Revta Tecnología em Marcha 24(5):89-90.

Vilela R.A. 2013. Efeito do ambiente térmico na fisiologia adaptativa de bubalinos. Tese de Doutorado, Faculdade de Zootecnia e Engenharia de Alimentos, Universidade de São Paulo, São Paulo, SP. 110p.

PESQUISA VETERINÁRIA BRASILEIRA
Brazilian Journal of Veterinary Research
ISSN 0100-736X (Print)
ISSN 1678-5150 (Online)

Pesq. Vet. Bras. 40(12):1054-1062, December 2020
DOI: 10.1590/1678-5150-PVB-6608

Original Article
Animal Morphophysiology
BY-NC

Macroscopic and microscopic morphology of the trachea and lungs of giant anteater (*Myrmecophaga tridactyla*)[1]

Evelyn Oliveira[2], Eduardo P. Nascente[2], Leiny P. Oliveira[2], Jair M. Santiago Neto[3], Júlio C. Roquete[4], Ana Paula I. Santin[5] and Veridiana M.B.D. Moura[5]*

ABSTRACT.- Oliveira E., Nascente E.P., Oliveira L.P., Santiago Neto J.M., Roquete J.C., Santin A.P.I. & Moura V.M.B.D. 2020. **Macroscopic and microscopic morphology of the trachea and lungs of giant anteater (*Myrmecophaga tridactyla*).** *Pesquisa Veterinária Brasileira 40(12):1054-1062*. Setor de Patologia Animal, Departamento de Medicina Veterinária, Escola de Veterinária e Zootecnia, Universidade Federal de Goiás, Rodovia Goiânia Km 8, Campus Samambaia, Goiânia, GO 74001-970, Brazil. E-mail: vdmoura@hotmail.com

Giant anteater (*Myrmecophaga tridactyla*) is a wild mammal distributed in Central and South America; nowadays, it is classified as an endangered species. Research about the macroscopic and histomorphological aspects of its respiratory tract is scarce, and, sometimes, it limits the treatment provided to sick animals and impairs species preservation. Thus, the present study aims to describe the macroscopic and microscopic morphology of its lower respiratory tract, including trachea and lungs. To do so, 12 adult giant anteaters from "Centro de Triagem de Animais Silvestres de Goiânia" (CETAS-GO), Goiás State, Brazil, were used in the research after natural death or euthanasia. Three of these animals were used for macroscopic assessments; they were fixed in 10% buffered formalin and dissected. Trachea and lung tissue samples were collected from nine animals right after death and fixed in 10% buffered formalin for histomorphological analysis; they were processed, embedded in paraffin, and inked with hematoxylin-eosin (HE), periodic acid-Schiff (PAS), and Masson's trichrome. The macroscopic analysis showed that the trachea in this species is proportionally short and presents from 19 to 27 tracheal cartilages. The right lung presents four lobes and the left one, two. The microscopic analysis evidenced respiratory epithelium of the ciliated cylindrical pseudostratified type, without evident goblet cells in the mucosa layer of the trachea and bronchi. The pulmonary visceral pleura is thick, similar to other large domestic mammals - complete septa extend from the pulmonary visceral pleura. In conclusion, the macroscopy and histomorphology of giant anteater's lower respiratory tract, represented by trachea and lungs, are similar to that of other domestic and wild mammals. Pulmonary histomorphology is mainly similar to that of pigs and ruminants: it has thick visceral pleura that emits complete septa of conjunctive tissue, which enable lobular parenchymal architecture.

INDEX TERMS: Morphology, trachea, lungs, giant anteater, *Myrmecophaga tridactyla*, anatomy, histology, respiratory tract, Xenarthras, wild animals.

RESUMO.- [**Morfologia macroscópica e microscópica da traqueia e pulmões do tamanduá-bandeira (*Myrmecophaga tridactyla*).**] O tamanduá-bandeira (*Myrmecophaga tridactyla*) é um mamífero silvestre com distribuição na América Central e do Sul e, atualmente, encontra-se classificado como ameaçado de extinção. Pesquisas acerca dos aspectos macroscópicos e histomorfológicos do seu sistema respiratório são escassas, o que, por vezes, limita o tratamento e o manejo de eventuais

[1] Received on August 19, 2020.
Accepted for publication on November 2, 2020.
[2] Veterinarian, Graduate Program in Animal Science (PPGCA), Escola de Veterinária e Zootecnia (EVZ), Universidade Federal de Goiás (UFG), Rodovia Goiânia Km 8, Campus Samambaia, Goiânia, GO 74001-970, Brazil.

[3] Programa de Iniciação Científica e Graduação em Medicina Veterinária, Escola de Veterinária e Zootecnia (EVZ), Universidade Federal de Goiás (UFG), Rodovia Goiânia Km 8, Campus Samambaia, Goiânia, GO 74001-970, Brazil.

[4] Docente, Anatomia Animal, Departamento de Morfologia, Instituto de Ciências Biológicas (ICB), Universidade Federal de Goiás (UFG), Rodovia Goiânia Km 8, Campus Samambaia, Goiânia, GO 74001-970, Brazil.

[5] Docente, Setor de Patologia Animal, Departamento de Medicina Veterinária, Escola de Veterinária e Zootecnia (EVZ), Universidade Federal de Goiás (UFG), Rodovia Goiânia Km 8, Campus Samambaia, Goiânia, GO 74001-970, Brazil. *Corresponding author: vdmoura@hotmail.com

animais doentes, bem como a preservação da espécie. Desse modo, o objetivo deste estudo foi descrever a morfologia macroscópica e microscópica do aparelho respiratório inferior do tamanduá-bandeira, incluindo traqueia e pulmões. Para tanto, foram utilizados 12 tamanduás-bandeiras adultos, provenientes do Centro de Triagem de Animais Silvestres de Goiânia (CETAS-GO), Goiás, Brasil, após morte natural ou eutanásia. Destes, três foram utilizados para o estudo macroscópico, sendo fixados em formalina tamponada a 10% e dissecados. Para a análise histomorfológica, amostras teciduais da traqueia e do pulmão foram colhidas de nove animais logo após o óbito, fixadas em formalina tamponada a 10%, processadas, incluídas em parafina e coradas com hematoxilina e eosina (HE), ácido periódico-Schiff (PAS) e tricrômico de Masson. À análise macroscópica notou-se que a traqueia é proporcionalmente curta, apresentando 19 a 27 cartilagens traqueais. O pulmão direito apresenta quatro lobos e o esquerdo dois. À análise microscópica foi constatado epitélio respiratório do tipo pseudoestratificado cilíndrico ciliado, sem células caliciformes evidentes na camada mucosa da traqueia e dos brônquios. A pleura visceral pulmonar é espessa, assim como nos grandes mamíferos domésticos, e, a partir desta, estendem-se septos completos. Conclui-se que a macroscopia e a histomorfologia do sistema respiratório inferior do tamanduá-bandeira, representado pela traqueia e pulmões, são semelhantes àquelas de outros mamíferos domésticos e silvestres. A histomorfologia pulmonar é especialmente semelhante à de suínos e ruminantes, com a pleura visceral espessa e emitindo septos completos de tecido conjuntivo, que conferem arquitetura parenquimal lobular.

TERMOS DE INDEXAÇÃO: Morfologia, macroscópica, traqueia, pulmões, tamanduá-bandeira, *Myrmecophaga tridactyla*, anatomia, animais silvestres, aparelho respiratório, histologia, Xenarthras.

INTRODUCTION

Giant anteater (*Myrmecophaga tridactyla* Linnaeus, 1758) is a wild mammal belonging to the super order Xenarthras, previously called Edentata, and order Pilosa featured by lack of teeth, dense coat, and strong claws in the hands (Chebez & Cirignoli 2008, Miranda 2014). This species is natural to Central and South America in Brazil. It is widely distributed in almost all biomes, mainly in field and "Cerrado" regions (Wetzel 1985).

However, nowadays, it is considered an endangered species classified as vulnerable by the International Union for Conservation of Nature (IUCN) (Miranda et al. 2015). Factors such as deforestation, wildfires, and agricultural development reduce these animals' habitat and significantly affect countless wild species populations; giant anteaters are among the main mammals affected by wildfires and run overs (Cáceres et al. 2010, Superina et al. 2010).

Animals belonging to this species have anatomical and physiological specificities yet little explored, including those concerning the respiratory tract. The scarcity of studies focused on this topic negatively influences the clinical treatment provided to animals who are victims of accidents since the respiratory tract is responsible not only for air conduction and gas exchange but also for phonation, smell, and body temperature regulation, and excretion.

Thus, knowing the anatomy and physiology of this tract is of paramount importance for giant anteater's preservation and conservation (Lange et al. 2013), since previous studies have evidenced some anatomical features specific of this species. However, only the macroscopy and pulmonary segmentation of these animals were evidenced in these studies (Giraldi et al. 2017) therefore, there are some remaining gaps that still have to be approached in detail.

It is essential segmenting the organs composing the respiratory tract in order to simplify the understanding about its structures and functions; so, it is worth dividing it into upper (nasal cavity, pharynx and larynx) and lower (trachea and lungs) portions (López 2013). Airways, hematogenic pathway and direct extension are the main entrances to the respiratory tract. Airways and hematogenic pathway can become the viable access to toxins and microorganisms in case of accidents (López 2013, König & Liebich 2016). Yet, the detailed description of organs and tracts makes it easier to understand this species' behavior and evolution (Giraldi et al. 2017) because it clarifies diagnostic and treatment questions, as well as favors species conservation (Sanders & Feijó 2007).

Accordingly, the aim of the present study was to describe the macroscopic and histomorphological features of giant anteater's trachea and lungs in order to provide biological information about this species.

MATERIALS AND METHODS

The present study was approved by the Ethics Committee on Animal Use of "Universidade Federal de Goiás" (ECAU-UFG), under no. 010/2018, and authorized by "Sistema de Autorização e Informação em Biodiversidade" (SISBIO-IBAMA), no. 61810-1/2018. Twelve adult giant anteaters used in this study, being four females and eight males, weighing an average of 23kg, all from free-living, and captured or rescued by the "Centro de Triagem de Animais Silvestres de Goiânia", Goiás (CETAS-GO). These nine died due to injuries caused by run overs, and three were euthanized due to multiple fractures and unlikely recovery.

Macroscopic analysis. Three animals were fixed in 10% buffered formalin after death for further dissection in the lower respiratory tract's macroscopic analysis. The skin was removed, and buffered formalin intramuscular injections were administered in the whole extension of the corpses for fixation. Next, the corpses were immersed in vats filled with fixing solution for 72 hours. Subsequently, they were washed in running water for 12 hours and transferred to the supersaturated saline solution (30%) to achieve conservation and handling throughout dissection.

The fasciae and muscles of the chest's ventral surface were moved for trachea and lungs access; next, the sternum was removed by disarticulating the costochondral junctions. The costal sternum railings were manually taken apart for photo-documentation with a digital camera (Camera Nikon D3300). Subsequently, the trachea dissected close to the mediastinum, and the whole set was removed from the larynx until mediastinum and lungs. These structures were subjected to microscopic analyses and the mesoscopic analysis of the trachea and lungs, tracheal cartilage count, and lung lobe identification through interlobular fissures.

Microscopic analysis. Nine animals were subjected to necroscopic examination after death to collect samples for the microscopic analysis. From the right lung were collected, two samples of the middle and accessory lobes and three samples were obtained of the

cranial and caudal lobes. From the trachea, samples were obtained of the cranial, middle, and caudal segments. All samples were fixed in 10% buffered formalin for 48 hours, processed in increasing ethyl alcohol solutions, clarified in xylol, embedded in paraffin, and cut to 5µm. Cuts were unbend over the histologic slide and inked with hematoxylin and eosin (HE), periodic acid-Schiff (PAS), and Masson's trichrome, based on Tolosa et al. (2003). Trachea fragments were descaled in 8% formic acid and hydrochloric acid solution for 72 hours before the histological processing.

The histological cuts were analyzed in a bright-field optical microscope (Leica DM 4000®), and a system provided the digital photomicrographs to capture images (Leica Application Site - LAS) coupled to the microscope. The different strata composing the trachea were described, and the structure of both the parenchyma and pulmonary stroma, including the bronchial tree components.

RESULTS

Trachea

In macroscopic terms, the trachea is a flexible tubular organ that goes from the caudal portion of the cricoid laryngeal cartilage, by the sixth cervical vertebra, until the bronchial bifurcation (carina), by the fifth thoracic vertebra; it is the origin of the principal, right and left bronchi. The ventral portion and the trachea sides were formed by incomplete-cartilage-ring-shaped entangled by fibroelastic tissue (the annular ligaments). The dorsal portion was formed by muscle tissue (tracheal muscle), more flexible, which bonds the rings' edges. The cervical portion of the trachea was short since the larynx in this species is close to the thorax entrance (Fig.1A). In this study's animals, the size of the trachea ranged from 8.0 to 10.8cm, with an average tracheal size of 9.24cm. The tracheal lumen diameter varied from 1.45 to 1.55cm, and the average of 1.5cm in diameter. The number of tracheal cartilages ranged from 19 to 27, with an average of 22 cartilages (Fig.1B).

Three different tunics were observed in the histomorphological analysis applied to the trachea: mucosa, submucosa, and adventitious. Mucosa surface was coated by the ciliated cylindrical pseudostratified epithelium (Fig.2A); without evidence of goblet cells throughout the whole extension of the respiratory epithelium (Fig.2B). The lamina propria and the submucosa were deep in the respiratory epithelium; however, the difference between these two structures was not established. They presented loose conjunctive tissue with collagen fibers, serous glands, tubuloacinous mucous

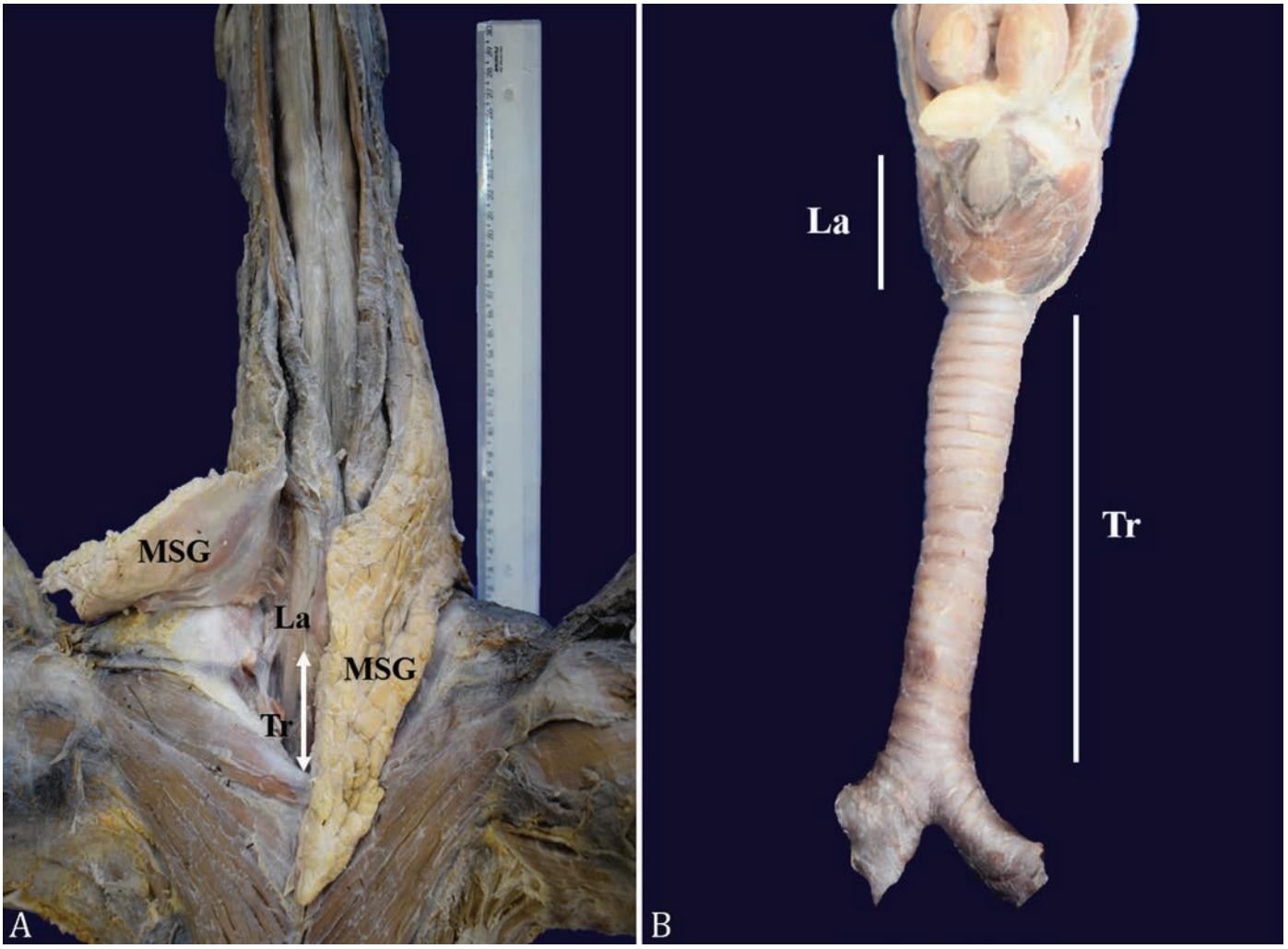


Fig.1. (**A**) Ventral face of neck and thorax (**B**) and ventral view of the trachea and larynx of the giant anteater (*Myrmecophaga tridactyla*). (**A**) Mandibular salivary glands (MSG), Larynx (La) and the cervical part of the trachea (Tr). (**B**) Larynx (La) and trachea (Tr).

membranes (at different sizes). Sometimes, the glandular duct would open to the trachea (Fig.2C) and blood vessels (at different calipers) (Fig.2D).

C-shaped incomplete cartilage ring deeper inside; it was composed of hyaline cartilage coated by perichondrium, the edges were free and had an opening in them. The hyaline

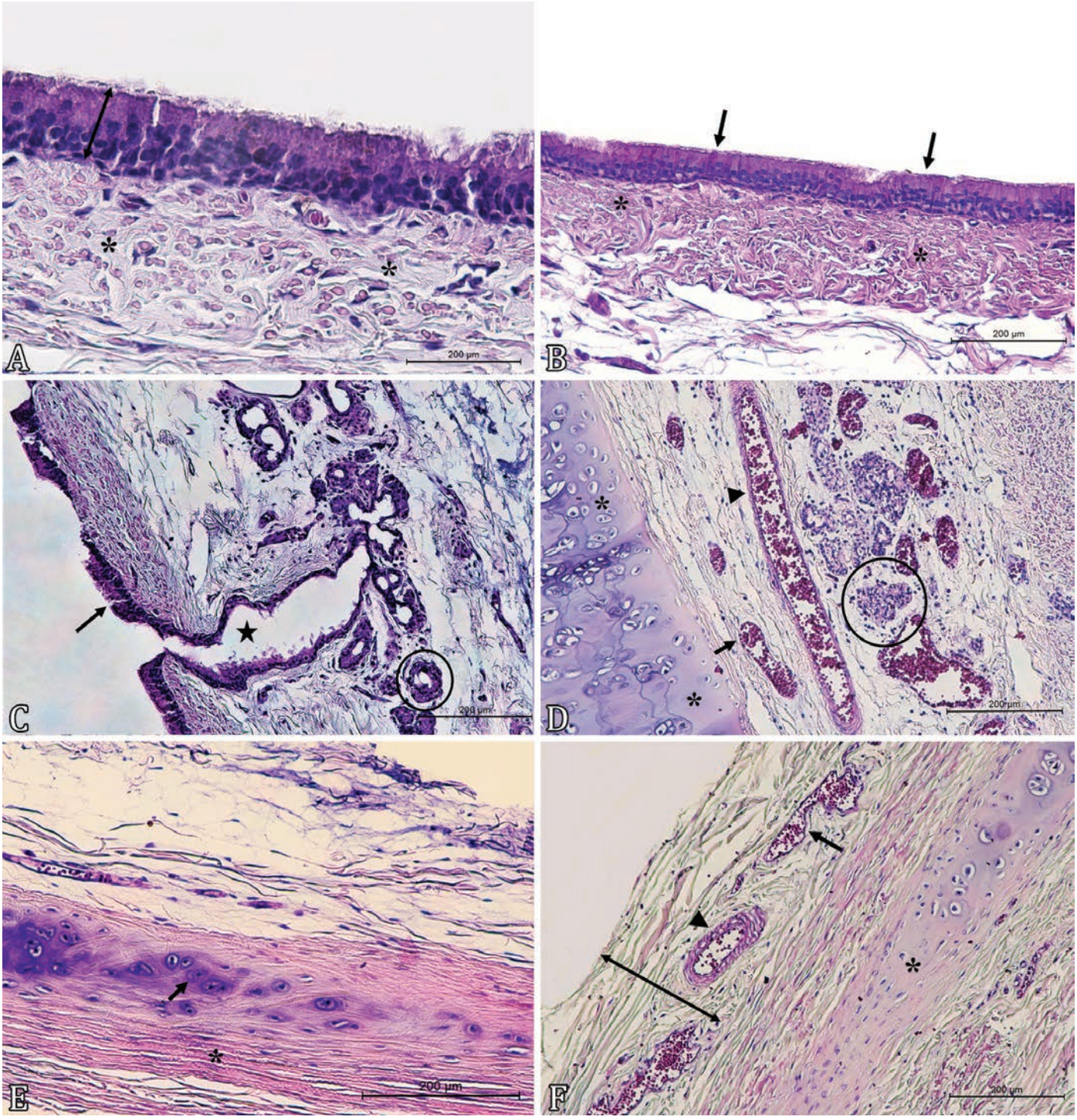


Fig.2. Photomicrographs of giant anteaters' trachea (*Myrmecophaga tridactyla*. (**A**) Cylindrical pseudo-stratified epithelium (double arrow) and lamina propria submucosa (asterisks), HE, bar = 200µm. (**B**) Cylindrical pseudo-stratified epithelium (arrows), without evidence of goblet cells, PAS, bar = 200µm. (**C**) Cylindrical pseudo-stratified epithelium (arrow) and lamina propria-submucosa composed of loose conjunctive tissue with collagen fibers, serous glands (circle) at different sizes, with glandular duct open to the trachea (star), HE, bar = 200µm. (**D**) Arterioles (arrowhead), venules (arrow) and serous glands (circle) distributed on in the submucosal layer, close to the hyaline cartilage (asterisk), HE, bar = 200µm. (**E**) Hyaline cartilage (arrow) and smooth muscle (asterisk) interspersed, HE, bar = 200µm. (**F**) Adventitia layer (double arrow) composed of loose connective tissue with collagen fibers, arterioles (arrowhead) and venules (arrow) dispersed in its whole extension, close to the hyaline cartilage (asterisk), HE, bar = 200µm.

cartilage and smooth muscle were interspersed (Fig.2E), which was featured by spindle fibers in parallel, at the cross-sectional position, this muscle filled the gaps between tracheal cartilage. There was an adventitious tunic heading outside (Fig.2F); the tunic was composed of loose connective tissue, collagen fibers, and arterial and venous vessels (at different calibers).

Lungs

The right lung of giant anteater was bigger and split in four lobes: cranial, middle, caudal and accessory. The cranial lobe was sub-divided into the cranial and caudal parts. The left lung, in its turn, had two lobes called 'cranial' and 'caudal' (Fig.3A,B). They were both covered by the pleura, which was also covered by a thick layer of subserous tissue - the interlobular septa spread out from this tissue.

In microscopic terms, the histological lung samples (at the magnitude of 10x) showed pulmonary parenchyma of the typical lacy aspect. The pulmonary histological structure could be divided into visceral pleura, bronchi, bronchioles, alveolar ducts, and alveolar sacs. The visceral pleura was relatively thick and composed of the mesothelium in its external portion; the mesothelium, in its turn, was composed of simple squamous epithelium. There were loose conjunctive tissue and blood vessels of different calipers deeper inside (Fig.4A). There were complete septa composed of loose conjunctive tissue from the pleura (Fig.4B) and extending to inside the organ; it separated the pulmonary parenchyma into lobes (Fig.4C). These septa also had blood vessels (at different calipers) throughout their full extension.

Bronchi were large (Fig.4D) and coated by ciliated cylindrical pseudostratified epithelium, with a moderate amount of goblet cells (Fig.4E); epithelium height was proportional to the caliper of the assessed bronchus. Adjacent lymphoid tissue was featured by the accumulation of lymphocytes close to the respiratory epithelium, known as bronchus-associated lymphoid tissue (BALT). The division between the lamina propria and the submucosa was evident, and both were composed of conjunctive tissue rich in collagen fibers. The mucosa's muscle layer had fibers of smooth muscle distributed in an oblique or circular form, as well as scarce plates of hyaline cartilage (Fig.4F), serous glands, and small arterial and venous vessels.

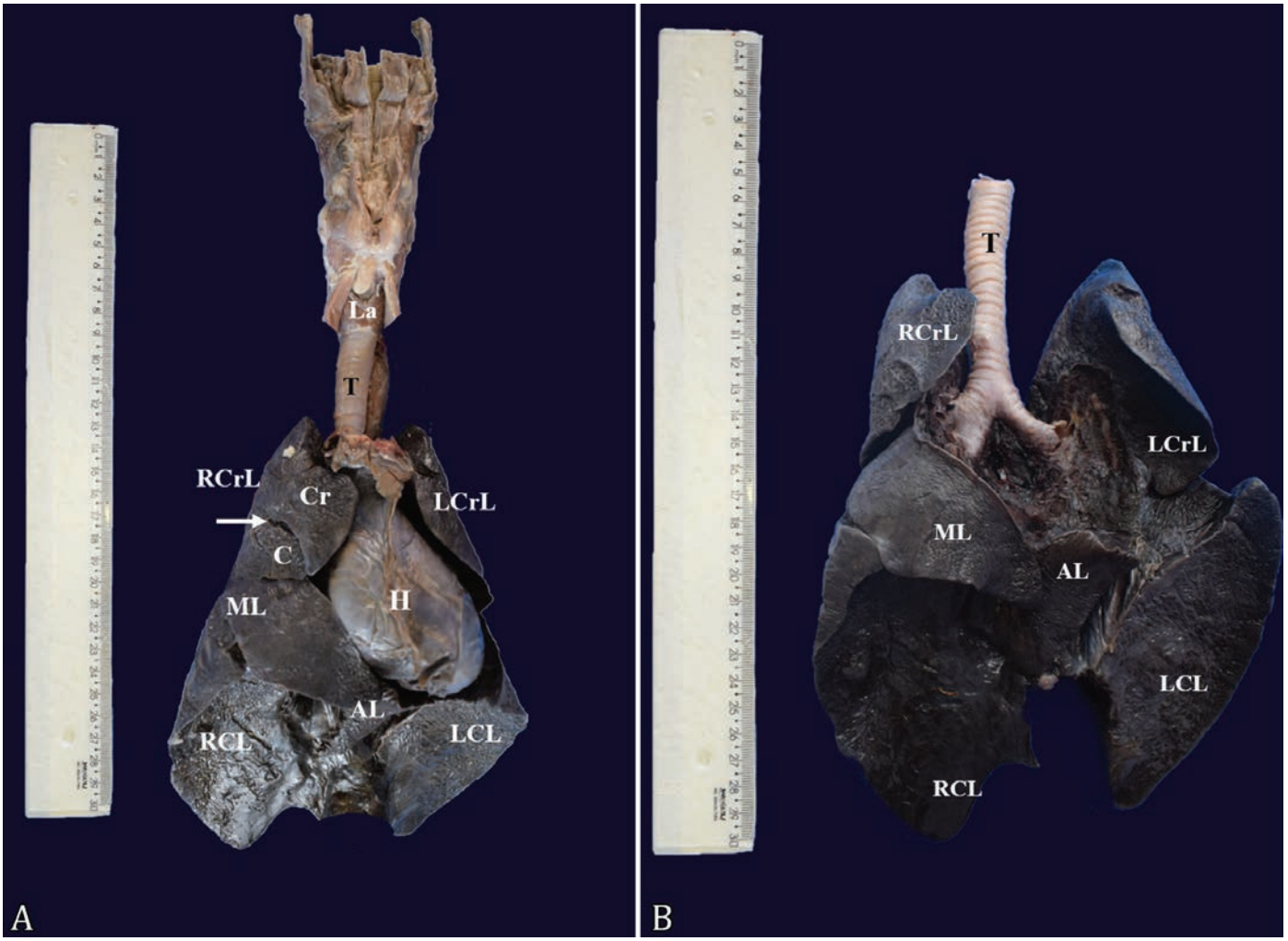


Fig.3. (**A**) Ventral face of the lower respiratory tract of giant anteater (*Myrmecophaga tridactyla*). (**B**) The same structures described in Figure A, with the absence of the heart to show the accessory lobe. Larynx (La), trachea (T), right cranial lobe (RCrL), cranial part of the right cranial lobe (Cr), caudal part of the right cranial lobe (C), interlobular fissure (arrow), middle lobe (ML), accessory lobe (AL), right caudal lobe (RCL), Heart (H), left cranial lobe (LCrL) and left caudal lobe (LCL).

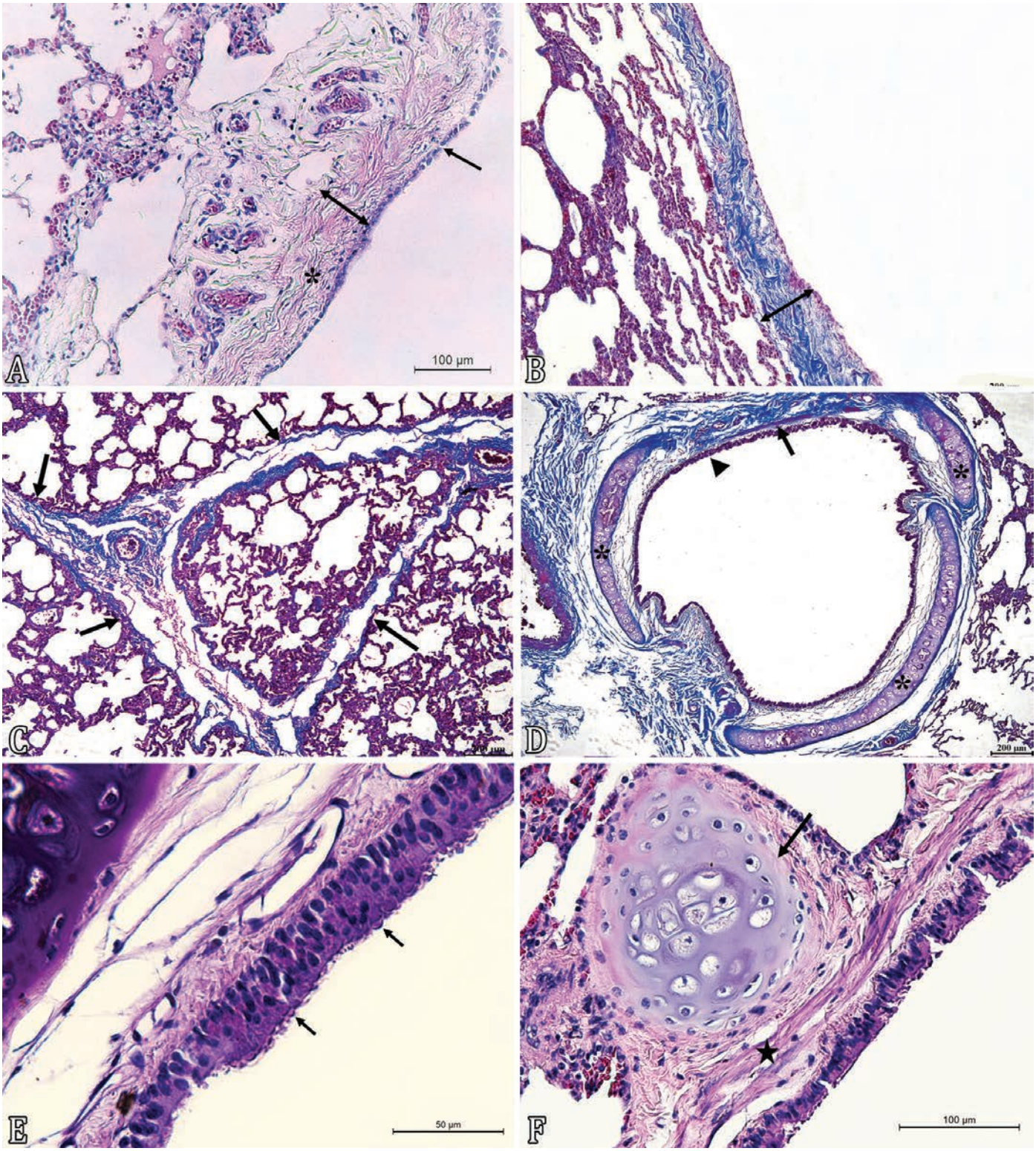


Fig.4. Photomicrographs of the lung of giant anteater *(Myrmecophaga tridactyla)*. (**A**) Thick pulmonary pleura (double arrow), formed by simple pavement epithelium (arrow) and loose connective tissue (asterisk). HE, bar = 100µm. (**B**) Pulmonary pleura (double arrow) with blue collagen highlighted. Masson's trichrome, bar = 200µm. (**C**) Blue connective tissue septa (arrows), separating the lung parenchyma into lobes. Masson's trichrome, bar = 200µm. (**D**) Pulmonary bronchus with ciliated cylindrical pseudostratified epithelium (arrowhead), lamina propria formed by connective tissue followed by muscular layer of the mucosa, with smooth muscle (arrow). Typical submucosa and hyaline cartilage plaques (asterisk) adjacent to connective tissue. Masson's Trichrome, bar = 200µm. (**E**) Bronchus showing ciliated cylindrical pseudo-stratified epithelium without evidence of goblet cells. PAS, bar = 50µm. (**F**) Hyaline cartilage plaque (arrow) typical of the pulmonary bronchus. Deeply to the epithelium, its own submucosal lamina with emphasis on the muscular layer of the mucosa of circular orientation (star), HE, bar = 100µm.

Bronchioles were smaller than (Fig.5A) and different from the bronchi, mainly because they did not present hyaline cartilage plates on the submucosa. The mucosa was coated by simple epithelium (at different heights); it could be cylindrical or cubic and present lashes or not. The lamina propria and the submucosa were in a deeper layer; therefore, it was not possible to set a partition between them; they were relatively thin and composed of loose conjunctive tissue, small amounts of arterial vessels, smaller venous vessels, and by few areas with smooth muscle fibers distributed in circular orientation (Fig.5B). There was lymphoid tissue in the bronchioles (Fig.5C), which was featured by the accumulation of lymphocytes close to the bronchiolar epithelium region.

Alveolar sacks did not present smooth muscle on the wall, which was formed by alveoli. These alveoli were covered by a thin layer of simple squamous epithelium, which formed the alveolar wall (Fig.5D). The alveoli were separated by interalveolar septa composed of conjunctive and capillary tissue in its inner side and by the alveoli's simple squamous epithelium in its external side.

DISCUSSION

The lower respiratory tract is featured by tubes that widespread - the so-called "tracheobronchial airways," and reach the alveolar gas exchange apparatus (Eurell & Frappier 2006). The trachea is the longest of these tubes; it goes from the larynx's cricoid cartilage to the bifurcation in the thoracic cavity (König & Liebich 2016). However, the length of this organ in giant anteater representatives was shorter than in species such as ruminants and horses, which show from 48 to 60 tracheal cartilages;

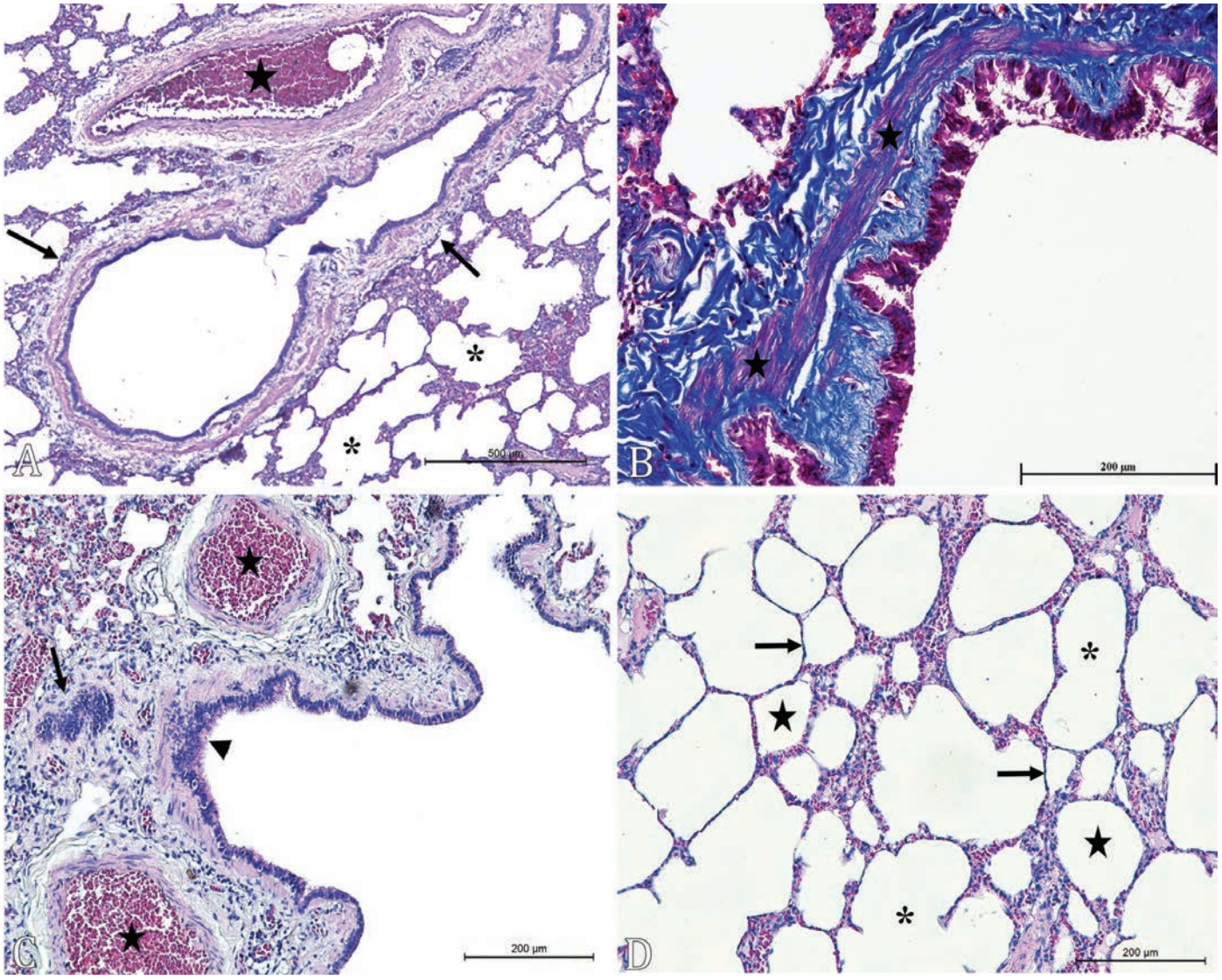


Fig.5. Photomicrographs of bronchioles and pulmonary alveoli of giant anteater (*Myrmecophaga tridactyla*). (**A**) Pulmonary bronchioles (arrow) characterized by the absence of hyaline cartilage plaques, with artery (star), alveolar sacs (asterisks) and adjacent alveoli, HE, bar = 500µm. (**B**) Muscle layer, eosinophilic color (star), in circular orientation in the bronchiolar wall, Masson's Trichrome, bar = 200µm. (**C**) Lymphoid tissue (arrow) characterized by the accumulation of lymphocytes close to the region of the bronchiolar epithelium (arrowhead) and arterioles (stars), HE, bar = 200µm. (**D**) Alveolar sacs (asterisks) and pulmonary alveoli (stars) covered by a thin layer of squamous epithelial cells (arrow), forming the alveolar wall. HE, bar = 200µm.

dogs, who have 42 to 46 cartilages; cats, who have 38 to 43 cartilages (König & Liebich 2016), capybaras have from 35 to 46 cartilages (Moreto et al. 2017) and 34 cartilages in the coatis, on average (Oliveira et al. 2011). On average, giant anteaters have 22 tracheal cartilages; this number was close to the one reported for skunks, which present 25 cartilages, on average (Bertassoli et al. 2013). The fact that the larynx is more caudal in giant anteaters contributes to their shorter trachea, making the cervical portion of the trachea exiguous. This is relevant knowledge in emergencies or anesthetic procedures since inhalation anesthesia in this species is more complex given a hard time intubating these animals. Tracheostomy would be a plausible alternative, as reported by Brainard et al. (2008); however, this procedure requires proper knowledge about the region's topographic anatomy. Although this segment is short, it is also covered by the mandibular salivary gland.

The lower respiratory tract is featured by tubes that widespread, the so-called "tracheobronchial airways", and reach the alveolar gas exchange apparatus (Eurell & Frappier 2006). The trachea is the longest of these tubes; it goes from the larynx's cricoid cartilage to the bifurcation in the thoracic cavity (König & Liebich 2016). However, the length of this organ in giant anteater representatives was shorter than in species such as ruminants and horses, which show from 48 to 60 tracheal cartilages; dogs, who have 42 to 46 cartilages; cats, who have 38 to 43 cartilages (König & Liebich 2016), capybaras have from 35 to 46 cartilages (Moreto et al. 2017) and 34 cartilages in the coatis, on average (Oliveira et al. 2011). On average, giant anteaters have 22 tracheal cartilages; this number was close to the one reported for skunks, which present 25 cartilages, on average (Bertassoli et al. 2013). The fact that the larynx is more caudal in giant anteaters contributes to their shorter trachea, making the cervical portion of the trachea exiguous. This is relevant knowledge in emergencies or anesthetic procedures since inhalation anesthesia in this species is more complicated given a hard time intubating these animals. Tracheostomy would be a plausible alternative, as reported by Brainard et al. (2008); however, this procedure requires proper knowledge about the region's topographic anatomy. Although this segment is short, it is also covered by the mandibular salivary gland. In the present study, tracheal mucosa was coated by the respiratory epithelium and had serous glands, similar to the description made for domestic (Banks 1993) and wild species (Moussa & Hassan 2015, Rocha et al. 2017, Mario et al. 2018). The tracheal muscle was inserted in the tracheal cartilage's internal face, similar to horses, pigs, and ruminants, but different from carnivores and humans, whose muscle fixation occurs on the external surface of the tracheal cartilages (Bacha & Bacha 2012, König & Liebich 2016).

Overall, pulmonary lobe subdivisions are similar in different species of mammals. The right lung is formed by the cranial, middle, caudal and accessory lobes, and the left one by the cranial and caudal lobes. The same features are observed in dogs, cats, pigs (König & Liebich 2016), capybaras (Moreto et al. 2017), coatis (Oliveira et al. 2011), and giant anteaters. However, different from these animals, and similar to cattle, goats, and sheep, the cranial lobe of the right lung in *Myrmecophaga tridactyla* is divided into cranial and caudal parts, as described by Giraldi et al. (2017).

Lungs can be split into intrapulmonary airways (bronchi and bronchioles), gas exchange areas (ducts and alveolar sacs and alveoli), and pleura (Eurell & Frappier 2006). Giant anteaters' pleura forms a serous membrane that covers the lungs; it is formed by mesothelium on its surface and, deeper inside, by loose conjunctive tissue and blood vessels, as reported for domestic animals (Banks 1993). However, different from dogs and cats, who present thin pleura, animals in the present study showed thick pleura, as described for large mammals such as cattle, horses, and pigs (Eurell & Frappier 2006, Bacha & Bacha 2012, König & Liebich 2016).

Besides being thicker, the pleura tissue in giant anteaters is continuous, septa form lobes; similar to pigs, ruminants (Bacha & Bacha 2012), and ringed seal (*Phoca hispida*), septa are complete. This pattern is different from that observed in horses, who show incomplete septa of conjunctive tissue, which features this species' little lobulated lungs (Eurell & Frappier 2006).

In domestic animals and humans, bronchi are histologically similar to the trachea; however, they present thinner extracts. The mucosa is coated with typical respiratory epithelium; lamina propria and submucosa are composed of loose conjunctive tissue, glands, smooth muscle, blood vessels, hyaline cartilage, and, sometimes, accumulated lymphoid tissue (Eurell & Frappier 2006, Junqueira & Carneiro 2013). All these features were also observed in pulmonary tissue collected from giant anteaters in the present research. The assessed bronchioles presented simpler morphology; cartilage and glands, similar to domestic animals (Bacha & Bacha 2012), human beings (Junqueira & Carneiro 2013), and to animals such as quaint (*Monodelphis domestica*) (Cope et al. 2012) and red fox (Moussa & Hassan 2015), the absence of these structures is the primary way of differentiating bronchioles from the bronchi.

Pulmonary structures composing the gas exchange apparatus are similar to those described for domestic (Banks 1993) and wild animals (Smodlaka et al. 2006, Oliveira et al. 2011, Cope et al. 2012, Moussa & Hassan 2015, Rocha et al. 2017). However, different from what was reported for such animals, there were no alveolar macrophages in giant anteaters. However, the microscopic evaluation under hematoxylin and eosin ink did not exclude the likelihood of finding these cells in the species mentioned above. Therefore, immunophenotyping tests would be an alternative to confirm or not the presence of these cells in giant anteaters' pulmonary gas exchange apparatus.

CONCLUSIONS

Giant anteaters' trachea presents 22 tracheal cartilages, on average. The trachea is smaller and more caudal than in other species of domestic and wild mammals. Its cervical portion is tiny and coated by salivary glands. The histomorphology of the lower portion of the respiratory tract in giant anteaters is equal to that of other domestic and wild mammals.

The pulmonary histomorphology is quite similar to that of pigs and ruminants. The visceral pleura is thick and emits complete septa formed by conjunctive tissue, enabling lobular parenchymal architecture.

Acknowledgments.- Evelyn de Oliveira thanks the "Conselho Nacional de Desenvolvimento Científico e Tecnológico" (CNPq) for granting scholarship. We thank the "Centro de Triagem de Animais Silvestres" (CETAS) of the State of Goiás, Brazil, for providing institutional support.

Conflict of interest statement.- The authors declare that there are no conflicts of interest.

REFERENCES

Bacha W.J. & Bacha L.M. 2012. Color Atlas of Veterinary Histology. 3rd ed. Wiley-Blackwell, London, p.195-210.

Banks W.J. 1993. Applied Veterinary Histology. 3rd ed. Mosby, St. Louis, p.390-407.

Bertassoli B.M., Santos A.C., Oliveira F.D., Oliveira D.M., Assis-Neto A.C. & Carvalho A.F. 2013. Morfologia da laringe e traqueia de gambás (*Didelphis* sp.). Ciênc. Anim. Bras. 14(2):222-229. <https://dx.doi.org/10.5216/cab.v14i2.17044>

Brainard B.M., Newton A., Hinshaw K.C. & Klide A.M. 2008. Tracheostomy in the Giant Anteater (*Myrmecophaga tridactyla*. J. Zoo Wildl. Med. 39(4):655-658. <https://dx.doi.org/10.1638/2007-0124.1> <PMid:19110713>

Cáceres N.C., Hannibal W., Freitas D.R., Silva E.L., Roman C. & Casella J. 2010. Mammal occurrence and roadkill in two adjacent ecoregions (Atlantic Forest and Cerrado) in south-western Brazil. J. Zoologia, Curitiba, 27(5):709-717. <https://dx.doi.org/10.1590/S1984-46702010000500007>

Chebez J. & Cirignoli Y. 2008. Mamíferos, p.31-40. In: Chebez J.C. (Ed.), Los que se Van, Fauna Argentina Amenazada. Vol.3. Albatros, Argentina.

Cope L.A., Henry R.W. & Reed Jr R.B. 2012. Microscopic anatomy of the lower respiratory tract of the Grey Short-Tailed Opossum (*Monodelphis domestica*). Anat. Histol. Embryol. 41(2):96-105. <https://dx.doi.org/10.1111/j.1439-0264.2011.01107.x> <PMid:21919952>

Eurell J.A. & Frappier B.L. 2006. Dellmann's Textbook of Veterinary Histology. 6th ed. Blackwell Publishing, Iowa, p.153-169.

Giraldi A.C.C., Aires L.P.N., Rodrigues R.F., Cruvinel T.M.A. & Melo A.P.F. 2017. Anatomia e segmentação pulmonar de tamanduá-bandeira (*Myrmecophaga tridactyla* - Linnaeus, 1758) de vida livre. Arq. Bras. Med. Vet. Zootec. 69(1):22-28. <https://dx.doi.org/10.1590/1678-4162-9197>

Junqueira L.C. & Carneiro J. 2013. Histologia Básica, Texto e Atlas. 12ª ed. Guanabara Koogan, Rio de Janeiro, p.676-712.

König H.E. & Liebich H.G. 2016. Anatomia dos Animais Domésticos, Texto e Atlas Colorido. 6ª ed. Artmed, Porto Alegre, p.377-398.

Lange R., Lang A., Allgayer M., Albuquerque I., Rossi Júnior J. & Chiesorin Neto L. 2013. Das práticas em zoológico à especialização dos dias atuais. Revta CFMV 19(59):13-15.

López A. 2013. Sistema respiratório, mediastino e pleuras, p.1183-1407. In: Zachary J.F. & McGavin M.D. (Eds), Bases da Patologia em Veterinária. 5ª ed. Elsevier Brasil, Rio de Janeiro.

Mario L.C., Borghesi J., Hayashi R.G., Favaron P.O., Rodrigues M.N., Carvalho R.C. & Miglino M.A. 2018. Morphology of the *Oligoryzomys nigripes* respiratory system. Anat. Histol. Embryol. 47(4):364-371. <https://dx.doi.org/10.1111/ahe.12363> <PMid:29869399>

Miranda F.R. 2014. Cingulata (tatus) e Pilosa (preguiças e tamanduás), p.707-722. In: Cubas Z.S., Silva J.C.R. & Catão-Dias J.L. (Eds), Tratado de Animais Selvagens Medicina Veterinária. 2ª ed. Roca, São Paulo.

Miranda F.R., Chiarello A.G., Rohe F., Braga F.G., Mourão G.M. & Miranda G.H.B. 2015. Avaliação do risco de extinção de *Myrmecophaga tridactyla* Linnaeus, 1758 no Brasil. Avaliação do Risco de Extinção de Xenartros Brasileiros, Instituto Chico Mendes de Conservação da Biodiversidade, ICMBio, Brasília, p.89-105.

Moreto A.O., Oliveira F.D., Bertassoli B.M. & Neto A.C.A. 2017. Morfologia comparada do aparelho respiratório de capivaras (*Hydrochoerus hydrochoeris*). Pesq. Vet. Bras. 37(3):269-277. <https://dx.doi.org/10.1590/s0100-736x2017000300011>

Moussa E.A. & Hassan S.A. 2015. Histology and scanning electron microscopy of the lower respiratory tract in the adult Red Fox (*Vulpes vulpes*). Int. J. Morphol. 33(1):267-274. <https://dx.doi.org/10.4067/S0717-95022015000100042>

Oliveira V.C., Souza A.F., Santos A.C., Bertassoli B.M., Rosa R.A., Carvalho A.F., Martins J.F.P. & Mançanares C.A.F. 2011. Estudo morfológico do sistema respiratório de quati (*Nasua nasua*). Biotemas 25(1):81-92. <https://dx.doi.org/10.5007/2175-7925.2012v25n1p81>

Rocha M.P., Nunes A.P., Minello L.F., Cruz L.A.X., Albano A.P.N. & Mondadori R.G. 2017. Histological description of *Cerdocyon thous* (Linnaeus, 1766) respiratory system. Pesq. Vet. Bras. 37(5):531-535. <https://dx.doi.org/10.1590/s0100-736x2017000500018>

Sanders A. & Feijó A.G.S. 2007. Uma reflexão sobre animais selvagens cativos em zoológicos na sociedade atual. Revta SORBI 1(4):1-10.

Smodlaka H., Reed R.B. & Henry R.W. 2006. Microscopic anatomy of the ringed seal (*Phoca hispida*) lower respiratory tract. Anat. Histol. Embryol. 35(1):35-41. <https://dx.doi.org/10.1111/j.1439-0264.2005.00635.x> <PMid:16433671>

Superina M., Miranda F.R. & Abba A.M. 2010. The 2010 anteater red list assessment. Edentata 11(2):96-114. <https://dx.doi.org/10.5537/020.011.0201>

Tolosa E.M.C., Rodrigues C.J., Behmer O.A. & Freitas Neto A.G. 2003. Manual de técnicas para histologia: normal e patológica. Manole, São Paulo. 341p.

Wetzel R.M. 1985. The identification and distribution of recent Xenarthra (Edentata), p.5-21. In: Montgomery G. (Ed.), The Evolution and Ecology of Armadillos, Sloths, and Vermilinguas. Smithsonian Institution Press, Washington, D.C.

PESQUISA VETERINÁRIA BRASILEIRA
Brazilian Journal of Veterinary Research
ISSN 0100-736X (Print)
ISSN 1678-5150 (Online)

Pesq. Vet. Bras. 40(12):1063-1072, December 2020
DOI: 10.1590/1678-5150-PVB-6491

Original Article
Animal Morphophysiology
BY-NC

Epigenetic characterization of the H19/IGF2 *locus* in calf clones placenta[1]

Natalia S. Costa[2,3]*, Márcia M. Silveira[2], Luna N. Vargas[2], Alexandre R. Caetano[4], Rodolfo Rumpf[5] and Maurício M. Franco[2,3]

ABSTRACT.- Costa N.S., Silveira M.M., Vargas L.N., Caetano A.R., Rumpf R. & Franco M.M. 2020. **Epigenetic characterization of the H19/IGF2 *locus* in calf clones placenta.** *Pesquisa Veterinária Brasileira 40(12):1063-1072*. Laboratório de Reprodução Animal, Embrapa Recursos Genéticos e Biotecnologia-Cenargen, Parque Estação Biológica, Avenida W/5 Norte (final), Cx. Postal 02372, Brasília, DF 70770-917, Brazil. E-mail: natalia.souzacosta15@gmail.com

Somatic Cell Nuclear Transfer (SCNT-Cloning) is a promising technique in many areas and is based on genetically identical individuals. However, its efficiency is low. Studies suggest that the leading cause is inadequate epigenetic reprogramming. This study aimed to characterize the methylation pattern of the exon 10 regions of the IGF2 gene and the Imprinting Control Region (ICR) of the H19 gene in the placenta of cloned calves. For this study, female and male cloned calves presenting different phenotypes were used. Genomic DNA from these animals' placenta was isolated, then treated with sodium bisulfite and amplified to the ICR/H19 and IGF2 loci. PCR products were cloned into competent bacteria and finally sequenced. A significant difference was found between controls and clones with healthy phenotypes for the ICR/H19 region. In this region, controls showed a hemimethylated pattern, as predicted in the literature due to this region has an imprinted control, while clones were showed less methylated. For the IGF2, no significant differences were found between controls and clones. These results suggest that different genomic regions in the genome may be independently reprogrammed and that failures in reprogramming the DNA methylation patterns of imprinted genes may be one of the causes of the low efficiency of SCNT.

INDEX TERMS: Epigenetic, H19, IGF2, *locus,* placenta, calf, cloning, imprinting, bovine.

RESUMO.- [**Caracterização epigenética do *locus* H19/IGF2 na placenta de bezerros clones.**] A Transferência Nuclear de Células Somáticas (TNCS-Clonagem) é uma técnica promissora em várias áreas, e se baseia na produção de indivíduos geneticamente idênticos. No entanto, sua eficiência é baixa. Estudos sugerem que a principal causa seja uma reprogramação epigenética inadequada. O objetivo desse trabalho é caracterizar o padrão de metilação da região éxon 10 do gene *IGF2* e da Região Controladora de *Imprinting* (ICR) do gene *H19* na placenta de bezerros clonados. Para a execução do trabalho foram selecionados clones bovinos fêmeas e machos, apresentando diferentes fenótipos. O DNA da placenta desses animais foi extraído, e em seguida foi tratado com bissulfito de sódio e amplificado para os loci ICR/H19 e IGF2. Os produtos da PCR foram clonados em bactérias competentes e, por fim, sequenciados. Foi encontrada uma diferença significativa entre os controles e os clones com fenótipos saudáveis para a região da ICR/H19. Nesta região, os controles tiveram um padrão hemimetilado, como previsto pela literatura, devido essa região ser *imprinted*. Enquanto os clones encontravam-se menos metilados. Para a região do éxon 10 do IGF2, não foi encontrada diferença significativa entre controles e clones. Estes resultados sugerem que as diferentes regiões do genoma podem se reprogramar independente umas das outras e que falhas na reprogramação do padrão de metilação do DNA de genes *imprinted* podem ser uma das causas da baixa eficiência da TNCS.

TERMOS DE INDEXAÇÃO: Epigenética, *locus,* H19, IGF2, placenta, bezerros, clonagem, imprinting, bovino.

[1] Received on August 25, 2019.
Accepted for publication on January 16, 2020.

[2] Laboratório de Reprodução Animal, Embrapa Recursos Genéticos e Biotecnologia, Parque Estação Biológica, Avenida W/5 Norte (final), Cx. Postal 02372, Brasília, DF 70770-917, Brazil. *Corresponding author: natalia.souzacosta15@gmail.com

[3] Graduate Program in Veterinary Sciences, Faculdade de Medicina Veterinária, Universidade Federal de Uberlândia (UFU), Rodovia BR-050 Km 78, Campus Glória, Uberlândia, MG 38410-337, Brazil.

[4] Embrapa Recursos Genéticos e Biotecnologia, Parque Estação Biológica, Avenida W/5 Norte (final), Cx. Postal 02372, Brasília, DF 70770-917, Brazil.

[5] Geneal Genética e Biotecnologia Animal, Rodovia BR-050, Km 184, Uberaba, MG 38038-050, Brazil.

INTRODUCTION

Somatic Cell Nuclear Transfer Cloning (SCNT) is one of the promising biotechniques in reproduction. This technique is based on the production of genetically identical individuals. This is because the oocyte cytoplasm contains specific epigenetic machinery that can reprogram the nucleus of somatic cells in an undifferentiated state, which can generate a viable embryo (Wilmut et al. 1997). The SCNT has potential applications, such as in the production of animals of high commercial value, in biomedicine with the use of xenotransplants, in the maintenance of animals at risk of extinction (Cibelli et al. 1998), and in the production of transgenic and genetically edited animals (Petersen 2017).

After Dolly, the first mammal to be cloned, several species have already been successful with NT. (Wilmut et al. 1997). However, its efficiency remains low (Rodriguez-Osorio et al. 2012). The rates of embryos with full-term development and birth are mainly below 5% (Wells et al. 1999). The main cause for the aberrant phenotypes found in cloning is believed to be related to failures in the epigenetic reprogramming of the nucleus donor cell, leading to changes in global gene expression and imprinted genes (Mann et al. 2003).

Epigenetics is an area of genetics that studies gene function changes that are not directly related to changes in the primary DNA sequence (Dupont et al. 2009). Epigenetic profiles can persist for generations, so they are inheritable. However, external factors can be altered, such as nutrition, environment, use of drugs, toxins, etc. (Reik 2007).

Research has shown that assisted reproduction techniques (ARTs) cause epigenetic changes in the conceptuses. For example, at SCNT, embryos are exposed to different microenvironments, in vitro maturation, and in vitro cultivation, which can interfere with their development (Wells et al. 1999). It can be concluded that these techniques also act as an external factor, assessing the potential for term development or even in the conception of healthy animals (Lucifero et al. 2004, Smith et al. 2012, Urrego et al. 2014).

DNA methylation is one of the prominent epigenetic marks responsible for epigenetic inheritance between generations (Migicovsky & Kovalchuk 2011). This epigenetic mark is characterized by the methyl group (CH3), linked to a cytosine that precedes guanine in a place called 5'-CpG-3 '(Smith & Meissner 2013). DNA methylation plays a fundamental role in controlling gene expression, maintaining genome integrity, regulating genomic imprinting, and inactivating the X chromosome, indispensable in cell differentiation and early development (Dean et al. 2003).

Gametes are responsible for transmitting genetic and epigenetic information to the next generation. They undergo extensive epigenetic reprogramming, making these cells suitable for fertilization and embryogenesis (Reik 2007). Stable patterns of genomic methylation are generally inherited in differentiated somatic cells, but only in gametogenesis, and during the beginning of embryogenesis, these patterns are reprogrammed in two waves of demethylation remethylation (Fig.1), (Reik 2007). In clones, this reprogramming is done in a shorter period and a different cellular context when compared to normal development, increasing the probabilities of failures in the process (Murrell et al. 2001).

Genomic imprinting is an epigenetic mechanism that causes monoallelic expression of genes according to the allele's parental origin. That is, of the two inherited copies, only one allele is expressed. Its main epigenetic mark is DNA methylation, established during gametogenesis (Barlow & Bartolomei 2014). Imprinted genes are generally related to behavior, metabolism, fetal growth, and postnatal development (Daelemans et al. 2010). Two imprinted genes essential in embryonic growth and development are IGF2 and H19 (Gebert et al. 2006). The IGF2 is responsible for inducing fetal growth and development and is related to the placenta's development by its mitogenic power, promoting cell division and differentiation (O'dell & Day 1998, Gebert et al. 2006). The H19 gene, on the other hand, regulates a non-coding RNA molecule responsible for inhibiting IGF2 expression (Brannan et al. 1990). As it has an imprinted pattern, only the maternal allele is transcribed. The opposite is true with IGF2, for which only the paternal allele is expressed (Fig.2) (Daelemans et al. 2010).

This study aimed to characterize the methylation pattern of the differentially methylated region of exon 10 of the IGF2 gene and the imprinting controlling region of the IGF2/H19 *locus* in the fetal placenta of cloned calves.

MATERIALS AND METHODS

The experiment was developed at "Laboratório de Reprodução Animal" of "Embrapa Recursos Genéticos e Biotecnologia" in Brasília, Distrito Federal, Brazil.

Experimental design. This study's biological material was fetal cotyledon of the bovine placenta of the Nellore breed (*Bos taurus indicus*). All the material was collected at "Geneal Genética e Biotecnologia Animal", in Uberaba/MG. With this material, the DMR methylation pattern of exon 10 of the IGF2 gene and ICR H19 was analyzed in the placenta of female and male clones, with healthy and aberrant phenotypes. The clones were aberrant when they presented at least one of the following phenotypes: thick umbilical cord, mortality in the first week, LOS, placental edema, large placentoma, meconium-tinged placental fluid. As controls, placentas from two animals, one male, and one female, produced by artificial insemination, were used (Table 1). The Ethics Committee on Animal Use (protocol CEUA No. 078/16) of the "Universidade Federal de Uberlândia", Minas Gerais, Brazil, approved all procedures performed.

Isolation of genomic DNA. Genomic DNA was isolated by the salting-out method as described by Biase et al. (2002). Then, it was submitted to quality evaluation by electrophoresis in 1% agarose gel. Concentration and purity were assessed with a NanoDrop spectrophotometer (Thermo Fisher Scientific, Waltham/MA, EUA). Genomic DNA samples were stored at -20°C.

Treatment of genomic DNA with sodium bisulfite. This technique allows DNA methylation analysis, as it converts unmethylated cytosines into uracils through sodium bisulfite. The kit used for this treatment was EZ DNA Methylation® (Zymo Research, Irvine/CA, USA), following the manufacturer's recommendations. The treated DNA was stored at -80°C. According to Zhang et al. (2016), the methylation pattern is classified as hypomethylated (0% to 20%), hemimethylated (21% to 50%), and hypermethylated (51% to 100%).

DNA samples treated with sodium bisulfite were subjected to PCR using the thermal cycler T100 Thermal Cycler (Bio-Rad). The regions of interest were the ICR of the H19 gene and the DMR of exon 10 of the IGF2 gene. The sequences of the primers used for DNA amplification, the *GenBank* access number, the CpG island position, the location and size of the amplified fragments are shown in Table 2.

PCR reactions for both regions were performed using 1x buffer solution; 2.0mM $MgCl_2$; 0.4 mM dNTP; 1U of Taq DNA Polymerase Platinum (Invitrogen, Carlsbad/CA, USA) and 1uM of each of the primers (forward and reverse), the volume being adjusted to 20uL with Milli-Q water. The amplification conditions are described in Table 3.

The amplicons were subjected to electrophoresis in 1.8% agarose gel, stained with ethidium bromide (10 mg/ml) at a constant electric current of 50mA in 0.5 X TBE medium. The marker used was 1 Kb Plus molecular weight DNA Ladder® (Invitrogen, Carlsbad/CA, USA). The gel was photographed on a photo documenter (BioRad). According to the manufacturer, the amplicons were cut out of the gel and purified using the Wizard® SV Gel and PCR Clean-Up System kit (Promega, Madison/WI, USA) standards. The samples were then quantified on a NanoDrop® spectrophotometer (ND-1000) (Thermo Scientific, Asheville/NC, USA).

Cloning of PCR products and extraction of plasmid DNA. The TOPO TA Cloning® (Invitrogen) vector was used to clone the amplicons. DH5α cells were transformed using a heat shock protocol. Then they were placed in a 90x15mm petri dish containing agar with 100ug/mL ampicillin, 40µL of 20mg/mL X-Gal (Sigma), and 4µL of 0.1 M IPTG (Sigma), followed by plate inversion and incubation in an oven at 37°C for 14 hours.

The white colonies were selected to be grown in Luria Bertani (LB) medium plus ampicillin at 100ug/mL. With a sterile wooden toothpick, the colonies were removed and deposited inside a 15mL collection tube containing 3mL of LB medium. The tubes were stirred at 250rpm at 37°C for 16 hours in a shaker (New Brunswick Scientific Co, NJ, USA). According to the plasmid mini-preparation protocol, half the contents of the tubes were used for the extraction of plasmid DNA. The dry pellets were eluted in 20µL of deionized water and the DNA quantified in a spectrophotometer. NanoDrop® (ND- 1000) (Thermo Scientific, Asheville/NC, USA).

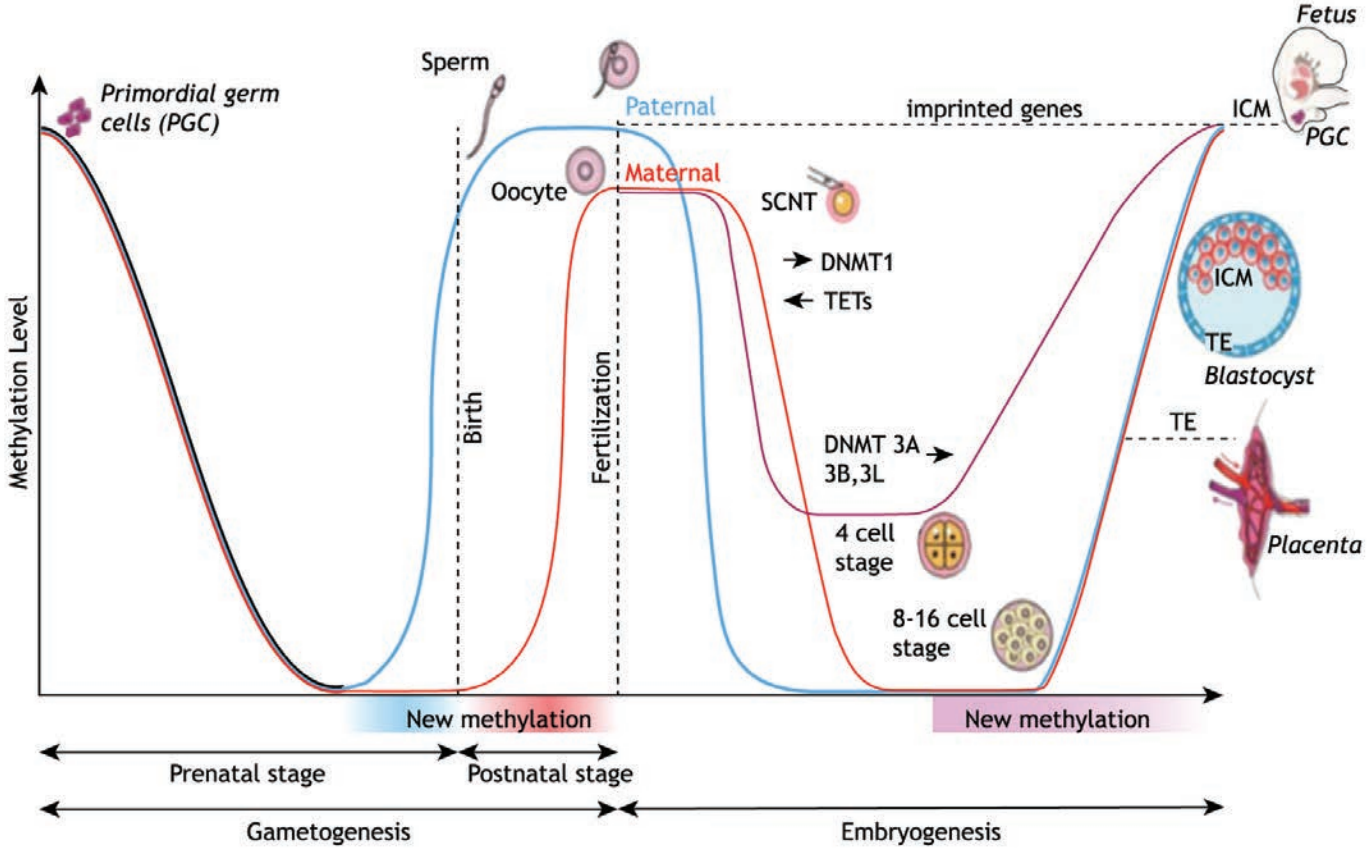


Fig.1. Epigenetic reprogramming in mammals. In gametogenesis, the primordial germ cells (PGC), paternal and maternal genomes (blue and red lines, respectively) undergo global demethylation of the genome, including also in differentially methylated regions of germline (gDMRs) (black line). In male fetuses, methylation again begins during fetal life (prenatal stage), and at birth, the paternal genome already has a high level of methylation (postnatal stage) (blue line). In female fetuses, the acquisition of methylation again begins whenever an oocyte is recruited to proceed with oogenesis but is only completed after puberty, with appropriate hormonal stimuli (postnatal stage) (red line). In embryogenesis, after fertilization and before DNA replication, TETs enzymes actively demethylate the paternal genome (blue line). Global remodeling occurs with the exchange of protamines for maternal histones (not shown). In contrast, the maternal genome is demethylated after several cell divisions by a passive mechanism (red line) due to the removal of DNMT1 from the nucleus. In bovine embryos, starts again, methylation of the two parental genomes, catalyzed by DNMTs 3A, 3B, and 3L, begins around the 8-16 cell stage. The purple line represents the reprogramming of DNA methylation in clone embryos, showing that an inefficient loss of methylation occurs after nuclear transfer, and the methylation starts again early, in the 4-cell stage. The first cell differentiation occurs in the blastocyst phase, generating the trophoblast cells (TE), which will originate from the placenta, and the internal cell mass (ICM), originating from the fetus. The dashed gray lines represent the imprinted genes' alleles, with the upper line representing the methylated alleles and the lower, the non-methylated alleles. The graph is not represented in scales and does not show the exact proportion of methylation. Adapted from Vargas (2018).

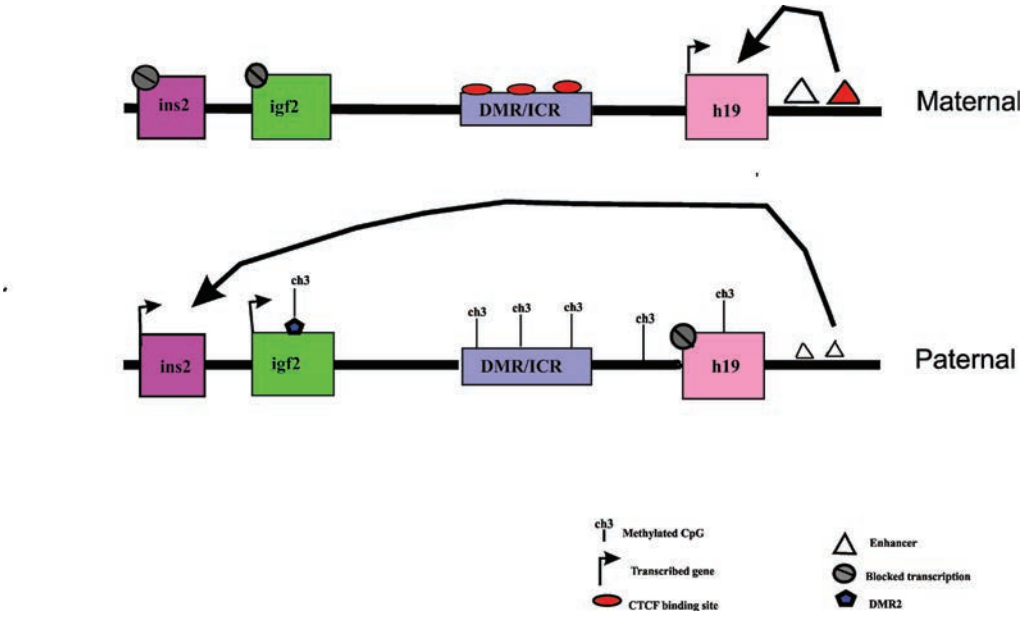


Fig.2. Regulation mechanism of the H19 and IGF2 gene. This figure depicts the maternal and paternal alleles for the IGF2/H19 *locus*. In the maternal allele, CTCF binds to the demethylated region of ICR/H19, blocking enhancers' binding to the promoter region of the IGF2 gene, silencing it. Enhancers promote the transcription of the H19 gene in the maternal allele. In the paternal allele, the ICR/H19 region is methylated. Therefore, there is no binding of the CTCF, and the enhancers approach the IGF2 promoter, triggering the IGF2 transcription. Adapted from Bartolomei (2009).

Table 1. Animals selected for the study, according to sex, phenotypes and viability (survival in the first week of birth)

Animals selected for the study				
Individual	Sex	Phenotypes	Viability	Classification
Clone	Female	No changes	Survived the 1st week	Healthy
Clone	Female	Large placentoma, LOS, thick umbilical cord	1st week mortality	Aberrant
Clone	Male	No changes	Survived the 1st week	Healthy
Clone	Male	LOS, placenta edema, thick umbilical cord, large placentoma, placental-meconium fluid	1st week mortality	Aberrant
A.I.	Female	No changes	Survived the 1st week	Healthy
A.I.	Male	No changes	Survived the 1st week	Healthy

Material provided by the company "Geneal Genética and Biotecnologia Animal", Uberaba/MG; A.I. = artificial insemination.

Table 2. Identification of the gene, primer sequences, GenBank access code, location of the primers, position of the CpG island and size of the amplified fragment

Gene	Sequence of primers (5' - >3')	Access to GenBank	Number of CpGs sites	Island position CpG	Amplicon size
ICR/H19	F: GGTGATATAGGGTAGTGTGTAGAGGATATTGGGG	Nc-037356.1	23	DMR1	423bp
	R: ATACTACTAAAAATCCCATAAAAAAAATCTCTCTC			ICR/H19*	
IGF2	F: TGGGTAAGTTTTTTTAATATGATATT	X53553.1	28	Exon 10	455bp
	R: TTTAAAACCAATTAATTTTATACATT				

F = forward, R = reverse, bp = base pairs, DMR1 = differentially methylated region 1 within the ICR/H19*, Primer IGF2 = Gebert et al. (2006), Primer ICR/H19 = Jenna et al. (2014).

Table 3. Amplification conditions used in the PCR for the ICR/H19 imprinting controlling region and for the differentially methylated region of the IGF2 gene

Locus	Initial denaturation	Cycles (40 for ICR and 45 for IGF2)			Final extension
		Denaturation	Annealing	Extension	
ICR/H19	94°C	94°C	58°C	72°C	72°C
	3 min	40s	1 min	1 min	15 min
DMR IGF2	94°C	94°C	45°C	72°C	72°C
	3 min	40s	1 min	1 min	15 min

CRI = controlling region of *imprinting,* DMR = differentially methylated region.

Plasmidial DNA sequencing and sequence analysis. The digestion of the miniprep samples for confirmation of cloning used the ECOR1 enzyme (5U), the H buffer (1X), and the miniprep DNA (2ul) adjusted with Milli-Q water to 10uL. The samples were incubated in a water bath at 37°C overnight. The digestion products were submitted to electrophoresis in 1.5% agarose gel stained with ethidium bromide 10mg/mL to confirm fragments' presence. Plasmidial DNA samples (~300ng) were sequenced using the universal primer M13 reverse by the Sanger method.

The Chromas® program verified the quality of the sequencing. For the quantification of the methylation pattern, the QUMA program was used, comparing the sequences obtained with the reference deposited in *GenBank*, both for ICR/H19 (X53553.1) and IGF2 (Nc-037356.1). In this study, only rows that presented at least 97% of conversion by sodium bisulfite - when the conversion rate of cytosines not followed by guanine and lines with at least 95% identity was observed - when compared with the reference sequence.

Statistical analysis. For statistical analysis, the GraphPad Prism software[5] was used. Kruskal-Wallis or Mann-Whitney analysis compared the animals experimental treatments. The means and standard deviations were verified using the Action version 2.9 program. The results were described as mean ± standard error of the mean. *P*-value ≤0.05 denotes a statistically significant difference.

RESULTS

The ICR/H19 showed the following methylation percentages: 20.916±7.016% for a female clone with a healthy phenotype, 24.907±9.785% for a male clone with a healthy phenotype, 32.592±10.598% for a female clone with aberrant phenotype, and 28.584±9.771% for clone male with aberrant phenotype. The percentage of methylation for the control group was 30.06±10.910% for females and 75.016±10.667% for males (Fig.3).

Concerning exon 10 of IGF2, the following percentages of methylation were found: 20.644±11.968% for a female clone with a healthy phenotype, 35.571±16.065% for a male clone with a healthy phenotype, 34.34±13.909% for a female clone with aberrant phenotype, and 10.727±8.288% for a male clone with aberrant phenotype. The percentage of methylation for the control group was 44.65±41.05% for females and 30.858±8.928% for males (Fig.4).

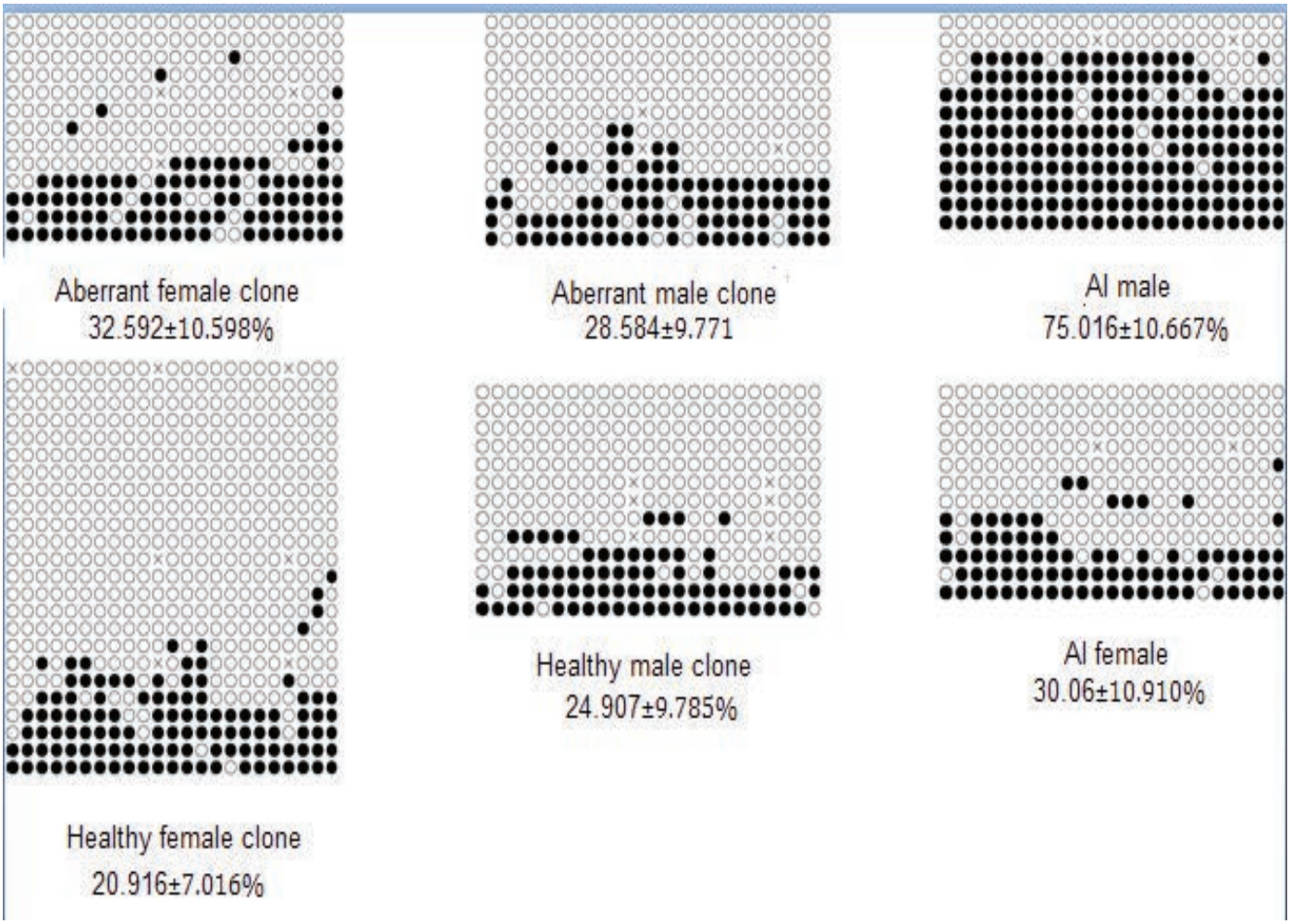


Fig.3. Methylation pattern of ICR/H19 in the placenta (cotyledon) of healthy and aberrant female and male bovine clones, and female and male conceived by artificial insemination (AI, controls). Each line represents one, where each circle is equivalent to a cytosine in the context of CpG dinucleotide. White circles represent unmethylated cytosines, and black circles represent methylated cytosines. An X represents cytosines that could not be analyzed. The animals and the DNA methylation percentages are represented under each group and were presented as mean.

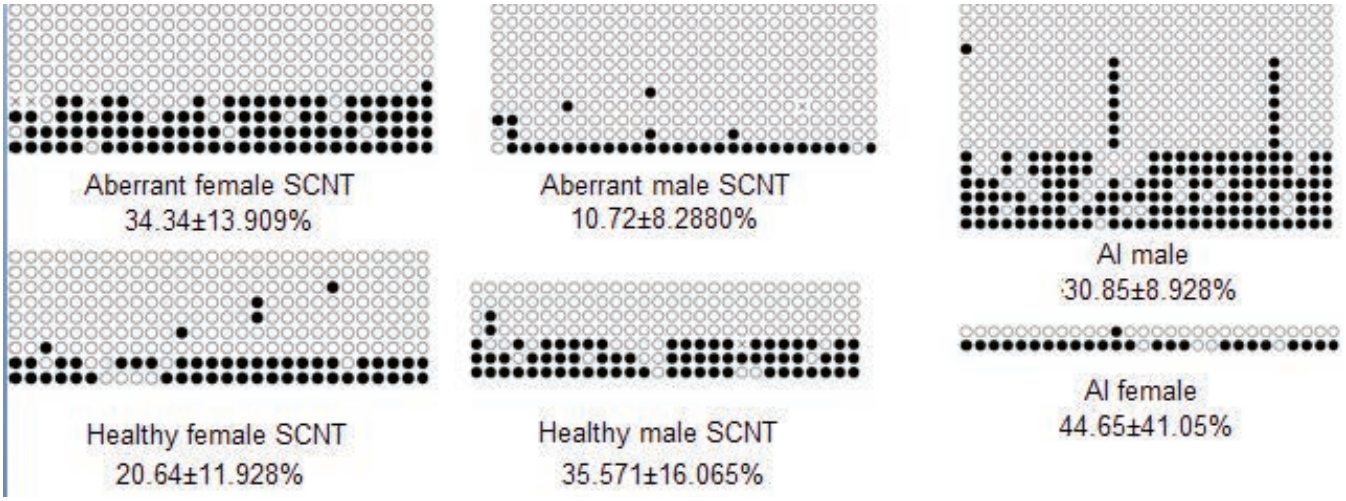


Fig.4. Methylation pattern of exon 10 of the IGF2 gene in the placenta (cotyledon) of healthy and aberrant female and male bovine clones, and females and males conceived by artificial insemination (AI, controls). Each line represents one, where each circle is equivalent to a cytosine in the context of CpG dinucleotide. White circles represent unmethylated cytosines, and black circles represent methylated cytosines. An X represents cytosines that could not be analyzed. The animals and the DNA methylation percentages are represented under each group and were presented as mean.

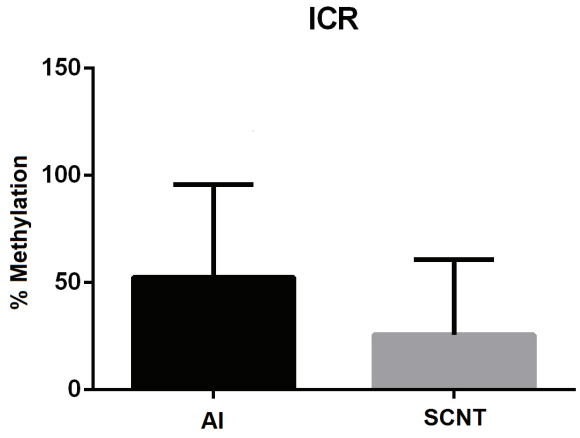


Fig.5. Methylation rate for the ICR/H19 region. Each bar represents a group studied: AI (controls by artificial insemination) and Somatic Cell Nuclear Transfer (SCNT, all clones studied for ICR/H19-aberrant and healthy). The results are represented as mean ± standard deviation from the mean (p<0.05).

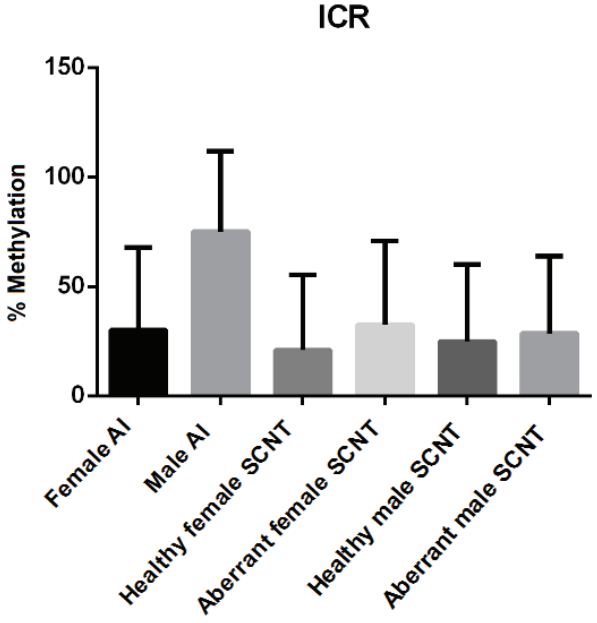


Fig.6. Methylation rate for the ICR/H19 region. Each bar represents a studied group: female artificial insemination (AI), male AI, healthy female Somatic Cell Nuclear Transfer (SCNT), aberrant female SCNT, healthy male TNCS and, aberrant male SCNT. The results are represented as mean ± standard deviation from the mean (p<0.05).

According to the results obtained for the ICR/H19 region, the control animals, as predicted by the literature, obtained, on average, a methylation pattern of approximately 50%, while the clones are less methylated (Fig.5 and 7).

Furthermore, individualizing the comparison of clones with controls, H19 of ICR was found in placenta calf clones, a significant difference from controls only with healthy phenotype clones (0.0089) (Fig.6 and 7), the other clones did not show significant differences in the control. When comparing the aberrant clones and healthy clones, for the H19 of ICR, there was no significant difference in the methylation pattern (Fig.6 and 7).

Evaluating the methylation pattern of exon 10 of IGF2 in the placenta of clones compared to the control group conceived by artificial insemination, there was no significant difference between them (Fig. 8 and 10). The comparison of the methylation pattern of aberrant clone X healthy clone, for exon 10 of IGF2, also had no significant changes (Figures 9 and 10). However, a hypomethylated pattern can be observed in the aberrant clones for the exon 10 region of IGF2 (Fig.8-10).

The methylation pattern of both ICR/H19 and exon 10 of IGF2 for the clones used in this study showed a lesser methylated pattern than the controls (Fig.11-13).

DISCUSSION

Despite the significant advance of the nuclear transfer cloning technique, its efficiency remains low (Rodriguez-Osorio et al. 2012). It is possible to verify high rates of losses during the whole pregnancy and after birth in several species due to placental disorders and aberrant phenotypes in clone animals (Chavatte-Palmer et al. 2004). Among the several disorders that clones present in their embryonic attachments are: very thick umbilical cord, edema in the placenta, large placentomas (Hashizume et al. 2002). The leading cause of these problems in fetuses and their placentas is believed to be related to epigenetic errors involved in embryonic development, such as failures in the nuclear reprogramming process (Chavatte-Palmer et al. 2004). For example, genomic imprinting is indispensable for the individual's normal development (Reik et al. 2003). If not established correctly, it can damage the regulation of growth and development of the fetus and the placenta (Reik et al. 2003).

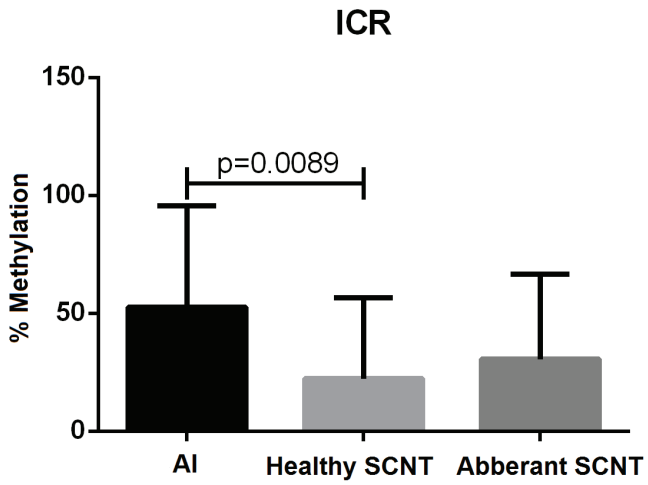


Fig.7. Methylation standard for the ICR/H19 region. Each bar represents a studied group: artificial insemination (AI), healthy Somatic Cell Nuclear Transfer (SCNT), aberrant SCNT. The results are represented as mean ± standard deviation from the mean (p<0.05).

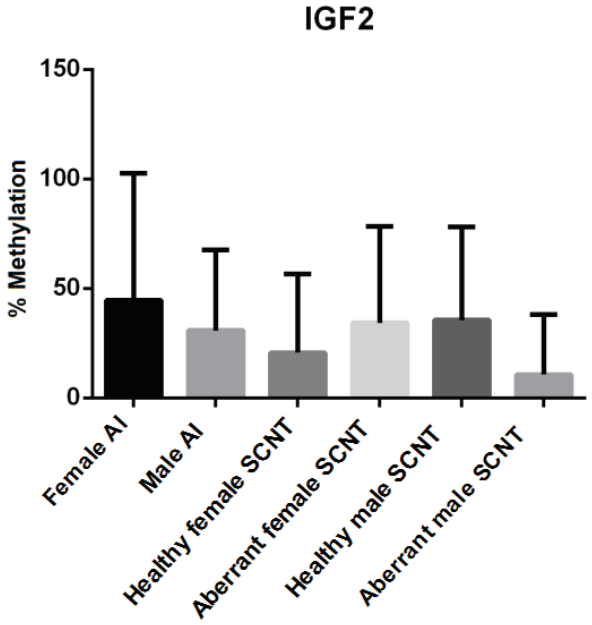


Fig.9. Methylation rate for exon 10 region of IGF2. Each bar represents a studied group: female artificial insemination (AI), male AI, healthy female Somatic Cell Nuclear Transfer (SCNT), aberrant female SCNT, healthy male SCNT, and aberrant male SCNT. The results are represented as mean ± standard deviation from the mean (p<0.05).

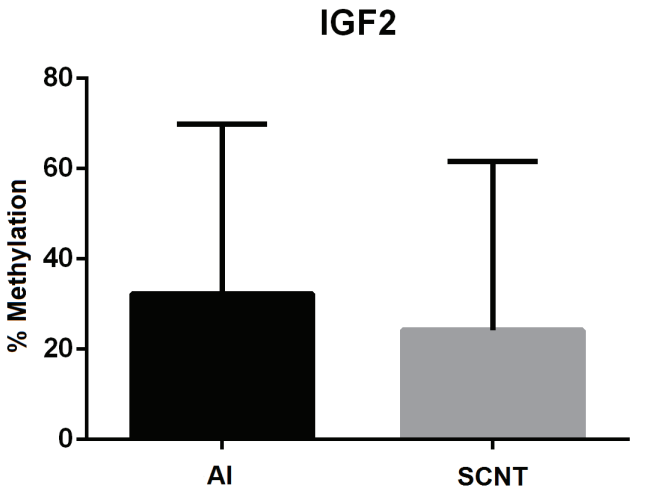


Fig.8. Methylation rate for exon 10 region of IGF2. Each bar represents a group studied: AI (controls by artificial insemination) and, Somatic Cell Nuclear Transfer (SCNT, all clones studied for exon 10 of IGF2 - aberrant and healthy). The results are represented as mean ± standard deviation from the mean (p<0.05).

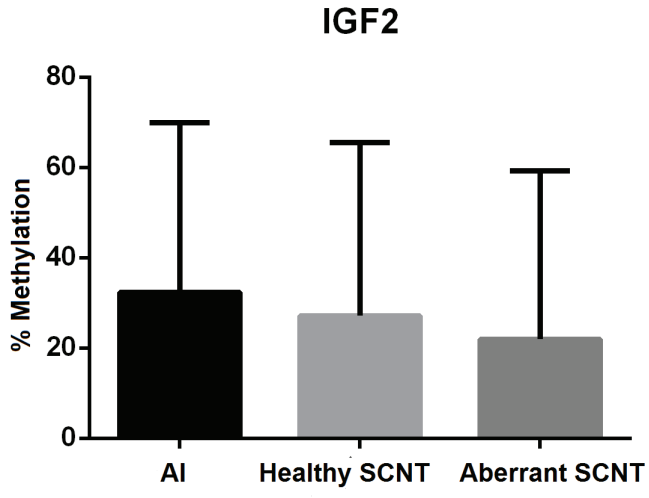


Fig.10. Methylation pattern for the exon 10 region of IGF2. Each bar represents a studied group: artificial insemination (AI), healthy Somatic Cell Nuclear Transfer (SCNT), aberrant SCNT. The results are represented as mean ± standard deviation from the mean (p<0.05).

According to the results of this work, when comparing the methylation pattern of all clones with the control animals (conceived by artificial insemination), for the ICR/H19 region, we observed an imprinted pattern in the control animals with a percentage methylation rate of around 50%. This methylation pattern can be confirmed in the study by Park et al. (2009) with somatic pig cells, specifically the lung tissue, a hemimethylated pattern, proving an imprinted model, with the expression of only one allele depending on the parental origin. On the other hand, in that study, the clones were less methylated. As already shown in other works, this pattern may be due to incomplete reprogramming that occurs in clones, which may be the cause of the technique's low efficiency. (Xuexiong et al. 2017). In the work of Xuexiong et al. (2017), with fibroblasts from cloned porcine fetuses, while the controls (originated from natural fertilization) showed a 50% methylated pattern for that same region, the clones were evaluated using a hypomethylated methylation pattern. In the study by Silveira et al. (2018), in satellite, I, the placenta of cloned calves also showed less methylated than control animals.

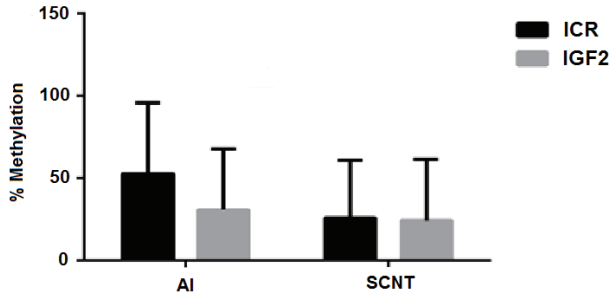


Fig.11. Comparison between methylation rate for the IC19 region of H19 and exon 10 of IGF2. Each bar represents a group studied: AI (controls by artificial insemination) and Somatic Cell Nuclear Transfer (SCNT, all clones studied for the two regions). The results are represented as mean ± standard deviation from the mean (p<0.05).

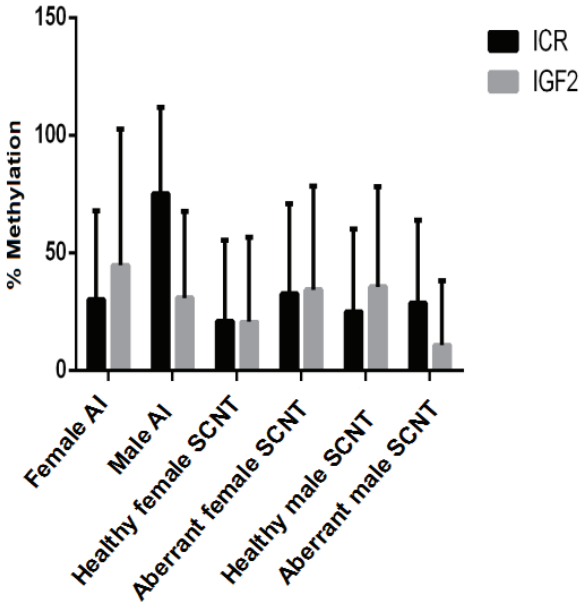


Fig.12. Comparison of the methylation rate for the ICR region of H19 and Exon 10 of IGF2. Each bar represents a studied group: female artificial insemination (AI), male AI, healthy female Somatic Cell Nuclear Transfer (SCNT), aberrant female SCNT, healthy male SCNT, and aberrant male SCNT, for both regions. The results are represented as mean ± standard deviation from the mean (p<0.05).

In the study by Yang et al. (2005), with neonatal bovine clones, half of the animals showed a significant increase in the pattern of H19 expression; that is, the H19 ICR that controls this region was little methylated in these clones, as we found in our study. As has already been reported, the biallelic expression of this same gene (Zhang et al. 2004).

In the study of Yamazaki (2006) on the mechanism of genomic imprinting in the placenta of bovine clones, he found an incomplete nuclear reprogramming in the placenta of viable term-born clones. What may justify this work is that the controls present a significant difference in clones with healthy phenotypes for the region of ICR/H19.

No significant difference was found for exon 10 of IGF2 between controls X clones and aberrant clones X healthy clones. The drop in IGF2 activity in bovine placentas can lead to placental abnormalities, such as decreased numbers of placentomas, hypovascularization of the placenta, and rudimentary development of some placental attachments (Yamazaki 2006). However, its elevation can lead to a range of syndromes, such as Beckwith-Wiedemann syndrome (BWS), characterized by exacerbated growth (Engel et al. 2000, Robbins et al. 2012). Probably, with a larger sample number, a significant difference would be found between the groups evaluated here in this study.

The study by Yamazaki (2006) revealed that a significant change in the pattern of expression of the H19 and IGF2 genes was revealed in the placenta of bovine clones compared to controls, with less expression of these "imprinted" genes, contributing to increased postnatal mortality. The rate of loss is believed to be a consequence of placental disorders, which

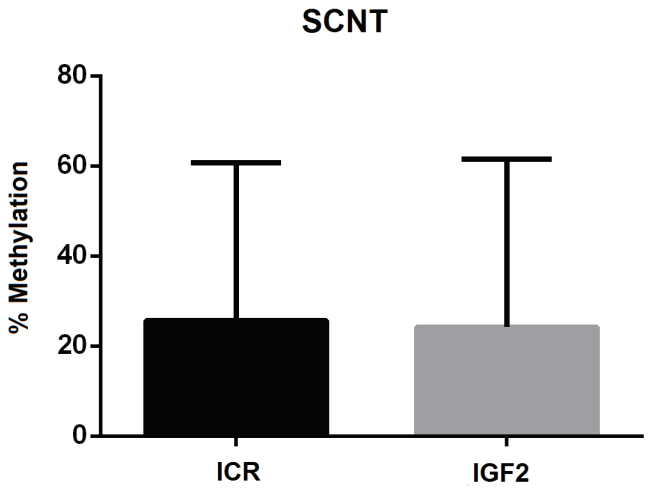


Fig.13. Comparison of the methylation pattern of the clones selected for the ICR/H19 region and of the clones selected for the exon 10 region of IGF2. The results are represented as mean ± standard deviation (p<0.05). Somatic Cell Nuclear Transfer (SCNT).

can be explained by the fact that the placenta is responsible for the exchange of gases and nutrients between mother and fetus, in addition to being important in the implantation process and early recognition of pregnancy by mother (Cross 2006). Therefore, a placenta different from the ideal, with the presence of phenotypic disorders, can interfere more in reprogramming the nucleus and regulating the fetus' gene expression. Contrary to the Yamazaki study, in the placenta of murine clones, an expression pattern for this elevated region was found (Inoue et al. 2002), suggesting a specific species change, including the different placentation process between mice and cattle (Kato et al. 1998, Humpherys et al. 2001).

This study shows a positive correlation between the two regions studied, with similar methylation patterns. Regarding expression, in mice, a negative correlation was found between IGF2 and H19. In many species (Humpherys et al. 2001), different from the study by Yamazaki (2006), it was possible to notice a positive correlation between genes. In the latter case, the decrease in H19 did not lead to an increase in IGF2, suggesting that the mechanism of regulation of imprinted genes may differences between species (Yamazaki 2006) or indicates that IGF2 is not just regulated by H19 even though there are few studies of these genes in the placenta of bovine clones, analysis of tissues from neonates clones and dead clones shortly after birth demonstrated that IGF2 expression patterns were significantly higher than in control calves (Yang et al. 2005). However, in the tissue analysis of newborn sheep clones, no difference was detected to express the IGF2 and H19 genes concerning the controls (Young et al. 2003). There is a diversity in the results of research related to these regions for clones, indicating an incomplete gene reprogramming, varying according to the epigenetic stability of the donor nucleus (Humpherys et al. 2001) or it can also indicate that it is not just these regions that determine success in embryonic development, but rather a set of genes, being well reprogrammed (Chavatte-Palmer et al. 2004).

Although efficient production of bovine clones is possible, a high mortality rate is noted during pregnancies and afterbirths (Chavatte-Palmer et al. 2004), the consequence of a set of factors, which are not reflected only in an incorrect reprogramming of the IGF2 and H19 genes, located in the study regions, but in an incomplete reprogramming of several genes involved in the development of the placenta (Hill et al. 1999, Heyman et al. 2002, Chavatte-Palmer et al. 2004). Therefore, more information is needed to clarify the epigenetic control mechanism during the development of clone animals.

CONCLUSION

The low efficiency in Somatic Cell Nuclear Transfer (SCNT) may be related to errors in nuclear reprogramming, mainly for the ICR/H19 region.

Acknowledgment.- To "Embrapa Recursos Genéticos e Biotecnologia" for providing the entire structure for carrying out this work. To "Geneal Genética e Biotecnologia Animal", for having given in to the biological samples used in this study.

Conflict of interest statement.- The authors have no conflicts of interest to declare.

REFERENCES

Barlow D.P. & Bartolomei M.S. 2014. Genomic imprinting in mammals. Cold Spring Harbor Perspectives in Biology, Cold Spring Harbor NY. 6(2)018382. <https://dx.doi.org/10.1101/cshperspect.a018382>

Bartolomei M.S. 2009. Genomic Impression: employing and avoiding epigenetic processes. Genes & Development, Cold Spring Harbor NY. 23(18):2124-2133. <https://dx.doi.org/10.1101/gad.1841409> <PMid:19759261>

Biase F.H., Franco M.M., Goulart L.R. & Antunes R.C. 2002. Protocol for extraction of genomic DNA from swine solid tissues. Genet. Mol. Biol., Ribeirão Preto, 25(3):313-315. <https://dx.doi.org/10.1590/S1415-47572002000300011>

Brannan C.I., Dees E.C., Ingram R.S. & Tilghman S.M. 1990. The product of the h19 gene may function as na RNA. Mol. Cell. Biol., Washington, 10(1):28-36. <https://dx.doi.org/10.1128/mcb.10.1.28> <PMid:1688465>

Chavatte-Palmer P., Remy D. & Cordonnier N. 2004. Health status of cloned cattle at different ages. Cloning Stem Cells, Larchmont, 6(2):94-100. <https://dx.doi.org/10.1089/1536230041372274> <PMid:15268782>

Cibelli J.B., Stice S.L., Golueke P.J., Kane J.J., Jerry J., Blackwell C., Ponce de León F.A. & Robl J.M. 1998. Cloned transgenic calves produced from nonquiescent fetal fibroblasts. Science, Washington, 280(5367):1256-1258. <https://dx.doi.org/10.1126/science.280.5367.1256> <Pmid:9596577>

CROSS J.C. 2006 Nutritional influences on implantation and placental development. Nutr. Rev., New York, 64(5 Pt 2):S512-S18. <https://dx.doi.org/10.1301/nr.may.s12-s18> <PMid:16770948>

Daelemans C., Ritchie M.E., Smits G., Abu-Amero S., Sudbery I.M., Forrest M.S., Campino S., Clark T.G., Stanier P., Kwiatkowski D., Deloukas P., Dermitzakis E.T., Tavaré S., Moore G.E. & Dunham I. 2010. High-throughput analysis of candidate imprinted genes and allele-specific gene expression in the human term placenta. BMC genetics, London, 11:25. <https://dx.doi.org/10.1186/1471-2156-11-25> <PMid:20403199>

Dean W., Santos F. & Reik W. 2003. Epigenetic Reprogramming in early mammalian development and following somatic nuclear transfer. Semin Cell Develop. Biol., Palo Alto, 14(1):93-100. <https://dx.doi.org/10.1016/s1084-9521(02)00141-6> <PMid:12524012>

Dupont C., Armant D.R. & Brenner C.A. 2009. Epigenetics: definition, mechanisms and clinical perspective. Semin. Semin Reprod. Med., New York, 27(5):351-357. <https://dx.doi.org/10.1055/s-0029-1237423> <PMid:19711245>

Engel J.R., Smallwood A., Harper A., Higgins M.J., Oshimura M., Reik W., Schofield P.N & Maher E.R. 2000. Epigenotype-phenotype correlations in Beckwith-Wiedemann syndrome. J. Med. Genet., New York, 37(12):921-926. <https://dx.doi.org/10.1136/jmg.37.12.921>

Gebert C., Wrenzycki C., Herrmann D., Gröger D., Reinhardt R., Hajkova P., Lucas-Hahn A., Carnwath J., Lehrach H. & Niemann H. 2006. The bovine IGF2 gene is differentially methylated in oocyte and sperm DNA. Genomics, San Diego, 88(2):222-229. <https://dx.doi.org/10.1016/j.ygeno.2006.03.011>

Hashizume K., Ishiwata H., Kizaki K., Yamada O., Takahashi T., Imai K., Patel O.V., Akagi S., Shimizu M. & Takahashi S. 2002. Implantation and placental development in somatic cell clone recipient cows. Cloning Stem Cells 4(3):197-209. <https://dx.doi.org/10.1089/15362300260339485> <PMid:12398801>

Heyman Y., Zhou Q., Lebourhis D., Chavatte-Palmer P., Renard J.P. & Vignon X. 2002. Novel approaches and hurdles to somatic cloning in cattle. Cloning Stem Cells, Larchmont, 4(1):47-55. <https://dx.doi.org/10.1089/153623002753632048> <PMid:12006156>

Hill J. R., Roussel A.J., Cibelli J.B., Edwards J.F., Hooper N.L., Miller M.W., Thompson J.A., Looney C.R., Westhusin M. E., Robl J.M. & Stice S.L. 1999. Clinical and pathologic features of cloned transgenic calves and fetuses (13 case studies). Theriogenology, Stoneham, 51(8):1451-1465. <https://dx.doi.org/10.1016/s0093-691x(99)00089-8> <PMid:10729073>

Humpherys D., Eggan K., Akutsu H., Hochedlinger K., Rideout W.M., Biniszkiwicz D., Yanagimachi R. & Jaenisch R. 2001. Epigenetic instability in ES cells and cloned mice. Science, Washington, 293(5527):95-97. <https://dx.doi.org/10.1126/science.1061402> <PMid:11441181>

Inoue K., Kohda T., Lee J., Ogonuki N., Mochida K., Noguchi Y., Tanemura K., Kaneko-Ishino T., Ishino F. & Ogura A. 2002. Faithful expression of imprinted genes in cloned mice. Science, Washington, 295(5553):297. <https://dx.doi.org/10.1126/science.295.5553.297> <Pmid:11786635>

Jena S.C., Kumar S., Rajput S., Roy B., Verma A., Kumaresan A., Mohanty T.K., Rakesh Kumar S. & Datta T.K. 2014. Differential methylation status of IGF2-H19 locus does not affect the fertility of crossbred bulls but some of the CTCF binding sites could be potentially important. Mol Reprod Dev. New York, 81(4):350-362. <https://dx.doi.org/10.1002/mrd.22303> <PMid:24436206>

Kato Y., Tani T., Sotomaru Y., Kurokawa K., Kato J., Doguchi H., Yasue H. & Tsunoda Y. 1998. Eight calves cloned from somatic cells of a single adult. Science, Washington, 282(5396):2095-2098. <https://dx.doi.org/10.1126/science.282.5396.2095> <PMid:9851933>

Lucifero D., Mann M.R.W., Bartolomei M.S. & Trasler J.M. 2004.Gene-specific timing and epigenetic memory in oocyte imprinting. Human Mol. Genet., Oxford, 13(8):839-849. <https://dx.doi.org/10.1093/hmg/ddh104>

Mann M.R., Chung Y.G., Nolen L.D., Verona R.I., Latham K.E. & Bartolomei M.S. 2003. Disruption of imprinted gene methylation and expression in cloned preimplantation stage mouse embryos. Biol. Reprod., New York, 69(3):902-914. <https://dx.doi.org/10.1095/biolreprod.103.017293> <PMid:12748125>

Migicovsky Z. & Kovalchuk I. 2011. Epigenetic memory in mammals. Front. Genet. 2:1-7. <https://dx.doi.org/10.3389/fgene.2011.00028> <PMid:22303324>

Murrell M., Heeson S., Bowden L., Constância M., Dean W., Leksey G. & Reik W. 2001. An intragenic methylated region in the imprinted igf2 gene augments transcriptions. EMBO Reports, London, 2(12)1101-1106. <https://dx.doi.org/10.1093/embo-reports/kve248> <PMid:11743023>

O'dell S.D. & Day I.N. 1998. Molecules in focus Insulin-like growth factor II (IGF-II). Int. J. Biochem. Cell Biol. 30(7):767-771. <https://dx.doi.org/10.1016/S1357-2725(98)00048-X>

Park C.H., Kim H.S., Lee S.G. & Lee C.K. 2009. Methylation status of differentially methylated regions at Igf2/H19 locus in porcine gametes and preimplantation embryos. Genomics, San Diego, 93(2):179-186. <https://dx.doi.org/10.1016/j.ygeno.2008.10.002> <PMid:18983907>

Petersen B. 2017. Basics of genome editing technology and its application in livestock species. Reprod. Domest. Anim., Zuchthygiene, 52(Supl.3):4-13. <https://dx.doi.org/10.1111/rda.13012> <PMid:28815851>

Reik W. 2007. Stability and flexibility of epigenetic gene regulation in mammalian development. Nature, London, 24:425-432. <https://dx.doi.org/10.1038/nature05918> <PMid:17522676>

Reik W., Constancia M., Fowden A., Anderson N., Dean W., Ferguson-Smith A., Tycko B. & Sibley C. 2003. Regulation of supply and demand for maternal nutrients in mammals by imprinted genes. J. Physiology, Bethesda, 547(Pt 1):35-44. <https://dx.doi.org/10.1113/jphysiol.2002.033274> <PMid:12562908>

Robbins K.M., Chen Z., Wells K.D. & Rivera R.M. 2012. Expression of KCNQ1OT1, CDKN1C, H19, and PLAGL1 and methylation patterns with the KvDMR1 and H19/IGF2 imprinting control regions is conserved between human and bovine. J Biomed Sci. 19:95. <https://dx.doi.org/10.1186/1423-0127-19-95> <PMid:23153226>

Rodriguez-Osorio N., Urrego R., Cibelli J.B., Eilertsen K. & Memili E. 2012. Reprogramming mammalian somatic cells. Theriogenology, Stoneham, 78(9):1869-1886. <https://dx.doi.org/10.1016/j.theriogenology.2012.05.030> <PMid:22979962>

Silveira M.M., Salgado B., Henrique X., Dos Santos M.A., Borges N.A., Vargas L.N., Caetano A.R., Rumpf R. & Franco M.M. 2018. DNA methylation profile at a satellite region is associated with aberrant placentation in cloned calves. Placenta, Washington, 70:25-33. <https://dx.doi.org/10.1016/j.placenta.2018.08.007>

Smith L.C., Suzuki J., Goff A.K., Filion F., Therrien J., Murphy B.D., Kohan-Ghadr H.R., Lefebvre R., Brisville A.C., Buczinski S., Fecteau G., Perecin F. & Meirelles F.V. 2012. Developmental and epigenetic anomalies in cloned cattle. Reprod. Domest. Anim., Berlin, 47(Supl.4):107-114. <https://dx.doi.org/10.1111/j.1439-0531.2012.02063.x> <PMid:22827358>

Smith Z.D. & Meissner A. 2013. DNA methylation: roles in mammalian development. Nat. Rev. Genet., London, 14(3):204-220. <https://dx.doi.org/10.1038/nrg3354> <PMid:23400093>

Urrego R., Rodriguez-Osorio N. & Niemann H. 2014.Epigenetic disorders and altered gene expression after use of Assisted Reproductive Technologies in domestic cattle. Epigenetics Chromatin, London, 9(6):803-815. <https://dx.doi.org/10.4161/epi.28711> <PMid:24709985>

Vargas L.M. 2018. Perfil transcricional de genes relacionados com a reprogramação da metilação do DNA em placenta de bovinos clones. Master's Thesis in Genetics and Biochemistry, Instituto de Genética e Bioquímica, Universidade Federal de Uberlândia. Avalaible at <https://repositorio.ufu.br/bitstream/123456789/22391/3/PerfilTranscricionalGenes.pdf> Accessed on Dec. 15, 2018.

Wells D.N., Misica P.M. & Tervit H.R. 1999. Production of cloned calves following nuclear transfer with cultured adult mural granulosa cells. Biol. Reprod., New York, 60(4):996-1005. <https://dx.doi.org/10.1095/biolreprod60.4.996> <PMid:10084977>

Wilmut I., Schnieke A.E., Mcwhir J., Kind A.J. & Campbell K.H.S. 1997. Viable offspring derived from fetal and adult mammalian cells. Nature, London, 385(6619):810-813. <https://dx.doi.org/10.1038/385810a0> <PMid:9039911>

Xuexiong S., Li F., Jiang Z., Sun Y., Li H., Gao S., Zhang L., Xue B., Zhao G., Li J., Liu Z., He H. & Huan Y. 2017. Imprinting disorder in donor cells is detrimental to the development of cloned embryos in pigs. Oncotarget, London, 8(42)72363-72374. <https://dx.doi.org/10.18632/oncotarget.20390> <PMid:29069793>

Yamazaki W. 2006. Estudo do "genomic imprinting" na placenta de clones bovinos. Doctoral Dissertation in Veterinary Sciences, Faculdade de Ciências Agrárias e Veterinárias, Universidade Estadual Paulista, Availabe at <http://fcav.unesp.br/download/pgtrabs/ra/d/1263.pdf> Accessed on Mar. 2, 2019.

Yang L., Chavatte-Palmer P., Kubota C., O'Neill M., Hoagland T., Renard J.P., Taneja M., Yang X. & Tian X.C. 2005. Expression of imprinted genes is aberrant in deceased newborn cloned calves and relatively normal in surviving adult clones. Biol. Reprod., New York, 71(4):431-438. <https://dx.doi.org/10.1002/mrd.20311> <PMid:15895469>

Young L.E., Schnieke A.E., Mccreath K.J., Wieckowski S., Konfortova G., Fernandes K., Ptak G., Kind A.J., Wilmut I., Loi P. & Feil R. 2003. Conservation of IGF2-H19 and IGF2R imprinting in sheep: effects of somatic cell nuclear transfer. Mechanisms Develop., Limerick. 120(12):1433-1442. <https://dx.doi.org/10.1016/j.mod.2003.09.006>

Zhang J., Qu P., Zhou C., Liu X., Ma X., Wang M., Wang Y., Su J., Liu J. & Zhang Y. 2017. MicroRNA-125b is a key epigenetic regulatory factor that promotes nuclear transfer reprogramming. J. Biol. Chemistry, Rockville, 292(38):15916-15926. <https://dx.doi.org/10.1074/jbc.M117.796771> <PMid:28794155>

Zhang S., Chen X., Wang F., An X., Tang B., Zhang X., Sun L. & Li Z. 2016. Aberrant DNA methylation reprogramming in bovine SCNT preimplantation embryos. Scient. Rep., London, 6:30345. <https://dx.doi.org/10.1038/srep30345> <PMid:27456302>

Zhang S., Kubota C., Yang L., Zhang Y., Page R., O'Neill M., Yang X. & Tian X.C. 2004. Genomic imprinting of H19 in naturally reproduced and cloned cattle. Biol. Reprod., New York, 71(5):540-1544. <https://dx.doi.org/10.1095/biolreprod.104.031807> <PMid:15240429>

PESQUISA VETERINÁRIA BRASILEIRA
Brazilian Journal of Veterinary Research
ISSN 0100-736X (Print)
ISSN 1678-5150 (Online)

Pesq. Vet. Bras. 40(12):1073-1076, December 2020
DOI: 10.1590/1678-5150-PVB-6668

Original Article
Animal Morphophysiology
BY-NC

Acute-phase protein concentration in bronchoalveolar lavage fluid from healthy horses[1]

Paula Alessandra Di Filippo[2]*, Luiza Maria F. Ribeiro[2], Marcos Aurélio D. Meireles[3], Francielli P. Gobbi[2] and Andressa Francisca S. Nogueira[4]

ABSTRACT.- Di Filippo P.A., Ribeiro L.M.F., Meireles M.A.D., Gobbi F.P. & Nogueira A.F.S. 2020. **Acute-phase protein concentration in bronchoalveolar lavage fluid from healthy horses.** *Pesquisa Veterinária Brasileira 40(12):1073-1076.* Laboratório de Clínicas e Cirurgia Veterinária, Centro de Ciências e Tecnologias Agropecuárias, Universidade Estadual do Norte-Fluminense Darcy Ribeiro, Av. Alberto Lamego 2000, Campos dos Goytacazes, RJ 28013-602, Brazil. E-mail: pdf@uenf.br

Bronchoalveolar lavage fluid (BALF) was analyzed to obtain information on leakage of acute-phase proteins from the blood into the respiratory lumen and about local synthesis. Ceruloplasmin, transferrin, albumin, α_1-antitripsin, immunoglobulin G heavy, immunoglobulin G light, immunoglobulin A, haptoglobin, acidic glycoprotein, and P23 were measured in BALF from 30 horses without inflammatory disease by sodium dodecyl sulfate polyacrylamide gel electrophoresis (SDS-PAGE). In serum, the same proteins were identified except for α_1-antitrypsin. In conclusion, this study demonstrated that polyacrylamide gel electrophoresis (SDS-PAGE) can be used for the determination of acute-phase proteins in BALF samples from horses. In healthy horses, the values are very low, but they can be compared with reference values to assist in the diagnosis of animals with respiratory diseases.

INDEX TERMS: Acute-phase, protein, bronchoalveolar lavage, healthy horses, inflammatory airway disease, inflammatory biomarker, electrophoresis, equine.

RESUMO.- [**Proteínas de fase aguda do lavado broncoalveolar de equinos hígidos.**] O líquido obtido através da lavagem broncoalveolar (LBA) foi analisado para obter informações sobre as proteínas da fase aguda. Ceruloplasmina, transferrina, albumina, α1-antitripsina, imunoglobulina G pesada, imunoglobulina G leve, imunoglobulina A, haptoglobina, glicoproteína ácida e P23 foram medidas nos LBA de 30 cavalos sem doença inflamatória por eletroforese em gel de poliacrilamida com dodecilsulfato de sódio (SDS-PAGE). No soro, as mesmas proteínas foram identificadas, exceto a α1-antitripsina. Em conclusão, este estudo demonstra que a eletroforese em gel de poliacrilamida (SDS-PAGE) pode ser usada para a determinação de proteínas de fase aguda em amostras de LBA em cavalos. Em cavalos saudáveis, os valores são muito baixos, no entanto, podem ser comparados e auxiliar no diagnóstico de animais com doenças respiratórias.

TERMOS DE INDEXAÇÃO: Proteína, fase aguda, lavado, broncoalveolar, equinos hígidos, inflamação das vias aéreas, biomarcador inflamatório, eletroforese equina.

INTRODUCTION

The lungs and airways are mucosal surfaces commonly exposed to invading pathogens and environmental contaminants (Kyd et al. 2001). As a result, the airway inflammatory airway disease (IAD) is a common cause of poor performance, exercise intolerance, interruption of training, and premature retirement of horses (Sweeney et al. 1992, Wilkins 2003, Couëtil et al. 2007). However, recognition of IAD in a horse usually requires more than just clinical assessment, because many horses do not display obvious clinical signs. In these cases, the implementation of biomarkers specific for lung inflammation can facilitate its diagnosis (Bullone et al. 2015).

[1]Received on June 9, 2020.
Accepted for publication on September 10, 2020.
[2]Laboratório de Clínicas e Cirurgia Veterinária (LCCA), Centro de Ciências e Tecnologias Agropecuárias (CCTA), Universidade Estadual do Norte Fluminense Darcy Ribeiro (UENF), Av. Alberto Lamego 2000, Parque Califórnia, Campos dos Goytacazes, RJ 28013-602, Brazil. E-mails: f.feitosaribeiro@gmail.com, franci_gobbi@hotmail.com; *Corresponding author: pdf@uenf.br

[3]Instituto Federal de Minas Gerais (IFMG), Campus Bambuí, Fazenda Varginha, Rodovia Bambuí/Medeiros Km 5, Bambuí, MG 38900-000, Brazil. E-mail: marcosadmeireles@yahoo.com.br

[4]Universidade Federal do Tocantins (UFT), Rua Dois 34, Conj. Res. Patrocínio, Araguaína, TO 65907-230, Brazil. E-mail: dessafsn@yahoo.com.br

In equine medicine, measurement of acute-phase proteins (APPs) is used to determine of the presence, prognosis, degree and time course of inflammation, since these proteins are released in large quantities to the bloodstream in response to infection or traumatic injury (Hultén & Demmers 2002).

Acute-phase proteins modulate leukocyte function and migration, activating the complement cascade, preventing the loss of iron through the formation of stable complexes with free hemoglobin, and in some cases presenting anti-inflammatory properties (Crisman et al. 2008). While the main source is the liver, some acute-phase proteins are also produced in the lungs (Yang et al. 1995, Upragarin et al. 2005). Measuring local levels of APP increases the accuracy of diagnosis by providing information on the inflammatory/infectious status of the organ of specific interest (Jacobsen 2007). However, this potential has been little explored in horses. The aim of this study was to measure the acute-phase proteins in bronchoalveolar lavage fluid (BALF) of healthy horses, to identify and quantify local markers that can help discriminate horses with and without airway inflammation.

MATERIALS AND METHODS

This study was approved by the ethics committee on animal experiments of Darcy Ribeiro Norte Fluminense State University (CEUA-UENF) under protocol number 901139. Horses were examined for 3 successive days from the day of admission until discharge. A total of 30 crossbreed female horses (age 5±2 years, BDW 400±25kg) were examined, which had no clinical signs or history of respiratory disease. All horses were kept in semi-confinement, in 10m^2 stalls with cement floor and no bedding. Feeding included 3 to 4kg/day of commercial horse concentrate per animal, containing 12% total protein, 4kg of Coast-Cross hay/animal per day, mineral salt, and water *ad libitum*. The animals were dewormed every four months and vaccinated against influenza, tetanus, rabies, equine adenitis, and leptospirosis. The horses had no history of respiratory disease, no acute signs of infection (leukocytosis, fever, depression), no tracheal secretions, low cellular density and neutrophils ≤10% in BALF cytology or medical treatment during the 30 days preceding data collection. The animals included were considered healthy after a routine physical evaluation, pulmonary auscultation and percussion, endoscopic examination, complete blood count, and cytological analysis of bronchoalveolar lavage fluid, according to the values described by Viscardi et al. (2015), and Couëtil et al. (2016).

Bronchoalveolar lavage was performed with the horses standing using a special silicone BAL catheter (BIVONA®), under mild sedation (detomidine, 0.5mg/kg bwt i.v). The catheter was placed through the nostril, advanced through the trachea until it became trapped in a distal bronchus. The cuff was then filled with 8mL of air, and 250mL of warm (37°C) sterile 0.9% saline, divided into 3 boluses, were sequentially instilled and immediately aspired. Samples were considered adequate if at least 40% of the infused liquid was recovered and when surfactant action and turbidity were observed. After collection, the aliquots of BALF were pooled and macroscopically examined to evaluate the color, transparency, and presence of flocculent debris. Flocculent samples were filtered through two layers of gauze to remove excess mucus strands and other debris.

The samples were maintained at -4°C in sterile test tubes for cytological processing and at -20°C for APP determination. Within 1 hour of collection, the samples used in the cytological analysis were cytocentrifuged (Cytopro 7620, Wescor®) at 110*g* for 5 min and stained with May-Grunwald Giemsa solution (Merck®). Differential cell counts were performed by counting 500 cells, excluding epithelial cells.

Venous blood samples (7mL) were collected from the jugular vein with a Vacutainer (BD) into plain tubes. Samples were centrifuged (1500*g*, 10 min) and the serum separated and stored at -20°C for subsequent laboratory analysis.

Total protein levels in serum (g/dL) and BALF (mg/dL) were measured according to the biuret protein assay using a set of diagnostic reagents (Labtest, Sistema de Diagnósticos Ltda., Lagoa Santa, Brazil) and spectrophotometric readings (Biosystem® - BTS-350). After protein measurements, the BALF samples were submitted to lyophilization (LioTop L-101). Protein fractions were determined by sodium dodecyl sulfate polyacrylamide gel electrophoresis (SDS-PAGE). Molecular weights and concentrations of protein fractions were determined by computed videodensitometry (CS 9000, Shimadzu Corp., Kyoto, Japan). Reference markers (Sigma Chemical Co., St Louis, USA) were used to characterize proteins, with molecular weights of 29, 45, 66, 97.4, 116, and 205kDa. Also, electrophoretic migration of proteins was compared with that of pure proteins including albumin, transferrin, haptoglobin, ceruloplasmin, IgA, IgG, α1-antitripsin, and acidic glycoprotein.

The data obtained were submitted to descriptive analysis, and means, maximum and minimum values were determined using the SAS statistical program.

RESULTS

The BALF cytology profiles of the healthy horses are summarized in Table 1 and were characterized by the prevalence of alveolar macrophages and lymphocytes, followed by neutrophils, mast cells, eosinophils and a small percentage of epithelial cells. These results are similar to the findings described by Viscardi et al. (2015), Wysocka & Kluciński (2015) and in a Consensus Statement of the American College of Veterinary Internal Medicine (Couëtil et al., 2016) for healthy horses.

Twenty-five proteins with molecular weights between 21 and 230kDa were identified in BALF of horses. BALF levels of proteins of 174kDa (immunoglobulin A), 106 kDa (ceruloplasmin), 80kDa (transferrin), 63kDa (albumin), 58kDa (α_1-antitripsin), 54kDa (immunoglobulin G heavy), 42kDa (haptoglobin), 34kDa (acidic glycoprotein), 24kDa (immunoglobulin G light), and 23kDa (P23) were nominally identified (Table 2).

In serum, 21 proteins with molecular weights between 21 and 255kDa were identified in all animals. Serum levels of proteins of 171kDa (immunoglobulin A), 106kDa (celuloplasmin), 80 kDa (transferrin), 59kDa (albumin), 51kDa (immunoglobulin G heavy), 41kDa (haptoglobin), 35kDa (acidic glycoprotein), 24kDa (immunoglobulin G light), and 23kDa (P23) were nominally identified (Table 2).

Table 1. Percentage of cells recovered from bronchoalveolar lavage fluid of healthy horses

Percentage of cells					
Macrophages	Lymphocytes	Neutrophils	Eosinophils	Mast cells	Epithelial cells
43.80 ± 17.01	36.4 ± 21.54	4.6 ± 3.80	1.8 ± 0.84	1.60 ± 0.84	0.70 ± 1.90

Table 2. Serum and bronchoalveolar fluid protein concentrations (mean ± SD) in healthy horses determined by sodium dodecyl sulfate-polyacrylamide gel electrophoresis

Protein	Horses					
	Serum (g/dL)			BALF (mg/dL)		
	M ± SD	Max	Min	M ± SD	Max	Min
Total serum protein	9.63 ± 0.86	11.64	8.71	18.52 ± 10.93	39.0	7.97
Albumin	5.63 ± 0.63	7.18	5.01	9.94 ± 7.66	24.44	2.59
Ceruloplasmin	0.028 ± 0.007	0.015	0.041	0.04 ± 0.03	0.11	0.005
Transferrin	0.72 ± 0.12	0.93	0.55	1.43 ± 0.74	2.87	0.63
Haptoglobin	0.06 ± 0.01	0.09	0.04	0.29 ± 0.15	0.50	0.03
Acid glycoprotein	0.011 ± 0.002	0.015	0.009	0.90 ± 0.54	1.64	0.09
IgA	0.23 ± 0.04	0.29	0.15	0.96 ± 0.08	0.32	0.01
IgG heavy	1.19 ± 0.21	1.65	0.82	1.17 ± 0.83	2.32	0.03
IgG light	1.11 ± 0.28	1.54	0.68	2.12 ± 1.74	5.83	0.27
α1-antitripsin	-	-	-	1.22 ± 0.87	2.43	0.29
P23	0.43 ± 0.002	1.54	0.68	0.12 ± 0.10	0.36	0.04

DISCUSSION

In this study, we evaluated healthy horses without clinical signs of respiratory disease and found that by applying electrophoresis (SDS-PAGE), the concentrations in BALF of ceruloplasmin, transferrin, albumin, α_1-antitripsin, immunoglobulin G heavy, immunoglobulin G light, immunoglobulin A, haptoglobin and acidic glycoprotein can be assessed. These proteins can also be measured in BALF or serum by ELISA, as described by Out et al. (1987) and Barton et al. (2017). Albumin, ceruloplasmin and alpha-2-macroglobulin were measured in paired BALF and serum samples from human patients with acute pneumonitis or asthma. The results indicated that abnormal leakage of proteins from the blood rather than local synthesis causes the increased concentrations of these proteins in BALF and that the determination of ceruloplasmin and alpha-2-macroglobulin yields more detailed information on leakage of proteins from the blood into the airway compartment than that of albumin (Out et al. 1987). Fibrinogen (Fb) and serum amyloid A (SAA) concentrations were measured in BALF of horses with respiratory disease. Although no significant differences were found between control groups compared to groups with recurrent airway obstruction, inflammatory airway disease or chronic interstitial pneumopathy, the fibrinogen concentration was positively correlated with the percentage of neutrophils in BALF cytology (Barton et al. 2017). Several functions have been ascribed to Fb, including providing a substrate for fibrin formation during tissue repair and providing a matrix for migration of inflammatory-related cells. Fb binds to cell surface integrins (CD11/CD18) of phagocytes, initiating a cascade of intracellular signals and promoting the enhancement of degranulation, phagocytosis, and antibody-dependent cytotoxicity (Borges et al. 2007).

In IAD-affected horses, high BALF albumin and IgG concentrations were consistent with leakage of plasma proteins into the airway lumen, but local Ig production cannot be excluded in IAD-affected horses. In fact, the magnitude of increase in BALF IgA concentrations was higher than expected from exudation of plasma proteins, which may indicate the presence of local IgA production (Moore et al. 1997). Exudation of plasma proteins into the airway lumen results from loss of vascular integrity of the subepithelial plexus secondary to subepithelial inflammation. Plasma exudation occurs independent of cellular diapedesis and migration and is not necessarily observed in all types of pulmonary inflammatory diseases (Persson 1991). Secretoglobin expression in BALF was significantly higher in horses with recurrent airway obstruction (RAO) compared to that in the control horses and inflammatory airway disease-affected horses (Miskovic Feutz et al. 2015). Secretoglobin is an anti-inflammatory protein that inactivates phospholipase A2, decreases proinflammatory cytokine production, alters phagocyte function, and may decrease the inflammatory response to endotoxin (Snyder et al. 2010). In this same study, the expression of transferrin in BALF was significantly lower in RAO-affected horses compared to airway disease-affected horses (IAD) and control horses. Because transferrin is a negative acute-phase protein, a decrease in response to inflammation is expected with both RAO and IAD. The relationship between transferrin and pulmonary inflammation is not as clear as that of secretoglobin. Transferrin concentrations may change with the duration and severity of inflammation, and thus the discrepancy in results between studies is not surprising. These differences suggest that secretoglobin and transferrin may be useful as biomarkers or as possible treatment targets for RAO (Miskovic Feutz et al. 2015).

Other studies, however, have used ELISA to measure concentrations of some acute-phase proteins in isolation or only in serum. In these cases, local production cannot be assessed. In horses with heaves, haptoglobin was a marker of both acute and chronic systemic inflammation, whereas high concentrations of SAA indicated acute inflammation. There was no difference in serum concentrations of C-reactive protein between healthy horses and horses with heaves (Lavoie-Lamoureux et al. 2012). In this study, the control horses also showed an increase in haptoglobin serum concentrations after hay exposure. This suggests that the magnitude, but not the uniqueness of the systemic inflammatory response distinguishes heaves-affected from healthy horses. The primary role to haptoglobin is to scavenge hemoglobin released into the circulation because of hemolysis or normal red blood cell turnover (Quaye 2008). Serum amyloid A concentrations were determined in horses with equine influenza virus (EIV), equine herpesvirus-4 (EHV-4), *Streptococcus equi* subspecies *equi* (*S. equi ss equi*), inflammatory airway disease (IAD),

and healthy controls in serum using a stall-side lateral flow immunoassay test. The results showed that the serum amyloid A levels were significantly greater for infectious respiratory diseases (EIV, EHV-4, *S. equi ss equi*) and horses with IAD compared to control horses. There was a significant difference between viral and bacterial infections and IAD (Viner et al., 2017). A peak in SAA and fibrinogen levels was observed in horses 24 hours after inoculation with *S. zooepidemicus.* In this study, the SAA value also reached peak value earlier than the fibrinogen value (Hobo et al. 2007).

CONCLUSIONS

This seems to be the first study in which ceruloplasmin, transferrin, albumin, α1-antitripsin, immunoglobulin G heavy, immunoglobulin G light, immunoglobulin A, haptoglobin and acidic glycoprotein concentrations were evaluated in BALF of healthy horses by sodium dodecyl sulfate polyacrylamide gel electrophoresis (SDS-PAGE).

Since only healthy horses were studied, the reference values for acute-phase proteins obtained can be a basis for studies of pulmonary pathologies. In healthy horses, the values are very low, but changes in clinical condition can cause a rapid response and the rate of synthesis is the only factor that affects blood concentration.

Acknowledgements.- The authors thank Dr. J.J. Fagliari for the assistance in developing and conducting the assays. This study was financed in part by the "Coordenação de Aperfeiçoamento de Pessoal de Nível Superior" (CAPES) - Finance Code 001, and the "Conselho Nacional de Desenvolvimento Científico e Tecnológico" (CNPq).

Conflict of interest statement.- The authors have no conflicts of interest to declare.

REFERENCES

Barton A.K., Wirth C., Bondzio A., Einspanier R. & Gehlen H. 2017. Are pulmonary hemostasis and fibrinolysis out of balance in equine chronic pneumopathies? J. Vet. Sci. 18(3):349-357. <https://doi.org/10.4142/jvs.2017.18.3.349> <PMid:28057902>

Borges A.S., Divers T.J., Stokol T. & Mohammed O.H. 2007. Serum iron and plasma fibrinogen concentrations as indicators of systemic inflammatory diseases in horses. J. Vet. Intern. Med. 21(3):489-494. <http://dx.doi.org/10.1892/0891-6640(2007)21[489:siapfc]2.0.co;2> <PMid:17552456>

Bullone M., Lagarde M., Vargas A. & Lavoie J.P. 2015. Serum surfactant protein D and haptoglobin as potential biomarkers for inflammatory airway disease in horses. J. Vet. Intern. Med. 29(6):1707-1711. <http://dx.doi.org/10.1111/jvim.13602> <PMid:26289543>

Couëtil L.L., Cardwell J.M., Gerber V., Lavoie J.P., Léguillette R. & Richard E.A. 2016. Inflammatory airway disease of horses - revised consensus statement. J. Vet. Intern. Med. 30(2):503-515. <http://dx.doi.org/10.1111/jvim.13824> <PMid:26806374>

Couëtil L.L., Hoffman A.M., Hodgson J., Buechner-Maxwell V., Viel L., Wood J.L. & Lavoie J-.P. 2007. Inflammatory airway disease of horses. J. Vet. Intern. Med. 21(2):356-361. <http://dx.doi.org/10.1892/0891-6640(2007)21[356:iadoh]2.0.co;2> <PMid:17427403>

Crisman M.V., Scarratt W.K., & Zimmerman K.L. 2008. Blood proteins and inflammation in the horse. Vet. Clin. N. Am., Equine Pract. 24(2):285-297. <http://dx.doi.org/10.1016/j.cveq.2008.03.004> <PMid:18652956>

Hobo S., Niwa H. & Anzai T. 2007. Evaluation of serum amyloid A and surfactant protein I sera for identification of the clinical condition of horses with bacterial pneumonia. J. Vet. Med. Sci. 69(8):827-830. <http://dx.doi.org/10.1292/jvms.69.827> <PMid:17827889>

Hultén C. & Demmers S. 2002 Serum amyloid A (SAA) as an aid in the management of infectious disease in the foal: comparison with total leucocyte count, neutrophil count and fibrinogen. Equine Vet. J. 34(7):693-698. <http://dx.doi.org/10.2746/042516402776250360> <PMid:12455840>

Jacobsen S. 2007. Review of equine acute-phase proteins. Proceedings of 53th Annual Convention of the American Association of Equine Practitioners, Orlando, FL, p.230-235.

Kyd J.M., Foxwell A.R. & Cripps A.W. 2001. Mucosal immunity in the lung and upper airway. Vaccine 19(17/19):2527-2533. <http://dx.doi.org/10.1016/s0264-410x(00)00484-9> <PMid:11257388>

Lavoie-Lamoureux A., Leclere M., Lemos K., Wagner B. & Lavoie J.P. 2012. Markers of systemic inflammation in horses with heaves. J. Vet. Intern. Med. 26(6):1419-1426. <http://dx.doi.org/10.1111/j.1939-1676.2012.00993.x> <PMid:22925172>

Miskovic Feutz M., Couetil L.L., Riley C.P., Zhang X., Adamec J. & Raskin R.E. 2015. Secretoglobin and transferrin expression in bronchoalveolar lavage fluid of horses with chronic respiratory disease. J. Vet. Intern. Med. 29(6):1692-1699. <http://dx.doi.org/10.1111/jvim.13604> <PMid:26332291>

Moore B.R., Krakowka S., Mcvey D.S., Cumminss J.M. & Robertson J.T. 1997. Inflammatory markers in bronchoalveolar lavage fluid of Standardbred racehorses with inflammatory airway disease: response to interferon-alpha. Equine Vet. J. 29(2):142-147. <http://dx.doi.org/10.1111/j.2042-3306.1997.tb01656.x> <PMid:9104564>

Out T.A., Jansen H.M., van Steenwijk R.P., Nooijer M.J., van de Graaf E.A. & Zuijderhoudt F.M.J. 1987. ELISA of ceruloplasmin and alpha-2-macroglobulin in paired bronchoalveolar lavage fluid and serum samples. Clin. Chim. Acta 165(2/3):277-288. <http://dx.doi.org/10.1016/0009-8981(87)90172-0> <PMid:2443279>

Persson C.G.A. 1991. Plasma exudation in the airways: mechanisms and function. Eur. Respir. J. 4(10):1268-1274. <PMid:1804675>

Quaye I.K. 2008. Haptoglobin, inflammation and disease. Trans. R. Soc. Trop. Med. Hyg. 102(8):735-742. <http://dx.doi.org/10.1016/j.trstmh.2008.04.010> <PMid:18486167>

Snyder J.C., Reynolds S.D., Hollingsworth J.W., Zhuowei Li., Kaminski N. & Stripp B.R. 2010. Clara cells attenuate the inflammatory response through regulation of macrophage behavior. Am. J. Respir. Cell Mol. Biol. 42(2):161-171. <http://dx.doi.org/10.1165/rcmb.2008-0353OC> <PMid:19423773>

Sweeney C.R., Humber K.A. & Roby K.A.W. 1992. Cytologic findings of tracheobronchial aspirates from 66 Thoroughbred racehorses. Am. J. Vet Res. 53(7):1172-1175. <PMid:1497188>

Upragarin N., Landman WJ., Gaastra W. & Gruys E. 2005. Extrahepatic production of acute-phase serum amyloid A. Histol. Histopathol. 20(4):1295-1307. <http://dx.doi.org/10.14670/HH-20.1295> <PMid:16136510>

Viner M., Mazan M., Bedenice D., Mapes S. & Pusterla N. 2017. Comparison of serum amyloid A in horses with infectious and noninfectious respiratory diseases. J. Equine Vet. Sci. 49:11-13. <http://dx.doi.org/10.1016/j.jevs.2016.09.005>

Viscardi V., Lopes A.C.G., Beling J.C.F., Gioia G.V., Torres Filhos R.A., Lessa D.A.B. & Alencar N.X. 2015. Effects of single and duplicate infusions of 250mL of saline solution in the cytological evaluation of bronchoalveolar lavage in equines. Braz. J. Vet. Med. 37(1):33-35.

Wilkins P.A. 2003. Lower airway diseases of the adult horse. Vet. Clin. N. Am., Equine Pract. 19(1):101-121. <http://dx.doi.org/10.1016/s0749-0739(02)00069-x> <PMid:12747664>

Wysocka B. & Kluciński W. 2015. Cytological evaluation of tracheal aspirate and broncho-alveolar lavage fluid in comparison to endoscopic assessment of lower airways in horses with recurrent airways obstruction or inflammatory airway disease. Pol. J. Vet. Sci. 18(3):587-597. <http://dx.doi.org/10.1515/pjvs-2015-0076> <PMid:26618592>

Yang F., Friedrichs W.E., Navarijo-Ashbaugh A.L., de Graffenried L.A., Bowman B.H. & Coalson J.J. 1995. Cell type-specific and inflammatory-induced expression of haptoglobin gene in lung. Lab. Invest. 73(3):433-440. <PMid:7564277>

PESQUISA VETERINÁRIA BRASILEIRA
Brazilian Journal of Veterinary Research
ISSN 0100-736X (Print)
ISSN 1678-5150 (Online)

Pesq. Vet. Bras. 40(12):1077-1087, December 2020
DOI: 10.1590/1678-5150-PVB-6421

Original Article
Animal Morphophysiology
BY-NC

Histomorphometric and immunohistochemical evaluation of the frontal cerebral cortex in diabetic rats after treatment with melatonin[1]

Marina G.P. Baptista[2]*, Cintia G.M. Ferreira[2], Yuri M.L. Albuquerque[2], Carolline G. D'assunção[2], Rebeca C. Alves[2], Valéria Wanderley-Teixeira[3] and Álvaro A.C. Teixeira[3]

ABSTRACT.- Baptista M.G.P., Ferreira C.G.M., Albuquerque Y.M.L., D'assunção C.G., Alves R.C., Wanderley-Teixeira V. & Teixeira A.A.C. 2020. **Histomorphometric and immunohistochemical evaluation of the frontal cerebral cortex in diabetic rats after treatment with melatonin.** *Pesquisa Veterinária Brasileira 40(12):1077-1087.* Departamento de Morfologia e Fisiologia Animal, Universidade Federal Rural de Pernambuco, Rua Dom Manoel de Medeiros s/n, Dois Irmãos, Recife, PE 52171-900, Brazil. E-mail: marinaabaptistaa@gmail.com

The central nervous system is vulnerable to complications caused by diabetes. These complications lead to increased oxidative stress in the brain, resulting in damage to the cerebral cortex, among other regions. Insulin and hypoglycemic agents are still the most widely used treatments. However, current research with an experimental model of diabetes suggests the use of antioxidants, such as melatonin. Thus, we tested the hypothesis that exogenous melatonin may decrease or prevent the effects of diabetes in the frontal cortex of the rat brain. Fifty albino rats were allocated into five groups: GC = rats without diabetes induction, GD = diabetic rats induced by streptozotocin, GDM = streptozotocin-induced and melatonin-treated diabetic rats, GDI = diabetic rats induced by streptozotocin and treated with insulin, GDMI = diabetic rats induced by streptozotocin and treated with melatonin and insulin simultaneously. Diabetes was induced by intraperitoneal administration of streptozotocin (60mg/kg). Insulin (5U/day) was administered subcutaneously and melatonin (10mg/kg) by drinking water; both treatments last days after. We analyzed animals' weight, the cytokines IL-6 and TNF-α, apoptosis, glycogen, and did morphometry and histopathology of the frontal cortex were analyzed. The results showed that the cerebral cortex of the diabetic animals presented axonal degeneration, reduced number of neurons in the cortex, reduced glycogen, increased IL-6 and TNF-α expression, high apoptotic index, and reduced animal weight and the brain. Treatment with melatonin associated or not with insulin prevented such effects. Thus, we conclude that melatonin associated with insulin may be an alternative for avoiding the impact of diabetes in the brain's frontal cortex.

INDEX TERMS: Frontal cerebral cortex, diabetes, brain, melatonin, cytokines, apoptosis, morphometry, rats, Brazil.

RESUMO.-[**Avaliação histomorfométrica e imuno-histoquímica do córtex cerebral frontal em ratos diabéticos após o tratamento com melatonina.**] O sistema nervoso central é vulnerável a complicações originadas pelo diabetes estresse oxidativo no cérebro e resultando em lesões no córtex cerebral, dentre outras regiões. A insulina e hipoglicemiantes ainda são os tratamentos mais utilizados, entretanto, pesquisas atuais com modelo experimental do diabetes sugerem a utilização de antioxidantes como, por exemplo, a melatonina. Assim, testamos a hipótese de que a melatonina exógena pode diminuir ou prevenir os efeitos do diabetes no córtex frontal do cérebro de ratos. Foram utilizados 50 ratos albinos, divididos em 5 grupos: GC = ratos sem indução ao diabetes, GD = ratos induzidos ao diabetes pela estreptozotocina, GDM = ratos induzidos ao diabetes pela estreptozotocina e

[1] Received on September 10, 2019.
Accepted for publication on November 6, 2019.
[2] Laboratório de Histologia, Departamento de Morfologia e Fisiologia Animal, Universidade Federal Rural de Pernambuco (UFRPE), Rua Dom Manoel de Medeiros s/n, Dois Irmãos, Recife, PE 52171-900, Brazil. *Corresponding autor: marinaabaptistaa@gmail.com

[3] Departamento de Morfologia e Fisiologia Animal, Universidade Federal Rural de Pernambuco (UFRPE), Rua Dom Manoel de Medeiros s/n, Dois Irmãos, Recife, PE 52171-900, Brazil.

tratados com melatonina, GDI = ratos induzidos ao diabetes pela estreptozotocina e tratados com insulina, GDMI = ratos induzidos ao diabetes pela estreptozotocina e tratados com melatonina e insulina simultaneamente. O diabetes foi induzido pela administração intraperitoneal de estreptozotocina (60mg/kg). A insulina (5U/dia) foi administrada por via subcutânea e a melatonina (10mg/kg) pela água de beber. Ambos tratamentos foram realizados durante 30 dias após a indução. Foram analisados o peso dos animais, do cerebro, as citocinas IL-6 e TNF-α, apoptose, glicogênio, além da morfometria e histopatologia do córtex frontal. Os resultados mostraram que o córtex cerebral dos animais diabéticos apresentou degeneração axonal, redução do número de neurônios no córtex, redução do glicogênio, aumento da expressão do IL-6 e TNF-α, elevação do índice apoptótico, além da redução do peso dos animais e do cérebro. O tratamento com melatonina associada ou não a insulina preveniu tais efeitos. Assim, concluímos que a melatonina associada ou não a insulina pode ser uma alternativa na prevenção dos efeitos do diabetes no córtex frontal do cérebro.

TERMOS DE INDEXAÇÃO: Córtex cerebral frontal, diabetes, cérebro, melatonina, citocinas, apoptose, morfometria, ratos.

INTRODUCTION

For several years, interest in the effects of diabetes on the brain has increased significantly. The central nervous system is vulnerable to complications caused by diabetes caused by chronic hyperglycemia (Van-Harten et al. 2006, Francis et al. 2008, Kodl et al. 2008, Yau et al. 2009, Yang et al. 2011, Huang et al. 2012, Yoon et al. 2017). Several studies have shown that vascular and metabolic changes associated with chronic hyperglycemia can cause brain damage, cerebral atrophy, structural and electrophysiological changes, and impairment of cognitive function (Van-Elderen et al. 2010, Franc et al. 2011, Louzada & Vargas 2015). Although several studies report adverse effects of diabetes mellitus on the hippocampus, hypothalamus, and cerebellum (Jackson-Guilford et al. 2000, Piotrowski et al. 2001, Beauquis et al. 2006, Khaksar et al. 2010, Ahmadpour & Haghir 2011), research has shown that diabetic patients have lesions in the white matter of the frontal cortex of the brain (Hsu et al. 2012).

Diabetes stimulates neuron damage, increasing the number of apoptotic cells and cognitive impairment followed by a marked increase in oxidative stress in the brain (Wang et al. 2010). In addition, patients with diabetes have higher levels of plasma concentrations of pro-inflammatory cytokines such as IL-6 and TNF-α, where they can potentiate inflammation. With significant advances made in our knowledge, it is possible to understand the mechanisms involved in the origin of brain complications so that new treatment modalities are being explored (Edwards et al. 2008). Thus, recent strategies for the prevention and treatment of complications resulting from diabetes have been studied. Insulin and hypoglycemic agents are still the most used treatments. However, current research with an experimental model of diabetes points to new antioxidants as a therapeutic approach for the prevention and treatment of neurological damage (Louzada & Vargas 2015). Several studies point to melatonin as an antioxidant and a free radical scavenger, as it stimulates the activity of antioxidant enzymes such as superoxide dismutase and glutathione reductase (El-Sokkary et al. 2003).

This hormone also plays an important role in the neuroprotection of several neurodegenerative disorders whose pathogenesis involves reactive oxygen species (Baydas et al. 2001), in addition to having anti-inflammatory effects and modulating the tumor necrosis factor-alpha (TNF-α) and the interleukin 6 (IL-6) (Hernandez-Velázquez et al. 2016). We then tested the hypothesis that exogenous melatonin may decrease or prevent the effects of diabetes on the frontal cortex of the rat brain.

MATERIALS AND METHODS

Experimental rats. The experiment was carried out at the "Laboratório de Histologia" of the "Departamento de Morfologia e Fisiologia Animal" of the "Universidade Federal Rural de Pernambuco" (UFRPE). Fifty 60 days old, virgin, albino rats (*Rattus norvegicus* albinus) of the Wistar lineage, weighing approximately 250g, were used The rats came from the vivarium of the UFRPE. The animals were kept in cages with food and water ad libitum, remaining in standard conditions of ±22°C with a light period between 6 a.m. - 18 p.m., divided into the following groups: control group (GC) = rats without diabetes induction, diabetic group (GD) = streptozotocin diabetes-induced rats, GDI = streptozotocin diabetes-induced rats treated with insulin, GDM = streptozotocin diabetes-induced rats treated with melatonin, GDMI = streptozotocin diabetes-induced rats treated with melatonin and insulin simultaneously. The experimental protocol was approved by the institutional Ethics Committee, protocol no. 36/2017.

Experimental rats. Diabetes was induced by intraperitoneal administration of a streptozotocin solution (Sigma Chemical Co., USA) after a 14-hour fast. Streptozotocin was diluted in 10mM sodium citrate buffer and pH 4.5, in a single dose of 60mg/kg of animal weight. GC group rats received equivalent doses of saline solution in the same way, and after 30 minutes of treatment, all rats were fed typically (Dall'Ago et al. 2002). Diabetes diagnosis was confirmed after seven days of streptozotocin administration. Only rats that had blood glucose above 200mg/dL (Glucometer Kit Accu-Chek Activ) were included in the study (Spadella et al. 2005). The fasting glycemia was monitored during the experimental period on days 0 (before induction), 7 (confirmation of diabetes), 15, and 30 days after administration of melatonin or insulin.

Melatonin treatment. Melatonin (Sigma, St. Louis/MO, USA) treatment was carried out for 30 days. Melatonin (10mg/kg) was dissolved in ethanol and diluted in saline and added to drinking water. The 700mL bottles were covered with aluminum foil and placed in the cages at the beginning of the night 1039 (6 p.m.) and removed the following morning (6 a.m.). During the day, water was restricted.

Insulin treatment. Insulin was administered subcutaneously for 30 days, at a dose of 5U/day, with two units of insulin at 10 a.m. and three remaining units at 7 p.m. (Pinheiro et al. 2011).

Weighing of animals and their brains. The rats in the experimental groups were weighed daily in the course of the experiment. After 30 days of treatment, the animals were euthanized with ketamine hydrochloride (80mg/kg) and xylazine (6mg/kg), intramuscularly, associated with 100mg/kg intraperitoneal thiopental. Subsequently, the brains were removed and weighed on an analytical scale. Frontal cortex fragments were fixed in 10% buffered formaldehyde and processed for inclusion in paraffin.

Histology and Histopathology. Cross-sections of the frontal cortex were stained for histopathology with hematoxylin and eosin

(HE) for routine analysis and periodic acid-Schiff stain (PAS) for glycogen evaluation. The glycogen content was quantified through images captured using a Sony®1061 Video camera, coupled to the Olympus® 1062 Bx50 microscope, which was submitted to the Gimp 2.0 application to elaborate an RGB (Red-Green-Blue) histogram. (Oberholzer et al. 1996).

Morphometry. We evaluated three slides per animal/group. The estimate of volume [V (ref)] of the cortex was by the Cavalieri Method (Gundersen et al. 1988) the one of the neurons' numerical density (Nv) in the cortex by a previously described method (Gundersen et al. 1988, Villeda-Hernández et al. 2006). The estimate of the total numbers of neurons (N) was calculated using the following formula: N = V (ref) - Nv (Korbo et al. 1990, West 1993). In the white matter, a morphometric evaluation of the percentage of nerve fibers was performed using a 10x eyepiece containing a 25-point Waibel reticulum internally (Weibel et al. 1966) and a 40x objective, where six fields were counted, all at random and clockwise, taking into account only the points that affected the fibers. In total, 150 points were counted per animal totaling 450 points per group.

Immunohistochemistry (IL-6 and TNF-α). The expression of inflammatory cytokines was determined using antibodies to IL-6 and TNFα (Santa Cruz Biotechnology) at the 1:30 dilution. The slides were deparaffinized and rehydrated in xylol and alcohols. The antigenic recovery was carried out using a solution of citrate buffer (pH 8.0) at a high temperature in the microwave for 5 minutes. Endogenous peroxidase was inhibited by a solution of hydrogen peroxide (3%) in methanol. The nonspecific antigen-antibody reaction was blocked by incubating the slides in PBS and 5% bovine serum albumin (BSA) for one hour. All antibodies (Santa Cruz Biotechnology Inc., Santa Cruz/CA, USA) were diluted in PBS/BSA 1% for one hour. Subsequently, the slides were treated with the secondary antibody for thirty minutes. The antigen-antibody reaction was observed through a brown precipitate after applying 3-3-diaminobenzidine for four minutes and counterstained with hematoxylin. The images were captured using a Sony® Video camera, coupled 1089 to the Olympus® Bx 50 microscope, which was subjected to the Gimp 2.0 application for quantification by means of RGB Histogram (Red-Green-Blue) (Oberholzer et al. 1996. For apoptosis, the TUNEL method (Kit Apoptag - Millipore) was used. The cuts were initially dewaxed and hydrated and then immediately incubated in PBS (pH 7.4) for 5 minutes at room temperature. Then, proteinase K was applied to the slides for 15 minutes. The slides were washed in distilled water and incubated in hydrogen peroxide for 5 minutes at room temperature. The sections were washed in PBS and incubated in equilibrium buffer for 60 minutes at 4°C. The sections were then incubated in TdT at 37°C for 1 hour in a humid chamber. The stop solution was applied for 10 minutes at room temperature, and then the slides were washed in PBS and incubated in anti-digoxigenin. The slides were rinsed in PBS, and the sections were revealed with a chromogenic diaminobenzidine substrate (DAB, DakoCytomationTM) (±20 min), and counterstained with hematoxylin for 20 to 30 seconds. Then, the slides were washed in running water, dehydrated in increasing alcohol concentrations, and placed in xylol to be assembled and observed under a light microscope. The apoptotic index was determined by counting the percentage of positive cells from at least 500 nuclei subdivided into ten fields chosen at random using the 40X objective (Wu et al. 2013).

Statistical analysis. The following parameters were statistically analyzed: morphometry, animal weight, brain weight, glycogen quantification, apoptotic index, TNFα, and IL-6 expression. The method used was Ruskal-Wallis non-parametric method with Dunn's posthoc (P<0.05).

RESULTS

Glycemic levels

Before the process of inducing diabetes, all animals in the experimental groups had blood glucose levels below 120mg/dL, with no significant differences. At seven days, all groups, except for control, had blood glucose above 300mg/dL. After 15 and 30 days of treatment, only the animals in the diabetic group (GD) continued to have a very high mean glucose (474mg/dL), while the groups treated with insulin (GDI), melatonin (GDM), and melatonin/insulin (GDMI) exhibited glucose values statistically similar to the control group (GC) (Table 1).

Weight of rats and their brains

There was progressive weight loss in the GD groups of rats compared to the control and the other treated groups. The treated groups (GDI, GDM, and GDMI) also showed weight reduction compared to the control, but without significant differences (Table 2). In analyzing the weight of brains from rats of the experimental groups, the GD rats showed a significantly lower value compared with other groups (Table 2). The groups treated with insulin (GDI), melatonin (GDM), and melatonin/insulin (GDMI) showed no relevant differences when compared to the GC group (Table 3).

Histopathology and histochemistry

In the cortical region, histopathological, there was no degeneration, atrophy, or neuronal vacuolization. However, in the white matter, a significant number of regions showed several nerve fibers devoid of axons in animals in the GD group (Fig.1). Histochemical analysis by PAS revealed a significant reduction in glycogen in animals' cortex in the

Table 1. Serum glucose levels (mg/dL) in rats the control and experimental groups

Groups	Day 0 Induction	Day 7 Confirmation	Day 15 After induction	Day 30 After induction
GC	960.75 ± 5.17a	99.17 ± 2.14b	102.30 ± 3.47b	110.80 ± 7.46b
GD	95.00 ± 3.36a	349.06 ± 12.02a	348,80 ± 11.43a	474.00 ± 9.87a
GDI	92.25 ± 4.38a	338.77 ± 9.43a	110.30 ± 7.59b	128.30 ± 10.23b
GDM	92.00 ± 3.55a	343.91 ± 7.88a	117.50 ± 9.80b	120.30 ± 8.16b
GDMI	91.64 ± 3.09a	335.48 ± 11.22a	108.44 ± 8.12b	119.58 ± 7.39b
P	0.0763	0.0223	0.0066	0.0132

[a,b] Means followed by the same letter in the columns do not differ significantly by Dunn's test (p<0.05); GC = control group, GD = diabetic group, GDI = diabetic group treated with insulin, GDM = diabetic group treated with melatonin, GDMI = diabetic group treated with insulin and melatonin

Table 2. Weight (mg/dL) of the rats in the control and experimental groups

Groups	Day 0 Induction	Day 7 Confirmation	Day 15 After induction	Day 30 After induction
GC	245.30 ± 7.54a	273.80 ± 2.50a	284.50 ± 19.82a	305.50 ± 6.85a
GD	247.80 ± 9.28a	202.50 ± 7.72c	144.30 ± 7.18c	118.00 ± 3.55c
GDI	246.30 ± 6.39a	241.30 ± 11.59b	242.00 ±10.03b	264.30 ± 3.40b
GDM	240.00 ± 7.07a	237.30 ± 8.84b	235.00 ± 10.98b	255.30 ± 9.81b
GDMI	239.80 ± 5.56a	243.00 ± 3.74b	238.50 ± 17.82b	259.30 ± 3.20b
P value	0.4242	0.0101	0.0323	0.0004

[a,b,c] Means followed by the same letter in the columns do not differ significantly by Dunn's test ($p<0.05$); GC = control group, GD = diabetic group, GDI = diabetic group treated with insulin, GDM = diabetic group treated with melatonin, GDMI = diabetic group treated with insulin and melatonin.

Table 3. Weight (g) of the brains from rats the control and experimental groups

Groups	GC	GD	GDI	GDM	GDMS	*P* value
	1.29 ± 0.07a	1.10 ± 0.02b	1.35 ± 0.05a	1.31 ± 0.04a	1.32 ± 0.01a	0.0112

[a,b] Means followed by the same letter in the columns do not differ significantly by Dunn's test ($p<0.05$); GC = control group, GD = diabetic group, GDI = diabetic group treated with insulin, GDM = diabetic group treated with melatonin, GDMI = diabetic group treated with insulin and melatonin.

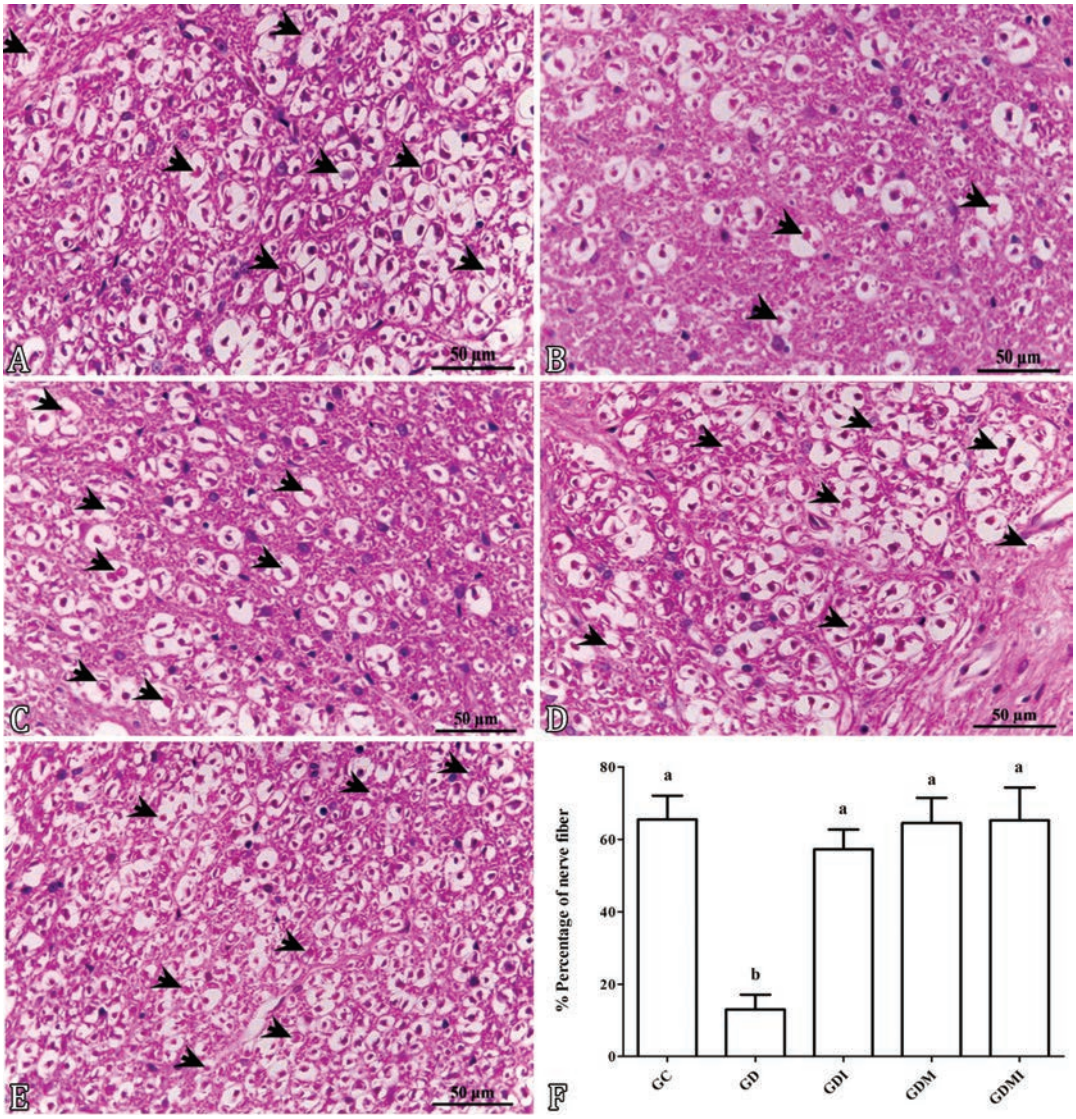


Fig.1. Photomicrograph of white matter of the brain from the rats of the experiment.(**A**) Control group (GC), (**B**) diabetic group (GD), (**C**) diabetic group treated with insulin (GDI), (**D**) diabetic group treated with melatonin (GDM) and (**E**) diabetic group treated with insulin and melatonin (GDMI). Note in (**A**), (**C**-**E**) predominance of nerve fibers (arrowhead), in (**B**) scares nerve fibers suggesting a degenerative process. HE, obj.20x. Insert: marked neuronal vacuolization. Nerve fibers without axon (arrows). HE, obj.20x. (**F**) Percentage of nerve fibers. Means followed by the same letter do not differ significantly from each other by Dunn's test ($p<0.05$).

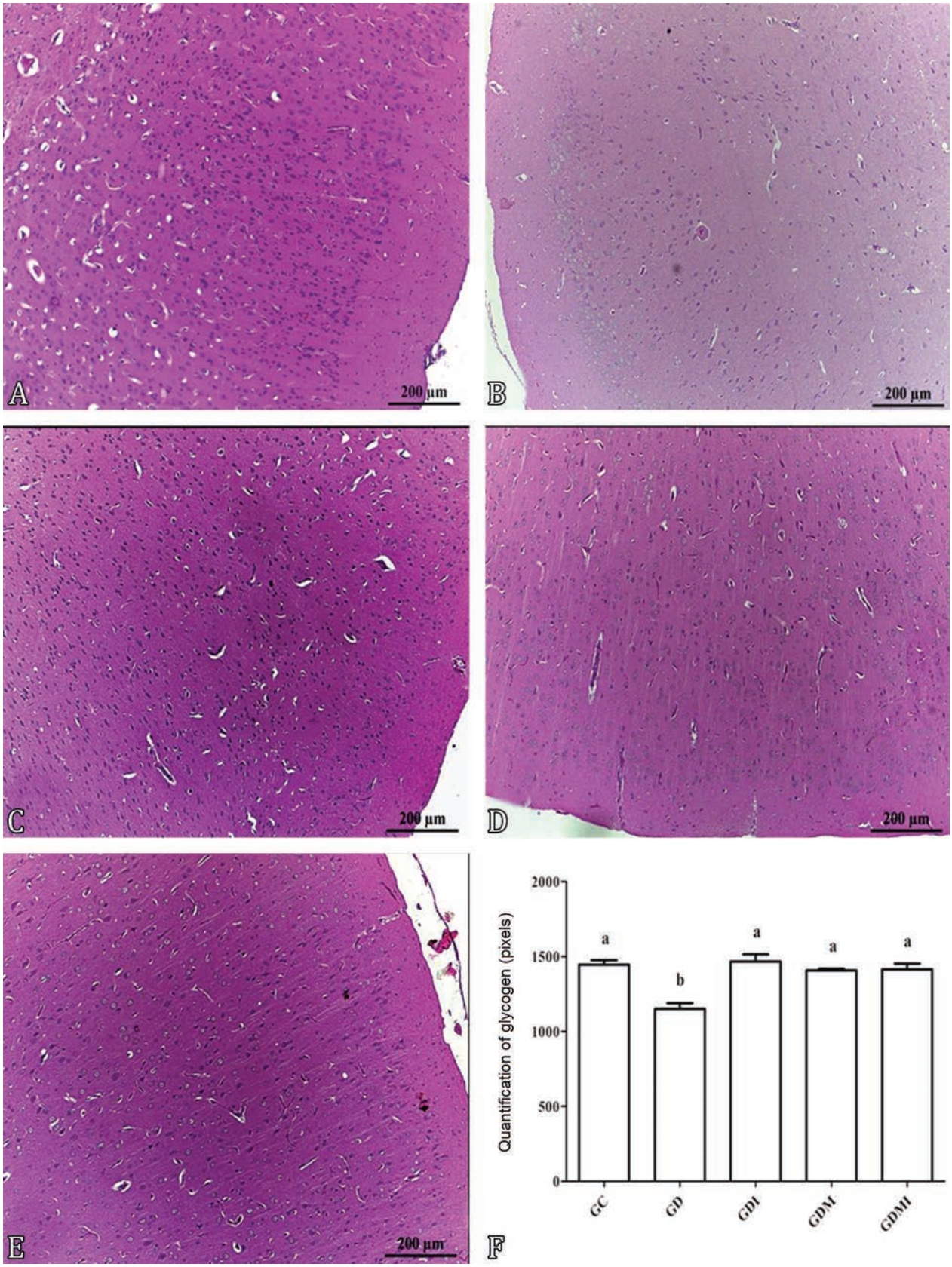


Fig.2. Photomicrograph of the cerebral cortex of animals in the experimental groups. (**A**) Control group (GC), (**B**) diabetic group (GD), (**C**) diabetic group treated with insulin (GDI), (**D**) diabetic group treated with melatonin (GDM) and (**E**) diabetic group treated with insulin and melatonin (GDMI). PAS, obj.20x. (**F**) Pixel quantification of glycogen content. Note a significant reduction in the GD group. Means followed by the same letter do not differ significantly by Dunn's test ($p<0.05$).

GD group compared to the other groups. The animals in the groups treated with melatonin associated or not with insulin showed characteristics similar to those observed in the control animals (Fig.2).

Morphometry

The quantification of neurons in the frontal cortex of the brain of animals in the experimental groups revealed a significant reduction in animals in the GD group compared to the other groups. There were no significant differences between the GC and those treated with melatonin with or without insulin (Fig.3).

Immunohistochemistry (IL-6, TNF-α) and apoptosis

Immunohistochemistry for IL-6 revealed that the animals in the diabetic group (GD) had a strong marking in the cerebral cortex (Fig.4B) However, in the control group (GC) (Fig.4A), treated with insulin (GDI) (Fig 4C), melatonin (GDM) (Fig.4D) and melatonin/insulin (GDMI) (Fig.4E) showed a similar marking, with no significant difference between these groups (Fig.4F). For the TFN-α, the GC (Fig.5A), GDI (Fig.5C), GDM (Fig.5D), and GDMI (Fig.5E) had an equivalent mark, showing no significant difference. On the other hand, the GD (Fig.5B) showed a strong marking in the cortical region, differing significantly from the other groups (Fig.5F). The TUNEL test revealed a high rate of apoptosis in the GD group's cerebral cortex compared to animals in the other groups (Fig.6).

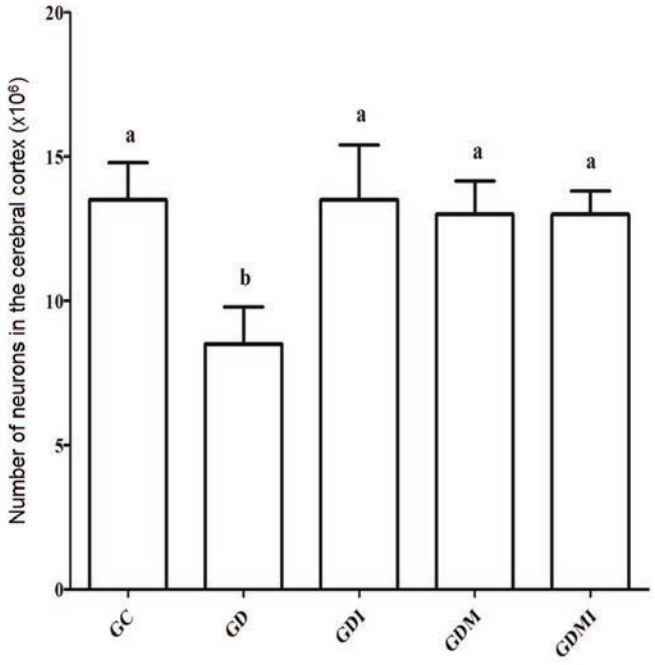


Fig.3. Estimation of the number of neurons in the cerebral cortex of animals in the experimental groups. Control group (GC), diabetic group (GD), diabetic group treated with insulin (GDI), diabetic group treated with melatonin (GDM), diabetic group treated with insulin and melatonin (GDMI). Means followed by the same letter do not differ significantly from each other by the Dunn test (p<0.05).

DISCUSSION

Regarding glycemic values, studies indicate that melatonin does not reduce hyperglycemic values in a state of diabetes (Cam et al. 2003). However, research on experimental models suggests that there is a positive relationship between melatonin and insulin. Sartori et al. (2009) showed that melatonin increased insulin sensitivity, in addition to stimulating the secretion of this hormone. This corroborates our findings that the animals in the group treated with melatonin and insulin had glucose values similar to those in the control group.

It is known that the loss of muscle mass is a characteristic of the diabetic state. This is believed to be the result of a change in protein metabolism in the state of hyperglycemia, in which this can be characterized by an increase in the catabolism of proteins and fats, leading to a decrease in the animals' body mass (Luciano & Mello 1998, Moura et al. 2012), which may justify the results observed in animals in the diabetic group. On the other hand, the animals in the groups treated with insulin associated or not with melatonin also showed weight loss in relation to the animals in the control group, but with less intensity than those in the diabetic group. This demonstrates that both insulin and melatonin can regulate body weight through energy balance, in which all energy captured by food is used and stored as energy storage (Sbem 2017).

The brain is hugely dependent on glucose and hyperglycemia (Yamada et al. 2002, Blurton-Jonesa et al. 2009), and disorders of neuronal glucose transport and metabolism in hyperglycemia can induce an increased number of free radicals in diabetic conditions and subsequently negatively affect the production of the brain-derived neurotrophic factor (BDNF). BDNF plays an essential role in the survival of neurons, their growth (axons and dendrites), and synapses' formation and function (Yamada et al. 2002, Blurton-Jonesa et al. 2009). This could explain the axonal degeneration of the in white matter and reduced levels of glycogen in the cortex of the diabetic rats, which was prevented in animals treated with melatonin regardless of the association with insulin, probably due to the ability of this indoleamine to promote the expression of BDNF (Luo et al. 2017). Concerning insulin, it was reported (Ghasemi et al. 2013), the presence of more significant numbers of receptors for this hormone in several sites such as the olfactory bulb, cerebral cortex, hippocampus, cerebellum, and choroid plexus, suggesting its importance in neuronal survival, synaptic plasticity and glucose absorption (Banks 2004).

There was a reduction in the number of neurons in the rats' frontal cortex from the diabetic group without treatment. This is undoubtedly related to the high apoptotic index observed in these animals, explaining the reduction in brain weight concerning rats in the other groups. Apoptosis is a series of processes programmed to carry out cell death and plays a significant role in maintaining tissue homeostasis. When deregulated, this process is associated with several pathological states such as neurodegenerative diseases and diabetes mellitus (Lee & Pervaiz 2007, Dorsemans et al. 2017).

In previous studies related to the central nervous system, the administration of exogenous melatonin resulted in a decrease in TUNEL-positive cells, indicating the neuroprotective effect of this hormone and suggesting that melatonin could act in the prevention of neurodegenerative diseases by inhibiting the intrinsic pathway of apoptosis (Lima et al. 2005, Tuzcu & Baydas 2006, Ferreira et al. 2010). Regarding insulin, it can

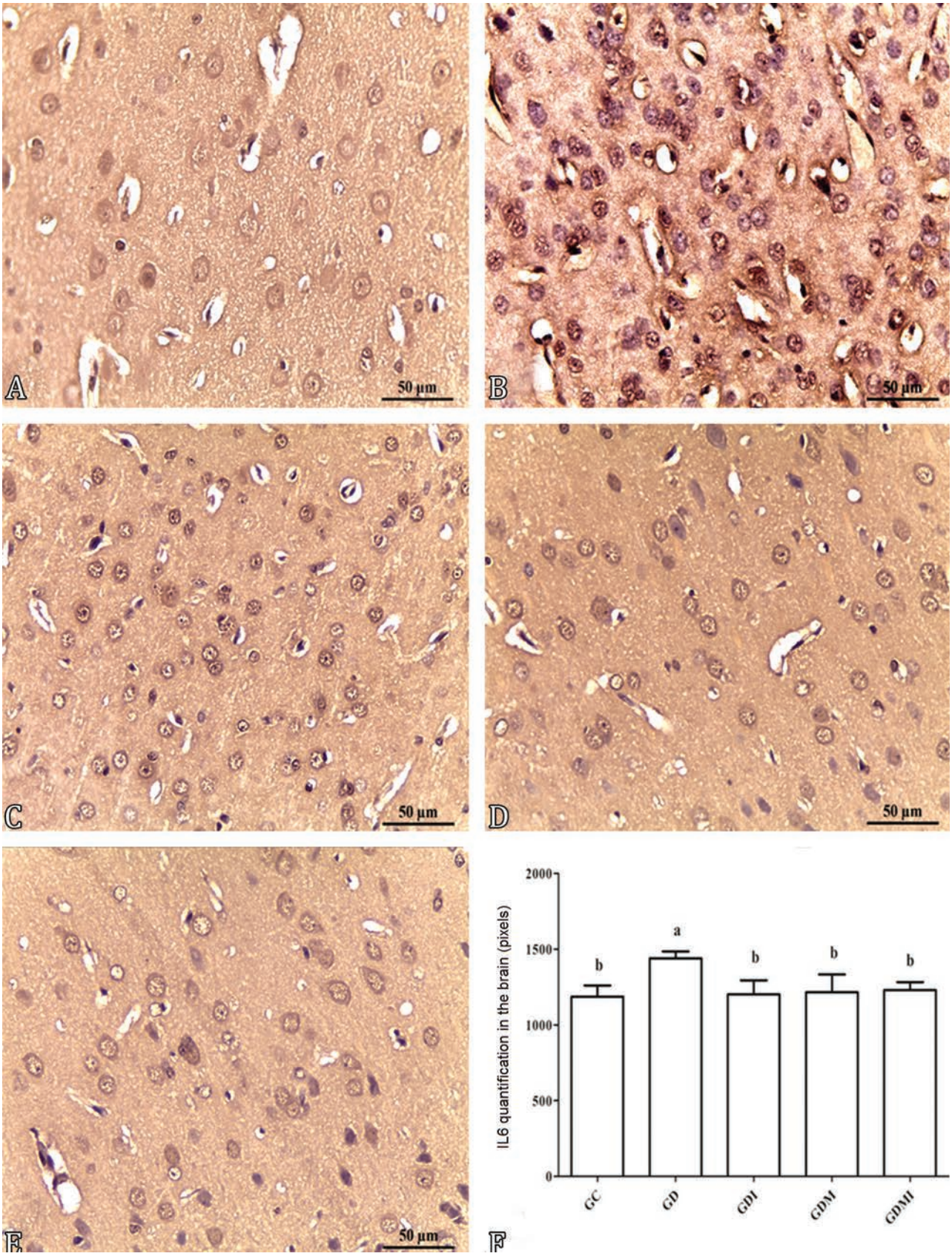


Fig.4. Immunohistochemistry for IL-6 in the brain of the rats. Observe in (**A**) control group (GC), (**C**) diabetic group treated with insulin (GDI), (**D**) diabetic group treated with melatonin (GDM) and (**E**) diabetic group treated with insulin and melatonin (GDMI) weak marking, and in (**B**) diabetic group (GD) strong marking in the cortical layer. (**F**) Quantification in pixels. Note a significant increase in the GD group. Means followed by the same letter do not differ significantly by Dunn's test (p<0.05).

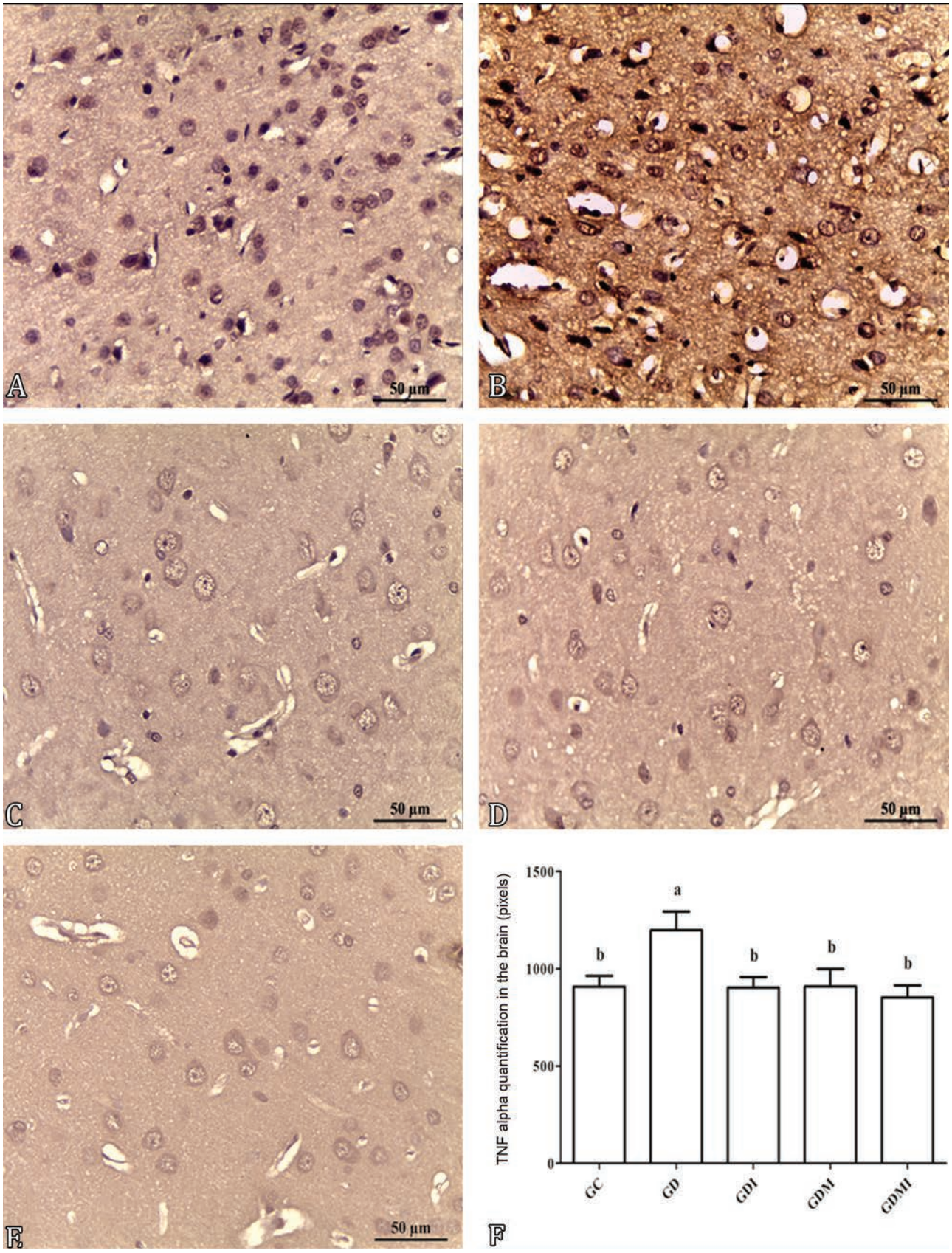


Fig.5. Immunohistochemistry for TNF-α in the brain of the rats. Observe in (**A**) control group (GC), (**C**) diabetic group treated with insulin (GDI), (**D**) diabetic group treated with melatonin (GDM) and (**E**) diabetic group treated with insulin and melatonin (GDMI) weak marking, and in (**B**) diabetic group (GD) strong marking in the cortical layer. (**F**) Quantification in pixels. Note a significant increase in the GD group. Means followed by the same letter do not differ significantly by Dunn's test ($p<0.05$).

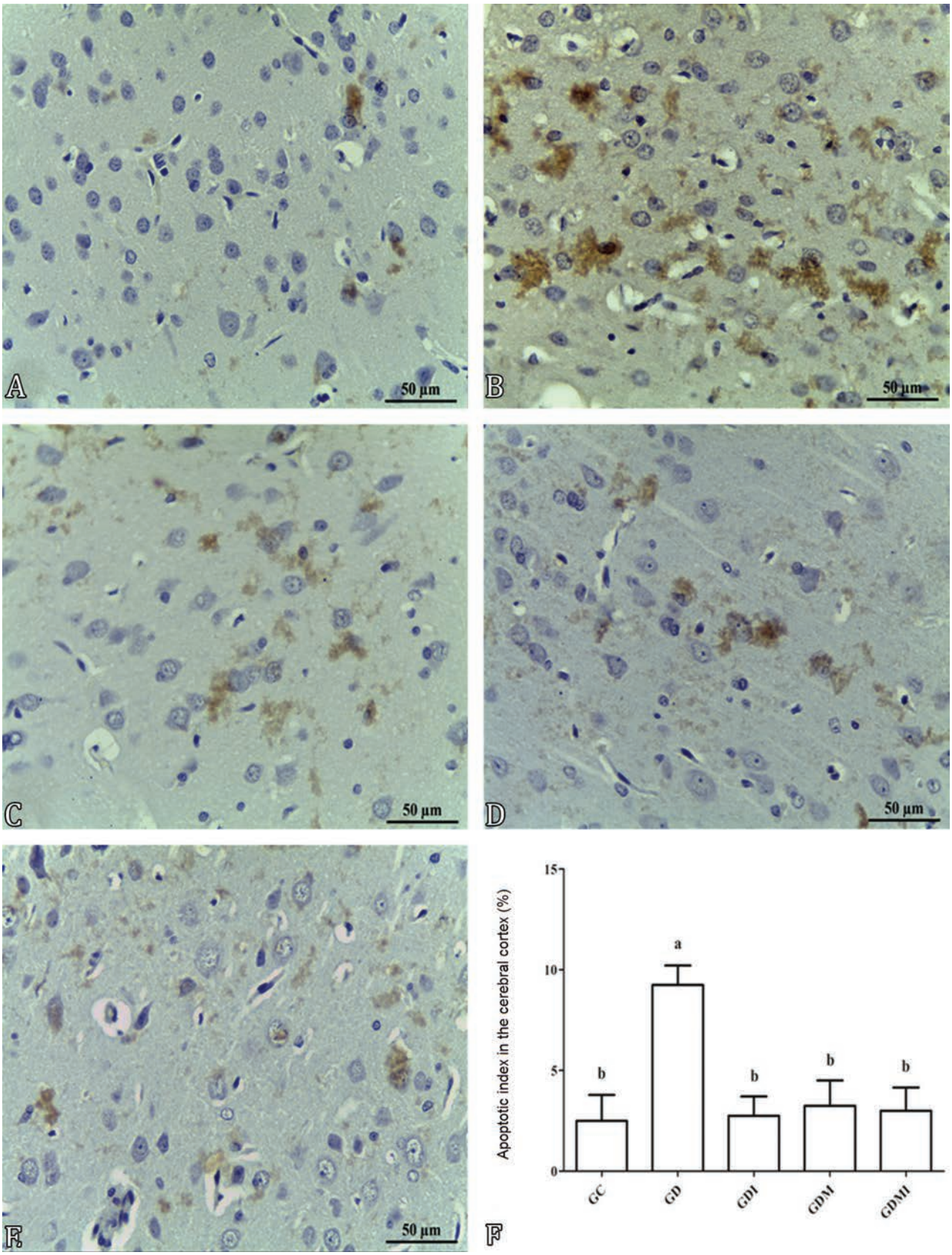


Fig.6. Immunohistochemistry for apoptosis in the brain. Observe in (**A**) control group (GC), (**C**) diabetic group treated with insulin (GDI), (**D**) diabetic group treated with melatonin (GDM) and (**E**) diabetic group treated with insulin and melatonin (GDMI) weak marking, and in (**B**) diabetic group (GD) strong marking in the cortical layer. (**F**) Apoptotic index. Note a significant increase in the GD group. Means followed by the same letter do not differ significantly by Dunn's test (p<0.05).

inhibit apoptosis in situations of oxidative stress, ischemia, and toxicity of the β-amyloid peptide (Ghasemi et al. 2013).

Pro-inflammatory cytokines play a crucial role in the pathogenesis of diabetes (Ghosh et al. 2015). Our results indicate a strong marking of IL-6 and TNF-α in the cortical area of the rats' frontal brain in the diabetic group compared to rats in the other groups. This points out to a neurodegenerative process that can compromise brain functions (Wajant et al. 2003, Cutando et al. 2015). However, these effects were prevented by melatonin with or without insulin, indicating this hormone is a potent inhibitor of inflammatory interleukins (Kumar & Sharma 2010, Seraphim et al. 2000). Other studies link the binding of insulin to the regulation of the inflammatory response since this hormone participates in processes that inhibit the production of inflammatory cytokines such as IL-6 and TNF-α .

CONCLUSION

The treatment with melatonin associated with insulin proved to be beneficial in preventing the effects of diabetes on the rat brain's frontal cortex. However, this administration's clinical and physiological importance requires further clarification to understand better the mechanisms by which melatonin exerts these beneficial effects.

Conflict of interest statement.- The authors have no conflicts of interest to declare.

REFERENCES

Ahmadpour S.H. & Haghir H. 2011. Diabetes mellitus type 1 induces dark neuron formation in the dentate gyrus: a study by Gallya's method and transmission eléctron microscopy. Rom. J. Morphol. Embryol. 52(2):575-579. <PMid:21655645>

Banks W.A. 2004. The source of cerebral insulin. Eur. J. Pharmacol. 490(1/3):5-12. <https://dx.doi.org/10.1016/j.ejphar.2004.02.040> <PMid:15094069>

Baydas G., Erçel E., Canatan H., Donder E. & Akyol A. 2001. Effect of melatonina on oxidative status of rat brain, liver and kidney tissues under constant light exposure. Cell. Biochem. Funct. 19(1):37-41. <https://dx.doi.org/10.1002/cbf.897> <PMid:11223869>

Beauquis J., Roig P., Homo-Delarche F., De-Nicola A. & Saraiva F. 2006. Reducced hipocampal neurogenesis and number hilar neurones in streptozotocin induced diabetic mice: reversion by antidepressant treatment. Eur. J. Neurosci. 23(6):1539-1546. <https://dx.doi.org/10.1111/j.1460-9568.2006.04691.x> <PMid:16553617>

Blurton-Jonesa M., Kitazawaa M., Martinez-Coriaa H., Castelloa N.A., Mallerb F., Loring J.F., Yamasakia T.R., Poona W.W., Greena K.N. & Laferla F.M. 2009. Neural stem cells improve cognition via BDNF in a transgenic model of Alzheimer disease. Proc. Natl. Acad. Sci. 106(32):13594-13599. <https://dx.doi.org/10.1073/pnas.0901402106> <PMid:19633196>

Cam M., Yavuz O., Guven A., Ercan F., Bukan N. & Ustündag N. 2003. Protective effects of chronic melatonin treatment against renal injury in streptozotocin-induced diabetic rats. J. Pineal Res. 35(3):212-220. <https://dx.doi.org/10.1034/j.1600-079x.2003.00082.x> <PMid:12932206>

Cutando A., Montero J., Gomez-de-Diego R., Ferrera M.J. & Lopez-Valverde A. 2015. Effect of topical application of melatonin on serum levels of C-reactive protein (CRP), interleukin-6 (IL-6) and tumor necrosis factor-alpha (TNF-α) in patients with type 1 or type 2 diabetes and periodontal disease. J. Clin. Exp. Dent. 7(5):e628-33. <https://dx.doi.org/10.4317/jced.52604> <PMid:26644840>

Dall'ago P., Silva V.O., De-Angelis K.L., Irigoyen M.C., Fazan R.J. & Salgado H.C. 2002. Reflex control of arterial pressure and heart rate in short-term streptozotocin diabetic rats. Braz. J. Med. Biol. Res. 35(7):843-849. <https://dx.doi.org/10.1590/S0100-879X2002000700013>

Dorsemans A.C., Couret D., Hoarau A., Meihac O., Lefebvre D.C. & Diotel N. 2017. Diabetes, adult neurogenesis and brain remodeling: New insights from rodent and zebrafish models. Neurogenesis 4(1):e1281862. <https://dx.doi.org/10.1080/23262133.2017.1281862> <PMid:28439518>

Edward J.L., Vicent A.M., Cheng H.T. & Feldman E.L. 2008. Diabetic neuropathy: mechanisms to management. Pharmcol. Ther. 120(1):1-34. <https://dx.doi.org/10.1016/j.pharmthera.2008.05.005> <PMid:18616962>

El-Sokkary G.H., Kamel E.S. & Reiter R.J. 2003. Prophylactic effect of melatonin in reducing lead-induced neurotoxicity in the rat. Cell. Mol. Biol. Lett. 8(2):461-470. <PMid:12813579>

Ferreira C.S., Maganhin C.C., Simões R.S., Girão M.J.B.C., Baracat E.C. & Soares-Jr J.M. 2010. Melatonina: modulador de morte celular. Revta Assoc. Med. Bras. 56(6):715-718. <https://dx.doi.org/10.1590/S0104-42302010000600024>

Franc D.T., Kodl C.T., Mueller B.A., Muetzel R.L., Lim K.O. & Seaquist E.R. 2011. High connectivity between reduced cortical thickness and disrupted white matter tracts in long-standing type 1 diabetes. Diabetes 60(1):315-319. <https://dx.doi.org/10.2337/db10-0598> <PMid:20980455>

Francis G.J., Martinez J.A., Liu W.Q., Xu K., Ayer A., Fine J., Tuor U.I., Glazner G., Hanson L.R., Frey II.W.H. & Touth C. 2008. Intranasal insulin prevents cognitive decline, cerebral atrophy and whitematter changes inmurine type I diabetic encephalopathy. Brain 131(Pt 12):3311-3334. <https://dx.doi.org/10.1093/brain/awn288> <PMid:19015157>

Ghasemi R., Haeri A., Dargahi L., Mohamed Z. & Ahmadiani A. 2013. Insulin in the brain: sources, localization and functions. Mol. Neurobiol. 47(1):145-171. <https://dx.doi.org/10.1007/s12035-012-8339-9> <PMid:22956272>

Ghosh S., Banerjee S. & Parames P. 2015. The beneficial role of curcumin on inflammation, diabetes and neurodegenerative disease: A recent update. Food Chem. Toxicol. 83:111-24. <https://dx.doi.org/10.1016/j.fct.2015.05.022> <PMid:26066364>

Gundersen H.J.G., Bendtsen T. F., Korbo L., Marcussen N., Moller A., Nielsen K., Nyengaard J.R., Pakkenberg B., Sorensen F.B., Vesterby A. & West M.J. 1988. Some new, simple and efficient stereological methods and their use in pathological research and diagnosis. APMIS 96(5):379-394. <https://dx.doi.org/10.1111/j.1699-0463.1988.tb05320.x> <PMid:3288247>

Hernandez-Velázquez B., Camara-Lemarroy C.R., González-González J.A., Garcia-Compean D., Monreal-Robles R., Cordero-Perez P. & Munõz-Espinosa L.E. 2016. Efectos de la melatonina en la respuesta inflamatória aguda associada con la colangiopancreatografia retrógrada endoscópica: un ensayo clínico aleatorizado, doble ciego y controlado con placebo. Revta Gastroenterol. Méx. 81(3):141-148. <https://dx.doi.org/10.1016/j.rgmx.2016.03.003>

Hsu J.L., Chen Y.L., Leu J.G., Jaw F.S., Lee C.H., Tsai Y.F., Hsu C.Y., Bai C.H. & Leemans A. 2012. Microstructural white matter abnormalities in type 2 diabetes mellitus: a diffusion tensor imaging study. NeuroImage. 59(2):1098-1105. <https://dx.doi.org/10.1016/j.neuroimage.2011.09.041> <PMid:21967726>

Huang M., Gao L., Yang L., Lin F. & Lei H. 2012. Abnormalities in the brain of streptozotocin-induced type 1 diabetic rats revealed by diffusion tensor imaging. NeuroImage Clin. 1(1):57-65. <https://dx.doi.org/10.1016/j.nicl.2012.09.004>

Jackson-Guilford J., Leander J.D. & Nisenbaum L.K. 2000. The effect of streptozotocin-induced diabetes on cell proliferation in the rat dentate gyrus. Neurosci. Lett. 293(2):91-94. <https://dx.doi.org/10.1016/s0304-3940(00)01502-0> <PMid:11027841>

Khaksar Z., Jelodar G. & Hematian H. 2010. Effect of maternal diabetes on cerebellum histomorphometry in neonatal rats. J. Shaheed Sadoughi Univ. Med. Sci. Health Serv. 18(1):56-63.

Kodl C.T., Franc D.T., Rao J.P., Anderson F.S., Thomas W., Mueller B.A., Lim K.O. & Seaquist E.R. 2008. Diffusion tensor imaging identifies deficits in White matter microstructure in subjects with type 1 diabetes that correlate

with reduced neurocognitive function. Diabetes 57(11):3083-3089. <https://dx.doi.org/10.2337/db08-0724> <PMid:18694971>

Korbo L., Pakkenberg B., Ladefoged O., Gundersen H.J., Arlien-Søborg P. & Pakkenberg H. 1990. An efficient method for estimating the total number of neurons in rat brain cortex. J Neurosci. Methods 31(2):93-100. <https://dx.doi.org/10.1016/0165-0270(90)90153-7> <PMid:2181205>

Kumar A. & Sharma S.S. 2010. NF-kappa B inhibitory action 1301 of resveratrol: a probable mechanism of neuroprotection in experimental diabetic neuropathy. Biochem. Biophysic Res. 394(2):360-365. <https://dx.doi.org/10.1016/j.bbrc.2010.03.014> <PMid:20211601>

Lee S.C. & Pervaiz S. 2007. Review Apoptosis in the pathophysiology of diabetes mellitus. Int. J. Biochem. Cell Biol. 39(3):497-504. <https://dx.doi.org/10.1016/j.biocel.2006.09.007> <PMid:17074529>

Lima E., Soares J.M.J., Del-Carmen S.G.Y., Gomes V.S., Priel M.R., Baracat E.C., Carvalheiro E.A., Naffah-Mazzacoratti M.G. & Amado D. 2005. Effects of pinealectomy and the treatment with melatonin on the temporal lobe epilepsy in rats. Brain Res. 1043(1/2):24-31. <https://dx.doi.org/10.1016/j.brainres.2005.02.027> <PMid:15862514>

Louzada S.M. & Vargas C.R. 2015. Encefalopatia diabética e depressão: dano oxidativo no cérebro. Clin. Biomed. Res. 35(4):184-195. <https://dx.doi.org/10.4322/2357-9730.59313>

Luciano E. & Mello M.A.R. 1998. Atividade física e metabolismo de proteínas em músculo de ratos diabéticos experimentais. Revta Paul. Educ. Fís. 12(2):202-209.

Luo Y., Peng M. & Wei H. 2017. Melatonin promotes brain-derived neurotrophic factor (BDNF) expression and anti-apoptotic effects in neonatal hemolytic hyperbilirubinemia via a phospholipase (PLC) - mediated mechanism. Med Sci Monit. 23:5951-5959. <https://dx.doi.org/10.12659/msm.907592> <PMid:29247156>

Moura L.P., Gomes R.J., Leme J.A., Voltarelli F.A., Ribeiro C., Moura R.F., Araújo M.B., Luciano E. & Mello M.R. 2012. Insulina pancreática de ratos diabéticos tipo 1 submetidos a um protocolo de treinamento físico individualizado. Motricidade. 8(1):23-32. <https://dx.doi.org/10.6063/motricidade.8(1).234>

Pinheiro L.S., Melo A.D., Andreazzi A.E., Caires Júnior L.C., Barros Costa M.& Gonzalez-Garcia R.M. 2011. Protocol of Insulin therapy for streptozotocin-diabetic rats based on a study of food ingestion and glycemic variation. Scand. J. Lab. Anim. Sci. 38(2):117-127.

Piotrowski P., Wierzbicka K. & Smialek M. 2001. Neuronal death in the rat hippocampus in experimental diabetes and cerebral ischaemia treated with antioxidants. Folia Neuropathol. 39(3):147-154. <PMid:11770125>

Sartori C., Dessen P., Mathieu C., Monney A., Bloch J., Nicod P., Scherrer U. & Duplain H. 2009. Melatonin Improves glucose homeostasis and endothelial vascular function in high-fat diet-fed insulin-resistant mice. Endrocrinology 150(12):311-317. <https://dx.doi.org/10.1210/en.2009-0425> <PMid:19819971>

Sbem 2017. Posicionamento da SBEM sobre a melatonina Sociedade Brasileira de Endocrinologia e Metabologia. Available at <https://www.endocrino.org.br/media/uploads/PDFs/posicionamento_sobre_melatonina_sbem.pdf> Accessed on Dec. 29, 2019.

Seraphim P.M., Sumida D.H., Nishide F.Y., Lima F.B., Neto Cipolla J. & Machado U.F. 2000. A glândula pineal e o metabolismo de carboidratos. Arq. Bras. Endocrinol. Metab. 44(4):331-338. <https://dx.doi.org/10.1590/S0004-27302000000400009>

Tuzcu M. & Baydas G. 2006. Effect of melatonin and vitamin E on diabetes-induced learning and memory impairment in rats. Eur. J. Pharmacol. 537(1/3):106-110. <https://dx.doi.org/10.1016/j.ejphar.2006.03.024> <PMid:16626697>

Van-Elderen S.G.C., De-Roos A., De-Craen A.J.M., Westendorp R.G.J., Blauw G.J., Jukema J.W., Bollen E.L.E.M., Middelkoop H.A.M., Van-Buchem M.A. & Van-Der-Grond J. 2010. Progression of brain atrophy and cognitive decline in diabetes mellitus. Neurology 75(11):997-1002. <https://dx.doi.org/10.1212/WNL.0b013e3181f25f06> <PMid:20837967>

Van-Harten B., De-Leeuw F.E., Weinstein H.C., Scheltens P. & Biessels G.J. 2006. Brain imaging in patients with diabetes - a systematic review. Diabetes Care 29(11):2539-2548. <https://dx.doi.org/10.2337/dc06-1637> <PMid:17065699>

Villeda-Hernández J., Méndez-Armenta M., Barroso-Moguel R., Trejo-Solis M.C., Guevara J. & Rios C. 2006. Morphometric analysis of brain lesions in rat fetuses prenatally exposed to low-level lead acetate: correlation with lipid peroxidation. Histol. Histopathol. 21(6):609-617. <https://dx.doi.org/10.14670/HH-21.609> <PMid:16528671>

Wajant H., Pfizenmaier K. & Scheurich P. 2003. Tumor necrosis factor signaling. Cell Death Differ. 10(1):45-65. <https://dx.doi.org/10.1038/sj.cdd.4401189> <PMid:12655295>

Wang C.F., Li D.Q., Xue H.Y. & Hu B. 2010. Oral supplementation of catalpol ameliorates diabetic encephalopathy in rats. Brain Res. 1307:158-165. <https://dx.doi.org/10.1016/j.brainres.2009.10.034> <PMid:19852947>

Weibel E.R., Kistler G.S. & Scherle W.F. 1966. Practical stereological methods for morphometric cytology. J. Cell Biol. 30(1):23-38. <https://dx.doi.org/10.1083/jcb.30.1.23> <PMid:5338131>

West M.J. 1993. Regionally specific loss of neurons in the aging human hippocampus. Neurobiol. Aging 14(4):287-293. <https://dx.doi.org/10.1016/0197-4580(93)90113-p> <PMid:8367010>

Wu X., Cheng B., Cai Z.D. & Lie-Ming L. 2013. Determination of the apoptotic index in osteosarcoma tissue and its relationship with patients prognosis. Cancer Cell Int. 13(1):56. <https://dx.doi.org/10.1186/1475-2867-13-56> <PMid:23734671>

Yamada K., Mizuno M. & Nabeshima T. 2002. Role for brain-derived neurotrophic factor in learning and memory. Life Sci. 70(7):735-744. <https://dx.doi.org/10.1016/s0024-3205(01)01461-8> <PMid:11833737>

Yang C., De-Visser A., Martinez J.A., Poliakov I., Rosales-Hernandez A., Ayer A., Garven A., Zaver S., Ricon N., Xu K., Tuor U.I., Schmidt A.M. & Toth C. 2011. Differential impact of diabetes and hypertension in the brain: adverse effects in white matter. Neurobiol. Disease 42(3):446-458. <https://dx.doi.org/10.1016/j.nbd.2011.02.007> <PMid:21324363>

Yau P.L., Javier D., Tsui W., Sweat V., Bruehl H., Borod J.C. & Convit A. 2009. Emotional and neutral declarative memory impairments and associated white matter microstructural abnormalities in adults with type 2 diabetes. Psychiatry Res. 174(3):223-230. <https://dx.doi.org/10.1016/j.pscychresns.2009.04.016> <PMid:19906514>

Yoon S., Cho H., Kim J., Lee D.W., Kim G.H., Hong Y.S., Moon S., Park S., Lee S., Bae S., Simonson D.C., Simonson D.C. & Lyoo I.K. 2017. Brain changes in overweight/obese and normal-weight adults with type 2 diabetes mellitus. Diabetologia. 60(7):1207-1217. <https://dx.doi.org/10.1007/s00125-017-4266-7> <PMid:28447116>

Colégio Brasileiro de Patologia Animal

Em 15 de agosto de 2019

INSTRUÇÕES AOS AUTORES

A submissão de artigos à revista "Pesquisa Veterinária Brasileira" (PVB) deve ser feita em Word, através do Sistema ScholarOne, *link* <https://mc04.manuscriptcentral.com/pvb-scielo>

A tramitação somente pode ter início se o seu artigo estiver rigorosamente dentro das normas de apresentação da revista, de acordo com as Instruções aos Autores, o modelo no site da revista e os últimos fascículos publicados (www.pvb.com.br). Na verificação de falhas de apresentação, o artigo será devolvido aos autores para as devidas correções.

Os autores podem submeter seus artigos em **Inglês** ou em **Português**, mas sempre com um Resumo em português. No caso de artigos aceitos escritos em **Português**, estes serão traduzidos para o **Inglês** pela Editora Cubo; pois todos os artigos publicados na PVB serão em inglês. Para os artigos já submetidos em **Inglês**, os autores devem apresentar via ScholarOne um Certificado de Tradução de uma empresa habilitada ou de um Tradutor Nativo. **Essa regra vale para artigos submetidos a partir de 1 de janeiro de 2018.**

Os pagamentos da taxa de publicação (*Paper Charge*) serão cobrados na ocasião do envio da comunicação de aceite por e-mail:

(1)Artigos submetidos em inglês, R$ 1.500,00 (*US$ 480.00*) por artigo;

(2)Artigos submetidos em português, R$ 1.500,00 (*US$ 800.00*) mais R$ 0,32 por palavra (o valor total cobrado por será enviado por e-mail pela tesouraria do CBPA).

A partir de 2019, **todos os autores deverão criar um registro no ORCID** (Open Researcher and Contributor ID - https://orcid.org/register) e vinculá-lo ao seu perfil no ScholarONE. O vínculo pode ser feito editando o perfil do usuário no ScholarONE na opção **Associate your existing ORCID iD**. Os identificadores ORCID contribuem para a identificação única dos autores e, portanto, para os processos interoperacionais e bibliométricos que envolvem autores. Usando um ORCID, os pesquisadores são fácil e corretamente conectados com seus resultados de pesquisa, publicações e afiliações.

O **texto** deve ser formatado, em todos os pormenores, de acordo com as normas de apresentação da revista (www.pvb.com.br).

Se o artigo for submetido fora das normas de apresentação da PVB, a tramitação somente ocorrerá após as devidas correções feitas pelo autor.

A PVB publica Artigos Originais, Artigos de Revisão Crítica e Tópicos de Interesse Geral; não publica artigos com a denominação de *Short Communications*.

Relatos de Caso serão aceitos somente em artigos classificados como pertencentes à área de Animais Selvagens (*Wildlife Medicine*).

Os Artigos Originais devem conter resultados de pesquisa ainda não publicados ou submetidos para outros periódicos.

Artigos de Revisão de Literatura, submetidos a convite, devem constituir-se de análise crítica, de assuntos na área de experiência dos autores, isto é, quando os autores já tiverem publicado anteriormente artigos sobre o assunto.

Os raros Tópicos de Interesse Geral devem constituir-se de assuntos de grande importância atual baseado na vasta experiência dos autores.

As opiniões e conceitos emitidos nos artigos submetidos são de responsabilidade dos autores. O Conselho Editorial da PVB, com a assistência da Assessoria Científica, pode sugerir ou solicitar modificações. Os artigos submetidos são avaliados pelos pares (*peer review*) e, aceitos para publicação com dois pareceres favoráveis, ou rejeitados por dois pareceres desfavoráveis.

Os direitos autorais dos artigos aceitos para publicação permanecem com os autores.

1. **Os artigos devem ser organizados em TÍTULO, ABSTRACT, RESUMO, INTRODUÇÃO, MATERIAL E MÉTODOS, RESULTADOS, DISCUSSÃO, CONCLUSÕES (de preferência os últimos três separadamente), Agradecimentos, Declaração de conflito de interesse e REFERÊNCIAS:**

a) O **TÍTULO** deve ser conciso e indicar o conteúdo do artigo; pormenores de identificação científica devem ser colocados em MATERIAL E MÉTODOS.

b) O(s) Autor(es) com numerosos primeiros nomes e sobrenomes, deve(m) padronizar o seu "nome para publicações científicas", como por exemplo: Cláudio Severo Lombardo de Barros, escreve Cláudio S.L. Barros ou Barros C.S.L.; Franklin Riet-Correa Amaral escreve Franklin Riet-Correa ou Riet-Correa F. **Os artigos devem ter no máximo 8 (oito) autores**. O autor para correspondência deve ser um autor que garanta o contato com o Conselho Editorial da PVB. Asteriscos de chamadas para o rodapé não devem ser sobrescritos.

c) O **Cabeçalho do ABSTRACT** deve conter além dos nomes dos autores abreviados invertido, o ano, o TÍTULO, o endereço postal do laboratório (inclusive o CEP) ou instituição principal onde foi desenvolvida a pesquisa. Endereços postais brasileiros

não devem ser traduzidos para o inglês, mesmo em artigos escritos na língua inglesa, a fim de evitar dificuldade na postagem. Deve-se conferir os nomes dos autores do artigo e do Cabeçalho do Abstract para evitar discrepâncias.

d) O **Rodapé da primeira página** deve conter os endereços profissionais postais completos dos autores (evitando-se traços horizontais), na língua do país do respectivo autor (em português, espanhol, inglês) e seus e-mails; o e-mail do autor para correspondência deve ser sublinhado. Os sinais de chamada para os nomes dos autores devem ser números arábicos, colocados em sobrescrito, sem o uso automático de "Inserir nota de fim", do Word (essas chamadas devem ser contínuas por todo artigo, isto é, em todas as notas de rodapé das outras páginas).

e) O **ABSTRACT** deve ser uma versão do RESUMO, mas pode ser mais explicativo, seguido de "INDEX TERMS" que devem incluir termos do título, por não se tratar somente de "ADDITIONAL INDEX TERMS".

f) O **RESUMO** deve conter o que foi feito e estudado, indicando a metodologia e dando os mais importantes resultados e conclusões, seguido dos "TERMOS DE INDEXAÇÃO" que incluem têrmos do título, por não se tratar somente de "TERMOS DE INDEXAÇÃO ADICIONAIS".

g) A **INTRODUÇÃO** deve ser breve, com citação bibliográfica específica sem que a mesma assuma importância principal e deve finalizar com a indicação do objetivo do artigo.

h) MATERIAL E MÉTODOS deve reunir a totalidade dos dados que permitam o desenvolvimento de trabalho semelhante por outros pesquisadores.

i) Em **RESULTADOS** devem ser apresentados concisamente os dados obtidos.

j) Na **DISCUSSÃO** devem ser confrontados os resultados diante da literatura. Não convém mencionar artigos em desenvolvimento ou planos futuros, de modo a evitar uma obrigação do autor e da revista de publicá-los.

k) CONCLUSÕES devem basear-se somente nos resultados obtidos e devem ser apresentados em diferentes parágrafos (uma Conclusão somente deve ser apresentada em parágrafo único).

l) Os **Agradecimentos** não devem aparecer no texto ou em notas de rodapé; devem ser sucintos e colocados antes da Declaração de conflito de interesse e da Lista de Referências.

m) A **Declaração de conflito de interesse** é obrigatória e deve ser mencionada nos casos positivos ou negativos; deve ser sucinta e colocada imediatamente antes da Lista de Referências.

n) A Lista de **REFERÊNCIAS** deve incluir todas as citações apresentadas no texto e que tenham servido como fonte para consulta. A Lista deve ser ordenada alfabética e cronologicamente, pelo sobrenome do primeiro autor, seguido de todos os demais autores (em caixa alta e baixa), do ano, do título da publicação citada, e abreviado (por extenso em casos de dúvida) o nome do periódico. Sugerimos consultar exemplos dos últimos fascículos (www.pvb.com.br).

(Notem: (1) As Referências citadas no texto devem ser colocadas em ordem cronológica, mas alfabética tratando-se de referências do mesmo ano; (2) Quando utilizados programas de formatação (p.ex. Endnote X7), remover o fundo automático cinzento antes da submissão, para não dificultar eventuais correções.

2. **Na elaboração do texto devem ser atendidas as seguintes normas:**

a) Fonte **Cambria, corpo 10, entrelinha simples; página formato A4, com 2cm de margens** (superior, inferior, esquerda e direita), texto corrido em uma coluna justificada, com as Legendas das Figuras no final (logo após a Lista de REFERÊNCIAS) sem repetir as legendas junto com as Figuras.

b) ABSTRACT e RESUMO serão escritos em um só parágrafo corrente e não devem conter citações bibliográficas.

c) A redação dos artigos deve ser concisa, com a linguagem, tanto quanto possível, no passado e impessoal.

d) Os nomes científicos usados no manuscrito devem ser apresentados por extenso (p.ex. *Palicourea marcgravii*), no início de cada capítulo (**TÍTULO, ABSTRACT, RESUMO, INTRODUÇÃO, etc.**), quando aparecem pela primeira vez, seguido da abreviação do gênero (p.ex. *P. marcgravii*).

e) Nos títulos dos Quadros e nas Legendas das Figuras os nomes científicos devem ser apresentados por extenso, já que estes são independentes do texto.

f) No texto, os sinais de chamada para notas de rodapé devem ser números arábicos colocados em sobrescrito após a palavra ou frase que motivou a nota. Essa numeração será contínua por todo o artigo; as notas deverão ser lançadas ao pé da página em que estiver o respectivo número de chamada, sem o uso do "Inserir nota de fim", do Word.

Notem: para evitar a separação em duas linhas, os numerais devem ser apresentados junto com suas unidades, ou seja, sem espaçamento, por exemplo: 100ppm, 10mm, 50cm, 18x10cm, (P<0,05), 15h. A abreviação de número é "nº" e não "nº"; grau Celsius é "ºC" e não "ºC".

g) Os Quadros (não usar o termo Tabela) e as Figuras devem ser citados no texto, pelos respectivos números, em ordem crescente e devem ser submetidos separadamente do texto!

h) Siglas e abreviações das instituições, ao aparecerem pela primeira vez, deverão ser colocadas entre parênteses, após o nome da instituição por extenso;

i) Citações bibliográficas serão feitas pelo sistema "autor e ano", p.ex. (Caldas 2005); artigos de até dois autores serão citados pelos nomes dos dois (Pedroso & Pimentel 2013); e com mais de dois, pelo nome do primeiro, seguido de "et al.", mais o ano (Brito et al. 2015); se dois artigos não se distinguirem, a diferenciação será feita através do acréscimo de letra minúscula ao ano (Barros 2017a, 2017b). A ordem de citação deve ser cronológica (Barbosa et al. 2003, Armién et al. 2004).

j) Recomenda-se consultar na íntegra todos os artigos citados; se isto não for possível, deve-se colocar no texto a referência original (não consultada na íntegra) seguida do ano, p.ex. (Bancroft 1921); na Lista de Referências deve ser incluída a referência original como: Bancroft 1921. ..... título. ... periódico. (Apud Suvarna & Layton 2013). A referência consultada também deve ser incluída na Lista de Referências.

k) O uso de "comunicação pessoal" e de "dados não publicados" deve ser feito apenas em casos excepcionais; no texto com citação de Nome e Ano, e na Lista de Referências como: Barbosa 2016. Comunicação pessoal (Universidade Federal do Pará, campus Castanhal).

l) As **Legendas das Figuras** devem conter informações suficientes para sua compreensão (independente do texto); e devem ser precedidas de "Fig." seguida do número sem espaço, p.ex. "Fig.8. ...". Para elaboração das legendas sugerimos consultar exemplos nos últimos fascículos (www.pvb.com.br).

(Notem: Na legenda de Figuras compostas deve-se colocar a letra de cada "subfigura" em **negrito** com parênteses claros antes do texto correspondente e devem ser mencionados letras ou sinais, que estão dentro de cada "subfigura", em parêntees e claros após o respectivo texto da legenda.)

m) O Título dos **Quadros** devem ser em **negrito**, sem ponto, e a "garganta" (título das colunas) deve ser escrita em claro e separada por dois traços longos horizontais; o Título dos Quadros e da "garganta" devem ser escritas em caixa alta e baixa. Os Quadros (não usar o termo Tabela) devem conter os resultados mais relevantes. Não há traços verticais, nem fundos cinzentos; excepcionalmente pode conter traços horizontais. Os sinais de chamada serão alfabéticos, recomeçando, com "a" em cada Quadro. As chamadas de rodapé deverão ser lançadas logo abaixo do Quadro respectivo, do qual serão separadas por um traço curto à esquerda; e devem evitar números arábicos. Os títulos não têm ponto no final, ao passo que as legendas terminam com um ponto. Os Quadros devem ser apresentados em Word e ser editáveis, a fim de inserirmos eventuais alterações de apresentação, dentro das normas da revista.

n) Dados complexos devem ser expressos por Gráficos (devem ser chamados de **Figuras**). Os gráficos devem ser produzidos em 2D, sem fundo e sem linhas horizontais. Em gráficos contendo texto a fonte deve ser Cambria tamanho 10.

3. **Apresentação das Figuras:**

a) As figuras devem ser salvas em 300dpi, arquivo TIF.

b) Enviar cada figura separadamente.

c) Identificar as figuras em ordem conforme a menção no texto.

d) As figuras solitárias devem ter seus arquivos identificados como (Fig.1, Fig.2 ...)

e) As figuras que serão destinadas a formar uma prancha devem ter seus arquivos identificados como (Fig.1A, Fig.1B ...). As pranchas devem ser compostas por múltiplas subfiguras. Imagens destinadas a uma prancha devem ser de mesmo tamanho.

f) Para micrografias usar, de preferência, barras de escala para indicar o aumento; apresentar na legenda sempre o método de coloração e a objetiva, p. ex.: HE, obj.40x.

g) As legendas de figuras devem conter inicialmente o que se observa na imagem, seguida das informações adicionais (Formato típico da legenda: Fig.1. (**A**) Descrição da imagem. Diagnóstico, órgão ou tecido, espécie animal, número do caso. Método de coloração e objetiva.).

h) As legendas de figuras devem ser apresentadas junto com o texto do artigo, após as Referências.

4. **Todas as referências citadas no texto devem ser incluídas na Lista de Referências e vice-versa**; **na revisão final do artigo pelos autores,** antes da submissão, **isto deve ser conferido criteriosamente, para evitar discrepâncias (o sistema ScholarOne bloqueia automaticamente artigos com discrepâncias).**

Exemplos de Referências

➢ Artigos publicados em periódicos:

Martins K.P.F., Fonseca T.R.S., Silva E.S., Munhoz T.C.P., Dias G.H.S., Galiza G.J.N., Oliveira L.G.S. & Boabaid F.M. 2018. Bócio em bovinos. Pesq. Vet. Bras. 38(6):1030-1037.

Rondelli L.A.S., Silva G.S., Bezerra K.S., Rondelli A.L.H., Lima S.R., Furlan F.H., Pescador C.A. & Colodel E.M. 2017. Doenças de bovinos no Estado de Mato Grosso diagnosticadas no Laboratório de Patologia Veterinária da UFMT (2005-2014). Pesq. Vet. Bras. 37(5):432440.

Hooiveld M., Smit L.A., Wouters I.M., Van Dijk C.E., Spreeuwenberg P., Heederik D.J. & Yzermans C.J. 2016. Doctor-diagnosed health problems in a region with a high density of concentrated animal feeding operations: a cross-sectional study. Environ. Health 17:15-24.

Colégio Brasileiro de Patologia Animal

Em 15 de agosto de 2019

(Notem: Os iniciais dos autores devem ser colocados sem espaço. O sinal "&" é usado para separar o penúltimo do último autor. As primeiras letras das palavras do título de artigos publicados em periódicos científicos devem ser de preferência minúsculas. A palavra "Revista" deve ser abreviada como "Revta" em diferença a "Rev.", do inglês "Review". Deve-se indicar o número do respectivo volume do periódico e, se possível, também do fascículo. Somente abreviações tem um ponto, exceto as que terminam com a última letra da palavra em extenso. O traço entre as páginas é curto (-) e não comprido. Não devem ser usados "pontovírgulas" (;) em lugar de vírgulas.

- Livros:

Tokarnia C.H., Brito M.F., Barbosa J.D., Peixoto P.V. & Döbereiner J. 2012. Plantas Tóxicas do Brasil para Animais de Produção. 2ª ed. Helianthus, Rio de Janeiro, p.305-348.

Marsh P. & Martin M. 1992. Oral Microbiology. 3rd ed. Chapman and Hall, London, p.167-196.

(Notem: A primeira letra de termos do título de livros deve ser maiúscula. Devem ser mencionadas as páginas que foram consultadas, em vez do total de páginas do livro.

- Capítulos de livros:

Barros C.S.L. 2007. Doenças víricas: leucose bovina, p.159-169. In: Riet-Correa F., Schild A.L., Lemos R.A.A. & Borges J.R.J. (Eds), Doenças de Ruminantes e Equídeos. Vol.1. 3ª ed. Pallotti, Santa Maria.

Tokarnia C.H., Brito M.F., Barbosa J.D., Peixoto P.V. & Döbereiner J. 2012. Plantas que afetam o funcionamento do coração, p.27-94. In: Ibid. (Eds), Plantas Tóxicas do Brasil para Animais de Produção. 2ª ed. Helianthus, Rio de Janeiro.

(Notem: As primeiras letras das palavras do título de capítulos de livros são minúsculas, mas as de livros são maiúsculas.)

- Dissertações e Teses:

Rech R.R. 2007. Alterações no encéfalo de bovinos submetidos à vigilância das encefalopatias espongiformes transmissíveis. Tese de Doutorado, Universidade Federal de Santa Maria, Santa Maria. 228p.

(Notem: (1) Deve-se evitar citações de Dissertações ou Teses; deve-se preferir citar artigos baseados nas mesmas e publicados em periódicos científicos que são de mais fácil acesso. (2) Não deve-se tentar de publicar o texto de Dissertação ou Tese praticamente na íntegra sem escrever um artigo conciso de seus resultados.

- Resumos publicados em eventos:

Mendonça F.S., Almeida V.M., Albuquerque R.F., Chaves H.A.S., Silva Filho G.B., Braga T.C., Lemos B.O. & Riet Correa F. 2016. Paralisia laríngea associada à deficiência de cobre em caprinos no semiárido de Pernambuco (IX Endivet, Salvador, BA). Pesq. Vet. Bras. 36(Supl.2):50-51. (Resumo)

Pierezan F., Lemos R.A.A., Rech R.R., Rissi D.R., Kommers G.D., Cortada V.C.L.M., Mori A.E. & Barros C.S.L. 2007. Raiva em equinos. Anais XIII Encontro Nacional de Patologia Veterinária, Campo Grande, MS, p.145-146. (Resumo)

(Note: Evitar na consulta o uso de Resumos ao invés de artigos na íntegra!)

Colégio Brasileiro de Patologia Animal

Em 15 de agosto de 2019

GUIDE FOR AUTHORS

Papers to "Pesquisa Veterinária Brasileira" (PVB), a Brazilian Journal of Veterinary Research, are submitted in Word online through ScholarOne, link <https://mc04.manuscriptcentral.com/pvb-scielo>

The authors should submit their papers in English, with a Portuguese Summary. To prove the quality of the English, a certificate of the English language is required, with exception of authors native in English.

With the communication of acceptance of the paper, the author for correspondence will be asked for payment of a Paper Charge of US$ 480.00 (*R$ 1.500,00*) for each article submitted in English.

As of 2019, **all authors should register in the ORCID** (Open Researcher and Contributor ID https://orcid.org/register) and link it to their ScholarONE profile. The link can be done by editing the user profile on ScholarONE in the option **Associate your existing ORCID iD**. The ORCID identifiers contribute to the singular identification of the authors and to the interoperational and bibliometric processes. Using an ORCID, researchers are easily and correctly connected with their research results, publications and affiliations.

Papers should be prepared in all details according to the style of the journal (www.pvb.com.br), in order to be peer reviewed. Tables and Figures should be submitted separately from the text.

PVB publishes Original Articles, but also Critical Literature Reviews and Topics of General Interest; no Short Communications are accepted.

Case Reports will be accepted only in articles classified as Wildlife Medicine.

The Original Papers should contain research results not yet published and not submitted to other journals.

Literature Reviews should be critical and consist of subjects of the author's research line.

Topics of General Interest should be of great importance and based on large experience of the authors.

The opinions and concepts emitted are of the responsibility of the authors. The Editorial Board of the journal, assisted by the peer review, may suggest or ask for modification of the text.

The author rights of the accepted papers are preserved.

1. **The submitted article should be organized in TITLE, ABSTRACT, RESUMO (the last when authors are from a Portuguese speaking country), INTRODUCTION, MATERIALS AND METHODS, RESULTS, DISCUSSION, CONCLUSION(S) (the last three preferably as separate chapters), Acknowledgements, Conflict of interest statement and REFERENCES:**

a) The **TITLE** should be concise and indicate the content of the article; details of scientific identification should be put into MATERIALS AND METHODS.

b) Authors with several first and family names should shorten their names for scientific publication, as for example: Cláudio Severo Lombardo de Barros writes Cláudio S.L. Barros or Barros C.S.L., and Franklin Riet-Correa Amaral writes Franklin Riet-Correa or Riet-Correa F. **The papers should not have more than 8 (eight) authors.** Corresponding author should be one who guarantees the contact with the Editorial Board of PVB. Asterisks for call to the footnotes should be elevated once more, in order to appear larger.

c) The **heading of the ABSTRACT** should contain the shortened and inverted names of the authors, the year, the Title (in brakes when translated), and the postal address of the laboratory or institution where the main part of the research was done (Always compare the authors of the paper and their shortened and inverted in the heading of the Abstract to avoid discrepancies).

d) The **footnote of the first page** should contain the complete professional address of each author (in the language of the author's country where to correspondence could be posted, Portuguese, Spanish, English, etc.) as well as the underlined e-mail of the corresponding author.

e) The **ABSTRACT** should be a well explained version of the Portuguese RESUMO, followed by "INDEX TERMS" which should include terms of the title, as they are not only Additional Index Terms.

f) The **RESUMO** should contain (1) what have been investigated, indicating (2) materials and methods used, (3) the most important results, and (4) the conclusion, followed by "TERMOS DE INDEXAÇÃO" (which include also words of the title, as they are not only Additional Index Terms).

g) The **INTRODUCTION** should be short, with citation of the specific literature without assuming main importance, followed by the objective of the research.

h) In **MATERIALS AND METHODS** should be given all data necessary for other research workers to repeat the research.

i) In **RESULTS** are presented the data obtained in a concise form.

j) In **DISCUSSION** the results should be confronted with the literature. Research in development or future planning should not be mentioned, to avoid the obligation for the journal to publish the results.

k) The **CONCLUSIONS** should be based only on the results obtained.

l) Acknowledgements should not be mentioned in the text or in footnotes.

m) Conflict of interest or none should be mentioned.

n) The **REFERENCES** include all citations consulted and presented chronologically in the text. The List of References should be written in alphabetical and chronological order, beginning with the family name of the first author, followed by the names of all other authors of the respective reference, in capital and small letters, and each author divided only by a comma, followed by year, title and the data of the publication (extensively in case of doubt about abbreviation) according to www.pvb.com.br.

2. During the elaboration of the paper, **the style of the journal has to be attended**, as follows:

a) Font **Cambria at 10 pitch, simple space between lines;** page **format A4, with 2cm margins** (superior, inferior, left and right), text in one column justified, with Figure captions below the list of References; without repeating the captions with the images of the Figures. Figures and Tables should be separately submitted.

b) ABSTRACT and **RESUMO** are written in only one paragraph and should not contain references.

c) The articles should be concise, always when possible in past tense and impersonal.

d) The scientific names should be presented in full (p.ex. *Palicourea marcgravii)* at the beginning of each chapter (Title, Abstract, Resumo, Introduction, etc.) when they appear for the first time, followed with abbreviation of the genus (p.ex. *P. marcgravii*).

e) In the Title of Tables and in Figure captions the scientific names are written in full.

f) In the text, calls to footnotes are given in Arabic numbers, in crescent order through the whole paper, without use of "Insert final note" of Word.

Note: To avoid separation in two lines, numbers should be presented without space to their units (p.ex.: 100ppm, 10mm, 50cm, 18x10cm, P<0.05.

The abbreviation for number is "nº" and not "nº"; for degree Celsius "ºC" and not "ºC".

g) Tables and Figures should be cited in the text with their respective numbers in crescent order.

h) Abbreviations of institutions when presented in the first place should be put within parentheses, after the full name of the institution.

i) Citations of the literature in the text are given by "author and year" (p.ex. Caldas 2005); papers with two authors are cited with the two names (p.ex. Pedroso & Pimentel 2013); citations with more than two authors are cited in the text by the name of the first author followed by "et al." and the year (p.ex. Brito et al. 2015). If two articles are not to distinguish, the differentiation is obtained through the addition of small letters after the year (p.ex. Barros 2017a, 2017b). The order of citation in the text should be chronological (p.ex. Barbosa et al. 2003, Armién et al. 2004).

j) All cited articles should be consulted in full text; if not possible, the original reference is put into the text as p.ex. Bancroft (1921); but in the List of References this should appear as: Bancroft 1921. ..... title. ... journal .... (Apud Suvarna & Layton 2013). The consulted reference should be also included in full in the List.

k) The use of "personal communication" and "non-published data" should be exceptional and cited in the text as Author and Year, and in the List of References as p.ex. Barbosa 2016. Personal Communication (Universidade Federal do Pará, campus Castanhal, Brazil).

l) Figure captions (p.ex. "Fig.3. ……..") should be sufficiently informative for understanding (because Figures are independent from the text).

m) The **Title of Tables** should be written in **bold** and the **Heading** (titles of the columns) should be in clear (not bold), written in capital and small letter and separated by two long horizontal lines. There are no vertical lines and no grey bottom; exceptionally can exist horizontal lines. The calls for footnotes should be in small letters or other signs, but not in Arabic numbers. Tables should be submitted in Word (not as images) to allow corrections according to the style of the journal.

n) Complex data should be presented as **graphics (but named Figures)** in 2D without grey bottom and horizontal lines. Graphics including text should be written with Cambria at 10 pitch.

3. **Figure presentation:**

a) Save images at 300 dpi, TIF files.

b) Send each figure separately.

c) Identify figures in the order in which they are mentioned in the text.

d) Individual figures must have their files named as (Fig.1, Fig.2, …).

e) Images that will compose a plate must have their files identified as (Fig.1A, Fig.1B,). Plates should be comprised by multiple images, and all images must have the same dimensions.

f) Use preferably scale bars for micrographs. For optical micrographs indicate at the legend finally the staining method and the objective used, for example: HE, obj.40x.

g) Figure legends should contain initially what is seen on the image, followed by additional information (Legend example: Fig.1. (**A**) Sentence description. Diagnosis, organ or tissue, animal species, case number. Staining method and objective used.).

h) Figure legends should be presented in the main document, after the **References**.

4. **All references cited in the text should be included in the List of References**; before the submission of the paper, discrepancies have to be corrected by the author (as the system ScholarOne blocks automatically if such discrepancies exist).

Exemples for References:

➢ Articles published in scientific journals:

Ubiali D.G., Cruz R.A., De Paula D.A., Silva M.C., Mendonça F.S., Dutra V., Nakazato L., Colodel E.M. & Pescador C.A. 2013. Pathology of nasal infection caused by *Conidiobolus lamprauges* and *Pythium insidiosum* in sheep. J. Comp. Pathol. 149(2/3):137-145.

Hooiveld M., Smit L.A., Wouters I.M., Van Dijk C.E., Spreeuwenberg P., Heederik D.J. & Yzermans C.J. 2016. Doctor-diagnosed health problems in a region with a high density of concentrated animal feeding operations: a cross-sectional study. Environ. Health 17:15-24.

(Note: The first letters of the words in the title of papers published in journals are small. It is preferable to indicate the number of the respective issue.)

➢ Books:

Marsh P. & Martin M. 1992. Oral Microbiology. 3rd ed. Chapman and Hall, London, p.167-196.

Tokarnia C.H., Brito M.F., Barbosa J.D., Peixoto P.V. & Döbereiner J. 2012. Plantas Tóxicas do Brasil para Animais de Produção. 2ª ed. Helianthus, Rio de Janeiro, p.305-348.

(Note: The first letter in the words of the title of books should be capital.)

➢ Chapters of books:

Uzal F.A., Plattner B.L. & Hostetter J.M. 2016. Alimentary system, p.1-257. In: Maxie M.G. (Ed.), Jubb, Kennedy and Palmer´s Pathology of Domestic Animals. Vol.2. 6th ed. Elsevier, St Louis, Missouri.

Barros C.S.L. 2007. Doenças víricas: leucose bovina, p.159-169. In: Riet-Correa F., Schild A.L., Lemos R.A.A. & Borges J.R.J. (Eds), Doenças de Ruminantes e Equídeos. Vol.1. 3ª ed. Pallotti, Santa Maria, RS.

Tokarnia C.H., Brito M.F., Barbosa J.D., Peixoto P.V. & Döbereiner J. 2012. Plantas que afetam o funcionamento do coração, p.27-94. In: Ibid. (Eds), Plantas Tóxicas do Brasil para Animais de Produção. 2ª ed. Helianthus, Rio de Janeiro.

➢ Dissertations and Theses:

Rech R.R. 2007. Alterações no encéfalo de bovinos submetidos à vigilância das encefalopatias espongiformes transmissíveis. Tese de Doutorado, Universidade Federal de Santa Maria, Santa Maria. 228p.

(Note: Use articles which originated from dissertations or theses instead of these).

➢ Abstracts published in Events:

Massa A.T., Potter K.A. & Bradway D. 2016. Epizootic bovine abortion outbreak in Eastern Nevada cattle. Annual Meeting American College of Veterinary Pathologist (ACVP), New Orleans, Lousiana. (Abstract D-50)

Colégio Brasileiro de Patologia Animal

Em 15 de agosto de 2019

Mendonça F.S., Almeida V.M., Albuquerque R.F., Chaves H.A.S., Silva Filho G.B., Braga T.C., Lemos B.O. & Riet Correa F. 2016. Paralisia laríngea associada à deficiência de cobre em caprinos no semiárido de Pernambuco (IX Endivet, Salvador, BA). Pesq. Vet. Bras. 36(Supl.2):50-51. (Resumo)

Pierezan F., Lemos R.A.A., Rech R.R., Rissi D.R., Kommers G.D., Cortada V.C.L.M., Mori A.E. & Barros C.S.L. 2007. Raiva em equinos. Anais XIII Encontro Nacional de Patologia Veterinária, Campo Grande, MS, p.145-146. (Resumo)

(Note: Consult entire papers instead of only Abstracts)

Pesquisa Veterinária Brasileira

Brazilian Journal of Veterinary Research

CONTENTS Volume 40, Number 12, December 2020

Livestock Diseases

Gangrenous mastitis in sheep caused by multidrug-resistant *Staphylococcus haemolyticus* [Gangrenous mastitis in sheep caused by multidrug-resistant *Staphylococcus haemolyticus*]. Moura G.S., Mota R.A., Marques M.F.S., Abad A.C.A., Costa L.B.B.C., Souza F.N., Almeida V.M., Silva Filho G.B., Bom H.A.S.C., Klaumann F., Souza F.A.L. & Mendonça F.S. 947-954

Lesions of the sheep reproductive system found in a slaughterhouse in the state of Bahia, Brazill [Lesões do sistema reprodutor em ovelhas de abatedouros frigoríficos no estado da Bahia]. Silva R.M.M., Macêdo J.T.S.A., Lacerda M.S.C., Azevedo J.P.M.V.B., Ferreira Júnior J.A., Cerqueira R.B. & Pedroso P.M.O. 955-962

Testicular and seminal evaluation of goats fed hay *Cenostigma pyramidale* [Avaliação testicular e seminal de caprinos alimentados com feno de *Cenostigma pyramidale*]. Santos M.V.B., Cavalcante A.K.S., Macêdo J.T.S.A., Santos M.C., Rocha L.F., Machado A.L. & Pedroso P.M.O. 963-969

Use of oral fluids to detect anti *Lawsonia intracellularis* antibodies in experimentally infected pigs [Utilização de fluidos orais para detecção de anticorpos anti *Lawsonia intracellularis* em suínos experimentalmente infectados]. Gabardo M.P., Sato J.P.H., Resende T.P., Otoni L.V.A., Rezende L.A., Daniel A.G.S, Pereira C.E.R. & Guedes R.M.C. 970-976

Indirect ELISA (iELISA) standardization for the diagnosis of bovine enzootic leukosis [Padronização de um ELISA indireto (iELISA) para diagnóstico da leucose enzoótica bovina]. Resende C.F., Galinari G.C.F., Victor R.M., Kassar T.C., Arcebispo T.L.M., Delarmelina E., Leite R.C., Reis J.K.P. 977-984

Welfare during pre-slaughter handling and carcass lesions of beef cattle submitted to different loading densities[Bem-estar durante o manejo pré abate e lesões em carcaça de bovinos submetidos às diferentes densidades de carregamento]. Brennecke K., Zeferino C.P., Soares V.E., Orlandi C.M.B., Bertipaglia L.M.A., Sgavioli S., Dian P.H.M. & Amâncio W.D.C. 985-991

Physiological and biochemical responses and hydration status in equines after two barrel racing courses [Respostas fisiológicas e bioquímicas e status de hidratação em equinos após dois percursos de três tambores]. Gomes C.L.N., Alves A.M., Ribeiro Filho J.D., Moraes Júnior F.J., Barreto Júnior R.A., Fucuta R.S., Ribeiro B.M. & Miranda L.M. 992-991

Small Animal Diseases

Clinical-pathological and immunohistochemical evaluations of cardiac lesions in cats with chronic kidney disease [Avaliações clínico-patológica e imuno-histoquímica de lesões cardíacas em gatos com doença renal crônica]. Cid G.C., Jardim M.P.B., Jesus A.C., Costa S.Z.R., Gonçalves I.N., Peixoto T.C., Souza H.J.M. & Nogueira V.A. 1002-1009

Evaluation of galectins 1 and 3 expression in canine melanoma [Avaliação da expressão das galectinas 1 e 3 no melanoma canino]. Garcia J.S., Hazarbassanov N.G.T.Q., Nakamura J.C., Nowosh V., Cogliati B., Marques de Sá L.R. & Massoco C.O. 1010-1017

Effects of canine adipose-derived mesenchymal stem cells on the epithelialization of rabbits' skin autograft (*Oryctolagus cuniculus*) [Efeitos das células-tronco mesenquimais derivadas do tecido adiposo de cães na epitelização de autoenxertos de pele em coelhos (*Oryctolagus cuniculus*)]. Alvarez Gómez J.L., Pazzini J.M., Barros M.A., Morais B.P., Firmo B., Matsui A., Ampuero R. & De Nardi A.B. 1018-1028

Neoplasms in domestic hamsters in Southern Brazil: epidemiological and pathological aspects of 40 cases [Neoplasias em hamsters domésticos no Sul do Brasil: aspectos epidemiológicos e patológicos de 40 casos]. Wentz M.F., Bianchi M.V., Mello L.S., Pietzsch C.A., Alievi M.M., Driemeier D., Sonne L. & Pavarini S.P. 1029-1038

Animal Morphophysiology

Assessment of fetal lung maturity using analysis of amniotic fluid from ewes that gave birth prematurely and at term [Avaliação da maturidade pulmonar fetal utilizando a análise de líquido amniótico de ovelhas que deram à luz prematuramente e a termo]. Souza N.C., Bovino F., Avilla L.G., Deschk M., Alcindo J.F., Fink M.F.C.B., Mendes L.C.N. & Feitosa F.L.F. 1039-1047

Influence of seasonality on the physiological and seminal parameters of buffaloes in the western region of Pará [Influência da sazonalidade nos parâmetros fisiológicos e seminais de búfalos da região oeste do Pará]. Castro S.R.S., Rebelo L.S., Fernandes Junior O.S., Belo-Reis A.S., Neves K.A.L., Silva W.C. & Vale W.G. 1048-1053

Macroscopic and microscopic morphology of the trachea and lungs of giant anteater (*Myrmecophaga tridactyla*) [Morfologia macroscópica e microscópica da traqueia e pulmões do tamanduá-bandeira (Myrmecophaga tridactyla)]. Oliveira E., Nascente E.P., Oliveira L.P., Santiago Neto J.M., Roquete J.C., Santin A.P.I. & Moura V.M.B.D. 1054-1062

Epigenetic characterization of the H19/IGF2 *locus* in calf clones placenta [Caracterização epigenética do *locus* H19/IGF2 na placenta de bezerros clones]. Costa N.S., Silveira M.M., Vargas L.N., Caetano A.R. & Franco M.M. 1063-1072

Acute-phase protein concentration in bronchoalveolar lavage fluid from healthy horses [Proteínas de fase aguda do lavado broncoalveolar de equinos hígidos].Di Filippo P.A., Ribeiro L.M.F., Meireles M.A.D., Gobbi F.P. & Nogueira A.F.S. 1073-1076

Histomorphometric and immunohistochemical evaluation of the frontal cerebral cortex in diabetic rats after treatment with melatonin [Avaliação histomorfométrica e imuno-histoquímica do córtex cerebral frontal em ratos diabéticos após o tratamento com melatonin].Baptista M.G.P., Ferreira C.G.M., Albuquerque Y.M.L., D'assunção C.G., Alves R.C., Wanderley-Teixeira V. & Teixeira A.A.C. 1077-187

Grillo Tecnologia

ISSN 0100-736X *(Print)*
ISSN 1678-5150 *(Online)*